Spring 2010

The white cell pheromone response pathway in Candida albicans provides insights into the evolution of new signal transduction pathways

Nidhi Sahni
University of Iowa

THE WHITE CELL PHEROMONE RESPONSE PATHWAY IN *CANDIDA ALBICANS* PROVIDES INSIGHTS INTO THE EVOLUTION OF NEW SIGNAL TRANSDUCTION PATHWAYS

by

Nidhi Sahni

An Abstract

Of a thesis submitted in partial fulfillment
of the requirements for the Doctor of
Philosophy degree in Biology
in the Graduate College of
The University of Iowa

May 2010

Thesis Supervisor: Professor David R. Soll

ABSTRACT

Candida albicans is the most common fungal pathogen that infects humans. The research described in this thesis focuses on an in-depth characterization of the regulatory pathways controlling white-opaque switching, mating and biofilm formation, and the relationships among these programs in this pathogen. It was demonstrated in 2006 that minority opaque cells of *C. albicans* release pheromone to signal majority white cells of the opposite mating type to form enhanced biofilms. The white cell biofilms in turn facilitate opaque cell chemotropism, an essential step in mating. The white cell pheromone response is a general characteristic of *C. albicans*, occuring in all tested strains and in all common lab media. By generation of deletion mutants of select genes in the opaque cell mating pathway, it was demonstrated that the pathway regulating the white cell response shares all of the components of the opaque mating pathway, from the pheromone receptor through the MAP kinase cascade with the exception of the downstream transcription factor. In addition, it was demonstrated that a *C. albicans*-specific region in the first intracellular loop, IC1, of the α-pheromone receptor is required for the white, but not the opaque, pheromone response. Furthermore, the *cis*-acting element in the promoters of genes induced by pheromone in white cells was identified. The white-specific pheromone response element, WPRE, is important for the regulation of the white pheromone response and induction of white-specific genes by pheromone. Finally, based on a misexpression library screening of transcription factors previously implicated in adhesion, cell wall biogenesis, filamentation or biofilm formation, the transcription factor Tec1 was identified to be the key regulator in the white pheromone response pathway. Tec1 binds to the WPRE in the promoters of genes induced by pheromone in white cells to mediate the white cell response. The white pheromone response pathway appears to be a relatively young pathway that borrowed the upstream components from the opaque mating pathway, the transcription factor from the ancestral

filamentation pathway, and the downstream genes from the pathway regulating biofilm formation in **a**/α cells of *C. albicans*. Therefore, the configuration of the white response pathway provides a unique glimpse and possibly a paradigm for the evolution of signal transduction pathways in eukaryotes.

Abstract Approved: _____
Thesis Supervisor

_____
Title and Department

_____
Date

THE WHITE CELL PHEROMONE RESPONSE PATHWAY IN *CANDIDA ALBICANS* PROVIDES INSIGHTS INTO THE EVOLUTION OF NEW SIGNAL TRANSDUCTION PATHWAYS

by

Nidhi Sahni

A thesis submitted in partial fulfillment
of the requirements for the Doctor of
Philosophy degree in Biology
in the Graduate College of
The University of Iowa

May 2010

Thesis Supervisor: Professor David R. Soll

Graduate College
The University of Iowa
Iowa City, Iowa

CERTIFICATE OF APPROVAL

_____

PH.D. THESIS

_____

This is to certify that the Ph.D. thesis of

Nidhi Sahni

has been approved by the Examining Committee
for the thesis requirement for the Doctor of Philosophy
degree in Biology at the May 2010 graduation.

Thesis Committee: _____
David R. Soll, Thesis Supervisor

_____
Gary Gussin

_____
Jim Lin

_____
Scott Moye-Rowley

_____
Christopher Stipp

To my parents, grandparents, sister, and friends for their constant encouragement, love and support!

ACKNOWLEDGMENTS

First, I would express my sincere thanks to my advisor Dr. David R. Soll. I would not have gone this far without his constant support, encouragement and guidance. David was always motivating and encouraging me to work hard. His enthusiasm for writing and publishing is commendable. It is because of his efforts and motivation that I was able to publish papers very quickly. I am also grateful to my committee members, Dr. Gary Gussin, Dr. Jim Lin, Dr. Scott Moye-Rowley and Dr. Christopher Stipp, for their advice and support during my Ph.D. study.

Dr. T. Srikantha has been my molecular biology guru over the last few years. I learnt many of the molecular techniques from him when I first joined the lab. It was great fun having both science and non-science discussions with him. I am also indebted to Dr. Karla Daniels for her great help all through my projects. She contributed immensely to the study of biofilms using confocal microscopy, a vital part of my thesis work. She also helped a lot with figure editing and assembling manuscripts for publication. I would like to express my sincere thanks to Dr. Claude Pujol. Claude has been invaluable in editing my thesis and most of my manuscripts. He contributed new ideas and provided important critiques throughout my thesis projects in the lab. I would also thank Dr. Deborah Wessels for having taught me some of the writing skills in the cancer class initiated by David in Spring, 2008. I would also like to thank Ms. Diana Kruse, Mr. Phil Ecklund, Dr. Guanghua Huang, Dr. Daniel Lusche, Ms. Ning Ma, Ms. Terra Simon, Dr. Brent Raisley, Ms. Katie Ekvall, Ms. Amanda Scherer, Mr. Phil Gibson, Mr. Bruce Ritchie and Dr. Wei Wu for their help and support. I am also indebted to my parents and my younger sister for their love and support. Last, but not the least, I would not have finished my Ph.D. without the constant support and encouragement of my great friend Dr. Song Yi. His constant hard work and intellect was a major factor in publishing so many good papers in a very short time. Anyone that I may have missed is purely due to space constraints.

ABSTRACT

Candida albicans is the most common fungal pathogen that infects humans. The research described in this thesis focuses on an in-depth characterization of the regulatory pathways controlling white-opaque switching, mating and biofilm formation, and the relationships among these programs in this pathogen. It was demonstrated in 2006 that minority opaque cells of *C. albicans* release pheromone to signal majority white cells of the opposite mating type to form enhanced biofilms. The white cell biofilms in turn facilitate opaque cell chemotropism, an essential step in mating. The white cell pheromone response is a general characteristic of *C. albicans*, occuring in all tested strains and in all common lab media. By generation of deletion mutants of select genes in the opaque cell mating pathway, it was demonstrated that the pathway regulating the white cell response shares all of the components of the opaque mating pathway, from the pheromone receptor through the MAP kinase cascade with the exception of the downstream transcription factor. In addition, it was demonstrated that a *C. albicans*-specific region in the first intracellular loop, IC1, of the α-pheromone receptor is required for the white, but not the opaque, pheromone response. Furthermore, the *cis*-acting element in the promoters of genes induced by pheromone in white cells was identified. The white-specific pheromone response element, WPRE, is important for the regulation of the white pheromone response and induction of white-specific genes by pheromone. Finally, based on a misexpression library screening of transcription factors previously implicated in adhesion, cell wall biogenesis, filamentation or biofilm formation, the transcription factor Tec1 was identified to be the key regulator in the white pheromone response pathway. Tec1 binds to the WPRE in the promoters of genes induced by pheromone in white cells to mediate the white cell response. The white pheromone response pathway appears to be a relatively young pathway that borrowed the upstream components from the opaque mating pathway, the transcription factor from the ancestral

filamentation pathway, and the downstream genes from the pathway regulating biofilm formation in **a**/α cells of *C. albicans*. Therefore, the configuration of the white response pathway provides a unique glimpse and possibly a paradigm for the evolution of signal transduction pathways in eukaryotes.

TABLE OF CONTENTS

LIST OF TABLES

Table

LIST OF FIGURES

Figure

CHAPTER 1

OVERVIEW OF *CANDIDA ALBICANS* PHENOTYPIC SWITCHING, MATING, AND BIOFILM DEVELOPMENT

Candida albicans is the most common fungal pathogen that infects humans (Edmond *et al.*, 1999; Wisplinghoff *et al.*, 2004). It can grow both as a benign commensal, carried by a majority of healthy people, and as an opportunistic pathogen causing a wide range of infections from superficial cutaneous colonization to serious life-threatening systemic infections (Odds, 1988; Scherer and Magee, 1990; Soll, 1992; Calderone, 2002). The ability of *C. albicans* to adapt to various environmental conditions within the host is acquired by phenotypic plasticity. In response to environmental cues, *C. albicans* is able to undergo phenotypic changes through elaborate developmental programs (Odds, 1988; Soll, 1992). *C. albicans* possesses several major developmental programs. The first is known as filamentation, which allows *C. albicans* cells to reversibly change from a budding yeast form to a filamentous form (true hyphae or pseudohyphae) (Soll, 1986; Calderone, 2002; Sudbery *et al.*, 2004). Filamentation is important for *C. albicans* pathogenesis since mutants that are unable to undergo this transition exhibit diminished virulence (Brown and Gow, 1999; Whiteway and Oberholzer, 2004). The second program is the 3153A-type switching system, through which cells can generate multiple and reversible phenotypes distinguished by colony morphology (Slutsky *et al.*, 1985). The third developmental program is the white-opaque transition, which enables a cell to switch spontaneously and reversibly between two major cell types, white and opaque (Slutsky *et al.*, 1987). White cells are small and their shape is round to oval, while opaque cells are larger and elongated. In addition, white cells form white, hemispherical colonies, while opaque cells form grey flat colonies (Slutsky *et al.*, 1987; Anderson and Soll, 1987; Anderson *et al.*, 1990; Soll, 1992). The white-opaque transition has profound effects on virulence (Soll, 2002; Anderson *et al*., 1989, 1990; Kvaal *et al*., 1997, 1999). Finally,

C.albicans undergoes homozygosis and mating (Miller and Johnson, 2002; Lockhart *et al*., 2002, 2003a; Hull *et al*., 2000; Magee and Magee, 2000), which also affects virulence (Wu *et al*., 2007; Lockhart *et al*., 2005; Lachke *et al*., 2003b). *C. albicans*, therefore has a variety of developmental programs that afford it phenotypic plasticity, which contributes to its success as both a commensal and pathogen.

This thesis focuses on one of these programs, the white-opaque transition. The white-opaque transition was discovered in 1987 in a *C. albicans* strain, WO-1, isolated from a patient with a life-threatening bloodstream infection at the University of Iowa Hospitals and Clinics (Slutsky *et al.*, 1987). But it was soon discovered that, only 8% of *C. albicans* strains underwent this transition (Soll D.R., personal communication), even though all strains carry opaque-specific genes (Slutsky *et al.*, 1987; Srikantha *et al.*, 1998; Soll, 1992, 2002; Lockhart *et al.*, 2002). The white-opaque transition was found to be sensitive to temperature (Slutsky *et al*., 1987). Both high (above 35^{o}C) and low (below 8^{o}C) temperatures caused mass conversion of opaque cells to white (Rikkerink *et al.,* 1988; Bergen *et al.,* 1990). This white-opaque transition was remarkable not only because it represented a complex cellular differentiation with dramatic effects on both physiology and morphology (Slutsky *et al.*, 1987; Anderson *et al.*, 1990; Rikkerink *et al*, 1988; Soll, 1992, 2002), but also because it involved the expression of multiple virulence factors (Soll, 1992, 2002). Through a microarray analysis, it was further revealed that this transition affected the expression of approximately six percent of the genes in the *C. albicans* genome (Lan *et al.*, 2002). It therefore seemed reasonable to assume that the white-opaque transition played a role in the virulence and pathogenesis of *C. albicans*. But the characteristics of the transition led to a number of questions. First, why did the white-opaque transition occur only in a minority of natural strains? Second, what is the exact role of so complex a developmental program in the life history of *C. albicans*? Third, why was the opaque phenotype unstable at physiological temperatures (37^{o}C), given that the animal host is the main environmental niche of *C. albicans*. The discoveries made

in the past decade or so in this field, including several key findings presented in this thesis, provide possible answers to these questions.

Until 1999, *C. albicans*, an obligate diploid, had been considered an asexual organism. In 1999, however Hull and Johnson discovered that *C. albicans* possessed a single mating type-like (*MTL*) locus (Hull and Johnson, 1999). The *MTL* locus contained four mating type genes, *MTL***a**1, **a**2, α1 and α2 (Hull and Johnson, 1999, Tsong et al., 2003). Evidence of mating between **a** and α cells was demonstrated both *in vivo* and *in vitro* (Hull *et al.*, 2000, Magee *et al.*, 2000). In nature, however, a majority of strains were heterozygous (**a**/α) at the *MTL* locus (Lockhart *et al.*, 2002; Tavanti *et al*., 2005; Legrand *et al.*, 2004) and didn't undergo the white-opaque transition. They had to undergo homozygosis to **a**/**a** or α/α to switch (Lockhart *et al.*, 2002; Miller and Johnson, 2002), because the **a**1-α2 protein complex repressed the white-opaque transition (Lockhart *et al.*, 2002; Miller and Johnson, 2002). In 2006, three groups simultaneously identified the master switch gene *WOR1* (*TOS9*), which encoded a transcription factor that induced switching to the opaque phase (Huang *et al*., 2006, Zordan *et al*., 2006; Srikantha *et al*., 2006). In *MTL*-heterozygous **a**/α strains, the **a**1-α2 repressor inhibited *WOR1* expression, and hence maintained the white phenotype and blocked the white-opaque transition (Huang *et al*., 2006, Zordan *et al*., 2006, 2007; Srikantha *et al*., 2006). These results provided an answer to the puzzling question of why only a minority of natural strains underwent the white-opaque transition.

In order to mate, *MTL*-heterozygous **a**/α strains of *C. albicans* must first undergo homozygosis to **a**/**a** or α/α, then switch from the white to opaque phenotype (Miller and Johnson, 2002; Lockhart *et al.*, 2002). An opaque cell is mating-competent and releases pheromone, which induces mating-associated changes in opaque cells of the opposite mating type and which also serves as the chemoattractant in the mating-associated process of chemotropism (Bennett *et al.*, 2003; Lockhart *et al.*, 2003a, b; Panwar *et al.*, 2003; Daniels *et al.*, 2006). The general mating process of *C. albicans* is similar to that of

haploid cells of *Saccharomyces cerevisiae,* the baker's yeast (Soll, 2004; Bennett and Johnson, 2005), but the requirement to switch from white to opaque was specific to *C. albicans*. Why did *C. albicans*, but not *S. cerevisiae*, require such a complex phenotypic transition to be mating-competent (Soll, 1992, 2004; Lan *et al.*, 2002)? The early observations that opaque cells, but not white cells, colonize skin (Kvaal *et al.*, 1999), and that skin facilitates mating (Lachke *et al.*, 2003b) seemed to provide an answer. But there was a problem with this explanation. Why restrict mating to skin? Skin represented only a minor site of colonization or infection (Odds, 1988). The unexpected finding that mating-incompetent white cells responded to the mating pheromones provided a possible resolution of this paradox (Lockhart *et al.*, 2003b; Daniels *et al.*, 2006). In opaque cells, pheromone induced a cell cycle arrest in G1, polarization, chemotropism, shmoo formation, fusion between opaque cells of the opposite mating type and up-regulation of mating-associated genes (Hull *et al.*, 2000; Magee and Magee, 2000; Bennett *et al.*, 2003; Lockhart *et al.*, 2003a, b; Daniels *et al.*, 2006; Zhao *et al.*, 2005b). Pheromone induced none of these responses in white cells; rather, it induced cohesion, adhesion and enhanced biofilm development (Daniels *et al.*, 2006; Yi *et al.*, 2008). It also up-regulated a number of white phase-specific genes (Daniels *et al.*, 2006; Yi *et al.*, 2008; Sahni *et al.*, 2009a, b). In turn, the white cell response facilitated opaque cell mating by providing a 3D environment, the white cell biofilm matrix which stabilized pheromone gradients and promoted chemotropism over extended periods of time and over extended distances, to facilitate fusion between minority opaque cells of opposite mating types (Daniels *et al.*, 2006). This unique signaling system was similar to that between germ cells and surrounding somatic cells in higher eukaryotes (Buccione *et al.*, 1990), and carried out a similar function. In both cases, sex cells signalled surrounding non-sex (somatic) cells to form a protective tissue that facilitated the mating process. In the case of *C. albicans*, the protective environment facilitated cellular fusion, and in the case of higher eukaryotes, the protective environment favored germ cell development. This novel white cell biofilm

response was demonstrated to be a general characteristic of *C. albicans*, and occuring in a majority of natural *MTL*-homozygous strains and homozygous strains generated in the laboratory (Sahni *et al.*, 2009a).

And how was this unique white cell biofilm response regulated? In *C. albicans* opaque cells, the pheromone signal was transduced by a classic mitogen-activated protein (MAP) kinase cascade to regulate mating, which was conserved in the hemiascomycetes which includes both *C.albicans* and *S.cerevisiae* (Chen *et al.*, 2002; Magee *et al.*, 2002; Sprague *et al.*, 1983; Leberer *et al.*, 1997; Errede *et al.*, 1995; Elion, 2000). The α- and **a**-pheromones interacted with the α and **a** receptors, Ste2 and Ste3, respectively (Bennett *et al.*, 2003; Daniels *et al.*, 2006). The activated pheromone receptors then caused the dissociation of the βγ complex from the α subunit of the heterotrimeric G-protein complex, which in turn activated the MAP kinase pathway and the downstream transcription factor Cph1 (Chen *et al.*, 2002; Magee *et al.*, 2002). Cph1 bound to the promoters of mating-associated genes, inducing transcription, resulting in the mating response (Chen *et al.*, 2002; Magee *et al.*, 2002). The MAP kinase cascade also activated the gene *FAR1*, which encoded a G1-cycline dependent protein kinase that mediated cell cycle arrest and directed polarization (Yi *et al.*, 2008; Cote and Whiteway, 2008). Interestingly, in white cells, the pheromone-mediated biofilm response was found to be regulated by the same receptors, heterotrimeric G-protein complex and MAP kinase cascade, but different downstream transcription factors regulating genes (Yi *et al.*, 2008). The opaque downstream regulator Cph1, however, was not induced by pheromone in white cells and did not play a role in the white cell biofilm response (Yi *et al.*, 2008; Sahni *et al.*, 2009b). The white downstream regulator, has recently been identified as Tec1 (Sahni *et al.*, in preparation). Tec1 is selectively induced by pheromone in white cells. Tec1 is the key regulator of the biofilm response.

An additional difference between the white and opaque responses to pheromone was found in the functional dependencies on an intracellular loop IC1, extracellular loop

EC2, intracellular loop IC3 and the C-terminus of the α-pheromone receptor (Yi *et al.*, 2009). The IC1 region was found to be specific to *C. albicans*, and to play a selective role in the white cell biofilm response (Yi *et al.*, 2009).

Through screening by Northern analysis of 103 genes encoding proteins that had been directly or indirectly implicated in adhesion, hydrophobicity, biofilm formation or cell wall biogenesis, we discovered 12 genes that were up-regulated by pheromone in white cells, but not opaque cells (Sahni *et al.*, 2009b). The genes that were selectively up-regulated by pheromone in white cells played a role in pheromone-induced adhesion and biofilm development (Daniels *et al.*, 2006; Sahni *et al.*, 2009b). Moreover, in white cells, the white-specific transcription factor Tec1 activated these biofilm-associated genes through a common *cis*-acting motif, the white pheromone response element (WPRE), while in opaque cells, the transcription factor Cph1 activated mating-associated genes through a different *cis*-acting motif, the opaque pheromone response element (OPRE) (Sahni *et al.*, 2009b; Sahni *et al.*, in preparation).

The discoveries of the white cell biofilm response and the signaling system between white and opaque cells provide an explanation for the function of white-opaque switching. Nevertheless, the instability of opaque cells of opposite mating type at 37^{o}C, the physiological temperature of the host, remained baffling. *In vitro*, this temperature induced opaque cells to switch *en masse* to white cells (Rikkerink *et al.,* 1988; Bergen *et al.,* 1990; Morrow *et al.*, 1993; Srikantha and Soll, 1993). This led to the paradox that if white-opaque switching and mating were important for commensalism and pathogenesis, then opaque cells should not be unstable *in vivo*. We recently found that high CO_2 and N-acetylglucosamine (GlcNAc), both molecules found in the host, were not only potent inducers of the white-to-opaque transition, but maintained the opaque phenotype at physiological temperature (Huang *et al.*, 2009; Huang *et al.*, submitted). These results suggested that high CO_2 and GlcNAc, induced and stabilized the opaque phenotype, in order to facilitate mating. These discoveries have strengthened the relevance of the

white-opaque transition and its associated phenomena (i.e. mating and biofilm formation) in the human host.

Outline of the Thesis Projects

Research described in this thesis has focused on key questions pertaining to the regulation of the white cell biofilm response and the white-opaque switching in *C. albicans*. The pertinent literature on these subjects is reviewed in detail in Chapter 2.

The foundation of my thesis work was laid out by Daniels *et al.* (2006), who discovered a novel signaling system between cells of the two switch phenotypes, white and opaque, in *C. albicans*. It was shown for the first time that rare opaque cells signaled majority white cells, through the release of mating pheromones, to form a white cell biofilm that facilitated rare opaque cell mating (Daniels *et al.*, 2006).

When initially reported the generality of this unique white cell biofilm response had been questioned (Bennett and Johnson, 2006). We therefore tested many natural strains and laboratory derivatives, as well as several different media for this response, and found that the white cell pheromone response was a general characteristic of *MTL*-homozygous strains of *C. albicans* (Sahni *et al.*, 2009a). This work is presented in Chapter 3.

We performed mutational analysis to identify the signal transduction pathway that mediates this unique white cell pheromone response (Yi *et al.*, 2008). The results revealed that the alternative white and opaque pheromone responses utilized the same upstream components, including the pheromone receptors, the heterotrimeric G protein complex and the MAP kinase cascade, but different downstream transcription factors (Yi *et al.*, 2008). This discovery had significant implications, because it identified for the first time in the fungal kingdom that two cell types of the same species employ the same signal, receptor, and signaling pathway to elicit two distinct responses, a configuration that has been found in higher eukaryotes (Yi *et al.*, 2008). This work is presented in Chapter 4.

We then focused on the pheromone receptors, one of the upstream components in the signaling pathway. We discovered a unique region, specific to *C. albicans*, in the first intracellular loop of the α-pheromone receptor, played a selective role in the white cell pheromone response, marking another distinction between the alternative white and opaque response circuitry (Yi *et al.*, 2009). The deletion and effects on signalling of a number of different domains in the α-pheromone receptor are described in Chapter 5.

In the white cell response, pheromone upregulates select white-specific biofilm-associated genes (Yi *et al.*, 2008, 2009; Sahni *et al.*, 2009a). We identified 12 such genes by northern blot screening, and demonstrated that these genes were regulated through a common white-specific *cis*-acting pheromone response element (WPRE), distinct from the opaque-specific *cis*-acting pheromone response element (OPRE) (Sahni *et al.*, 2009b). We further found that the genes up-regulated by pheromone in white cells played essential roles in biofilm formation (Sahni *et al.*, 2009b). This work is discussed in Chapter 6.

The white cell biofilm response had been shown to be mediated by a transcription factor different from Cph1, the transcription factor for the opaque mating response but the white-specific transcription factor had not been identified (Yi *et al.*, 2008). Through construction of a misexpression library of 106 putative transcription factors, we searched for a candidate white-specific transcription factor that, when misexpressed, induced adhesion in the absence of pheromone. We identified one gene, *TEC1*, which met this criterion. We characterized this gene and found that *TEC1* was induced by pheromone only in white cells, functioned through the MAPK pathway, and regulated biofilm-associated genes through WPRE (Sahni *et al.*, in preparation). This work is discussed in Chapter 7.

In Chapter 8, I discuss the significance of my thesis work and the impact it should have on future research. Perspectives on the unique interdependencies between the

white-opaque switching, mating and biofilm development are discussed. Finally, the roles of these programs in the pathogenesis and evolution of *C. albicans* are discussed.

It is clear that the white-opaque transition has an intimate relationship with mating and biofilm formation, which provides a clue for the role of white-opaque switching in nature. It is, however, unclear why opaque cells are sensitive to 37^{o}C, the body temperature of the host, which is the major niche of *C. albicans* colonization. How could the opaque phenotype play any role in the host if high temperature induced mass-conversion to white? My colleagues and I recently identified two molecules present in the gut of humans, CO_2 and GlcNAc, as potent inducers for the white-to-opaque switching at their physiological levels, therefore favoring the opaque phenotype and facilitating mating (Huang *et al.*, 2009; Huang *et al.*, submitted). These findings provide a clue for resolving the above paradox, and for understanding the role of switching and mating in the pathogenesis of *C. albicans*. These data are presented in Appendix A and B.

CHAPTER 2

INTRODUCTION AND BACKGROUND

The Human Fungal Pathogen *Candida albicans*

Candida and Candidiasis

Candida albicans is an opportunistic fungal pathogen (Odds, 1988). It is routinely carried by a majority of healthy individuals as a benign commensal in the mouth (Peters *et al.*, 1966; Martin and Wilkinson, 1983), in the gastrointestinal tract (Gorbach *et al.*, 1969; Cohen *et al.*, 1969), the genitourinary tract (Barlow and Chattaway, 1969) and on the skin (Simuangco *et al.*, 1957). However, *C. albicans* can overgrow its niche when the host immue system is compromised due to a predisposing condition, including bacterial infection (Odds, 1988), human immunodeficiency virus (HIV) infection (Maksymiuk *et al.*, 1984), diabetes mellitus (Skoglund, 1971), cancer chemotherapy (Edwards *et al.*, 1974), antibiotic therapy (Seelig *et al.*, 1974), immunosuppressive therapy following organ or bone marrow transplant (Hill *et al.*, 1964), and aging (Russell and Lay, 1973; Wilkieson *et al.*, 1991). Overgrowth of *C. albicans* leads to a wide range of diseases, from superficial infections, such as vaginitis (Morris, 1969; Singh *et al*., 1972), to severe surface infections of the mouth and esophagus (Powderly *et al.*, 1992; Miyasaki *et al.*, 1992), and to life-threatening blood stream infections (Umazume *et al.*, 1995; Kao *et al.*, 1999). Infections by *C. albicans* and other related species are often referred to as “candidiasis” (Odds, 1988). In the United States, candidiasis is the fourth most common cause of hospital-acquired infections (Edmond *et al.*, 1999; Beck-Sague and Jarvis, 1993), with approximately 10,000 deaths a year due to serious bloodstream infections (Kao *et al.*, 1999; Wisplinghoff *et al.*, 2004). Among all *Candida* species, *C. albicans* is the most prevalent (Odds, 1988; Scherer and Magee, 1990; Soll *et al.*, 1991; Soll, 1992; Calderone, 2002), accounting for the majority (approximately 54%) of candidiasis cases in humans (Wisplinghoff *et al.*, 2004). Clearly, such a high rate of infections is a major public health

concern. Although a number of antifungal drugs have been developed to treat candidiasis (Odds *et al.*, 1986; Kuhn *et al.*, 2002), the efficacy of these drugs is often limited, and recurrent infections are not infrequent (Odds, 1988; Soll *et al.*, 1989; Soll, 2002).

The capacity of *C. albicans* as a human pathogen to evade the host immune defense and survive drug therapy, stemsin part from its high level of phenotypic plasticity (Odds, 1988; Soll, 1992). Phenotypic plasticity can be achieved in several ways. One way is to generate genetic variations within a population by recombination through a sexual cycle and meiosis, as it occurs in a variety of prokaryotic and eukaryotic pathogens (Görtz and Fujishima, 1983; Bähler *et al.*, 1991; Honigberg *et al.*, 1993; Reedy *et al.*, 2009). Although recent studies have demonstrated the completion of a complex sexual cycle in *C. albicans* (Bennett and Johnson, 2003; Lockhart *et al.*, 2003a), meiosis has not yet been identified, thus limiting an estimate of its role in creating genetic diversity (Bennett and Johnson, 2005; Reedy *et al.*, 2009). Another way of acquiring phenotypic plasticity is to modulate gene expression in response to environmental challenges. Such responses are usually rapid because they are at the level of transcriptional regulation and do not rely on DNA replication (Enjalbert *et al.*, 2003). A third way of acquiring phenotypic plasticity is by cellular differentiation through developmental programs. Developmental programs can be triggered by various environmental cues, such as nutrient availability (Madhani and Fink, 1998b; Messenguy and Scherens, 1990), alteration in environmental pH and temperature (Buffo *et al.*, 1984), or host hormones (Bramley *et al.*, 1991; Kinsman *et al.*, 1988; Zhao *et al.*, 1995). *C. albicans* is known for possessing elaborate developmental programs, including filamentation (Soll, 1986), 3153A-type switching (Slutsky *et al.*, 1985), the white-opaque transition (Slutsky *et al.*, 1987) and mating (Hull *et al.*, 2000; Magee and Magee, 2000). All of these developmental programs provide phenotypic plasticity, and hence can be considered as representing virulence factors that can contribute to pathogenicity. Understanding the basic biology of *C. albicans* and the roles these

developmental programs play is, therefore, pivotal to the development of better therapies to treat candidiasis.

Developmental Programs and Virulence in *C. albicans*

In the filamentation program, *C. albicans* cells switch between a round-to-oval budding yeast form and a long filamentous form (Odds, 1988; Gow, 1997). The filamentous form can either be a hypha, which is a compartmentalized tube-like structure with no constriction at the mother-bud neck and compartment junctions, or a pseudohypha, with a constriction at the mother-bud neck and subsequent septal junctions (Sudbery *et al.*, 2004). Filamentation is an important virulence factor and plays a critical role in *C. albicans* infections (Mitchell, 1998; Sudbery *et al.*, 2004). The involvement of filamentation in pathogenesis was initially documented in 1958, when Young observed that yeast cells, which were inoculated in mice intraperitoneally, underwent filamentation to form hyphae (germ tubes) that invaded host pancreatic tissue (Young, 1958). In the host, when yeast cells of *C. albicans* are engulfed by macrophages, they produce germ tubes that extrude out through the plasma membrane of macrophages, bursting them from inside-out in the process (Lorenz and Fink, 2002). Yeast cells also appear to play an important role early in the infectious process by extravasating blood vessels and disseminating to target organs as has been shown in a murine model of systemic infection (Saville *et al.*, 2003). The switch from the budding yeast to the hyphal form of growth is important in the invasion of epithelial cells (Scherwitz, 1982; Sherwood *et al.*, 1992), while the switch from hyphae back to the budding yeast form allows efficient dessimination of yeast cells into the bloodstream for systemic infection (Corner and Magee, 1997; San-Blas *et al.*, 2000).

The filamentation program is coupled with differential expression of a number of genes involved in virulence (Lane *et al.*, 2001; Bensen *et al.*, 2002; Nantel *et al.*, 2002). Cph1 and Efg1 are two transcription factors that regulate hyphal morphogenesis. The

cph1efg1 double mutant strain, which is impaired in hyphal formation under most conditions, has reduced virulence in a murine model of candidiasis (Lo *et al.*, 1997). Hyphae of *C. albicans* express a cell wall-associated protein, Hwp1, which acts as a substrate for mammalian transglutaminase and is specific to *C. albicans* (no homolog of *HWP1* exists in *S. cerevisiae*) (Staab *et al.*, 1999; Sharkey *et al.*, 1999). The null mutant of *HWP1* is unable to form stable attachments to buccal epithelial cells (Staab *et al.*, 1999) and cannot maintain a normal infection in a murine model of systemic candidiasis (Tsuchimori *et al.*, 2000). The expression of Als3 is also under the regulation of the bud-hypha transition and is hypha-specific (Hoyer, 2001). Als3-mediated filamentation is important for host-pathogen interaction *in vivo*, by promoting binding and subsequent endocytosis of *C. albicans* cells by host phagocytes (Phan *et al.*, 2007; Coleman *et al.*, 2009). Interestingly, mutants that are constitutively filamentous also display a defect in virulence. Deletion of *PDE2*, which encodes a phosphodiesterase that degrades cellular cAMP, results in a hyperfilamentous phenotype and dramatically impairs virulence in a systemic murine model of candidiasis (Bahn *et al.*, 2003). Deletion of *TUP1*, which encodes a repressor of filamentous growth, leads to constitutive filamentation, with a significantly reduced capacity to invade endothelial cells and reduced virulence in a murine model of systemic candidiasis (Phan *et al.*, 2000; Braun *et al.*, 2000; Zhao *et al.*, 2002). Finally deletion of *NRG1*, which encodes another filamentation repressor, locks the cells predominantly in the hyphal form, resulting in diminished virulence (Braun *et al.*, 2001; Murad *et al.*, 2001). These results indicate that the bud-hypha transition is indispensible for virulence during *C. albicans* infections, but neither the yeast nor hyphal form alone is sufficient.

Besides filamentation, the developmental programs of phenotypic switching, including the 3153A-like switching system and the white-opaque transition, also play an important role in virulence and pathogenesis of *C. albicans* (Calderone and Fonzi, 2001; Soll, 2002; Liu, 2002). In the 3153A-like switching system, a *C. albicans* strain switches

among seven distinct colony phenotypes (Slutsky *et al.*, 1985). Phenotypic switching is more frequent during *C. albicans* infections (Malavasic *et al.*, 1991; Jones *et al.*, 1994; Soll, 1992, 2002). Superficial and invasive isolates of *C. albicans* differ markedly in the frequency of phenotypic switching, with invasive isolates having higher frequencies (Jones *et al.*, 1994). In addition, cells of different switch phenotypes in the 3153A-like switching system exhibit different adhesive properties to buccal epithelium and stratum corneum (Vargas *et al.*, 1994). Finally, cells from different switch phenotypes also differ in their drug susceptibility. Low and high susceptibility to azoles correlate with the "o-smooth" and the "irregular wrinkle" phenotype, respectively (Soll *et al.*, 1989).

In the white-opaque transition which occurs in *C. albicans* cells that are homozygous at the *MTL* locus (Miller and Johnson, 2002; Lockhart *et al*.,2002), two switch phenotypes, white and opaque, differ in their abilities to express various virulence traits, including the presentation of antigens, adhesion, hydrophobicity, filamentation, drug susceptibility, and virulence in different infection models (Soll, 2002). White and opaque cells express different antigens on their surface (Anderson *et al.*, 1990). Adhesive properties differ between white and opaque cells. White cells are significantly more adhesive to buccal epithelial cells than opaque cells, while opaque cells exhibit significantly more hydrophobicity (Kennedy *et al.*, 1988), a trait that is linked to adhesion during virulence (Cutler, 1991). White cells are able to form hyphae under most of the hypha-inducing conditions, whereas opaque cells are able to do so at significant frequencies only in a culture together with a monolayer of human epithelial cells (Anderson *et al.*, 1989). White cells are more resistant than opaque cells to the antifungal drug amphotericin B (Soll *et al.*, 1991; Vargas *et al.*, 2000), and they are also more resistant to white blood cells and oxidants (Kolotila and Diamond, 1990). White cells are far more virulent than opaque cells in a mouse model for systemic infection (Kvaal *et al.*, 1997), whereas opaque cells are more virulent than white cells in a mouse model for skin colonization (Kvaal *et al.*, 1999). In addition, white and opaque cells differ in their

interaction with host phagocytic cells. White cells are more susceptible to phagocytosis than opaque cells in both Drosophila and mouse phagocytosis models (Lohse and Johnson, 2008). Furthermore, recent studies have shown that white cells, but not opaque cells, can undergo pheromone-enhanced biofilm formation (Daniels *et al.*, 2006; Yi *et al.*, 2008), a pathogenic trait that will be discussed in the next section.

The white-opaque transition involves differential expression of a battery of genes, many of which play a role in drug resistance and virulence (Soll, 2002; Lan *et al.*, 2002; Tsong *et al.*, 2003). Several genes that play an important role in drug efflux are regulated in a phase-specific manner. For instance, the gene *CDR1*, induced in response to antifungal drug treatment, regulates drug resistance in *C. albicans* (Prasad *et al.*, 1995; Hernaez *et al.*, 1998). *CDR1* is expressed in white but not opaque cells (Balan *et al.*, 1997; Soll, 2002). In addition, white-opaque switching has a dramatic impact on the secretion of different secreted aspartyl proteinases (Saps). The expression of Saps is also regulated in a phase-specific manner and is believed to play a role in tissue invasion (Hube and Naglik, 2001; Naglik *et al.*, 2003). The ability of opaque cells to specifically express four *SAP* genes (*SAP1*, *SAP2*, *SAP3*, and *SAP8*) (Morrow *et al.*, 1992, 1993; White *et al.*, 1993; Hube *et al.*, 1994) is believed to account for the better capacity of opaque cells but not white cells, to colonize skin (Kvaal *et al.*, 1999). Taken together, it seemed reasonable to conclude that the white-opaque transition in *C. albicans* provided variability within colonizing populations of *MTL*-homozygous cells for the rapid adaptations to environmental challenges, including different host niches (Soll, 1992, 2002; Odds, 1997).

The role of mating in *C. albicans* virulence is less clear, but several studies have presented evidence for its possible involvement in virulence (Hull *et al.*, 2000; Lachke *et al.*, 2003b). The diploid genome of *C. albicans* possesses a mating type locus, *MTL* (Whelan and Magee, 1981; Riggsby *et al.*, 1982; Hull and Johnson, 1999). Mating between *MTL***a** and *MTL*α strains has been demonstrated *in vitro* (Magee and Magee, 2000) and in a mouse host (Hull *et al.*, 2000; Dumitru *et al.*, 2007). Mating can occur *in*

vivo in the kidney (Hull *et al.*, 2000) and in the gastrointestinal tract (Dumitru *et al.*, 2007), two major host sites of *C. albicans* infection (Simuangco *et al.*, 1957; Eras *et al.*, 1972). In addition, *C. albicans* **a** and α opaque cells can fuse efficiently on skin in a cutaneous infection model (Lachke *et al.*, 2003b). The mating type locus, *MTL*, may also play a role in virulence (Lockhart *et al.*, 2005; Wu *et al.*, 2007). *MTL*-heterozygous **a**/α strains, which are majortity in nature, exhibit a competitive edge compared to *MTL*-homozygous **a**/**a** and α/α offspring in invading hosts in a systemic infection mouse model (Lockhart *et al.*, 2005). *In vivo*, it appears that the heterozygosity of the *MTL* locus plays a minor role in virulence, but in contrast, the heterozygosity of non-*MTL* genes along the sex chromosome plays a more important role (Wu *et al.*, 2007). Finally, Daniels *et al.* (2006) suggested another relationship between mating and virulence in *C. albicans*. Opaque cells can signal majority mating-incompetent white cells to form an enhanced biofilm, which not only serves a role as a virulence factor, but also facilitates mating between minority opaque cells (Daniels *et al.*, 2006).

Biofilm Formation Is Associated with *C. albicans* Infections

There are more than 40 million medical devices implanted in surgeries every year in the United States. Infections from implanted devices occur in approxiately 30% of the patients, and *Candida* species are responsible for up to 20% of these infections (Kojic and Darouiche, 2004). Many *C. albicans* infections in humans are associated with biofilm formation (Hawser *et al.*, 1998; Douglas, 2003). Biofilms are structured communities in which cells bind tightly to a living or inert surface, and become embedded in an extracellular matrix of polymeric substances (Hawser *et al.*, 1998; Ramage *et al.*, 2001, 2005; Soll, 2008). *C. albicans*, like many other microbial pathogens, forms biofilms on medical devices and human tissues (Douglas, 2003), in order to gain access to the bloodstream and eventually colonize viturally every internal organ, leading to systemic infections (Kojic and Darouiche, 2004). Biofilms formed on the surface of implanted

devices, such as plastic prosthetics and catheters, are a serious clinical problem because of their increased resistance to the host immune system and to conventional antifungal drug therapies (Ramage *et al.*, 2002; Mukherjee *et al.*, 2003; Kuhn and Ghannoum, 2004).

Biofilm formation is a complex process that involves several stages (Chandra *et al.*, 2001; Douglas, 2003; Soll, 2008). This process begins with adherence of cells to a surface, forming a basal layer. Cells then grow, proliferate and undergo cohesion with each other, resulting in large aggregates. Finally, cells undergo filamentation to form hyphae in all directions, and produce an extracellular polymeric substance (EPS) matrix, leading to a highly-structured three-dimensional biofilm architecture (Hawser and Douglas, 1994; Blankenship and Mitchell, 2006). Adhesion plays an important role throughout biofilm developmental stages (Gow *et al.*, 1999), and is mediated by cell surface-associated proteins, adhesins (Chaffin, 2008). An important adhesin implicated in biofilm formation is Eap1 (Li *et al.*, 2007). The *eap1* null mutant, which forms a defective biofilm *in vitro*, exhibits a defect in adherence to a human embryonic kidney cell line (Li *et al.*, 2003). Hwp1, which is another cell wall-associated adhesin located on hyphae (Staab and Sundstrom, 1998), can form covalent links to buccal epithelial cells *in vitro* by interacting with mammalian transglutaminases (Staab *et al.*, 1999; Sharkey *et al.*, 1999). The *hwp1* null mutant, which forms a fragile biofilm (Nobile *et al.*, 2006a, b), fails to establish stable attachments to human buccal epithelial cells (Staab *et al.*, 1999), and is compromised in virulence in a mouse model of systemic candidiasis (Tsuchimori *et al.*, 2000; Sundstrom *et al.*, 2002). In addition, the agglutinin-like sequence (*ALS*) family genes encode cell surface adhesin proteins necessary for adherence to fibronectin and host epithelial cells (Hoyer, 2001; Hoyer *et al.*, 2008). The *als1* and *als3* null mutants, both of which produce fragile biofilms with an aberrant hyphal architecture (Nobile *et al.*, 2006a), exhibit reduced adherence to vascular endothelial cells and oral epithelial cells (Fu *et al.*, 2002; Zhao *et al.*, 2004; Sheppard *et al.*, 2004).

Mating can also play a role in promoting biofilm development. Indeed, mating-competent opaque cells can release mating pheromones to signal mating-incompetent white cells to form a biofilm in *MTL*-homozygous strains (Daniels *et al.*, 2006; Sahni *et al.*, 2009a). This pheromone-mediated white cell biofilm response includes an increase in cell-surface adhesion, cell-cell cohesion and an enhancement of biofilm formation, which, in turn, provides a protective environment for opaque cell mating (Daniels *et al.*, 2006). A majority white cell biofilm has been shown to promote chemotropism of rare opaque mating partners to facilitate mating (Daniels *et al.*, 2006). The MAP kinase pathway that regulates mating in *C. albicans*, is also involved in the regulation of the white cell biofilm response (Yi *et al.*, 2008). However, the downstream transcription factor differs, with Cph1 mediating the opaque response (Chen *et al.*, 2002; Magee *et al.*, 2002; Yi *et al.*, 2008), and Tec1 mediating the white response (Sahni *et al.*, in preparation). In addition, a specific region in the first intracellular loop (IC1) of the α-pheromone receptor plays a selective role in the white cell response, but is not involved in the opaque response (Yi *et al.*, 2009). Moreover, in *MTL*-homozygous strains, deletion of each of the genes *EAP1*, *PGA10*, *CSH1* and *PBR1*, which are activated by pheromone specifically in white cells, causes a dramatic defect in biofilm development both in the absence and presence of mating pheromones (Sahni *et al.*, 2009b). Finally, two recent observations in the Soll laboratory demonstrate that i.) white cells of a *MTL*-hemizygous **a**/- strain, derived from deleting the α2 gene or the entire *MTL*α locus of the **a**/α strain P37037, form a thinner and more fragile biofilm (Soll and colleagues, unpublished observations); ii.) deletion of one copy of all three genes, *OBP*, *PAP*, and *PIK*, from the *MTL*α locus of the **a**/α parent strain P37037, results in a defect in biofilm formation (Soll and colleagues, unpublished observations). These results support the hypothesis that the mating type locus (*MTL*) contributes to the regulation of biofilm development.

C. albicans Genome and Genomic Stability

C. albicans is an obligate diploid (Whelan and Magee, 1981; Riggsby *et al.*, 1982). Although mating occurs, meiosis has not been identified (Hull *et al.*, 2000; Magee and Magee, 2000; Bennett and Johnson, 2003). *C. albicans* possesses eight pairs of chromosomes ($n = 8$), as shown in a study using pulsed-field gel electrophoresis (Chibana *et al.*, 2000). The genome of *C. albicans* has been sequenced in two independent commonly used strains, the **a**/α lab strain SC5314 and the α/α natural strain WO-1. The sequencing of *C. albicans* genome in the **a**/α strain SC5314, which is available at the *Candida* Genome Database (http://www.candidagenome.org/), was first completed at the Stanford DNA Sequencing and Technology Center (Jones *et al.*, 2004; Braun *et al.*, 2005). Up until December 1st, 2009, as documented in the newest Assembly 21 of the genome sequencing project (van het Hoog *et al.*, 2007), the *C. albicans* genome contains approximately 6,177 total ORFs, out of which 4,770 are still uncharacterized, and contains 14.2 Mb of nuclear DNA and 40.4 Mb of mitochondrial DNA (*Candida* Genome Database). The genome for the α/α strain WO-1, on the other hand, was independently sequenced by the Broad Institute of MIT and Harvard, and the results can be accessed at (http://www.broad.mit.edu/annotation/genome/candida_albicans/MultiHome.html).

The easy accessibility of the genome sequences has paved the way for the implementation of post-genomic approaches. Microarrays have been developed and used to study the *C. albicans* transcriptome (Lorenz and Fink, 2001). Proteomic methods have also been employed to complement transcriptional analyses (Pitarch *et al.*, 2003). Furthermore, systematic approaches are becoming available to study the contribution of each gene in different natural contexts (Selmecki *et al.*, 2005). The genome of *C. albicans* was subsequently anotated by Braun *et al.* (2005). Since then, more efforts have been contributed to comprehensive genome-wide analysis, including an accurate annotation for *C. albicans* introns (Mitrovich *et al.*, 2007). Mitrovich *et al.* (2007) found that introns were not randomly distributed across the entire genome; instead, they were over-

represented in genes involved in specific cellular processes, such as translation and respiration.

Comparative genome hybridization (CGH) analyses that assess gene copy number on a genome-wide scale reveal that several common laboratory strains of *C. albicans* are characterized by widespread "aneuploidy", which is defined as loss or gain of one chromosome, or a portion of one chromosome (Selmecki *et al.*, 2005). This suggests high levels of genome instability, probably as a result of stress that could be associated with gene transformation and/or selection strategies that involve the use of toxic markers (Selmecki *et al.*, 2005; Ketel *et al.*, 2009). For example, loss of one homolog of chromosome 5 often occurs in strains growing in medium containing sorbose as the only carbon source (Janbon *et al.*, 1998). Sorbose-induced loss of chromosome 5, in which the mating-type locus (*MTL*) is harbored, is commonly used to generate *MTL*-homozygous strains in studies of *C. albicans* mating (Magee and Magee, 2000; Magee *et al.*, 2002; Bennett and Johnson, 2006) and biofilm formation (Sahni *et al.*, 2009a). Noteworthy, these karyotypic alterations and chromosomal rearrangements can lead to changes in phenotype, which in turn may provide an adaptative strategy for this fungus (Ciudad *et al.*, 2004; Magee *et al.*, 2008). For example, loss of one homolog of chromosome 4 and triploidy of chromosome 3 are associated with fluconazole resistance (Perepnikhatka *et al.*, 1999). Moreover, increases and decreases in azole drug resistance are strongly associated with gain and loss, respectively, of an isochromosome composed of the two left arms of chromosome 5 (Selmecki *et al.*, 2006). Together, these results suggest that one of the most interesting features of the *C. albicans* genome is the occurrence of chromosomal rearrangements (Selmecki *et al.*, 2006), such as chromosome length polymorphisms (Magee and Magee, 1987), reciprocal translocations, chromosome loss, and trisomy of individual chromosomes (Wu *et al.*, 2005; Selmecki *et al.*, 2005, 2006).

Molecular Strategies in *Candida* Research

Gene Disruption and Reporter Systems

Although the pathogen *C. albicans* has become the object of intensive investigations over the past three decades, two genetic characteristics of *C. albicans* have made the investigations difficult. First, it is an obligate diploid (Riggsby *et al.*, 1982; Whelan and Magee, 1981). Second, it employs the non-canonic CUG codon, which decodes it as a serine instead of a leucine (Ohama *et al.*, 1993). As a consequence of diploidy, null mutants of *C. albicans* are difficult to obtain. Non-canonical codon usage makes it difficult to develop reporter systems and to use gene homologs from other organisms.

In order to overcome the problems of diploidy and alternative codon usage, *Candida* researchers had to invent new tools based on the existing techniques in related yeast species (De Backer *et al.*, 2000). Targeted gene disruption is now possible and highly efficient through the sequential disruption of both copies of a gene on homologous chromosomes. One of the most widely used gene disruption strategies was pioneered by Fonzi and Irwin (1993), who developed the two-step gene disruption "URA blaster" protocol to create the first isogenic gene knockout in *C. albicans*. This strategy uses a URA blaster cassette that comprises direct repeat elements of the *Salmonella typhimurium hisG* gene, which are separated by a copy of *C. albicans URA3* (*hisG-URA3-hisG*) (Fonzi and Irwin, 1993). Target gene sequences flanking this cassette can be used to efficiently integrate at the target gene locus by homologous recombination in a *ura3*$^{-}$ derivative of *C. albicans*. Integration is selected by screening for rescue of *URA3* auxotrophy in transformants. After confirmation of the heterozygotes by either PCR or Southern blotting, *URA3* auxotrophy is re-established in a heterozygote clone. The *hisG* repeats play a role in providing an efficient homologous recombination-mediated excision of *URA3*, leaving the heterozygote with *URA3* auxotrophy, which can then be used for a

second round of disruption. Obtaining heterozygotes that have lost the *URA3* cassette is accomplished through negative selection based on growth on 5-fluoroorotic acid containing medium that selects against the *URA3*$^{+}$ phenotype and selectively allows the growth of *ura3*$^{-}$ auxotrophs (Fonzi and Irwin, 1993).

In 2000, Aaron Mitchell's group developed an improved strategy that eliminates the use of *hisG* repeats and allows efficient creation of a knockout cassette tailored to any gene of interest by a simple PCR-based amplification method (Wilson et al., 2000). They constructed a single UAU1 genetic construct that specifically targets the two copies of genes of interest in one round of transformation, based on a series of recombination events (Enloe *et al.*, 2000). The *UAU1* cassette contains three fragments, the *URA3* ORF with a 3' deletion, the *ARG4* marker and the *URA3* ORF with a 5' deletion. The two nonfunctional *URA3* fragments share 200 bp of common sequence that is sufficient to mediate intra-chromosomal recombination to excise the *ARG4* fragment (Enloe *et al.*, 2000). To generate a knockout strain, the deletion construct, in which the *UAU1* cassette is flanked by sequences flanking the gene to be deleted, is introduced into *arg*$^{-}$ *ura*$^{-}$ cells. Heterozygotes are selected for acquired arginine (*ARG4)* prototrophy. Homozygous deletion mutants are then obtained by two successive recombinations, an inter-chromosomal recombination between the two homologous chromosomes to replace the functional allele with the first deleted allele, and an intra-chromosomal recombination between the two nonfunctional *URA3* fragments, which excises the *ARG4* marker on one of the two chromosomes and results in *URA3* prototrophy (Enloe *et al.*, 2000). Mitchell's group further exploited this UAU cassette by incorporating it into a Tn7 transposon that is, in turn, used to create a set of random homozygous insertional mutants (Davis *et al.*, 2002). They used the system to identify several essential *C. albicans* genes that have no homologs in *S. cerevisiae* (Davis *et al.*, 2002). In a separate study, Johnson's group used a large scale loss of function forward genetic screen based on transposon-mediated haploinsufficiency to identify 146 genes that affect the bud-hypha transition in *C. albicans*

(Uhl *et al.*, 2003). The advantage of this latter approach is evident in the fact that only six of these 146 genes were previously known in the context of bud-hypha transition, while 39 genes were found to lack close homologs in *S. cerevisiae* and also had not been predicted from previous genetic studies of filamentation in *C. albicans*.

In 2004, a *SAT1*-flipper-based gene disruption system, which makes use of the *S. cerevisiae FLP* recombinase to excise the nourseothricin resistance gene *SAT1*^{r}, was developed to increase knock-out efficiency (Reuss *et al.*, 2004). In this method, the deletion construct contains the drug resistance marker *SAT1*^{r}, and a *FLP* ORF with its regulatory sequence incorporated between two direct repeats of the *FLP* recognition target (FRT). The deletion construct also contains 5' and 3' flanking sequences of the gene to be deleted. Heterozygous mutants are selected for *SAT1* resistance and then *FLP* expression is induced, which mediates excision of the *SAT1*^{r} marker, allowing for a second round of gene deletion (Reuss *et al.*, 2004). The advantage of this strategy is that, it is suitable for generating gene deletion mutants in wild-type strains independently of auxotrophic markers.

In addition to these strategies, there have been great advancements in customizing reporters of gene expression in *C. albicans* (Soll and Srikantha, 1998). Cormack and colleagues (1997) developed modified GFPs that could be used in *C. albicans*. To circumvent the problem posed by alternative codon usage, Soll and colleagues (1996) used a luciferase gene from a sea pansy, *Renilla reniformis*, which lacked CUG codons, as a reporter of gene expression. This luciferase-based enzyme assay provides an extremely sensitive method for quantitating promoter function and has been successfully used in the functional characterization of the promoters ofseveral phase-specific genes (Srikantha *et al.*, 1997; Lockhart *et al.*, 1998; Lachke *et al.*, 2003a; Lockhart *et al.*, 2003b).

Genome-wide Molecular Tools

The completion of the *C. albicans* genome sequencing and annotation made it possible to develop microarrays to monitor the expression of thousands of genes in parallel. Several versions of *C. albicans* expression arrays have been constructed and applied in studies, such as the evolution of drug resistance (Cowen *et al.*, 2002; De Backer *et al.*, 2001), the mechanisms for host-pathgen interaction (Lorenz and Fink, 2002), filamentation (Nantel *et al.*, 2002), phenotypic switching (Lan *et al.*, 2002) and the opaque pheromone response and mating (Bennett *et al.*, 2003; Bennett and Johnson, 2006; Zhao *et al.*, 2005b). Although genome-wide microarray analyses can provide a global view of gene expression and the regulation of the biological processes studied, they fall short of directly revealing the underlying molecular mechanisms, since they simply monitor the transcription levels. Such information can only provide hints for further studies. Follow-up functional analyses must be performed to better interpret these expression data.

An emerging genome-wide approach is proteomics, which can measure thousands of proteins, both qualitatively and quantitatively, in parallel. Although using two-dimensional gel electrophoresis to analyze protein differences in studying developmental programs such as dimorphism (Brummel and Soll, 1982) and phenotypic switching (Finney *et al.*, 1985) is not new in *C. albicans* research, the recent combination of high-resolution 2-D gel electrophoresis and mass spectrometry offers researchers an opportunity not only to recognize differences, but also to determine the identities of differentially expressed proteins. For protein separation, a large 2-D gel is used to resolve up to thousands of proteins (Haynes *et al.*, 1998) and detect protein levels as low as 1 pg (James, 1997). For protein identification, proteins of interest are extracted from 2-D gels, cleaved into shorter peptides, and subjected to mass spectrometry to generate peptide mass fingerprints (Aebersold and Mann, 2003). Proteins are then identified in a fingerprint database (Aebersold and Mann, 2003). Post-translational modifications of proteins, such as phosphorylation and acetylation, can also be detected (Fey *et al.*, 1997).

Proteomics-based methods have been applied to *C. albicans* to identify cell wall proteins specific to yeast and hyphae (Pitarch *et al.*, 1999).

Mophogenesis of *C. albicans*

Filamentation: Dimorphism or Trimorphism?

C. albicans can grow as a budding yeast, or a pseudohypha, or a true hypha (germ tube) (Brown and Gow, 1999; Sudbery *et al.*, 2004). Cells in the budding yeast form are spherical or ellipsoidal in shape (Soll, 1986), and bud in a bipolar fashion similar to diploid *S. cerevisiae* cells (Soll and Herman, 1983; Chaffin, 1984). Hyphal and pseudohyphal cells are two distinct morphological forms; hence, the bud-pseudohypha-hypha transition may be more correctly described as trimorphism, rather than dimorphism (Sudbery *et al.*, 2004). In the hyphal form, cells begin with an outgrowth (germ tube) followed by apical extension to generate a hypha that is unconstricted at the mother-daughter junction and subsequent junctions (Odds, 1988). In the pseudohyphal form, in contrast, the morphology of cells ranges from chains of undetached yeast cells with constrictions at the mother-daughter junction to tube structures resembling true hyphae, except for only mild constrictions at the junction (Odds, 1988). Interestingly, Carlisle *et al.* (2009) recently demonstrated that ectopic expression of *UME6*, a gene encoding a zinc-finger transcription factor involved in morphogenesis, induces filamentation to produce pseudohyphae and hyphae. Lower levels of *UME6* expression specify cell growth largely in the pseudohyphal form, whereas high levels of *UME6* expression specify cell growth exclusively in the hyphal form (Carlisle *et al.*, 2009). Indeed, by increasing *UME6* expression levels, cell morphology transitions gradually through the yeast to pseudohyphal to hyphal morphology (Carlisle *et al.*, 2009; Bastidas and Heitman, 2009). Pseudohypha is, therefore, an intermediate, but distinct, growth morphology between those of yeast and hypha (Sudbery *et al.*, 2004).

There are a number of additional differences between the yeast, pseudohyphal and hyphal forms. First, nuclear divison pattern is different among these three types of cells. In yeast and pseudohyphal cells, the nucleus divides at the mother-daughter junction, whereas in hyphae, nuclear division occurs within the tube-like structure at the place where the septum is formed (Whiteway and Bachewich, 2007). Second, septum localization also differs among yeast, pseudohyphal and hyphal cells. In a study of the temporal and spatial dynamics of septum formation, Mitchell and Soll (1979) stained *C. albicans* cells with the dye calcofluor, which binds chitin, a septal component, and monitored septum formation over time (Mitchell and Soll, 1979). In budding yeast cells, the septum is formed at the time of evagination, and localized at the mother-bud junction (Mitchell and Soll, 1979; Whiteway and Bachewich, 2007). In pseudohyphae, the septum is at the mother-bud junction, which is not the case for hyphae (Sudbery, 2001). In hyphae, however, the septum is formed 20-30 minutes after evagination, and away from the mother-bud junction (Mitchell and Soll, 1979; Whiteway and Bachewich, 2007). In addition to nuclear divison and septum formation, the cytoskeleton arrangement and cell growth pattern provide additional differences between yeast and hyphal cells. Actin polarization occurs in hyphal tips while actin-mediated tip elongation is shut down in budding yeast (Anderson and Soll, 1986). During hyphal growth, the expansion zone is limited to a small region called the spitzenkorper at the hyphal tip, while bud growth involves both apical and isotropic wall expansion that does not require a spitzenkorper (Staebell and Soll, 1985).

Microarrays have been used to study large-scale gene expression profiles during the transition from bud to hypha in a number of strains (Lane *et al.*, 2001; Nantel *et al.*, 2002; Bensen *et al.*, 2002). A number of hypha-specific genes have been identified, including those encoding secreted aspartyl proteases (*SAP4*, *SAP5*, and *SAP6*) (Hube and Naglik, 2001), cell wall adhesins (*HWP1*, *ALS1* and *ALS3*) (Staab and Sundstrom, 1998; Hoyer, 2001; Nobile *et al.*, 2006a, b), proteins required for virulence and host infection (*RBT1* and *RBT4*) (Kadosh and Johnson, 2001; Nobile *et al.*, 2006a), a cell wall

modulating protein (*CHS2*) (Gow *et al.*, 1994b), and a protein involved in biofilm formation (*ECE1*) (Birse *et al.*, 1993; Nobile *et al.*, 2006a).

Regulation of Filamentation by Multiple Factors

Filamentation is condition-dependent, and can be triggered by multiple environmental factors. A commonly used environmental factor regulating the filamentation is pH, because pH represents a simple and defined signal (Soll, 1986; Buffo *et al*., 1984). When yeast cells are released from saturation phase at 37 ºC into fresh Lee's medium at pH 4.5, they continue to grow in the yeast form. In contrast, when grown at pH 6.7, they are induced to form hyphae (Soll, 1986). In a study of yeast and hypha development, Soll and Herman tested the time of commitment to yeast and hypha formation (Soll and Herman, 1983). Commitment to yeast is defined as the time point at which cells incubated in yeast-inducing medium (pH 4.5) can no longer become hyphae when transferred back to hypha-inducing medium (pH 6.7). Hypha commitment is defined as the time point at which cells incubated in hypha-inducing medium (pH 6.7) can no longer make buds when transferred back to yeast-inducing medium (pH 4.5). Commitment to yeast occurs at the time of cell evagination, while commitment to hypha formation occurs 20-30 minutes after evagination (Soll and Herman, 1983). These results suggest that the molecular mechanisms underlying the two commitment points are different.

In addition to pH, the filamentation program can be regulated by a variety of environmental factors, such as serum (Gow and Gooday, 1982), N-acetylglucosamine (GlcNAc) (Hrmová and Drobnica, 1982; Sullivan and Shepherd, 1982), temperature (Buffo *et al.*, 1984), anaerobic conditions (Kaminishi *et al.*, 1994), growth surface and host immune factors (Sherwood-Higham *et al.*, 1994; Gow *et al.*, 1994a), nutrient availability (Madhani and Fink, 1998b), agar matrix (Brown *et al.*, 1999), farnesol (Oh *et al.*, 2001),

oxidative stress (Alonso-Monge *et al.*, 2003), cell cycle (Loeb *et al.*, 1999; Zheng *et al.*, 2004) and carbon dioxide (Klengel *et al.*, 2005).

Serum-containing liquid medium can also induce hypha formation (Mickle and Jones, 1940; Taschdjian *et al*., 1960). The hypha phenotype is maintained for extended periods of time in the presence of serum (Gow and Gooday, 1982), while hyphae induced in Lee's medium revert rapidly to the yeast form (Lee *et al.*, 1975). The hypha-inducible component of serum has recently been purified and characterized (Xu *et al.*, 2008). The essential component, muramyl dipeptides (MDPs), can strongly promote *C. albicans* hyphal growth (Xu *et al.*, 2008). MDPs, mediate hypha formation by activating the cyclic AMP-PKA pathway (Rocha *et al.*, 2001; Xu *et al.*, 2008), which will be discussed in the next section. Nitrogen starvation media containing N-acetyl-glucosamine (GlcNAc) is also known to induce the yeast-to-hypha transition in *C. albicans* (Cannon *et al.*, 1994). GlcNAc promotes germ tube formation within 3 h (Hrmová and Drobnica, 1982). Experiments with immobilized GlcNAc indicated that sensing of GlcNAc is at the cell surface, rather than intracellularly (Sullivan and Shepherd, 1982). However, it remains unclear what receptor is involved in GlcNAc sensing.

Lower temperatures (< 35 ºC) favor yeast growth while higher temperatures do not (Buffo *et al.*, 1984). Anaerobic conditions also affect hyphal development (Kaminishi *et al.*, 1994). When yeast cells, cultured on agar medium supplemented with magnesium chloride and sodium phosphate, are shifted from an aerobic condition to an anaerobic condition, the hyphae formed on the agar surface undergo a morphological change from a straight, elongated form to a spiral form (Kaminishi *et al.*, 1994). Furthermore, growth surface and host immune factors can stimulate and direct hyphal growth (Sherwood-Higham *et al.*, 1994; Gow *et al.*, 1994a). Topological features of the growth surface can control the direction of growth in vitro (Sherwood-Higham *et al.*, 1994). Guidance by the complex topology of epithelia may play a role in infections (Gow *et al.*, 1994a).

Nutrient limited media (minimal media), such as synthetic low-ammonium dextrose, Spider medium (Liu *et al*., 1994) and RPMI medium, are often used to induce the transition from the budding to the filamentous hyphal form and have become the standard media in morphogenesis studies performed to assess the effect of specific gene disruptions in *C. albicans* (Messenguy and Scherens, 1990; Madhani and Fink, 1998b). Glucose as a sole carbon source, on the other hand, promotes yeast growth (Madhani and Fink, 1998a, b).

When yeast cells are embedded in an agar matrix, they are induced to form hyphae (Brown *et al.*, 1999). Farnesol is another signal that triggers conversion of hyphae to yeast cells (Oh *et al.*, 2001). When farnesol, a chemical secreted by hyphal cells, is added toa hyphal culture in medium containing serum, cells switch rapidly to the yeast morphology (Oh *et al.*, 2001). 3-oxo-C12 homoserine lactone, a chemical secreted by *P. aeruginosa* with structural similarity to farnesol, maintains *C. albicans* in the yeast form even in the presence of multiple hyphal-inducing factors (Hogan *et al.*, 2004). Oxidative stress plays an indirect role in the regulation of the bud-hypha transition (Alonso-Monge *et al.*, 2003). Adaptive responses to oxidative stress are mediated by the Hog1 MAPK pathway in *C. albicans* (Alonso-Monge *et al.*, 2003). The HOG pathway represses the serum-induced yeast-to-hypha transition and also represses filamentous growth under other conditions, such as low temperature, low pH, or nitrogen starvation (Eisman *et al.*, 2006). The *hog1* null mutant exhibits a hyperfilamentous phenotype on different agar media (Alonso-Monge *et al.*, 1999).

Furthermore, filamentation is also regulated by the cell cycle (Loeb *et al.*, 1999; Zheng *et al.*, 2004; Chapa y Lazo *et al.*, 2005), as reported for *S. cerevisiae* (Garí *et al.*, 2001; Moffat and Andrews, 2004). In *C. albicans*, G_1 cyclins have also been shown to regulate filamentous growth. In the homozygous deletion mutant of *CLN1*, a G_1 cyclin gene, hyphal growth did not take place in liquid Lee's medium, but did in a serum-containing medium (Loeb *et al.*, 1999). Another G_1 cyclin gene, *CLN3*, was also

required for normal hyphal development, since the *cln3* mutant developed abnormal morphology under hypha-inducing conditions, such as serum-containing medium and neutral pH (Chapa y Lazo *et al.*, 2005). In addition, a hypha-specific G1 cyclin-related gene, *HGC1*, was demonstrated to be essential for hyphal morphogenesis by interacting with the cyclin-dependent kinase (Cdk) Cdc28 (Zheng *et al.*, 2004). The mutant *hgc1*/*hgc1* was incapable of under going hyphal growth in all laboratory conditions tested (Zheng *et al.*, 2004).

In addition, carbon dioxide (CO_2) also plays an important role as a filamentation signal (Klengel *et al.*, 2005; Bahn and Muhlschlegel, 2006). CO_2 concentrations in an animal host can be more than 100-fold higher (5%) than in air (0.033%) (Levitt and Bond, 1970; Stenni *et al.*, 2001). The presence of 5% CO_2 strongly induces pseudohyphal development and invasion of an agar medium (Klengel *et al.*, 2005), a response that requires adenylate cyclase (Cdc35) and the cAMP-PKA pathway, but not the GTPase Ras1 (Klengel *et al.*, 2005). Whether there is indeed a specific CO_2 sensor protein on the cell membrane remains elusive.

Molecular Mechanisms Controlling Filamentation

pH-mediated Filamentation Response Pathways

Studies employing *S. cerevisiae* (Su and Mitchell, 1993) and *Yarrowia lipolytica* (Lambert *et al.*, 1997) as models have identified a pH-response pathway in filamentation, comprising three genes, *RIM20*, *RIM8* and *RIM101*. The homologous pathway in *C. albicans* also regulates the pH-mediated filamentation response (Davis *et al.*, 2000) (Figure 1). *RIM101* is induced in alkaline conditions, and this induction depends on *RIM20* and *RIM8* (Davis *et al.*, 2000). The homozygous deletion mutants of each of the genes, *RIM20*, *RIM8* and *RIM101* exhibit a complete defect in alkaline-regulated filamentation in liquid medium, and exhibit a change in the pH-regulated gene expression pattern when compared to the parental control (Davis *et al.*, 2000). These mutants,

Figure 1. Regulation of morphogenesis in *C. albicans*. Morphogenesis can be triggered by a number of environmental factors and involves a network of multiple signaling pathways. The pathways promoting filamentation include the MAPK pathway, the cAMP-PKA pathway, and Rim101-dependent pH response pathway. The pathways inhibiting filamentation include the Tup1- and Rbf1-mediated pathways. This figure is adapted from Biswas *et al*. (2007).

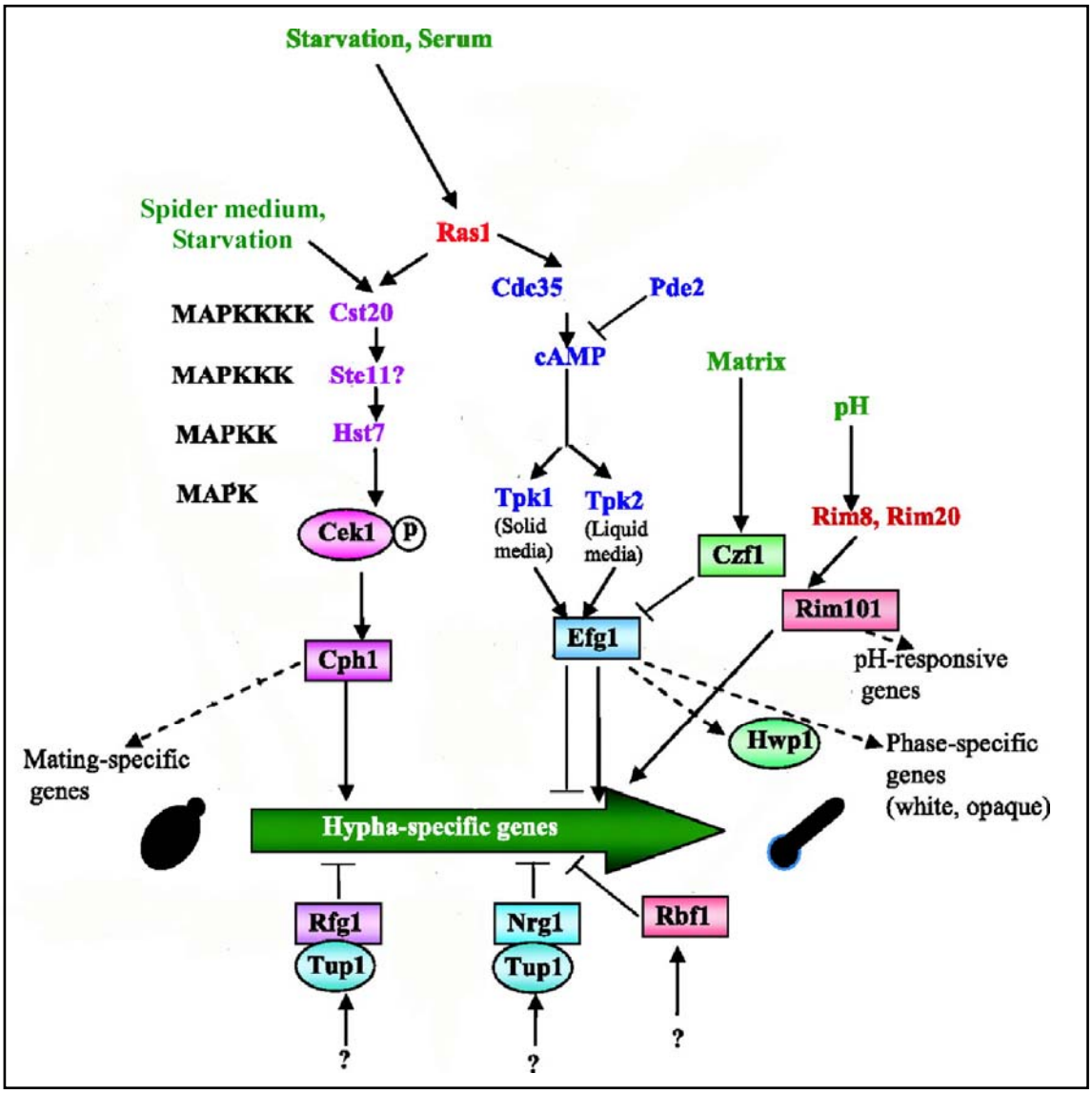
Starvation, Serum
Spider medium,
Starvation
Ras1
Cdc35
Pde2
MAPKKK Cst20
MAPKKK Ste11?
MAPKK Hst7
MAPK
cAMP
Matrix
pH
Cek1
P
Tpk1
(Solid
media)
Tpk2
(Liquid
media)
Czf1
Rim8, Rim20
Rim101
Efg1
Cph1
pH-responsive
genes
Hwp1
Phase-specific
genes
(white, opaque)
Mating-specific
genes
Hypha-specific genes
Rfg1
Tup1
Nrg1
Tup1
Rbf1
?
?
?

however, undergo normal filamentation in the presence of serum at 38^{o}C (Davis *et al.*, 2000). These results suggest that the *RIM101*-dependent pathway plays an important role in alkaline-induced filamentation, but not in serum-induced filamentation. Surprisingly, in the homozygous deletion mutants of *RIM20*, *RIM8* or *RIM101*, the gene *PHR2* can still be alkaline-induced, suggesting that *RIM101*-independent pathways exist to regulate this gene (Davis *et al.*, 2000). Indeed, the calcineurin signal transduction pathway is also involved in the response of *C. albicans* cells to environmental pH changes (Kullas *et al.*, 2007). Calcineurin is a protein phosphatase devoted to the transduction of Ca(2+)-signals (Santos and De Larrinoa, 2005), which plays a role in hyphal formation in *C. albicans* (Brand *et al.*, 2009). The Rim101 pH-sensing pathway acts in parallel to the calcineurin pathway, which targets Crz1, a calcineurin- regulated transcription factor (Karababa *et al.*, 2006), for adaptation to alkaline pH (Kullas *et al.*, 2007). At acidic pH, on the other hand, basal levels of Rim101can act in parallel to Crz2, a calcineurin-independent transcription factor, to repress filamentation (Kullas *et al.*, 2007).

Mitogen-Activated Protein (MAP) Kinase Pathway

The MAP kinase pathway plays a role in the regulation of *C. albicans* filamentous growth under certain conditions, including growth on solid Spider medium (Kohler and Fink, 1996; Liu *et al.*, 1994) and nutrient-limiting medium (Csank *et al.*, 1998) (Figure 1). The main components of this pathway include the kinase Cst20 (Leberer *et al.*, 1996), the MAP kinase kinase (MAPKK) Hst7 (Leberer *et al.*, 1996), the MAP kinase (MAPK) Cek1 (Csank *et al.*, 1998) and the transcription factor Cph1 (Liu *et al.*, 1994) (Figure 1). The homozygous deletion mutants of each of the genes *CST20*, *HST7*, *CEK1* and *CPH1*, exhibit a defect in hypha formation on solid Spider medium (Liu *et al.*, 1994; Csank *et al.*, 1998). The effect of these genes on filamentation on Spider medium may be dosage-dependent, since deletion of one copy of the gene *CST20* or *HST7* also reduces the ability of cells to undergo hypha formation (Kohler and Fink, 1996). On agar medium

containing serum, however, the *CST20*, *HST7* and *CPH1* homozygous deletion strains form normal hyphae, similar to their parental strains (Kohler and Fink, 1996). In contrast, the *cek1* homozygous deletion mutant is severely impaired in serum-induced hyphal growth (Csank *et al.*, 1998). These results suggest that other pathways are involved in regulating the induction of hyphae by serum. In addition, on solid medium when nutrient is limiting, such as medium with mannitol as the only carbon source or glucose medium with limiting nitrogen, the homozygous deletion mutants of *CST20*, *HST7*, *CEK1* and *CPH1*, have severe defects in hypha formation (Csank *et al.*, 1998). None of these mutants, however, exhibits a similar defect in liquid medium (Csank *et al.*, 1998). Although the downstream targets for the transcription factor Cph1 have not been identified, *INT1,* a gene encoding a surface protein with a cytoplasmic tail, may be a candidate. Overexpression of *INT1* leads to filamentous growth in the *S. cerevisiae* null mutant of *STE12*, the homolog of *C. albicans CPH1* (Gale *et al.*, 1996). In addition, disruption of *INT1* in *C. albicans* suppresses hyphal growth on Spider or milk-Tween solid medium, but not on Lee's medium or in the presence of serum (Gale *et al.*, 1998). Finally, despite numerous studies performed on the role of the MAP kinase cascade in hypha formation, little is known about the precise signal(s) that activates the MAP kinase filamentation pathway or the identity of the receptor(s).

Cyclic AMP-dependent Protein Kinase (PKA) Pathway

The cyclic adenosine 3',5'-monophosphate (cAMP)-dependent protein kinase (PKA) signaling pathway regulates filamentation in *C. albicans* under most *in vitro* conditions, including, but not limited to, growth in liquid inducing medium, on solid medium, and serum-induced conditions (Whiteway and Bachewich, 2007) (Figure 1). This pathway includes the upstream GTPase Ras1 (Feng *et al.*, 1999; Leberer *et al.*, 2001), the adenylyl cyclase Cdc35 (Rocha *et al.*, 2001), the cAMP activated protein kinases Tpk1 and Tpk2 (Cloutier *et al.*, 2003) and the transcription regulator Efg1 (Stoldt *et al.*, 1997)

(Figure 1). Disruption of *RAS1*, results in a defect in hyphal formation under all conditions tested, including liquid and solid Spider medium or Lee's medium, 37^{o}C in liquid YPD medium containing 10% serum, 37^{o}C on YPD agar plates containing 10% serum, and induction by N-acetyl glucosamine (Leberer *et al.*, 2001). Disruption of the gene *CDC35*, encoding an adenylyl cyclase that catalyzes the conversion of cytosolic ATP to cAMP, abolishes hyphal formation under all tested hyphal-inducing conditions, including liquid or solid medium, and serum induction (Rocha *et al.*, 2001). Consistently, the null mutant cells of *PDE2*, encoding a phosphodiesterase that degrades cellular cAMP levels, exhibit an enhanced filamentous morphology under all conditions examined (Bahn *et al.*, 2003; Jung and Stateva, 2003). Both of the two PKA protein kinases, Tpk1 and Tpk2, act positively by promoting filamentation under many hypha-inducing conditions (Cloutier *et al.*, 2003). The *tpk1* null mutant is significantly defective in hyphal morphogenesis on solid inducing media with or without serum (Bockmuhl *et al.*, 2001), but is only slightly defective by delaying hyphal development in liquid inducing media (Bockmuhl *et al.*, 2001; Souto *et al.*, 2006). Similarly, the *tpk2* null mutant also exhibits a strong defect in hyphal formation on solid Spider medium and on agar containing 5% serum (Sonneborn *et al.*, 2000). However, in contrast to the *tpk1* mutant, the *tpk2* mutant is severely impaired in hyphal growth in liquid inducing media, including Spider medium and serum-containing medium (Sonneborn *et al.*, 2000; Bockmuhl *et al.*, 2001). The downstream transcription factor Efg1 is regulated through direct phosphorylation by the two kinases, Tpk1 and Tpk2 (Bockmuhl and Ernst, 2001). Disruption of *EFG1* suppresses filamentous growth, while overexpression of *EFG1* enhances filamentous growth under most hypha-inducing conditions examined *in vitro*, including common solid and liquid inducing media and serum-containing media. These data strongly suggest a positive role for this regulator in the filamentation program (Stoldt *et al.*, 1997). Mutation of the single PKA phosphorylation site (T206) in Efg1 from threonine to alanine impairs filamentation, whereas a mutational change to glutamate results in hyperfilamentation

under all conditions examined (Bockmuhl and Ernst, 2001). In some cases, however, Efg1 represses hyphal growth, for instance, during embedded growth on agar matrix at low temperatures (Giusani *et al.*, 2002). This process may be mediated by Czf1, since the repressive effect of Efg1 is abolished in the *czf1* null mutant (Giusani *et al.*, 2002).

Efg1 may not however, be the only target of the cAMP-PKA pathway in hyphal morphogenesis. *RAS1*^{V13}, a dominant active allele of *RAS1*, can stimulate hyphal development in the *efg1* mutant strain (Chen *et al.*, 2000). This indicates that additional genes are involved in the signal transduction downstream of the cAMP pathway. The putative candidates include the two genes *FLO8* and *CRK1*. *FLO8* encodes a transcription factor that physically interacts with Efg1 under hypha-inducing conditions (Cao *et al.*, 2006). Deleting *FLO8* in *C. albicans* blocks hyphal development and hypha-specific gene expression (Cao *et al.*, 2006). However, it is not known if *FLO8* is induced by the cAMP signal or upregulated in the *RAS1*^{V13} mutant. On the other hand, overproducing the Cdc2-related protein kinase Crk1 in *C. albicans* rescues the *efg1* mutant defect in hyphal formation, similar to the phenotype of the *RAS1*^{V13} mutant (Chen *et al.*, 2000). The *crk1/crk1* mutant is significantly impaired in hyphal formation in serum as well as many other hypha-inducing media, a defect typical of mutants in the cAMP pathway. The cAMP pathway in *C. albicans* may include additional transcription factors, such as Mnl1, whose homolog Msn2 in *S. cerevisiae*, is regulated directly by PKAs and is important for cell morphogenesis and pseudohyphal growth (Gorner *et al.*, 1998; Ho and Bretscher, 2001). It would be worthwhile to determine whether these genes are important for hyphal development in *C. albicans*.

Efg1 and Cph1 are the two key transcription factors in the cAMP and MAP kinase pathway, respectively, and function in an independent manner under most hypha-inducing conditions (Lo *et al.*, 1997; Braun and Johnson, 2000). Expression of *HWP1*, a hypha-specific gene that encodes a cell surface protein involved in adhesion to host epithelial cells, is dependent on *EFG1*, but not on *CPH1* (Sharkey *et al.*, 1999). The *hwp1*

mutant is not able to form hyphae on solid medium and produces reduced levels of peripheral hyphae on agar in the presence of serum (Sharkey *et al.*, 1999). Although *HWP1* appears to function downstream of *EFG1* (Figure 1), constitutive expression of *HWP1* is not sufficient to suppress the *efg1* null mutant defect in filamentation, which indicates that Efg1 regulates additional genes required for hyphal development (Sharkey *et al.*, 1999). The complex gene regulation patterns in the Efg1- or Cph1-mediated pathways, therefore, suggest that hyphal development involves multiple, distinct regulators under a specific hypha-inducing condition. Notably, the double mutant *efg1cph1* is unable to undergo filamentation under most tested laboratory conditions. However, this mutant strain is able to filament under certain *in vitro* (Brown *et al.*, 1999; Phan *et al.*, 2000) and *in vivo* (Riggle *et al.*, 1999) conditions. The *efg1cph1*mutant cells undergo filamentous growth when embedded in agar (Brown *et al.*, 1999) and form pseudohyphae in liquid culture in the presence of human endothelial cells (Phan *et al.*, 2000). Cells of this mutant also produce filaments on the tongues of immunosuppressed gnotobiotic piglets *in vivo* (Riggle *et al.*, 1999). These results suggest that additional signaling transduction pathways that are independent of the Efg1- and Cph1-mediated circuits do regulate filamentation.

Pathways that Negatively Regulate Filamentation

Filamentation in *C. albicans* is under both positive and negative regulation. Pathways involving *TUP1* and *RBF1*, for instance, play a role in the repression of filamentation (Braun and Johnson, 1997; Ishii *et al.*, 1997; Zhao *et al.*, 2002) (Figure 1). The Tup1-mediated pathway acts independent of the Efg1- and Cph1-mediated pathways (Braun and Johnson, 2000). Deletion of *TUP1* leads to constitutive filamentation on all tested solid and liquid media, including YPD, Lee's, Spider, minimal nutrient medium, and 20% calf serum (Braun and Johnson, 1997; Zhao *et al.*, 2002). The *tup1* mutant cells form pseudohyphae, but not true hyphae under these conditions (Braun and Johnson, 1997;

Zhao *et al.*, 2002). Tup1 functions through interaction with Rfg1 and Nrg1, two DNA binding proteins involved in the repression of filamentation (Khalaf and Zitomer, 2001; Braun *et al.*, 2001) (Figure 1). Tup1 represses the expression of a number of filamentation-associated genes, including *HWP1* and *SWI1* (Braun and Johnson 1997; Sharkey *et al.*, 1999; Kadosh and Johnson, 2001). Interestingly, deletion of *SWI1*, encoding an activator for the yeast-hypha transition (Mao *et al.,* 2006), in the *tup1* null mutant, completely blocks hypha growth under all of the conditions examined (Mao *et al.*, 2008). This result suggests that Swi1 is a downstream target of the Tup1-mediated pathway that plays a positive role in the regulation of filamentation in *C. albicans* (Mao *et al.*, 2008). Finally, deletion of *RBF1*, encoding another negative regulator of hyphal development, also results in constitutive filamentous growth in both liquid and solid media (Ishii *et al.*, 1997). Unlike the Tup1 pathway, Rbf1 represses filamentation through a different pathway that does not involve Hwp1 regulation (Sharkey *et al.*, 1999).

The Protein Kinase C (PKC) Pathway

The protein kinase C (PKC) pathway mediates hyphal development under a number of conditions, such as embedded and semisolid conditions, oxidative stress, changes in osmotic pressure, cell wall damage, and growth on agar surface (Navarro-Garcia *et al.*, 1995, 1998). Mkc1, which is a major downstream target of protein kinase C, regulates invasive hyphal growth under embedded and semisolid conditions (Navarro-Garcia *et al.*, 1995). Filamentation under these conditions is mediated by Mkc1 phosphorylation, which largely depends on the protein kinase C (Navarro-Garcia *et al.*, 1998; Biswas *et al.*, 2007). The *mkc1* mutant is defective in hypha formation under embedded conditions (Navarro-Garcia *et al.*, 1998). Moreover, ectopic expression of the *CZF1* gene, encoding a transcription factor regulating filamentous growth, restores the filamentation defect of the *mkc1* mutant (Brown *et al.*, 1999). This result indicates that Czf1 is a downstream target of the Mkc1-mediated PKC signaling pathway.

Emerging Genes Involved in the Filamentation Program

A number of genes have recently emerged as new regulators involved in the filamentation program. Some of these genes play a positive role in filamentation, such as *BIG1*, *YAK1*, *MSS11*and *UME6*, whereas others play a negative role to inhibit filamentous growth, such as *SSN6*, *SFL1* and *RAD52*. Deletion of *BIG1*, encoding a protein involved in β-1,6-glucan biosynthesis, reduces filamentation on a solid agar medium and in YPD liquid medium containing 10% serum (Umeyama *et al.*, 2006). Deletion of the gene *YAK1*, encoding a protein of the family of dual-specificity tyrosine-phosphorylated and regulated kinases (DYRKs; Becker and Joost, 1999), results in a defect in filamentous growth on solid agar media, including RPMI and YPD plus 20% serum (Goyard *et al.*, 2008). Deletion of the gene *MSS11*, encoding a protein that interacts with the transcription factor Flo8, causes a profound defect in hyphal development on solid and in liquid medium containing serum (Su *et al.*, 2009). The gene *UME6* encodes a transcription factor, whose homolog in *S. cerevisiae* is involved in regulating filamentation. The *ume6* null mutant displays a dramatic defect in hyphal extension under a variety of filament-inducing conditions *in vitro*, including agar plates containing spider medium and YPD medium plus 10% serum, and *in vivo*, in a murine model of systemic candidiasis (Banerjee *et al.*, 2008; Carlisle *et al.*, 2009). While these genes play a role in promoting morphogenesis towards the filamentous form of *C. albicans*, the following ones serve an opposite function to repress filamentation. The gene *SSN6* encodes a putative global transcriptional co-repressor. Disruption of *SSN6* results in a pseudohyphal growth morphology, but not true hyphae, in liquid medium at 37 ºC (Hwang *et al.*, 2003). Disruption of *SFL1*, which encodes a *C. albicans* homolog of the *S. cerevisiae* Sfl1 (suppressor of flocculation) protein, results in hyphal formation even in non-inducing liquid medium (Bauer and Wendland, 2007; Li *et al.*, 2007). Disruption of *RAD52*, which encodes a protein involved in homologous recombination and DNA damage repair, leads

to slow growth, hyphal and pseudohyphal formation in liquid YPD medium, and significantly enhanced filamentation on solid agar medium (Andaluz *et al.*, 2006).

Although extensive studies have been conducted towards dissecting the molecular mechanisms regulating filamentation in *C. albicans*, most of the mutants defective in hyphae formation were often characterized on a limited set of specialized media (Ernst, 2000). Given that filamentation is a condition-specific process which depends on a variety of environmental cues, mutant strains in *C. albicans* that were reported to exhibit a defect in hyphal formation must be tested under multiple hypha-inducing conditions. The results will provide important clues to determine if a given gene plays a critical role in the regulation of filamentation in general or merely in a context-dependent manner. In addition, since there are an increasing number of genes reported to be involved in filamentation in the last several years, it will be necessary to integrate these genes into the existing filamentation pathways, such as the MAP kinase pathway and the cAMP-PKA pathway. The integration of these new genes into the classical filamentation signaling pathways will not only reveal how these genes are regulated, but it will also provide a more comprehensive regulatory network controlling filamentation under different conditions.

Phenotypic Switching

The success of *C. albicans* as an opportunistic pathogen lies in its high levels of phenotypic plasticity. Up until 1985, the only developmental program that had been demonstrated to generate this plasticity and contribute to *C. albicans* virulence, was the filamentation program. In 1985 and 1987, however, two fundamental discoveries that provided alternative sources for phenotypic plasticity, were made in Dr David Soll's lab at University of Iowa. First, the 3153A-like switching system was discovered in the strain 3153A, which was able to switch among seven distinct colony phenotypes (Slutsky *et al.*, 1985). Second, the white-opaque transition, was discovered in the strain WO-1, a natural *C. albicans* strain isolated from a patient with systemic candidiasis at the University of

Iowa Hospitals and Clinics (Slutsky *et al.*, 1987). Both of these phenotypic switching systems allow cells to generate morphological variants, resulting in a heterogenous population that increases the chance of possessing a phenotype suitable for survival and host infection, hence improving the fitness of the population as a whole. Since the discoveries, the phenotypic switching systems have reveived tremendous attention in the *Candida* community. They are remarkable, not only because the phenotypic consequence is pleotropic, but also because they affect a number of virulence genes (Lan *et al.*, 2002; Soll, 2002; Tsong *et al.*, 2003) and are associated with the infection process (Kolotila and Diamond, 1990; Soll *et al.*, 1991; Kvaal *et al.*, 1997, 1999; Vargas *et al.*, 2000; Lohse and Johnson, 2008).

3153A-like Switching System

Yeast cells of the *C. albicans* strain 3153A normally form smooth, white dome-shaped colonies (O-smooth). However, at low frequency, cells in an O-smooth colony spontaneously and reversibly convert to phenotypes that form variant colony morphologies (i.e. star, ring, irregular wrinkle, hat, stipple and fuzzy) (Slutsky *et al.*, 1985) (Figure 2A-I). Switching among phenotypes occurs at frequencies between 10^{-4} and 10^{-2} per cell generation (Figure 2J), much higher (~1000 fold) than the rate of random genetic point mutations (Slutsky *et al.*, 1985). More importantly, when cells of a particular phenotype are replated, the majority of colonies formed maintain that phenotype, demonstrating heritability, but a minority display other phenotypes, demonstrating reversibility (Slutsky *et al.*, 1985). A change in the proportions of cellular morphology (yeast, pseudohypha, hypha) also occurs during colony switching (Slutsky *et al.*, 1985). The variant colonies are composed of different mixtures of yeast, pseudohyphal and hyphal cells, which show different distribution patterns (Slutsky *et al.*, 1985; Soll, 1992, 2002). In addition, cells in the various switch phenotypes can be induced to form hyphae without losing their identity (Anderson *et al.*, 1990).

Figure 2. The 3153A-like switching system. Different switch phenotypes of *C. albicans*. Each panel depicts a colony representative of each of the several phenotypes. A) “o-smooth”; B) “star”; C) “ring”; D) “irregular wrinkle”; E) “stipple”; F) “hat”; G) “fuzzy”; and H) “r-smooth”. I) A switch from ring to star. J) Switching frequencies among the different phenotypes. All of the clones originated from a star clone following UV treatment. This figure is obtained from Slutsky *et al*. (1985).

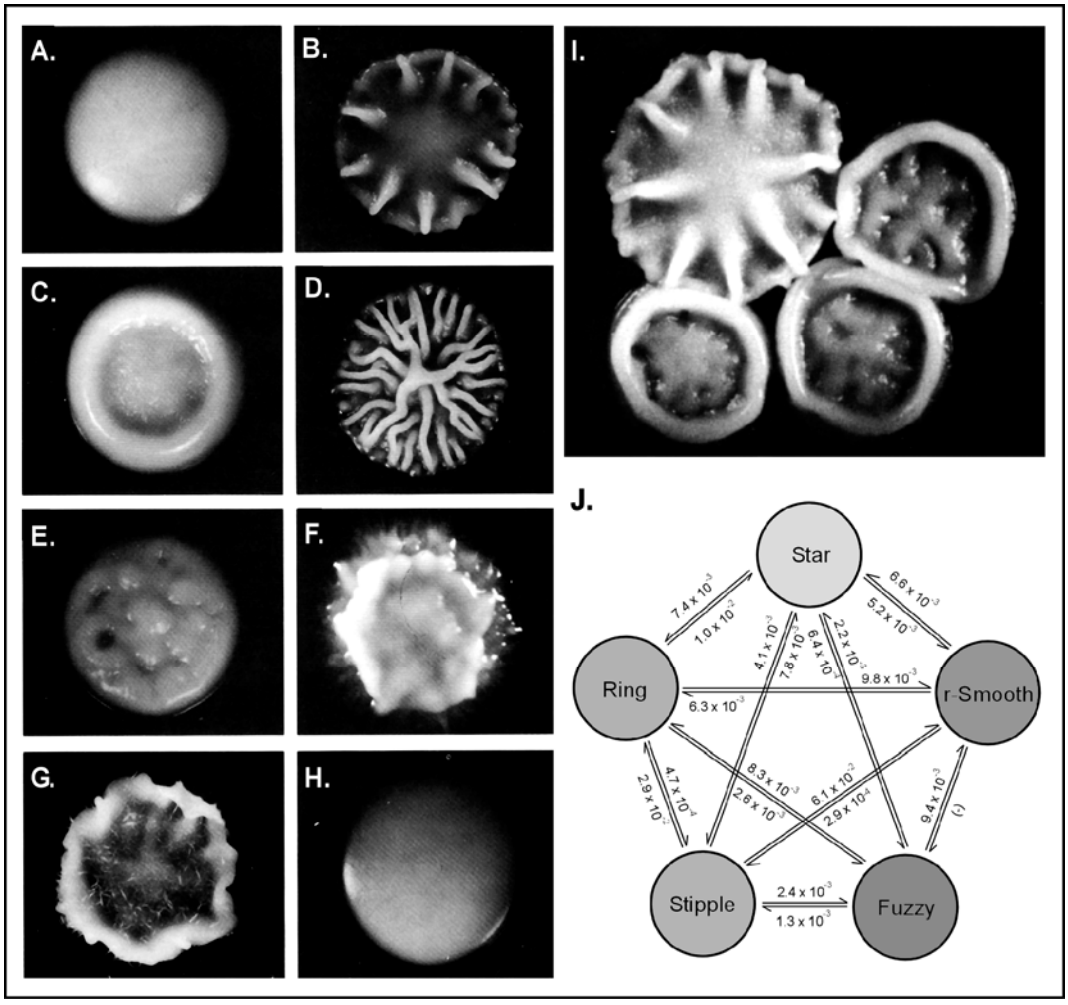
A.
B.
C.
D.
E.
F.
G.
H.
I.
J.
Star
Ring
r-Smooth
Stipple
Fuzzy
7.4 x 10-3
1.0 x 10-2
6.6 x 10-3
5.2 x 10-3
4.1 x 10-3
7.8 x 10-3
6.4 x 10-3
2.2 x 10-2
9.8 x 10-3
6.3 x 10-3
4.7 x 10-4
2.9 x 10-4
8.3 x 10-3
2.8 x 10-3
6.1 x 10-2
2.9 x 10-4
9.4 x 10-3
(-)
2.4 x 10-3
1.3 x 10-3

Discovery of the White-Opaque Transition

The white-opaque transition is a spontaneous, reversible and heritable switch between two metastable phenotypes, designated "white" and "opaque" (Soll, 1992, 2002). In 1987, the white-opaque transition was discovered in strain WO-1 by a graduate student Bernice Slutsky in Dr. David R. Soll's lab at the University of Iowa (Slutsky *et al.*, 1987). The strain WO-1 was isolated from the bloodstream of a patient with systemic candidiasis (Slutsky *et al.*, 1987). The frequency of white-opaque switching was estimated to be between 10^{-2} to 10^{-3} (Figure 3A) (Rikkerink *et al.*, 1988; Bergen *et al.*, 1990; Soll *et al.*, 1991). Frequency was affected by a variety of environmental conditions (Rikkerink *et al.*, 1988; Morrow *et al.*, 1989; Kolitila & Diamond, 1990; Dumitru *et al.*, 2007; Ramirez-Zavala *et al.*, 2008; Huang *et al.*, 2009). When cells from a colony exhibiting one phenotype, either white or opaque, are plated on agar, they produce primarily colonies of that original phenotype (about 97-99%), and rarely switch to produce colonies (about 0.1%) or sectors (about 3%) of the alternative phenotype (Slutsky *et al.*, 1987; Soll, 1992, 2002; Srikantha and Soll, 1993) (Figure 3A). White and opaque phenotypes can be distinguished in many ways, including, but not limited to, colony morphology, cellular morphology and gene expression profile. Opaque colonies differentially stain red when phloxine B is supplemented into the supporting agar medium. The white colonies are small and dome-shaped, whereas the opaque colonies are larger and flat (Slutsky *et al.*, 1987). Cells from the white colonies are round with uniform surfaces (Figure 3B, D, F), whereas cells from the opaque colonies are twice as large as white cells (Figure 3C), and have unique surface pimples and a large vacuole in the cytoplasm (Anderson and Soll, 1987; Anderson *et al.*, 1990) (Figure 3E, G).

Opaque cells express a unique antigen, a 14.5 kDa protein associated with the pimple structures on the cell surface (Anderson *et al.*, 1990). A number of phase-specific genes have been identified. In 1992, the first opaque phase-specific gene, *PEP1* (*SAP1*),

Figure 3. The white-opaque transition in *C. albicans*. A) When white cells are plated on agar containing phloxine B, majority of the colonies formed are white but a few ($\sim 10^{-3}$) are opaque. On the other hand when opaque cells are plated on agar, majority of colonies are opaque but few are white. B) White cells in liquid Lee's medium. C) Opaque cells in liquid Lee's medium. D) Scanning electron micrograph (SEM) of a white cell. E) Scanning electron micrograph (SEM) of an opaque cell. Note that the white cell is round while the opaque cell is elongated and about twice the size of the white cell. F) Transmission electron micrograph (TEM) of a white cell. G) Transmission electron micrograph (TEM) of an opaque cell. Note the presence of cell surface pimples as indicated by arrows on opaque cells. This figure is adapted from Soll (2004, 2009).

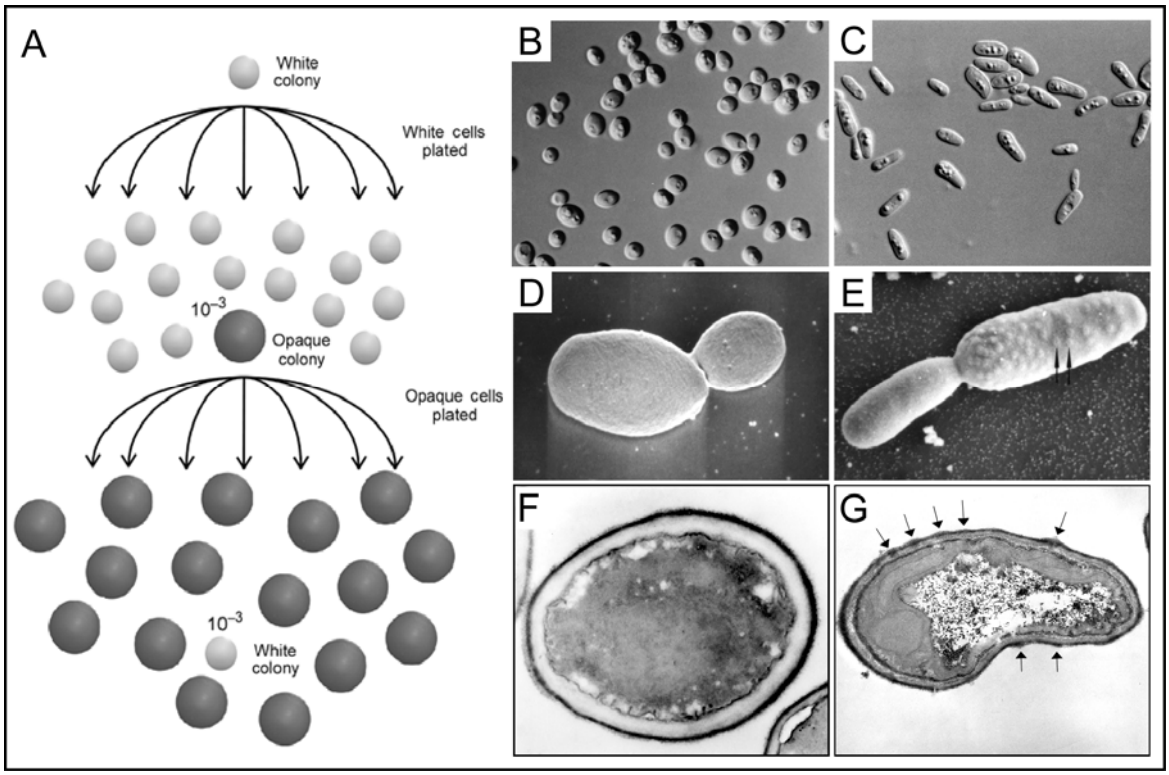
A
White colony
White cells plated
10^{-3}
Opaque colony
Opaque cells plated
10^{-3}
White colony
B
C
D
E
F
G

for secreted aspartyl proteinase 1, was identified (Morrow *et al.*, 1992). In 1993, another opaque-specific gene, *OP4* (Morrow *et al.*, 1993), and the first white phase-specific gene, *WH11* (Srikantha and Soll, 1993), were identified. In addition, *EFG1* was found to exhibit a phase-dependent pattern in transcript size (Srikantha *et al.*, 2000). *EFG1* expresses a low molecular weight transcript in opaque cells, but a higher molecular weight transcript in white cells (Srikantha *et al.*, 2000). The list of phase-specific genes expanded dramatically through analysis of expression microarrays (Lan *et al.*, 2002; Tsong *et al.*, 2003; Zhao *et al.*, 2005b). Approximately 400 genes, roughly 6% of the *C. albicans* genome, were differentially regulated during the white-opaque transition, with about 170 genes upregulated in the white phase and about 230 genes upregulated in the opaque phase (Lan *et al.*, 2002). Based on transcriptional profiling studies, it was further suggested that the white-opaque transition is associated with metabolic specialization. White cells express genes involved in fermentative metabolism, while opaque cells express genes involved in oxidative metabolism (Lan *et al.*, 2002). This difference occurs both under aerobic and anaerobic conditions, indicating that it is inherent to both the phenotypes (Lan *et al.*, 2002).

There existed, however, two paradoxes in the white-opaque transition? First, why does the white-opaque transition occur only in approximately 8% of natural strains, while all strains contain phase-specific genes (Slutsky *et al.*, 1987; Srikantha *et al.*, 1998; Soll, 1992, 2002; Lockhart *et al.*, 2002)? And second, why are opaque cells unstable at the host physiological temperature (~37^{o}C), when the main niche of C.albicans is the animal host (Cohen *et al*., 1969; Martin and Wilkinson, 1983; Barlow and Chattaway, 1969; Odds, 1988)? Opaque cells undergo a switch *en masse* to white cells when the environmental temperature is shifted to above 35^{o}C (Slutsky *et al.*, 1987; Rikkerink *et al.*, 1988; Srikantha and Soll, 1993; Soll, 2002).

White-Opaque Transition Depends on *MTL*-homozygosis

Miller and Johnson (2002) derived **a** and α strains from an **a**/α laboratory strain CAI4, and discovered that the **a** and α derivatives, but not the **a**/α parent, underwent the white-opaque transition and formed opaque sectors. Cells from these opaque sectors were found to be true "opaque" cells, because they expressed the opaque-specific gene *OP4*, but not the white-specific gene *WH11* (Miller and Johnson, 2002). This study suggested that the **a**1-α2 complex represses switching in addition to its role in the repression of mating (Miller and Johnson, 2002). To universalize this observation, Lockhart *et al.* (2002) analyzed the relationship between the *MTL* genotype and the ability to switch in 220 natural strains. Their results indicated that the majority of *C. albicans* strains in nature, which are **a**/α, are not capable of switching between white and opaque phenotypes, unless they first undergo *MTL*-homozygosis (Lockhart *et al.*, 2002). Consistently, two other studies also reported that around 90% of natural strains are **a**/α, and 10% **a**/**a** or α/α (Legrand *et al.*, 2004; Tavanti *et al.*, 2005).

Interestingly, it was demonstrated that deletion of a single allele of the *HBR1* (hemoglobin response gene 1) allowed **a**/α cells to undergo the white-opaque transition and acquire mating competency (Pendrak *et al.*, 2004), probably through repression of *MTL*α1 and α2 gene expression and activation of *MTL***a**1 expression. Since *HBR1* is a host factor-regulated gene, this study indicated that **a**1-α2 repression in *C. albicans* can be relieved through host-pathogen interactions. These results, however, were never corroborated, and the research was discontinued.

Epigenetic Mechanisms for Switching

The white-opaque transition is an epigenetic phenomenon, in which genetically identical cells can exist in two distinct cell types, white and opaque (Slutsky *et al.*, 1987; Soll, 1992). In *S. cerevisiae*, histone deacetylases play critical roles in epigenetic mechanisms regulating gene silencing (Hassig *et al.*, 1998; Kadosh and Struhl, 1998;

Rundlett *et al.*, 1998; Suka *et al.*, 1998; Grozinger *et al.*, 1999). In *C. albicans*, an indication that gene-silencing mechanisms might play a role in switching was provided by several studies. Treatment with trichostatin A, a deacetylase inhibitor, causes a dramatic and selective increase in the frequency of switching from white to opaque (Klar *et al.*, 2001). Deletion of the deacetylase gene *HDA1*, a presumed target of trichostatin A (Carmen *et al.*, 1996), also causes a dramatic increase in the frequency of switching from white to opaque, and deletion of the deacetylase gene *RPD3* causes a dramatic increase in the frequency of switching from both opaque to white and white to opaque (Srikantha *et al.*, 2001). The increase in the frequency of switching in deacetylase mutants suggests that spontaneous switching may involve a metastable, epigenetic transition between active (expressed) and inactive (suppressed) chromatin states at a master switch locus (Soll, 1992). Recently, Hnisz *et al.* (2009) have shown that the Set3/Hos2 histone deacetylase complex plays a regulatory role in white-opaque switching, and involves the methylation of histone H3.

Identification of the Master Switch Locus, *WOR1*

In 2006, three groups independently identified the master switch locus, *WOR1* (*TOS9*). The gene *WOR1*, which is homologous to the *S. cerevisiae* gene *TOS9*, encodes a transcription factor that plays a fundamental role in the white-opaque transition (Huang *et al.*, 2006; Zordan *et al.*, 2006; Srikantha *et al.*, 2006). Huang *et al.* (2006) identified *WOR1* through a screen for *C. albicans* genes that could suppress the defect of a *S. cerevisiae flo8* mutant, which was incapable of invading solid medium. They then generated a *wor1* null mutant in an **a**/**a** strain, and found that cells of this mutant could not switch to opaque (Huang *et al.*, 2006). Zordan *et al.* (2006) generated null mutants for six genes, previously identified as targets of the **a**1-α2 complex in **a**/α cells (Tsong *et al.*, 2003). They found that deletion of *WOR1* abolished switching and locked cells in the white phase. Finally, Srikantha *et al.* (2006) performed a chromatin

immunoprecipitation-microarray (ChIP-chip) analysis to identify genes with **a**1-α2 binding sites (Srikantha *et al.*, 2006). They then screened these genes by northern analysis for an opaque-specific expression pattern, and found that the gene *WOR1* (*TOS9*) fit the putative criteria. The *wor1* null mutant blocked cells in the white state (Srikantha *et al.*, 2006).

WOR1 has an extremely long 5'-untranslated upstream region, and an **a**1-α2 binding site. Zordan *et al.* (2006) demonstrated that the promoter of *WOR1* has five Wor1 binding sites between −2000 and −8000 bp. The *WOR1* transcription start site is approximately 2000 bp upstream of the *WOR1* ORF and 3647 bp downstream of the putative **a**1-α2 binding site (Srikantha *et al.*, 2006). Hence, the estimated *WOR1* transcript is relatively large, approximately 4530 bases (Huang *et al.*, 2006; Srikantha *et al.*, 2006). Northern analyses and green fluorescence protein (GFP)-tagging experiments revealed selective *WOR1* expression in opaque cells (Huang *et al.*, 2006; Srikantha *et al.*, 2006; Zordan *et al.*, 2006). Wor1 localizes in the nucleus of opaque cells, but is undetectable in white cells (Srikantha *et al.*, 2006). When opaque cells undergo mass conversion to the white phenotype as a result of an increase in temperature higher than 35 °C, Wor1 is degraded (Srikantha *et al.*, 2006). When *WOR1* is overexpressed ectopically in α/α cells in the white phase, they convert *en masse* to the opaque phase (Srikantha *et al.*, 2006). Misexpression of WOR1 in **a**/α cells leads to unstable expression of the opaque phenotype (Huang *et al.*, 2006; Srikantha *et al.*, 2006; Zordan *et al.*, 2006), and a pulse of *WOR1* expression in white cells is sufficient to induce a metastable switch from white to opaque (Zordan *et al.*, 2006). *WOR1* misexpression in opaque cells also prevents temperature-induced mass conversion to white (Srikantha *et al.*, 2006). In addition, removal of the potential PKA phosphorylation site impairs opaque cell formation (Huang *et al.*, submitted), suggesting that the white-opaque transition is under the regulation of cAMP-PKA pathway.

Regulatory Feedback Loops Controlling Switching

The white-opaque transition is a complex process that has been proposed to be controlled by multiple regulators in a network of feedback loops (Srikantha *et al.*, 2006; Vinces and Kumamoto, 2007; Zordan *et al.*, 2007; Soll, 2009). These feedback loops involve, but are not limited to, four transcription factors, Efg1, Czf1, Wor1 and Wor2 (Zordan *et al.*, 2007). Efg1, a protein with homology to Myc-type transcription factors, was initially demonstrated to play a role in filamentation (Stoldt *et al.*, 1997). Overexpression of *EFG1* leads to enhanced filamentous growth, while low levels of Efg1 cause the formation of elongated cells that superficially resemble opaque cells (Stoldt *et al.*, 1997). Indeed, *EFG1* is also involved in the regulation of the white-opaque transition (Sonneborn *et al.*, 1999; Srikantha *et al.*, 2000; Zordan *et al.*, 2007). *EFG1* is abundantly expressed in white cells, but it is expressed at a much lower level in opaque cells (Srikantha *et al.*, 2000). Overexpression of *EFG1* in opaque cells induces switching to white cells (Doedt *et al.*, 2004). Deletion of *EFG1* in *MTL*-homozygous **a**/**a** or α/α, but not *MTL*-heterozygous **a**/α cells, leads to an opaque-like morphology (Srikantha *et al.*, 2000; Zordan *et al.*, 2007). These mutant cells possess characteristic pimples on the cell surface, and express the opaque-specific markers *OP4* and *SAP1*, but not the white-specific marker *WH11* (Srikantha *et al.*, 2000). However, the mutant cells can also form white colonies (Zordan *et al.*, 2007), and undergo mass conversion from opaque to white at 42^{o}C (Srikantha *et al.*, 2000). During mass conversion, the opaque-specific genes *OP4* and *SAP1* are downregulated, and the white-specific gene *WH11* is upregulated (Srikantha *et al.*, 2000). Surprisingly, the *efg1* "white" cells are elongated in shape, but do not possess pimples on the cell wall (Srikantha *et al.*, 2000). The *efg1* null mutant is, therefore, impaired in its ability to generate the complete white cell phenotype (Srikantha *et al.*, 2000; Zordan *et al.*, 2007).

Czf1, which was initially found to play a role in promoting hyphal growth under embedded conditions (Brown *et al.*, 1999), is another important regulator in the

white-opaque transition (Vinces and Kumamoto, 2007; Zordan *et al.*, 2007). While overexpression of *EFG1* induces the switch from opaque to white, overexpression of *CZF1* stimulates the reverse switch, from white to opaque (Vinces and Kumamoto, 2007). In wild-type *MTL*-homozygous cells, *CZF1* is expressed specifically in opaque, but not white cells (Lan *et al.*, 2002; Tsong *et al.*, 2003). The *czf1* null mutant is defective in opaque cell formation (Zordan *et al.*, 2007). Hence, these two transcription regulators, Efg1 and Czf1, seem to exhibit antagonistic effects in white-opaque switching. This antagonistic effect is probably mediated through a physical interaction between Efg1 and Czf1, as demonstrated by Giusani *et al.* (2002) *in vitro* in a yeast two-hybrid system. The transcription factor Wor2 also promotes switching from white to opaque (Zordan *et al.*, 2007). *WOR2* is specifically expressed in opaque, but not white, cells. The *wor2* null mutant is severely impaired in switching to the opaque phase (Zordan *et al.*, 2007).

As mentioned in the previous section of "Identification of the Master Switch Locus", the master switch gene *WOR1* plays a key role in the white-opaque transition (Huang *et al.*, 2006; Zordan *et al.*, 2006; Srikantha *et al.*, 2006). Wor1 regulates the expression of a number of phase-specific genes by directly binding to their promoters (Zordan *et al.*, 2007). Wor1 can function as either an activator or a repressor to regulate gene transcription. For instance, binding of Wor1 positively regulates the expression of *CZF1* and *WOR2*, but negatively regulates the expression of *EFG1* (Zordan *et al.*, 2007). Interestingly, Wor1 can also bind to its own promoter and positively regulate its own expression (Zordan *et al.*, 2006, 2007). To better describe the regulation of white-opaque switching, Zordan *et al.* (2007) proposed a model involving a network of regulatory feedback loops. In this model, expression of *EFG1* induces the white phenotype, while expression of *WOR1* induces the opaque phenotype. In white cells, *WOR1* is not expressed, but *EFG1* is. In opaque cells, expression of *WOR1* activates *CZF1* and *WOR2*, and represses *EFG1*. Expression of *CZF1* represses *EFG1*, and expression of *WOR2* activates *WOR1* in a feedback manner (Zordan *et al.*, 2007). Indeed, the autoregulation of

Wor1 is the key to understanding the regulation of these interlocking loops. Once *WOR1* expression is established, it is maintained by a positive-feedback loop that stabilizes the cells in the opaque state (Zordan *et al.*, 2007). However, if Wor1p levels drop below a critical threshold, this positive-feedback loop is disrupted and the cells revert to the white phenotype (Zordan *et al.*, 2007). Together, these results suggest that multiple phase-specific transcription factors are at play in establishing and maintaining the alternative phases of the white-opaque transition (Srikantha *et al.*, 2006; Zordan *et al.*, 2007; Soll, 2009).

Stability of the Opaque Phenotype in the Host

Low oxygen has been recently reported to play a role in stabilizing opaque cells in the host (Dumitru *et al.*, 2007; Ramirez-Zavala *et al.*, 2008). In the human host, the gastrointestinal tract and the vaginal cavity contain reduced levels of oxygen (Levitt and Bond, 1970; Stenni *et al.*, 2001; Avunduk, 2002; Hill *et al.*, 2005). Dumitru *et al.* (2007) demonstrated that under anaerobic conditions when the temperature was raised from 25 to 37 °C, the frequency at which opaque cells switched to white cells was far lower than under aerobic conditions, suggesting that hypoxia stabilized the opaque phenotype at 37 °C. The reason for this decrease in the frequency of opaque to white switching, however, could have been due either to a decrease in the rate of switching, or to the associated decrease in the rate of cell division. It has been shown previously that when the temperature was raised from 25 to 37 °C, opaque cells had to divide a minimum of two times before switching to white (Srikantha and Soll, 1993). In another study, Ramirez-Zavala *et al.* (2008) presented evidence that under anaerobic conditions generated *in vitro* at 37 °C, the frequency of switching from white to opaque increased and the opaque phenotype was stabilized. They also found that passage of white *MTL*-homozygous cells through the gastrointestinal tract of a mouse, induced switching from white to opaque. Their method for experimentally reducing O_2 levels *in vitro*,

however, caused an increase in CO_2 to levels much higher than in air (Ramirez-Zavala *et al.*, 2008). This latter study did not, therefore, distinguish between induction by low O_2 and induction by high CO_2. Huang *et al.* (2009) appear to have resolved this question. They found that physiological levels of CO_2, which are over 100 times higher than the levels in air (Levitt and Bond, 1970; Stenni *et al.*, 2001; Avunduk, 2002), induced white to opaque switching in the presence as well as in the absence of O_2. High CO_2 stabilized the opaque phenotype and inhibited opaque to white switching at 37 °C (Huang *et al.*, 2009). These results provided a better explanation for how opaque cells may be stabilized in the animal host in order to facilitate mating. These results also suggested that opaque cells may be more prevalent in *MTL*-homozygous cell populations at sites of colonization than originally considered. The observation (Ramirez-Zavala *et al.*, 2008) that white cells are induced to switch to opaque in the gut of a host would be explained by the very high levels of CO_2 (Huang *et al.*, 2009).

Alternative Pheromone Responses in White and Opaque Cells

In the white-opaque transition, cells undergo a spontaneous and reversible switch between the white and opaque cell types (Slutsky *et al.*, 1987). This transition is observed only in *MTL*-homozygous cells (Miller and Johnson, 2002; Lockhart *et al.*, 2002). Opaque cells secrete mating-type specific pheromone that induces a mating response in opaque cells of the opposite mating type, characterized by a cell cycle arrest, cellular polarization, production of mating projections (shmoo formation), and mating (Bennett *et al.*, 2003; Lockhart *et al.*, 2003a, b; Dignard *et al.*, 2007; Yi *et al.*, 2008). White cells do not produce pheromone and do not undergo a mating response in response to pheromone. Pheromone does, however, induce white cells to undergo a unique cellular response, which includes cell-cell cohesion, cell-surface adhesion, enhanced biofilm formation and upregulation of white-specific genes (Daniels *et al.*, 2006; Yi *et al.*, 2008). The enhanced

biofilm in turn facilitates chemotropism and mating between opaque cells by stabilizing pheromone gradients (Daniels *et al.*, 2006; Yi *et al.*, 2008; Sahni *et al.*, 2009a, b). The alternative opaque and white pheromone responses are discussed in detail below.

Opaque Cell Mating Response

The Mating-Type Locus in *S. cerevisiae* and *C. albicans*

The mating process has been extensively studied in the baker's yeast *S. cerevisiae* (Sprague, 1991; Haber, 1992; Elion, 2000). *S. cerevisiae* can exist as either in a haploid or a diploid state (Sprague, 1991). In *S. cerevisiae*, there are three mating-type loci (*MAT*), one expression locus that is either *MAT***a** or *MAT*α and defines the mating type in haploids, and two silent loci, *HMR* and *HML*, that contain a copy of the *MAT***a** and *MAT*α genes, respectively (Nasmyth, 1982; Hicks *et al.*, 1977; Haber, 1998). In haploid **a** or α cells, the mating type can be switched from **a** to α or α to **a** through a cassette system, in which a gene conversion event occurs at the *MAT* locus with a replacement by a copy of the silent locus of the opposite mating type (Hicks *et al.*, 1977; Haber, 1998). This process referred to as "mating-type switching" is initiated by a double-stranded DNA break at the *MAT* locus mediated by the *HO* gene, which encodes an endonuclease (Hicks *et al.*, 1977; Strathern *et al.*, 1982). Thus, this cassette system ensures that a haploid **a** or α strain still retains the opposite mating-type information.

In *S. cerevisiae*, all three *MAT* loci reside on Chromosome 3 (Strathern *et al.*, 1979; Klar *et al.*, 1979). The *MAT***a** locus carries the gene *MAT***a**1, while the *MAT*α locus carries the genes *MAT*α1 and α2 (Strathern *et al.*, 1979) (Figure 4A). In a haploid **a** cell, **a**-specific genes are expressed by default. In contrast, in an α cell, α2 represses **a**-specific genes and **a**-mating competence, while α1 activates α-specific genes and confers α-mating competence (Nasmyth, 1982; Bardwell *et al.*, 1994). In a diploid **a**/α cell, the **a**1-α2 repressor complex suppresses both **a**- and α-mating competence, and α2 alone again represses **a**-mating competence (Nasmyth, 1982; Bardwell *et al.*, 1994). Haploid cells of

Figure 4. Comparison of the *S. cerevisiae* mating-type (*MAT*) locus and the *C. albicans* mating type-like (*MTL*) locus. A) The *S. cerevisiae MAT***a** locus contains the gene **a**1, and the *MAT*α locus contains the genes α1 and α2. B) The *C. albicans MTL***a** locus contains the genes **a**1, **a**2, a phosphatidylinositol kinase gene PIK**a,** an oxysterol binding protein gene OBP**a,** and a poly(A) polymerase gene PAP**a**. The *MAT*α locus contains the genes α1, α2, a phosphatidylinositol kinase gene PIKα**,** an oxysterol binding protein gene OBPα**,** and a poly(A) polymerase gene PAPα. This figure is obtained from Hull and Johnson (1999).

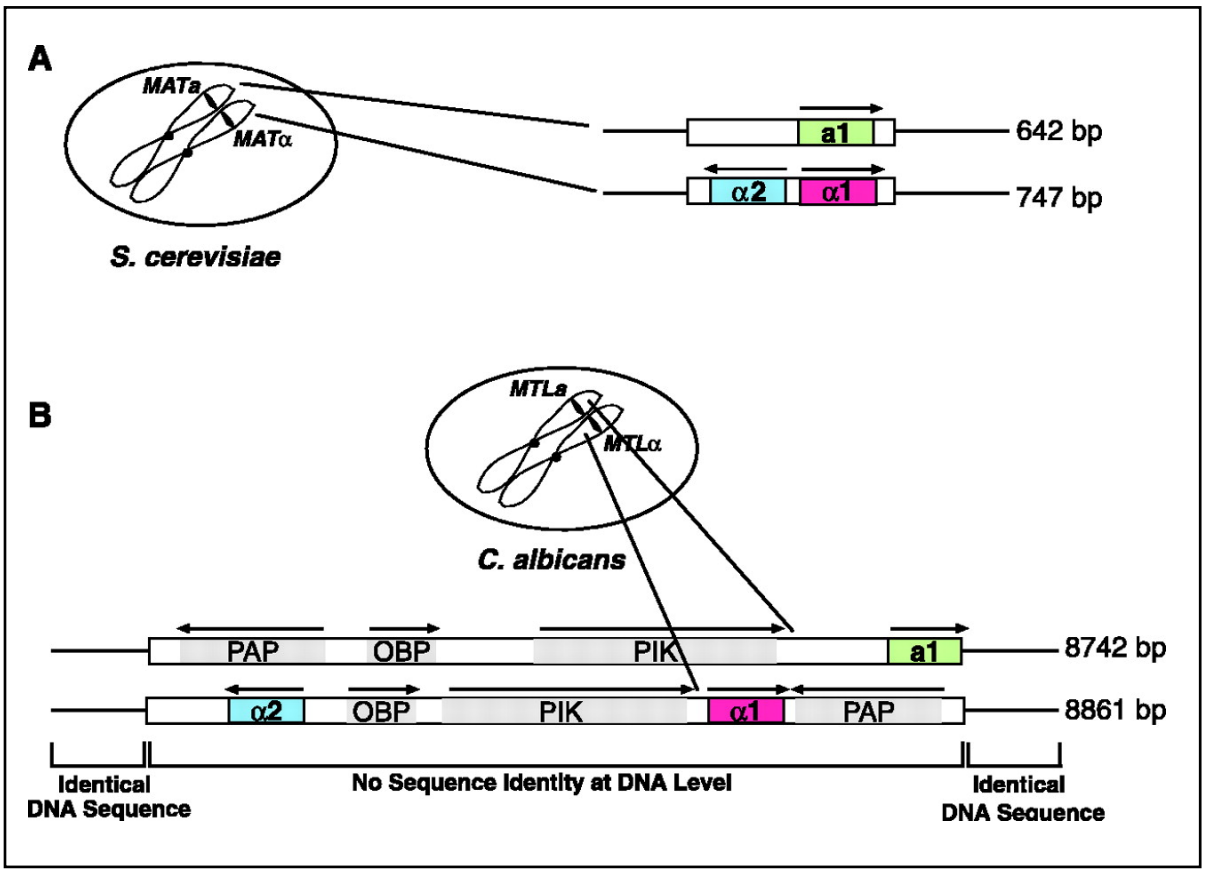
A
MATa
MATα
a1
α2
α1
642 bp
747 bp
S. cerevisiae
B
MTLa
MTLα
C. albicans
PAP
OBP
PIK
a1
8742 bp
α2
OBP
PIK
α1
PAP
8861 bp
Identical
DNA Sequence
No Sequence Identity at DNA Level
Identical
DNA Sequence

*MAT***a** and *MAT*α strains are both mating-competent, and undergo mating to generate diploid **a**/α daughter cells, which are mating-incompetent (Sprague, 1991; Haber, 1992) (Figure 5A). To become mating-competent, a diploid **a**/α cell has to undergo meiosis to return to a haploid state through the process of sporulation (Sprague, 1991). The diploid **a**/α cell gives rise to four spores, two **a** and two α haploid daughter cells (Sprague, 1991) (Figure 5A).

C. albicans is an obligate diploid (Whelan *et al.*, 1980; Whelan and Magee, 1981; Whelan and Soll, 1982). Meiosis and a haploid form of *C. albicans* have not yet been discovered, although aneuploidy has been reported (Chen *et al.*, 2004; Selmecki *et al.*, 2005). In 1999, Hull and Johnson (1999) identified a single mating-type locus (*MTL*) in the *C. albicans* genome. This locus resides on Chromosome 5, and can be either **a** or α (Hull and Johnson, 1999). The **a** locus and α locus exhibit distinct gene compositions, gene sequence and molecular sizes (Hull and Johnson, 1999). Hence, they are often referred to as "idiomorphs", rather than "alleles" (Butler *et al.*, 2004). The gene *MTL***a**1 at the **a** idiomorph and the genes *MTL*α1 and *MTL*α2 at the α idiomorph are homologous to the *S. cerevisiae* genes *MAT***a**1, α1 and α2, respectively (Hull and Johnson, 1999) (Figure 4B). The *MTL***a**2 gene at the **a** idiomorph, however, does not have a close homolog in *S. cerevisiae*, suggesting that *S. cerevisiae* has lost **a**2 during evolution (Tsong *et al.*, 2003, 2006; Reedy *et al.*, 2009; Soll *et al.*, 2009). In **a**/α cells of *C. albicans*, the **a**1-α2 complex represses **a**- and α-mating competence, similar to *S. cerevisiae*, but α2 does not directly repress **a**-specific genes, as it does in *S. cerevisiae* (Tsong *et al.*, 2003). In *C. albicans* α/α cells, α1 activates α-specific genes and α-mating competence, as it does in *S. cerevisiae.* In *C. albicans* **a**/**a** cells, however, **a**2 positively regulates **a**-specific genes and **a**-mating competence, unlike the default system in *S. cerevisiae* **a** cells (Tsong *et al.*, 2003). Hence, *MTL*-homozygous **a**/**a** and α/α strains, but not *MTL*-heterozygous **a**/α strains, are mating-competent. Mating competency, however, requires a switch from white to opaque (Miller and Johnson, 2002; Lockhart *et al.*, 2003a), as will be discussed in

Figure 5. A comparison of mating between *S. cerevisiae* and *C. albicans*. A) In *S. cerevisiae*, mating between haploid **a** and α cells generates an **a**/α diploid cell, which then undergoes meiosis to return to the haploid state. Following meiosis, the resulting haploid cells of *S. cerevisiae* are immediately mating-competent. B) In *C. albicans*, to mate, *MTL***a**/α cells first undergo homozygosis at the *MTL* locus to become either **a**/**a** or α/α. Following *MTL*-homozygosis, *C. albicans* is not immediately mating-competent. It needs to switch from white to opaque. Mating between opaque cells generates a tetraploid **a**/**a**/α/α, which then returns to the diploid state by random chromosome loss or meiosis (the latter has not been identified yet). This figure is obtained from Soll (2009).

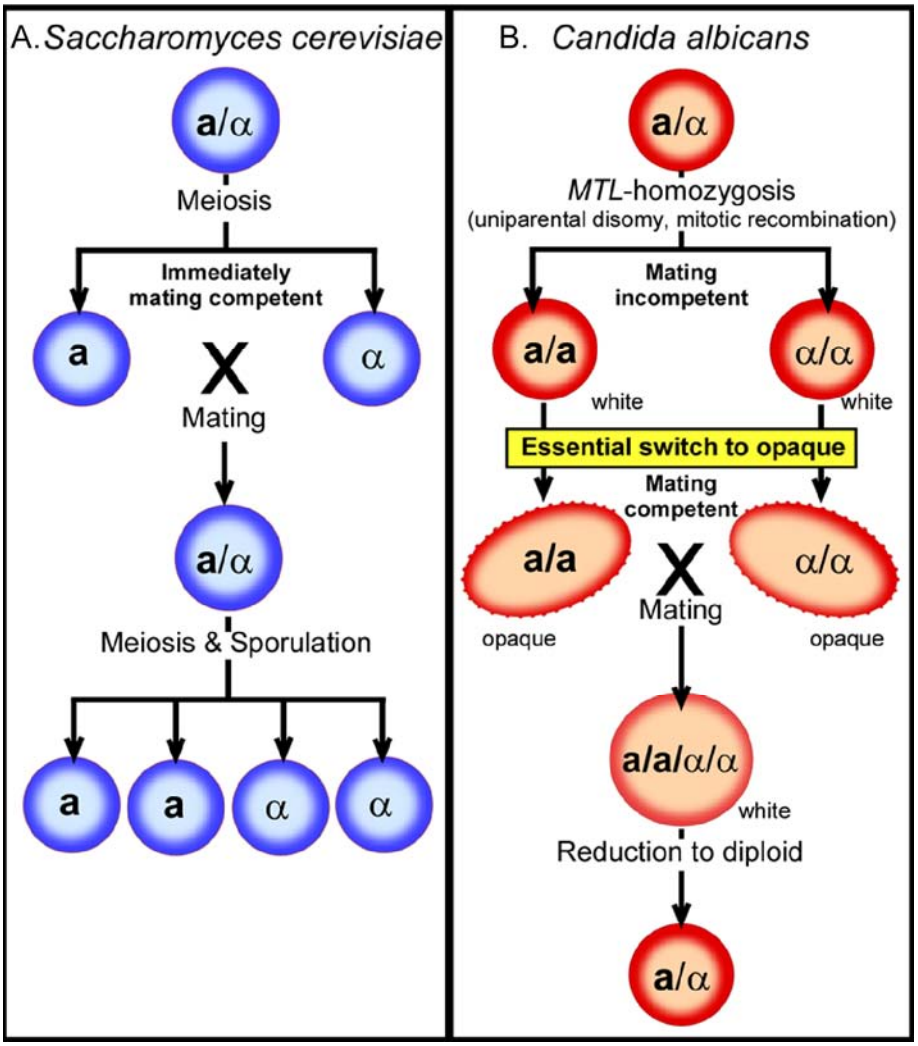
A. Saccharomyces cerevisiae
a/α
Meiosis
Immediately mating competent
a
X
α
Mating
a/α
Meiosis & Sporulation
a
a
α
α
B. Candida albicans
a/α
MTL-homozygosis
(uniparental disomy, mitotic recombination)
Mating incompetent
a/a
white
α/α
white
Essential switch to opaque
Mating competent
a/a
opaque
X
Mating
α/α
opaque
a/a/α/α
white
Reduction to diploid
a/α

the next section. In addition, in contrast to *S. cerevisiae* (Butler *et al.*, 2004, 2009), *C. albicans* possesses three additional genes at each *MTL* locus: *PAP*, *PIK* and *OBP* (Hull and Johnson, 1999) (Figure 4B), which encode a poly(A) polymerase, an ortholog of the *S. cerevisiae* phosphatidylinositol kinase Pik1, and an ortholog of the human oxysterol binding protein, respectively (Bennett and Johnson, 2005). Interestingly, the pairs of alleles for these three genes at the *MTL***a** and *MTL*α loci differ dramatically in their DNA sequence and in their positions on thd mating type locus (Hull and Johnson, 1999; Butler *et al.*, 2004; Bennett and Johnson, 2005) (Figure 4B). These pairs of alleles are far more divergent than alleles for most of the genes in the *C. albicans* genome (Butler *et al.*, 2004; Bennett and Johnson, 2005; Soll *et al.*, 2009). It is not clear why these non-mating-type genes reside in the *MTL* locus, as they do not seem to be directly associated with the mating process or play a role in mating-type specificity (Bennett and Johnson, 2005; Soll *et al.*, 2009). The dramatic allelic difference of these non-mating-type genes, however, suggests that they may have acquired different functions in *MTL***a** and α cells. This hypothesis is now being actively explored in our lab.

To assess the *MTL* genotype of natural strains, Lockhart *et al.* (2002) analyzed 220 independent clinical isolates of *C. albicans*, which included members of the five major clades of *C. albicans* that had been fingerprinted by Southern blot hybridization with the complex DNA probe Ca3 (Pujol *et al.*, 1997, 2002; Blignaut *et al.*, 2002; Soll and Pujol, 2003). They found that about 97% of the tested natural strains are *MTL*-heterozygous (**a**/α) and about 3% are *MTL*-homozygous (**a**/**a** or α/α). They also found that about 4% of the **a**/α strains undergo high-frequency *MTL*-homozygosis to **a**/**a** or α/α (Lockhart *et al.*, 2002). Together with several subsequent studies (Legrand *et al.*, 2004; Tavanti *et al.*, 2005), it seems reasonable to conclude that in nature, approximately 90% of the strains are **a**/α, and approximately 10% **a**/**a** or α/α. It was further demonstrated *in vitro* that the majority of the *MTL*-homozygosis events arise through the loss of one Chromosome 5 homolog followed by duplication of the other homolog, resulting in homozygosity along

the entire length of Chromosome 5 (Wu *et al.*, 2005). *In vivo* in host niches, however, *MTL*-homozygosis to **a**/**a** or α/α arises primarily by multiple mitotic cross-over events outside the *MTL* locus (Wu *et al.*, 2007).

The Mating Cycle of *C. albicans* and the Dependency on Switching

In order to mate, *MTL*-heterozygous **a**/α strains have to undergo *MTL*-homozygosis to **a**/**a** or α/α, because the **a**1-α2 complex in **a**/α cells represses mating (Hull *et al.*, 2000; Magee and Magee, 2000; Tsong *et al.*, 2003) (Figure 5B). However, this is not sufficient. *MTL*-homozygous strains must undergo an extra step, namely the transition from the white to opaque pheenotype, to become mating-competent (Miller and Johnson, 2002) (Figure 5B). The mating efficiency between opaque **a** and opaque α cells is several orders of magnitude higher than that between white **a** and opaque α cells, between opaque **a** and white α cells, or between white **a** and white α cells (Miller and Johnson, 2002). These data suggest that only opaque cells, but not white cells, are mating-competent in *MTL*-homozygous strains (Miller and Johnson, 2002). Indeed, mating in *C. albicans MTL*-homozygous or hemizygous strains has been demonstrated both *in vivo* (Hull *et al.*, 2000) and *in vitro* (Magee and Magee, 2000). Hull *et al.* (2000) constructed functional **a** and α strains from the **a**/α laboratory strain SC5314, by deleting the *MTL*α1 and α2 genes, or the *MTL***a**1 gene, respectively. They also generated **a** and α strains in which the entire *MTL*α or *MTL***a** locus was deleted (Hull *et al.*, 2000). The derived *MTL*-hemizygous **a/-** and α**/-** strains carried different auxotrophic markers, one being *ade2*$^-$ and the other being *ura3*$^-$ (Hull *et al.*, 2000). These engineered strains were mixed and co-injected into the tail veins of mice. After 24 hours, the mice were euthanized, the kidneys were removed and homogenized, and the macerates were plated on agar medium lacking both auxotrophic markers (*ade2*$^-$ and *ura3*$^-$) (Hull *et al.*, 2000). The colonies that grew on such media were interpreted to be the result of mating. Cells of these strains contained single nuclei, but exhibited substantially higher DNA content

indicative of tetraploids (Hull *et al.*, 2000). Magee and Magee (2000) constructed **a** and α strains by growing an **a**/α laboratory strain on agar plates containing sorbose, a condition that had been previously shown to induce the loss of one of the two homologs (monosomy) of Chromosome 5 where the *MTL* genes are located (Janbon *et al.*, 1999). Chromosome 5 monosomy is associated with an increased expression of *SOU1*, a gene on a different chromosome encoding an L-sorbose reductase that allows cells to utilize sorbose (Janbon *et al.*, 1998). The sorbose-derived **a** and α strains, which carried different auxotrophic markers, were then cross-streaked on agar media lacking both auxotrophic ingredients (Magee and Magee, 2000), and the resulting colonies isolated from such selection media were **a**/α mating products with increased DNA content (Magee and Magee, 2000). Furthermore, high-frequency mating has also been demonstrated in a gastrointestinal murine model *in vivo* (Dumitru *et al.*, 2007). Mating in the host is probably facilitated by high physiological levels of CO_2 that promotes and stabilizes the opaque phenotype (Huang *et al.*, 2009).

Opaque cells of **a**/**a** and α/α strains of *C. albicans* undergo efficient mating with each other (Lockhart *et al.*, 2003a; Daniels *et al.*, 2003, Bennett and Johnson, 2005). The mating product is tetraploid (**a**/**a**/α/α), and has to undergo a reduction division to return to the diploid or near diploid state (Figure 5B) (Bennett and Johnson, 2003; Forche *et al.*, 2008). This reduction could be achieved by meiosis or a parasexual cycle that involves random chromosome loss (Bennett and Johnson, 2003; Forche *et al.*, 2008). Bennett and Johnson (2003) demonstrated that growth of tetraploid strains on sorbose-containing medium or *S. cerevisae* pre-sporulation medium, induced the formation of diploid or near-diploid strains, as a result of chromosome loss (Janbon *et al.*, 1999). While the reduction from tetraploidy to diploidy, or near diploidy, can be accomplished by certain inducing media, it does not rule out the possibility that meiosis can occur. Indeed, *C. albicans* possesses homologs of genes involved in meiosis, recombination, and the formation of synaptic complexes (Tzung *et al.*, 2001). In *Candida lusitaniae*, another

Candida species, meiosis has recently been identified during its sexual cycle (Reedy *et al.*, 2009). After meiosis, the majority of progeny cells of *C. lusitaniae* are euploid, but approximately one-third are aneuploid/diploid (Reedy *et al.*, 2009). The aneuploidy in the parasexual mating progeny cells of *C. albicans* is, therefore, similar to that in certain meiotic progeny cells of *C. lusitaniae*. It is likely that meiosis exists in *C. albicans*, but the evidence for a meiotic process has not been discovered.

The Cell Biology of Mating

Mating-competent **a**/**a** and α/α opaque cells release **a** and α pheromones, respectively, during the mating process (Bennett et al., 2003,2005; Bennett and Johnson, 2005; Lockhart et al., 2003a, b), just as haploid cells of *S. cerevisiae* do (Duntze *et al.*, 1970; Wilkinson and Pringle, 1974; Shimoda and Yanagishima, 1975). Pheromone of one mating type forms a concentration gradient that induces polarization, G1 arrest, and shmoo formation in opaque cells of the opposite mating type (Bennett *et al.*, 2003; Lockhart *et al.*, 2003a; Tsong *et al.*, 2003; Panwar *et al.*, 2003). The shmoo extends in the direction of increasing pheromone concentration, through a process called chemotropism (Arkowitz, 1999, Daniels *et al.*, 2003, 2006). When the extending shmoos of the two opposite mating-type cells make apical contact, they fuse to form a conjugation bridge into which the nuclei of the two mother cells migrate and fuse (Lockhart *et al.*, 2003a; Daniels *et al.*, 2003). On that bridge, a nascent daughter cell forms. As the daughter cell grows, the tetraploid nucleus in the bridge divides, and one nucleus moves into the daughter cell (Lockhart *et al.*, 2003a). The other nucleus left in the bridge again undergoes mitosis and the two daughter nuclei migrate back to the mother cells (Lockhart *et al.*, 2003a).

Pheromone-mediated Opaque Mating Response

The *C. albicans* α mating pheromone gene, *MFα1*, was identified in the genome sequence database as a homolog of the *S. cerevisiae* α-pheromone gene (Bennett *et al.*, 2003; Lockhart *et al.*, 2003b; Panwar *et al.*, 2003). The *MFα1* gene encodes an

oligopeptide α-pheromone of 13 to 14 amino acids in length (Bennett *et al.*, 2003; Lockhart *et al.*, 2003b). The *mfα1* null mutant in α/α cells is not capable of mating, while the *mfα1* mutant in **a**/**a** cells retains mating capability (Bennett *et al.*, 2003; Panwar *et al.*, 2003). A similar strategy was used to identify the **a** mating pheromone gene, but was not successful (Bennett *et al.*, 2003; Lockhart *et al.*, 2003b; Panwar *et al.*, 2003). Subsequently, using a comparative genomics approach which involved several fungal genomes, Dignard *et al.* (2007) identified the **a**-pheromone gene, *MFA1*, which encodes a highly prenylated 14-amino-acid peptide pheromone. The *mfa1* null mutant is completely defective in mating in **a**/**a**, but not α/α, cells (Dignard *et al.*, 2007).

α-pheromone is produced by α/α opaque cells, and binds to the α-pheromone receptor encoded by the gene *STE2* on **a**/**a** cells (Bennett *et al.*, 2003; Lockhart *et al.*, 2003b; Tsong *et al.*, 2003; Panwar *et al.*, 2003). **a**-pheromone is produced by **a**/**a** opaque cells, and binds to the **a**-pheromone receptor encoded by the gene *STE3* on α/α cells (Lockhart *et al.*, 2003b; Tsong *et al.*, 2003; Dignard *et al.*, 2007). Since α-pheromone is an unmodified peptide, unlike the **a**-pheromone, which has extensive post-translational modifications, α-pheromone can easily be chemically synthesized as a handy pheromone source (Bennett *et al.*, 2003; Lockhart *et al.*, 2003b; Panwar *et al.*, 2003). Synthetic 13-mer α-pheromone induces shmoo response in **a**/**a** opaque cells (Bennett *et al.*, 2003; Lockhart *et al.*, 2003b).

The pheromone-induced opaque cell response includes polarization, shmoo formation, G1 arrest and mating (Lockhart *et al.*, 2003a, b; Daniels *et al.*, 2003, 2006; Yi *et al.*, 2008). α-pheromone induces the formation of a conjugation tube (shmoo) at one end of an **a**/**a** opaque cell at an angle to the long cellular axis (Lockhart *et al.*, 2003b), a pattern similar to that of a budding cell (Shannon and Rothman, 1971, Slutsky *et al.*, 1987). With incubation of α-pheromone for an extended period of time, opaque **a**/**a** cells extend the conjugation tube to lengths equivalent to several cell diameters (Lockhart *et al.*, 2003b, Zhao *et al.*, 2005b). These long tubes resemble true hyphae, they do not, however,

compartmentalize through the formation of septae, and the nucleus does not migrate into the conjugation tube, either (Lockhart *et al.*, 2003b; Daniels *et al.*, 2003). When α-pheromone is depleted over time, these conjugation tubes revert by budding at the tip of the tubes, producing a daughter cell. The unique morphology of long shmoos in *C. albicans*, different from that in *S. cerevisiae* (Elion, 2000; Lengeler *et al.*, 2000; Schwartz and Madhani, 2004), suggests that the *C. albicans* mating process may have borrowed at least part of the signaling machinery of the filamentation program. Indeed, Daniels *et al.* (2003) demonstrated that the *HWP1* gene, which encodes a hyphal wall protein, is upregulated by α-pheromone in opaque **a**/**a** cells, and expressed exclusively in the **a**/**a** portion, but not the α/α portion, of the conjugation tube during the mating process (Daniels *et al.*, 2003). Large-scale gene expression profiling studies showed that several hypha-regulated genes are induced in mating pheromone-treated opaque cells in *C. albicans* (Nantel *et al.*, 2002; Bennett *et al.*, 2003; Zhao *et al.*, 2005b). One important gene is *CPH1*, which encodes a transcription factor that regulates both hyphal growth and the opaque mating response in *C. albcians* (Lane *et al.*, 2001; Chen *et al.*, 2002; Magee *et al.*, 2002). Moreover, the four genes *DDR48*, *CZF1*, *RIM101* and *RBT1*, previously reported to be upregulated during hyphal development (Staab *et al.*, 1996; Brown *et al.*, 1999; Davis *et al.*, 2000; Nantel *et al.*, 2002), are all induced during the mating process as well (Bennett *et al.*, 2003; Zhao *et al.*, 2005b).

The opaque mating response to pheromone also involves a G1 arrest in the cell cycle. Zhao *et al.* (2005) performed a kinetic analysis of shmoo formation in mating mixures of **a**/**a** and α/α opaque cells derived from either mid-log phase or saturation phase cultures, and found that these shmooing cells underwent growth arrest. They further quantitated the DNA content of individual nuclei in shmooing cells versus budding cells. The results showed that in response to pheromone, opaque cells are arrested in G1 in the cell cycle (Zhao *et al.*, 2005b). Indeed, cells from a saturation phase culture, which are predominantly in the G1 phase, undergo efficient shmoo formation (>90%) when treated

with pheromone, while cells from mid-log phase shmoo at a much lower frequency (20-40%) (Zhao *et al.*, 2005b). In *S. cerevisiae*, mating pheromone blocks haploid cells of opposite mating types in G1 through the activation of Far1, a cyclin-dependent protein kinase inhibitor (Chang and Herskowitz, 1990, 1992). In *C. albicans*, however, the *FAR1* homolog is not induced by mating pheromone (Zhao *et al.*, 2005b), but it does play a role in the opaque mating response (Yi *et al.*, 2008; Cote and Whiteway, 2008). Deletion of *FAR1* dramatically reduces the mating efficiency (Yi *et al.*, 2008; Cote and Whiteway, 2008), while overproduction of Far1 hypersensitizes cells to G1 arrest (Cote and Whiteway, 2008). Furthermore, our recent work indicates that phosphorylation and ubiquitination of Far1 plays an important role in the mating process (Sahni *et al.*, in preparation).

Molecular Mechanisms of the Mating Response

In *S. cerevisiae*, the α- and **a**-pheromone receptors, Ste2 and Ste3, respectively, interact with a heterotrimeric G-protein complex, composed of a Gα, Gβ and Gγ subunit, which are encoded by the genes *GPA1*, *STE4*, and *STE18*, respectively (Lengeler *et al.*, 2000; Schwartz and Madhani, 2004). Receptor occupancy by a specific mating pheromone leads to dissociation of the dimeric Gβγ subunits from the Gα subunit (Schwartz and Madhani, 2004), but the Gα and Gβγ subunits remain at the plasma membrane (Elion, 2000; Dohlman and Thorner, 2001). The Gα subunit negatively regulates the mating response by promoting an adapative recovery from pheromone exposure (Miyajima *et al.*, 1987; Nakayama *et al.*, 1988). This requires the gene *SGV1*, encoding a cyclin-dependent kinase (Irie *et al.*, 1991). The dissociated Gβγ complex activates the kinase Ste20 (Ramer and Davis, 1993), which then transduces the mating signal to the MAP kinase cascade (Whiteway *et al.*, 1988, 1989). Activation of the MAP kinase pathway involves consecutive phosphorylations of the sequential kinase components, which include Ste11 (Rhodes *et al.*, 1990), Ste7 (Chaleff and Tatchell, 1985;

Fields *et al.*, 1988) and Fus3 (Fujimura, 1990; Elion *et al.*, 1991). When Fus3 is inactivated or deleted, another kinase Kss1, which is normally involved in filamentation (Maleri *et al.*, 2004), can substitute functionally for Fus3 (Elion *et al.*, 1991; Ma *et al.*, 1995; Madhani *et al.*, 1997). The activated MAP kinase cascade finally targets and activates Ste12 (Elion *et al.*, 1993), which encodes a transcription factor that upregulates mating-associated gene expression and hence mediates the mating response (Tyers and Futcher, 1993; Elion, 2000; Lengeler *et al.*, 2000). Fus3 activates Ste12 indirectly, by inactivating the two redundant inhibitors of Ste12, Dig1 and Dig2 (Cook *et al.*, 1996; Tedford *et al.*, 1997). The activated downstream transcription factor Ste12 also induces expression of the genes in the MAP kinase cascade, forming a positive feedback loop (Roberts *et al.*, 2000; Paliwal *et al.*, 2007). In addition, the protein Ste5 functions as a scaffold to tether the components of the MAPK cascade, increasing the signaling specificity and efficiency in the mating process (Choi *et al.*, 1994; Elion, 1995).

C. albicans possesses homologs for most of the components of the *S. cerevisiae* mating pathway (Tzung *et al.*, 2001). To study the regulation of the opaque cell mating response in *C. albicans*, Chen *et al.* (2002) and Magee *et al.* (2002) analyzed the deletion mutants of select genes in the conserved MAP kinase pathway for their mating efficiency. They constructed mutants in *MTL*-homozygous (**a**/**a** or α/α) strains derived by growing the **a**/α parental strains on sorbose-containing medium and assessing mating efficiency based on auxotrophic complementation (Chen *et al.*, 2002; Magee *et al.*, 2002). Deletion of *CST20*, the homolog of *S. cerevisiae STE20*, results in a decrease in the frequency of mating (Chen *et al.*, 2002). Deletion of *HST7* and *CPH1*, the homologs of *S. cerevisiae STE7* and *STE12*, respectively, leads to a complete loss of mating in both *MTL***a** and *MTL*α cells (Chen *et al.*, 2002; Magee *et al.*, 2002). A double deletion mutant of *CEK1* and *CEK2*, the homologs of *S. cerevisiae KSS1* and *FUS3*, respectively, is incapable of mating, while the single deletion mutants, *cek1*/*cek1* and *cek2*/*cek2*, are still able to mate, but with reduced efficiency (Chen *et al.*, 2002). In addition, Bennett *et al.* (2003) found that

deletion of the α-pheromone receptor gene, *STE2*, causes a complete defect in mating (Bennett *et al.*, 2003). It was further demonstrated by other groups that disruption of *STE4*, the homolog of the *S. cerevisiae* Gβ subunit *STE4*, also completely blocks the mating response (Yi *et al.*, 2008; Dignard *et al.*, 2008). Together, these results suggest that the *C. albicans* mating response is regulated through a conserved MAP kinase pathway, similar to that found in *S. cerevisiae* (Elion, 2000; Lengeler *et al.*, 2000; Schwartz and Madhani, 2004).

There are, however, several differences in the pheromone response pathway between *C. albicans* and *S. cerevisiae*. First, disruption of *C. albicans CAG1*, the homolog of the *S. cerevisiae* Gα subunit *GPA1*, blocks pheromone-induced gene expression and abolishes the opaque cell mating response (Dignard *et al.*, 2008). Therefore, in contrast to the *S. cerevisiae* Gpa1, which acts as a negative regulator of the mating response (Miyajima *et al.*, 1987; Nakayama *et al.*, 1988), the *C. albicans* Cag1 is required for the transmission of the mating signal in opaque cells (Dignard *et al.*, 2008). Second, homologs of *S. cerevisiae* Dig1 and Dig2 have not been identified in the *C. albicans* genome, suggesting that the mating-specific transcription factor Cph1 in *C. albicans* might not be under the negative regulation of similar inhibitors. Third, a homolog of the *S. cerevisiae* scaffold protein Ste5 (Choi *et al.*, 1994; Elion, 1995) has not been identified in *C. albicans*. However, since Ste5 in *S. cerevisiae* plays a critical role in the activation of the MAP kinase cascade (Mahanty *et al.*, 1999) and signaling specificity (Flatauer *et al.*, 2005), it is possible that in *C. albicans*, a protein that plays this role diverged from *S. cerevisiae* Ste5 or another protein replaced Ste5 function.

Pheromone-dependent Gene Expression in Mating

High-throughput microarray-based transcription profiling studies have identified genes that are upregulated or downregulated by α-pheromone in opaque **a** cells (Bennett *et al.*, 2003; Bennett and Johnson, 2006). Among these differentially regulated genes,

several upregulated genes are similarly induced by pheromone in *S. cerevisiae*, including the α-pheromone receptor gene *STE2*, components of the MAP kinase pathway, and genes involved in karyogamy, pheromone processing and adaptation (Bennett *et al.*, 2003; Bennett and Johnson, 2006). Another group of genes upregulated by pheromone in *C. albicans*, but not upregulated in *S. cerevisiae*, include *RAM1*, *RAM2* and *KAR9* (Bennett *et al.*, 2003; Bennett and Johnson, 2006). By northern blot analysis, Lockhart *et al.* (2003b) also analyzed gene expression in opaque **a**/**a** cells in response to α-pheromone. In addition to the upregulation of mating-associated genes reported in previous microarray studies (Bennett *et al.*, 2003; Bennett and Johnson, 2006), Lockhart *et al.* (2003b) found that three opaque-specific genes, *OP4*, *SAP1* and *SAP3*, were downregulated by pheromone. The reason for this downregulation is not obvious, but it is not due to pheromone-induced phenotypic switching (Zhao *et al.*, 2005b). Moreover, to study gene expression pattern during mating between opaque cells of opposite mating types, Zhao *et al.* (2005) employed both a microarray and northern blot analysis, and identified several new genes that are upregulated in mating, including *RCE1*, encoding a CaaX prenyl proteinase involved in pheromone maturation, and *MPT5*, a gene involved in re-entry into the mitotic cycle. However, *CST20*, a mating-associated gene, is constitutively expressed in *C. albicans* (Zhao *et al.*, 2005b), an expression pattern different from that of *S. cerevisiae*, in which the homolog *STE20* is induced by pheromone (Ramer and Davis, 1993). The *C. albicans* mating process, therefore, involves a complex gene regulation pattern, probably because it incorporates the unique white-opaque transition and contributes to the virulence of this fungal pathogen.

White Cell Biofilm Response

Discovery of a "Sexy" Biofilm System

As mentioned in the last section, mating between *C. albicans MTL*-homozygous strains depends on a switch from white to opaque (Miller and Johnson, 2002; Lockhart *et*

al., 2002). Opaque is the mating-competent phenotype. Thus, opaque cells, but not white cells, were initially believed to respond to pheromone of the opposite mating type (Miller and Johnson, 2002; Lockhart *et al.*, 2002). Based on this assumption, only opaque cells were employed in initial studies of pheromone responses (Bennett *et al.*, 2003; Lockhart *et al.*, 2003b; Zhao *et al.*, 2005b). However, Lockhart *et al.* (2003b) used α-pheromone-treated white cells as a presumed negative control in a northern analysis of pheromone-induced gene expression. Surprisingly, they found that α-pheromone upregulates select mating-associated genes in white **a**/**a** cells, and to the same extent as it does in opaque **a**/**a** cells (Lockhart *et al.*, 2003b). White **a**/**a** cells also express α-pheromone receptors, as opaque **a**/**a** cells do (Daniels *et al.*, 2006). The receptors on white cells are, however, distributed evenly on the cell surface, whereas on opaque cells, the receptors are localized in a punctate manner (Daniels *et al.*, 2006). Upon α-pheromone treatment, the receptors of both white and opaque cells are downregulated, but the redistribution is different (Daniels *et al.*, 2006). In white cells, the receptors do not relocalize after pheromone treatment, but in opaque cells, the receptors relocalize to the tip of the shmoo (Daniels *et al.*, 2006), as they do in *S. cerevisiae* haploid cells (Schandel and Jenness, 1994; Stefan and Blumer, 1999). Furthermore, in response to pheromone, white cells do not undergo G1 cell cycle arrest, shmoo formation or mating (Daniels *et al.*, 2006), as opaque cells do in the mating response (Bennett *et al.*, 2003; Lockhart *et al.*, 2003a, b).

It seems paradoxical that white cells express pheromone receptors, upregulate select mating-associated genes in response to pheromone, but do not undergo the mating response. Daniels *et al.* (2006) proposed a possible interactive system between opaque and white cells. They hypothesized that opaque cells might signal white cells through the release of pheromone, to form a biofilm that would in turn protect opaque cell chemotropism and hence mating (Daniels *et al.*, 2006). This hypothesis was based on the following speculations. First, in overlapping white **a**/**a** and α/α populations at the same site of colonization, a switch to opaque would occur at a really low frequency (Figure 6A).

Figure 6. Unique communication between the two switch phenotypes white and opaque in *C. albicans*. In *MTL*-homozygous strains opaque cells through the release of mating pheromone signal white cells of the opposite mating type to become cohesive, adhesive and form an enhanced 3D biofilm that in turn facilitates opaque cell chemotropism and mating (Daniels *et al*., 2006). A) Rare opaque cells result from spontaneous switching in overlapping populations of white **a**/**a** and α/α cells. B) **a**-pheromone released by opaque **a**/**a** cells signals white α/α cells to form a biofilm. α-pheromone released by opaque α/α cells signals white **a**/**a** cells to form a biofilm. C) The **a**-pheromone gradient decreases in the direction of the opaque α/α cell and the α-pheromone gradient decreases in the direction of the opaque **a**/**a** cell. D) **a**/**a** and α/α opaque cells shmoo and extend long conjugation tubes up the opposing gradients of pheromone. This figure is adapted from Soll (2009).

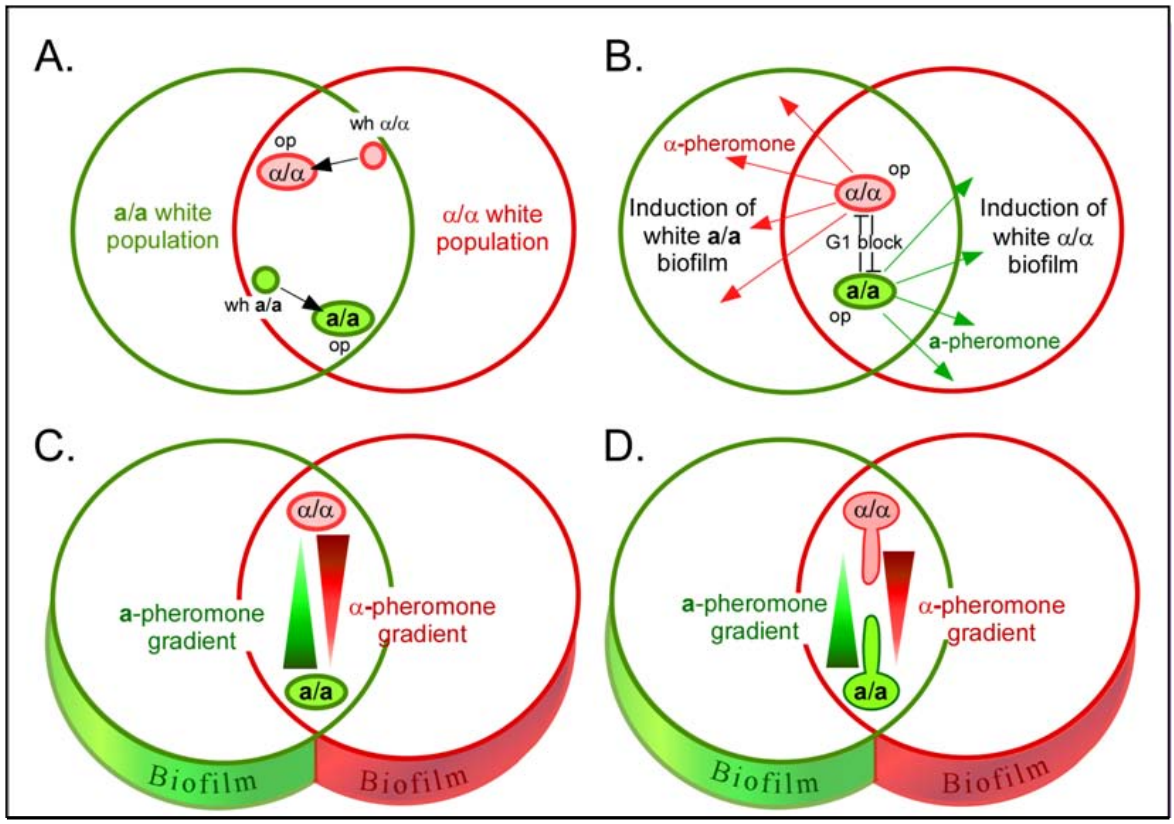
A.
wh α/α
op
α/α
a/a white population
α/α white population
wh a/a
a/a
op
B.
α-pheromone
op
α/α
Induction of white a/a biofilm
G1 block
Induction of white α/α biofilm
a/a
op
a-pheromone
C.
α/α
a-pheromone gradient
α-pheromone gradient
a/a
Biofilm
Biofilm
D.
α/α
a-pheromone gradient
α-pheromone gradient
a/a
Biofilm
Biofilm

Second, rare opaque cells secrete pheromones that induce a G1 block in opaque cells of opposite mating type (Figure 6B). Third, opaque cells would have to accurately sense the pheromone gradient emanating from opaque cells of the opposite mating type, in order to extend the conjugation tube in the correct direction and fuse in the mating process (Figure 6C, D). Finally, these pheromone gradients would have to be protected since they are prone to dissipation by diffusion and mechanical perturbation (Daniels *et al.*, 2006).

To test this hypothesis, Daniels *et al.* (2006) performed a number of experiments and found that: i.) α-pheromone induces white **a**/**a** cells, but not opaque **a**/**a** cells, to become cohesive to each other in suspension, and become adhesive to a plastic substratum; ii.) **a**-pheromone has a similar effect on white α/α cells, but not opaque α/α cells, based on a transwell assay; iii.) 1-10% of opaque cells in an overlapping white cell population serve as a pheromone source that enhances the thickness of biofilms formed by white cells of the opposite mating type; and finally iv.) a majority white cell biofilm protects the pheromone gradients in chemotropism, and hence facilitates chemotropism between rare opaque cells of opposite mating types (Daniels *et al.*, 2006) (Figure 6A-D). Together, these observations collectively lend support to the initial hypothesis of an opaque-white signaling system in the formation of biofilms. Given that biofilm formation is a pathogenic trait (Hawser *et al.*, 1998; Douglas, 2003; Kuhn and Ghannoum, 2004), the above results suggest that the white-opaque transition and mating may both be involved in pathogenesis, and provide an important insight into the role of the white-opaque transition in *C. albicans*. The interaction between mating-incompetent white cells (non-sex cells) and mating-competent opaque cells (sex cells) is unique in the fungal kingdom, but resembles the inductive events between germ cells and somatic cells during embryogenesis in higher eukaryotes, and represents an antecedent in the evolution of multicellularity in higher eukaryotes (Gilchrist *et al.*, 2004).

Biofilm Development and Characteristics in *C. albicans*

C. albicans, the most pervasive fungal pathogen, is remarkable in its ability to form biofilms on tissues, prosthetics and catheters (Hawser *et al.*, 1998; Douglas, 2003; Kojic and Darouiche, 2004). Biofilms are surface-associated communities of cells surrounded by an extracellular matrix (Hawser *et al.*, 1998; Ramage *et al.*, 2001, 2005; Blankenship and Mitchell, 2006). Notably, most of the *C. albicans* infections in humans are associated with biofilm formation (Hawser *et al.*, 1998; Douglas, 2003). Biofilms represent an important clinical problem because of increased resistance of the cells within a biofilm to antimicrobial drugs (Mukherjee *et al.*, 2003; Kuhn and Ghannoum, 2004).

The generation of a *C. albicans* biofilm involves a series of developmental stages (Chandra *et al.*, 2001; Douglas, 2003; Soll, 2008). Biofilm formation begins with the attachment of yeast cells to a surface and to one another to form a basal layer of cells (Douglas, 2003) (Figure 7A). This step is followed by proliferation of yeast cells across the surface and hyphal development (Douglas, 2003) (Figure 7B). Between hyphal filaments, an extracellular matix, also known as extracellular polymeric substance (EPS), forms that envelopes the cells in the mature biofilm (Hawser and Douglas, 1994; Nobile and Mitchell, 2006) (Figure 7C). In addition, recent studies have indicated another step in *C. albicans* biofilm development, a dispersal step in which daughter cells bud as non-adherent yeast cells (Granger *et al.*, 2005; Sellam *et al.*, 2009). Noteworthy, adhesion plays a vital role throughout biofilm development. Adhesion is not only essential for substratum attachment and for cell-cell binding, but also important for the interaction between hyphae, which serve to stabilize the biofilm (Gow *et al.*, 1999; Chaffin, 2008).

Drug resistance is one of the most prominent features of *C. albicans* biofilms (Mukherjee *et al.*, 2003; Kuhn and Ghannoum, 2004). Mechnisms known for the regulation of drug resistance are summarized as follows. At early stages of biofilm development, biofilm extracellular matrix EPS prohibits drug access (Al-Fattani and Douglas, 2004). In addition, upregulation of genes encoding drug efflux pumps

Figure 7. Steps in biofilm development in *C. albicans*. Biofilm formation involves the following steps. A) Binding of yeast cells to a surface. B) Cohesion between yeast cells resulting in the formation of a basal layer. C) Hyphae or germ tubes originate from the basal layer. In the space between the yeast cells and germ tubes an extrapolymeric matrix is formed that serves to stabilize the biofilm architecture. This figure is obtained from Soll (2008).

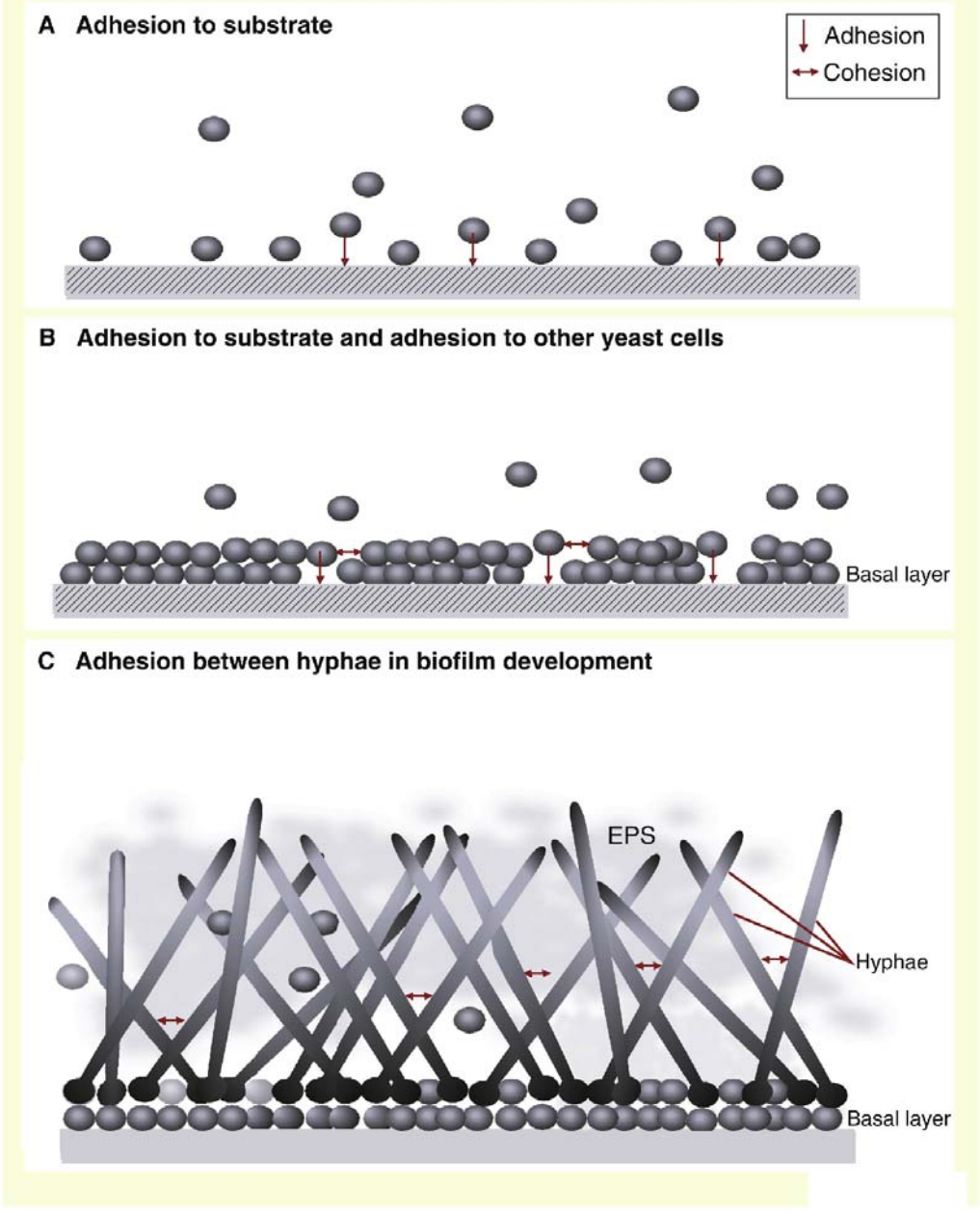
A Adhesion to substrate
Adhesion
Cohesion
B Adhesion to substrate and adhesion to other yeast cells
Basal layer
C Adhesion between hyphae in biofilm development
EPS
Hyphae
Basal layer

contributes to the drug resistance of cells in early biofilms (Ramage *et al.*, 2002; Mateus *et al.*, 2004; Cowen and Steinbach, 2008). *C. albicans* possesses two different types of efflux pumps: ATP binding cassette (ABC) transporters and facilitators, which are encoded by *CDR* and *MDR* genes, respectively (Prasad *et al.*, 1995; Balan *et al.*, 1997; Ramage *et al.*, 2002). Deletion of *CDR1* or *CDR2* increases drug sensitivity of adherent cells in biofilms (Mateus *et al.*, 2004). Deletion of *MDR1* also increases the sensitivity of biofilm cells to antifungal drugs (Wirsching *et al.*, 2000). A transcription factor, Tac1, targets the genes *CDR1* and *CDR2* to mediate drug resistance. A Tac1 hyperactive mutant harbors a N977D mutation, and confers drug resistance by upregulating the expression of *CDR1* and *CDR2* (Coste *et al.*, 2006). In contrast, at late stages of biofilm development (biofilm maturation), the regulatory mechanism of drug resistance is very different. Drug resistance in mature biofilms is conferred by a change in the sterol content in the fungal membrane (Mukherjee *et al.*, 2003). Common antifungal drugs, such as azoles (Odds *et al.*, 1986; Pfaller *et al.*, 2001; Mukherjee *et al.*, 2003), decrease ergosterol synthesis and cause growth inhibition in *C. albicans* (Sanglard *et al.*, 2003), by inhibiting the lanosterol-14-α-D-methylase encoded by *ERG11* (Sanglard *et al.*, 1998; Marichal *et al.*, 1999). Resistance to antifungal drugs in mature biofilms is, therefore, often associated with increased expression of *ERG11* (Perea *et al.*, 2001; Akins, 2005). This drug resistance mechanism also involves calcineurin, a calcium-dependent protein phosphatase which is essential for *C. albicans* survival from membrance stress (Cruz *et al.*, 2002; Bader *et al.*, 2006). The null mutant of the gene *CNB1*, encoding calcineurin B regulatory subunit, is markedly sensitive to drugs (Cruz *et al.*, 2002). The molecular chaperone Hsp90 stabilizes calcineurin, which in turn activates multiple transcription factors involved in drug resistance (Singh *et al.*, 2009). Together, these results suggest that drug resistance in *C. albicans* biofilms is a complex property that may involve alternative mechanisms depending on the developmental stage.

The presence of an extracellular polymeric substance (EPS) is a defining characteristic of fungal biofilms (Hawser *et al*., 1998). The EPS consists of carbohydrates and proteins, and is in part secreted by cells within the biofilm, but also contains materials from dead biofilm cells (Baillie and Douglas, 2000). The EPS serves many functions including defense against phagocytic cells, a scaffold for maintaining biofilm integrity, and limiting diffusion of toxic substances into the biofilms (Baillie and Douglas, 2000; Chandra *et al.*, 2001; Douglas, 2003). The regulation of EPS in biofilm development, however, is poorly understood. A recent study identified a transcription factor, Zap1, as a negative regulator of biofilm matrix formation. Zap1 functions through inhibition of the biogenesis of β-1,3 glucan, a major matrix component. The *zap1* null mutant forms a glistening biofilm with enhanced matrix, which contains 2- to 3-fold greater soluble β-1,3 glucan than the parental strain, in both *in vitro* and *in vivo* biofilm models (Nobile *et al.*, 2009). Two Zap1 target genes, *GCA1* and *GCA2*, encoding glucoamylases, have positive roles in matrix production via hydrolysis of insoluble β-1,3 glucan chains (Nobile *et al.*, 2009). The alcohol dehydrogenase genes, *ADH5*, *CSH1* and *IFD6*, are also regulated by Zap1 and have roles in matrix production. The *adh5* null mutant produces less matrix, whereas the *csh1* and *ifd6* null mutants produce significantly more matrix than their parental control strain (Nobile *et al.*, 2009). Taken together, these results suggest that as biofilms undergo maturation, the expression or activity of Zap1 declines, and that a number of matrix-related genes play roles in the regulation of matrix production in biofilms.

Critical Adhesion Proteins in Biofilms: Adhesins

Most of the biofilm studies have been carried out in *MTL*-heterozygous strains (Hawser *et al*., 1998; Hoyer *et al.*, 2008; Soll, 2008). Among these studies, adhesin proteins have been identified that are important for adhesion in biofilm formation, such as the Als protein family, Hwp1 and Eap1 (Hoyer, 2001; Hoyer *et al.*, 2008; Garcia-Sanchez *et al.*, 2004; Li *et al.*, 2007). All fungal adhesins share a common three-domain structure.

The N-terminal part of adhesins protrudes from the cell surface and often contains a carbohydrate or peptide binding domain (Kobayashi *et al.*, 1998; Groes *et al.*, 2002; Rigden *et al.*, 2004). The C-terminal part of adhesins contains a glycosylphosphatidylinositol (GPI)-anchor addition site and links the adhesin to the cell wall (Kapteyn *et al.*, 1999). The large middle domain of adhesins is characterized by the presence of serine- and threonine-rich repeats encoded by conserved DNA sequences. The number of these repeats can vary in different alleles and can represent a source of variability to generate new adhesin genes (Hoyer, 2001; Hoyer *et al.*, 2008).

The Als (agglutinin-like sequences) proteins are adhesins that resemble *S. cerevisiae* mating agglutinins (Cappellaro *et al.*, 1991, 1994). There are at least eight different *ALS* genes in the *C. albicans* genome (Braun *et al.*, 2005). Six of the *ALS* genes, *ALS1*, *ALS2*, *ALS3*, *ALS4*, *ALS5*, *ALS9*, are expressed throughout *C. albicans* biofilm development *in vitro* (Green *et al.*, 2004). Several of these genes have been deleted in **a**/α strains to assess their function in biofilm development. The *als1* null mutant exhibits a partial defect in biofilm formation (Nobile *et al.*, 2006a), while the *als3* null mutant produces fragile biofilms with primarily yeast cells and few hyphae (Nobile *et al.*, 2006a; Zhao *et al.*, 2006). In contrast, the *als4* null mutant (Zhao *et al.*, 2005a) and the *als9* null mutant (Zhao *et al.*, 2007) do not display a significant defect in biofilm formation. In addition, decreased expression of *ALS2* in a conditional knockout strain, in which one allele of the gene *ALS2* is deleted and the other allele is placed under the control of the *MAL2* promoter, leads to a marked defect in biofilm formation (Zhao *et al.*, 2005a).

Another adhesin gene, *HWP1*, is also upregulated during biofilm development in **a**/α cells (Garcia-Sanchez *et al.*, 2004). The *hwp1* null mutant has a partial defect in biofilm formation, similar to the *als1* null mutant (Nobile *et al.*, 2006a). Finally, the adhesin gene, *EAP1*, is involved in biofilm formation. The *eap1* null mutant forms a fragile biofilm with reduced thickness (Li *et al.*, 2003, 2007).

Role of Hyphal Formation in Biofilm Development

Numerous lines of evidence indicate that hyphal morphogenesis is pivotal for biofilm formation. In a screen of a transposon-based insertion mutant library for biofilm defects, the transcription factors, Tec1 and Bcr1 (biofilm and cell wall regulator), were identified (Nobile and Mitchell, 2005). *TEC1* and *BCR1* are both expressed in a hypha-specific manner (Nobile and Mitchell, 2005). Tec1 regulates *BCR1* transcription, which in turn regulates genes involved in hyphal differentiation. Both the *tec1* null mutant and the *bcr1* null mutant are unable to undergo normal hyphal growth, and exhibit a severe biofilm defect (Nobile and Mitchell, 2005). In addition, Tec1 has a Bcr1-independent role in biofilm morphogenesis because overexpression of *BCR1* in a *tec1* mutant only partially restores biofilm formation (Nobile and Mitchell, 2005).

A microarray transcription profiling analysis of Bcr1 target genes showed that, the expression of a number of adhesin genes, including *HYR1*, *HWP1*, *CHT2*, *ECE1*, *RBT5*, *ALS1* and *ALS3*, is reduced in the *bcr1* null mutant compared to the wild type parental strain (Nobile and Mitchell, 2005). Overexpression of one target gene, *ALS3*, rescues the biofilm defect of the *bcr1* mutant *in vitro* and *in vivo* (Nobile *et al.*, 2006a). In contrast, overexpression of other Bcr1 target genes, *ALS1*, *ECE1*, or *HWP1*, only partially restores biofilm formation in the *bcr1* mutant background. These results suggest that Als3 is an important target of the Bcr1-mediated biofilm signaling pathway, while Als1, Hwp1 and Ece1 also contribute to biofilm formation, but play a minor role (Nobile *et al.*, 2006a).

A number of genes involved in the regulation of filamentation play a role in biofilm development. *GCN4*, encoding a bZIP transcription factor, mediates filamentous growth in response to environmental starvation signals (Tripathi *et al.*, 2002). The *gcn4* null mutant fails to undergo filamentation under starvation conditions and forms a defective biofilm with a reduced biomass (Tripathi *et al.*, 2002; Garcia-Sanchez *et al.*, 2004; Murillo *et al.*, 2005). A null mutant of the gene *ACE2,* which encodes a transcription factor that regulates filamentous growth on solid medium (Kelly *et al.*, 2004;

Mulhern *et al.*, 2006), exhibits reduced adherence to polystyrene and reduced biofilm formation (Kelly *et al.*, 2004). A null mutant of the gene *NOT4*, which encodes a putative E3 ubiquitin ligase involved in filamentation on solid Spider medium and serum-containing medium (Krueger *et al.*, 2004), fails to attach firmly to a serum-coated plastic surface and is defective in biofilm formation (Krueger *et al.*, 2004). Another positive regulator important for biofilm development is Efg1, which also plays a role in hyphal formation under most hypha-inducing conditions (Ramage *et al.*, 2002). The *efg1* null mutant exhibits a dramatic defect in biofilm formation *in vitro* (Ramage *et al.*, 2002). Further evidence for the role of hyphal differentiation in biofilm development comes from the study of four unrelated genes *SUV3*, *NUP85*, *MDS3* and *KEM1*, which are required for both hyphae and biofilm formation (Richard *et al.*, 2005).

Interestingly, the hypha-specific proteins may interact with each other, and play complementary roles in biofilm development in *C. albicans* (Nobile *et al.*, 2008). The heterotypic interaction between Als1/3 and Hwp1 on the surfaces of adjacent cells served to maintain the integrity of a developing biofilm (Nobile *et al.*, 2008). Given that Als proteins are structurally similar to α-mating agglutinin (Sheppard *et al.*, 2004), and Hwp1 is selectively expressed in the **a**/**a** portion of the conjugation tube (Daniels *et al.*, 2003), suggests that the interaction between these proteins may resemble mating agglutinin interactions (Nobile *et al.*, 2008), drawing an indirect relationship between biofilm formation and mating.

White Cell Biofilm Response in *MTL*-homozygous Strains

The White Cell Response Signaling Pathway

In *MTL*-homozygous strains, minority mating-competent opaque cells signal majority mating-incompetent white cells of the opposite mating type to undergo a unique white cell pheromone response and form thicker biofilms (Daniels *et al.*, 2006; Sahni *et al.*, 2009a). These biofilms may be different from the biofilms formed by *MTL*-heterozygous

strains (Soll and colleagues, unpublished observations), the latter representing the predominant genotype in nature (Lockhart *et al.*, 2002; Legrand *et al.*, 2004; Tavanti *et al*., 2005; Odds and Jacobsen, 2008).

Although the signal transduction pathway of the opaque mating response had been identified (Chen *et al.*, 2002; Magee *et al.*, 2002; Bennett *et al.*, 2003), the signal transduction pathway of the white response was not known. Mutational analyses were, therefore, performed to test whether the components of the opaque response pathway were also employed in the white response pathway (Yi *et al.*, 2008). The results revealed that the opaque and white responses shared the same upstream components of the pathway, including the pheromone receptor, the heterotrimeric G-protein complex and the MAP kinase cascade (Yi *et al.*, 2008). The two responses, however, target different *trans*-acting regulators, Cph1 in the opaque response (Chen *et al.*, 2002; Magee *et al.*, 2002; Yi *et al.*, 2008), and Tec1, a recently identified transcription factor (Sahni *et al.*, in preparation), in the white response.

The Pheromone Receptors and Biofilm Regulation

Pheromone receptors belong to the superfamily of G-protein-coupled receptors (GPCRs). Like other GPCRs, the pheromone receptors present a structural topology of seven transmembrane domains connected by hydrophilic loops. In general, the third intracellular (IC3) loop is involved in G-protein coupling, and the cytoplasmic carboxy-terminal domain mediates ligand-induced endocytosis and desensitization (Leberer *et al.*, 1997; Hicke, 1999). While yeast pheromone receptors are not similar in sequence to mammalian receptors, their functions are conserved in evolution. For instance, some ectopically expressed mammalian receptors are capable of directly activating the yeast G protein (Price *et al.*, 1995, 1996). Furthermore, the yeast α-pheromone receptor is capable of activating at least one mammalian G protein (Crowe *et al.*, 2000).

The expression of the pheromone receptors is upregulated following exposure to pheromones (Hartwell, 1980; Roberts *et al.*, 2000). In *S. cerevisiae*, pheromone binding triggers modifications of the receptors, including ubiquitination (Hicke and Riezman, 1996; Roth and Davis, 1996), phosphorylation (Chen and Konopka, 1996) and conformational changes (Bukusoglu and Jenness, 1996). This binding activates the G protein complex, the IC3 loop (Boone *et al.*, 1993; Stefan and Blumer, 1994) and specific residues in the sixth transmembrane region (Konopka *et al.*, 1996). The IC3 loop of the α-pheromone receptor Ste2 plays an important role in signal transduction. Extensive mutagenesis of the IC3 loop has uncovered both unresponsive and hyperactive alleles that influence ligand discrimination, G-protein coupling and receptor endocytosis (Boone *et al.*, 1993; Clark *et al.*, 1994; Stefan and Blumer, 1994). Amino acid substitutions in IC3 that reduce the overall positive charge cause defects in gene induction in response to α-pheromone (Celic *et al.*, 2003). In addition, three point mutations in IC3, G237R, G237A, and K239N, render the α-receptor hypersensitive to pheromone (Stefan and Blumer, 1994). The carboxy-terminal tail of the Ste2 receptor is the site of ubiquitination required for proper endocytosis and subsequent vacuolar degradation of the receptor (Hicke and Riezman, 1996; Hicke, 1999; Shih *et al.*, 2000). The Ste2 carboxyl terminus is also a site of serine/threonine phosphorylation, deletion of this domain results in a loss of morphological changes in response to pheromone, and a loss of signal desensitization. Removal of the four phosphorylation sites at the carboxyl terminus decreases the rate of adaptation to pheromone-mediated cell cycle arrest, but has only a minor defect in morphogenesis (Chen and Konopka, 1996), suggesting that receptor desensitization and cellular morphogenesis are two separate functions of the Ste2 carboxy-terminus. Moreover, the distal half of the carboxy tail domain of Ste2 forms a pre-activation complex with the Gα subunit of the G-protein complex, and this interaction regulates pheromone signaling (Dosil *et al.*, 2000). Finally, mutational analysis suggested a possible role of the first intracellular (IC1) loop of Ste2 in G protein coupling, but the defects in IC1

mutants were only observed in strains in which the carboxy tail of the receptor was truncated (Chinault *et al.*, 2004).

In *C. albicans*, however, functional analysis of different domains of the pheromone receptors has not been well characterized. Yi *et al.* (2009) reported two unique regions in the *C. albicans* Ste2 receptor. While overall *C. albicans* Ste2 is homologous to *S. cerevisiae*, it possesses a much longer IC1 and EC2 loop, an additional 55-amino-acids in the former and an additional 17-amino-acids in the latter (Yi *et al.*, 2009). Since in *C. albicans*, Ste2 plays a role not only in the opaque cell mating response (Bennett *et al.*, 2003; Panwar *et al.*, 2003; Yi *et al.*, 2008), but also in the white cell biofilm response (Daniels *et al.*, 2006; Yi *et al.*, 2008), which is unique in *C. albicans*, it was hypothesized that these two unique regions in Ste2 might be involved in the white response (Yi *et al.*, 2009). In support of the hypothesis, through a series of mutational analyses, Yi *et al.* (2009) demonstrated that the *C. albicans*-specific IC1 region, but not the EC2 region, of Ste2 plays a selective role in the white cell biofilm response. The Ste2 IC1 domain deletion mutant exhibits a complete defect in pheromone-induced cohesion, adhesion and biofilm enhancement, similar to the mutant phenotype of the *ste2* null mutant (Yi *et al.*, 2008). However, the pheromone-induced opaque cell mating response is not affected in the IC1 domain deletion mutant (Yi *et al.*, 2009). Moreover, the upregulation of white-specific biofilm-associated genes by pheromone is abolished in the Ste2 IC1 deletion mutant. The IC1 loop of Ste2 functions primarily through the classic MAP kinase cascade, but additional pathways emanating from this loop have not been excluded (Yi *et al.*, 2009). In contrast to the Ste2 IC1 mutant, the IC3 and carboxy terminal domain deletion mutants display a severe defect in both the opaque and white pheromone responses, suggesting a critical role of these two domains of the Ste2 receptor in the regulation of pheromone signaling (Yi *et al.*, 2009), as is the case in *S. cerevisiae* (Stefan and Blumer, 1994; Dosil *et al.*, 2000). Finally, it is not clear why the IC1 loop of Ste2 is selectively involved in the white response. The IC1 loop of Ste2 contains a long stretch

(~18 amino acids) of glutamines or asparagines, which could play a role as "polar zippers" in protein-protein interactions (Perutz *et al.*, 1994; Michelitsch and Weissman, 2000). The interacting partners of the Ste2 IC1 loop, however, remain unidentified.

Although the **a**- and α-pheromone receptors, Ste3 and Ste2, respectively, are not homologous at the amino acid level, they are structurally similar in that they both contain seven hydrophobic transmembrane segments, typical for the GPCR family (Nakayama *et al.*, 1985; Burkholder and Hartwell, 1985, Hagen *et al.*, 1986). Both are known to activate the same G protein complex and MAP kinase pathway in response to pheromone (Tsong *et al.*, 2003; Bennett *et al.*, 2003; Yi *et al.*, 2008). However, there are no sequences in the intracellular loops of *C. albicans* Ste3 that are similar to the protein binding motifs in the IC1 region of Ste2 (Yi *et al.*, 2009). Therefore, the selective role of the IC1 region of Ste2 in the white cell biofilm response would have to be fulfilled by a nonhomologous region in Ste3, or involve a different mechanism, in the white cell response to **a**-pheromone.

The Pheromone Response Element Mediating Biofilm Response

In *S. cerevisiae* haploid cells, pheromone induces the transcription of a number of mating-associated genes via a *cis*-acting element in their promoters (Dolan *et al.*, 1989; Sengupta and Cochran, 1990; Elion, 2000). This element is designated as the "pheromone response element" (PRE), consisting of the sequence 5'-ATGAAACA-3' (Hagen *et al*., 1991). The PRE is the binding site for Ste12, the *S. cerevisiae* transcription factor that mediates gene induction in the pheromone response (Dolan *et al.*, 1989; Errede and Ammerer, 1989). Interestingly, Ste12 participates in an autoregulatory circuit whereby it binds to its own promoter and upregulates its own expression (Lee *et al.*, 2002; Ren *et al.*, 2000). Ste12 is constitutively bound to the PREs in some promoters in untreated cells, and binds to the PREs in other promoters only after pheromone stimulation (Ren *et al.*, 2000; Zeitlinger *et al.*, 2003).

FUS1 is one of the most extensively studied pheromone-inducible genes in *S. cerevisiae* (Trueheart *et al.*, 1987; McCaffrey *et al.*, 1987; Roberts *et al.*, 2000; Nolan *et al.*, 2006). PRE elements in the *FUS1* upstream control region are both necessary and sufficient for pheromone-induced *FUS1* transcription (Hagen *et al.*, 1991). In particular, the expression of *FUS1* is abolished when the PREs in the *FUS1* upstream region are deleted. This result is further supported by the finding that a DNA fragment including the PREs of *FUS1* confers *FUS1*-like expression to a *CYC1-lacZ* reporter gene, which is normally not induced by pheromone (Hagen *et al.*, 1991). Furthermore, a simple cluster of synthetic PREs can substitute for the *FUS1* promoter activity either in the reporter gene constructs or in the natural *FUS1* context (Hagen *et al.*, 1991). Although PRE sequences alone can act as upstream activation sequence (UAS) elements, most genes inducible by pheromone have additional UAS elements contributing to the overall activity of their promoters. For instance, the *BAR1* and *STE2* genes contain PREs in close proximity to a P box (Errede and Ammerer, 1989; Hwang-Shum *et al.*, 1991; Keleher *et al.*, 1989), a known UAS element to which the Mcm1 protein binds (Ammerer, 1990; Bender and Sprague, 1987; Jarvis *et al.*, 1989; Keleher *et al.*, 1989). In **a** cells, these genes are only moderately inducible by α-factor. When the P box is deleted and the PREs are left intact, their expression is highly induced in response to α-factor; and when the PREs are deleted, their expression is no longer induced (Keleher *et al.*, 1989; Kronstad *et al.*, 1987). Thus, PREs can either act alone or in concert with other UAS elements to modulate gene induction in response to pheromone.

In *C. albicans*, the opaque-specific genes upregulated by pheromone contain a putative “opaque pheromone response element” (OPRE) with the consensus sequence of 5’-GTGAGGGGA-3’ in their promoter, whereas the white-specific pheromone-inducible genes contain a “white pheromone response element” (WPRE) with the consensus sequence of 5’-AAAAAAAAAAGAAAG-3’ in their promoter (Sahni *et al.*, 2009b). Genes that are upregulated by α-pheromone in both white and opaque cells contain both

OPRE and WPRE elements in their promoters (Sahni *et al.*, 2009b). Selective deletion of OPRE from the promoters of opaque-specific genes, or WPRE from the promoters of white-specific genes, results in the loss of α-pheromone upregulation of gene expression in opaque and white cells, respectively (Sahni *et al.*, 2009b). These results indicate that the alternative transcription factors of the opaque and white pheromone response pathways, activate phase-specific pheromone-inducible genes through the *cis*-acting sequence, OPRE and WPRE, respectively (Sahni *et al.*, 2009b).

The Key Transcription Factor Tec1 and the Filamentation Program

The transcription factor Tec1 belongs to a protein superfamily that contains an evolutionarily conserved "TEA" DNA-binding domain (Burglin, 1991). The TEA superfamily not only includes the Tec1 homologs in *S. cerevisiae* (Gavrias *et al.*, 1996) and *C. albicans* (Schweizer *et al.*, 2000), as will be discussed below, but it also includes the human homolog, TEF-1 (Xiao *et al.*, 1991), which is involved in the activation of SV40 promtoter by large T antigen (Casaz *et al.*, 1991), and the *Aspergillus nidulans* homolog, AbaA, which is involved in phialide differentiation in development (Sewall *et al.*, 1990). In *S. cerevisiae*, Tec1 regulates filamentous growth in both diploid and haploid cells (Gavrias *et al.*, 1996; Mosch and Fink, 1997). It functions in cooperation with Ste12 (Baur *et al.*, 1997) as a complex, and binds to promoter elements, termed filamentation response elements (FREs), that have been defined in the promoters of filamentation-associated genes (Mosch and Fink, 1997; Madhani and Fink, 1997). A FRE contains both a Ste12-binding site, PRE, and a Tec1-binding site, TCS (TEA consensus sequence), and the two sites are often adjacent to each other (Madhani and Fink, 1997). Tec1 harbors a TEA superfamily DNA-binding domain that recognizes the target TCS sequence, 5'-AGAATG-3' (Gavrias *et al.*, 1996). Interestingly, the *TEC1* promoter

contains a FRE as well, suggesting an autoregulation mechanism for *TEC1* activation (Madhani and Fink, 1997).

In *S. cerevisiae*, *TEC1* transcription can be induced by mating pheromone and is dependent on the MAP kinase signal transduction pathway (Madhani and Fink, 1997; Oehlen and Cross, 1998). The upregulation of *TEC1* expression by pheromone is not surprising, since the promoter of *TEC1* contains a Ste12-binding site in the FRE (Oehlen and Cross, 1998). Tec1 protein contains a consensus MAP kinase phosphorylation site at threonine 273, the mutation of which disrupts the activation of FRE-*lacZ* expression (Bao *et al.*, 2004; Chou *et al.*, 2004). Tec1 is, however, not involved in mating. In the mating process, Tec1 is rapidly degraded, and this degradation is dependent on Fus3 kinase activity and the MAP kinase phosphorylation site both *in vitro* and *in vivo* (Bao *et al.*, 2004; Chou *et al.*, 2004, 2008). Finally, the pheromone-mediated degradation of Tec1 in *S. cerevisiae* is mediated by an SCF ubiquitin ligase (Bao *et al.*, 2004; Chou *et al.*, 2004).

In *C. albicans*, *TEC1* is expressed predominantly in hyphal cells (Schweizer *et al.*, 2000), as it is in *S. cerevisiae* (Gavrias *et al.*, 1996; Mosch and Fink, 1997). *In vitro*, serum-induced hypha formation is affected in the *tec1* null mutant cells (Schweizer *et al.*, 2000). In addition, *TEC1* transcription in *C. albicans* is selectively induced by pheromone in white, but not opaque, cells, and is dependent on the MAP kinase pheromone response pathway (Sahni *et al.*, in preparation). Pheromone also selectively upregulates the expression of Tec1 at the protein level only in white cells (Sahni *et al.*, in preparation). Tec1 is the unique white-specific transcription factor that mediates the white cell pheromone response, in constrast to Cph1 in the opaque response (Sahni *et al.*, in preparation). The *tec1* null mutant is severely defective in the pheromone-induced adhesion response and enhancement of biofilm formation (Sahni *et al.*, in preparation). Furthermore, Tecl is also involved in adhesion and biofilm formation in **a**/α cells (Li *et al.*, 2005; Nobile and Mitchell, 2005).

TEC1 upregulates the white-specific biofilm-associated genes through binding to the WPRE element in their promoters (Sahni *et al.*, in preparation). The WPRE element in *C. albicans*, exhibits homology with the Tec1-binding site, TCS, in *S. cerevisiae* (Gavrias *et al.*, 1996) which is involved in the induction of filamentation associated genes. This result suggests that the *C. albicans* transcription factor Tec1, which mediates the white cell pheromone response, may have evolved from the ancestral filamentation pathway.

The White-specific Biofilm-associated Genes

In a northern blot screen of 103 genes, 12 were identified as selectively upregulated by α-pheromone in white but not opaque cells (Sahni *et al.*, 2009b). These 12 genes are *PBR1*, *CSH1*, *EAP1*, *PGA10*, *PHR1*, *PHR2*, *WH11*, *SUN41*, *CIT1*, *LSP1*, *RBT5*, and *Orf19.2077*. All 12 genes contain a WPRE in their promoters. The WPRE and homozygous deletion mutants of the four genes, *PBR1*, *CSH1*, *EAP1* and *PGA10*, all exhibit a reduction in α-pheromone induced adhesion, but not a complete loss of the response (Sahni *et al.*, 2009b). In addition, all these mutants form defective biofilms in the absence of minority opaque cells, and none of them exhibit biofilm enhancement in the presence of minority opaque cells (Sahni *et al.*, 2009b), the source of pheromone (Daniels *et al.*, 2006; Yi *et al.*, 2008). All the mutants, however, undergo a normal opaque cell response to pheromone (Sahni *et al.*, 2009b). These results suggest that the genes upregulated by pheromones in white, but not opaque, cells play a role in biofilm formation in *MTL*-homozygous cells both in the absence and presence of pheromone. Indeed, the genes that are upregulated by pheromone specifically in white cells, may also play a role in biofilm formation in *MTL*-heterozygous **a**/α strains as well. For instance, disruption of *PGA10* or *RBT5* in an **a**/α strain results in a defect in biofilm formation on plastic (Perez *et al.*, 2006). Disruption of *SUN41* in an **a**/α strain causes a severe defect in biofilm development on silicone elastomer squares (Norice *et al.*, 2007; Hiller *et al.*, 2007). In

addition, the discovery that the WPRE and homozygous deletion mutants of the four genes, *PBR1*, *CSH1*, *EAP1* and *PGA10*, all have a defect in biofilm development in the absence of minority opaque cells, suggests an autocrine system in which white cells release pheromone of the opposite mating type, which in turn binds to the pheromone receptors on the same cells that secrete the pheromone to elicit a pheromone response (Sahni *et al.*, 2009b). This latter hypothesis is now being tested in our laboratory.

Summary: Rationale and Scope of the Thesis Research

My thesis project has focused on the relationship between white-opaque switching, mating and biofilm formation in the human fungal pathogen *C. albicans*. *MTL*-homozygous strains of *C. albicans* can undergo the white-opaque transition. In 2006, Daniels *et al*. identified a novel form of communication between the two switch phenotypes, white and opaque, in *C. albicans* (Daniels *et al*., 2006). It was demonstrated that opaque cells, through the release of pheromone, signal majority white cells of the opposite mating type to form a biofilm. In turn, white cell biofilms facilitate opaque cell chemotropism required for mating. However, the generality of the white cell biofilm response was initially questioned (Bennett and Johnson, 2006). Hence, validation of the generality of the white response was performed in a number of different *MTL*-homozygous strains (Sahni *et al.*, 2009a). This work is described in Chapter 3.

The signaling circuitry regulating this unique white cell pheromone response was not known. Chapter 4 focuses on the identification and characterization of the signaling pathway mediating this response (Yi *et al.*, 2008). This pathway has significant implications in the evolution of multicellularity in higher eukaryotes.

The pheromone receptor is one of the upstream components of the white cell biofilm response pathway. Chapter 5 focuses on the role of a unique *C. albicans*-specific 55 amino acid region in the first intracellular loop (IC1) of the α-pheromone receptor, Ste2,

in the white response, based on an extensive mutational analysis of key domains in the receptor (Yi *et al.*, 2009).

In response to pheromone, the unique white cell biofilm response pathway specifically activates biofilm-associated genes. Chapter 6 focuses on the identification of genes that are specifically upregulated by pheromone in white cells of *C. albicans* (Sahni *et al.*, 2009b). These genes are activated through a common *cis*-acting sequence, WPRE, distinct from the *cis*-acting sequence, OPRE, responsible for the up-regulation of mating-associated genes in opaque cells. Moreover, these white-specific genes are essential for biofilm formation (Sahni *et al.*, 2009b).

Yi *et al.* (2008) demonstrated that the downstream transcription factor in the white cell response is different from that in the opaque mating response. Chapter 7 covers the identification of the unique transcription factor, Tec1, in the white pheromone response pathway, distinct from Cph1 that mediates the opaque pheromone response (Sahni *et al.*, in preparation). Tec1 is activated by the pheromone-activated MAPK pathway in *C. albicans* white cells. Moreover, it regulates the downstream biofilm-associated genes through binding to the WPRE (white pheromone response element) in their promoters (Sahni *et al.*, in preparation).

Chapter 8 discusses the significance of my thesis work and provides future perspectives. Evolutionary implications of the novel white cell biofilm response signal transduction pathway are discussed, with unique insights into how new signal transduction pathways may evolve and adapt in general. The interdependencies of switching, mating and biofilm development are emphasized in terms of their role in *C. albicans* pathogenesis.

CHAPTER 3
GENERALITY OF THE WHITE CELL PHEROMONE RESPONSE IN *C. ALBICANS*

Introduction

As mentioned in Chapter 2, in *Candida albicans MTL*-homozygous strains, minority opaque cells signal majority white cells through the release of pheromone to become more cohesive, adhesive and form enhanced biofilms. However, skepticism has been voiced formally concerning the validity and generality of the white cell response. This stemmed from a recent microarray analysis by Bennett and Johnson (2006) comparing α-pheromone-induced gene expression in white cells of two strains, RBY717, an **a**/**a** derivative of the laboratory strain SC5314 (Bennett *et al*., 2003), and P37005, a natural **a**/**a** strain (Lockhart *et al*., 2002). Although their study focused primarily on the expression of genes induced in opaque cells in response to pheromone, they reported that the pheromone-induced response in terms of gene expression in white cells of strain RBY717 was weaker than that of strain P37005 (Bennett and Johnson, 2006). Additionally, they provided evidence that the α-pheromone-induced gene expression profile was affected by the composition of the supporting medium (Bennett and Johnson, 2006). Taken together, their results suggested that the white cell pheromone response was conditional and did not occur in all strains or in all media.

Since the white cell pheromone response provides a key to understanding the role of white-opaque switching in *C. albicans* mating, we went on to test the generality of the white cell response in a large number of strains belonging to the five major clades of *C. albicans* and also in a number of lab media. We used two characteristics to assay the white cell pheromone response, an increase in adhesion to a plastic surface in response to pheromone (Daniels *et al*., 2006) and induction of a number of genes induced specifically in white cells (Yi *et al*., 2008, 2009). Our results demonstrated that the response occured

in all tested media (Lee's, RPMI, SpiderM, yeast extract-peptone-dextrose, and a synthetic medium) and in all of the 27 tested strains, including **a**/**a** and α/α strains, derivatives of the common laboratory strain SC5314, and representatives from all of the five major clades. The white cell response to pheromone is therefore a general characteristic of *MTL*-homozygous strains of *C. albicans*.

Materials and Methods

Strains and Media

All yeast strains were clonally derived from clinical isolates or from the laboratory strain SC5314. Their origins and genotypes are listed in Table 1. Cells from all strains were stored at 20% glycerol at -80°C. For experimental purposes they were grown on agar plates containing supplemented Lee's medium (Bedell and Soll, 1979) at 25 °C. **a**/**a** strains RBY717 and RBY731, and α/α strains RBY722 and RBY734 were derivatives of the **a**/α laboratory strain SC5314. They were generous gifts of Dr. Richard Bennett from Brown University. Except for spontaneous *MTL*-homozygous strains, **a**/**a** or α/α derivatives of natural **a**/α strains were obtained by growth in Lee's medium supplemented with sorbose, as described by Bennett *et al.* (2003). After 5 days, cells were plated on Lee's agar plates supplemented with phloxine B (5 μg/ml) to screen for opaque cells (Anderson and Soll, 1987), which are either **a**/**a** or α/α. The mating-type was then determined by PCR (Miller and Johnson 2002; Wu *et al.*, 2005).

Laboratory media were prepared as described in relevant references: supplemented Lee's medium (Bedell and Soll, 1979), RPMI medium (Daniels *et al.*, 2006), SpiderM medium (Bennett *et al.*, 2006), YPD medium (Bennett *et al.*, 2006; Srikantha *et al.*, 2006) and SCD medium (Bennett *et al.*, 2006).

Table 1. *C. albicans* strains used in the generality analysis of the white pheromone response

Strain	Parent	*MTL*	Genotype	Reference or source
P37005	–	**a**/**a**	Wild type	Lockhart *et al.* (2002)
L26	–	**a**/**a**	Wild type	Lockhart *et al.* (2002)
P87	–	**a**/**a**	Wild type	Blignaut *et al.* (2002)
P60002	–	**a**/**a**	Wild type	Wu *et al.* (2007)
P78042(**a**/**a**)	P78042	**a**/**a**	Wild type	This study
P76068(**a**/**a**)	P76068	**a**/**a**	Wild type	This study
P75006(**a**/**a**)	P75006	**a**/**a**	Wild type	This study
P57096(**a**/**a**)	P57096	**a**/**a**	Wild type	This study
P76067(**a**/**a**)	P76067	**a**/**a**	Wild type	This study
P76055(**a**/**a**)	P76055	**a**/**a**	Wild type	This study
GH1011	SC5314	**a**/**a**	Wild type	Huang *et al.* (in prep.)
WO-1	–	α/α	Wild type	Slutsky *et al.* (1987)
P89011	–	α/α	Wild type	This study
P80001(α/α)	P80001	α/α	Wild type	Lockhart *et al.* (2002)
P34048(α/α)	P34048	α/α	Wild type	Wu *et al.* (2007)
P37039(α/α)	P37039	α/α	Wild type	Pujol *et al.* (2003)
P75063(α/α)	P75063	α/α	Wild type	Lockhart *et al.* (2002)
GC75	–	α/α	Wild type	Blignaut *et al.* (2002)
P48076(α/α)	P48076	α/α	Wild type	Pujol *et al.* (2002)
19F	–	α/α	Wild type	Lockhart *et al.* (1996)
P75010(α/α)	P75010	α/α	Wild type	This study
P75006(α/α)	P75006	α/α	Wild type	This study
P57072	–	α/α	Wild type	Pujol *et al.* (2002)

White Cell Adhesion Assay

The adhesion assay was performed according to methods described previously (Daniels *et al.*, 2006; Yi *et al.*, 2008). α-pheromone (13-mer) was synthesized by Open Biosystems (Huntsville, AL) and dissolved in dimethyl sulfoxide (DMSO) for use. For experiments in the absence of α-pheromone, an equivalent amount of DMSO was added. In brief, **a**/**a** cells at stationary phase were resuspended in fresh medium at 5×10^7/ml and inoculated in wells of a Costar six well cluster plate (Corning Life Sciences, Lowell, MA) in the absence or presence of 10^{-6} M α-pheromone. After 16 h at 25 °C, the wells were gently washed and photographed. A 0.05% trypsin-EDTA solution (Invitrogen, Carlsbad, CA) was then added into each well to release adhering cells from the well bottom. The number of cells was quantitated. **a**-pheromone induced adhesion in α/α cells was performed in a similar fashion, except that instead of pheromone, 1% of an opaque cell mixture was added to 99% white α/α test cells. The opaque cell mixture contained 50% opaque **a**/**a** cells of strain P37005 and 50% opaque α/α cells of strain WO-1. The combination of majority white and minority opaque cells was then added to the wells of a Costar six well cluster plate.

Northern Analysis

For northern analyses, cells from saturation phase cultures were diluted into fresh medium in the absence or presence of 3×10^{-6} M α-pheromone, and pelleted after 4 hr. Total RNA was extracted using the RNeasy Mini Kit (Qiagen Sci., MA). Polymerase chain reaction (PCR) products were used for probing northern blots.

Clade Analysis by DNA Fingerprinting

Isolates included in the dendrogram were fingerprinted by Southern blot hybridization with the complex DNA fingerprinting probe Ca3 (Sadhu *et al.*, 1991; Pujol *et al.*, 1997; Blignaut *et al.*, 2002; Lockhart *et al.*, 2002; Pujol *et al.*, 2002) by methods

previously described in detail (Schmid *et al.*, 1990; Soll, 2000; Soll *et al.*, 2007). The Ca3 banding patterns of all test isolates were compared in a pairwise fashion, and similarity coefficients (S_{AB}) computed by the DENDRON software program according to the formula for the Dice coefficient (Soll, 2000; Soll *et al.*, 2007). The dendrogram was generated from a matrix of pairwise S_{AB}s using the Unweighted Pair Group Method with Arithmetic averages (UPGMA; Rohlf, 1963). The dendrogram includes 50 strains previously fingerprinted that included 10 strains from each of the five major clades (Soll and Pujol, 2003), and 25 of the 27 strains analyzed for the white response. The latter included at least two **a**/**a** and two α/α strains in each clade.

Results

α-pheromone Induction of Adhesion

α-pheromone induces adhesion and cohesion in white, but not opaque **a**/**a** cells (Daniels *et al*., 2006). White cells of 13 **a**/**a** strains (Table 1) were tested for α-pheromone-induced adhesion to the plastic bottoms of wells in a cluster well plate according to the methods of Daniels *et al.*, 2006. Adhesion to well bottoms was negligible in the absence of α-pheromone ($<10^6$ cells per well bottom), but high in its presence (1.5 to 2.7 x 10^8 per well bottom) for the 13 tested strains (Figure 8A). The increase was well over 100 fold for every tested strain (Figure 8A). The well bottoms for white cells of the natural **a**/**a** strain L26 (Lockhart *et al*., 2002) in the absence (-) and presence (+) of α-pheromone were representative of all tested **a**/**a** strains (Figure 8B). In control experiments, we found that α-pheromone did not stimulate adhesion in white cells of five tested α/α strains or in cells of five tested **a**/α strains; in all of these controls, adhesion to the well bottom was comparable in the absence or presence of α-pheromone (data not shown).

Figure 8. α-pheromone induces a dramatic increase (> 100 fold) in adhesion in white cells of all tested **a**/**a** strains of *C. albicans*. The methods of Daniels *et al.* (2006) were employed. In brief, white cells were incubated for 16 hr at 25 °C in supplemented Lee's medium (Bedell and Soll, 1979) in the wells of cluster-well plates in the absence (-) or presence (+) of 10^{-6} M α-pheromone (13-mer). Well bottoms were then gently rinsed and photographed, then scraped and the suspended cells counted. A. Histogram of the average number of cells adhering to the well bottom for each of 10 **a**/**a** strains. Those strains with a/a in parenthesis were obtained by treating the noted wild type **a**/α strain with sorbose (Janbon *et al.*, 1998), screening for opaque sectors (*MTL*-homozygous offspring) and genotyping for a/a strains by PCR (Miller and Johnson, 2002; Wu *et al.*, 2005). Three **a**/**a** derivatives of the laboratory strain SC5314 were also tested. The origins and genotypes of the tested **a**/**a** strains are provided in Table 1. The mean of three well bottoms plus standard deviation (error bar) are presented for each strain: α-ph, α-pheromone. B. The well bottoms for strain L26 in the absence (-) or presence (+) of α-pheromone were representative of all a/a strains tested.

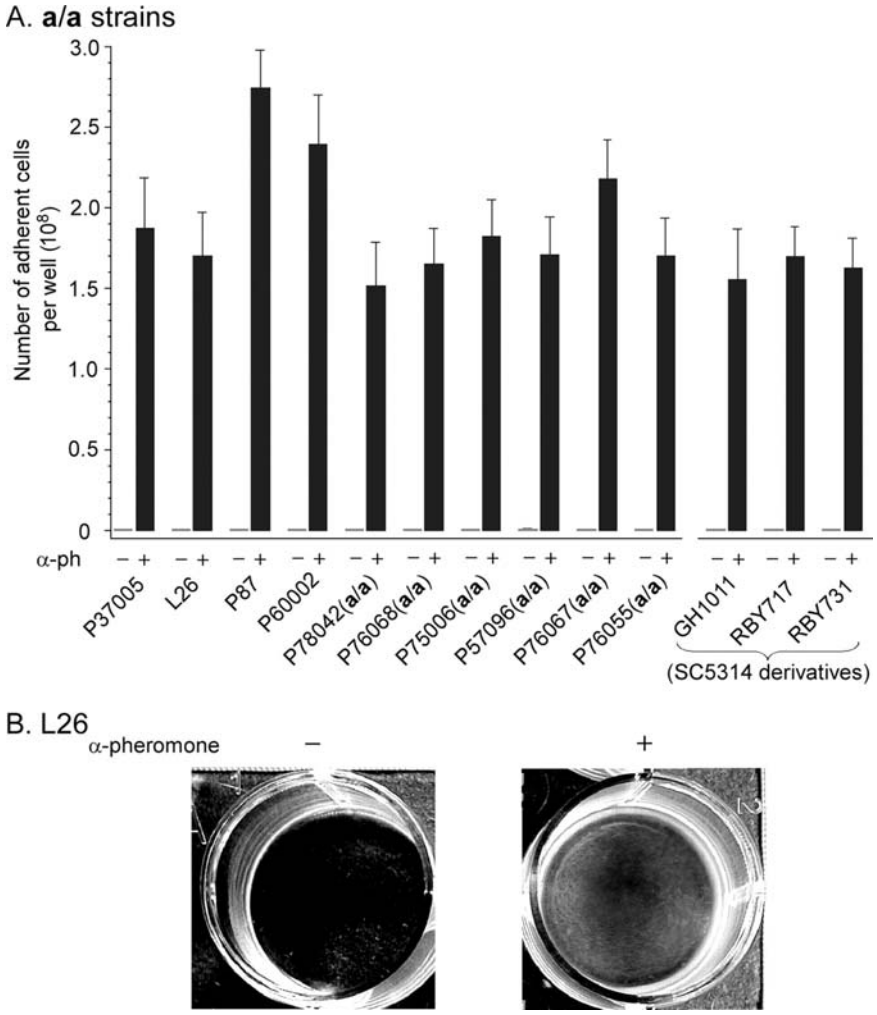
A. a/a strains
Number of adherent cells per well (10^8)
3.0
2.5
2.0
1.5
1.0
0.5
0
α-ph
− + − + − + − + − + − + − + − + − + − + − + − + − +
P37005
L26
P87
P60002
P78042(a/a)
P76068(a/a)
P75006(a/a)
P57096(a/a)
P76067(a/a)
P76055(a/a)
GH1011
RBY717
RBY731
(SC5314 derivatives)
B. L26
α-pheromone
−
+

a-pheromone Induction of Adhesion

a-pheromone induces adhesion and cohesion in white, but not opaque, α/α cells (Daniels *et al.*, 2006). White cells of 14 α/α strains were tested for **a**-pheromone-induced adhesion to a plastic surface by a modification of the procedure of Daniels *et al.* 2006. **a**-pheromone was generated by adding 1% opaque cells, consisting of a 50:50 mixture of opaque α/α cells (strain WO-1) and opaque **a**/**a** cells (strain P37005), to 99% white test cells. Presumably, the release of α-pheromone by minority opaque α/α cells up-regulated **a**-pheromone production by minority opaque **a**/**a** cells, which in turn signaled majority white α/α cells. Adhesion of white cells to the substrate was negligible in the absence of the opaque cell mixture (< 10^6 cells per well bottom), but high in its presence (1.0 to 2.2 x 10^8 per well bottom) for all 14 strains (Figure 9A). The increase was well over 100 fold for every tested strain (Figure 9A). The well bottoms for white cells of the natural α/α strain WO-1 (Slutsky *et al*., 1987) in the absence (-) and presence (+) of the minority opaque cell mixture were representative of all tested α/α strains (Figure 9B). In control experiments, we found that the 1% mixture of opaque cells did not stimulate adhesion in five tested **a**/α strains; adhesion to the dish bottom in the absence or presence of minority opaque cells was comparable. We could not test the effects of **a**-pheromone on white **a**/**a** cells since the opaque cell mixture, which is the source of **a**-pheromone, also produces α-pheromone.

Pheromone Induction of Gene Expression

We next tested whether α-pheromone up-regulated *STE2*, the α-pheromone receptor gene, and three white-specific genes, *CSH1* (Yi *et al*., 2008), *orf19.2077* (Sahni *et al.*, 2009b) and *orf19.6274* (Sahni *et al.*, 2009b), in white cells of seven **a**/**a** strains and whether **a**-pheromone up-regulated *STE3*, the **a**-pheromone receptor gene, and the same three white-specific genes in white cells of seven α/α strains. α-pheromone up-regulated *STE2* and the three white-specific genes in all tested **a**/**a** strains (Figure 10A),

Figure 9. **a**-pheromone induces a dramatic increase (> 100 fold) in adhesion in white cells of all tested α/α strains of *C. albicans*. A modified version of the methods of Daniels *et al.* (2006) was employed. In brief, majority white cells (99%) of each strain were mixed with minority opaque cells (1%), the latter composed of a 50:50 mixture of opaque **a**/**a** (P37005) and opaque α/α (WO-1) cells. Presumably the α/α opaque cells in the mixture produced α-pheromone, which up-regulated **a**-pheromone production in the opaque **a**/**a** cells (Daniels *et al.*, 2006). White cells of each test strain alone or mixed with the minority opaque cell mixture, were then assayed for adhesion as described in the legend to Figure 9 for the α-pheromone response of **a**/**a** cells. A. Histogram of the average number of cells adhering to the well bottom for each of 14 α/α strain. The three α/α strains P48076, P75010 and P75006 were obtained by growing the natural **a**/α strains with sorbose (Janbon *et al.*, 1998), screening for opaque sectors (*MTL*-homozygous offspring), and genotyping for α/α strains by PCR (Miller and Johnson, 2002, Wu *et al.*, 2005). The four α/α strains P80001, P34048, P37039 and P75063, were spontaneous α/α derivatives of natural **a**/α strains. The mean of three well bottoms plus standard deviation are presented for each strain: 1% Op, 1% opaque cell mixture. B. The well bottoms for strain WO-1 in the absence (-) or presence (+) of the mixture of minority opaque cells were representative of all α/α strains tested.

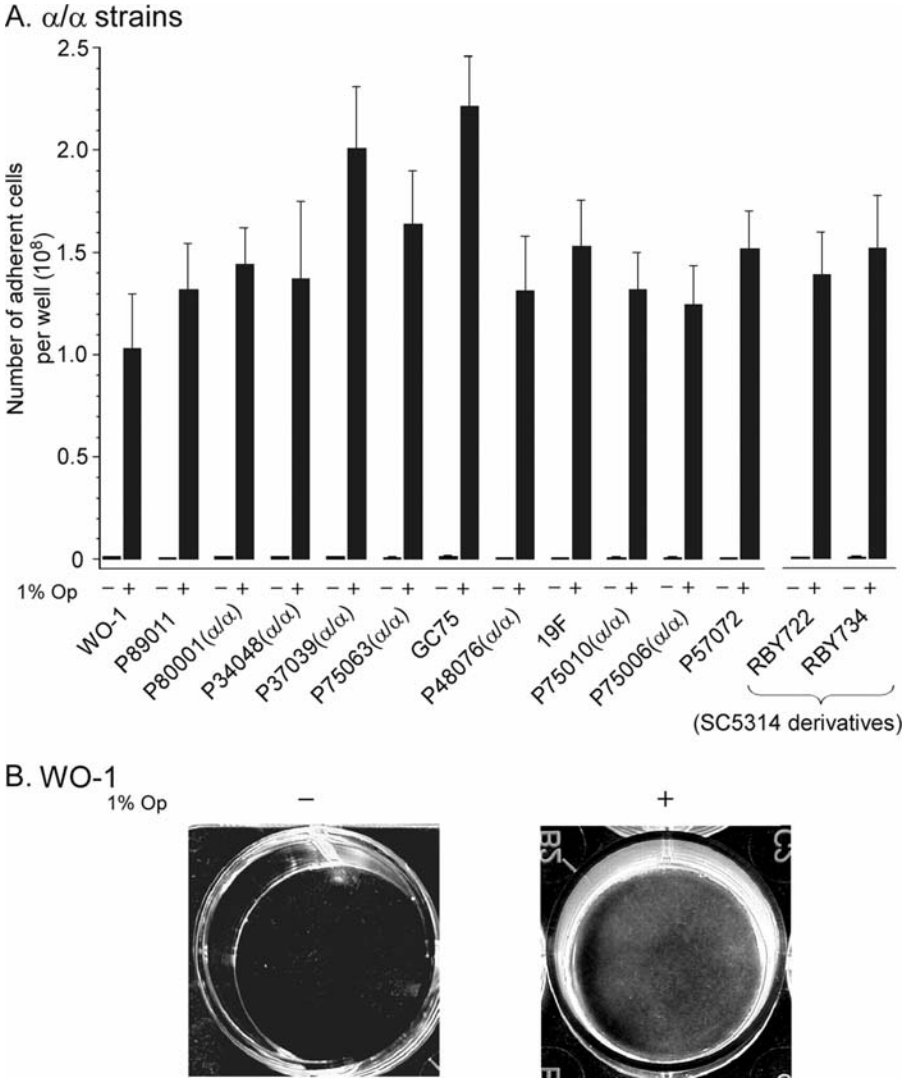
A. α/α strains
Number of adherent cells per well (10^8)
2.5
2.0
1.5
1.0
0.5
0
1% Op
− + − + − + − + − + − + − + − + − + − + − + − + − + − +
WO-1
P89011
P80001(α/α)
P34048(α/α)
P37039(α/α)
P75063(α/α)
GC75
P48076(α/α)
19F
P75010(α/α)
P75006(α/α)
P57072
RBY722
RBY734
(SC5314 derivatives)
B. WO-1
1% Op
−
+

Figure 10. Pheromone induces the expression of the pheromone receptor genes and white-specific genes in white cells of all tested strains. Saturation phase white cells of **a**/**a** strains were released into supplemented Lee's medium in the absence or presence of 10^{-6} M α-pheromone (13-mer) and incubated for 4 hr. Saturation phase white cells of α/α strains were mixed 99:1 with a 50:50 mixture of opaque **a**/**a** P37005 and opaque α/α WO-1 cells and incubated for 4 hrs. Northern analyses were performed as previously described (Srikantha *et al.*, 2006, Yi *et al.*, 2008). A. Northern analysis of the expressions of *STE2* and the white-specific, pheromone-induced genes *CSH1*, *orf19.6274*, and *orf19.2077*, in white cells of seven **a**/**a** test strains in the absence (-) or presence (+) of α-pheromone (α-ph). Three **a**/**a** derivatives of the laboratory strain SC5314 were tested. B. Northern analysis of the expressions of *STE3* and the white-specific genes *CSH1*, *orf19.6274*, and *orf19.2077* in white cells of seven α/α strains in the absence (-) or presence (+) of 1% opaque cell mixture (1% Op). The patterns to the left and right of each panel represent independent experiments and, therefore, each has one common strain, P37005 for **a**/**a** strains and WO-1 for α/α strains. The ethidium bromide-stained 18S rRNA patterns are provided to demonstrate uniform loading.

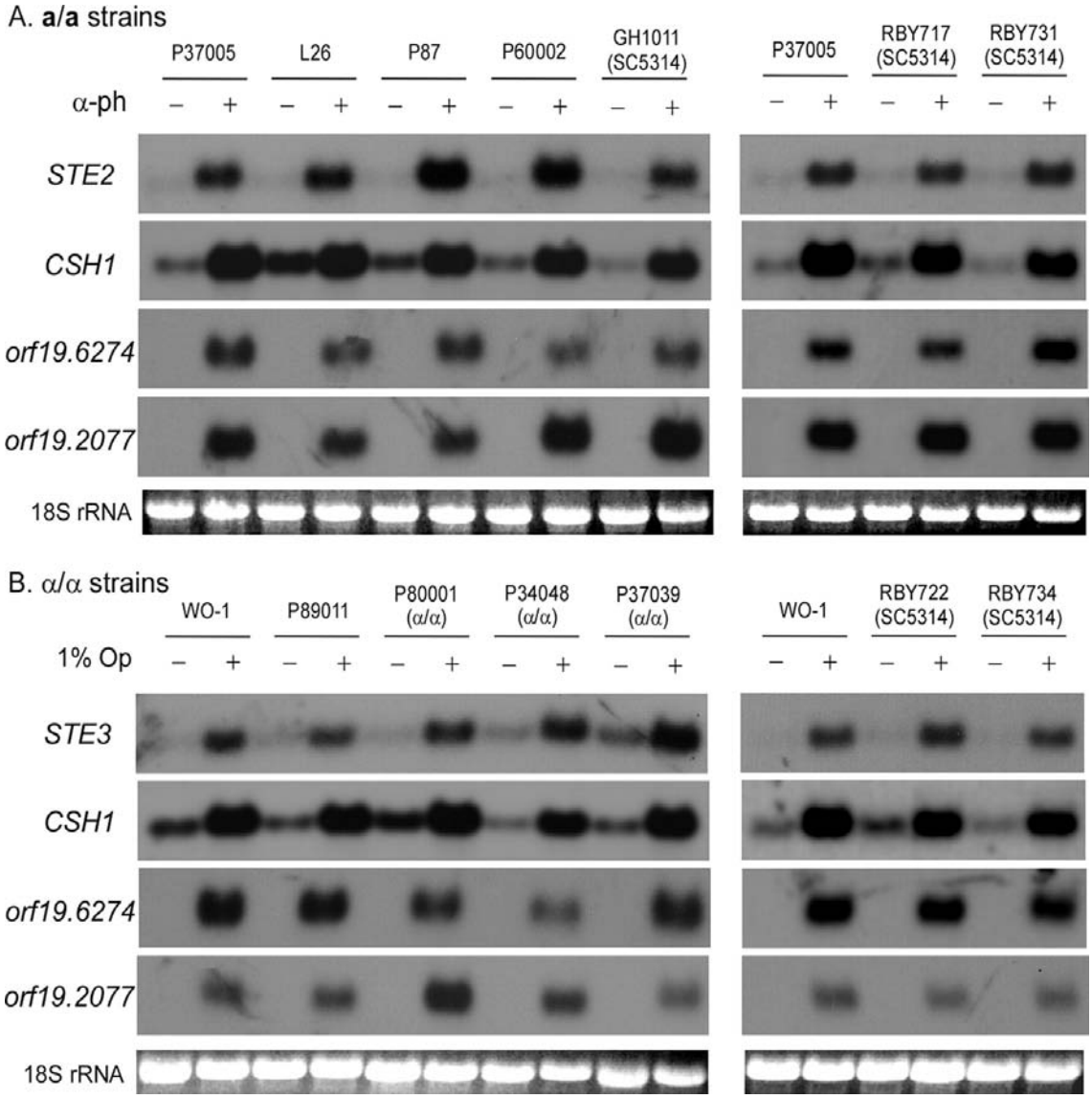
A. a/a strains
P37005
L26
P87
P60002
GH1011 (SC5314)
P37005
RBY717 (SC5314)
RBY731 (SC5314)
α-ph
– + – + – + – + – + – + – + – +
STE2
CSH1
orf19.6274
orf19.2077
18S rRNA
B. α/α strains
WO-1
P89011
P80001 (α/α)
P34048 (α/α)
P37039 (α/α)
WO-1
RBY722 (SC5314)
RBY734 (SC5314)
1% Op
– + – + – + – + – + – + – + – +
STE3
CSH1
orf19.6274
orf19.2077
18S rRNA

and **a**-pheromone up-regulated *STE3* and the three white-specific genes in all α/α strains (Figure 10B). α-pheromone up-regulated *STE2* but not the three white-specific genes in opaque cells of the tested **a**/**a** strains (data not shown), and **a**-pheromone up-regulated *STE3*, but not the three white-specific genes, in opaque cells of the seven α/α test strains (data not shown). Strain variation was observed in the expression levels of the assayed genes upon pheromone induction, but most importantly pheromone up-regulated every tested gene in every tested strain.

The White Cell Response of SC5314 Derivatives

In the Bennett and Johnson study, the α-pheromone-induced pattern of gene expression was stronger in white cells of the natural **a**/**a** strain P37005 than in the SC5314 **a**/**a** derivative RBY717. We therefore compared the white cell response to α-pheromone between RBY717 and natural **a**/**a** strains. We also compared a second SC5314 **a**/**a** derivative generated by Bennett and Johnson, RBY731. Similarly, we compared the white cell response to **a**-pheromone of two SC5314 α/α derivatives also generated by Bennett and Johnson (2006), RBY722 and RBY734. All of these strains were generous gifts of Richard Bennett of Brown University. Finally, we tested the white cell response to α-pheromone of the SC5314 **a**/**a** derivative, GH1011, which we independently generated (Huang *et al*., 2009). α-pheromone induced adhesion (Figure 8A) and up-regulated gene expression (Figure 10A) in white cells of the three SC5314 **a**/**a** derivatives, and **a**-pheromone induced adhesion (Figure 9A) and up-regulated gene expression (Figure 10B) in white cells of the two SC5314 α/α derivatives. All of the SC5314 derivatives responded to pheromone as robustly, on average, as the other *MTL*-homozygous strains (Figures 8, 9, 10). No significant difference was observed between P37005 and the SC5314 **a**/**a** derivatives, including strain RBY717, in the level of adhesion (p values < 0.05) or the levels of gene expression induced by pheromone.

The White Response in Different Media

Bennett and Johnson observed marked differences in the effect of α-pheromone on the global expression patterns of white cells of strain P37005 and RBY717 in different nutrient media, and noted that the effect of medium composition was more pronounced for strain RBY717 than strain P37005. They found that Lee's medium was better than SpiderM medium for the white response (Bennett and Johnson, 2006). We therefore tested whether growth medium influenced the white cell response to pheromone of the natural **a**/**a** strain P37005 and RBY717. In five test media (Lee's, RPMI, SpiderM, YPD, SCD), α-pheromone induced adhesion over 100 fold for both P37005 (Figure 11A) and RBY717 (Figure 11B). Differences in the fold increase induced by α-pheromone in the different media ranged from 1.0 to 2.1 x 10^8 cells per well bottom (Figure 11A, B). Pheromone induction was higher in Lee's and RPMI media than in SpiderM, YPD and SCD media for both P37005 and RBY717 white cells (Figure 11A and B, respectively). We found, as did Bennett and Johnson, that Lee's medium was better in supporting the pheromone response than SpiderM medium. More importantly, a robust white cell response to α-pheromone occurred in both strains in all tested media.

Distribution between Clades

DNA fingerprinting studies with the complex probe Ca3 have separated the majority of *C. albicans* isolates into five major clades, I, II, III, SA and E (Soll and Pujol, 2003). To assess the generality of the white response, we selected a minimum of two **a**/**a** and two α/α test strains from each of the major clades in testing for the response. Four of the **a**/**a** strain (P37005, L26, P87, P60002) possessed this genotype at the time of collection, six (P78042, P76068, P75006, P57096, P76067, P76055) were natural **a**/α strains that were induced by sorbose treatment (Bennett *et al*., 2003; Janbon *et al*., 1998) to undergo *MTL*-homozygosis, and three (GH1011, RBY717, RBY731) were derived from the laboratory strain SC5314 by sorbose treatment (Bennett and Johnson, 2006). Five of

Figure 11. The increase in white cell adhesion induced by pheromone occurs in five common media used in *C. albicans* research. White a/a cells of natural strain P37005 (A) and strain RBY 717 (B), an **a**/**a** derivative of laboratory strain SC5314, were grown and tested with α-pheromone as described in the legend of Figure 8, but the media in which they were tested included one of the following: supplemented Lee's (Bedell and Soll, 1979), RPMI (Daniels *et al.*, 2006), SpiderM (Bennett and Johnson, 2006), YPD (Bennett and Johnson, 2006, Srikantha *et al*., 2006) or SCD (Bennett and Johnson, 2006). The increase in adhesion induced by pheromone varied between > 100 fold in SCD and > 200 fold in RPMI.

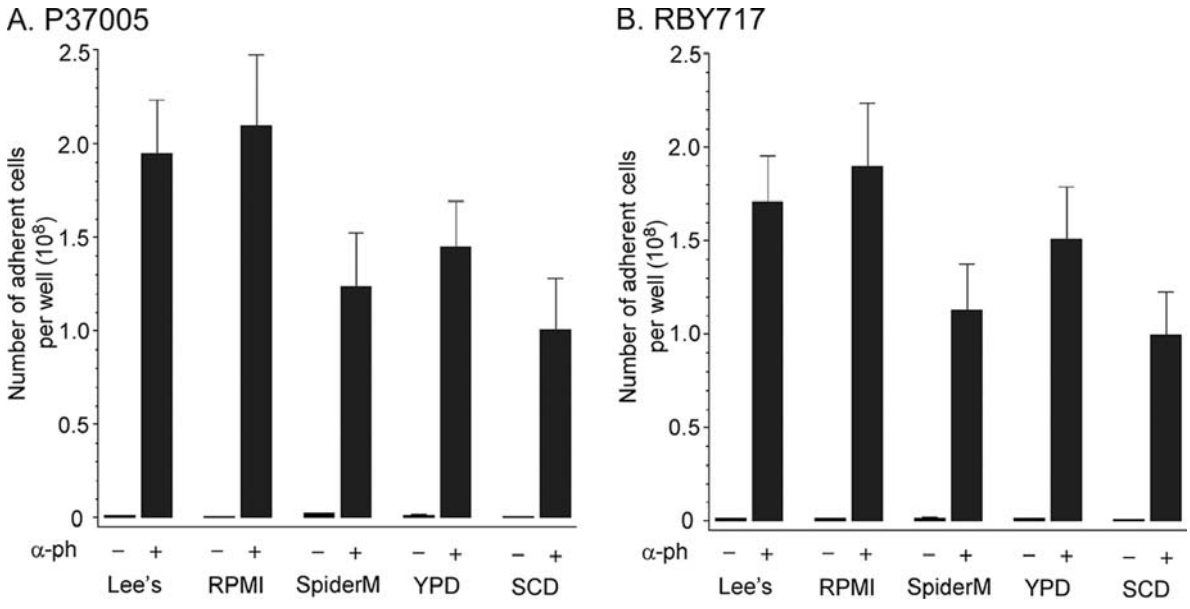
A. P37005
B. RBY717
Number of adherent cells per well (10^8)
2.5
2.0
1.5
1.0
0.5
0
α-ph
− +
Lee's
RPMI
SpiderM
YPD
SCD

the α/α strains (WO-1, P89011, P57072, GC75, 19F) possessed this genotype at the time of collection, four (P80001, P34048, P37039, P75063) were natural **a**/α strains that underwent spontaneous *MTL*-homozygosis, three (P48076, P75010, P75006) were natural **a**/α strains induced to undergo *MTL*-homozygosis by sorbose treatment, and two (RBY722, RBY734) were derived from laboratory strain SC5314 by sorbose treatment (Bennett and Johnson, 2006). As noted, white cells of every **a**/**a** and α/α test strain, representing all of the five major clades, responded to pheromone with an increase in adhesion of greater than 100 fold (Figures 8, 9). A dendrogram was generated that was based on the similarity coefficients (S_{AB}s) (Blignaut *et al.*, 2002; Soll and Pujol, 2003; Soll *et al.*, 2007) computed amongst 25 DNA fingerprinted test strains and 50 other previously DNA fingerprinted strains that were distributed among the five major clades in order to emphasize the generality of the white cell response (Figure 12).

Discussion

We have, therefore, found that a robust white cell response to pheromone occurred in all of the 27 *MTL*-homozygous strains tested, both in **a**/**a** and α/α representatives of the five major clades of *C. albicans*. We have found that white **a**/**a** cells responded to α-pheromone similarly to white α/α cells to **a**-pheromone, and that the basic white cell response occurred in a variety of nutrient media. Moreover, we found that all of the tested **a**/**a** and α/α derivatives of the common laboratory strain SC5314 underwent the white response to their respective pheromones, and did so with a robustness similar to that of white cells of strain P37005 and the other strains tested. Variation was observed in the strength of the response amongst strains and media, but the level of induction by pheromone was still robust for each tested strain and in every medium. The changes in the global expression pattern induced by α-pheromone in white cells of laboratory strain RBY717 were demonstrated by Bennett and Johnson, using microarray technology, to be weaker than the changes induced in the global expression pattern of the natural strain

Figure 12. Strains exhibiting the white response to α-pheromone or **a**-pheromone are distributed throughout the major clades of *C. albicans*. Two or more strains from each of the five major clades of *C. albicans*, I, II, III, E and SA (Soll and Pujol, 2003), were tested for and found to exhibit the white cell response to pheromone. A dendrogram was generated in which the Ca3 hybridization patterns of 25 of the test strains or substrains that exhibited the white cell response and had been genetically fingerprinted with the DNA fingerprinting probe Ca3 (Soll *et al*., 2007) were compared to the patterns of 50 strains representing the five major clades, by computing similarity coefficients (SAB), using the DENDRON software program (Soll *et al*., 2007). The *MTL*-homozygous strains that were tested for the white response are presented in bold print. The five major clades are labeled to the right of the dendrogram. The dashed line represents the threshold for clades (Soll and Pujol, 2003).

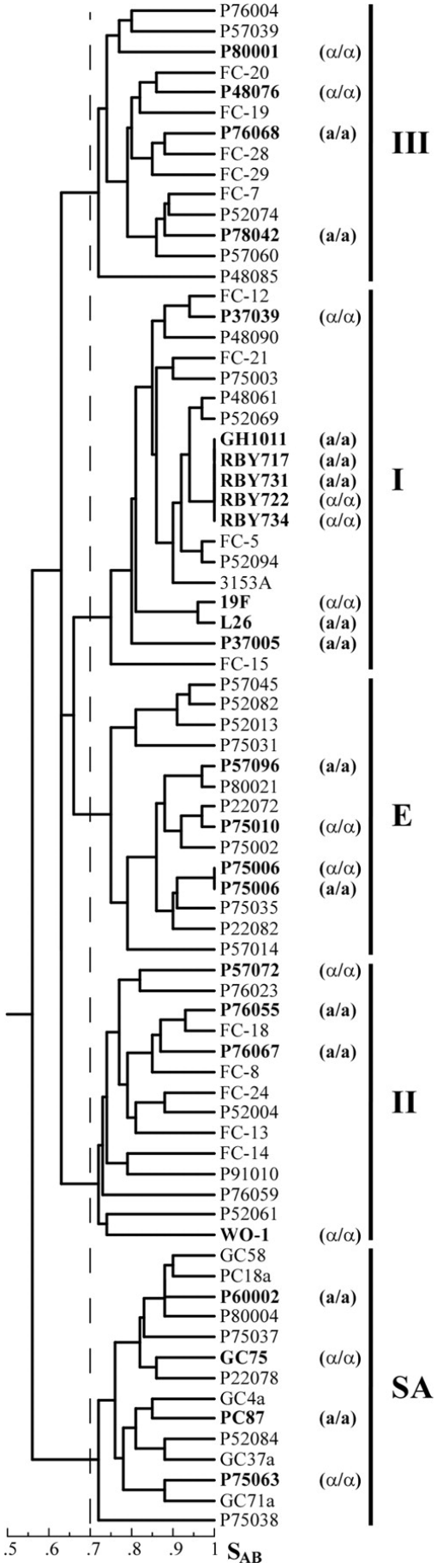
P76004
P57039
P80001 (α/α)
FC-20
P48076 (α/α)
FC-19
P76068 (a/a)
FC-28
FC-29
FC-7
P52074
P78042 (a/a)
P57060
P48085
III
FC-12
P37039 (α/α)
P48090
FC-21
P75003
P48061
P52069
GH1011 (a/a)
RBY717 (a/a)
RBY731 (a/a)
RBY722 (α/α)
RBY734 (α/α)
FC-5
P52094
3153A
19F (α/α)
L26 (a/a)
P37005 (a/a)
FC-15
I
P57045
P52082
P52013
P75031
P57096 (a/a)
P80021
P22072
P75010 (α/α)
P75002
P75006 (α/α)
P75006 (a/a)
P75035
P22082
P57014
E
P57072 (α/α)
P76023
P76055 (a/a)
FC-18
P76067 (a/a)
FC-8
FC-24
P52004
FC-13
FC-14
P91010
P76059
P52061
WO-1 (α/α)
II
GC58
PC18a
P60002 (a/a)
P80004
P75037
GC75 (α/α)
P22078
GC4a
PC87 (a/a)
P52084
GC37a
P75063 (α/α)
GC71a
P75038
SA
.5 .6 .7 .8 .9 1
S_AB

P37005 in either of two media. The expression patterns of RBY717 were also demonstrated to be sensitive to the composition of the supporting medium. The combined results, however, suggest that the increase in adhesion and up-regulation of receptor genes and white specific genes provide more specific indicators of the white response to pheromone than changes in global expression patterns assessed by microarrays. More importantly, our results demonstrate that the white cell response to pheromone is a general characteristic of *C. albicans*, as is the opaque cell response to pheromone (Bennett *et al*., 2003; Lockhart *et al*., 2003a).

CHAPTER 4
IDENTIFICATION OF THE SIGNAL TRANSDUCTION PATHWAY THAT REGULATES THE WHITE PHEROMONE RESPONSE OF *C. ALBICANS*

Introduction

While the *C. albicans* opaque cell pheromone response (Bennett *et al*., 2003; Lockhart *et al*., 2003b; Panwar *et al*., 2003) is similar to that of haploid cells of *S.* cerevisiae (Sprague, 1994; Elion, 2000), the white cell pheromone response is unique (Daniels *et al*., 2006; Yi *et al*., 2008), and proves to be a general characteristic of *MTL*-homozygous strains of *C. albicans* (Sahni *et al*., 2009a). However, it was not known how the pheromone induced white cell biofilm response is regulated.

The MAP kinase pathways have evolved as highly efficient, multipurpose signal transduction systems. *S. cerevisiae* utilizes multiple MAP kinase pathways, each one for a distinct signaling system, including the mating process, the filamentation process, cell wall integrity, ascospore formation and osmoregulation (Chen and Thorner, 2007; Gustin *et al.*, 1998; Saito and Tatebayashi, 2004; Levin and Errede, 1995). Several of these pathways share a limited number of components, but all are presumed to utilize different receptors to elicit quite different responses.

C. albicans, like *S. cerevisiae*, utilizes MAP kinase pathways in the mating process (Magee *et al.*, 2002; Chen *et al.*, 2002), filamentation (Csank *et al.*, 1998; Liu *et al.*, 1994; Navarro-Garcia *et al.*, 1998), and osmoregulation (Smith *et al.*, 2004; Alonso-Monge *et al.*, 1999). Mutational studies using auxotrophic complementation as an assay for mating showed that the α-pheromone receptor Ste2, the MAP kinases Cek1 and Cek2, and a key transcription factor, Cph1, were necessary for mating in *C. albicans* **a**/**a** opaque cells (Bennett *et al.*, 2003; Chen *et al.*, 2002; Magee *et al.*, 2002). However the receptors,

signal transduction pathways, and downstream transcription factor(s) that mediate the unique white cell response to pheromone remained unknown.

There existed at least three possibilities. First, the same receptor, G-protein complex, MAP kinase pathway and transcription factor could mediate both the opaque cell mating response and the white response. Second, select components of the signal transduction pathway regulating the opaque pheromone response could be shared with the pathway regulating the white pheromone response. Third, completely different receptors and transduction pathways, with no overlap, could mediate the alternative opaque and white responses.

To distinguish between these possible scenarios, I along with the senior author Song Yi generated deletion derivatives in a natural **a**/**a** strain for components mediating the mating response, including the α-pheromone receptor gene, *STE2*, the gene for the β-subunit of the heterotrimeric G-protein, *STE4*, the genes for the MAP kinases, *CEK1* and *CEK2*, the gene for the downstream *trans*-acting factor *CPH1*, and the gene for the downstream cyclin-dependent kinase inhibitor, *FAR1*. We also generated deletion derivatives in a natural α/α strain for the **a**-pheromone receptor gene, *STE3*, and for *FAR1*. The mutant and complemented strains were then analyzed for both the opaque and white pheromone responses.

Our results demonstrated that the pathways regulating the alternative responses in opaque and white cells to the same pheromone share the same receptor, heterotrimeric G-protein and MAP kinase cascade, but not the same downstream transcription factor(s). This configuration, which has no analogous example in *S. cerevisiae*, is found in a variety of multicellular systems in which the same signal is transduced in different cell types by the same signal transduction pathway, but results in different cellular responses (Rincón and Pedraza-Alva, 2003). We argue that several aspects of the signaling system between opaque and white cells suggest that it may represent an antecedent to multicellularity in higher eukaryotes.

Materials and Methods

Strain Maintenance and Growth

Strains used in this study as well as their origins and genotypes are listed in Table 2. Cells of the natural strains P37005 (**a**/**a**) (Lockhart *et al*., 2002), P57072 (α/α) (Lockhart *et al.*, 2002) and WO-1 (α/α) (Slutsky *et al*., 1987), the derived mutants, and complemented strains were maintained at 25°C on agar containing modified Lee's medium (Bedell and Soll, 1979) or YPD medium (Sherman *et al*., 1986). For distinguishing between white- and opaque phase sectors or colonies, colonies were grown on modified Lee's agar medium supplemented with phloxine B (5 μg/ml), which differentially stained opaque phase cells red (Anderson and Soll, 1987). Prior to use, white- and opaque-phase cells were verified microscopically for the unique differences in cell shape and vacuole formation (Anderson and Soll, 1987; Slutsky *et al.*, 1987).

Generation of Null Mutants

In this study, the following null mutants were generated: *ste2/ste2*, *ste4/ste4*, *cek1/cek1*, *cek2/cek2*, *cek1*/*cek1 cek2*/*cek2*, *cph1/cph1* and *far1/far1* in the natural **a**/**a** strain P37005; and *ste3/ste3* in the natural α/α strain P57072. In addition, a *far1/far1* mutant was generated in the natural α/α strain WO-1. The recyclable flipper cassette from pSFS2A (Reuss *et al.*, 2004), containing a dominant nourseothricin resistance marker (*CaSAT1*), was used to create all mutants. The plasmid pSFS2A was a generous gift from Joachim Morschhauser, The University of Würzburg, Germany. The 4.2 kb XhoI-SacII fragment, SAT1-2A, of the cassette was blunt-ended with T4 polymerase prior to its use in ligations to create the deletion cassettes.

All of the primers used to create gene deletions are provided in Table 3. To obtain a homozygous mutant strain for a particular gene, deletion cassettes I and II were generated in a two-step disruption strategy. Deletion cassette I was constructed as follows: 5' and 3' flanking regions of each target gene were amplified by PCR using the primers provided in

Table 2. *C. albicans* strains used in the analysis of the white cell pheromone response pathway

Strain	Parent	*MTL*	Relavant Genotype	Reference or source
P37005	–	**a**/**a**	Wild type	Lockhart *et al.* (2002)
WO-1	–	α/α	Wild type	Slutsky *et al.* (1987)
P57072	–	α/α	Wild type	Lockhart *et al.* (2002)
ste2/*ste2*	P37005	**a**/**a**	*ste2*Δ::FRT/*ste2*Δ::FRT	This study
ste3/*ste3*	P57072	α/α	*ste3*Δ::FRT/*ste3*Δ::FRT	This study
ste4/*ste4*	P37005	**a**/**a**	*ste4*Δ::FRT/*ste4*Δ::FRT	This study
cek1/*cek1*	P37005	**a**/**a**	*cek1*Δ::FRT/*cek1*Δ::FRT	This study
cek2/*cek2*	P37005	**a**/**a**	*cek2*Δ::FRT/cek*2*Δ::FRT	This study
cek1/*cek1 cek2*/*cek2*	*cek2*/*cek2*	**a**/**a**	*cek1*Δ::FRT/*cek1*Δ::FRT *cek2*Δ::FRT/*cek2*Δ::FRT	This study
cph1/*cph1*	P37005	**a**/**a**	*cph1*Δ::FRT/*cph1*Δ::FRT	This study
far1/*far1*	P37005	**a**/**a**	*far1*Δ::FRT/*far1*Δ::FRT	This study
far1/*far1* (WO-1)	WO-1	α/α	*far1*Δ::FRT/*far1*Δ::FRT	This study
ste2/*ste2-STE2*	*ste2*/*ste2*	**a**/**a**	*ste2*Δ::FRT/*STE2-GFP-SAT*^{R}	This study
ste3/*ste3-STE3*	*ste3*/*ste3*	α/α	*ste3*Δ::FRT/*STE3-GFP-SAT*^{R}	This study
ste4/*ste4-STE4*	*ste4*/*ste4*	**a**/**a**	*ste4*Δ::FRT/*STE4-GFP-SAT*^{R}	This study
cek1/*cek1-CEK1*	*cek1*/*cek1*	**a**/**a**	*cek1*Δ::FRT/*CEK1-GFP-SAT*^{R}	This study
cek2/*cek2-CEK2*	*cek2*/*cek2*	**a**/**a**	*cek2*Δ::FRT/*CEK2-GFP-SAT*^{R}	This study
cph1/*cph1-CPH1*	*cph1*/*cph1*	**a**/**a**	*cph1*Δ::FRT/*CPH1-GFP-SAT*^{R}	This study
far1/*far1-FAR1*	*far1*/*far1*	**a**/**a**	*far1*Δ::FRT/*FAR1-GFP-SAT*^{R}	This study

Table 3. Oligonucleotides used in the analysis of the white cell pheromone response pathway

Primer	Gene/Purpose	Sequence
STE2f1	*STE2* heterozygote	5'-TCTATTGTGTAAACTATTAC-3'
STE2r1	*STE2* heterozygote	5'-GTGTCCCGGGAATCAATGCCTAGTCGATC-3'
STE2f2	*STE2* heterozygote	5'-TGTACCCGGGCAAATCACCATCAAAAGA-3'
STE2r2	*STE2* heterozygote	5'-CTTGTACTGGTTCAGCAACC-3'
STE2f3	*STE2* homozygote	5'-GATCGACTAGGCATTGATTTTTG-3'
STE2r3	*STE2* homozygote	5'-TCATCCCGGGTCTTCTTATGTTGAACAC-3'
STE2f4	*STE2* homozygote	5'-TCTTCCCGGGCTCAAACTGCTAATAAT-3'
STE2r4	*STE2* homozygote	5'-CACTCTTTTGATGGTGATTTG-3'
STE3f1	*STE3* heterozygote	5'-TGAATCTACTTTGGGCAGAG-3'
STE3r1	*STE3* heterozygote	5'-CCAACCCGGGATTTTCCTCTTGGTTTT-3'
STE3f2	*STE3* heterozygote	5'-ACAACCCGGGGTCTTCGCCTGCAACATTA-3'
STE3r2	*STE3* heterozygote	5'-CACAAATGCAGATGTTGTCG-3'
STE3f3	*STE3* homozygote	5'-AAAACCAAGAGGAAAATCCC-3'
STE3r3	*STE3* homozygote	5'-ACTTCCCGGGTGCCATAAAAATGGCGG-3'
STE3f4	*STE3* homozygote	5'-ACAGCCCGGGCAACTGTATTCTTTCTGT-3'
STE3r4	*STE3* homozygote	5'-GCAGGCGAAGACTGGAGTTG-3'
STE4f1	*STE4* heterozygote	5'-ATGGTTAACTCGAACAT-3'
STE4r1	*STE4* heterozygote	5'-TCACCCGGGTTGTAAAACAGATCCCA-3'
STE4f2	*STE4* heterozygote	5'-TCACCCGGGAAGAGCGAGACTGAGGGTA-3'
STE4r2	*STE4* heterozygote	5'-AAGGTGCCATGAAAGGTA-3'
STE4f3	*STE4* homozygote	5'-ATGTCCGATTATCTTGC-3'
STE4r3	*STE4* homozygote	5'-TCACCCGGGCATTTGATAGGTTCCATT-3'
STE4f4	*STE4* homozygote	5'-TCACCCGGGCTGATCCGGTTATTCGAT-3'
STE4r4	*STE4* homozygote	5'-GACGGACCAAACTTTGAT-3'
CEK1f1	*CEK1* heterozygote	5'-ATTCCCGAGAATATATGA-3'
CEK1r1	*CEK1* heterozygote	5'-TCGCCCGGGTAAATAATATATAAGTTGA-3'
CEK1f2	*CEK1* heterozygote	5'-TCGCCCGGGTAAAGTTGAAGTTAAGTA-3'

Table 3 --- continued

CEK1r2	*CEK1* heterozygote	5'-GAGAGGTTTATTTGGTAGA-3'
CEK1f3	*CEK1* homozygote	5'-TTAAATTTACTATCCCAAA-3'
CEK1r3	*CEK1* homozygote	5'-TCGCCCGGGTGAGTTCTAATGACTCGAT-3'
CEK1f4	*CEK1* homozygote	5'-TCGCCCGGGTTGGTCAGTTGGTTGTAT-3'
CEK1r4	*CEK1* homozygote	5'-TCAAAACCTATACAACAA-3'
CEK2f1	*CEK2* heterozygote	5'-TAACGACAACTGCAGGAC-3'
CEK2r1	*CEK2* heterozygote	5'-TCACCCGGGTTGGTCAGGTATTGTAA-3'
CEK2f2	*CEK2* heterozygote	5'-TCACCCGGGCTTTACTTAATTAATTAC-3'
CEK2r2	*CEK2* heterozygote	5'-ACAATGGAGCACAATGCT-3'
CEK2f3	*CEK2* homozygote	5'-CTTCCTGTTACCATGTTA-3'
CEK2r3	*CEK2* homozygote	5'-TCACCCGGGCATGTATTCCTGAATAA-3'
CEK2f4	*CEK2* homozygote	5'-TCACCCGGGTTGAGTGCATCCAATTAT-3'
CEK2r4	*CEK2* homozygote	5'-CGACATGACTATTTCGA-3'
CPH1f1	*CPH1* heterozygote	5'-TTGAAATTAATCTAGAATC-3'
CPH1r1	*CPH1* heterozygote	5'-TCGCCCGGGCTAAAACTAAGACCAAAAC-3'
CPH1f2	*CPH1* heterozygote	5'-TAACCCGGGTAGATGAATAGATACAGA-3'
CPH1r2	*CPH1* heterozygote	5'-AACGTGAGGTGATGTTTC-3'
CPH1f3	*CPH1* homozygote	5'-TCTTAGTTTTAGTTTGAC-3'
CPH1r3	*CPH1* homozygote	5'-TCGCCCGGGTAAACAATACAACGGACA-3'
CPH1f4	*CPH1* homozygote	5'-TCGCCCGGGAACAAGCCCAACCAATAA-3'
CPH1r4	*CPH1* homozygote	5'-TGGAATTCACAACATCAT-3'
FAR1f1	*FAR1* heterozygote	5'-TTGATAATGTCACCCAA-3'
FAR1r1	*FAR1* heterozygote	5'-TCACCCGGGGTCTAACACTTTAAGTGGT-3'
FAR1f2	*FAR1* heterozygote	5'-TCACCCGGGTTGTGCTGGTGCAACCAT-3'
FAR1r2	*FAR1* heterozygote	5'-TTGATTTGATCCGTAGA-3'
FAR1f3	*FAR1* homozygote	5'-ATGCGCAAACTGTTCCA-3'
FAR1r3	*FAR1* homozygote	5'-TCACCCGGGATAGACACACCAATGCCA-3'
FAR1f4	*FAR1* homozygote	5'-TCACCCGGGTCAGTTGACACTTACTAT-3'
FAR1r4	*FAR1* homozygote	5'-TATTAAACTATTCATCA-3'
STE2Q1XhF	*STE2* complementation	5'-TCCCTCGAGTCTATTGTGTAAACTATTAC-3'
STE2Q1BhR	*STE2* complementation	5'-TCCGGATCCCACTCTTTTGATGGTGATTT-3'

Table 3 --- continued

STE2Q2BhF	*STE2* complementation	5'-TCCGGATCCAAATCGTATTCAAGTATCTT-3'
STE2Q2XhR	*STE2* complementation	5'-TCCCTCGAGCTTGCTCCATTGGGAAGTTT-3'
STE3Q1XhF	*STE3* complementation	5'-TCCCTCGAGTGAAGAGGCTAAAGACGTTG-3'
STE3Q1BhR	*STE3* complementation	5'-TCCGGATCCGTTATCATACGATTTCAGTT-3'
STE3Q2BhF	*STE3* complementation	5'-TCCGGATCCTCCATCGTATCCTGTTACTT-3'
STE3Q2XhR	*STE3* complementation	5'-TCCCTCGAGGAAACCAGAGGCTGGAATG-3'
STE4Q1XhF	*STE4* complementation	5'-TCACTCGAGATGGTTAACTCGAACAT-3'
STE4Q1BhR	*STE4* complementation	5'-TCAGGATCCGACGGACCAAACTTTGAT-3'
STE4Q2BhF	*STE4* complementation	5'-TCAGGATCCAAGAGCGAGACTGAGGGTA-3'
STE4Q2XhR	*STE4* complementation	5'-TCACTCGAGAAGGTGCCATGAAAGGTA-3'
CEK1Q1XhF	*CEK1* complementation	5'-TCCCTCGAGATTCCCGAGAATATATGA-3'
CEK1Q1BgR	*CEK1* complementation	5'-TCCAGATCTTAATGGCTTCATAATCTCT-3'
CEK1Q2BgF	*CEK1* complementation	5'-TCCAGATCTTAAAGTTGAAGTTAAGTA-3'
CEK1Q2XhR	*CEK1* complementation	5'-TCCCTCGAGGAGAGGTTTATTTGGTAGA-3'
CEK2Q1XhF	*CEK2* complementation	5'-TCACTCGAGTAACGACAACTGCAGGAC-3'
CEK2Q1BhR	*CEK2* complementation	5'-TCAGGATCCCGACATGACTATTTCGA-3'
CEK2Q2BhF	*CEK2* complementation	5'-TCAGGATCCCTTTACTTAATTAATTAC-3'
CEK2Q2XhR	*CEK2* complementation	5'-TCACTCGAGACAATGGAGCACAATGCT-3'
CPH1Q1StF	*CPH1* complementation	5'-TCGAGGCCTTTGAAATTAATCTAGAATC-3'
CPH1Q1BhR	*CPH1* complementation	5'-TCGGGATCCTGTTTGTGACTGTTTTACTT-3'
CPH1Q2BhF	*CPH1* complementation	5'-TCGGGATCCTAGATGAATAGATACAGA-3'
CPH1Q2StR	*CPH1* complementation	5'-TCGAGGCCTAACGTGAGGTGATGTTTC-3'
FAR1Q1StF	*FAR1* complementation	5'-TCAAGGCCTTTGATAATGTCACCCAA-3'
FAR1Q1BgR	*FAR1* complementation	5'-TCAAGATCTTATTAAACTATTCATCA-3'
FAR1Q2BgF	*FAR1* complementation	5'-TCAAGATCTTTGTGCTGGTGCAACCAT-3'
FAR1Q2StR	*FAR1* complementation	5'-TCAAGGCCTTTGATTTGATCCGTAGA-3'
SATBgF1	*GFP-SAT1* PCR	5'-TCAAGATCTTCCATCATAAAATGTCGA-3'
GFBhF1	*GFP-SAT1* PCR	5'-TCAGGATCCATGTCTAAAGGTGAAGAA-3'
STE2f	Deletion probe for Southern	5'-GTGTTCAACATAAGAAGA-3'
STE2r	Deletion probe for Southern	5'-ATTATTAGCAGTTTGAGC-3'
STE3f	Deletion probe for Southern	5'-CCGCCATTTTTATGGCAC-3'

Table 3 --- continued

STE3r	Deletion probe for Southern	5'-TACAGTTGACCAATCTGT-3'
STE4f	Deletion probe for Southern	5'-AGGCAACTTTTATCAATC-3'
STE4r	Deletion probe for Southern	5'-AGCACAAAACATCTCCTGA-3'
CEK1f	Deletion probe for Southern	5'-ATCTGATGATCATATACA-3'
CEK1r	Deletion probe for Southern	5'-ACATCAATAGCAGTAGTA-3'
CEK2f	Deletion probe for Southern	5'-AAGGATTAAAGATGATTC-3'
CEK2r	Deletion probe for Southern	5'-TGATTTCTGGAGCTCGATA-3'
FAR1f	Deletion probe for Southern	5'-ACTAGTTAACCAAACATC-3'
FAR1r	Deletion probe for Southern	5'-TGATGTTGTACGTGGAAT-3'
CPH1f	Southern and Northern probe	5'-AGCATTATCATTCCATTA-3'
CPH1r	Southern and Northern probe	5'-TATTGACTTGGTGTGGCTT-3'
MFA1f	Northern probe	5'-ATGGCTGCTCAACAACAA-3'
MFA1r	Northern probe	5'-TTACATAACAGAACAAGT-3'
CSH1f	Northern probe	5'-TCGACTCTGAAAAAACTA-3'
CSH1r	Northern probe	5'-CATGCCAATGAAACTTGC-3'

Table 3. The 5' region and 3' region were then each digested by SmaI and ligated together using T4 ligase. The 5'-3' fusion product was amplified by PCR and subcloned into the pGEM-T Easy vector (Promega Corp., Madison, WI). The SAT1-2A fragment was then inserted into the SmaI-digested, dephosphorylated plasmid. This plasmid was digested with SacI plus SphI to generate the deletion cassette, which was then used to transform *C. albicans* strain P37005, P57072 or WO-1 by electroporation (De Backer *et al.*, 1999). For each gene, two independent transformants were confirmed as heterozygous by both PCR and Southern analysis. The heterozygotes were then subjected to a pop-out strategy in the maltose-containing medium YPM (1% yeast extract, 2% Bacto-peptone, 2% maltose) to excise the *CaSAT1* marker. Deletion cassette II was constructed in a similar fashion. The new 5' and 3' flanking regions which contained sequences deleted in the first step were amplified by PCR, using the primers noted for each gene in Table 3. The resulting plasmid was digested with SacI and SphI, and used to transform the heterozygous mutant derivatives. Two independent null mutants were confirmed by both PCR and Southern analysis for each gene.

Mutant Complementation

Complementation was performed for the mutants *ste2/ste2*, *ste4/ste4*, *cek1/cek1*, *cek2/cek2*, *cph1/cph1* and *far1/far1*, generating *ste2*/*ste2-STE2*, *ste4*/*ste4-STE4*, *cek1*/*cek1-CEK1*, *cek2*/*cek2-CEK2*, *cph1*/*cph1-CPH1* and *far1*/*far1-FAR1*. The *CaSAT1* marker was deleted by a pop-out protocol from each null mutant as described for heterozygous mutants. The 5' and 3' regions flanking the stop codon were amplified by PCR with the primers noted for each gene in Table 3. The 5'-3' fusion product was amplified by PCR and subcloned into pGEM-T Easy (Promega Corp). For complemented strains, a DNA fragment containing both *GFP* (green fluorescent protein) and *CaSAT1* was amplified by PCR with the primers noted in Table 3, using plasmid pK91.6 (T. Srikantha and D.R. Soll, unpublished data) as template. *GFP* was inserted into the plasmid for

future experiments and not utilized in this study. The *GFP-CaSAT1* fragment was digested with BamHI plus BglII, and ligated into the Bg1II- or BamHI-digested, dephosphorylated plasmid containing the 5'-3' fusion product of the gene. This plasmid contained the transformation module for targeting to the gene locus. The in-frame *GFP*-gene fusion was confirmed by sequencing. This plasmid was digested with XhoI or StuI and used for transformation into the null mutant of each gene. Transformants were verified by both PCR sequencing and Southern analysis.

Opaque Cell Shmooing and Mating

Opaque cells were grown in liquid modified Lee's medium in a rotary water bath shaker (250 rpm) at 25°C to early saturation phase (~5 x 10^7 cells/ml) (Lockhart *et al.*, 2003b). Cells were then pelleted, resuspended at 10^6 cells/ml in fresh medium containing 3 x 10^{-6} M synthetic 13-mer α-pheromone (Panwar *et al.*, 2003; Bennett *et al.*, 2003) and incubated at 25°C in a shaker (250 rpm). The 13-mer peptide (GFRLTNFGYFEPG), synthesized by Open Biosystems Inc. (Huntsville, AL), was dissolved in DMSO. In controls not treated with pheromone, equivalent amount of DMSO was added. Shmooing and conjugation tube growth were monitored microscopically. Cell concentration was also monitored over time. To test for **a**-pheromone-induced shmoo formation, a transwell assay was performed according to Daniels *et al.* (2006).

To test for mating (Lockhart *et al.*, 2003a), opaque cells of an **a**/**a** or α/α mutant were grown to early saturation phase and mixed with an equal concentration of WO-1 (α/α) or P37005 (**a**/**a**) opaque cells, respectively, in liquid culture. The mating mixtures were incubated at 25°C in a rotary shaker (250 rpm) and monitored for fusants microscopically over a 48 hr period.

White Cell Cohesion and Adhesion Assays

To test for α-pheromone-induced cohesion according to the methods of Daniels *et al.* (2006), **a**/**a** white cells from a saturation phase culture (~ 4 x 10^8 cells per ml) of strain

P37005 or mutant derivatives were resuspended in fresh medium at a concentration of 5 x 10^7 per ml. The medium was supplemented with the 13-mer synthetic α-pheromone at a concentration of 3 x 10^{-6} M. The culture was rotated at 250 rpm at 25°C. Samples were taken from the suspension culture after 6 hr and examined microscopically for cell aggregates. To test for **a**-pheromone-induced cohesion of white cells of strain P57072 and the mutant derivative *ste3/ste3*, a 50:50 mixture of opaque P37005 and WO-1 cells were added to a suspension of either white P57072 or *ste3/ste3* cells so that the former inducing mixture made up 1% of cells. Opaque P37005 cells (**a**/**a**), stimulated by opaque WO-1 (α/α) cells, released **a**-pheromone.

To test for α-pheromone-induced adhesion of white cells of the natural **a**/**a** strain P37005 and its mutant derivatives to plastic, the methods of Daniels *et al*. (2006) were employed. Two ml of cells (5 x 10^7 per ml) were incubated in a well of a Costar™ 6-cluster well plate (Costar, Cambridge, MA) in the presence of 3 x 10^{-6} M synthetic 13-mer α-pheromone. After 16 hr at 25°C, the wells were gently washed with phosphate buffer solution and photographed. Gray scale images were subsequently pseudocolored for clarity. Three hundred μl of a 0.05% trypsin-EDTA solution (Invitrogen-GIBCO, Carlsbad, CA) were added to each well. After 15 min, the cells on the dish bottom were released into 300 μl of supplemental Lee's medium containing 10% calf serum, and the number of adhering cells determined in a hemocytometer. To test for **a**-pheromone-induced adhesion of α/α strain P57072 and its mutant derivative *ste3/ste3*, 1% opaque cells of **a**/**a** strain P37005 and α/α strain WO-1 were added to the well culture. After 16 hr at 25°C, adhesion was analyzed as above.

Biofilm Thickness

Biofilm enhancement was quantitated in strain P37005 and mutant derivatives according to a protocol described previously (Daniels *et al.*, 2006) with one exception. Although in earlier experiments, a minority mixture (50:50) of opaque **a**/**a** and α/α cells

was found more stimulatory than opaque α/α cells alone in enhancing a majority (90%) white **a**/**a** cell biofilm formation, recent experiments proved that minority opaque α/α cells (WO-1) alone induced near maximum enhancement of majority white biofilms. Therefore, a mixture of 90% white **a**/**a** test cells and 10% opaque α/α WO-1 cells (a total of ~ 5 x 10^7 cells in 2.5 ml of RPMI medium) was distributed on a silicone elastomer square in a well and incubated for 90 min. To test for enhancement of white cell biofilms of strain P57072 and the mutant derivative *ste3/ste3*, opaque **a**/**a** cells (P37005) (10%) were added to majority α/α cells in the presence of 3 x 10^{-6} α-pheromone. The square was then rinsed and incubated in RPMI medium on a rocker at 29°C for the subsequent 48 hr. Biofilms were prepared in triplicate cultures. The biofilm was fixed, stained with calcofluor and the thickness measured using BioRad LaserSharp™ software in a BioRad Radiance 2100 MP laser scanning confocal microscope (LSCM) (BioRad, Hermel, Hamstead, UK).

Quantitative Fluorescence Analysis of DNA

Two methods were employed. In the first, previously described in detail (Zhao *et al.*, 2005b), opaque cells were grown to saturation phase, then resuspended in fresh medium at 10^6 cells per ml. Cells were treated with synthetic α-pheromone (13-mer) in suspension, then fixed after 3 hr in 70% ethanol and treated overnight with RNase. Nuclei were stained with 25 μM Sytox Green™ (Molecular Probes, Eugene, OR). Fluorescent quantitation of the staining of individual nuclei was performed using a confocal method we previously described in great detail (Zhao *et al.*, 2005b). Using the projected confocal image, a line profile of pixel intensity was measured across the center of each nucleus. In both control P37005 and *far1/far1* cell populations, only the nuclei of cells that had formed shmoos were scanned. That represented approximately 60 to 70% of the P37005 cell population and 25% of the *far1/far1* cell population. In a second method, cell cycle status was determined by fluorescence activated cell sorting (FACS). Cells were prepared as above, with modification. RNase treatment was followed by proteinase K digestion. The

final cell suspension was then stained overnight with 1 μM Sytox Green™. The cells were sonicated briefly to disrupt cell aggregates, and analyzed with a FACScan (Becton Dickinson, Mountain View, CA). Cell cycle status was analyzed using ModFitLT v2.0 software (Becton Dickinson).

Northern and Southern Analyses

Northern and Southern analyses were performed as previously described (Lockhart *et al.*, 2003b; Srikantha *et al.*, 2006). For northern analyses, cells from saturation phase cultures were diluted into fresh medium in the absence or presence of 3 x 10^{-6} M α-pheromone, and pelleted after 4 hr. Total RNA was extracted using the RNeasy Mini Kit (Qiagen Sci., MA). Polymerase chain reaction (PCR) products were used for probing northern and Southern blots. The primers used to generate the PCR probe for each gene are listed in Table 3.

Results

The Pheromone Response Pathway Plays No Role in Switching

The deletion mutants *ste2/ste2*, *ste4/ste4*, *cek1/cek1*, *cek2/cek2*, *cek1/cek1 cek2/cek2*, *cph1*/*cph1*and *far1/far1* were generated in the natural **a**/**a** strain P37005 (Lockhart *et al.*, 2002). The deletion mutant *ste3/ste3* (α/α) was generated in the natural α/α strain P57072 (Lockhart *et al.*, 2002) and a *far1/far1* deletion mutant was generated in the natural α/α strain WO-1 (Slutsky *et al.*, 1987). Each mutant and complemented derivatives were individually tested for spontaneous white-opaque switching by plating cells from single white colonies at low density on nutrient agar containing phloxine B, which differentially stained opaque cells red (Anderson and Soll, 1987). One thousand derivative colonies were scored for each strain. In every case, red colonies and/or sectors formed after 7 days at low frequencies similar to wild type (~ 10^{-3} opaque colonies). Cells

from every tested red colony or sector of each mutant were found to exhibit the unique elongate opaque cell shape (data not shown). When these opaque cells were in turn plated at low density on agar, they formed a majority of opaque colonies and a minority of white colonies, demonstrating reversibility for every mutant. The same was true for the complemented strains *ste2*/*ste2-STE2*, *ste3*/*ste3-STE3*, *ste4*/*ste4-STE4*, *cek1*/*cek1-CEK1*, *cek2*/*cek2-CEK2*, *cph1*/*cph1-CPH1*, and *far1*/*far1-FAR1* (**a**/**a**). Zordan *et al.* (2006) previously demonstrated that switching was unimpaired in deletion mutants of *STE2*, *CEK2* and *FAR1* generated in an **a** cell background in a laboratory strain derived from strain SC5314. Together, these results demonstrate that the genes in the pheromone response pathway are not essential for white-opaque switching. This allowed ready isolation of white and opaque cells for each mutant and complemented strain, which were then tested for the alternative pheromone responses.

Opaque Cell Pheromone Response of *ste2/ste2*, *ste3*/*ste3* and *ste4/ste4*

No shmoo formation was observed in opaque cells of parent strain P37005 in the absence of α-pheromone. Seventy-five percent formed shmoos after 4 hours of treatment with α-pheromone and 91% after 8 hours (Figure 13A, B, M). Neither opaque cells of the *ste2/ste2* mutant nor of the *ste4/ste4* mutant formed shmoos in response to α-pheromone (Figure 13C and D, respectively; Figure 13M). The complemented strains *ste2*/*ste2-STE2* and *ste4*/*ste4-STE4* regained the capacity to form shmoos in response to pheromone, and to the same extent as parental P37005 cells (data not shown). Bennett *et al.* (2003) also found that *STE2* was required for opaque **a** cells to undergo shmoo formation.

Opaque cells of the **a**-receptor mutant *ste3*/*ste3* could not be tested with synthetic pheromone, since **a**-pheromone is not readily synthesized chemically due to extensive post-translational modification (Chen *et al.*, 1997a, b; Huyer *et al.*, 2006). Mutant *ste3/ste3* cells were, therefore, compared with parent P57072 cells for their response to

Figure 13. α-Pheromone does not induce conjugation tube ("shmoo") formation in opaque cells of the mutants *ste2/ste2*, *ste4/ste4*, the *cek1*/*cek1 cek2*/*cek2* double mutant, or *cph1/cph1*, derived from the natural **a**/**a** strain P37005. (A and B) Representative images of P37005 cells in the absence (–) or presence (+) of α-pheromone, respectively. (C, D, I, and J) Representative images of mutants *ste2/ste2*, *ste4/ste4*, *cek1*/*cek1 cek2/cek2*, and *cph1/cph1*, which did not form shmoos after 4 h of pheromone treatment. The same was true after 8 h (data not shown). Selected images of shmoo formation after 4 and 8 h for mutants *cek1/cek1* (E and F), *cek2*/*cek2* (G and H), and *far1/far1* (K and L). It should be noted that in these cases, the proportion of cells that had shmooed ranged between 9 and 68%; therefore, the images were selected. (M) Quantitation of shmooing for different strains. The "percentage of reduction in induced shmoos" was computed by dividing the difference in percentage of shmooing between P37005 and mutant strain, by percentage of shmooing of P37005, and multiplying by 100%. Bar (A), 5 μm.

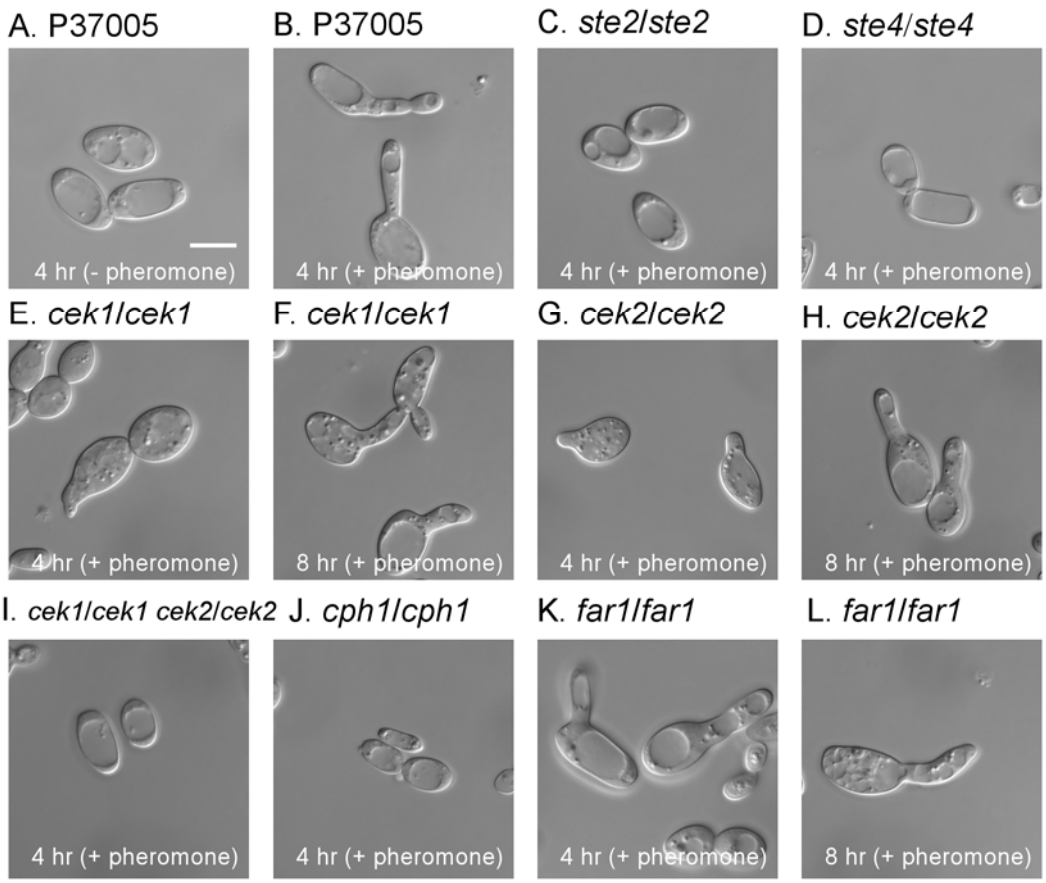

M. Shmoo formation in response to α-pheromone

Strain	Pheromone treatment	Treatment duration (hr)	Cell number	Percent of population			Reduction in induced shmoos (%)
				Unbudded cells (%)	Budded cells (%)	Shmoos (%)	
P37005	−	4	260	27	73	0	
	+	4	234	23	2	75	—
	+	8	274	7	2	91	—
ste2/ste2	−	4	280	35	65	0	
	+	4	275	29	71	0	100%
ste4/ste4	−	4	265	8	92	0	
	+	4	263	9	91	0	100%
cek1/cek1	−	4	242	14	86	0	
	+	4	238	57	34	9	88%
	+	8	209	35	20	45	51%
cek2/cek2	−	4	235	21	79	0	
	+	4	232	61	16	23	69%
	+	8	210	20	12	68	25%
cek1/cek1 *cek2/cek2*	−	4	245	33	67	0	
	+	4	243	18	82	0	100%
cph1/cph1	−	4	213	16	84	0	
	+	4	222	27	73	0	100%
far1/far1	−	4	241	18	82	0	
	+	4	238	17	51	32	57%
	+	8	215	40	43	17	81%

a-pheromone released by opaque **a**/**a** cells (P37005) mixed with wild type opaque α/α cells (P57072) that up-regulated **a**-pheromone production in the former. This inducing mixture was separated from opaque *ste3/ste3* cells or α/α wild type cells by a micropore filter in a trans-well chamber (Figure 14A) (Daniels *et al.*, 2006). Whereas opaque cells of parent strain P57072 cells were induced to form shmoos (Figure 14B), opaque cells of *ste3*/*ste3* were not (Figure 14C). Opaque cells of the complemented strain *ste3*/*ste3-STE3* regained shmoo formation in response to **a**-pheromone (data not shown).

Opaque cells of the mutants *ste2/ste2* and *ste4/ste4* were also compared with opaque cells of parent strain P37005 for their ability to mate with opaque cells of the α/α strain WO-1, using microscopically identified fusion as an assay (Lockhart *et al.*, 2003a). While 27% of opaque cells in a 50:50 mixture of opaque **a**/**a** P37005 cells and opaque α/α WO-1 opaque cells fused (Figure 15A, K), no fusions were observed between opaque *ste2/ste2* or *ste4/ste4* cells, and opaque WO-1 cells (Figure 15B and C, respectively; Figure 15K). Opaque cells of the complemented strains *ste2*/*ste2-STE2* and *ste4*/*ste4-STE4* regained the capacity to mate with opaque WO-1 cells (data not shown). Using complementation between **a** and α auxotrophs as a fusion assay, Bennett *et al.* (2003) had previously demonstrated that *STE2* was essential for mating.

The *ste3/ste3* mutant was also incapable of mating. Whereas the parent α/α strain P57072 mated readily with the natural **a**/**a** strain P37005 (Figure 15D, K), *ste3/ste3* did not (Figure 15E, K). Opaque cells of the complemented strain *ste3*/*ste3-STE3* mated with opaque cells of the **a**/**a** strain P37005 (data not shown). Together with the pheromone response data, these results indicated that the α-pheromone receptor, Ste2, and the β-subunit of the heterotrimeric G-protein, Ste4 were essential for α-pheromone-induced shmooing and fusion of opaque **a**/**a** cells, and that the **a**-pheromone receptor, Ste3, was essential for **a**-pheromone-induced shmooing and fusion of opaque α/α cells.

Figure 14. **a**-Pheromone does not induce conjugation tube formation in opaque cells of the mutant *ste3/ste3*, derived from the a/α strain P57072. (A) Transwell apparatus for **a**-pheromone induction of a/α cells. (B) Representative image of opaque P57072 cells after 7 h of incubation in the response well. (C) Representative image of *ste3/ste3* after 7 h in response well. Bar (C), 5 μm.

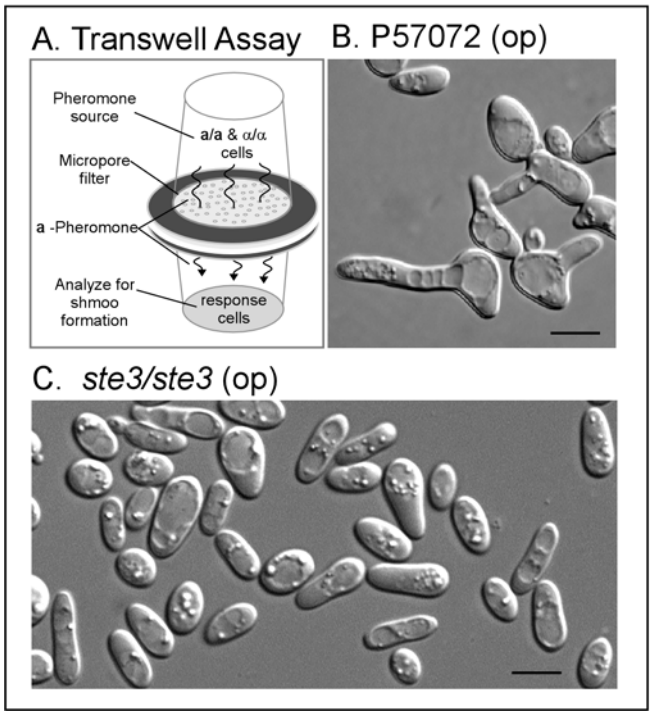
A. Transwell Assay
B. P57072 (op)
Pheromone source
a/a & α/α cells
Micropore filter
a -Pheromone
Analyze for shmoo formation
response cells
C. ste3/ste3 (op)

Figure 15. Opaque cells of the mutants *ste2/ste2*, *ste3/ste3*, *ste4/ste4*, the double mutant *cek1*/*cek1 cek2*/*cek2*, and *cph1/cph1* do not mate (i.e., undergo fusion) with opaque cells of opposite mating type in suspension cultures, whereas mutants *cek1/cek1*, *cek2/cek2*, and *far1/far1* mate, but at reduced frequency. (A and D) Selected image of mating opaque cells of parent strain P37005 (**a**/**a**) with opaque cells of strain WO-1 (α/α), and P57072 (α/α) with P37005 (**a**/**a**), respectively. Selected images of mixtures of opaque cells of *ste2/ste2* (B), *ste4/ste4* (C), *ste3/ste3* (E), the double mutant *cek1*/*cek1 cek2*/*cek2* (H), and *cph1/cph1* (I), with mating partners, none of which mated. Selected images of mixtures of opaque cells of *cek1/cek1* (F), *cek2/cek2* (G), and *far1/far1* (J), with mating partners, which underwent mating. (K) Quantitation of mating efficiency. "Percentage of reduction in mating" was computed as follows. The percentage of opaque cells of the different strains that fused with opaque cells of opposite mating type was subtracted from the percentage of the parent strain that fused with opaque cells of opposite mating type. The difference was then divided by the percentage of parent strain cells that fused, and the fraction multiplied by 100%. The percentage of mating cells of the complemented strains *ste2*/*ste2-STE2*, *ste3*/*ste3-STE3*, *ste4*/*ste4-STE4*, *cek1*/*cek1-CEK1*, *cek2*/*cek2-CEK2*, *cph1*/*cph1-CPH1*, and *far1*/*far1-FAR1* was similar to that of the parent wild type strains from which they were derived (data not shown). Bar (A), 5 μm.

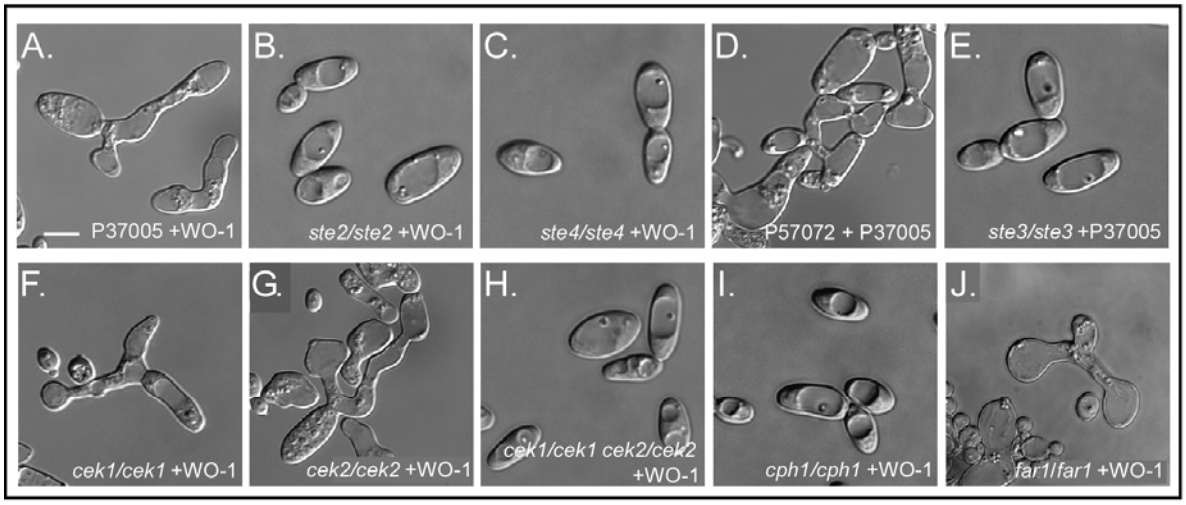

K. Mating efficiency (48 hr)

Strain	Mating Partner	No. of Cells analyzed[a]	No. of Cells in fusants	Percent of cells that mated	Percent reduction in mating
P37005	WO-1	3984	1078	27%	—
ste2/ste2	WO-1	3013	0	0%	100%
ste4/ste4	WO-1	3226	0	0%	100%
cek1/cek1	WO-1	5159	5	0.01%	99.96%
cek2/cek2	WO-1	3501	96	2.7%	90%
cek1/cek1 cek2/cek2	WO-1	3322	0	0%	100%
cph1/cph1	WO-1	3479	0	0%	100%
far1/far1	WO-1	5058	12	0.2%	99.26%
P57072	P37005	3890	823	21%	—
ste3/ste3	P37005	3537	0	0%	100%

[a] Sum of three independent experiments.

White Cell Pheromone Response of *ste2/ste2*, *ste3/ste3* and *ste4/ste4*

White cells of the mutants *ste2/ste2* and *ste4/ste4* were compared with white cells of the parental strain P37005 for the α-pheromone-stimulated white cell response, which included dramatic increases in cohesion, adhesion and enhanced biofilm development (Daniels *et al.,* 2006). To assess pheromone-induced cohesion, *ste2/ste2* and *ste4/ste4* cells were incubated in suspension either in the absence or in the presence of α-pheromone for six hours. Cells were then distributed on a slide and the average number of cells per aggregate calculated. As we previously described (Daniels *et al.*, 2006), the majority of white P37005 cells remained largely separated or formed small aggregates in the absence of α-pheromone (Figure 16I), but in the presence of α-pheromone, the majority of cells formed large aggregates (Figure 16A, I). In the absence (data not shown) or presence of α-pheromone, the majority of white *ste2/ste2* and *ste4/ste4* cells remained largely separated or formed small aggregates (Figure 16B, I, and 16C, I, respectively). White cells of the complemented strains *ste2*/*ste2-STE2* and *ste4*/*ste4-STE4* regained the aggregation response to α-pheromone (data not shown).

To assess pheromone-induced adhesion, *ste2/ste2* and *ste4/ste4* cells were incubated on a plastic surface in the absence or in the presence of 3×10^{-6} M synthetic α-pheromone for 16 hours. As previously described (Daniels *et al.*, 2006), in the absence of α-pheromone white P37005 cells did not form a tight adhesive film on the dish bottom (Figure 17A), but in the presence of pheromone they did (Figure 17B). In contrast, neither white *ste2/ste2* cells nor white *ste4/ste4* cells formed a tight adhesive film on the plastic dish bottom in the absence of pheromone (Figure 17J) or presence of α-pheromone (Figure 17C, D, respectively; Figure 17J). White cells of *ste2*/*ste2-STE2* and *ste4*/*ste4-STE4* regained the capacity to form an adhesive film in response to α-pheromone (Figure 17J).

Figure 16. White cells of the mutants *ste2/ste2*, *ste4/ste4*, and *cek1*/*cek1 cek2/cek2* do not form large aggregates in response to pheromone as do wild-type cells, but mutants *cph1/cph1* and *far1/far1* do. White cells of *cek1/cek1* and *cek2/cek2* form clumps of intermediate size. Cells of each strain from saturation phase cultures were diluted into fresh medium in the absence of pheromone (–) or in the presence of 3 x 10^{-6} M α-pheromone (+). Samples were incubated 6 h before analysis. (A–H) Representative images of cells from parent and mutant strains in the presence of pheromone. (I) Average number of cells (error bar represents standard deviation) in aggregates. In total, 20 cell aggregates were analyzed for each strain. Bar (A), 5 μm.

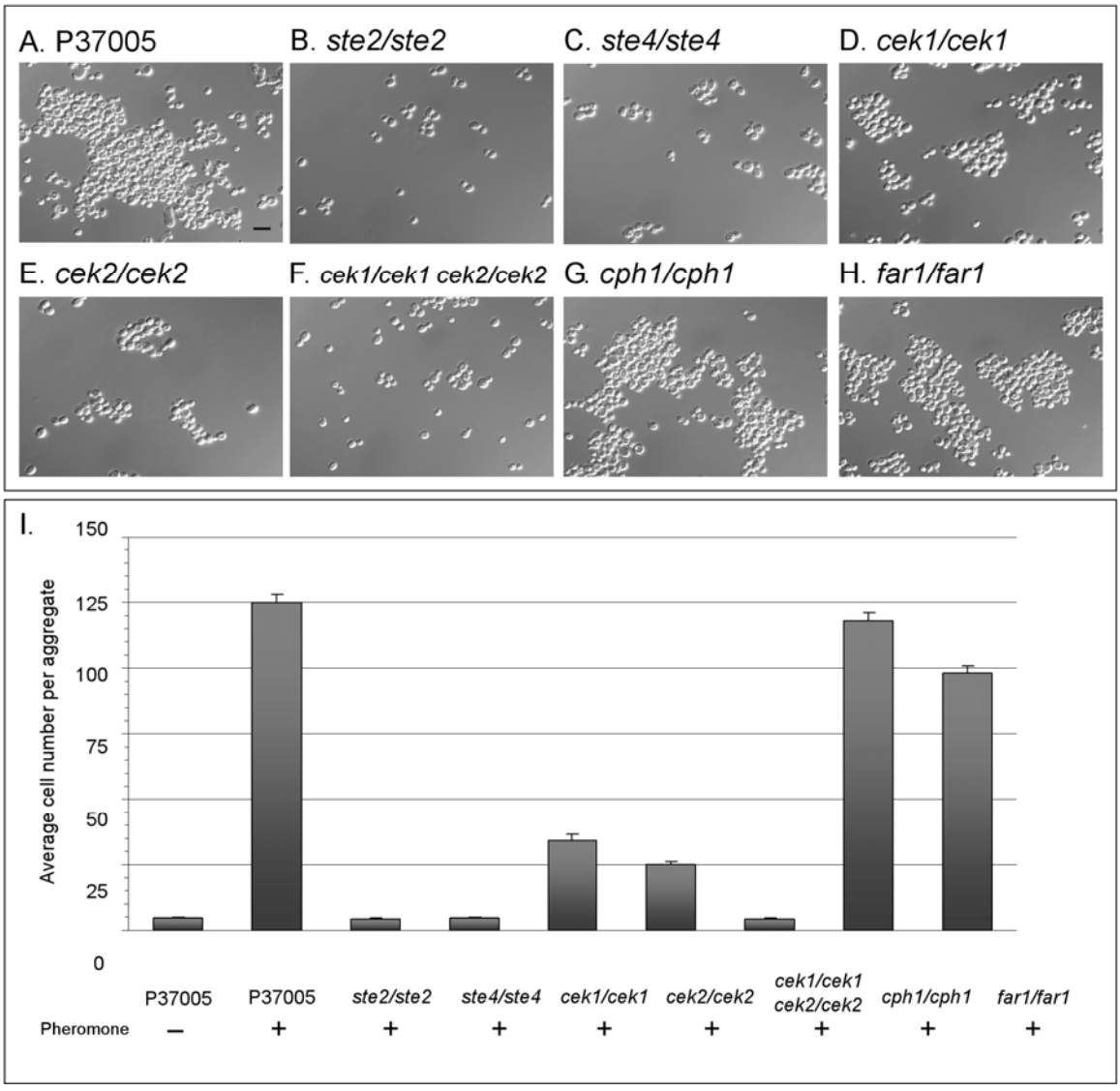
A. P37005
B. ste2/ste2
C. ste4/ste4
D. cek1/cek1
E. cek2/cek2
F. cek1/cek1 cek2/cek2
G. cph1/cph1
H. far1/far1
I.
Average cell number per aggregate
150
125
100
75
50
25
0
P37005
P37005
ste2/ste2
ste4/ste4
cek1/cek1
cek2/cek2
cek1/cek1 cek2/cek2
cph1/cph1
far1/far1
Pheromone
–
+
+
+
+
+
+
+
+

Figure 17. In response to pheromone, white cells of the mutants *ste2/ste2*, *ste4/ste4*, and the double mutant *cek1/cek1 cek2*/*cek2* do not form an adhesive film on the bottom of a plastic well. White cells of the individual mutants *cek1/cek1* and *cek2*/*cek2* form films nearly as dense as wild type, and white cells of the mutants *cph1/cph1* and *far1/far1* form normal films. Dish bottoms were examined for a cell film after 16 h. Pseudocolor images (in orange) are provided. (A and B) Representative images of the dish bottom of P37005 cultures in the absence (–) and presence (+) of pheromone. (C–I). Representative images of the dish bottom of mutant cultures in the presence (+) of α-pheromone. (J) Quantitation of cells adhering to the dish bottom. The "number of adherent cells" has been computed for the entire bottom of three separate wells. The average number is presented. Bar represents standard error. Data are also presented in J for complemented strains *ste2*/*ste2-STE2*, *ste4*/*ste4-STE4*, *cek1*/*cek1-CEK1*, and *cek2*/*cek2-CEK2*.

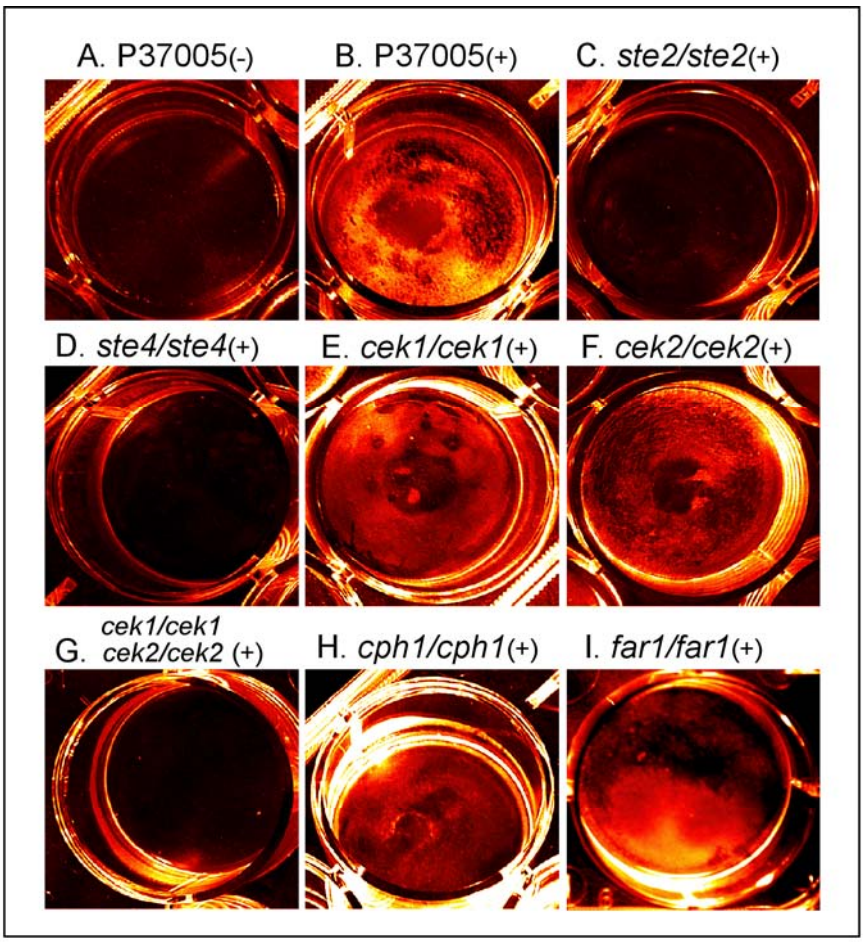
A. P37005(-)
B. P37005(+)
C. ste2/ste2(+)
D. ste4/ste4(+)
E. cek1/cek1(+)
F. cek2/cek2(+)
G. cek1/cek1 cek2/cek2 (+)
H. cph1/cph1(+)
I. far1/far1(+)

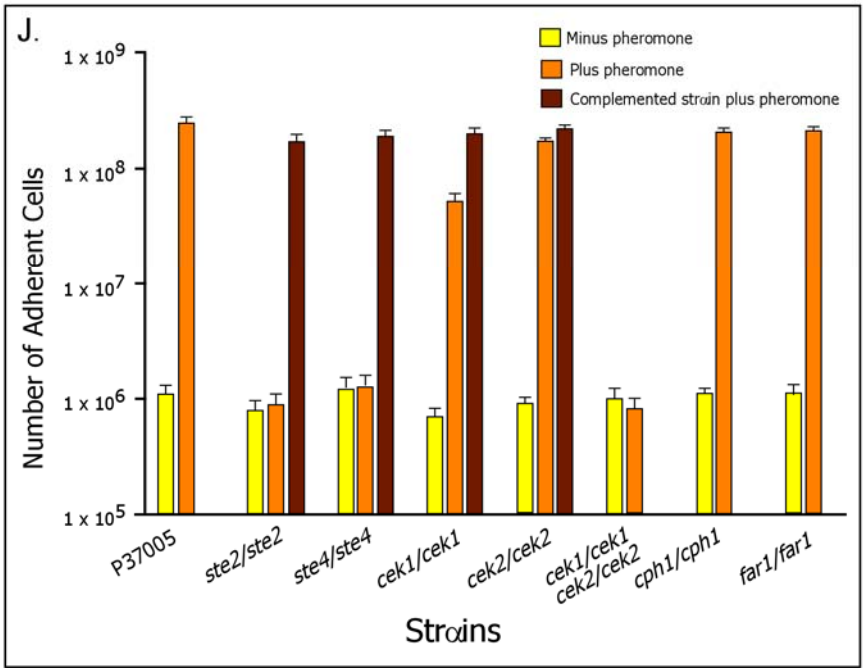
J.
Minus pheromone
Plus pheromone
Complemented strain plus pheromone
Number of Adherent Cells
1 x 10^9
1 x 10^8
1 x 10^7
1 x 10^6
1 x 10^5
P37005
ste2/ste2
ste4/ste4
cek1/cek1
cek2/cek2
cek1/cek1 cek2/cek2
cph1/cph1
far1/far1
Strains

To test for the enhancement of a majority white cell biofilm by minority opaque cells of opposite mating type, a mixture of 10% opaque WO-1 (α/α) cells and 90% *ste2/ste2* (**a**/**a**) or *ste4/ste4* white (**a**/**a**) cells were incubated on a silicone elastomer surface for 48 hours and biofilm thickness measured using LSCM (Daniels *et al.*, 2006). In the absence of opaque WO-1 (α/α) cells, white P37005 cells formed a biofilm with an average thickness of 21 ± 2 μm (Figure 18M). In the presence of minority opaque α/α cells, majority white **a**/**a** P37005 cells formed a biofilm with an average thickness of 61 ± 6 μm, over three times the thickness of biofilms formed by untreated cells (Figure 18A, M). In the absence of opaque α/α cells, white *ste2/ste2* or *ste4/ste4* cells formed biofilms of approximately the same thickness as untreated white P37005 cells (data not shown); in the presence of opaque α/α cells, majority white *ste2/ste2* or *ste4/ste4* still formed biofilms approximately half as thick as those formed by stimulated white cells of strain P37005 (Figure 18B and C, respectively, and Figure 18M). Majority white cells of both complemented strains *ste2*/*ste2-STE2* and *ste4*/*ste4-STE4* regained the capacity to form biofilms comparable to those of stimulated white cells of strain P37005 in the presence of minority opaque α/α cells (Figure 18I and J, respectively and Figure 18M). Together with the cohesion and adhesion data (Figure 16, 17), these results indicate that the same α-pheromone receptor and heterotrimeric G-protein that regulate the α-pheromone-induced opaque cell response also regulate the pheromone-induced white cell response.

Because of the unavailability of chemically synthesized **a**-pheromone, we tested whether natural **a**-pheromone released from opaque cells induced cohesiveness between white cells in a mixture maintained in suspension. In this protocol majority white α/α P57072 cells (99%) were mixed with minority opaque **a**/**a** P37005 (0.5%) and opaque α/α WO-1 (0.5%) cells, the latter opaque cells added to stimulate the former to release **a**-pheromone. Whereas white α/α P57072 cells were induced by minority opaque **a**/**a** cells to form large clumps, majority white *ste3/ste3* cells were not (Figure 19). The

Figure 18. The thickness of biofilms formed by white cells of mutants *ste2/ste2*, *ste4/ste4*, and *cek1/cek1*, *cek2/cek2*, and the double mutant *cek1*/*cek1 cek2*/*cek2*, is not enhanced by minority (10%) opaque cells of opposite mating types, as was the thickness of the biofilms of parent strain P37005, *cph1*/*cph1*and *far1far1*. A mixture of 90% white test cells and 10% opaque a/α cells was inoculated onto a silicone square and incubated for 48 h. The z-series projections were viewed from the side (90° tilt) of stacked multiphoton laser scanning confocal microscope scans. (A–L). Representative z-series projections of parental, mutant and complemented strain biofilms. (M) Average thickness (±standard deviation) of biofilms, computed from 10 measurements that included multiple cultures. Arrow span in A represents 75 μm. Enhancement returned in the complemented strains *ste2*/*ste2*-*STE2*, *ste4*/*ste4*-*STE4*, *cek1*/*cek1*-*CEK1*, and *cek2*/*cek2*-*CEK2*.

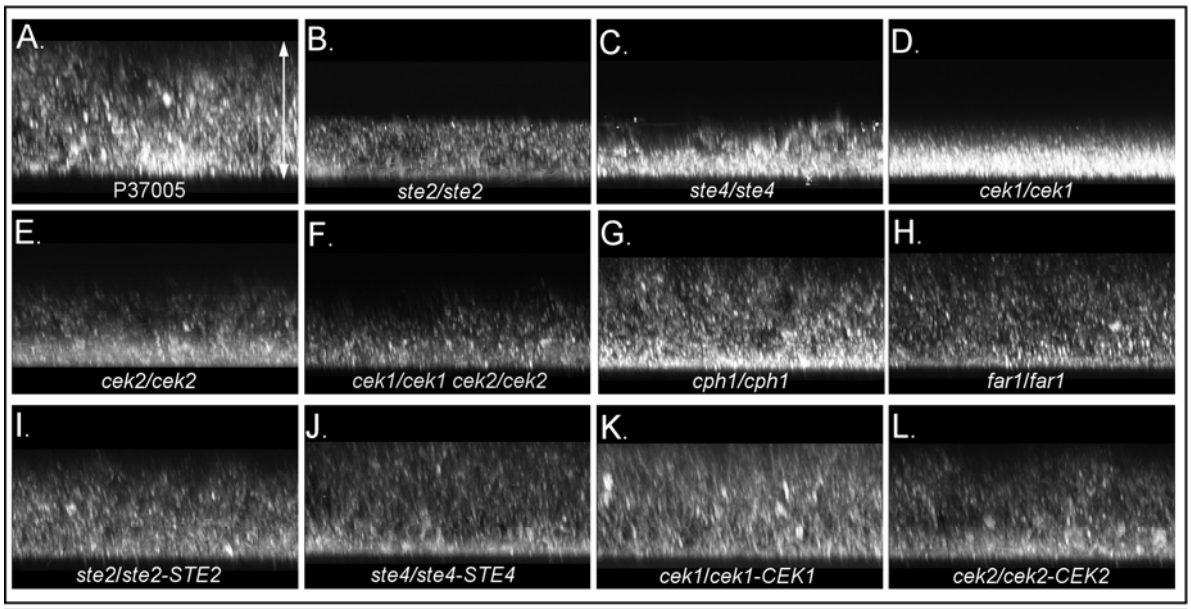

M. Biofilm Thickness (90% **a/a** wh + 10% WO-1 op)

Strain	10% op	Thickness (μm)	Strain	10% op	Thickness (μm)
P37005	–	21+2	*cph1/cph1*	+	63±9
P37005	+	61±6	*far1/far1*	+	60±9
ste2/ste2	+	34±4	*ste2/ste2-STE2*	+	62±3
ste4/ste4	+	31±3	*ste4/ste4-STE4*	+	62±3
cek1/cek1	+	25±2	*cek1/cek1-CEK1*	+	55±6
cek2/cek2	+	37±6	*cek2/cek2-CEK2*	+	67±2
cek1/cek1 cek2/cek2	+	28±4			

Figure 19. White cells of *ste3/ste3* lose the cohesion response to **a**-pheromone exhibited by wild type P57072 cells, and white *ste3*/*ste3*-*STE3* cells regain the response. A, B, C. Aggregation of white P57072, *ste3/ste3* and *ste3*/*ste3*-*STE3* cells, respectively, in the presence (+) of a 1% mixture of opaque P37005 (**a**/**a**) cells and opaque WO-1 (α/α) cells. D, E, F. Aggregation of white P57072, *ste3/ste3* and *ste3*/*ste3*-*STE3* cells, respectively, in the absence (-) of the 1% mixture of opaque cells. G. Average number of cells (error bar represents standard deviation) computed from 20 aggregates. Scale bar represents 5 μm.

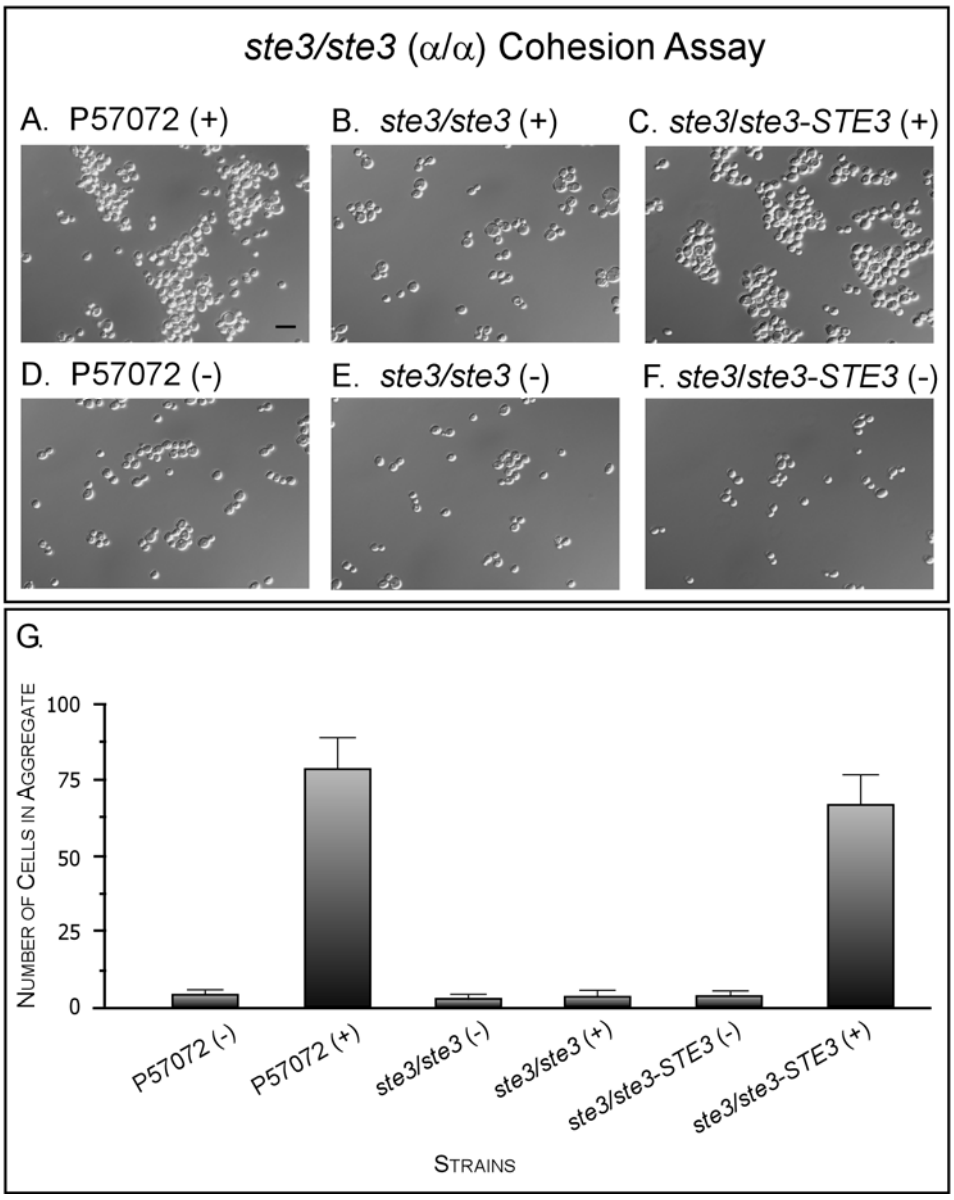
ste3/ste3 (α/α) Cohesion Assay
A. P57072 (+)
B. ste3/ste3 (+)
C. ste3/ste3-STE3 (+)
D. P57072 (-)
E. ste3/ste3 (-)
F. ste3/ste3-STE3 (-)
G.
Number of Cells in Aggregate
100
75
50
25
0
P57072 (-)
P57072 (+)
ste3/ste3 (-)
ste3/ste3 (+)
ste3/ste3-STE3 (-)
ste3/ste3-STE3 (+)
Strains

cohesive response to **a**-pheromone, similar to that of parent α/α strain P57072, was restored in the complemented strain *ste3/ste3-STE3* (Figure 19).

To test whether **a**-pheromone induced *ste3/ste3* cells to form a tight adhesive film on a plastic surface, majority white cells (99%) of either strain P57072 or strain *ste3/ste3*, were mixed with a minority (1%) of half opaque P37005 (**a**/**a**) cells and opaque WO-1 (α/α) cells. As in the previous strategy, opaque α/α cells stimulate the release of **a**-pheromone by opaque **a**/**a** cells, which then stimulates white-specific responses in white α/α cells (Daniels *et al.*, 2006). Whereas white P57072 cells were induced to form an adhesive film on the plastic well bottom, *ste3/ste3* cells were not (Figure 20). Pheromone-induced substrate adhesion was restored in the complemented strain *ste3*/*ste3-STE3* (Figure 20). Minority opaque **a**/**a** cells (P37005) stimulated by α-pheromone also enhanced biofilm formation by majority white P57072 cells, but not majority white *ste3/ste3* cells (Figure 21). The former were close to twice as thick as the latter (Figure 21). Enhancement of biofilm formation by minority opaque cells similar to that in parent strain P57072 was restored in the complemented strain *ste3*/*ste3-STE3* (Figure 21). Together, these results demonstrate that the same **a**-pheromone receptor (Ste3) regulates the **a**-pheromone-induced opaque cell response and white cell response, just as the same Ste2 receptor regulates the α-pheromone responses of opaque and white **a**/**a** cells.

Opaque Cell Pheromone Response of *cek1/cek1*, *cek2/cek2* and the *cek1*/*cek1 cek2*/*cek2* Double Mutant

Opaque cells of the individual MAP kinase mutants *cek1/cek1* and *cek2/cek2*, which were generated in the natural **a**/**a** strain P37005, formed shmoos in response to α-pheromone, but the response in both cases was delayed and the proportion of cells that responded after four hours reduced (Figure 13E and G, respectively, and Figure 13M). The percent of cells that shmooed in both mutants increased after eight hours of treatment

Figure 20. White cells of *ste3/ste3* lose the adhesive response to a-pheromone exhibited by wild type P57072, and white *ste3*/*ste3*-*STE3* cells regain the response. Pseudocolor images in orange are provided. A, B, C. Representative images of the dish bottoms of *ste3/ste3*, *ste3*/*ste3*-*STE3* and P57072 cultures, respectively, in the presence (+) of the 1% mixture of opaque P37005 and WO-1 cells. D, E. F. A repeat of A, B, C, respectively. G, H, I. Representative images of the dish bottoms of *ste3/ste3*, *ste3*/*ste3*-*STE3* and P57072 cultures, respectively, in the absence (-) of the 1% mixture of opaque cells. J. Quantitation of cells adhering to the dish bottom. The average number was computed from three wells. Error bar represents standard deviation. Note that the level attained by white P57072 cells is lower than that by white P37005 cells in response to pheromone. This may be due either to strain differences or **a**/**a**, α/α differences. The reason for the difference is now under investigation.

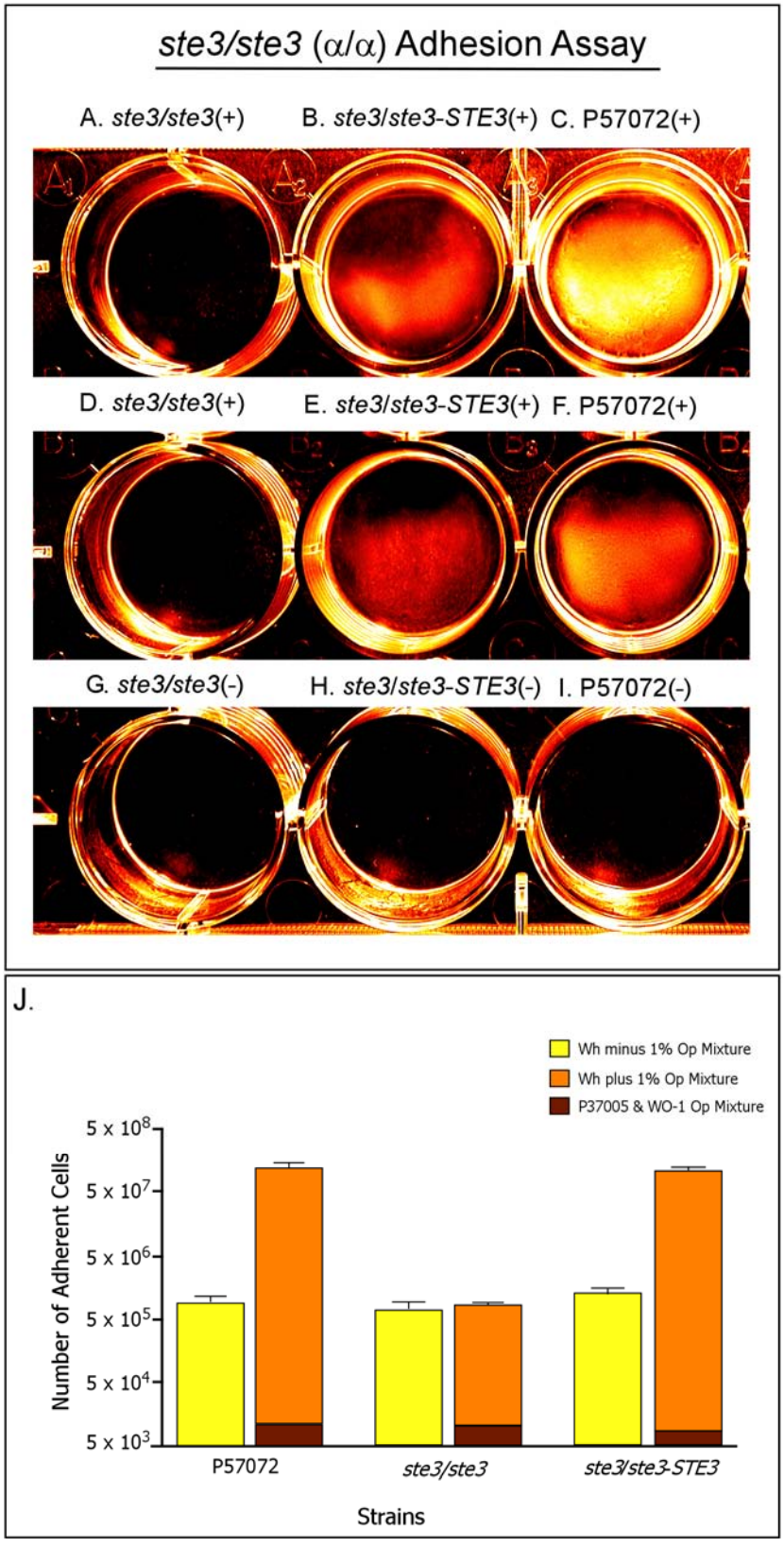
ste3/ste3 (α/α) Adhesion Assay
A. ste3/ste3(+)
B. ste3/ste3-STE3(+)
C. P57072(+)
D. ste3/ste3(+)
E. ste3/ste3-STE3(+)
F. P57072(+)
G. ste3/ste3(-)
H. ste3/ste3-STE3(-)
I. P57072(-)
J.
Wh minus 1% Op Mixture
Wh plus 1% Op Mixture
P37005 & WO-1 Op Mixture
Number of Adherent Cells
5 x 10^8
5 x 10^7
5 x 10^6
5 x 10^5
5 x 10^4
5 x 10^3
P57072
ste3/ste3
ste3/ste3-STE3
Strains

Figure 21. White cells of *ste3/ste3* lose enhancement of biofilm thickness in response to opaque cells of P37005, and white *ste3*/*ste3*-*STE3* cells regain the enhancement response. A, B, C. Representative LSCM Z-series projections of P57072, *ste3*/ste3 and *ste3*/*ste3*-*STE3* biofilms, respectively. D. Average thickness (± standard deviation) of biofilms, computed from 9 measurements.

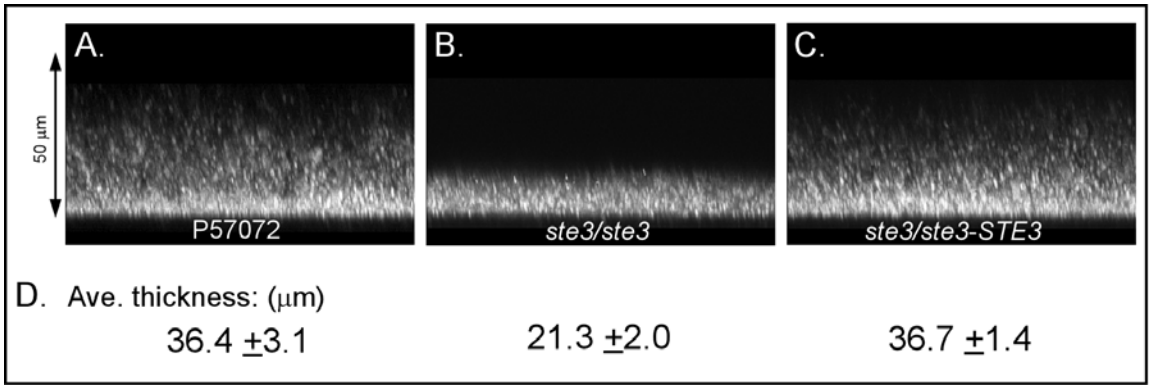
A.
B.
C.
50 µm
P57072
ste3/ste3
ste3/ste3-STE3
D. Ave. thickness: (µm)
36.4 ±3.1
21.3 ±2.0
36.7 ±1.4

(Figure 13F and H, respectively, and Figure 13M). Opaque cells of both mutants also underwent mating with opaque cells of the α/α strain WO-1 (Figure 15F and G, respectively), but the proportion of fusants was reduced by more than 99% for *cek1*/*cek1*and by 90% for *cek2/cek2* (Figure 15K). Pheromone-induced shmooing and mating of opaque cells was restored in the complemented strains *cek1*/*cek1*-*CEK1* and *cek2*/*cek2*-*CEK2* (data not shown).

Opaque cells of the double mutant *cek1*/*cek1 cek2*/*cek2*, however, neither shmooed in response to α-pheromone (Figure 13I, M) nor underwent mating with opaque cells of the α/α strain WO-1 (Figure 15H, K). These results were consistent with those obtained with null mutants of *KSS1* and *FUS3*, the respective orthologs of *CEK1* and *CEK2*, in *S. cerevisiae* (Elion *et al.*, 1991), and confirm and extend earlier observations by Chen *et al.* (2002) on *cek1/cek1*, *cek2/cek2* and the *cek1*/*cek1 cek2*/*cek2* double mutant of *C. albicans* strain CAI4, in which complementation was used between auxotrophic **a** and α strains as an assay for mating.

White Cell Pheromone Responses of *cek1/cek1*, *cek2/cek2* and the *cek1*/*cek1 cek*/*cek2* Double mutant

In the absence of α-pheromone, white *cek1/cek1* and *cek2/cek2* cells formed only small aggregates in suspension cultures (data not shown), as did white P37005 cells (Figure 16I). In response to α-pheromone, both white *cek1/cek1* and white *cek2/cek2* cells formed aggregates that were on average larger than in the absence of α-pheromone (Figure 16D and E, respectively), but still far smaller than those formed by α-pheromone treated P37005 cells (Figure 16A). The average number of cells per clump for treated white *cek1/cek1* and *cek2/cek2* cells was 35 and 25, respectively, compared to 125 for white P37005 cells (Figure 16I). In response to α-pheromone, white *cek1/cek1* and white *cek2/cek2* cells formed a film on a plastic surface (Figure 17E and F, respectively). Quantitation revealed that the number of adherent cells in these films was greater than that

in unstimulated cultures, but consistently smaller ($p < 0.001$) than that of pheromone-stimulated P37005 cells (Figure 17J). This adhesive response was regained in the complemented strains *cek1*/*cek1*-*CEK1* and *cek2*/*cek2*-*CEK2* (Figure 17J). A minority of α/α opaque cells of strain WO-1 did not enhance the thickness of biofilms formed by majority *cek1/cek1* or *cek2/cek2* white cells over a 48 hour period (Figure 18D and E, respectively), as it did white P37005 cells (Figure 18M). Enhancement of the thickness of white cell biofilms by minority α/α opaque cells returned in the complemented strains (Figure 18K and L, respectively; Figure 18M).

In the presence of α-pheromone, white cells of the double mutant *cek1*/*cek1 cek2*/*cek2* formed only small clumps (Figure 16F, I) like untreated cells (data not shown). White *cek1*/*cek1 cek2*/*cek2* cells also did not form a film on a plastic surface in response to α-pheromone (Figure 17G, J). Finally, minority α/α opaque cells of strain WO-1 did not stimulate an increase in the thickness of a majority **a**/**a** white cell biofilm of the *cek1*/*cek1 cek2*/*cek2* mutant on a silicone elastomer surface (Figure 18F, M). These results demonstrate that as was the case for *STE2*, *STE3* and *STE4*, the partially redundant functions of *CEK1* and *CEK2* are necessary for both the opaque and white cell responses, suggesting that the response pathways from receptor through the MAP kinase cascade are shared.

Opaque Cell Pheromone Response of *cph1/cph1*

Opaque cells of the *trans*-acting factor mutant *cph1/cph1*, which was generated in the natural **a**/**a** strain P37005, neither formed shmoos in response to α-pheromone (Figure 13J, M), nor mated with opaque cells of the α/α strain WO-1 (Figure 15I, K). The complemented strain *cph1*/*cph1*-*CPH1* reacquired these responses (data not shown). These results support and extend earlier observations by Magee *et al.* (2002) and Chen *et al.* (2002) in which complementation between auxotrophs was used as an assay to demonstrate that mating depends on *CPH1* function.

White Cell Pheromone Response of *cph1/cph1*

Although deletion of *CPH1* completely blocked pheromone-induced formation and mating of opaque cells, it did not block the white cell pheromone response. Treatment of white *cph1/cph1* cells with α-pheromone stimulated aggregation in suspension cultures (Figure 16G, I) to levels comparable to that of treated white P37005 cells (Figure 16A, I). Treatment with α-pheromone also induced *cph1/cph1* cells to form a tightly adhering film on a plastic surface (Figure 17H, J) comparable to that formed by treated white P37005 cells (Figure 17B, J). Finally, minority α/α opaque cells of strain WO-1 stimulated an approximate three-fold increase in the thickness of majority white *cph1/cph1* cell biofilms (Figure 18G, M), an increase comparable to that induced by α/α cells in white P37005 biofilms (Figure 18A, M). These results clearly demonstrate that the white cell response to pheromone does not require the downstream target Cph1, and, therefore, that although the pheromone response pathway from receptor through the MAP kinase pathway is shared, the downstream components of the pathways regulated by the MAP kinases differ.

Opaque Cell Pheromone Response of *far1/far1*

It was previously demonstrated that white cells do not shmoo (Bennett *et al.*, 2003; Lockhart *et al.*, 2003b) and do not arrest in G1 in response to α-pheromone (Zhao *et al.*, 2005b). Therefore, one might not expect *FAR1* to play a role in the white cell response, since the role *FAR1* plays in the analogous mating process of *S. cerevisiae* is in the polarization of cells in a gradient of pheromone and G1 arrest (Chang and Herskowitz, 1990; Butty *et al.*, 1998; Valtz *et al.*, 1995). However, in supplemental data to Roberts *et al.* (2000), it was reported that *STE12* was not up-regulated by pheromone in a *far1/far1* mutant, indicating that Far1 played a role in the up-regulation of pheromone-induced genes. We considered, therefore, the possibility that Far1 may also be involved in the up-regulation of genes by pheromone in the white cell response. The *far1/far1* mutant of *S. cerevisiae* shmoos in response to α-pheromone, but the shmoos do not polarize in a

gradient of pheromone, and *far1/far1* cells are not blocked in G1 by pheromone (Chang and Herskowitz, 1990; Valtz *et al.*, 1995; Dorer *et al.*, 1995). The *far1/far1* mutant of *S. cerevisiae* is capable of mating, but the frequency of mating is significantly reduced, presumably because *far1/far1* cells cannot efficiently find partners since they are defective in chemotropism (Valtz *et al.*, 1995).

Opaque cells of the *C. albicans far1/far1* mutant generated in the **a**/**a** strain P37005, exhibited mating-associated abnormalities similar to those in *S. cerevisiae*. Opaque cells of *C. albicans far1/far1* shmooed in response to α-pheromone (Figure 13K, L), but the percent of shmooing was reduced by 57% after four hours and 81% after eight hours (Figure 13M). The *C. albicans far1/far1* mutant also exhibited a strong mating defect (99.26% reduction) when compared to the parental strain P37005 (Figure 15J and K). To test whether bilateral mating between *far1/far1* (**a**/**a**) and a *far1/far1* (α/α) strain completely blocked mating, we generated a *far1*/*far1* mutant in the α/α strain WO-1. More than 4000 cells were scanned in mixtures of opaque *far1*/*far1* (**a**/**a**) and *far1*/*far1* (α/α). No mating was observed (data not shown). These results suggest that *FAR1* is not essential for shmooing in response to pheromone, although the frequency is reduced, but *FAR1* appears to be essential for fusion. Full shmooing and mating responses were restored in the complemented *C. albicans* strain *far1*/*far1-FAR1* (data not shown).

To test whether *FAR1* was required for a pheromone-induced block in G1 during shmoo formation in *C. albicans*, the DNA content of the nuclei of opaque cells of strain P37005, the *far1*/*far1* derivative and the complemented *far1*/*far1-FAR1* strain undergoing shmooing was assessed by measuring the pixel intensity of a line scan through the nucleus of cells stained with Sytox Green™ according to methods previously described (Zhao *et al.*, 2005b). At saturation phase in liquid culture, the distributions of maximum pixel intensities of the stained nuclei of 27 independently scanned opaque cells of each of strain P37005 (Figure 22A), *far1*/*far1-FAR1* (Figure 22B) and *far1*/*far1* (Figure 22C), which in all three cases were primarily unbudded, were similar, ranging between approximately 100

Figure 22. Opaque cells of *far1far1*, although induced by pheromone to form shmoos, are not arrested in G1. Parental P37005, complemented *far1*/*far1-FAR1*, and *far1/far1* cells were grown to saturation at 25°C in liquid culture (saturation phase), and then they were released into fresh medium in the absence of pheromone (– pheromone) or in the presence of pheromone (+ pheromone) and incubated for 3 h. Cells were then fixed, stained with Sytox Green for DNA, and the intensity of staining in the nucleus of cells forming shmoos quantitated by LSCM (Zhao *et al.*, 2005a). Alternatively, the same cell preparation was analyzed by FACS analysis. (A–C) Distributions of maximum intensity measurements of 27 individual nuclei from saturation phase cells and saturation phase cells diluted into fresh medium containing 3 x 10–6 M α-pheromone and incubated for 3 h, for P37005, *far1*/*far1-FAR1*, and *far1*/*far1* cells, respectively. (D and E) Examples of line profile scans of the intensity of nuclei of opaque *far1*/*far1-FAR1* cells that formed shmoos, with fluorescent nucleus overlaid on differential interference contrast (DIC) cell images. Similar results were obtained for opaque P37005 cells (data not shown). (F–I) Representative line profile scans of the intensity of nuclei of opaque *far1/far1* cells that formed shmoos, with fluorescent nucleus overlaid on DIC images. (J) FACS analysis of *far1*/*far1-FAR1* and *far1/far1*. The percent reduction due to the addition of α-pheromone in the proportion of cells undergoing DNA replication is presented at the two tested concentrations of α-pheromone. R, average replicated state estimate; U, average unreplicated state estimate.

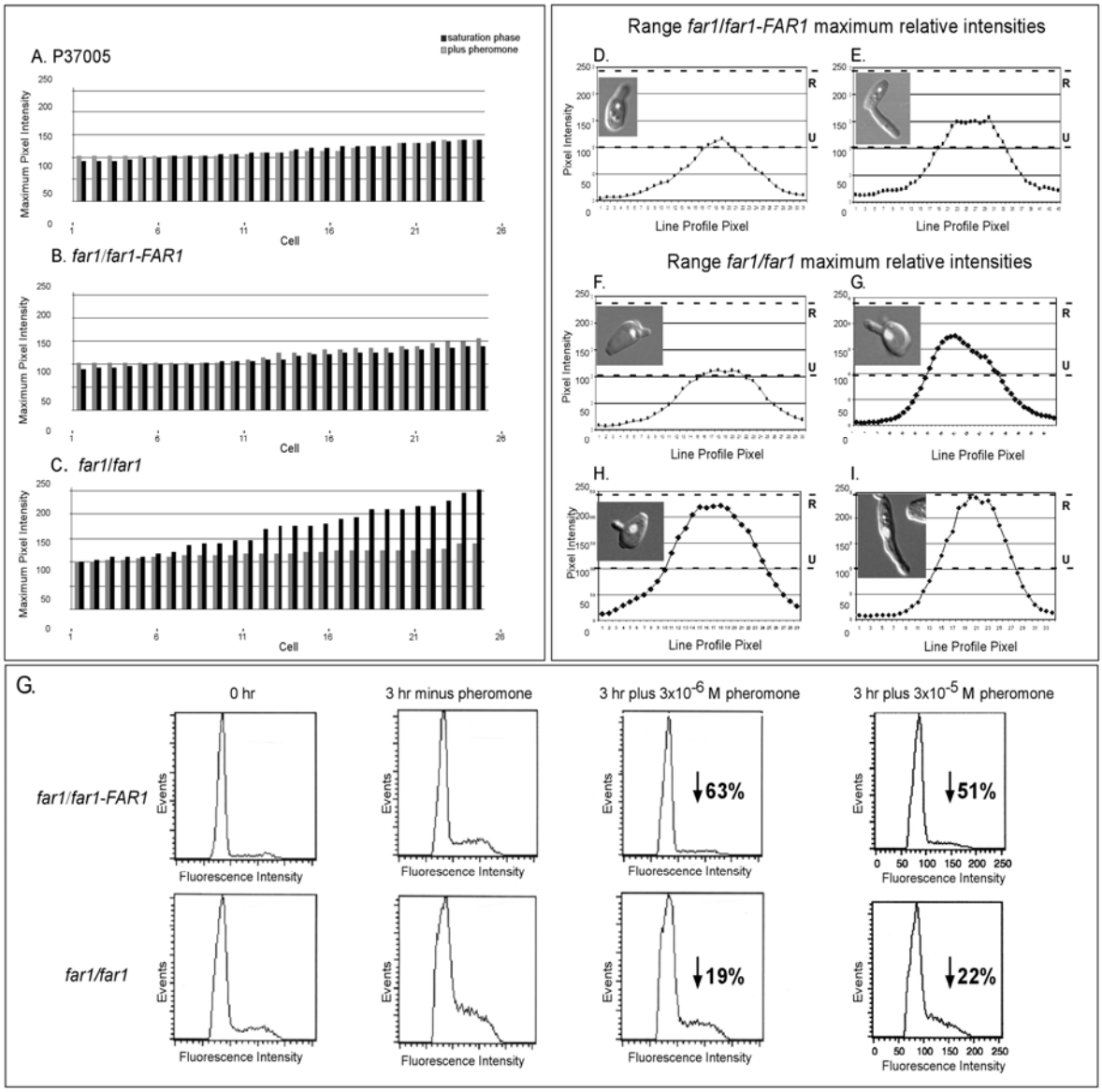
A. P37005
saturation phase
plus pheromone
Maximum Pixel Intensity
Cell
B. far1/far1-FAR1
C. far1/far1
Range far1/far1-FAR1 maximum relative intensities
D.
E.
Pixel Intensity
Line Profile Pixel
R
U
Range far1/far1 maximum relative intensities
F.
G.
H.
I.
G.
0 hr
3 hr minus pheromone
3 hr plus 3x10-6 M pheromone
3 hr plus 3x10-5 M pheromone
far1/far1-FAR1
far1/far1
Events
Fluorescence Intensity
63%
51%
19%
22%

and 150 relative units. When opaque cells from saturation phase cultures of P37005, *far1*/*far1-FAR1* or *far1*/*far1* were diluted into fresh medium and incubated for three hours in the absence of α-pheromone, the range of maximum pixel intensities in all cases increased. In the case of control P37005 or *far1*/*far1-FAR1*, the range increased to approximately 150 to 250 relative units, and in the case of *far1*/*far1*, to 110 to 250 units (data not shown), indicating a lag in *far1/far1* cells. If cells from the two control strains P37005 and *far1*/*far1-FAR1* were diluted into fresh medium containing α-pheromone and incubated for three hours, the increases in DNA content of cells forming shmoos in the population did not occur (Figure 22A, B). However, if cells from *far1/far1* were diluted into fresh medium containing α-pheromone, the increase still occurred (Figure 22C). In Figure 22D and E, examples are presented of representative line scans of the relative DNA content of nuclei of *far1*/*far1-FAR1* cells undergoing shmoo formation in response to pheromone. In Figure 22F through I, examples are presented of representative line scans of the relative DNA content of nuclei of *far1/far1* cells undergoing shmoo formation in response to pheromone. Note that the two cells in Figure 22H and I are undergoing DNA replication and, hence, are not blocked in G1. Together, these results indicate that just as in the case of *S. cerevisiae*, *FAR1* plays a role in the pheromone-induced G1 block in mating-competent opaque cells.

We employed confocal line scans of individual nuclei because the more common method for assessing cell cycle, fluorescence activated cell sorting (FACS), does not allow one to assess the DNA content of a morphologically identified cell. This proved to be an issue since the proportion of cells that formed shmoos differed between saturation phase opaque *far1/far1* cells and control cells that had been released into fresh medium containing α-pheromone (Figure 13M). Even so, a FACS analysis revealed that when saturation phase *far1/far1* opaque cells were released into fresh medium containing α-pheromone and incubated for three hours, a reproducibly higher proportion underwent DNA replication than control *far1*/*far1-FAR1* cells treated similarly. In the absence of

pheromone, the proportion of the control population undergoing DNA replication after three hours was 0.35, and the proportion of *far1/far1* cells was 0.32 (Figure 22J). In the presence of 3 x 10^{-6} or 3 x 10^{-5} M α-pheromone, the proportion in the control population undergoing DNA replication decreased by 63% and 51%, respectively, from that in the absence of pheromone (Figure 22J). For *far1/far1* cells, the decrease was 19 and 22%, respectively, from that in the absence of pheromone (Figure 22J). Similar results were obtained in repeat experiments. The difference in the proportion of opaque cells undergoing DNA replication in the absence and presence of α-pheromone was, therefore, approximately three fold higher in the *far1/far1* mutant than in the parental strain (data not shown) or complemented strain (Figure 22J). These results are consistent with the confocal microscopy line scan data of individual cells. The small decrease in the proportion undergoing DNA replication that did occur in opaque cells treated with pheromone, however, suggests that regulation other than through *FAR1* also has an effect on the cell cycle.

White Cell Pheromone Response of *far1/far1*

As one would expect given its characteristics, deletion of *FAR1* had no effect on the white cell pheromone response. When treated with α-pheromone, white cells of the *far1*/*far1* mutant formed large clumps in suspension (Figure 16H, I), like white parental P37005 cells (Figure 16A, I), and thick films on plastic surfaces (Figure 17I) with the number of cells adhering comparable to that of films formed by α-pheromone-treated white cells of strain P37005 (Figure 17J). Furthermore, minority opaque α/α cells stimulated approximately a three fold increase in the thickness of majority white cell biofilms of the *far1*/*far1* mutant on a silicone elastomer surface (Figure 18H, M), as they did biofilms of white cells of strain P37005 (Figure 18A, M). These results demonstrate that Far1 is not involved in the white cell response to pheromone.

Regulation of *CPH1* Expression

It had previously been demonstrated that *CPH1* was up-regulated by α-pheromone in opaque **a**/**a** cells (Bennett *et al.*, 2003; Zhao *et al.*, 2005b). In *S. cerevisiae*, the ortholog to *CPH1*, *STE12*, is expressed at a basal level in untreated **a** cells and, as in *C. albicans*, is up-regulated by α-pheromone (Roberts *et al.*, 2000; Crosby *et al.*, 2000). In the absence of α-pheromone, *CPH1* was expressed at a low but reproducible level in opaque cells of strain P37005 (Figure 23). In the presence of α-pheromone, *CPH1* was up-regulated (Figure 23). In opaque cells of the mutants *ste2/ste2*, *ste4/ste4* and *cek1*/*cek1 cek2*/*cek2*, *CPH1* expression was undetectable in the absence or presence of pheromone (Figure 23), indicating that basal level expression was dependent on *STE2*, *STE4*, and on *CEK1* and *CEK2*. *CPH1* was, however, expressed at a low basal level in *far1/far1* cells in the absence of pheromone, indicating that basal level expression of *CPH1* was not dependent on *FAR1*. However, *CPH1* expression was not up-regulated in *far1/far1* cells by pheromone, indicating that up-regulation was dependent on *FAR1*, as it is in *S. cerevisiae* (Roberts *et al.*, 2000) (Figure 23). Pheromone-induction of *CPH1* expression was regained in the complemented strain *far1*/*far1-FAR1* (Figure 24).

In white cells of strain P37005, *CPH1* was expressed at levels that were barely detectable, far below the basal levels observed in opaque cells (Figure 23). In addition, *CPH1* was not up-regulated in response to pheromone in white cells (Figure 23). Similar results were obtained for the mutants *ste2/ste2*, *ste4/ste4*, *cek1*/*cek1 cek2*/*cek2*, and *far1*/*far1* (Figure 23). These results indicate that the pheromone-response pathway functions in the basal level expression of *CPH1* in opaque cells, but not white cells.

Molecular Markers for the Alternative Phenotypic Responses to Pheromone

The alternative phenotypic responses to pheromone of white and opaque cells must depend upon the activation of alternative batteries of genes. Activation of such

Figure 23. Northern analysis of the expression of the downstream opaque cell regulator *CPH1*, the **a**-pheromone gene *MFA1*, and the cell surface hydrophobicity gene *CSH1* in the mutant strains *ste2*/*ste2*, *ste4*/*ste4*, the double mutant *cek1*/*cek1 cek2*/*cek2*, *cph1*/*cph1*, and *far1*/*far1*. Each gene was probed in white (Wh) and opaque (Op) cells grown to saturation phase in liquid medium at 25°C, and then released and incubated in fresh medium in the absence (–) or presence (+) of **a**-pheromone for 3 h. White and opaque samples were hybridized in unison on the same blot, and the sequence of images was separated for clarity. It should be noted that longer exposures reveal very low level up-regulation of *CSH1* in pheromone-treated *ste2/ste2* and *ste4/ste4* cells, but not *cek1*/*cek1 cek2*/*cek2*, an observation now being explored. To demonstrate equal loading of RNA among lanes, 18S rRNA levels are provided. In addition, hybridization was performed with the white and opaque blots for *ACT1*, a constitutively expressed actin gene. Furthermore, it should be noted that white and opaque samples were exposed to the probe on the same autoradiograms, scanned, and then digitally separated, so exposure times are equal.

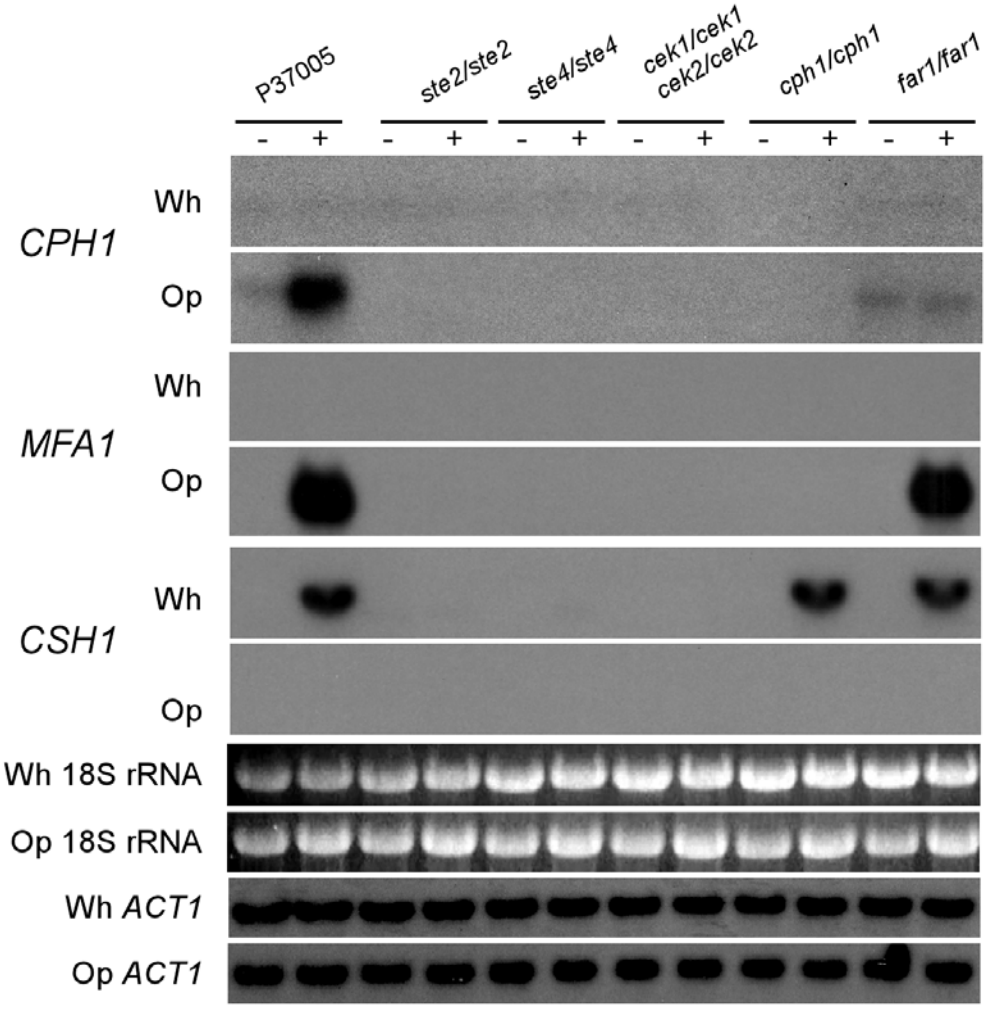
P37005
ste2/ste2
ste4/ste4
cek1/cek1
cek2/cek2
cph1/cph1
far1/far1
- + - + - + - + - + - +
CPH1
Wh
Op
MFA1
Wh
Op
CSH1
Wh
Op
Wh 18S rRNA
Op 18S rRNA
Wh ACT1
Op ACT1

Figure 24. Northern analysis reveals that pheromone up-regulation of *CPH1* is regained in the complemented strain *far1*/*far1-FAR1*. (-), absence of α-pheromone; (+) presence of α-pheromone. See legend to Figure 25 for details. 18S rRNA hybridization demonstrated equivalent loading (data not shown).

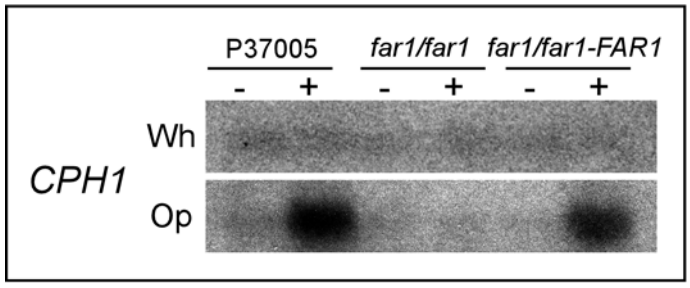
P37005
far1/far1
far1/far1-FAR1
- + - + - +
CPH1
Wh
Op

genes must exhibit the same dependencies on the components of the pheromone response pathways as the cell type-specific phenotypic responses. Hence, up-regulation of genes in the opaque battery must depend on an intact pathway from receptor (*STE2*) through transcription factor (*CPH1*); alternatively, genes in the white battery must depend on an intact pathway from receptor (*STE2*) through the MAP kinases (*CEK1* and *CEK2*), but not on *CPH1*.Genes exhibiting these alternative dependencies were identified.

In *S. cerevisiae*, there are two genes for the **a**-pheromone, *MFA1* and *MFA2* (Gething, 1985; Michaelis and Herskowitz, 1988). The expression of these genes is selectively up-regulated in **a** cells by α-pheromone (Roberts *et al.*, 2000). *C. albicans* has only one **a**-pheromone gene, *MFA1*, which is also selectively up-regulated in opaque **a**/**a** cells by α-pheromone (Dignard *et al.*, 2007). Up-regulation of this gene exhibited the same dependencies on components of the opaque pheromone response pathway as shmooing and mating. *MFA1* expression was undetectable by northern analysis in white cells of strain P37005 and white cells of all tested mutants in the absence or presence of α-pheromone (Figure 23). In opaque P37005 cells, *MFA1* was up-regulated by α-pheromone (Figure 23). It was not similarly up-regulated by α-pheromone in the mutants *ste2/ste2*, *ste4/ste4*, *cek1*/*cek1 cek2*/*cek2* or *cph1/cph1* (Figure 25). It was, however, up-regulated by α-pheromone in the mutant *far1/far1*. *MFA1* thus exhibits the dependencies expected of genes up-regulated by pheromone in opaque cells.

Since pheromone induces both cohesiveness and adhesiveness in white cells but not opaque cells, we screened a set of genes encoding cell surface proteins by northern analysis for an expression pattern consistent with the white cell pheromone response (Sahni *et al.*, submitted). The screen revealed that the cell surface hydrophobicity gene *CSH1* (Singleton and Hazen, 2004; Singleton *et al.*, 2005) was strongly up-regulated by α-pheromone in white cells, but not opaque cells, of parent strain P37005 (Figure 23). Up-regulation of this gene exhibited the same dependencies on components of the white pheromone-response pathway as increased cohesion, adhesion and biofilm development.

CSH1 was expressed at a very low to negligible level in opaque P37005 cells in the absence of α-pheromone and was not up-regulated by the addition of pheromone (Figure 23). In white P37005 cells, *CSH1* expression was low in the absence of α-pheromone, but up-regulated in the presence of α-pheromone (Figure 23). *CSH1* was expressed at low levels in white cells of the mutants *ste2/ste2*, *ste4*/*ste4* and *cek1*/*cek1 cek2*/*cek2* cells in the absence or presence of α-pheromone, demonstrating that normal pheromone-induced expression depended on the pheromone receptor, heterotrimeric G protein and MAP kinase cascade (Figure 23). *CSH1*, however, was fully up-regulated by α-pheromone in both the *cph1/cph1* and *far1/far1* mutants (Figure 23), demonstrating that pheromone-induced expression was independent of *CPH1* or *FAR1*.

The Effects of Low and High Concentrations of Pheromone

Suboptimal concentrations of α-pheromone that do not induce shmooing in haploid **a** cells of *S. cerevisiae* have been shown to induce invasive growth (Moore, 1983). We therefore entertained the possibilities that in *C. albicans* high concentrations of pheromone may be necessary to induce shmooing in white cells and suboptimal concentrations of α-pheromone may induce the white response or filamentous growth in opaque **a**/**a** cells. We discovered early in our studies that the chemically-synthesized α-pheromone 13-mer at a concentration of 3×10^{-6} M was sufficient to induce maximum opaque and white cell responses. Furthermore, a FACS analysis revealed that concentrations of α-pheromone between 10^{-5} and 10^{-6} M caused a maximum G1 block after three hours (*i.e.*, the DNA of approximately 90% of opaque **a**/**a** cells of natural strain P37005 remained in the unreplicated state), that a concentration of 10^{-7} M α-pheromone resulted in less than 90% of cells in the unreplicated state after three hours, and that concentrations ranging from 10^{-8} through 10^{-10} M, or no added pheromone, resulted in 60 to 70% of cells in the unreplicated state after 3 hours (data not shown). These results

supported our use of 3 x 10^{-6} M α-pheromone as the inducing concentration for both the opaque and white cell responses.

To test whether α-pheromone concentrations higher than 3 x 10^{-6} M induced shmooing in white cells, we diluted saturation phase white P37005 cells into fresh medium containing a ten-fold higher concentration of α-pheromone, 3 x 10^{-5} M. A FACS analysis revealed no decrease in the proportion of cells undergoing DNA replication (data not shown), and absolutely no shmoo formation (over 10,000 white cells were assessed after three and six hours of treatment).

To test whether suboptimal concentrations of pheromone induced filamentation or the white response among opaque cells, saturation phase P37005 opaque cells were diluted into fresh medium containing α-pheromone in the range of 10^{-7} to 10^{-10} M. Suboptimal concentrations did not induce cohesion in suspension or adhesion to plastic, and did not induce either pseudohypha or hypha formation (data not shown). These results demonstrate that high concentrations of pheromone do not block white cells in G1 or induce shmoo formation, and low concentrations do not induce opaque cells to undergo the white cell response or filamentation.

Discussion

The pheromones released by opaque *C. albicans* cells to induce mating response*s* in opaque cells of opposite mating type also signal white cells to become both cohesive and adhesive so that they can more readily form incipient biofilms that then develop into mature biofilms twice as thick as these formed by untreated white cells (Daniels *et al.*, 2006). We previously hypothesized, based on *in vitro* results, that these white cell biofilms might function as protective environments that facilitate mating between minority opaque cells of opposite mating type in nature (Daniels *et al.*, 2006). Using biotinylated α-pheromone, we further demonstrated that white cells bound pheromone to their surfaces, and that the binding of pheromone then down-regulated the receptors (Daniels *et al.*,

2006). However, the staining pattern of receptors on the surface differed between white and opaque cells, and reappearance of receptors after down-regulation occurred only in opaque cells (Daniels *et al.*, 2006). Here, we have presented evidence that the same pheromone signal, receptor, heterotrimeric G-protein and MAP kinase cascade, but different downstream regulators, mediate the disparate pheromone responses of opaque and white cells of *C. albicans*.

In the fungi, including plant pathogens, there are numerous examples of the conservation of components of MAP kinase cascades in different pathways regulating a variety of responses, but in the great majority of cases, the signals, receptors and differing numbers of components along the transduction pathways are distinct (Xu, 2000; Banuett, 1998). In *S. cerevisiae*, the signals and receptors triggering the mating response of the alternative mating types differ, as is also the case in a number of other yeast (Leberer *et al.*, 1997; Elion, 2000; Davidson *et al.*, 2003; Li *et al.*, 2004). In *S. cerevisiae*, the signals, receptors and a majority of components of the signal transduction pathways differ among a number of environmental responses, including the mating response to pheromones, filamentation, ascospore formation and osmoregulation (Gustin *et al.*, 1998; Chen and Thorner, 2007). However, we found no definitive example in other fungi of the scenario we have described for white and opaque cells of *C. albicans*, specifically, that the same signal interacts with the same receptor, activating the same upstream signal transduction pathway, but different downstream regulators in two different cell types, resulting in completely different responses. This is not to say that this scenario does not exist in other fungi, but simply that it has not yet been fully described, if it does. In higher eukaryotes, however, there are several examples of this signaling scenario. For instance, both $CD4^+$ and $CD8^+$ T cells respond to the same mitogenic signals, and through the same TCR receptor, MAPKK (MKK4/7) and MAPK (JNK2), induce IL-2 expression in the case of $CD4^+$ cells, but repress IL-2 expression in the case of $CD8^+$ cells (Rincon and Pedraza-Alva, 2003). In addition, both cell types transduce the same signal through the

same receptor MAPKK (MKK4/7) and MAPK (p38), but the response in $CD4^+$ cells is survival, while that in $CD8^+$ cells is apoptosis (Rincon and Pedraza-Alva, 2003). There appear to be a variety of additional examples in higher eukaryotes, especially in developing systems (Bacci *et al.*, 2005; Dailey *et al.*, 2005), of the same signal, receptor, and upstream components in the transduction pathway, but different downstream regulators in different cell types.

Common Upstream Components

Although we have presented evidence that the same upstream components, including receptors, heterotrimeric G-protein and MAP kinase cascade, are shared in the pheromone response pathways of opaque and white cells (Figure 25), we cannot exclude the possibility that additional, parallel pathways involved in the alternative pheromone responses are activated by the same or even different receptors. We can also not exclude the possibility that *CEK1* and *CEK2* have non-overlapping as well as overlapping functions in the opaque and white responses, given that the effects of neither *cek1/cek1* or *cek2*/*cek2* were complete for the majority of assayed pheromone responses in both white and opaque cells, in comparison to the double mutant *cek1*/*cek1 cek2*/*cek2*. The *cek1/cek1* mutant exhibited stronger defects than the *cek2/cek2* mutant in a majority of the measured responses. The individual roles of *CEK1* or *CEK2*, therefore, remain to be elucidated.

Difference in the Downstream Component(s)

Our evidence demonstrates that while the transcription factor Cph1 represents the downstream transcription factor in the opaque pheromone response pathway, it does not appear to play any distinct role in the white pheromone response pathway (Figure 25). Here, we have demonstrated that while *MFA1* is up-regulated by the opaque pheromone response pathway through *CPH1*, *CSH1* is up-regulated by the same pheromone response pathway, but through a different downstream transcription regulator, which is yet, to be identified. Recent experiments, employing both expression arrays, and northern analyses

Figure 25. Comparison of the pheromone response pathways of opaque and white cells (A and B, respectively). The roles of some of the components (the trimeric G protein α and γ subunits and *CST20*) in the models were not analyzed here, but they were inferred from the conserved and more thoroughly studied pheromone response pathway of *S. cerevisiae*. The distinctive points of the comparison are that the components of pathways from receptor through the MAP kinase cascade are shared, whereas the terminal regulatory component, the response-specific transcription factor, differs. Although *CPH1* is the downstream regulator in the opaque pheromone response pathway, the downstream regulator in the white pheromone response pathway remains unidentified, hence the question mark. Although *FAR1* plays a major role as a downstream regulator in the opaque pheromone response pathway, its functions have no analogies in the white pheromone response pathway, so it has not been represented in the opaque model. The checks in the figure denote deletions created for specific genes along the pathway.

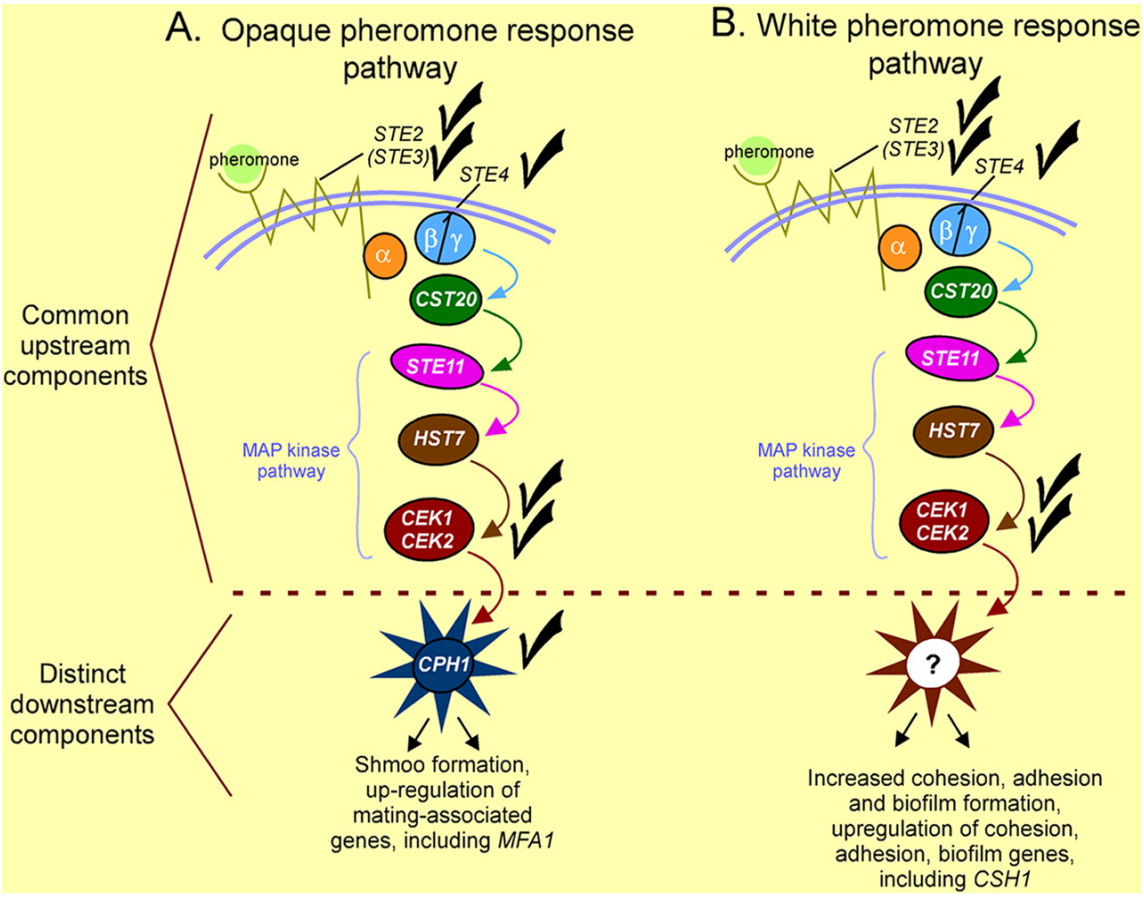
A. Opaque pheromone response pathway
B. White pheromone response pathway
pheromone
STE2 (STE3)
STE4
α
β/γ
CST20
STE11
HST7
CEK1 CEK2
MAP kinase pathway
Common upstream components
Distinct downstream components
CPH1
?
Shmoo formation, up-regulation of mating-associated genes, including MFA1
Increased cohesion, adhesion and biofilm formation, upregulation of cohesion, adhesion, biofilm genes, including CSH1

of both putative cell surface adhesion molecules and transcription factors, have revealed additional pheromone-induced genes in white cells, the up-regulation of which depends on the same pathway that regulates *CSH1* (Sahni *et al.*, submitted). Identification of the downstream transcription factor in the white pheromone response pathway represents our immediate challenge.

FAR1, which encodes a cyclin-dependent kinase inhibitor (Chenevert *et al.*, 1994; Valtz *et al.*, 1995), proved to play no apparent role in the white cell response. This was expected since white cells neither become blocked in G1 nor form shmoos in response to pheromone, the former response dependent on *FAR1* and the latter influenced by *FAR1* both in *S. cerevisiae* and *C. albicans*.

Regulation of *CPH1*

As is the case for the ortholog *STE12* in haploid *S. cerevisiae* (Roberts *et al.*, 2000), *CPH1* is up-regulated by pheromone in opaque cells of *C. albicans* (Zhao *et al.*, 2005b). Here, we have shown that it is not similarly up-regulated by pheromone in white cells. We have found that *CPH1* is expressed at a basal level in opaque cells in the absence of pheromone, and that basal expression depends on a functional receptor, heterotrimeric G-protein, and MAP kinase cascade, as was indicated by the results of Roberts *et al.* (2000). However, basal expression of *CPH1* is not dependent on *FAR1*. The possibility must, therefore, be considered that basal expression of *CPH1* may depend on a complete opaque pheromone response pathway, including *CPH1*, in which case, expression would depend on autoregulation at the level of transcription.

In contrast, pheromone induction of *CPH1* expression in opaque cells is dependent on *FAR1*, just as is pheromone induction of *STE12*, its ortholog in *S. cerevisiae* (see Supplement to Roberts *et al.*, 2000). This result, however, is paradoxical both for *S. cerevisiae* and *C. albicans*. If the target transcription factor of the pheromone response pathway is not up-regulated by pheromone in the *far1/far1* mutant of both haploid *S.*

cerevisiae and *MTL*-homozygous *C. albicans* cells, how does pheromone induce shmoo formation in a significant proportion of *far1* cells? The answer may lie in post-translational modification or stability. *STE12* activity has been demonstrated to be enhanced post-translationally by pheromone through *FUS3*-mediated phosphorylation (Elion *et al.*, 1993) and its stability decreased through the effect of pheromone on ubiquitin-mediated degradation (Esch *et al.*, 2006).

Evolutionary Implications of the Pheromone Response Pathways of *C. albicans*

We previously noted (Daniels *et al.*, 2006) that signaling of mating- incompetent white cells by mating-competent opaque cells to form a biofilm that facilitates mating, at least *in vitro*, was very much akin to the types of inductive events in embryogenic development, most notably between germ cells and somatically-derived follicle cells (Gilchrist *et al.*, 2004). Our demonstration here that white and opaque cells respond to the same signal through the same receptor, heterotrimeric G-Protein and MAP kinase cascade, but different target transcription factors (Figure 25), reveals a configuration more common in higher eukaryotes (Bacci *et al.*, 2005; Rincon and Pedraza-Alva, 2003), adding support to the suggestion (Daniels *et al.*, 2006) that the interactions between opaque and white cells may represent an antecedent to higher eukaryotic multicellularity.

CHAPTER 5
THE FIRST INTRACELLULAR LOOP OF THE ALPHA-PHEROMONE RECEPTOR REGULATES THE WHITE CELL PHEROMONE RESPONSE

Introduction

In Chapter 4, the molecular pathway regulating the *C. albicans* unique pheromone-induced white cell biofilm response was presented. Our results demonstrated that the pheromone-induced biofilm response pathway in white cells of *C. albicans* shared all of the upstream components, from the receptor through the MAP kinase cascade, with the opaque cell mating pathway (Yi *et al*., 2008). However, the key downstream transcription factor Cph1 mediating the opaque response, a different regulator (recently identified as Tec1) mediating the white response (Sahni *et al*., in preparation).

However, a discussion of my PI David R.Soll with Dr. Jeffrey Becker from the University of Tennessee made us aware of two peculiar differences in the α-pheromone receptor Ste2 of *C. albicans*. The *C. albicans* α-pheromone receptor is overall homologous to the α-pheromone receptor of *S. cerevisiae*. However, there are two interesting differences that exist. The *C. albicans* α-pheromone receptor has a long intracellular loop, IC1 of about 55 amino acids, whereas the IC1 loop in *S. cerevisiae* is 8 amino acids in length. The second difference is in the second extracellular loop, EC2, which is 30 amino acids long in *C. albicans*, whereas the EC2 loop in *S. cerevisiae* is 14 amino acids in length. Given that the pheromone-induced white cell biofilm response of *C. albicans* has no correlate in *S. cerevisiae*, we tested the possibility that one or both of the *C. albicans* (*Ca*)-specific regions might play a selective role in the white pheromone-induced biofilm response, but not opaque mating response.

To address this, we generated in an **a/a** strain mutations spanning different domains of the *C. albicans* α-pheromone receptor Ste2. Mutants were generated in the first

intracellular loop, IC1, the second extracellular loop, EC2, the third intracellular loop, IC3, and the C-terminus. These mutants were then tested both for the opaque pheromone responses, including shmoo formation, mating and cell cycle arrest, as well as the white pheromone responses including cohesion, adhesion and enhanced biofilm formation. Our results demonstrated that deletion of the IC1 domain selectively affected the white, but not the opaque cell pheromone responses. Deletion of the EC2 loop did not affect either white or opaque pheromone responses, whereas deletion of IC3 loop and the C-terminus affected both the white and opaque responses. Collectively, these results demonstrate that the *Ca*-specific IC1 region plays a selective role in the pheromone-induced white biofilm response unique to *C. albicans*. Furthermore, based on overexpression of the α or the β subunit of the G protein complex, we showed that the IC1 loop functions primarily through the pheromone responsive MAPK pathway. In this project, Song Yi and I shared equal senior authorship.

Materials and Methods

Strain Maintenance

Strains were maintained at 25 °C on agar containing modified Lee's medium (Bedell and Soll, 1979; Lee *et al.*, 1975) supplemented with 5 μg/ml phloxine B when differential staining of opaque sectors and colonies was required (Anderson and Soll, 1987). All strains used in this study are listed in Table 4.

Generation of Mutants

The parent strain P37005 was a natural **a**/**a** isolate from a bloodstream infection (Lockhart *et al.*, 2002). The *ste2/ste2* mutant, which was derived from strain P37005, and its complemented derivative *ste2*/*ste2*-*STE2* have been previously described (Yi *et al*., 2008). The following method was used to obtain mutants harboring deletions of different domains of the α-pheromone receptor Ste2 (Figure 26A, E-I), except for the C-terminal

Table 4. *C. albicans* strains used in the functional analysis of the Ste2 pheromone resceptor

Strain	Parent	*MTL*	Relevant Genotype	Reference or source
P37005	–	**a**/**a**	Wild type	Lockhart *et al.* (2002)
WO-1	–	α/α	Wild type	Slutsky *et al.* (1987)
ste2/*ste2*	P37005	**a**/**a**	*ste2*Δ::FRT/*ste2*Δ::FRT	Yi *et al.* (2008)
ste2/*ste2*-*STE2*	*ste2*Δ	**a**/**a**	*ste2*Δ::FRT/*STE2*-*GFP*::*SAT*^{R}	Yi *et al.* (2008)
ste2/*IC1p*Δ1	*ste2*Δ	**a**/**a**	*ste2*Δ::FRT/*STE2IC1p*Δ1-*GFP*::*SAT*^{R}	This study
ste2/*IC1p*Δ2	*ste2*Δ	**a**/**a**	*ste2*Δ::FRT/*STE2IC1p*Δ2-*GFP*::*SAT*^{R}	This study
ste2/*IC1f*Δ1	*ste2*Δ	**a**/**a**	*ste2*Δ::FRT/*STE2IC1f*Δ-*GFP*::*SAT*^{R}	This study
ste2/*EC2*Δ1	*ste2*Δ	**a**/**a**	*ste2*Δ::FRT/*STE2EC2*Δ-*GFP*::*SAT*^{R}	This study
ste2/*IC3*Δ1	*ste2*Δ	**a**/**a**	*ste2*Δ::FRT/*STE2IC3*Δ-*GFP*::*SAT*^{R}	This study
ste2/*CTer*Δ1	*ste2*Δ	**a**/**a**	*ste2*Δ::FRT/*STE2Cter*Δ-*GFP*::*SAT*^{R}	This study
P37005-tet*STE4*	P37005	**a**/**a**	*ADH1*/*adh1*Δ::ptet-*STE4*-*GFP*::*SAT*^{R}	This study
ste2/*IC1f*Δ1-tet*STE4*	*ste2*Δ/*IC1f*Δ1	**a**/**a**	*ste2*Δ::FRT/*STE2IC1f*Δ::FRT *ADH1*/*adh1*Δ::ptet-*STE4*-*GFP*::*SAT*^{R}	This study
P37005-tet*CAG1*	P37005	**a**/**a**	*ADH1*/*adh1*Δ::ptet-*CAG1*-*GFP*::*SAT*^{R}	This study
ste2/*IC1f*Δ1-tet*CAG1*	*ste2*Δ/*IC1f*Δ1	**a**/**a**	*ste2*Δ::FRT/*STE2IC1f*Δ::FRT *ADH1*/*adh1*Δ::ptet-*CAG1*-*GFP*::*SAT*^{R}	This study
vps34/*vps34*	P37005	**a**/**a**	*Vps34*Δ::FRT/*vps34*Δ::FRT	This study

Figure 26. Deletions of the α-pheromone receptor Ste2 generated in this study in order to test for a selective role in the white, but not opaque, pheromone response. A. Sequence comparison of *S. cerevisiae* Ste2 (ScSte2) and *C. albicans* Ste2 (CaSte2), and the locations of the generated deletions. The amino acid sequences were aligned with the Clustal W program (Thompson et al., 1994) available at http://align.genome.jp/clustalw/. Transmembrane domains were predicted with Split 4.0 (Juretic et al., 2002) at http://split.pmfst.hr/split/4/. Identical residues between the two proteins are denoted by stars, while conservative replacements of amino acid residues are denoted by either ":" (based on similar functional groups) or "." (based on similar effects on secondary structure). Predicted transmembrane domains are highlighted in red (TM1 to 7). Intracellular loops (IC1 to 3) and extracellular loops (EC1 to 3) are indicated by lines above the sequences: thick black lines denote regions that are predicted to be part of the loops in both ScSte2 and CaSte2; thick green lines denote regions predicted to make up part of a loop in one protein but are included in a predicted transmembrane region in the other. The *Ca*-specific 55 amino acid region of the IC1 loop is highlighted in blue. The regions deleted in different deletion mutants are indicated by thick purple lines below the targeted regions. B through J. Schematic diagram of Ste2 and deletion derivatives: B. *C. albicans* wild type; C. *S. cerevisiae*; D. *ste2*/*ste2-STE2*; E. *ste2*/*IC1p*Δ1; F. *ste2*/*IC1p*Δ2; G. *ste2*/*IC1f*Δ1; H. *ste2*/*EC2*Δ1; I. *ste2*Δ/*IC3*Δ1; and J. *ste2*/*CTer*Δ1. The different deletion derivatives of Ste2 and Ste2 of the complemented strain *ste2*/*ste2-STE2* were fused to *GFP* at their C-terminus.

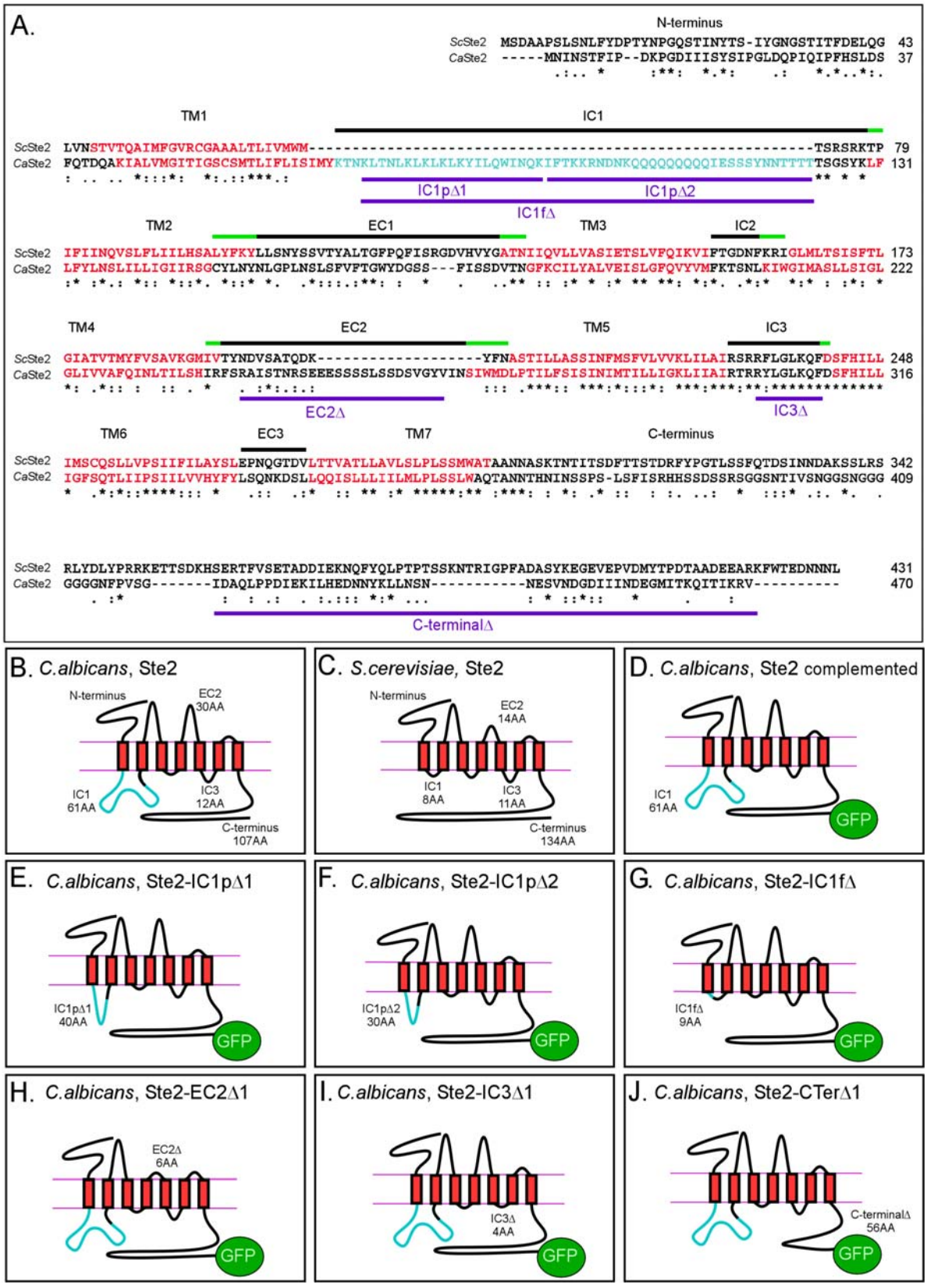
A.
N-terminus
ScSte2 MSDAAPSLSNLFYDPTYNPGQSTINYTS-IYGNGSTITFDELQG 43
CaSte2 -----MNINSTFIP--DKPGDIIISYSIPGLDQPIQIPFHSLDS 37
TM1
IC1
ScSte2 LVNSTVTQAIMFGVRCGAAALTLIVMWM----------TSRSRKTP 79
CaSte2 FQTDQAKIALVMGITIGSCSMTLIFLISIMYKTNKLTNLKLKLKLKYILQWINQKIFTKKRNDNKQQQQQQQQQIESSSYNNTTTTTSGSYKLF 131
IC1pΔ1
IC1pΔ2
IC1fΔ
TM2
EC1
TM3
IC2
ScSte2 IFIINQVSLFLIILHSALYFKYLLSNYSSVTYALTGFPQFISRGDVHVYGATNIIQVLLVASIETSLVFQIKVIFTGDNFKRIGLMLTSISFTL 173
CaSte2 LFYLNSLILLIGIIRSGCYLNYNLGPLNSLSFVFTGWYDGSS---FISSDVTNGFKCILYALVEISLGFQVYVMFKTSNLKIWGIMASLLSIGL 222
TM4
EC2
TM5
IC3
ScSte2 GIATVTMYFVSAVKGMIVTYNDVSATQDK----------YFNASTILLASSINFMSFVLVVKLILAIRSRRFLGLKQFDSFHILL 248
CaSte2 GLIVVAFQINLTILSHIRFSRAISTNRSEEESSSSLSSDSVGYVINSIWMDLPTILFSISININMTILLIGKLIIAIRTRRYLGLKQFDSFHILL 316
EC2Δ
IC3Δ
TM6
EC3
TM7
C-terminus
ScSte2 IMSCQSLLVPSIIFILAYSLEPNQGTDVLTTVATLLAVLSLPLSSMWATAANNASKTNTITSDFTTSTDRFYPGTLSSFQTDSINNDAKSSLRS 342
CaSte2 IGFSQTLIIPSIILVVHYFYLSQNKDSLLQQISLLLIILMLPLSSLWAQTANNTHNINSSPS-LSFISRHHSSDSSRSGGSNTIVSNGGSNGGG 409
ScSte2 RLYDLYPRRKETTSDKHSERTFVSETADDIEKNQFYQLPTPTSSKNTRIGPFADASYKEGEVEPVDMYTPDTAADEEARKFWTEDNNNL 431
CaSte2 GGGGNFPVSG-------IDAQLPPDIEKILHEDNNYKLLNSN----------NESVNDGDIIINDEGMITKQITIKRV---------- 470
C-terminalΔ
B. C.albicans, Ste2
N-terminus
EC2
30AA
IC1
61AA
IC3
12AA
C-terminus
107AA
C. S.cerevisiae, Ste2
N-terminus
EC2
14AA
IC1
8AA
IC3
11AA
C-terminus
134AA
D. C.albicans, Ste2 complemented
IC1
61AA
GFP
E. C.albicans, Ste2-IC1pΔ1
IC1pΔ1
40AA
GFP
F. C.albicans, Ste2-IC1pΔ2
IC1pΔ2
30AA
GFP
G. C.albicans, Ste2-IC1fΔ
IC1fΔ
9AA
GFP
H. C.albicans, Ste2-EC2Δ1
EC2Δ
6AA
GFP
I. C.albicans, Ste2-IC3Δ1
IC3Δ
4AA
GFP
J. C.albicans, Ste2-CTerΔ1
C-terminalΔ
56AA
GFP

deletion (Figure 26J). The plasmid pGEM-7Z (Promega Corp., Madison, WI) lacking the BamHI site was generated by digesting the plasmid with BamHI, followed by end repair with T4 DNA polymerase (Promega Corp.) and calf intestinal phosphatase (Promega Corp.). A DNA fragment spanning the *STE2* promoter and the 5′ end of the domain region to be deleted, was amplified using the primer pairs listed in Table 5. The underlined regions in each primer in Table 5 represent added restriction sites. Another DNA fragment spanning a region from the 3′ end of the region to be deleted to the last base of the *STE2* ORF was amplified by PCR using the primer pairs in Table 5. These two DNA fragments, bordering the targeted deletion sequence, were fused by PCR using the common primers IC1p1F1 and IC1p1R2, generating the 5′ flank sequence, including the in-frame *STE2* ORF lacking the truncated domain region. In the case of Ste2 C-terminal mutant, the 5′ flank sequence was obtained with a single PCR amplification, using the primer pair CterF1 and CterR1 (Table 5). Then, a 3′ flanking sequence, representing the 3′-untranslated region of *STE2*, which was common for all mutants including the C terminal deletion mutant, was amplified with the primers Ste2-3′F and Ste2-3′R (Table 5). The 5′ and 3′ flanking regions were then each digested with SbfI, fused together with T4 ligase, and ligated to the BamHI-minus pGEM-7Z derivative, to derive the plasmid pX1. A DNA fragment, containing both the green fluorescent protein (GFP) gene and the dominant selection marker *CaSAT1* (Reuss *et al.*, 2004), was amplified by PCR with the plasmid pK91.6 (Yi *et al*., 2008) as template and the primers GFCFSRB1 and SATBgF1 (Table 5). The *GFP-CaSAT1* fragment was digested with PstI and BglII, and ligated into the SbfI-BamHI digested, dephosphorylated plasmid pX1 to generate pX1-*GFP-SAT1*, which contained the different versions of the *STE2* ORF. *GFP* and the deletion sequences were demonstrated to be in frame by PCR sequencing. The plasmid, containing the *STE2* deletion derivative with *GFP* in-frame, was finally digested with XhoI and used to transform the *ste2/ste2* mutant, targeted to the *STE2* gene locus, according to the methods previously described (De Backer *et al*., 1999; Yi *et al*., 2008). At least three independent

Table 5. Oligonucleotides used in the functional analysis of the Ste2 pheromone resceptor

Primer	Gene/Purpose	Sequence
IC1p1F1	*IC1p*Δ1 mutant	5'-ATTGCTCGAGCTATTACTCGTTTTGATCGG-3'
IC1p1R1	*IC1p*Δ1 mutant	5'-ATTAGTTTTATACATTATAGAAATC-3'
IC1p1F2	*IC1p*Δ1 mutant	5'-TATAAAACTAATATCTTCACCAAAAAAAGGAAT-3'
IC1p1R2	*IC1p*Δ1 mutant	5'-CCATCCTGCAGGACACTCTTTTGATGGTGATTT-3'
IC1p2F1	*IC1p*Δ2 mutant	5'-ATTGCTCGAGCTATTACTCGTTTTGATCGG-3'
IC1p2R1	*IC1p*Δ2 mutant	5'-TTTTTGATTTATCCATTGCAAGATA-3'
IC1p2F2	*IC1p*Δ2 mutant	5'-ATAAATCAAAAAACGCTGGGGAGTTATAAATTA-3'
IC1p2R2	*IC1p*Δ2 mutant	5'-CCATCCTGCAGGACACTCTTTTGATGGTGATTT-3'
IC1fF1	*IC1f*Δ1 mutant	5'-ATTGCTCGAGCTATTACTCGTTTTGATCGG-3'
IC1fR1	*IC1f*Δ1 mutant	5'-ATTAGTTTTATACATTATAGAAATC-3'
IC1fF2	*IC1f*Δ1 mutant	5'-TATAAAACTAATACGCTGGGGAGTTATAAATTA-3'
IC1fR2	*IC1f*Δ1 mutant	5'-CCATCCTGCAGGACACTCTTTTGATGGTGATTT-3'
EC2F1	*EC2*Δ1 mutant	5'-ATTGCTCGAGCTATTACTCGTTTTGATCGG-3'
EC2R1	*EC2*Δ1 mutant	5'-GGAAAATCGAATATGAGATAAAATT-3'
EC2F2	*EC2*Δ1 mutant	5'-ATTCGATTTTCCATTAATTCAATATGGATGGA-3'
EC2R2	*EC2*Δ1 mutant	5'-CCATCCTGCAGGACACTCTTTTGATGGTGATTT-3'
IC3F1	*IC3*Δ1 mutant	5'-ATTGCTCGAGCTATTACTCGTTTTGATCGG-3'
IC3R1	*IC3*Δ1 mutant	5'-TCTTGTTCTAATAGCAATTATAAGT-3'
IC3F2	*IC3*Δ1 mutant	5'-TAATCTTGTTCTGATAGTTTCCATATTTTATT-3'
IC3R2	*IC3*Δ1 mutant	5'-CCATCCTGCAGGACACTCTTTTGATGGTGATTT-3'
CterF1	*CTer*Δ1 mutant	5'-ATTGCTCGAGCTATTACTCGTTTTGATCGG-3'
CterR1	*CTer*Δ1 mutant	5'-CCATCCTGCAGGAACCTGAAACAGGGAAATTC-3'

Table 5 --- continued

Ste2-3'F	3' flank (all mutants)	5'-ACACCTGCAGGCGGATCCTAATAAATATGGTGG TACAC-3'
Ste2-3'R	3' flank (all mutants)	5'-CTTGCTCGAGTGGGAAGTTTAGGTACTCTTC-3'
GFCFSRBF1	*GFP-SAT1* PCR	5'-TCGCCTGCAGGATGTCTAAAGGTGAAGAA-3'
SATBgF1	*GFP-SAT1* PCR	5'-TCAAGATCTTCCATCATAAAATGTCGA-3'
Ste4overexF	MAPK hyperactivation	5'-TCCGTCGACAAAGATGTCCGATTATCTTGCT-3'
Ste4overexR	MAPK hyperactivation	5'-TCCGTCGACAAGACGGACCAAACTTTGAT-3'
Cag1overexF	MAPK hyperactivation	5'-TCCGTCGACAAAGATGGGTTGTGGCGCTAGT-3'
Cag1overexR	MAPK hyperactivation	5'-TCCGTCGACAATATATAATACCACTCTTTTT-3'
KAR4F	Northern probe	5'-ATGTATACTTACAATAAGTTTGGG-3'
KAR4R	Northern probe	5'-TACCTCTGTAGCACCAGA-3'
CSH1F	Northern probe	5'-TCGACTCTGAAAAAACTA-3'
CSH1R	Northern probe	5'-CATGCCAATGAAACTTGC-3'
STE2F	Northern probe	5'-GTGTTCAACATAAGAAGA-3'
STE2R	Northern probe	5'-ATTATTAGCAGTTTGAGC-3'
VPS34F1	*VPS34* heterozygote	5'-AATAGACCTGGACTGCAA-3'
VPS34R1	*VPS34* heterozygote	5'-TCGCCCGGGCATTCCGGTTGTTGTTTT-3'
VPS34F2	*VPS34* heterozygote	5'-TCGCCCGGGATCTAGGGTAAATAGTAA-3'
VPS34R2	*VPS34* heterozygote	5'-CGAATGTGAGGTAATTGT-3'
VPS34F3	*VPS34* homozygote	5'-ACAAAGATAGCGACTACT-3'
VPS34R3	*VPS34* homozygote	5'-TCGCCCGGGTTAGAAGTAGTTTCAGTT-3'
VPS34F4	*VPS34* homozygote	5'-TCGCCCGGGTCGTCTTCATAGTCAAGA-3'
VPS34R4	*VPS34* homozygote	5'-TACTATAGAATCACGTGA-3'
VPS34F	Deletion probe	5'-ACTGGAGTGTTGATAAGT-3'
VPS34R	Deletion probe	5'-TGATCAGATCTTTCGCAA-3'

mutants were obtained for each deleted region in independent transformations. Each was verified by PCR sequencing and Southern analysis. In addition, a deletion mutant for the PI-3 kinase gene *vps34/vps34* was generated in the **a/a** strain P37005 using a two-step disruption strategy as previously reported (Yi *et al*., 2008). Three independent null mutants were obtained and confirmed by both PCR sequencing and Southern analysis. For every experiment performed, two or more independent mutants were tested and in every case found to give similar results.

Shmooing, Mating and G1 Arrest

The methods for quantitating shmoo formation in response to 3 x 10^{-6} M synthetic α-pheromone (13-mer) (Bennett *et al.*, 2003; Panwar *et al.*, 2003), synthesized by Open Biosystems (Huntsville, AL), have been described in detail (Lockhart *et al.*, 2003b; Yi *et al.*, 2008). The synthetic α-pheromone was dissolved in dimethyl-sulfoxide (DMSO). In all experiments not treated with pheromone, equal amount of DMSO was added. Cell cycle status was assessed by fluorescent-activated cell sorting (FACS), using 1 μM Sytox Green (Invitrogen, Carlsbad, CA) to stain nuclei, according to methods previously described (Yi *et al.,* 2008*)*. The methods for measuring mating frequencies between opaque **a**/**a** cells of a test strain and opaque α/α cells of strain WO-1 have also been described (Lockhart *et al.*, 2003a; Yi *et al.*, 2008).

Cohesion, Adhesion and Biofilm Formation

α-pheromone-induced cohesion in white cells suspension cultures was assessed according to the methods of Daniels *et al.* (2006). Samples were assessed for clumping after 6 hr. α-pheromone-induced adhesion on the bottoms of costar plastic six-cluster well plates (Corning Life Sciences, Lowell, MA) was assessed according to methods previously described (Daniels *et al.*, 2006; Yi *et al.*, 2008). Adhesion was assessed after 16 hr. White cell biofilm enhancement by minority opaque cells (5% opaque P37005 **a**/**a**

cells, and 5% opaque WO-1 α/α cells) was assessed according to the methods of Daniels *et al.* (2006). Biofilms were analyzed for thickness after 48 hr of incubation.

Immunolocalization of GFP-tagged Ste2 and Derivatives

White cells were grown in modified Lee's medium (Bedell and Soll, 1979) to saturation phase in suspension. Cells were pelleted, incubated in modified Lee's medium containing 3 x 10^{-6} M α-pheromone, fixed in 1% formaldehyde and washed in ice cold water. To produce spheroplasts, the methods of Liu *et al.* (2005) were used, with minor modifications. Cell pellets were resuspended in Z buffer (1 M sorbitol, 50 mM Tris-HCl, pH 7.4) containing 10 mM β-X mercaptoethanol and 10 mg per ml of zymolyase 20T (Seikagaku America, Falmouth, MA). After one hour, cells were pelleted, washed in 1 M sorbitol, resuspended in Z buffer plus 1% BSA, and permeabilized by the addition of 0.1% Triton-X 100. Spheroplasts were verified microscopically, and dispersed on a coverslip coated with poly-L-lysine (Sigma, St. Louis, MO). After attachment, the coverslip was washed with PBS-T (Gibco™ PBS-Invitrogen, Carlsbad, CA) containing 0.05% Tween-20 (Sigma). The coverslips were blocked with 10% normal goat serum (Sigma) in PBS for 1 hr at room temperature. Rabbit anti-GFP polyclonal antibody (Santa Cruz Biotechnology, Santra Cruz, CA) was diluted in 1% PBS containing goat serum and incubated on the coverslips overnight at 4 °C. The coverslips were washed three times with PBS-T and incubated with Alexa 488 goat anti-rabbit polyclonal antibody (Invitrogen) in 1% PBS containing goat serum at 37 °C for one hour. The secondary antibody was removed by three rinses with PBS-T and a final rinse with PBS. Coverslips were mounted using Prolong Gold™ (Invitrogen).GFP-localization was imaged through a Nikon TE2000 microscope attached to a BioRad MP2100 laser scanning confocal microscope. To ensure the validity of comparisons, confocal images were collected on the same day with identical acquisition parameters. Using LaserSharp™ software, Alexa 488 was excited using the 488 argon laser line at 10% power scan, images for each sample were collected through the

z-axis at the minimum aperture setting (0.7) with the gain set at 10.0 and the offset at 0. Each image presented in the figure represented a single scan at one optical plane. The control cell P37005 was analyzed at these settings and then with the aperture finally opened to be sure there was no cell surface autofluorescence. Phase images of the spheroplasts were gathered after the fluorescent image using a Microfire® digital camera (Optronics, Goleta, CA). All images were prepared for publication using Adobe Photoshop™ without image enhancement.

Western Blot

Cells were harvested 4 hr after pheromone treatment. Total cell protein was then extracted in a solution containing 50 mM HEPES (pH 7.6), 150 mM NaCl, 1 mM EDTA, 1% Triton-X-100, 0.1% sodium deoxycholate, 1 mM phenyl-methylsulfonyl fluoride and a protease inhibitor cocktail (Sigma, St. Louis, MO). Protein concentrations were determined according to the Bradford method using Coomassie Plus protein assay reagent (Pierce, Rockford, IL). An aliquot of each protein sample was then subjected to SDS-polyacrylamide gel electrophoresis as previously described (Srikantha *et al*., 2006). Following electrophoresis, the proteins were transferred to a PVDF membrane (Immobilon-P, Millipore Corporation, Bedford, MA) using an electrophoretic transfer cell (Bio-Rad, Hercules, CA). The membrane was blocked for 2 hr at room temperature in blocking buffer containing 3% nonfat dry milk in TBS-T (20 mM Tris-HCl , pH 7.5, 150 mM NaCl, 0.05% Tween-20). Rabbit anti-GFP polyclonal antibody (sc-8334, Santa Cruz Biotechnology, Santa Cruz, CA) was diluted 1:1000 in blocking buffer and then incubated with the membrane at 4 °C overnight. The membrane was gently washed five times in TBS-T. The primary antibody was detected with horseradish peroxidase-labeled goat anti-rabbit IgG (Promega, Madison, WI), diluted 1:20,000 in blocking buffer, developed with SuperSignal West Pico Chemiluminescent Substrate (Pierce, Rockford, IL), and exposed to autoradiography film (Molecular Technologies, St. Louis, MO).

Northern Analysis

For northern analyses, cells from saturation phase cultures were diluted into fresh medium in the absence or presence of 3 x 10^{-6} M α-pheromone, and pelleted after 4 hr. Total RNA was extracted using the RNeasy Mini Kit (Qiagen Sci., MA). Polymerase chain reaction (PCR) products were used for probing northern blots. The primers used to generate the PCR probe for each gene are listed in Table 5.

Inducible Expression of *STE4* and *CAG1*

The plasmid pNIM1 harboring the *CaSAT1* marker and doxycycline-regulated promoter was used in this study. This plasmid was a generous gift from Joachim Morschhäuser (University of Würzburg, Germany). The ORFs of the *STE4* and *CAG1* gene, amplified by PCR with primer pairs Ste4overexF, Ste4overexR, and Cag1overexF, Cag1overexR (Table 5), respectively, were digested with SalI and subcloned into the plasmid pNIM1, which had been digested with SalI and dephosphorylated, to derive pTet-STE4 and pTet-CAG1, respectively. These plasmids were then digested with ApaI plus SacII, and transformed into either the wild type strain P37005 or the Ste2p-IC1 full deletion mutant, in which the *CaSAT1* marker had been excised as described below. Activation of *STE4* and *CAG1* transcription by doxycycline was verified by Northern analysis. The IC1 full deletion construct pX1-*GFP-SAT1* containing the *STE2* IC1f orf was digested with SalI, followed by T4 polymerase repair and CIP dephosphorylation, then ligated together with the *SAT1*-2A flipper cassette (Yi *et al.*, 2008), generating plasmid pX1-*GFP-SAT1-2A*. This plasmid was used to transform *ste2*, to derive the *SAT1*-excisable IC1 full deletion mutant *ste2/IC1f*Δ*1-2*. Following incubation in YPM medium (Yi *et al.*, 2008), the *SAT1* marker was deleted from the IC1 full deletion mutant. This mutant derivative was found to behave similarly as the *ste2/ICf*Δ*1-1* strain for both the white and opaque response.

Results

Deletion Mutants

The *C. albicans* pheromone receptor Ste2 is 68% similar to that of *S. cerevisiae* (Figure 26A). Two notable differences, however, are an extra region of 55 amino acids in the first intracellular loop, ICl, and an extra region of 17 amino acids in the second extracellular loop, EC2 (Figure 26A, B, C). In *S. cerevisiae*, IC1, which is approximately eight amino acids in length, has been shown to play a weak role in G protein coupling and activation that could only be identified in a mutant background in which the carboxy terminal tail of the protein had been deleted (Chinault *et al.*, 2004). IC1 of *C. albicans* contains a six amino acid region at its carboxy end that is homologous to the IC1 loop of *S. cerevisiae* (Figure 26A). The role of *S. cerevisiae* EC2, which is approximately 14 amino acids in length, has not been determined. To investigate whether the extra *C. albicans*-specific regions in IC1 and EC2 play roles in the *C. albicans*-specific white cell response to pheromone, deletion mutants of the two regions were generated. In the case of IC1, partial deletion mutants lacking approximately the first two fifths (*ste2/IC1pΔ1*) or approximately the last three fifths (*ste2/IC1pΔ2*) of the *Ca*-specific region (Figure 26A, E, F) were generated. A nearly full deletion mutant, lacking the central 52 of 55 amino acids of the *Ca*-specific IC1 region (*ste2/IC1fΔ1*) (Figure 26A, G) was also generated. In both the partial and full deletion mutants, the six amino acids homologous to the *S. cerevisiae* IC1 loop, were retained. At the end of the *STE2* derivative of each deletion mutant of IC1, the *GFP* gene was placed in frame (Yi *et al.*, 2008) (Figure 26E, F, G). As a control, the *ste2/ste2* mutant (Yi *et al.*, 2008) used to generate the partial deletion mutants was complemented with a copy of the native *STE2* gene that included the *STE2* promoter, the *STE2* ORF, and the *GFP* gene fused in-frame at the carboxy terminus (Yi *et al.*, 2008) (Figure 26D). *STE2* was targeted to its native site in the genome in each mutant.

Deletion mutants were also generated for the extracellular loop EC2, the intracellular loop IC3 and the intracellular carboxy terminal tail of Ste2. IC3 and the tail have been demonstrated to play roles in G protein coupling and activation, ligand discrimination and endocytosis during signal transduction (Weiner *et al.*, 1993; Celic *et al.*, 2003; Stefan and Blumer, 1994; Konopka *et al.*, 1988; Rohrer *et al.*, 1993*;* Dosil *et al.*, 2000). For EC2 (amino acids 239 through 268), the central 24 of 30 amino acids were deleted to generate Ste2-EC2Δ1 (Figure 26H). This included 15 of the 17 amino acids in the *Ca*-specific EC2 region. For IC3, eight of the 12 amino acids were deleted to generate Ste2-IC3Δ1 (Figure 26I). And for the intracellular carboxy terminal tail of Ste2, the terminal 51 of 107 amino acids were deleted to generate Ste2-CTerΔ1 (Figure 26J). It should be noted that the deletion mutants generated for IC1, IC3, EC2 and the carboxy terminal tail of Ste2 all contained *GFP* fused in-frame with the derivative *STE2* gene. For brevity, the *GFP* tag has not been noted in the name of the mutants.

The Opaque Cell Responses of IC1 Deletion Mutants

Opaque cells of natural **a**/**a** strains respond to α-pheromone by arresting in G1, polarizing and forming mating projections (shmoo formation) (Miller and Johnson, 2002; Bennett *et al.,* 2003; Lockhart *et al.*, 2003a, b; Zhao *et al.*, 2005b; Daniels *et al.*, 2003, 2006). To test for shmoo formation, opaque cells of saturation phase cultures of the parent strain P37005, the null mutant *ste2/ste2*, the complemented *ste2* strain *ste2*/*ste2-STE2* and the three deletion mutants of the *Ca*-specific IC1 region were diluted into fresh liquid nutrient medium in the absence or in the presence of 3×10^{-6} M α-pheromone and analyzed for cellular phenotypes after four hours. At saturation phase, the majority of all tested strains had accumulated as unbudded singlets. After 4 hours in medium lacking α-pheromone, 81% of opaque P37005 cells and 76% of opaque *ste2*/*ste2-STE2* cells had formed buds; none of the cells of either strain had formed shmoos (Figure 27A, B). After four hours in the presence of α-pheromone, only 3 and 2%,

Figure 27. The *Ca*-specific regions of IC1 and EC2 of Ste2 are not necessary for shmoo formation by opaque cells in response to α-pheromone, but IC3 and the C-terminal intracellular tail are necessary. A. Quantitation of shmoo formation in response to 4 hr treatment with 3 x 10^{-6} M α-pheromone (chemically synthesized 13 mer). The total number of cells is the sum of four independent experiments. The "percent of population" represents the mean of the four experiments. Only the standard deviations for the population of shmoos are presented. B. Examples of shmoo formation in the parent strain P37005 and deletion mutants. Note that opaque cells of the mutants *ste2/ste2*, *ste2*/*IC3*1-1 and *ste2*/*CTer*1-1 do not form shmoos in response to α-pheromone, but the mutants *ste2*/*IC1p*Δ1-1, *ste2*/*IC1p*Δ2-1, *ste2*/*IC1f*Δ1-1 and *ste2*/*EC2*Δ1-1 do. The scale bar in panel B represents 5 μm.

A.

Shmoo formation in response to α-pheromone (4 hr)

Strain	alpha pheromone	Total No. of cells analyzed	Percent of Population: Unbudded cells (%)	Budded cells (%)	Shmoos (%)	Standard deviation for shmoos (%)
P37005	-	1025	19	81	0	0
	+	1207	28	3	69	8
ste2/ste2-STE2	-	1228	24	76	0	0
	+	1194	36	2	62	7
ste2/ste2	-	1143	37	63	0	0
	+	1276	30	70	0	0
ste2/IC1pΔ1-1	-	1090	22	78	0	0
	+	1244	34	2	64	6
ste2/IC1pΔ2-1	-	1152	29	71	0	0
	+	1098	26	4	70	7
ste2/IC1fΔ1-1	-	1200	39	61	0	0
	+	1311	24	3	73	8
ste2/EC2Δ1-1	-	1233	35	65	0	0
	+	1179	36	3	61	6
ste2/IC3Δ1-1	-	1137	32	68	0	0
	+	1086	36	64	0	0
ste2/CTerΔ1-1	-	1250	28	72	0	0
	+	1166	29	71	0	0

B.

Examples of major phenotypes

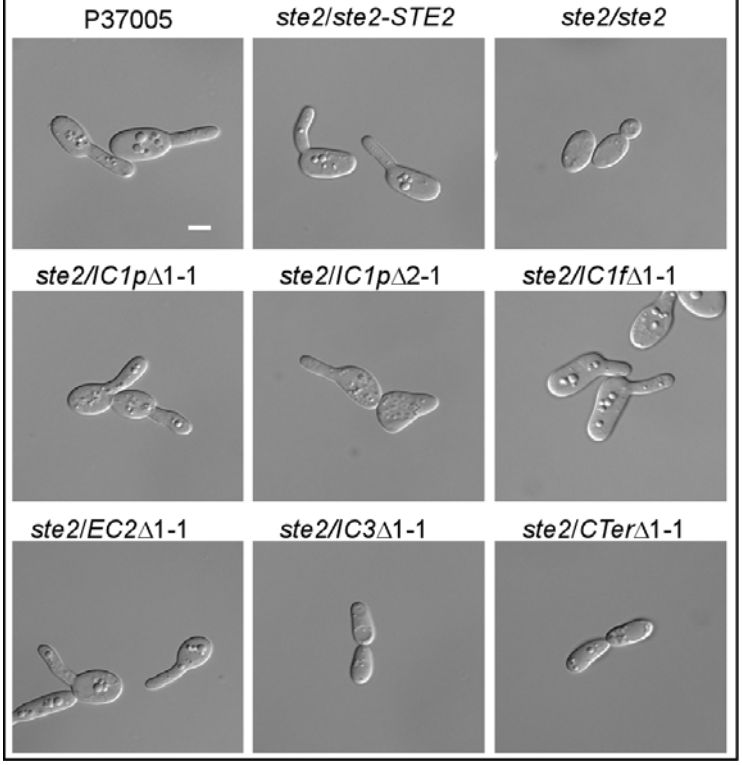

respectively, of opaque P37005 and *ste2*/*ste2*-*STE2* cells had formed buds, whereas 69% and 62% had formed shmoos (Figure 27A, B). Opaque cells of *ste2/ste2* formed buds exclusively after four hours in both the absence and presence of α-pheromone (Figure 27A, B), as previously demonstrated (Yi *et al.*, 2008). In the absence of α-pheromone, a majority of opaque cells of both the partial deletion mutants *ste2*/*IC1pΔ1-1* and *ste2*/*IC1pΔ2-1*, and the full deletion mutant *ste2*/*ICfΔ1-1*, formed buds after 4 hours, while in the presence of α-pheromone a majority of each mutant formed shmoos, and at levels comparable to those of opaque cells of the control strains P37005 and *ste2*/*ste2*-*STE2* (Figure 27A, B). Moreover, the conjugation tubes formed by opaque cells of the partial and full loop deletion mutants of the *C. albicans*-specific IC1 region were similar in length and shape to those of opaque cells of the control strains P37005 and *ste2*/*ste2*-*STE2* cells (Figure 27B). The induction of shmoo formation by α-pheromone was, therefore, unaffected by partial or full deletion of the *Ca*-specific IC1 region.

To test whether deletion mutants of the *Ca*-specific ICl region responded to α-pheromone by accumulating in G1 (Zhao *et al.*, 2005b), fluorescence activated cell sorting (FACS) was used to measure the proportion of a population that had undergone DNA replication four hours after release from stationary phase. In the absence of pheromone, the proportion of opaque cells of the control strains P37005 and *ste2*/*ste2*-*STE2* was 0.58 and 0.47, respectively (Figure 28A and B, respectively; Figure 28F). In the presence of α-pheromone, the proportions dropped to 0.20 in both strains, a decrease of 66% and 57%, respectively (Figure 28A and B, respectively; Figure 28F). The proportion of opaque cells of strain *ste2/ste2* that had undergone DNA replication was similar in the absence and presence of α-pheromone (Figure 28C), 37% and 35%, respectively (Figure 28F). In both the partial mutant *ste2/IC1pΔ2-1* and the full deletion mutants *ste2/IC1fΔ1-1*, α-pheromone caused a decrease in the proportion of cells that had undergone DNA replication (Figure 28D, E) that was similar to that of control strains (Figure 28A, B and F). These results demonstrate that the *Ca*-specific IC1 region does not

Figure 28. The *Ca*-specific IC1 region of Ste2 is not necessary for the G1 arrest caused by α-pheromone in opaque cells. A through E. Fluorescence activated cell sorting (FACS) analysis of control strains (P37005, *ste2*/*ste2-STE2*) and mutant strains (*ste2/ste2*, *ste2*/*IC1p*Δ2-1, *ste2*/*IC1f*Δ1-1). Saturation phase cells were released into fresh medium in the absence (-) and presence (+) of α-pheromone incubated for 3 hr, then fixed and stained with Sytox Green™ for DNA (Yi et al., 2008). The first peak represents unreplicated DNA, the second peak represents replicated DNA, and measurements in between represents replicating DNA. F. The proportion of the populations of control and mutant opaque cells that have undergone DNA replication in the absence and presence of pheromone. The proportions represent the mean of three replicates. The standard deviations were less than 10% of the mean in every case.

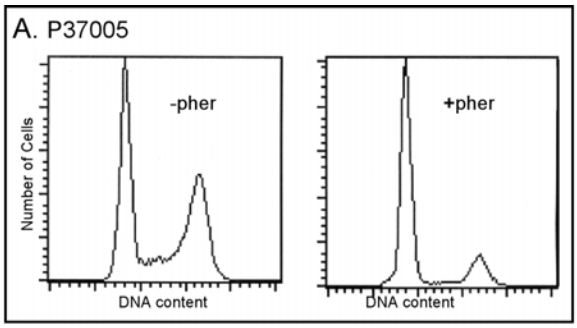

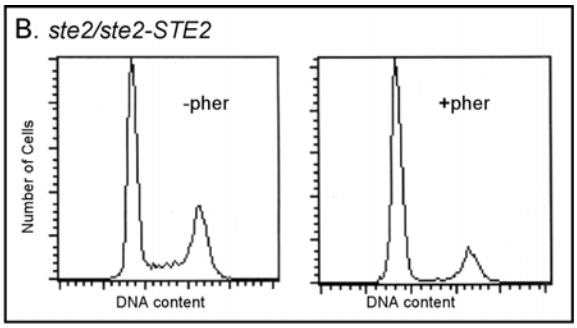

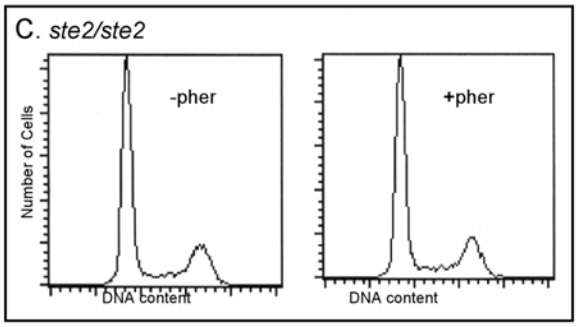

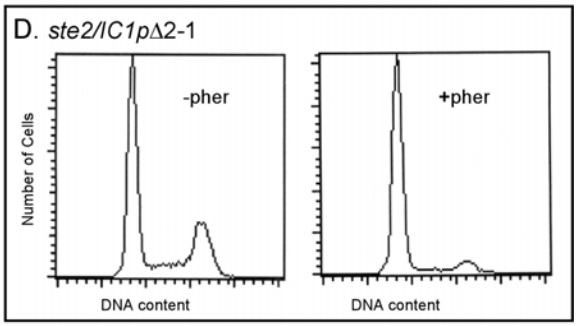

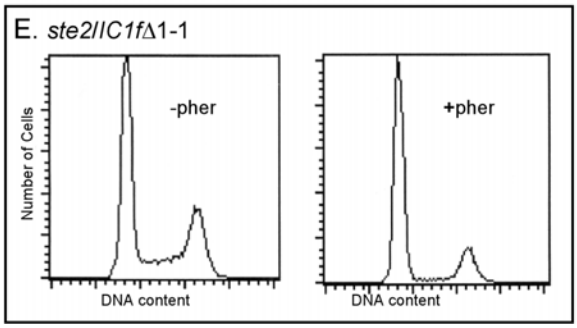

F. Quantitation

Strain	Proportion of population that has undergone DNA replication: -α-pheromone	Proportion of population that has undergone DNA replication: +α-pheromone	Percent decrease in proportion.
P37005	0.58	0.20	66%
ste2/ste2-STE2	0.47	0.20	57%
ste2/ste2	0.37	0.35	5%
ste2/IC1pΔ2-1	0.43	0.12	72%
ste2/IC1fΔ1-1	0.47	0.22	53%

play a role either in shmoo formation or in the α-pheromone-induced G1 block of opaque **a**/**a** cells.

To test if the *Ca*-specific IC1 region played a role in mating (*i.e.*, fusion with cells of opposite mating type), opaque cells of control strains P37005 and *ste2/ste2-STE2*, and the deletion mutants *ste2/IC1pΔ1-1*, *ste2/IC1pΔ2-1* and *ste2/IC1fΔ1-1*, which were all **a**/**a**, were mixed with opaque cells of the natural α/α strain WO-1. The mixtures were maintained in suspension for 12 hours (Lockhart *et al.*, 2003a). The proportion of fused cells was then determined for each mixture. In the absence of opaque WO-1 cells, 0% of control opaque cells of strains P37005 and *ste2*/*ste2-STE2* underwent fusion, and in the presence of opaque WO-1 cells, 24 and 20%, respectively, underwent fusion (Figure 29A). In the absence or presence of WO-1 cells, 0% of *ste2/ste2* cells underwent fusion (Figure 29A), as previously reported (Yi *et al.*, 2008). For the two partial and full IC1 deletion mutants, the results were similar to those for opaque cells of control strains P37005 and *ste2*/*ste2-STE2* (Figure 29A). Examples are presented in Figure 29B of fusions with WO-1 for opaque cells of strain P37005, *ste2/ste2-STE2*, *ste2*/*IC1pΔ1-1*, *ste2*/*IC1pΔ2-1* and *ste2*/*IC1fΔ1-1*. The fusants formed between WO-1 and the partial and full loop deletion mutants were morphologically similar to those formed between WO-1 and control strains (Figure 29B). Fusants of all the tested strains formed daughter buds from their conjugation bridges. These results indicate that the *Ca*-specific IC1 region is not essential for opaque cell fusion.

Opaque Cell Response of the EC2, IC3 and Tail Deletion Mutants

Deletion of the major portion of the *Ca*-specific region of the second extracellular loop EC2 had no effect on pheromone-induced shmoo formation in opaque cells (Figure 27A, B). In contrast, deletion of a major portion of the third intracellular loop or deletion of the carboxy terminal 51 amino acids of Ste2 blocked shmoo formation

Figure 29. The *Ca*-specific IC1 and EC2 regions of Ste2 are not necessary for mating (fusion) between opaque cells of opposite mating types, but the IC3 loop and C-terminal intracellular tail are necessary. A. Quantitation of fusion between control and mutant opaque **a**/**a** cells, and opaque α/α cells of the mating partner WO-1. The data of four independent experiments were pooled for quantitation. B. Examples of fusions. The scale bar in panel B represents 5 μm.

A. Mating efficiency

Strain	Mating partner WO-1 (α/α)	Total No. of cell analyzed	No. of cells in fusants	Percent of mating cells
P37005	-	3024	0	0%
	+	3540	842 ± 21	24%
ste2/ste2-STE2	-	3113	0	0%
	+	2994	610 ± 14	20%
ste2/ste2	-	2975	0	0%
	+	3122	0	0%
ste2/IC1pΔ1-1	-	3308	0	0%
	+	3611	926 ± 24	26%
ste2/IC1pΔ2-1	-	2946	0	0%
	+	3272	730 ± 17	22%
ste2/IC1fΔ1-1	-	3007	0	0%
	+	3483	802 ± 19	23%
ste2/EC2Δ1-1	-	2859	0	0%
	+	3015	806 ± 20	27%
ste2/IC3Δ1-1	-	3226	0	0%
	+	3228	0	0%
ste2/CTerΔ1-1	-	3264	0	0%
	+	3030	0	0%

B. Examples of fusants with α/α strain (WO-1)

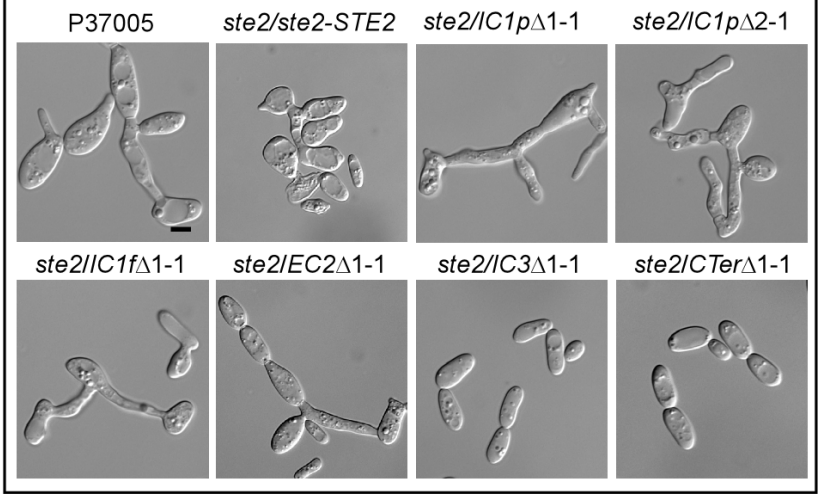

by opaque cells in response to α-pheromone (Figure 27A, B). Deletion of the major portion of the *Ca*-specific region of EC2 had no effect on fusion (Figure 29A, B). But as was the case for shmoo formation, deletion of a major portion of the IC3 or deletion of the C-terminal 51 amino acids of Ste2 blocked mating (Figure 29A, B).

White Cell Cohesion and Adhesion Responses of IC1 Deletion Mutants

To assess the effects of partial or full deletions of the *Ca*-specific IC1 region on the white cell response to α-pheromone, we first tested α-pheromone-induced cohesion (Daniels *et al.*, 2006). White cells of strain P37005, *ste2*/*ste2-STE2*, *ste2/ste2* , *ste2*/*IC1pΔ1-1*, *ste2*/*IC1p*Δ*2-1* and *ste2*/*IC1fΔ1-1* were incubated in suspension either in the absence or presence of 3 x 10^{-6} M α-pheromone for six hours, then distributed through a wide-bore pipette onto a slide and the average number of cells per aggregate counted. In the absence of pheromone, the majority of cells of control strains P37005 or *ste2*/*ste2-STE2* remained independent or formed only very small aggregates containing two to six cells (Figure 30J). In the presence of α-pheromone the majority of white cells of both control strains formed large aggregates, containing on average 170 and 150 cells, respectively (Figure 30A, B, J). α-pheromone did not induce aggregation in strain *ste2*/*ste2* (Figure 30C, J), as previously reported (Yi *et al.*, 2008). α-pheromone induced both partial deletion mutants of the *Ca*-specific IC1 region to form aggregates but at reduced average size (Figure 30D, E, J). The reduction in the average number of cells per aggregate for *ste2*/*IC1p*Δ*1-1* and *ste2*/*IC1p*Δ*2-1* was 50 and 73%. α-pheromone did not stimulate cohesion in the full IC1 deletion mutant *ste2*/*IC1f*Δ*1-1* (Figure 30F, J).

We then assessed whether partial or full deletion of the *Ca*-specific IC1 region affected α-pheromone-induced adhesion of white cells to a plastic surface, the first step in biofilm formation (Hawser and Douglas, 1994). White cells of control and deletion mutants were incubated in the wells of a 6-cluster well plate for 16 hours in the absence or

Figure 30. IC1, IC3 and C-terminal regions of Ste2 are essential for pheromone-induced white cell cohesion. Saturation phase cells of each strain were diluted into fresh medium in the absence (-) and presence (+) of 3 x 10^{-6} M α-pheromone, incubated for 6 hr, then distributed on slides to assess clump size. A through I. Representative fields of control strains (P37005, *ste2*/*ste2-STE2*) and mutant strains revealing the degree of cohesion in the presence of pheromone. J. Quantitation of clump size (cohesion). Error bars in the histograms represent standard deviations for measurements of 20 aggregates analyzed for each strain. The scale bar in panel A represents 5 μm.

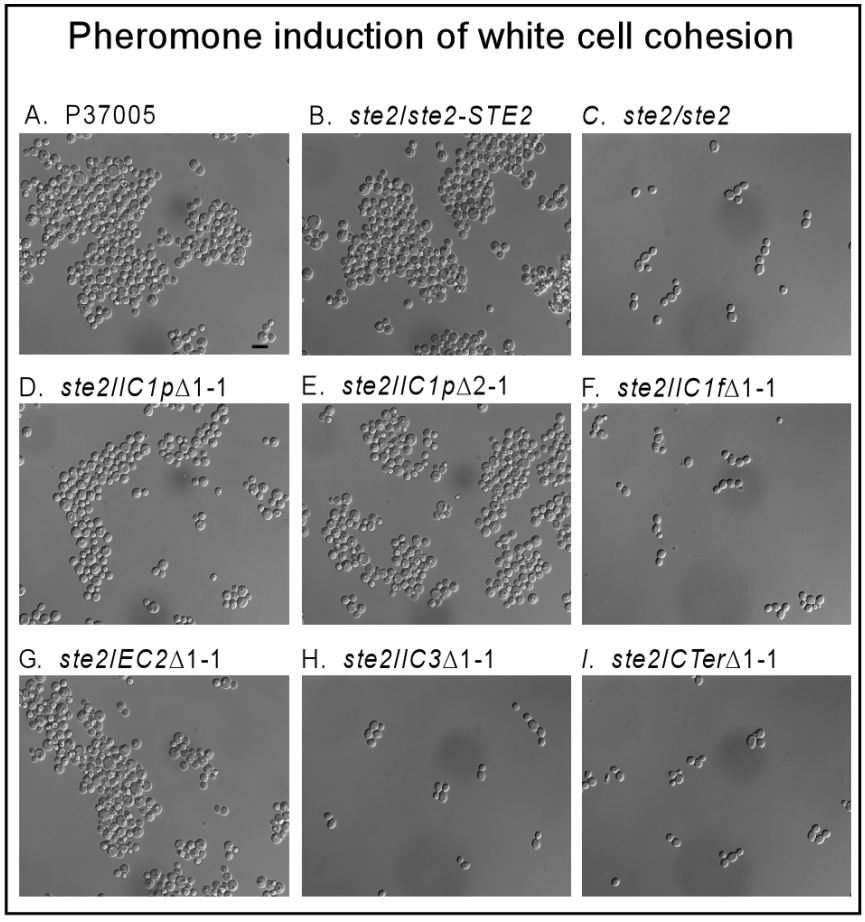
Pheromone induction of white cell cohesion
A. P37005
B. ste2/ste2-STE2
C. ste2/ste2
D. ste2/IC1pΔ1-1
E. ste2/IC1pΔ2-1
F. ste2/IC1fΔ1-1
G. ste2/EC2Δ1-1
H. ste2/IC3Δ1-1
I. ste2/CTerΔ1-1

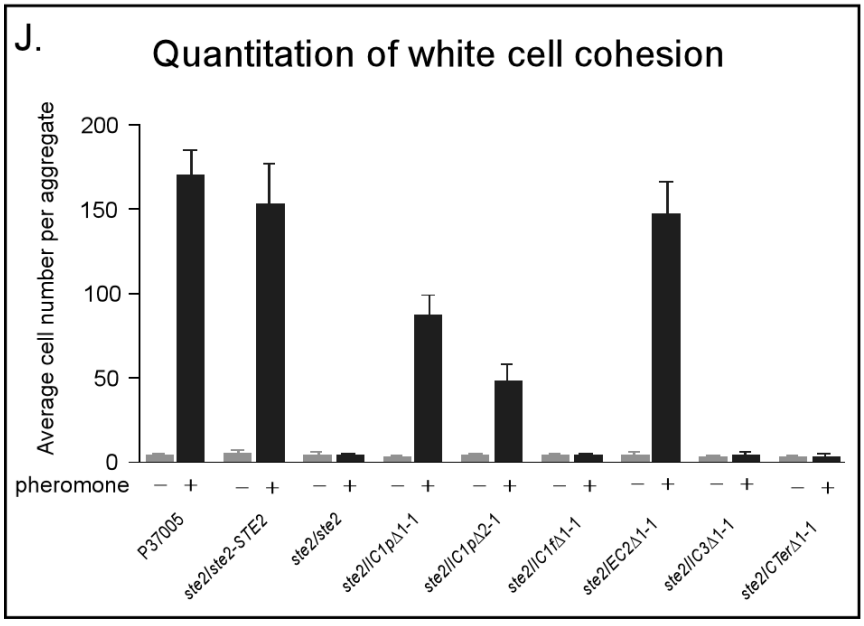
J.
Quantitation of white cell cohesion
Average cell number per aggregate
200
150
100
50
0
pheromone
– + – + – + – + – + – + – + – + – +
P37005
ste2/ste2-STE2
ste2/ste2
ste2/IC1pΔ1-1
ste2/IC1pΔ2-1
ste2/IC1fΔ1-1
ste2/EC2Δ1-1
ste2/IC3Δ1-1
ste2/CTerΔ1-1

presence of 3 x 10^{-6} M synthetic α-pheromone, the polystyrene well bottom gently washed and the cells adhering photographed. The cells on the well bottoms were then suspended and counted. In the absence of α-pheromone, white cells of the two control strains, the *ste2* strain and both the two partial and full deletion mutants of the *Ca*-specific IC1 region were non-adherent (Figure 31J). In the presence of α-pheromone, white cells of control strains P37005 and *ste2*/*ste2-STE2* formed thick films on the plastic well surface (Figure 31A and B, respectively), with densities of 2.1 x 10^8 and 2.3 x 10^8 cells per well bottom, respectively (Figure 31J). In the presence of α-pheromone, white cells of the mutant *ste2*/*ste2* were non-adherent (Figure 31C, J). In the presence of α-pheromone, white cells of the two partial deletion mutants *ste2/IC1pΔ1-1* and *ste2/IC1pΔ2-1* adhered, but adherence was reduced by 43 and 67 %, respectively, when compared with control cells (Figure 31D, E, J), roughly the same reductions observed for cohesion (Figure 30J). In the presence of α-pheromone, white cells of the full deletion mutant were non-adherent (Figure 31F, J).

White Cell Cohesion and Adhesion Responses of EC2, IC3 and Carboxy Terminal Deletion Mutants

In the absence of pheromone, white cells of the deletion mutants *ste2*/*EC2Δ1-1*, *ste2*/*IC3Δ1-1* and *ste2*/*CTerΔ1-1* were not cohesive (Figure 30J). In the presence of α-pheromone, white cells of *ste2*/*EC2Δ1-1* became cohesive at levels similar to that of control cells (Figure 30G, J), but white cells of *ste2*/*IC3Δ1-1* and *ste2/CTerΔ1-1*, did not (Figure 30H, I, J). Similar results were obtained for α-pheromone-induced adhesion to a plastic surface. Whereas α-pheromone induced adhesion in white cells of *ste2*/*EC2Δ1-1* (Figure 31G, J), it did not do so in white cells of *ste2*/*IC3Δ1-1* or *ste2*/*CTerΔ1-1* (Figure 31H, I, J).

Figure 31. The *Ca*-specific IC1 region, as well as the IC3 loop and the C-terminal tail of Ste2 are essential for pheromone-induced adhesion to plastic. Saturation phase cells of each strain were incubated in plastic wells in the absence (-) and presence (+) of 3 x 10^{-6} M pheromone. The wells were then gently washed and photographed. Adhering cells were released by trypsin and counted. A through I. Examples of the bottoms of wells after washing of control and mutant strains, that had been incubated in the presence of α-pheromone. J. Quantitation of the cells that adhered to the dish bottom. The mean ± standard deviation (error bar) of three dishes is presented.

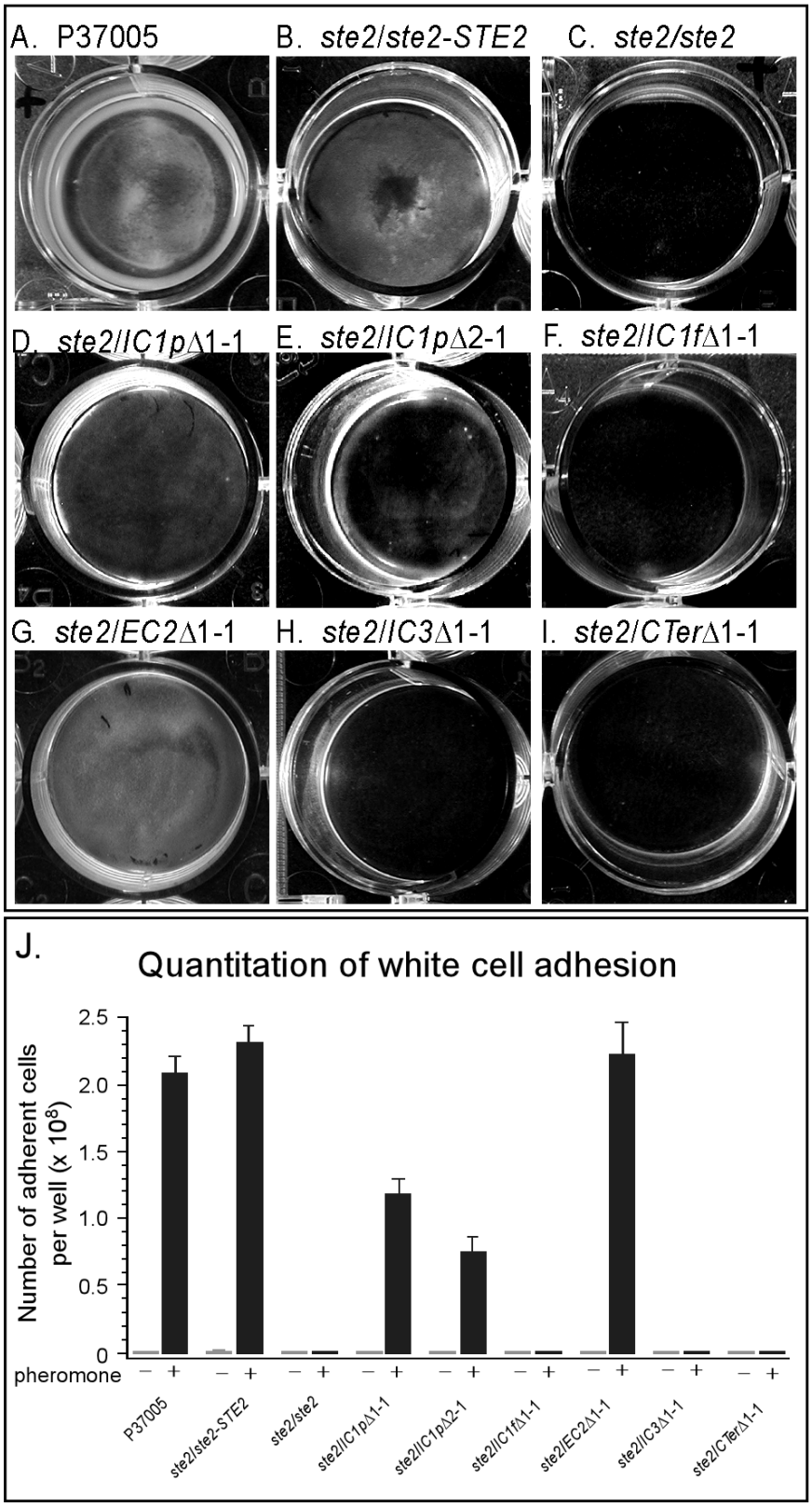
A. P37005
B. ste2/ste2-STE2
C. ste2/ste2
D. ste2/IC1pΔ1-1
E. ste2/IC1pΔ2-1
F. ste2/IC1fΔ1-1
G. ste2/EC2Δ1-1
H. ste2/IC3Δ1-1
I. ste2/CTerΔ1-1
J.
Quantitation of white cell adhesion
Number of adherent cells per well (x 10^8)
2.5
2.0
1.5
1.0
0.5
0
pheromone
– + – + – + – + – + – + – + – + – +
P37005
ste2/ste2-STE2
ste2/ste2
ste2/IC1pΔ1-1
ste2/IC1pΔ2-1
ste2/IC1fΔ1-1
ste2/EC2Δ1-1
ste2/IC3Δ1-1
ste2/CTerΔ1-1

White Cell Biofilm Response of the Deletion Mutants

Finally we tested whether partial or full deletion of the *Ca*-specific IC1 region played a role in the enhancement of majority white cell biofilm formation by minority opaque cells (Daniels *et al.*, 2006). To assess the enhancement effect, white **a**/**a** cells of control or deletion mutants were combined with a 50:50 mixture of opaque α/α cells of strain WO-1 and opaque **a**/**a** cells of strain P37005 at a ratio of 90:10, distributed on silicone elastomer squares, incubated for 90 minutes, rinsed to remove nonadherent cells, and incubated for an additional 48 hours (Daniels *et al.*, 2006). The addition of the mixture of opaque α/α and opaque **a**/**a** cells had been shown to stimulate the thickness of majority white **a**/**a** cell biofilm through the release of α-pheromone (Daniels *et al.*, 2006). It was presumed that opaque **a**/**a** cells stimulated α-pheromone production by opaque α/α cells, which in turn stimulated white **a**/**a** cells. Nine measurements of thickness were made that included three random ones for each of three independently formed biofilms of each strain alone (i.e., in the absence of opaque cells) or mixed with 10% opaque cells (Daniels *et al.*, 2006; Yi *et al.*, 2008).

In the absence of opaque cells, white cells of the control strains P37005 (Figure 32A) and *ste2*/*ste2*-*STE2* (data not shown) formed uniformly thick biofilms with average depths of 30 ± 2 and 30 ± 3μm, respectively (Figure 32K). Cells in the basal layer attached to the substratum were in the yeast phase. In the presence of opaque cells, the average depths of the two control strains were 57 ± 3 and 59 ± 4 μm, increases of 90% and 97%, respectively (Figure 32B, C, K). Cells in the basal layer were also in the yeast phase. In the absence or presence of opaque cells, white cells of the mutant *ste2/ste2* formed fragile, uneven, patchy biofilms, which attained maximum depths, at the apices of patches, of 25 ± 1 and 25 ± 3 μm, respectively (Figure 32K). Regions between patches frequently were less than 5μm thick and in some cases, contained no cells. A confluent basal layer of yeast cells did not form at the substratum. The patches usually contained

Figure 32. The *Ca*-specific IC1 region, as well as the IC3 loop and the C-terminal tail region of Ste2 are essential for normal biofilm development in the absence of α-pheromone, and the full *Ca*-specific IC1 region is necessary for complete pheromone enhancement. Majority white cells (90%) were mixed with a 50:50 mixture of opaque a/a and opaque α/α cells (10%), and the mixture incubated on a silicone elastomer square for 48 hr. A through J. z-series projections of laser scanning confocal microscope scans of biofilms viewed from the side for control (P37005, *ste2*/*ste2*-*STE2*) and mutant strains. In all cases but panel A the biofilms were developed in the presence (+) of 10% opaque cells (50:50 a/a and α/α). In panel A, the biofilm of P37005 was developed in the absence of opaque cells. For strains ste2 (D), *ste2*/*IC1f*Δ1-1 (G), *ste2*/*IC3*Δ1-1 (I) and *ste2*/*CTer*Δ1-1 (J), the biofilms were patchy, so scans through the thickest region of patches (left) and through the thin interpatch regions (right) are presented in these panels. K. Quantitation of average thickness. Average thickness of biofilms or in parenthesis the thickest portions of patches is presented as the mean ± standard deviation of nine measurements, three from each of three independent biofilms.

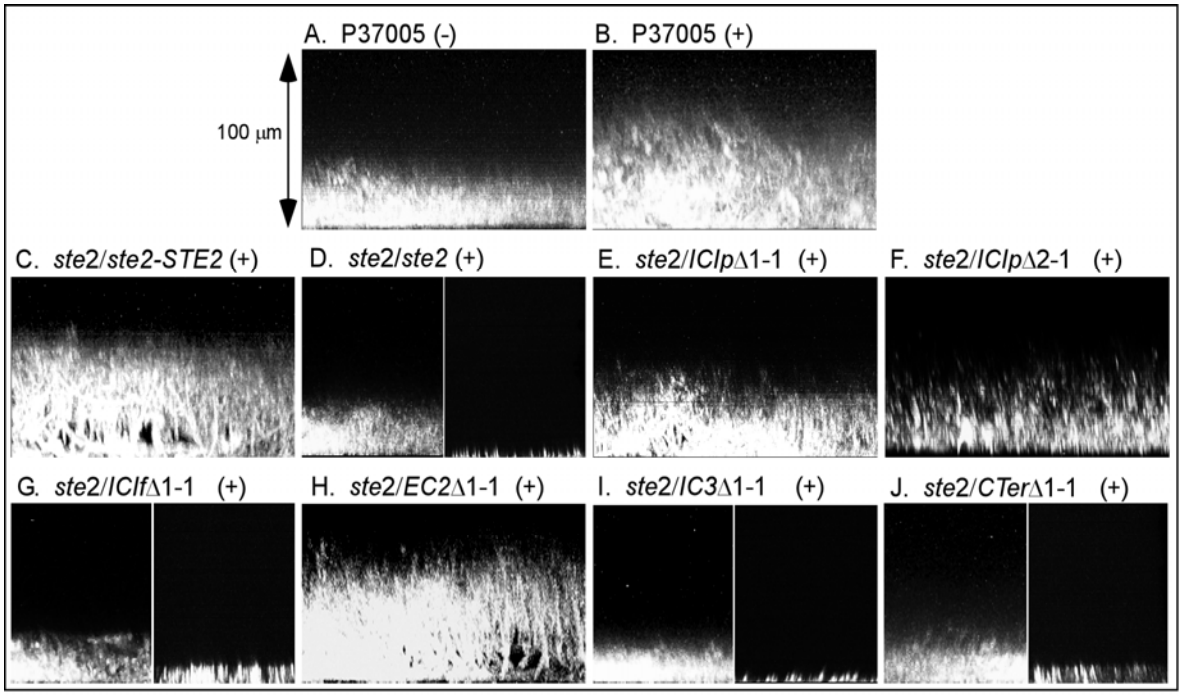

K.

Strain	Biofilm Thickness (μm) (-) opaque cells	(+) opaque cells	Percent increase
P37005	30±2	57±3	90%
ste2/ste2-STE2	30±3	59±4	97%
ste2/ste2	(25±1)	(25±3)	0%
*ste2/IC1p*Δ1-1	26±1	40±2	54%
*ste2/IC1p*Δ2-1	25±2	39±2	56%

Strain	Biofilm Thickness (μm) (-) opaque cells	(+) opaque cells	Percent increase
*ste2/IC1f*Δ1-1	(21±2)	(21±9)	0%
*ste2/EC2*Δ1-1	33±1	60±4	82%
*ste2/IC3*Δ1-1	(22±2)	(27±3)	23%
*ste2/CTer*Δ1-1	(23±2)	(23±3)	0%

hyphae, but on occasion they contained clumps of opaque cells. It was, therefore, far more difficult to compare their thickness with that of control cell biofilms the depths of which were relatively uniform across the elastomer surface, or to assess the enhancement of biofilm thickness by opaque cells. Images of a patchy and sparse surface of the film formed by *ste2/ste2* are presented in Figure 32D.

In the absence of opaque cells, the partial IC1 deletion mutants *ste2*/*IC1pΔ1-1* and *ste2*/*IC1pΔ2-1* formed uniformly thick biofilms with average depths of 26 ± 1 and 25 ± 2 μm, respectively (Figure 32K). In the presence of opaque cells, the average thickness of biofilms formed by the two partial mutants was 40 ± 2 and 39 ± 2 μm, respectively, increases of 54 and 56% (Figure 32E, F, K). The relative increases caused by opaque cells were roughly half those observed for control strains (Figure 32K). The biofilms of both partial deletion mutants contained basal layers of yeast cells in the absence or presence of α-pheromone. Interestingly, the percent reductions in opaque cell enhancement of the partial mutant biofilms were similar to the percent reductions exhibited by these two mutants for α-pheromone-induced cohesion and adhesion (Figure 30 and 31, respectively). In the absence and presence of opaque cells, white cells of the full deletion mutant *ste2/IC1fΔ1-1* formed fragile, uneven, patchy biofilms lacking uniform basal layers of yeast cells (Figure 32G, K), very much like those formed by white *ste2/ste2* cells (Figure 32D, K). The biofilms of *ste2/IC1fΔ1-1* cells attained maximum depths at patch apices in the absence and presence of opaque cells of 21 ± 2 and 21 ± 9 μm, respectively (Figure 32K).

Biofilms formed by white cells of the deletion mutant *ste2*/*EC2Δ1-1* in the absence and presence of opaque cells were similar to those formed by control strains (Figure 32H, K). In contrast, biofilms formed by the deletion mutants *ste2*/*IC3Δ1-1* and *ste2*/*CTerΔ1-1* in the absence and presence of opaque cells were similar to those formed by the *ste2* mutant and the *ste2*/*IC1fΔ1-1* mutant (Figure 32I, J, K).

Sensitivity to Varying Concentrations of Pheromone

In all of the preceding experiments in which we tested the effects of α-pheromone, we employed a concentration of 3 x 10^{-6} M. In earlier studies in our laboratory, this concentration had been found empirically to be the minimum which caused a maximum or near maximum response in both opaque and white cells (Lockhart *et al.*, 2003b; Daniels *et al.*, 2006; Yi *et al.*, 2008). The possibility was therefore entertained that partial or full deletion of the *Ca*-specific IC1 region selectively decreased the sensitivity of the receptor to the ligand in white, but not opaque, cells. If true, then a higher concentration of α-pheromone might rescue the defects of *Ca*-specific IC1 deletion mutants. To test this possibility, we performed experiments in which the opaque-specific shmoo response and the white-specific adherence response, were measured as functions of α-pheromone concentration for the control strain *ste2*/*ste2-STE2*, the partial deletion mutant *ste2*/*IC1pΔ2-1*, and the full deletion mutant *ste2*/*IC1fΔ1-1*.

The dose-response curves for shmoo formation were indistinguishable between opaque cells of strain *ste2*/*ste2-STE2*, *ste2*/*IC1pΔ2-1* and *ste2*/*IC1fΔ1-1* (Figure 33A). When normalized to maximum shmoo formation (the proportion at 3 x 10^{-5} M), the three curves were nearly superimposable (Figure 33B), indicating that opaque cells with partial or full deletions of the *Ca*-specific IC1 region exhibited the same sensitivity to α-pheromone concentrations as control cells. The dose-response curve for adhesion of white *ste2*/*ste2-STE2* cells to a plastic surface (Figure 33C) was similar to the dose-response curve for shmoo formation of opaque *ste2*/*ste2-STE2* cells (Figure 33A). The curve of the partial mutant *ste2/IC1pΔ2-1*, however, differed. Although sigmoidal, it was reduced by approximately half at all concentrations (Figure 33C). However, when the dose-response curves of white *ste2*/*ste2-STE2* and *ste2*/*IC1pΔ2-1* were normalized to the percent maximum response (the proportions at 3 x 10^{-5} M), they proved similar (Figure 33D). This indicated that deletion of approximately half the *Ca*-specific IC1 region of the α-pheromone receptor results in partial loss of the α-pheromone-induced adhesion

Figure 33. The sensitivity of white cells of the partial deletion mutant *ste2*/*IC1p*Δ2-1 to the concentration of α-pheromone is similar to that of control cells. Dose response curves were generated for pheromone-induced shmoo formation in opaque cells (A, B) and adhesion in white cells (C, D). A. Percent shmoo formation as a function of α-pheromone concentration. Cells were analyzed after 4 hr of incubation. B. Percent maximum shmoo formation; maximum was considered the proportion at 3 x 10^{-5} M α-pheromone (in panel A). C. Number of adhering cells per well as a function of α-pheromone concentration. D. Percent maximum adhesion; maximum adhesion was considered the number of adhering cells at 3 x 10^{-5} M α-pheromone (in panel C). The measurements in panels A and C represent the means and standard deviations of three independent experiments.

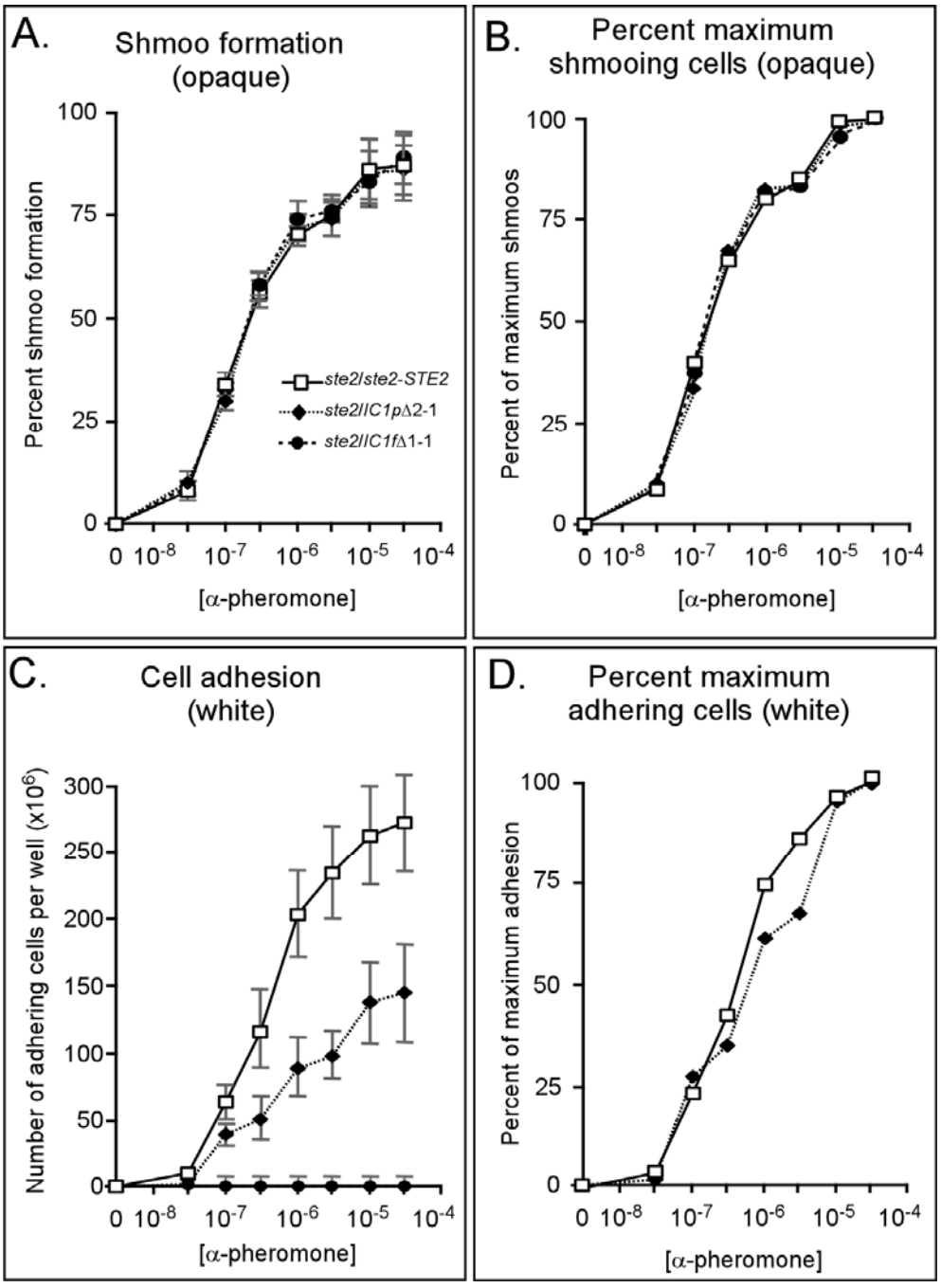
A.
Shmoo formation (opaque)
Percent shmoo formation
100
75
50
25
0
0 10-8 10-7 10-6 10-5 10-4
[α-pheromone]
ste2/ste2-STE2
ste2/IC1pΔ2-1
ste2/IC1fΔ1-1
B.
Percent maximum shmooing cells (opaque)
Percent of maximum shmoos
100
75
50
25
0
0 10-8 10-7 10-6 10-5 10-4
[α-pheromone]
C.
Cell adhesion (white)
Number of adhering cells per well (x10^6)
300
250
200
150
100
50
0
0 10-8 10-7 10-6 10-5 10-4
[α-pheromone]
D.
Percent maximum adhering cells (white)
Percent of maximum adhesion
100
75
50
25
0
0 10-8 10-7 10-6 10-5 10-4
[α-pheromone]

response, but it does not affect the sensitivity to ligand concentration. White cells of the full *Ca*-specific IC1 region exhibited no adhesion response to α-pheromone at any concentration (Figure 33C), even though opaque cells of this mutant exhibited a normal response curve for shmoo formation (Figure 33A). These results indicate that the selective decrease in the white cell response of partial or full deletion mutants of the *Ca*-specific IC1 region is not due to a selective decrease in the sensitivity of the receptor to the concentration of α-pheromone.

Insertion into the Plasma Membrane

The complete absence of a response to α-pheromone of white cells of the full deletion mutant *ste2*/*IC1fΔ1-1*, combined with the complete response to α-pheromone of opaque cells of the same mutant could reflect a selective white cell defect in membrane localization of the mutated receptor. We therefore tested membrane localization by indirect immunofluorescence imaging. Since native Ste2 expressed in the complemented strain *ste2*/*ste2-STE2*, and the Ste2 deletion derivatives expressed in *ste2/IC1pΔ1-1*, *ste2*/*1C1pΔ2-1* and *ste2*/*IC1fΔ1-1*, were all tagged at the carboxy terminus with GFP, we used anti-GFP antibody to label spheroplasts prepared from white cells exposed to 3×10^{-6} M α-pheromone. Antibody labeling was imaged by laser scanning confocal microscopy, at the same setting and scan number for comparison between strains. Similar levels of cell surface fluorescence were observed for α-pheromone-treated white cells of the complemented control strain *ste2/ste2-STE2* and the partial deletion mutants *ste2*/*IC1pΔ1-1* and *ste2/IC1pΔ2-1* (Figure 34A, B and C, respectively). The cell surface fluorescence of the full deletion mutant *ste2/IC1fΔ1-1*, was reduced but present at the established settings (Figure 34D). At the same settings there was no surface fluorescence in white cells of strain P37005 (Figure 34E), which did not have a *GFP* tag on Ste2, or white cells of strain *ste2/ste2* (data not shown). To demonstrate that the reduced surface fluorescence of white cells of *ste2*/*IC1fΔ1-1* was not an artifact (*i.e.*, not due to

Figure 34. Ste2 derivatives of the partial and full deletion mutants of the *Ca*-specific IC1 region of Ste2 localize normally in the plasma membrane. Laser scanning confocal microscopy was used to localize *GFP*-tagged Ste2 and its derivatives in the presence of α-pheromone in the control strain *ste2*/*ste2*-*STE2*. (A) and the partial and full deletion mutants *ste2*/*IC1p*Δ1-1 (B), *ste2*/*IC1p*Δ2-1 (C) and *ste2*/*IC1f*Δ1-1 (D). Note that Ste2 derivatives of the three deletion derivatives of the *Ca*-specific IC1 region localized in the plasma membrane of white cells, but the signal was much weaker in the full deletion mutant. No signal was observed in white cells of control strain P37005 (E), in which the Ste2 is not tagged with *GFP*. Opening the aperture, which allows low intensity light to be resolved, did not reveal a cell surface signal (F), supporting the conclusion that the lower surface fluorescence of *ste2*/*IC1f*Δ1-1 (D) does represent localization rather than autofluorescence. Similar staining intensities were obtained for 35 cells of each strain, and for one additional mutant of each deletion (data not shown). G. Western analysis revealed that the level of the Ste2 derivative in the mutant *ste2*/*IC1f*Δ1-1 was not up-regulated by a 3 hr exposure to α-pheromone in white cells. The scale bar in panel A represents 5 μm. The lines through the cell in each panel represented the trajectory of the scan.

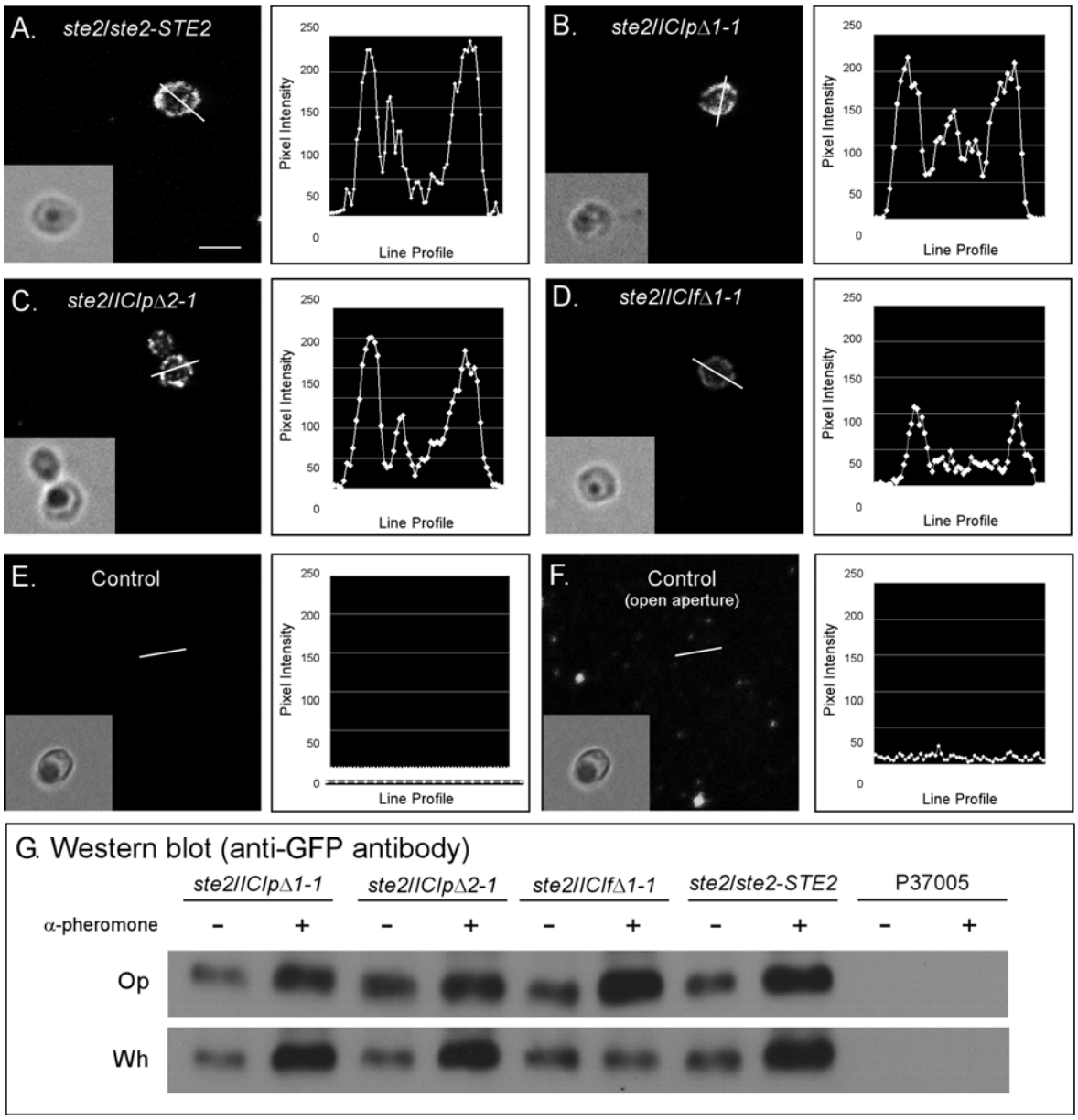
A. ste2/ste2-STE2
B. ste2/lClpΔ1-1
C. ste2/lClpΔ2-1
D. ste2/lClfΔ1-1
E. Control
F. Control
(open aperture)
Pixel Intensity
Line Profile
0
50
100
150
200
250
G. Western blot (anti-GFP antibody)
ste2/lClpΔ1-1
ste2/lClpΔ2-1
ste2/lClfΔ1-1
ste2/ste2-STE2
P37005
α-pheromone
–
+
Op
Wh

autofluorescence), we opened the aperture (iris) to view white cells of strain P37005. A larger aperture allows resolution of lower intensity fluorescence. Increasing the aperture did not result in detectable surface fluorescence of white cells of P37005 (Figure 34F). The same was true for strain *ste2/ste2* (data not shown). Increasing scan number, another method for visualizing low level fluorescence, also did increase surface fluorescence of white cells of strain *ste2/IC1fΔ1-1* significantly, but not white cells of strain P37005 (data not shown). Similar results were obtained for 35 cells of each strain analyzed, and for each condition. These results indicate that the α-pheromone receptor of the full deletion mutant *ste2/IC1fΔ1-1* inserts into the plasma membrane of white cells treated with α-pheromone, but at a lower density, than α-pheromone-treated white cells of the complemented strain or partial deletion mutants.

Cell surface labeling suggested that α-pheromone did not up-regulate the Ste2 derivative in white cells of the mutant *ste2/IC1fΔ1-1* (Figure 34D), but it did up-regulate the Ste2 derivatives in white cells of the partial deletion mutants *ste2/IC1pΔ1-1* and *ste2/IC1pΔ2-1* (Figure 34B and C, respectively). To test this suggestion at the protein level, a Western blot analysis was performed, using anti-GFP antibody to quantitate Ste2 among the tested strains. The results demonstrated that Ste2 was up-regulated by α-pheromone in white cells of the partial mutants *ste2/IC1pΔ1-1* and *ste2/IC1pΔ2-1* , as it was in white cells of the control strain *ste2*/*ste2-STE2*, but Ste2 was not up-regulated by α-pheromone in white cells of the full deletion mutant *ste2*/*IC1fΔ1-1* (Figure 34G). No staining was observed in the absence or presence of pheromone in white or opaque cells of strain P37005, which did not have a GFP tag on Ste2 (Figure 34G).

The cell surface fluorescence of white cells of the deletion mutants *ste2/IC3Δ1-1* and *ste2/CTerΔ1-1* treated with α-pheromone was also examined. In both cases low fluorescence was localized at the cell surface (data not shown), but the level was reduced in the presence of α-pheromone in comparison to the complemented control or partial

deletion mutants, as was the case for white cells of the IC1 full deletion mutant tested with α-pheromone (Figure 34D).

Pheromone Induction of *STE2*

The results of both the fluorescence and Western analyses (Figure 34) indicated that the *Ca*-specific region of the IC1 loop was necessary for α-pheromone induction of Ste2 expression in white, but not opaque, cells. To test whether this dependency was at the level of transcription, we performed a northern analysis. The transcript level of *STE2* was up-regulated by α-pheromone in both white and opaque cells of the partial deletion mutants of the *Ca*-specific region of IC1, as it was in control cells (Figure 35A). The transcript levels of *STE2*, however, was not up-regulated by α-pheromone in white cells of the full deletion mutant *ste2/IC1fΔ1-1*, but it was in opaque cells of this mutant (Figure 35A). These results were consistent with those of the Western analysis (Figure 34G). In the mutant *ste2*/*EC2Δ1-1*, α-pheromone up-regulated the transcript level of *STE2* in both white and opaque cells, as it did in control cells, but in the mutants *ste2*/*IC3Δ1-1* and *ste2*/*CTerΔ1-1*, α-pheromone did not up-regulate *STE2* expression in either white or opaque cells (Figure 35A). The latter results were consistent with the observed low level of surface fluorescence (data not shown).

Pheromone Induction of White- and Opaque-specific Genes

STE2 is up-regulated by α-pheromone in both white and opaque cells (Bennett *et al.*, 2003; Lockhart *et al.*, 2003b). There are, however, a number of genes that are selectively up-regulated by pheromone in white, but not opaque cells, just as there are a number of genes selectively up-regulated by pheromone in opaque, but not white cells (Lockhart *et al.*, 2003b; Daniels *et al.*, 2006; Bennett and Johnson, 2006; Yi *et al.*, 2008). We, therefore, tested whether up-regulation by α-pheromone of the opaque-specific gene *KAR4* (Bennett *et al.*, 2003; Lockhart *et al.*, 2003b; Dignard and Whiteway, 2006) or the white-specific gene *CSH1* (Singleton *et al.*, 2001; Yi *et al.*, 2008) was affected in any of the

Figure 35. Northern analysis reveals that the *Ca*-specific IC1 region is essential for up-regulation of genes by α-pheromone in white cells, but not opaque cells. Expression was analyzed in the absence (-) and presence (+) of 3 hr α-pheromone in control and mutant white (Wh) and opaque (Op) cells. A. Expression pattern of the gene *STE2*, which is up-regulated by α-pheromone in both opaque and white cells. B. Expression pattern of the gene *KAR4*, which is up-regulated by α-pheromone in opaque, but not white cells of the wild type strain (Lockhart *et al.*, 2003b; Bennett *et al.*, 2003). C. Expression pattern of the genes *CSH1*, which is up-regulated by α-pheromone in white, but not opaque, cells (Yi *et al.*, 2008). To demonstrate equal loading of RNA, 18 S rRNA levels in white and opaque cells are shown.

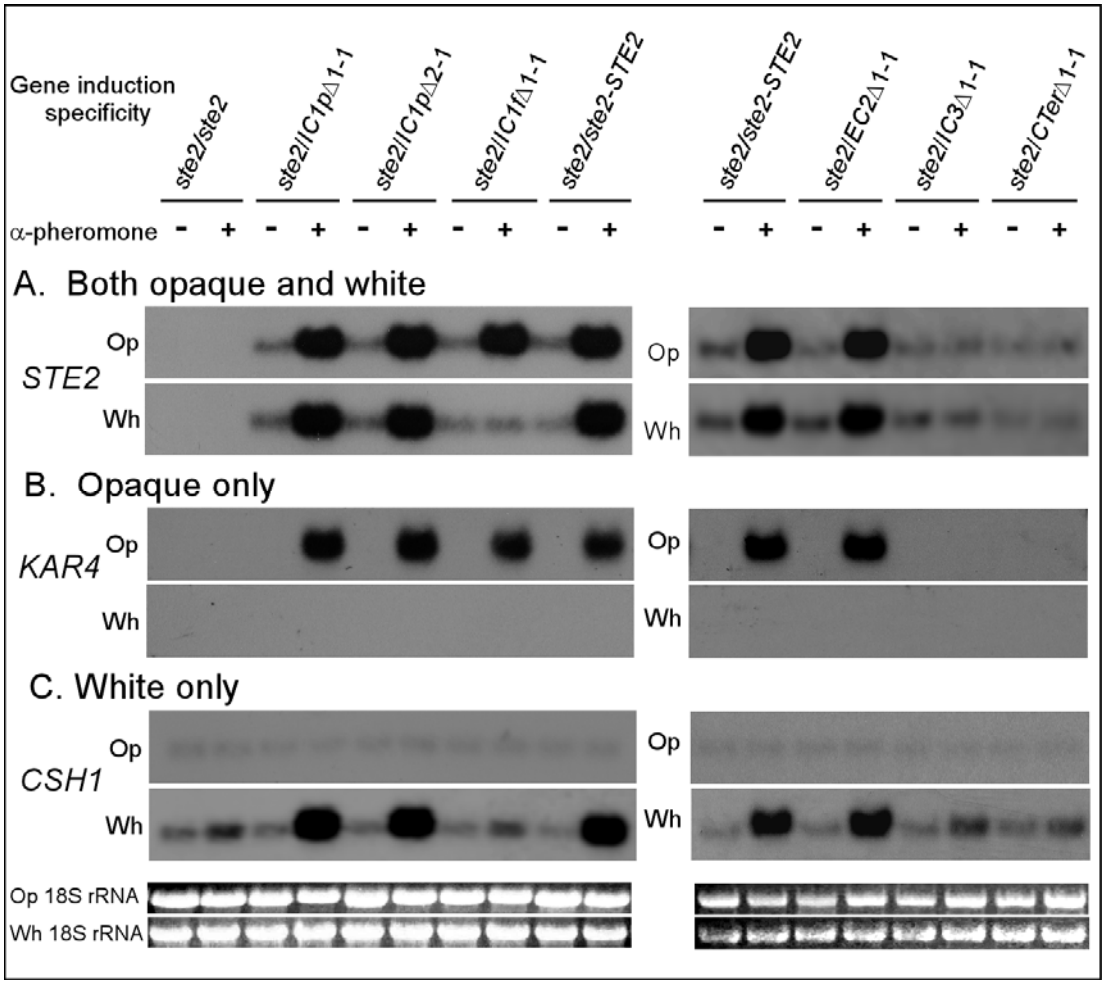
Gene induction specificity
ste2/ste2
ste2/IC1pΔ1-1
ste2/IC1pΔ2-1
ste2/IC1fΔ1-1
ste2/ste2-STE2
ste2/ste2-STE2
ste2/EC2Δ1-1
ste2/IC3Δ1-1
ste2/CTerΔ1-1
α-pheromone - + - + - + - + - + - + - + - + - +
A. Both opaque and white
STE2
Op
Wh
B. Opaque only
KAR4
C. White only
CSH1
Op 18S rRNA
Wh 18S rRNA

deletion mutants. *KAR4* was selectively up-regulated by α-pheromone in opaque, but not white cells, in the two partial and one full IC1 deletion mutants, and the EC2 deletion mutant, in a fashion similar to control cells (Figure 35B). *KAR4*, however, was not up-regulated in either opaque or white cells of the mutants *ste2*/*IC3Δ1-1* or *ste2*/*CTerΔ1-1* (Figure 35B).

In white cells of the control strain *ste2*/*ste2-STE2,* the white-specific gene *CSH1* was up-regulated from a low basal level in the absence of α-pheromone to a high level in the presence of α-pheromone (Figure 35C). In opaque cells of strain *ste2*/*ste2-STE2*, *CSH1* was expressed at a negligible level in the absence and presence of α-pheromone (Figure 35C). *CSH1* was fully up-regulated in white cells of the two partial deletion mutants *ste2/IC1pΔ1-1* and *ste2/IC1pΔ2-1*, just as it was in control cells, but it was only slightly up-regulated in white cells of the full deletion mutant *ste2/IC1fΔ1-1* (Figure 35C). These results indicate that the *Ca*-specific region of IC1 plays a selective role in α-pheromone up-regulation of white-specific genes, but not α-pheromone up-regulation of opaque-specific genes. Curiously, the level of the *CSH1* transcript was higher in cells treated with α-pheromone than untreated cells, not only in the IC1 deletion mutant *ste2/IC1fΔ1-1*, but also in the full *STE2* deletion mutant *ste2/ste2* (Figure 35C). This latter result was reproducible and suggests a low level pheromone effect not mediated by Ste2. The *CSH1* transcript level was also fully up-regulated by α-pheromone in white cells of the mutant *ste2*/*EC2Δ1-1*, but only slightly in *ste2*/*IC3Δ1-1* and *ste2/CTerΔ1-1*, the latter two in a manner similar to that in *ste2* and *ste2*/*IC1fΔ1-1* (Figure 35C).

The *Ca*-specific IC1 Region Functions through the MAP Kinase Pathway

We previously demonstrated that the white response to pheromone is transduced through the same MAP kinase pathway as the opaque response, but targets a different transcription regulator (Yi *et al.*, 2008). To test whether the *Ca*-specific IC1 region of

Ste2 also functions through this pathway, we generated a mutant in which *STE4*, the gene for the Gβ subunit of the G protein complex (Whiteway *et al.*, 1989, 1990), was placed under the regulation of an inducible promoter so that it could be up-regulated in a strain expressing the Ste2 deletion derivative that lacked the *Ca*-specific IC1 region. Upon receptor occupancy in *S. cerevisiae*, the Gβ subunit in combination with Gγ activates the MAP kinase pathway by dissociating from Gα as a result of the transition of the Gα-bound GDP to GTP (Kurjan, 1993; Bardwell *et al.*, 1994). If the IC1 loop functions through the MAP kinase pathway, then up-regulating Gβ might initiate the white response. To generate this mutant, we removed the *SAT1* marker from the full deletion mutant *ste2/IC1fΔ1-2*, and then transformed it with the gene, *STE4*, under the regulation of the tetracycline promoter (Park and Morschhaüser, 2005), generating strain *ste2/IC1fΔ1-tetSTE4*. This allowed us to up-regulate *STE4* in the absence or presence of α-pheromone in white cells of a strain expressing a Ste2 derivative missing the *Ca*-specific IC1 region by adding the tetracycline analog doxycycline.

In the absence or presence of α-pheromone, doxycycline induced *STE4* expression in a dose-dependent fashion (Figure 36A). However, up-regulation of *STE4* by doxycycline did not induce adhesion (Figure 36B, C) or up-regulate the gene *CSH1* (Figure 38A), which is up-regulated by α-pheromone in white cells of natural wild type strains (Yi *et al.*, 2008). Up-regulation of *STE4* did, however, induce adhesion (Figure 36B, C) and the expression of *CSH1* in the presence of α-pheromone. We also transformed the wild type parental strain P37005 with *STE4* under control of the tetracycline promoter, to test whether misexpression of *STE4* in the absence of α-pheromone in a cell containing an intact IC1 loop stimulated the white response. In the absence of α-pheromone, doxycycline-induced misexpression of *STE4*, did not induce adhesion in white cells of strain P37005-*tetSTE4* (Figure 36D). In the presence of α-pheromone, adhesion was stimulated approximately 100 fold in the absence of doxycycline (Figure 36D), and approximately 240 and 330 fold in the presence of 50 and

Figure 36. *STE4* overexpression in the full length deletion mutant *ste2*/*IC1f*Δ1-1, restores the white cell pheromone response, indicating that the *Ca*-specific IC1 region effect is mediated through the MAP kinase pathway. A. Northern analysis of the effects of doxycycline on *STE4* and *CSH1* expression in white cells of *ste2*/*IC1f*Δ1-tet*STE4* in the absence (-) or presence (+) of α-pheromone. B. The effects of doxycycline-induced *STE4* expression on adhesion to the bottoms of the wells of multicluster plates of white cells of *ste2*/*IC1f*Δ1-tet*STE4* incubated in the absence (-) or presence (+) of α-pheromone. C, D. Quantitation of the effects of doxycycline-induced *STE4* expression on the adhesion of white cells of strains *ste2*/*IC1f*Δ1-tet*STE4* (panel B) and P37005-tet*STE4*, respectively, on the well bottoms, in the absence (-) or presence (+) of α-pheromone. E, F. Quantitation of the effects of doxycycline-induced *CAG1* expression on the adhesion of white cells of strains *ste2*/*IC1f*Δ1-tet*CAG1* and P37005-tet*CAG1* on the well bottoms in the absence (-) or presence (+) of α-pheromone. For all quantitation experiments, the means and standard deviations are presented for adhesion to three separate wells.

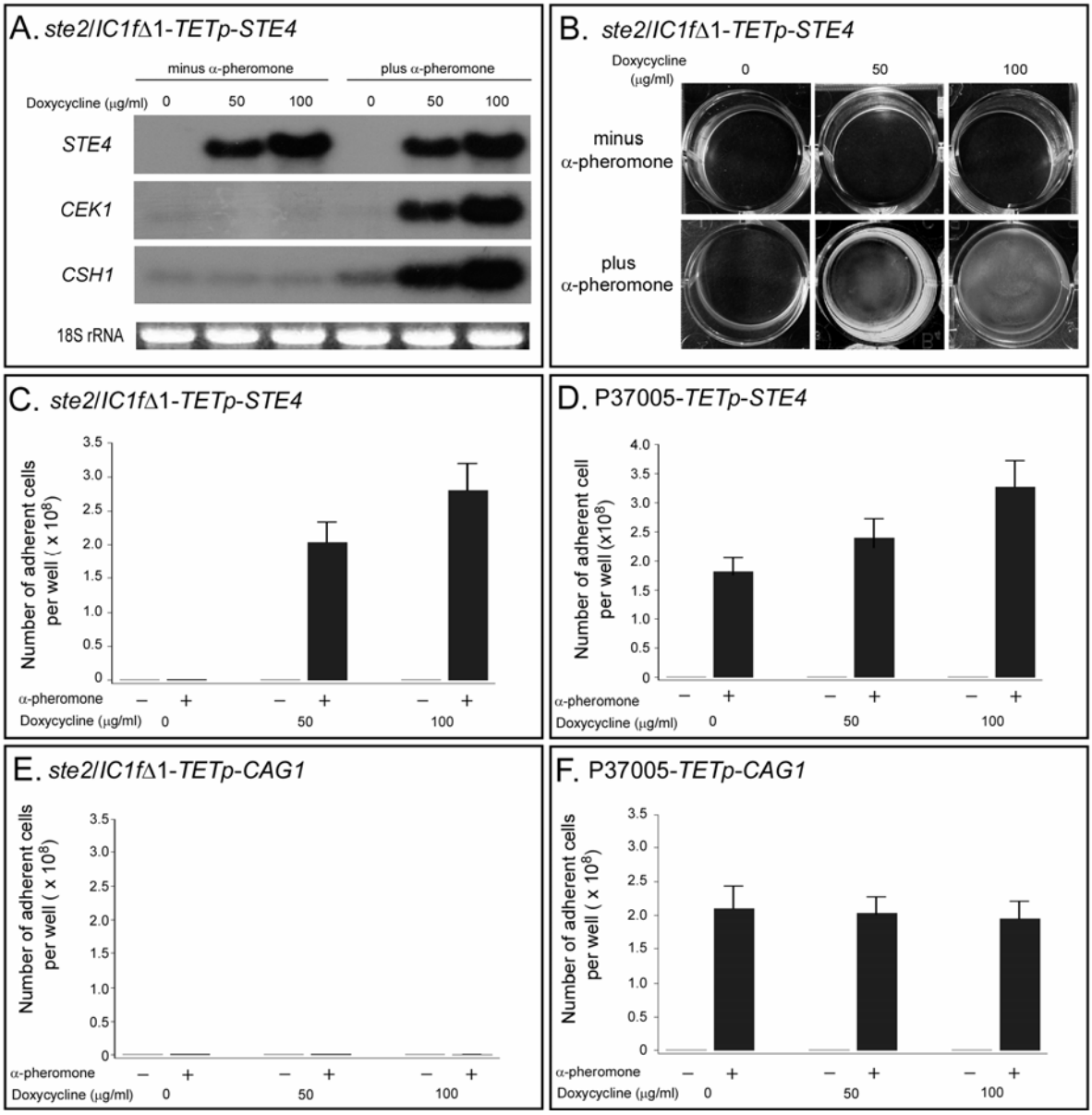
A. ste2/IC1fΔ1-TETp-STE4
minus α-pheromone
plus α-pheromone
Doxycycline (μg/ml) 0 50 100 0 50 100
STE4
CEK1
CSH1
18S rRNA
B. ste2/IC1fΔ1-TETp-STE4
Doxycycline (μg/ml)
0
50
100
minus α-pheromone
plus α-pheromone
C. ste2/IC1fΔ1-TETp-STE4
Number of adherent cells per well (x 10^8)
α-pheromone
Doxycycline (μg/ml)
D. P37005-TETp-STE4
Number of adherent cell per well (x10^8)
E. ste2/IC1fΔ1-TETp-CAG1
F. P37005-TETp-CAG1

180 µg per ml of doxycycline (Figure 36D). These results indicate that the *Ca*-specific IC1 region functions through the Gβ-induced MAP kinase pathway in the white cell pheromone response. They also suggest that a pheromone-dependent event that does not involve the loop, is required for *STE4* activation in white cells.

Recently, Dignard *et al.* (2008) demonstrated that in addition to the Gβ subunit, the Gα subunit of the receptor-coupled G protein complex of *C. albicans* is a necessary positive regulator of the opaque cell pheromone response. We, therefore, generated the mutant *ste2/IC1fΔ1-tetCAG1*, in which *CAG1*, the gene for the Gα subunit of the G protein complex (Sadhu *et al.*, 1992; Dignard *et al.*, 2008), could be up-regulated in a strain expressing the Ste2 deletion derivative that lacked the *Ca*-specific IC1 region. This mutant would allow us to test whether expression of *CAG1* initiates the white cell response, as was the case for *STE4* in the presence of α-pheromone. To generate this mutant, we transformed the full deletion mutant *ste2/IC1fΔ1-2* with the gene *CAG1* under the regulation of the tetracycline promoter (Park and Morschhaüser, 2005). In contrast to *STE4*, up-regulation of *CAG1* by the addition of doxycycline did not stimulate adhesion or cohesion in the presence, or absence, of α-pheromone (Figure 36E). When *CAG1* was placed under the regulation of the tetracycline-regulated promoter in the parental strain P37005, up-regulation in white cells by the addition of doxycycline in the absence or presence of α-pheromone did not induce the white cell response (Figure 36F).

In *S. cerevisiae*, there is evidence suggesting that the Gα subunit plays a role in signaling through a phosphatidylinositol phosphate signaling pathway (Slessareva and Dohlman, 2006; Slessareva *et al.*, 2006). This pathway is mediated by PI3 kinase (Dohlman and Slessareva, 2006). Since the mechanism by which *CAG1* regulates mating is not known (Dignard *et al.*, 2008) and since a second Gα subunit, Gpa2p, which plays a role in the pheromone block in G1, has been shown to function through the regulation of cAMP (Bennett and Johnson, 2006), we tested whether deleting the gene that encodes PI3 kinase, *VPS34* (Eck *et al.*, 2000; Gunther *et al.*, 2005), affected the white cell response to

pheromone. Deletion of *VPS34* had no effect on pheromone-induced shmoo function (Figure 37A) and no effect on mating efficiency (Figure 37B). It also had no effect on pheromone-induced cohesion (Figure 37C) or adhesion (Figure 37D) in the white cell response.

Discussion

In *S. cerevisiae*, the α and **a**-pheromone receptors appear to play a single role, activation of the mating response in the alternate mating types. In *C. albicans*, however, they play dual roles, activation of the mating response in mating-competent opaque cells and activation of a unique response in mating-incompetent white cells (Daniels *et al*, 2006; Yi *et al.*, 2008; Sahni *et al.*, 2009a). Our interest in exploring the role of the *Ca*-specific region of the IC1 loop of the α-pheromone receptor Ste2 stemmed from an observation communicated to us by Jeffrey Becker of the University of Tennessee. He noticed that although *C. albicans* Ste2 was overall homologous to *S. cerevisiae* Ste2, the first intracellular loop, IC1, contained, in addition to a short homologous region, a large 55 amino acid region unique to *C. albicans*. This additional region was noteworthy since the intracellular loops interact with the G protein complex to activate the pheromone response pathway (Weiner *et al.*, 1993; Celic *et al.*, 2003; Stefan and Blumer, 1994). Glutamine or asparagine constituted eighteen of these 55 unique amino acids, suggesting a role in protein aggregation (Michelitsch and Weissman, 2000). Such glutamine- and asparagine-rich regions have been shown to play roles as "polar zippers" in protein-protein interactions (Perutz *et al.*, 1994; Michelitsch and Weissman, 2000). In addition to the *Ca*-specific region in IC1, the second extracellular loop, EC2, also contained a unique region of 17 amino acids, although a role for this extracellular loop has not been ascertained. Based on the observation that the pheromone responses of opaque cells of *C. albicans* and haploid cells of *S. cerevisiae* were similar, but the pheromone response of white cells was unique,

Figure 37. Deletion of the gene for PI-3 kinase, *VPS34*, has no effect on either the opaque or the white cell response to α-pheromone. A. Representative images of shmoo formation in response to α-pheromone by opaque *vps34/vps34* cells, and quantitation, of shmooing by opaque cells of the parental strain P37005, and the mutant strain *vps34*/*vps34*. B. A representative image of an opaque cell of strain *vps34/vps34* mating with an opaque cell of the α/α strain WO-1, and quantitation of the efficiency of mating. C. A representative field containing cell clusters induced by α-pheromone in population of white *vps34/vps34* cells, and quantitation. D. A representative image of adhesion to a well surface of white *vps34/vps34* cells treated with α-pheromone, and quantitation.

A. Shmoo formation

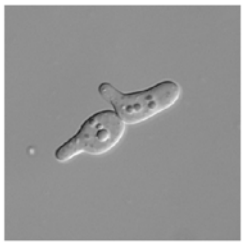

Strain	α-pheromone	No. of cells analyzed	Percent of population: Unbudded cells (%)	Budded cells (%)	Shmoo (%)	Standard deviation for shmoo (%)
P37005	–	1521	26	74	0	0
	+	1507	21	3	76	8
vps34/vps34	–	1553	31	69	0	0
	+	1530	24	3	73	7

B. Mating efficiency

Strain	Mating partner WO-1	No. of cells analyzed	No. of cells in fusants	Percent mating cells
P37005	–	3020	0	0%
	+	3112	770 ± 18	25%
vps34/ vps34	–	3208	0	0%
	+	3136	802 ± 20	26%

C. Cohesion

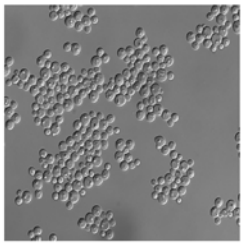

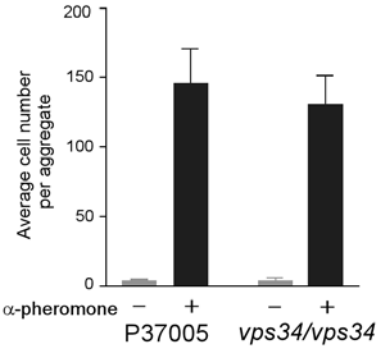

D. Adhesion

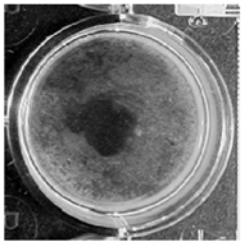

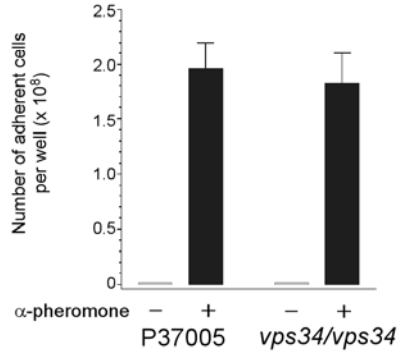

we explored the possibility that the two unique regions of the *C. albicans* Ste2 protein might play a selective role in the white but not opaque pheromone response.

The Selective Role of the *Ca*-specific IC1 Region in the White Response

Previous mutational studies in *S. cerevisiae* had revealed that multiple sites along the intracellular domains of the α-pheromone receptor were involved in G protein coupling and activation. Weiner *et al.* (1993) found three mutations in the third intracellular loop (IC3) that affected receptor function, but did not affect ligand binding or endocytosis, and Celic *et al.* (2003) demonstrated that the overall positive charges of this loop were necessary for G protein activation. Stefan and Blumer (1994) further demonstrated that IC3 was involved in activation and/or desensitization, ligand discrimination and endocytosis. A number of additional studies demonstrated that the intracellular C-terminal tail of Ste2 was involved in desensitization (Chen and Konopka, 1996), endocytosis (Rohrer *et al.*, 1993; Schandel and Jenness, 1994) and preactivation of the G-protein complex (Dosil *et al.*, 2000). The role of IC1 in G protein coupling and activation in *S. cerevisiae*, however, was less clear. Mutational analyses suggested that IC1 played a role in G protein coupling, but the defects in IC1 mutants could only be resolved in strains in which the C-terminal tail of the receptor was truncated (Chinault *et al.*, 2004).

Here we have analyzed the effects of deletion in the unique regions of IC1 and EC2, as well as deletions in IC3 and the carboxy terminal tail of *C. albicans* Ste2. Deletion of the central 24 amino acids of the EC2 loop, which included 15 of the 17 amino acids in the *Ca*-specific region, had no effect on either the white or opaque response to pheromone. Deletion of 8 of the 12 amino acids of IC3 or the last 51 amino acids of the carboxy terminal tail of Ste2 abolished the alternative pheromone responses of both white and opaque cells in a nondiscriminatory fashion. Only deletions in the unique *Ca*-specific IC1 region had a selective effect on the white, but not opaque, response.

Deletion of 52 of the 55 amino acids that comprise the *Ca*-specific IC1 region had no measurable effect on either pheromone-induced shmoo formation, the efficiency of mating or pheromone up-regulation of *STE2* or *KAR4* in opaque cells. It did, however, result in the complete elimination in white cells of the α-pheromone-induced cohesion and adhesion responses, and of α-pheromone induction of the white-specific response gene *CSH1* (Yi *et al.*, 2008). It eliminated the white cell response to opaque cells in biofilm development and selectively eliminated α-pheromone-induced up-regulation of *STE2* expression in white cells, but not opaque cells. Deletion of 21 of the first 24 amino acids of the *Ca*-specific IC1 region, or 31 of the last 37 amino acids, had no measurable effect on the opaque cell responses to α-pheromone, but both deletions reduced both the cohesion and adhesion response to pheromone in white cells, and reduced the response of white cells to opaque cells in biofilm development. These results demonstrate that the *Ca*-specific IC1 region is necessary for the white, but not the opaque, cell responses to α-pheromone, and suggest that the first third and last two thirds of the region play additive roles. If the *Ca*-specific IC1 region played a role in protein binding, then both the anterior (amino) third and the posterior (carboxy) two thirds should have protein binding characteristics. The first third did contain five mini-repeats of lysine (K)-leucine (L), which represents a highly charged region with the capacity to bind either phosphoserine-containing proteins, or glycolipids (Dalton *et al.*, 2007; Yeung and Grinstein, 2007; Wakelam *et al.*, 2007). The second two thirds contained a Q-box comprised of nine glutamines in sequence. Such sequences have been shown to be capable of binding proteins and clustering prions (Michelitsch and Weissman, 2000).

The Selective Effect on Transcription

Here, we have demonstrated that *STE2*, which is up-regulated by α-pheromone in both white and opaque cells, shows the same cell type-specific dependencies on the *Ca*-specific IC1 region. In addition, the phase-specific genes *KAR4* (opaque-specific) and

CSH1 (white-specific), which are up-regulated by α-pheromone, also show the same cell type-specific dependency on the *Ca*-specific IC1 region. But our observations on gene expression have also revealed two paradoxes that must still be resolved. First, Northern analyses have revealed that although *STE2* and *CSH1* are maximally up-regulated by α-pheromone in white cells of the partial mutants *ste2*/*IC1pΔ1* and *ste2*/*IC1pΔ2* to the transcript levels induced by α-pheromone in white cells of the control strain, the cellular responses (i.e., cohesion, adhesion and the biofilm response to opaque cells) are induced only half maximally. This suggests either that the genes that regulate these biological responses to pheromone in white cells are not maximally activated by α-pheromone as are the genes that we tested by Northern analysis, or that regulatory events other than transcription that effect adhesion, cohesion and biofilm enhancement are not maximally activated by α-pheromone in the partial mutants. Second, we have observed a common characteristic of *CSH1* expression in mutants in which the entire *STE2* gene (*ste2/ste2*), the *Ca*-specific region of IC1 (*ste2/IC1fΔ1*), a major portion of IC3 (*ste2*/*IC3Δ1*) or the last 51 amino acids of the intracellular carboxy terminal tail (*ste2*/*CTerΔ1*) are deleted. Although these deletions result in a nearly complete loss of α-pheromone up-regulation of *CSH1*, there is still a very minor, but reproducible, increase in *CSH1* expression when α-pheromone is added. These results, and especially those for the *ste2/ste2* mutant, suggest that α-pheromone may bind to a second, minor receptor that effects very low level activation.

The Role of Ste2 and the *Ca*-specific IC1 Region in Biofilm Development

To assess the role of the *Ca*-specific IC1 region in the formation of a white cell biofilm, we used an assay in which white cells first form a basal layer of yeast cells (Hawser and Douglas, 1994), which then develops into a thick biofilm that contains hyphae and extracellular polymeric substance (Hawser *et al.*, 1998; Baillie and Douglas, 1999).

The addition of a mixture of opaque cells of opposite mating types to these majority white cell biofilms enhances thickness, presumably by releasing pheromone (Daniels *et al.*, 2006; Yi *et al.*, 2008). In the absence or presence of majority opaque cells, majority white cells of the *ste2/ste2* mutant, however, formed uneven patchy films that, upon scrutiny, proved to be missing the basal layer of yeast cells and to be very fragile. The patches consisted mainly of hyphae, and were not enhanced by mixtures of minority opaque cells. In earlier studies of the mutant *ste2/ste2* (Yi *et al.*, 2008), we did not take notice of, and therefore did not report, the nonuniformity of *ste2* biofilms. The biofilm defect in *ste2/ste2* was surprising since it suggested that Ste2 may play a role in white cell biofilm development in the absence of pheromone. White cell biofilms of the mutants *ste2/IC1fΔ1-1*, *ste2Δ/IC3Δ1-1* and *ste2/CTerΔ1-1*, exhibited the same white cell biofilm defects as *ste2*. The partial deletion mutants *ste2/IC1pΔ1-1* and *ste2/IC1pΔ2-1* did, however, form relatively normal biofilms in the absence of opaque cells. These biofilms were enhanced by the addition of minority opaque cells, but to only half the extent of wild type white cell biofilms. Although these mutant results are consistent with those for cohesion and adhesion, they are harder to interpret given how little we know about biofilm development in general, and *MTL*-homozygous, white cell biofilm development in particular. What is intriguing is that the mating receptor may play a fundamental role in white cell biofilm development in the absence of opaque cells, and hence, in the absence of exogenously supplied pheromone.

Our results, therefore, suggest a relationship between the *C. albicans* mating process and white cell biofilm development, the latter being a pathogenic characteristic. We have found that at least for biofilms formed by *MTL*-homozygous strains of *C. albicans*, the pheromone receptor may be involved in white cell biofilm development, both in a pheromone-dependent and -independent manner. This, however, is not the first time a relationship between mating and biofilm development has been suggested. We initially suggested that opaque signaling of white cells through the release of pheromone induced

the formation of white cell biofilms in order to provide minority opaque cells an environment conducive for mating (Daniels *et al.*, 2006; Soll, 2008). Nobile *et al.* (2008) subsequently discovered that the Als proteins and Hwp1 played complimentary roles in cell adhesion in biofilms formed by **a**/α cells. Based on the characteristics of these molecules, they suggested that the complementary adhesions may have developed from primitive mating agglutinins. But the relationship between mating and biofilm development is not limited to *C. albicans*, or fungal, biofilms. A number of studies have demonstrated that the mating process is also intimately involved in the development of bacterial biofilms (Hausner and Wuertz, 1999; Ghigo, 2001; Reisner *et al.*, 2003; Soll, 2008).

IC1 and the MAP Kinase Pathway

There are at least two mechanistic hypotheses that are consistent with the selective role of the *Ca*-specific IC1 region in the white cell response to α-pheromone. First, this region may be necessary for the selective activation in white cells of a second essential pathway that is independent of the MAP kinase pathway. This pathway could be novel, given the uniqueness of the white cell response, or it could be related to activation of the G protein complex. Recently, Gα has been demonstrated to function as a positive regulator of the mating response in *C. albicans*, which is opposite to the antagonistic role that it plays to Ste4 in *S. cerevisiae* (Dignard *et al.*, 2008). In *S. cerevisiae*, Gα plays a role as an intracellular signal that activates the phosphatidyl inositol phosphate pathway, which includes the key enzyme PI3 kinase (Dohlman and Slessareva, 2006). In *C. albicans*, the mechanism by which Gα (Cag1) functions in the opaque cell mating response has not been elucidated (Dignard *et al.*, 2008), although a second Gα subunit, Gpa2, is required for a normal response to α-pheromone, and appears to function through the cAMP signaling pathway (Bennett and Johnson, 2006). Here, we have found that misexpression of *CAG1* in the absence or presence of α-pheromone in the full deletion mutant for the *Ca*-specific

IC1 region does not restore the white cell pheromone response. We have also found that deleting the gene for PI3 kinase, *VPS34*, has no effect on the white cell response to α-pheromone. Although our results indicate that the white cell response to α-pheromone is not mediated solely by Gα through the *Ca*-specific IC1 region of the α-pheromone receptor, they do not exclude a role in combination with Gβ, as has been shown to be the case for the opaque cell response to α-pheromone, and they do not exclude the role of an unidentified pathway activated by the occupied Ste2 receptor through the *Ca*-specific IC1 region.

In a second hypothesis, the *Ca*-specific IC1 region could play a selective role in the activation of the MAP kinase pathway of white cells through the release of Gβγ, that is not required for the activation of the MAP kinase pathway in opaque cells. We previously demonstrated that Gβ activates the MAP kinase pathway in an apparently similar fashion in the opaque and white cell response to α-pheromone (Yi *et al.*, 2008). Here we have shown that the α-pheromone response can be rescued in cells lacking the *Ca*-specific IC1 region by expressing *STE4* under the control of an inducible promoter. This result indicates that the *Ca*-specific IC1 loop region functions through the Gβ subunit of the G protein complex, and hence, effects the white cell response through the same MAP kinase pathway that activates the opaque cell response. Our results, however, do not provide a molecular mechanism for the selective white cell role of the IC1 loop, or an explanation for why the *Ca*-specific IC1 region is essential for the white cell, but not for the opaque cell, pheromone response. The loop may interact with one or more accessory proteins involved in coupling, preactivation or activation of the G protein complex in white cells, that are not involved in these processes in opaque cells (Lee and Dohlman, 2008), or it may be necessary for the clustering of receptors in white, but not opaque, cells. Clustering of receptors has been demonstrated to be a prerequisite for the activation of the G protein complex in *S. cerevisiae* (Overton *et al.*, 2003).

The **a**-pheromone Receptor, Ste3

We have focused here on the role of the α-pheromone receptor in the response of white **a**/**a** cells to α-pheromone, primarily because active 13-mer or 14-mer α-pheromone is readily available through chemical synthesis (Lockhart *et al.*, 2003b; Bennett *et al.*, 2003; Panwar *et al.*, 2003). This is not the case for the heavily modified and labile **a**-pheromone (Anderegg *et al.*, 1988; Michaelis *et al.*, 1992), which has also retarded studies of the **a**-pheromone mating response and the **a**-pheromone receptor in *S. cerevisiae*. The **a**-pheromone receptor, like the α-pheromone receptor, is a seven transmembrane protein which must function in α/α cells similarly to the α-pheromone receptor in **a**/**a** cells of *C. albicans*. But in contrast to *C. albicans* Ste2, Ste3, which is homologous to *S. cerevisiae* Ste3, (73% similarity), contains no major *Ca*-specific regions in the first intracellular loop, or the remaining two intracellular loops and carboxy terminal tail (C. Pujol and D.R. Soll, unpublished observations). In addition, there are no sequences in the first intracellular loop, or the other two intracellular loops and the tail of *C. albicans* Ste3 that are similar in nature to the protein binding motifs in the *Ca*-specific IC1 region of Ste2 (C. Pujol and D.R. Soll, unpublished observations). Hence, the selective role of the *Ca*-specific IC1 region of Ste2 in the white cell response to α-pheromone must be fulfilled by nonhomologous regions in *C. albicans* Ste3, or, possibly, by a different mechanism involving a necessary protein, in the white cell response to **a**-pheromone. A functional analysis of Ste3 is now in progress to identify such regions or an alternative mechanism.

A Unique Regulatory Model

Our results lead to a unique regulatory model for the manner in which two distinct cell types respond differently to the same extracellular signal (Figure 38). The same pheromone activates the same receptor, which in turn activates the same G protein complex. The G protein complex in turn activates the same MAP kinase pathway which in turn activates different downstream transcription factors (Yi *et al.*, 2008). In the

Figure 38. Models of the pathways regulating the pheromone-induced white and opaque responses. The red circles denote the differences between the two pathways. Note that the same pheromone activates the same receptor which in turn activates the dissociation of the α subunit from the βγ subunits of the G protein complex. The β subunit of the βγ complex then signals through the same MAP kinase pathway which activates the downstream Cph1 transcription factor in opaque cells and a different unidentified downstream transcription factor in white cells. Activation of the G protein complex, however, requires only the IC3 loop and the intracellular carboxy terminal Tail (I tail) in opaque cells, but the IC1 loop, the IC3 loop and the carboxy terminal tail in white cells. The requirement of an extra receptor domain to activate the same MAP kinase pathway in one but not the other cell type, and the fact that the dependency on the IC1 loop can be circumvented by overexpressing *STE4*, which encodes the Gβ subunit, suggest that the IC1 loop plays a role in Ste2 function, not downstream in the activation of the white-specific transcription factor.

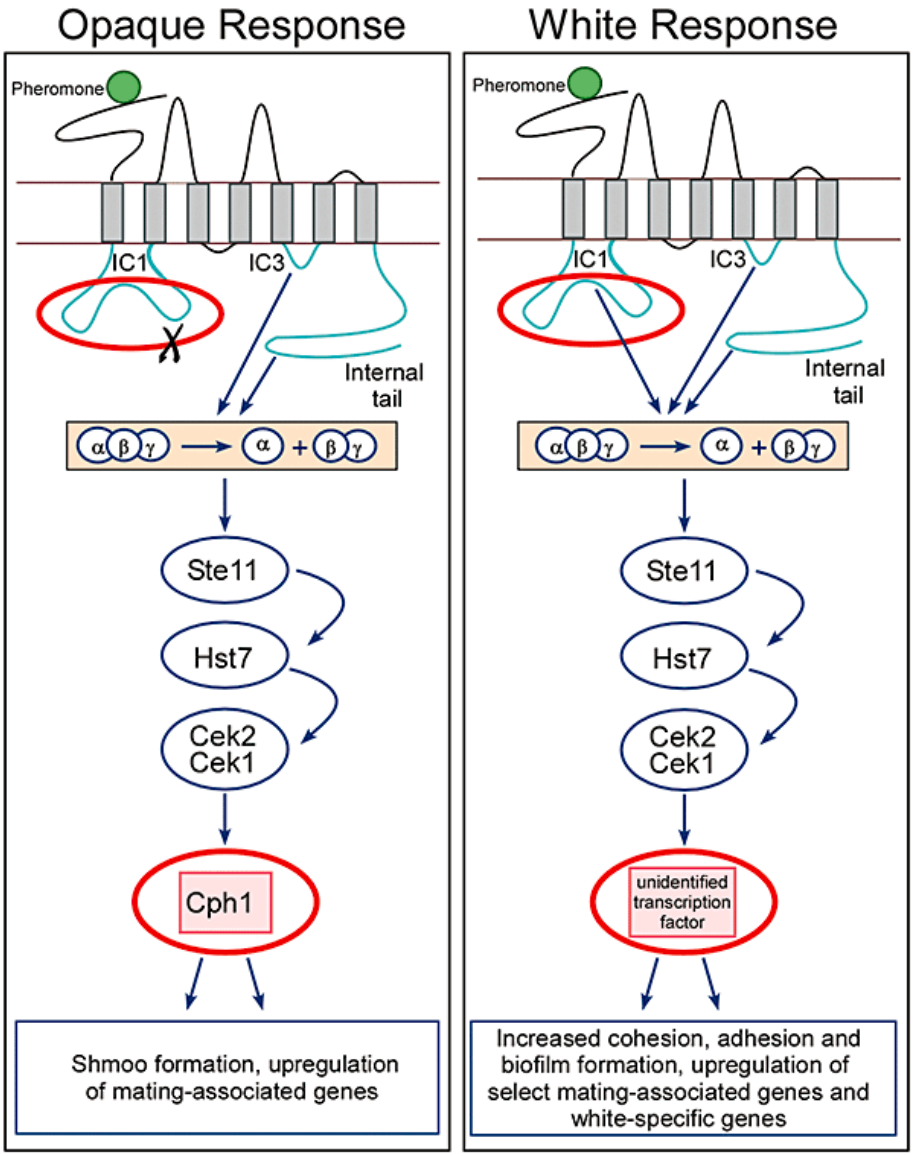
Opaque Response
White Response
Pheromone
IC1
IC3
Internal tail
α β γ → α + β γ
Ste11
Hst7
Cek2 Cek1
Cph1
unidentified transcription factor
Shmoo formation, upregulation of mating-associated genes
Increased cohesion, adhesion and biofilm formation, upregulation of select mating-associated genes and white-specific genes

activation of the G protein complex and subsequent MAP kinase pathway, two receptor domains (IC3, internal tail) are essential in the opaque cell, whereas a third domain (IC1) in addition to the two domains in white cells. Given that the same MAP kinase pathway is employed in both responses, but different transcription factors are activated at the end of the pathway, the reason for the selective dependency of the white cell response on the IC1 region is not obvious. Since this selective dependency can be circumvented by overexpressing the β subunit (Ste4) of the G complex, one can conclude that the IC1-dependent event precedes Ste4 function. IC1, therefore, may be necessary for receptor clustering or function in white but not opaque cells because of differences in the plasma membrane-cell wall milieu, which have been demonstrated morphologically and antigenically (Anderson and Soll, 1987; Anderson *et al.*, 1990). This possibility is now being pursued.

CHAPTER 6
GENES SELECTIVELY UP-REGULATED BY PHEROMONE IN WHITE CELLS ARE INVOLVED IN BIOFILM FORMATION IN *C. ALBICANS*

Introduction

In Chapters 4 and 5, mutational analyses have revealed that the white cell response to pheromone involves the same receptors and MAP kinase pathway as the opaque cell mating response (Yi *et al*., 2008, 2009). This pathway, however, activates a different downstream *trans*-acting factor (Yi *et al*., 2008). The downstream transcription factor targeted by the pheromone response pathway in white cells has recently been identified as Tec1, and will be discussed in chapter 7. In white cells, pheromone also induces the expression of a number of genes that are also induced in opaque cells, as well as a number of genes specific to white cells (Lockhart *et al*., 2003a; Daniels *et al*., 2006; Sahni *et al*., 2009b). Since the major effects of pheromone on white cells include increased cohesion, adhesion and enhanced biofilm formation, we predicted that pheromone-induced white-specific genes would play key roles in these processes. Our results demonstrated that white-specific genes are regulated through an AT-rich white-specific pheromone response element, WPRE (AAAAAAAAAAGAAAG), which is distinct from the GC-rich response element, OPRE (GTGAGGGGA), regulating genes in the opaque cell pheromone response. These results support our earlier conclusion that white genes are regulated by a single white-specific *trans*-acting factor (Yi *et al*., 2008). Furthermore, we show by mutational analysis that the white-specific genes play fundamental roles in adhesion and white cell biofilm formation. Interestingly, the white-specific genes up-regulated by pheromone in *MTL*-homozygous white cells have previously been demonstrated to play roles in biofilm formation in **a**/α cells, which represent a majority of the strains found in nature (Lockhart *et al*., 2002; Legrand *et al*., 2004; Tavanti *et al*., 2005; Odds and Jacobsen

2008). Together, these results provide clues to the evolution of the white cell pheromone response.

Materials and Methods

Strains and Strain Maintenance

Strain P37005, a natural clinical isolate from a blood stream infection with the *MTL* genotype **a**/**a** (Lockhart *et al.*, 2002), was used to derive the homozygous deletion mutants and the WPRE mutants. The WPRE mutants were used to generate the complemented strains. All strains were maintained on agar containing modified Lee's medium (Lee *et al.*, 1975; Bedell and Soll, 1979) supplemented with phloxine B, which differentially stains opaque sectors and colonies red (Anderson and Soll, 1987). The strains are listed in Table 6.

MEME Identification of WPRE and OPRE

To identify candidate white- and opaque-specific *cis*-acting pheromone response elements (PREs) in *C. albicans*, a set of white phase-specific and opaque phase-specific pheromone-inducible genes were submitted to the motif-finding program, MEME (Bailey and Elkan, 1994; Grundy *et al*., 1997; Bailey *et al*., 2006). All the selected genes were verified by northern analysis for induction by pheromone prior to motif analysis. One thousand base pairs upstream of the open reading frame of 12 white-specific and the 6 opaque-specific pheromone-up-regulated genes were pooled into two respective groups and subjected to MEME analysis. The website address for MEME is http://meme.sdsc.edu/meme/cgi-bin/meme.cgi. MEME program analyzes input promoter sequences for similarities among them and elicits consensus motifs, which may be present in some or all of the promoters analyzed. The parameters were set as follows: width of each motif between 6 and 15, a limit output of 3 different motif types, and other parameters with default values defined in the program. Results from the MEME analysis yields an E

Table 6. *C. albicans* strains used in the study of white-specific pheromone-regulated genes

Strain	Parent	*MTL*	Relevant Genotype	Reference or source
P37005	–	**a**/**a**	Wild type	Lockhart *et al.* (2002)
WO-1	–	α/α	Wild type	Slutsky *et al.* (1987)
eap1/eap1	P37005	**a**/**a**	*eap1*Δ::FRT/*eap1*Δ::FRT	This study
$EAP1_{WPRE\Delta}$/*eap1*	P37005	**a**/**a**	*eap1*Δ::FRT/*EAP1*-WPREΔ::FRT	This study
$EAP1_{WPRE\Delta}$-*EAP1*/*eap1*	$EAP1_{WPRE\Delta}$/*eap1*	**a**/**a**	*eap1*Δ::FRT/ *EAP1*-WPREΔ::FRT-WPRE-*EAP1*::*GFP*::SAT^R	This study
pga10/pga10	P37005	**a**/**a**	*pga10*Δ::FRT/*pga10*Δ::FRT	This study
$PGA10_{WPRE\Delta}$/*pga10*	P37005	**a**/**a**	*pga10*Δ::FRT/*PGA10*-WPREΔ::FRT	This study
$PGA10_{WPRE\Delta}$-*PGA10*/ *pga10*	$PGA10_{WPRE\Delta}$/*pga10*	**a**/**a**	*pga10*Δ::FRT/ *PGA10*-WPREΔ::FRT-WPRE-*PGA10*::*GFP*::SAT^R	This study
csh1/csh1	P37005	**a**/**a**	*csh1*Δ::FRT/*csh1*Δ::FRT	This study
$CSH1_{WPRE\Delta}$/*csh1*	P37005	**a**/**a**	*csh1*Δ::FRT/*CSH1*-WPREΔ::FRT	This study
$CSH1_{WPRE\Delta}$-*CSH1*/*csh1*	$CSH1_{WPRE\Delta}$/*csh1*	**a**/**a**	*csh1*Δ::FRT/ *CSH1*-WPREΔ::FRT-WPRE-*CSH1*::*GFP*::SAT^R	This study
pbr1/pbr1	P37005	**a**/**a**	*pbr1*Δ::FRT/*pbr1*Δ::FRT	This study
$PBR1_{WPRE\Delta}$/*pbr1*	P37005	**a**/**a**	*pbr1*Δ::FRT/*PBR1*-WPREΔ::FRT	This study
$PBR1_{WPRE\Delta}$-*PBR1*/*pbr1*	$PBR1_{WPRE\Delta}$/*pbr1*	**a**/**a**	*pbr1*Δ::FRT/ *PBR1*-WPREΔ::FRT-WPRE-*PBR1*::*GFP*::SAT^R	This study
P37005-tet*PBR1*	P37005	**a**/**a**	*ADH1*/*adh1*Δ::ptet-*PBR1*-*GFP*::SAT^R	This study
$EAP1_{WPRE\Delta}$/*eap1* -tet*PBR1*	$EAP1_{WPRE\Delta}$/*eap1*	**a**/**a**	*eap1*Δ::FRT/*EAP1*-WPREΔ::FRT *ADH1*/*adh1*Δ::ptet-*PBR1*-*GFP*::SAT^R	This study
$PGA10_{WPRE\Delta}$/*pga10* -tet*PBR1*	$PGA10_{WPRE\Delta}$/*pga10*	**a**/**a**	*pga10*Δ::FRT/*PGA10*-WPREΔ::FRT *ADH1*/*adh1*Δ::ptet-*PBR1*-*GFP*::SAT^R	This study

Table 6 --- continued

CSH1$_{WPRE\Delta}$/*csh1* -tet*PBR1*	*CSH1*$_{WPRE\Delta}$/*csh1*	**a**/**a**	*csh1*Δ::FRT/*CSH1*-WPREΔ::FRT *ADH1*/*adh1*Δ::ptet-*PBR1-GFP*::*SAT*^{R}	This study
PBR1$_{WPRE\Delta}$/*pbr1* -tet*PBR1*	*PBR1*$_{WPRE\Delta}$/*pbr1*	**a**/**a**	*pbr1*Δ::FRT/*PBR1*-WPREΔ::FRT *ADH1*/*adh1*Δ::ptet-*PBR1-GFP*::*SAT*^{R}	This study
eap1/eap1-tet*PBR1*	*eap1/eap1*	**a**/**a**	*eap1*Δ::FRT/*eap1*Δ::FRT *ADH1*/*adh1*Δ::ptet-*PBR1-GFP*::*SAT*^{R}	This study
csh1/csh1-tet*PBR1*	*csh1/csh1*	**a**/**a**	*csh1*Δ::FRT/*csh1*Δ::FRT *ADH1*/*adh1*Δ::ptet-*PBR1-GFP*::*SAT*^{R}	This study
cek1/cek1 cek2/cek2	P37005	**a**/**a**	*cek1*Δ::FRT/*cek1*Δ::FRT *cek2*Δ::FRT/*cek2*Δ::FRT	Yi *et al.* (2008)
cek1 cek2-tet*PBR1*	*cek1/cek1 cek2/cek2*	**a**/**a**	*cek1*Δ::FRT/*cek1*Δ::FRT *cek2*Δ::FRT/*cek2*Δ::FRT *ADH1*/*adh1*Δ::ptet-*PBR1-GFP*::*SAT*^{R}	This study

value defined as the probability of finding an equally well conserved pattern in random sequences (Bailey *et al*., 2006). The highest scoring hit in the analysis output for the white and opaque groups of genes represented the conserved DNA motifs, WPRE and OPRE, respectively. The WPRE or OPRE site was highlighted in each promoter and the distance from the translation start site shown.

To identify a strong WPRE or OPRE motif in the promoter, the parameter of "number of occurrences of a single motif" was set to be zero or one per sequence, and the result of MEME yielded one motif per promoter with the highest E value. To identify additional weaker WPRE or OPRE motifs in the promoter, the parameter of "number of occurrences of a single motif" was set to be any number of repetitions, and the result of MEME yielded more motifs, if any, per promoter with the same consensus but with lower E values. Noteworthy, the *S. cerevisiae* PRE (TGAAACA) (Hagen *et al.*, 1991) was not identified in our analysis with the same parameters, although a motif that contained a similar sequence to *S. cerevisiae* PRE was obtained with a poor E value of 10^{+2}. The result is consistent with the observation by Bennett and Johnson (2006), who reported that *S. cerevisiae* PRE was present in some, but not all, of genes that are induced by pheromone in opaque cells.

Construction of WPRE Mutants, WPRE-complemented Strains and Gene Disruption Mutants

The recyclable SAT1 flipper cassette SAT1-2A, containing a dominant nourseothricin resistance marker SAT^r (Reuss *et al*., 2004), was used for all mutant construction according to a protocol previously described (Yi *et al*., 2008). The original SAT1 flipper plasmid pSFS2A was a generous gift from Dr. Joachim Morschhäuser, the University of Würzburg, Germany. To generate WPRE mutants, a two-step strategy was employed. First, heterozygous mutants of the coding region were derived. In brief, 5' and 3' flanking regions of each gene were amplified by PCR using the primer pairs f1, r1, and

f2, r2, respectively (Table 7). The 5' and 3' fragments were then each digested with SmaI and ligated together using T4 DNA ligase. The fusion product was amplified by PCR and cloned into pGEM-T Easy vector (Promega, Madison, WI), generating the plasmid pGeneX1-T. The SAT1-2A cassette was then inserted into the SmaI-digested, dephosphorylated plasmid pGeneX1-T, yielding pGeneX1-2A. This plasmid was digested with SacI and SacII (or PvuII in the case of *CSH1*), then introduced into *C. albicans* strain P37005 by electroporation (De Backer *et al*., 1999). The derived heterozygotes were confirmed by PCR and Southern analysis. The heterozygotes were subjected to a pop-out protocol in YPM medium (Yi *et al*., 2008) to excise the *CaSAT1* marker prior to the next step. Second, WPRE elements were deleted directly from the endogenous promoters in the heterozygous background. The methods used were as follows. A 5' flanking DNA fragment, about 2 kb upstream of the start codon plus the ORF, was amplified using the primer pair pf1 and pr1 (Table 7). In addition, two DNA fragments spanning a promoter region on the 5' and 3' side, respectively, of the WPRE element to be deleted, were amplified by PCR with the primer pairs listed in Table S2. These two fragments, bordering the targeted WPRE element, were then fused by PCR using the primer pair pf2 and pr2 (Table 7), generating the 3' flanking DNA fragment. The 5' and 3' flanking DNA fragment were then each digested with SmaI, fused together with T4 DNA ligase, amplified by PCR using primers pf1 and pr2 (Table 7), and ligated into pGEM-T Easy vector (Promega, Madison, WI), generating the plasmid pGeneXw-T. The SAT1-2A cassette was inserted into the SmaI-digested, dephosphorylated plasmid pGeneXw-T, yielding pGeneXw-2A. This plasmid was digested with SacI and SacII (or PvuII in the case of *PGA10*), then introduced by electroporation (De Backer *et al*., 1999) into the heterozygous strains obtained in the first step. Two or more independent WPRE deletion mutants were obtained for each gene and verified by PCR sequencing and Southern analysis. We generated in this way the mutants $EAP1_{WPRE\Delta}/eap1$, $PGA10_{WPRE\Delta}/pga10$, $CSH1_{WPRE\Delta}/csh1$, and $PBR1_{WPRE\Delta}/pbr1$ (Table 6).

Table 7. Oligonucleotides used in the study of white-specific pheromone-regulated genes

Primer	Gene/Purpose	Sequence
EAP1f1	*EAP1* heterozygote	5'-TACCTTTTAGTACTCTGT-3'
EAP1r1	*EAP1* heterozygote	5'-TCCCCCGGGCAACTGAAGAGATCTTGA-3'
EAP1f2	*EAP1* heterozygote	5'-TCCCCCGGGTGTACCATATGGTGGTGA-3'
EAP1r2	*EAP1* heterozygote	5'-TCCTGTTGTTGATGTTCA-3'
PGA10f1	*PGA10* heterozygote	5'-TTCATTATGGACCCATTT-3'
PGA10r1	*PGA10* heterozygote	5'-TCCCCCGGGTTGCGAGAATAAGTTTGT-3'
PGA10f2	*PGA10* heterozygote	5'-TCCCCCGGGGTTTTTCATTAAATGATGAGA-3'
PGA10r2	*PGA10* heterozygote	5'-TCTAAGAAGAAGCCAGAT-3'
CSH1f1	*CSH1* heterozygote	5'-AAGTTGATGCTTTATCAG-3'
CSH1r1	*CSH1* heterozygote	5'-TCGCCCGGGTCGGAACAATTACTGTAT-3'
CSH1f2	*CSH1* heterozygote	5'-TCGCCCGGGTAACGAAATAATTTGTCA-3'
CSH1r2	*CSH1* heterozygote	5'-TGACATATTTTGGTTAGA-3'
PBR1f1	*PBR1* heterozygote	5'-TTCCATCAACCAGTTGCT-3'
PBR1r1	*PBR1* heterozygote	5'-TCCCCCGGGTTGTTGAGGTTTCAGTTT-3'
PBR1f2	*PBR1* heterozygote	5'-TCCCCCGGGTGTTGCCTATCCAAATTG-3'
PBR1r2	*PBR1* heterozygote	5'-TGATTATGTAATAAACTCCA-3'
EAP1pf1	WPRE deletion	5'-AGCCAAGTTTATACACAT-3'
EAP1pr1	WPRE deletion	5'-TCCCCCGGGCTATCATGCAACAGTGAT-3'
EAP1pf2	WPRE deletion	5'-TCCCCCGGGGTCAATTAATTAGCTAGAT-3'
EAP1pdelf	WPRE deletion	5'-CAATGAGGTGAACTTAATAAAAGGGTTCTA-3'
EAP1pdelr	WPRE deletion	5'-TTATTAAGTTCACCTCATTGTATTAATTC-3'
EAP1pr2	WPRE deletion	5'-TCCTGTTGTTGATGTTCA-3'
PGA10pf1	WPRE deletion	5'-CCAAATCGATCTAGAGGT-3'
PGA10pr1	WPRE deletion	5'-TCCCCCGGGTTAACATCAGTCTCCAGT-3'
PGA10pf2	WPRE deletion	5'-TCCCCCGGGACAGAAATTGGAGATGTC-3'
PGA10pdelf	WPRE deletion	5'-GATAGAGAATATGGCTGTTGTTCAATTC-3'
PGA10pdelr	WPRE deletion	5'-CAACAGCCATATTCTCTATCCGAGAATC-3'
PGA10pr2	WPRE deletion	5'-GTTTGTACCGTCTGAAGT-3'
CSH1pf1	WPRE deletion	5'-TTTTGCTCTTGTAGACAC-3'

Table 7 --- continued

CSH1pr1	WPRE deletion	5'-TCCCCCGGGACCTCAACAGTATAAACA-3'
CSH1pf2	WPRE deletion	5'-TCCCCCGGGTCGATGGTTCAGTATATT-3'
CSH1pdelf	WPRE deletion	5'-TATCGATTGAAGTTAAAGTTAAGTTGTAGTT-3'
CSH1pdelr	WPRE deletion	5'-AACTTTAACTTCAATCGATAAATCAAGAAT-3'
CSH1pr2	WPRE deletion	5'-TAGACTTCTCAACAACCC-3'
PBR1pf1	WPRE deletion	5'-AGGAAGATGACAATTCAT-3'
PBR1pr1	WPRE deletion	5'-TCCCCCGGGAGGAGAAAACATACACAAA-3'
PBR1pf2	WPRE deletion	5'-TCCCCCGGGACTTATTGATACACCAAT-3'
PBR1pdelf	WPRE deletion	5'-TGGTTATACCAGAGTTACCAATTGGTTA-3'
PBR1pdelr	WPRE deletion	5'-TGGTAACTCTGGTATAACCAACTAATAC-3'
PBR1pr2	WPRE deletion	5'-TAGTAGTTGTAATTAATGAATTAAT-3'
EAP1wQ1f	WPRE complementation	5'-TTCCATTTCTATAGGCTC-3'
EAP1wQ1r	WPRE complementation	5'-TCCGGATCCCATAAAGTAGACTAATGC-3'
EAP1wQ2f	WPRE complementation	5'-TCCGGATCCTGTACCATATGGTGGTGA-3'
EAP1wQ2r	WPRE complementation	5'-TCCTGTTGTTGATGTTCA-3'
PGA10wQ1f	WPRE complementation	5'-TGATGAACGTGGTATGAA-3'
PGA10wQ1r	WPRE complementation	5'-TCCGGATCCGATTAAGGCAGCAAATGC-3'
PGA10wQ2f	WPRE complementation	5'-TCCGGATCCCTACTGTTAATAGGTGAT-3'
PGA10wQ2r	WPRE complementation	5'-AGAACCGTCAGCATATAA-3'
CSH1wQ1f	WPRE complementation	5'-ATCTCTGTGCAATGTGAA-3'
CSH1wQ1r	WPRE complementation	5'-TCCAGATCTAGCAGCAACTCTTGCCAA-3'
CSH1wQ2f	WPRE complementation	5'-TCCAGATCTCTAAGTGATTCATAAGGA-3'
CSH1wQ2r	WPRE complementation	5'-CACGGTTAGAATTCATTT-3'
PBR1wQ1f	WPRE complementation	5'-CCATCATTACATGGTGAT-3'
PBR1wQ1r	WPRE complementation	5'-TCCGGATCCCAAGACAGCCCAATTGAGA-3'
PBR1wQ2f	WPRE complementation	5'-TCCGGATCCTGTTGCCTATCCAAATTG-3'
PBR1wQ2r	WPRE complementation	5'-TGATTATGTAATAAACTCCA-3'
SATBgF1	*GFP-SAT1* PCR	5'-TCAAGATCTTCCATCATAAAATGTCGA-3'
GFBhF1	*GFP-SAT1* PCR	5'-TCAGGATCCATGTCTAAAGGTGAAGAA-3'
EAP1f3	*EAP1* homozygote	5'-AGAGAAGATAGAACCCTT-3'
EAP1r3	*EAP1* homozygote	5'-TCCCCCGGGAGCTGGAGTACTTTCAGT-3'
EAP1f4	*EAP1* homozygote	5'-TCCCCCGGGTTATCCCAGGCACTGAAA-3'
EAP1r4	*EAP1* homozygote	5'-AGGTGATGGTGATAATCA-3'

Table 7 --- continued

PGA10f3	*PGA10* homozygote	5'-TCGCTTAAAATCCGAACA-3'
PGA10r3	*PGA10* homozygote	5'-TCCCCCGGGCCAATAGCACCACCAAAT-3'
PGA10f4	*PGA10* homozygote	5'-TCCCCCGGGCATGAAAGCAAAGTAGCT-3'
PGA10r4	*PGA10* homozygote	5'-GAAAACATTGGATAACAC-3'
CSH1f3	*CSH1* homozygote	5'-TGTTCCGATAACCACCACT-3'
CSH1r3	*CSH1* homozygote	5'-TCGCCCGGGTCAAGTGAACTGTCTTCT-3'
CSH1f4	*CSH1* homozygote	5'-TCGCCCGGGAGAGACGCAGATAAGATT-3'
CSH1r4	*CSH1* homozygote	5'-CAGTTTCAACAAATGGAAT-3'
PBR1f3	*PBR1* homozygote	5'-AACACACAGCTTTATAGT-3'
PBR1r3	*PBR1* homozygote	5'-TCCCCCGGGCTTACCATTGACTTCTTC-3'
PBR1f4	*PBR1* homozygote	5'-TCCCCCGGGAACCAGCTTATTCTGCTA-3'
PBR1r4	*PBR1* homozygote	5'-CAAATCAACGAGAGATCA-3'
TetPBR1f	*PBR1* overexpression	5'-TCCGTCGACAAAGATGTACAAATTCACTGTT-3'
TetPBR1r	*PBR1* overexpression	5'-TCCGTCGACAACAAGACAGCCCAATTGAG-3'

To obtain a complemented strain for each of the above WPRE deletion mutants, a DNA sequence containing an intact promoter region, the ORF and a C-terminal GFP fusion was designed to target the gene copy of each WPRE deletion mutant in which the WPRE was deleted. The SAT^r marker was first excised from the WPRE mutants in the medium YPM (Yi *et al*., 2008). The 5' region spanning the promoter and ORF was amplified by PCR with the primers wQ1f and wQ1r (Table 7). The 3' region spanning a region downstream of the stop codon was amplified using the primers wQ2f and wQ2r (Table 7). The 5'-3' fusion product was amplified by PCR and subcloned into pGEM-T Easy to derive pGeneXwQ-T. A fragment containing both *GFP* and the SAT^r marker was amplified by PCR with primers GFBhF1 and SATBgF1 (Table 7), using plasmid pK91.6 (T. Srikantha and D. R. Soll, unpublished) as template. This *GFP-SAT* fragment was digested with BamHI plus Bg1II and ligated into the BamHI (or BglII in the case of *CSH1*)-digested, dephosphorylated plasmid pGeneXwQ-T to derive plasmid pGeneXwQ-SAT. C-terminal GFP fusion was confirmed to be in-frame by sequencing. pGeneXwQ-SAT was then digested with SacI plus SacII and transformed into the WPRE deletion mutants. The resulting complemented strains were verified by PCR, sequencing and Southern analysis. We generated in this way the complemented control strains $EAP1_{WPRE\Delta}$-*EAP1/eap1*, $PGA10_{WPRE\Delta}$-*PGA10/pga10*, $CSH1_{WPRE\Delta}$-*CSH1/csh1*, and $PBR1_{WPRE\Delta}$-*PBR1/pbr1*.

Null mutants of each gene were also created. As described earlier, the heterozygous mutants were derived based on the selection marker SAT^r (Reuss *et al*., 2004). The deletion cassette for the second allele was then constructed using the same strategy to delete the first copy. The resulting plasmid pGeneX2-2A was digested with SacI and SacII, and transformed by electroporation into the heterozygous mutant strains for each gene. At least two independent null mutants for each gene were generated and confirmed by PCR and Southern analysis. We generated in this way the null mutants *eap1*/*eap1*, *pga10*/*pga10*, *csh1*/*csh1* and *pbr1*/*pbr1*.

Northern Analysis

The methods for northern blot hybridization have been described in detail (Srikantha *et al*., 2006; Yi *et al*., 2008). Probes were made by polymerase chain reaction (PCR) for genes that have been implicated in adhesion, cell wall biogenesis, biofilm formation and filamentation. The primers for synthesizing the probes for these genes are presented in Table 8. Quantitation for the signal intensity of each band in northern blots was performed by gray value analysis in the graphics program Adobe Photoshop™.

Imaging GFP-tagged Proteins

Fluorescence of GFP-tagged proteins was visualized through a ZEISS Axioplan2 upright optical microscope and a 63x Plan-Apochromat oil immersion objective (numerical aperture 1.4). GFP was excited at 475-nm with an Omega Set XF 100 filter by Attoarc HBO 100 epi-fluorescence lamp. The same acquisition parameters were used for all samples. AxioVision Release 4.6 software was used for image acquisition. Images were then prepared for publication using Adobe Photoshop™.

Western Analysis

The methods for western blot analysis have been described previously (Yi *et al*., 2009). Rabbit anti-GFP antibody (SC-8334, Santa Cruz Technology, Santa Cruz, CA) was used to detect GFP-tagged proteins.

Shmooing and Mating

The methods for analyzing shmoo formation in response to 3×10^{-6} M α-pheromone, the synthetic 13-mer, were previously described in detail (Lockhart *et al.*, 2003b; Yi *et al.*, 2008). The methods for testing mating with opaque α/α cells of strain WO-1 have also been described (Lockhart *et al*., 2003a).

Table 8. Oligos for genes analyzed by northern blot in the study of white-specific pheromone-regulated genes

Gene	Primer	Sequence
EAP1	EAP1f	5'-TAGCACTGATTGTACCAC-3'
EAP1	EAP1r	5'-AGCTGGTGTAGATTCAGT-3'
PGA10	PGA10f	5’-TGACTGTGTTGCTAAAAA-3’
PGA10	PGA10r	5’-TGCTGCGGAGGACTTTTC-3’
CSH1	CSH1f	5'-TCGACTCTGAAAAAACTA-3'
CSH1	CSH1r	5'-CATGCCAATGAAACTTGC-3'
PBR1	PBR1f	5’-AATGTGACTTTATACATT-3’
PBR1	PBR1r	5’-CAGCATATAAGTAATCAT-3’
RBT5	RBT5f	5'-TGATGCCGCTGCTGAAAC-3'
RBT5	RBT5r	5'-ACAGCGGCAATGACACCA-3'
PHR1	PHR1f	5'-TCATGAAGAGTGTATGAA-3'
PHR1	PHR1r	5'-TACATCCATATTCGGAGA-3'
PHR2	PHR2f	5'-TGAATCCATCAACAGAGA-3'
PHR2	PHR2r	5'-ATACCACCAGACCAAACT-3'
LSP1	LSP1f	5'-TGGTGAATTGGAAGATCA-3'
LSP1	LSP1r	5'-CTTTACCATAACCAGCAA-3'
CIT1	CIT1f	5'-AACTGTCATTGGTGAAGT-3'
CIT1	CIT1r	5'-ATTCCTTGTTGTCACCAA-3'
SUN41	SUN41f	5’-GCTTGCCAAAGTGGTATG-3’
SUN41	SUN41r	5’-ACCTCTCCAAGTGTAATA-3’
WH11	WH11f	5'-ATGTCCGACTTAGGTAGA-3'
WH11	WH11r	5'-TTATTTGGAGTCACCAAA-3'
19.2077	19.2077f	5'-TTAAAAGGAGCCAAGAGT-3'
19.2077	19.2077r	5'-TCAACACCTTTGTCGTCA-3'
INT1	INT1f	5'-CAAACCGAGTTTAGATCC-3'
INT1	INT1r	5'-TGACACTTTAGGAGTTGC-3'
UTR2	UTR2f	5'-AGTTAAAGAAATTGAATTA-3'
UTR2	UTR2r	5'-TCTTTAATGTGAGCATAA-3'
PDE2	PDE2f	5'-TACTACTACTACTAATAC-3'

Table 8 --- continued

PDE2	PDE2r	5'-AATAAACCAAATCGTCAT-3'
SSA2	SSA2f	5’-GTTCAGATCTACTTTGGA-3’
SSA2	SSA2r	5’-TTTGGTCATGATACCACC-3’
OCH1	OCH1f	5’-GATTAAAACCAGTTGATG-3’
OCH1	OCH1r	5’-TCAGTGAAAATCCCAGGA-3’
GPI8	GPI8f	5’-AGGTATAACGAAATATTT-3’
GPI8	GPI8r	5’-CTTCACTAACATTACGCT-3’
GPA2	GPA2f	5'-AATGAAATTTTAGATTAT-3'
GPA2	GPA2r	5'-GACCACCAACATCAAATA-3'
FGR23	FGR23f	5’-TACTCATTGTCCTGAATG-3’
FGR23	FGR23r	5’-AGTTGGACATGTAGTTAT-3’
RBT4	RBT4f	5'-TCTACTAAAGACGCTTCT-3'
RBT4	RBT4r	5'-GTACCAAGCTTGAAGAGC-3'
ALS1	ALS1f	5'-CATGTCAAGTTCAAAGAT-3'
ALS1	ALS1r	5'-CTAGTTACGATTGAGGAT-3'
ALS2	ALS2f	5'-CCGGGTGGTACTGACTCA-3'
ALS2	ALS2r	5'-ATTCAGTAGTGGTCACAG-3'
ALS3	ALS3f	5'-TATGACACCATGTCAAGT-3'
ALS3	ALS3r	5'-AGCAGTAGTAAAAGTAGA-3'
ALS4	ALS4f	5'-CACCAATAGTGTCATTAT-3'
ALS4	ALS4r	5'-ATAGAAGTTTGACAACCA-3'
ALS5	ALS5f	5'-TACAACTACAACCCAGTT-3'
ALS5	ALS5r	5'-TTCTCTAACAATGACTGA-3'
ALS6	ALS6f	5'-TCAAGTATGAGTTGTGTA-3'
ALS6	ALS6r	5'-AATCCGAGCACACCGGAT-3'
ALS7	ALS7f	5'-TCACGTAGAGTCCAGTAGT-3'
ALS7	ALS7r	5'-TGACGTAGTGTACAAATC-3'
ALS9	ALS9f	5'-ACCAAGTGTTTCCAGTTT-3'
ALS9	ALS9r	5'-AATGGAAGTGACCGCACT-3'
HYR1	HYR1f	5'-TCTCAACCTCAGTGCTGC-3'
HYR1	HYR1r	5'-AACAAGACCCGAAGAAG-3'
IFF4	IFF4f	5'-TCTTCTACAGCCGGAAGT-3'
IFF4	IFF4r	5'-TTCACTGGAGACAAATGA-3'

Table 8 --- continued

CSA1	CSA1f	5'-GCAGAAGCTGCTCATAAG-3'
CSA1	CSA1r	5'-AAACACGAAACTAGCGAC-3'
ECM33	ECM33f	5'-ATGCAAATTAAGTCATTTCT-3'
ECM33	ECM33r	5'-GATTGAAATTTAATGAGAC-3'
HSP12	HSP12f	5'-ACAAACACCATAAATCCC-3'
HSP12	HSP12r	5'-CATATTCTTGAGCTGTTT-3'
ECM331	ECM331f	5’-CGGTAATTTAACTATTCA-3’
ECM331	ECM331r	5’-TTCCATAGTCAAATTATC-3’
AAF1	AAF1f	5’-TGATGTAACGGTCAATTT-3’
AAF1	AAF1r	5’-ATTTTTATTTGTCAGTTT-3’
SAP1	SAP1f	5’-AGGAGTTATTGCCAAGAA-3’
SAP1	SAP1r	5’-GAAAGTATGACCTTGACC-3’
ECE1	ECE1f	5’-TAATGCCGTCGTCAGATT-3’
ECE1	ECE1r	5’-ATTGCTAAGTGCTACTGA-3’
BGL2	BGL2f	5’-CAAGTGTCCCAGTTGGTA-3’
BGL2	BGL2r	5’-CAGATACCTTTTTGCCAT-3’
PGA59	PGA59f	5'-ATGCAATTCTCATCCGCT-3'
PGA59	PGA59r	5'-AACAAACCGGCAGCAACG-3'
MSB1	MSB1f	5’-CTGTTTCTTAATCACAGA-3’
MSB1	MSB1r	5’-TAAACTCAGAATGTCATT-3’
CSE4	CSE4f	5’-ATCATCGCTACCACGAAG-3’
CSE4	CSE4r	5’-TGAATCGCACATAAATTT-3’
CHK1	CHK1f	5'-TACCAGACCAATATGAAC-3'
CHK1	CHK1r	5'-TTAGTGCAACAGTTGTAT-3'
KRE1	KRE1f	5'-TGAACGTTAACTCAGTCA-3'
KRE1	KRE1r	5'-TGAATGAAATGAATGCAA-3'
SSK1	SSK1f	5'-ACTACTAGAAAGAACAGA-3'
SSK1	SSK1r	5'-TAAACCTACACGAGTATT-3'
SMI1B	SMI1Bf	5'-ACCAAATTGTGTCATTCA-3'
SMI1B	SMI1Br	5'-ACATTGAAGTTGCGGTAT-3'
CRH1	CRH1f	5'-ATGATTTGGATGAAATTG-3'
CRH1	CRH1r	5'-ATACTTGTGTCCTTCATA-3'
IFF11	IFF11f	5’-GTCTATTACTATTGCTGG-3’

Table 8 --- continued

IFF11	IFF11r	5’-ACTAGTAGTTTTTGATTG-3’
GPI1	GPI1f	5’-TTACCTCAATTATTAAAT-3’
GPI1	GPI1r	5’-ATTAAATTAATCCCATCA-3’
GPI13	GPI13f	5’-TACGAGTACTGACAATGT-3’
GPI13	GPI13r	5’-ACATATGAATTAGATGCA-3’
CHS1	CHS1f	5’-CAGGGGCTGCTGGTGAAA-3’
CHS1	CHS1r	5’-GCCAAGTACATATTTGCT-3’
EXG1	EXG1f	5’-GTTGTTATTGGTATTGAA-3’
EXG1	EXG1r	5’-ACGTTCCAATGGGATTCC-3’
UAP1	UAP1f	5’-ATTCTAAGGGCATCAAAC-3’
UAP1	UAP1r	5’-TTTAAAAATTCCACTGAA-3’
RAM1	RAM1f	5’-TAGATAATTTAAGAGAAT-3’
RAM1	RAM1r	5’-GCAAGGGCACAATAAGTA-3’
PMT1	PMT1f	5'-GGCAAAGAAACCGTCACA-3'
PMT1	PMT1r	5'-ATCAGGAAATTTATCACCA-3'
ACE2	ACE2f	5'-TCCATTAACGGTGTCAACA-3'
ACE2	ACE2r	5'-TTGGCAACAATGTACTCGT-3'
PMT5	PMT5f	5’-TGATGACTGATCAAAGAG-3’
PMT5	PMT5r	5’-AGTTTCTGTTCGTGACTC-3’
MDR1	MDR1f	5'-TAATGATAATGATGTTGAT-3'
MDR1	MDR1r	5'-TTTAACCACATCAGCAAC-3'
ENO1	ENO1f	5’-TGGTAACGTCGGTGACGA-3’
ENO1	ENO1r	5’-GTGGACCCAAGCATCCCA-3’
ADH1	ADH1f	5'-ATGCAAGCAAGCTTATTC-3'
ADH1	ADH1r	5'-TATCAAAGACAACGGCTT-3'
RIX7	RIX7f	5’-CAGGTATAAGTGCTATTA-3’
RIX7	RIX7r	5’-GGAATAGTTGCGAATCCC-3’
MIG1	MIG1f	5’-CCGATGGTAATAAATTAT-3’
MIG1	MIG1r	5’-TTAGTATTAGATGTTGTT-3’
CDR1	CDR1f	5’-GCTGGTGCTTATCAATAT-3’
CDR1	CDR1r	5’-CTGGGAAATCAACACTTC-3’
CDR3	CDR3f	5’-GTATTGATGTGGTTAATC-3’
CDR3	CDR3r	5’-TCCTGACATTTTTGAACT-3’

Table 8 --- continued

YWP1	YWP1f	5’-ACTGTCCATTAAGTTCTT-3’
YWP1	YWP1r	5’-TTATAAGTAACATAATGA-3’
VPS1	VPS1f	5’-TCCTGCATCAATTGCATT-3’
VPS1	VPS1r	5’-ACATCTGATAGAAGGTTC-3’
NUP85	NUP85f	5’-CCGAAAAGCCGCCTTCGG-3’
NUP85	NUP85r	5’-GGTACCAATTCATGAATA-3’
KEM1	KEM1f	5’-TCAACCATTCCATTTACT-3’
KEM1	KEM1r	5’-TAGAAACTTCGGAACGGA-3’
SUV3	SUV3f	5’-AGTGGAAAAACTGAATAC-3’
SUV3	SUV3r	5’-AATTTTTCTACAGTAGAA-3’
SNF1	SNF1f	5’-TATGCCAGATTATTTGTT-3’
SNF1	SNF1r	5’-TGGACTTGGTGGTGGAGA-3’
RNH1	RNH1f	5'-ATGCCATATTACGCAGTT-3'
RNH1	RNH1r	5'-TCAGTATCTTCCTGTAGT-3'
CSC25	CSC25f	5’-GGTTAACTTATAAGTCGC-3’
CSC25	CSC25r	5’-ATAGAATAAAGGATCTTC-3’
NAG2	NAG2f	5’-TCGGATTATGACACAGCC-3’
NAG2	NAG2r	5’-ACCGATCGCCAGTCTTTA-3’
SHE3	SHE3f	5’-CTTGTCGATTTTGAATGA-3’
SHE3	SHE3r	5’-GAAACTTTTTCAATCATA-3’
RBF1	RBF1f	5’-TGAAAAGGATCAGAAAAG-3’
RBF1	RBF1r	5’-TTGCTGTTGTGCTTGGCT-3’
VAC1	VAC1f	5’-AGTTGAATTACACACACG-3’
VAC1	VAC1r	5’-CGTTCATTGTCTCTTGTG-3’
RFG1	RFG1f	5’-CTTCCTAATAATAAATCT-3’
RFG1	RFG1r	5’-AGTTTGTGGGTTGCTAGT-3’
DDR48	DDR48f	5’-AGAGAAGTAACGATTCAT-3’
DDR48	DDR48r	5’-TGTTGGAAGAGCCATAGG-3’
IRS4	IRS4f	5’-CAGTTTCTAGTCGTCTTC-3’
IRS4	IRS4r	5’-GATCCATATCACGATAGT-3’
IHD1	IHD1f	5’-CAAATGAAACTGGTTCTG-3’
IHD1	IHD1r	5’-CTGGTTCCATTAGTAAAT-3’
REG1	REG1f	5’-AATAATTTTGGGCCAGCA-3’

Table 8 --- continued

REG1	REG1r	5’-ATAAGATGCATACACTGA-3’
MNN2	MNN2f	5’-TGTTTGAAAGTGATTTAT-3’
MNN2	MNN2r	5’-TTGTAGTATAAACAAAGC-3’
SWI1	SWI1f	5’-TCATGGAGTTATTAGACG-3’
SWI1	SWI1r	5’-TGAAACTCAAGCACATCT-3’
NOT4	NOT4f	5’-CGAAGCCCATAAGGAACA-3’
NOT4	NOT4r	5’-GCGTACATTTCTTATATC-3’
ADR1	ADR1f	5’-CATCCTTCTAAATTGAAT-3’
ADR1	ADR1r	5’-TCCGTAAAGAACAGACAA-3’
CRK1	CRK1f	5’-GATAAAGAACGATTTAAA-3’
CRK1	CRK1r	5’-GAATATCCCTCCGTCTTT-3’
RAS1	RAS1f	5’-TAGAAACTTCTGCTAAAC-3’
RAS1	RAS1r	5’-GGAAGATTTGCTTGACCA-3’
RAS2	RAS2f	5’-GCAAACGTAATGGGAGTT-3’
RAS2	RAS2r	5’-CGAGTTAGTGTTGATAAT-3’
PTC1	PTC1f	5’-TACTGCTGCAGTGGCTGT-3’
PTC1	PTC1r	5’-CATATATGTGTTCACCAAG-3’
BIG1	BIG1f	5’-GATGATCGAGTCAAAGAA-3’
BIG1	BIG1r	5’-TTCATCTTTCTTTTTATT-3’
PLD1	PLD1f	5’-CATGTGGGCAGACCGCAA-3’
PLD1	PLD1r	5’-TCGATGAAACAAGCTGTT-3’
HSL1	HSL1f	5’-GCACCATCTTCTGGTATG-3’
HSL1	HSL1r	5’-CATTAGTATCAGTTGTAC-3’
NOT3	NOT3f	5’-CAAACACTTCCTCATCAA-3’
NOT3	NOT3r	5’-GTCTTCAGTTCTACCAGT-3’
YVH1	YVH1f	5’-AATGAAATATTGAAGAGC-3’
YVH1	YVH1r	5’-TCTAATTCTTGTTTCATC-3’
SPT6	SPT6f	5’-GGGTCAAAGGCGAATGTT-3’
SPT6	SPT6r	5’-GTCAAATTCACTCTTTAC-3’
FIG1	FIG1f	5’-TTTAGCAATATATGTCAT-3’
FIG1r	FIG1r	5’-CATCAATATAAAACTAAA-3’
RAX2	RAX2f	5’-GTCTTAATAATACTTTTG-3’
RAX2	RAX2r	5’-AATTATTGAAATTACCAC-3’

Table 8 --- continued

UPC2	UPC2f	5’-TCAATATGCTTGACTTGA-3’
UPC2	UPC2r	5’-ATATCAAGGCACTGGCAA-3’
CPH1	CPH1f	5’-CAATTACGATTCATTTTT-3’
CPH1	CPH1r	5’-TGCTGAAATTGGCGGCAC-3’
KEL1	KEL1f	5’-CGACTTGCCTTCAACTAC-3’
KEL1	KEL1r	5’-GACCAATTCGTTGGTGAG-3’
CDC5	CDC5f	5’-CTCAACCAGGTGTGCTTT-3’
CDC5	CDC5r	5’-AGCTGGAGGGTTTGCAAG-3’
GAL10	GAL10f	5’-GGAAAAGTGTACAAATTA-3’
GAL10	GAL10r	5’-TGAGTTGGAAACATTGAA-3’
HXK1	HXK1f	5’-TTGGAAACAACCGACTAC-3’
HXK1	HXK1r	5’-CGTAGCATCAGCCAACAT-3’
STE2	STE2f	5'-GTGTTCAACATAAGAAGA-3'
STE2	STE2r	5'-ATTATTAGCAGTTTGAGC-3'
MFA1	MFA1f	5'-ATGGCTGCTCAACAACAA-3'
MFA1	MFA1r	5'-TTACATAACAGAACAAGT-3'

Adhesion and Biofilm Formation

The methods for analyzing α-pheromone-induced adhesion to a plastic surface were previously described in detail (Daniels *et al*., 2006; Stoodley and Stoodley, 2005). Adhesion was assessed after 16 hr on the surface of a plastic Costar twelve-well cluster plate (Corning Life Sciences, Lowell, MA). The analysis of white cell biofilm enhancement by minority opaque cells (5% opaque **a**/**a** P37005 cells and 5% opaque α/α WO-1 cells) was previously described (Daniels *et al*., 2006). Biofilm thickness was analyzed by laser scanning confocal microscopy of calcofluor-stained biofilms after 48 hr of incubation on a silicone elastomer surface. The intensity of calcofluor staining through the depth of a biofilm was represented as a graph in which the mean pixel intensity (y-axis) was plotted as a function of depth (x-axis). The mean grayscale value (0-256) of all the pixels (512x512) in each X-Y optical section was calculated. To visualize the extrapolymeric substance (EPS), also referred to as "matrix", between cells in a biofilm, excitation of calcofluor was increased. Since the EPS was much dimmer than the cells in a biofilm, the laser power at 780 nm was increased to the point at which the cell pixels became saturated. Adobe Photoshop™ was then used to remove the saturated pixels (the cells), leaving behind an image of the EPS. Grayscale images were pseudocolored using Confocal Assistant software LUT.

Generating *PBR1*-misexpression Strains

The plasmid pNIM1 (Park *et al*., 2005), harboring a GFP gene and the tetracycline-regulated promoter, was employed in this study. The pNIM1 plasmid was also a generous gift from Joachim Morschhäuser. The ORF of the *PBR1* gene, amplified by PCR with primers listed in Table 7, was digested with SalI and subcloned into the plasmid pNIM1 that had been digested with SalI and dephosphorylated, to derive pTet-PBR1. The correct orientation of the *PBR1* ORF was confirmed by sequencing. The *GFP* gene was fused in-frame to the C-terminus of *PBR1* ORF. The plasmid pTet-PBR1

was then digested with ApaI plus SacII, and transformed into either wild-type or mutant strains. The transformants were verified by PCR and Southern analysis. Activation of the *PBR1* transcription by doxycycline was demonstrated by northern analysis. We generated in this way the derivative strains P37005-tet*PBR1*, *EAP1*$_{WPRE\Delta}$/*eap1*-tet*PBR1*, *PGA10*$_{WPRE\Delta}$/*pga10*-tet*PBR1*, *CSH1*$_{WPRE\Delta}$/*csh1*-tet*PBR1*, *PBR1*$_{WPRE\Delta}$/*pbr1*-tet*PBR1* and *cek1cek2-tetPBR1*.

Measurements Secreted (1, 3)-β-glucan Concentration from Biofilms

Equal numbers of cells ($5x10^7$) of mutant or parental strains were case without (-) and with (+) 1% opaque cells onto silicone elastomer squares in RPMI medium, as described previously (Daniels *et al*., 2006; Yi *et al*., 2008, 2009). After 48 hr, supernatants from biofilm culture were collected by pipetting off the supernatant without disturbing the culture, centrifuging at 4,000 rpm for 5 min, and removing the supernatant. Glucan concentration in the supernatants was then measure using Glucatell (1,3)-β-Glucan Detection Reagent Kit (Associates of Cape Cod, Falmouth, MA) (Nobile *et al.*, 2009). Optical density (OD) values were determined at 540 nm in a microplate reading (MDS Analytical Technologies, Sunnyvale, CA) and the glucan concentration assessed by an end-point assay according to the manufacturer's protocol. Four biofilms were employed for condition and strain. The means and standard deviation of glucan concentration are presented in a bar chart.

Results

Selective Induction of White-specific Genes

In past studies, the genes *CSH1* (Yi *et al*., 2009), orf19.2077 (Sahni *et al*., 2009a) and orf19.6274 (Sahni *et al*., 2009a) had been demonstrated to be selectively up-regulated by pheromone in white, but not opaque, cells. To identify additional genes similarly

up-regulated, we analyzed by northern blot hybridization the expression patterns of 103 genes that had been implicated in adhesion, cell wall biogenesis, biofilm formation, filamentation or switching (Table 9). Nine of these genes (*EAP1*, *PGA10*, *RBT5*, *PHR1*, *PHR2*, *LSP1*, *CIT1*, *SUN41*, *WH11*) were strongly up-regulated in white but not opaque cells (Figure 39A). With the genes *CSH1*, orf19.2077 and orf19.6274 (Figure 39A), the last renamed *PBR1* (Pheromone-induced Biofilm Regulator 1) for its role in white cell biofilm formation, which we demonstrate here, we had 12 genes for further analysis that were selectively up-regulated by pheromone in white but not opaque cells.

Putative Pheromone-regulated *cis*-acting Elements

To identify potential pheromone-regulated *cis*-acting elements, the promoters of the 12 white-specific test genes and the promoters of six genes that had previously been shown to be selectively up-regulated by pheromone in opaque cells, *MFA1*, *FUS1*, *CPH1*, *ECE1*, *KAR4* and *RAM1* (Bennett *et al*., 2003; Daniels *et al*., 2006; Yi *et al*., 2009; Bennett and Johnson, 2006 and N. Sahni, S. Yi, D. R. Soll, unpublished observations), were subjected to sequence analysis with the Multiple EM (model) for Motif Elicitation (MEME) software (Bailey *et al*., 2006) in order to identify among the white group and among the opaque group consensus sequences with the highest level of homology. The one thousand base pair upstream regions of the genes in the white and opaque sets were each analyzed for a common motif with an upper length limit of 15 bp at an E value of ≤0.001 as a threshold (Bailey and Elkan, 1994; Grundy *et al*., 1997; Bailey *et al*., 2006). At this stringent threshold, the E value represents the expected number of motifs with a score as good or better than the analyzed motif, in a set of similar sized random sequences (Bailey *et al*., 2006). The promoters of all 12 white-specific genes contained at least one copy of a putative white pheromone-regulated element (WPRE) with high homology to the consensus sequence AAAAAAAAAAGAAAG (Figure 39B; Table 10). Using the same stringent E value of ≤0.001 as a threshold, this DNA sequence was found to be absent in

Table 9. Genes screened for differential expression in *C. albicans* white cells in response to pheromone

A. Genes strongly induced by pheromone						
Adhesion:	*EAP1*	*PGA10*	*RBT5*			
Cell wall biogenesis	*PHR1*	*PHR2*				
Biofilm formation:	*CSH1*	*LSP1*	*CIT1*	*SUN41*		
Other:	*PBR1*	*WH11*	*19.2077*			
B. Genes slightly induced by pheromone						
Adhesion:	*INT1*					
Cell wall biogenesis:	*UTR2*	*PDE2*	*SSA2*	*OCH1*	*GPI8*	
Filamentation:	*GPA2*	*FGR23*	*RBT4*			
C. Genes not induced by pheromone						
Adhesion:	*ALS1*	*ALS2*	*ALS3*	*ALS4*	*ALS5*	*ALS6*
	ALS7	*ALS9*	*HYR1*	*IFF4*	*CSA1*	*ECM33*
	HSP12	*ECM331*	*AAF1*	*SAP1*	*ECE1*	*BGL2*
	PGA59	*MSB1*	*CSE4*			
Cell wall biogenesis:	*CHK1*	*KRE1*	*SSK1*	*SMI1B*	*CRH1*	*IFF11*
	GPI1	*GPI13*	*CHS1*	*EXG1*	*UAP1*	*RAM1*
Biofilm formation:	*PMT1*	*ACE2*	*PMT5*	*MDR1*	*ENO1*	*ADH1*
	RIX7	*MIG1*	*CDR1*	*CDR3*	*YWP1*	*VPS1*
	NUP85	*KEM1*	*SUV3*	*SNF1*		
Filamentation	*RNH1*	*CSC25*	*NAG2*	*SHE3*	*RBF1*	*VAC1*
	RFG1	*DDR48*	*IRS4*	*IHD1*	*REG1*	*MNN2*
	SWI1	*NOT4*	*ADR1*	*CRK1*	*RAS1*	*RAS2*
	PTC1	*BIG1*	*PLD1*	*HSL1*	*NOT3*	*YVH1*
	SPT6	*FIG1*	*RAX2*	*UPC2*	*CPH1*	*KEL1*
	CDC5	*GAL10*	*HXK1*			

Figure 39. Twelve genes were identified that were strongly up-regulated by α-pheromone in white **a**/**a**, but not opaque **a**/**a**, cells. Each of these genes contained one or more putative white-specific pheromone response elements (WPRE) in their promoters. A. Northern analysis of the expression of twelve genes in white and opaque **a**/**a** cells in the absence (-) and presence (+) of α-pheromone (α-ph) that were identified in a screen of 103 genes as strongly up-regulated. B. The sequence considered to represent the putative white-specific pheromone response element (WPRE) in the promoters of the 12 selected white-specific genes in panel A, using a high stringency E value threshold of ≤0.001 in the Multiple for Motif Elicitation (MEME) software. The consensus sequence for WPRE is given at the bottom of the panel. C. The sequence considered the putative opaque-specific pheromone response element (OPRE) in the promoters of six genes selectively up-regulated by pheromone in opaque cells, using a threshold of 0.001 in the MEME program. The consensus sequence for OPRE is presented at the bottom of the panel. D. Genes up-regulated by α-pheromone in both opaque and white cells contain both OPRE and WPRE. The positions of the OPRE and WPRE sequence with the highest homology to the consensus sequence is given relative to the start codon in panels B, C and D.

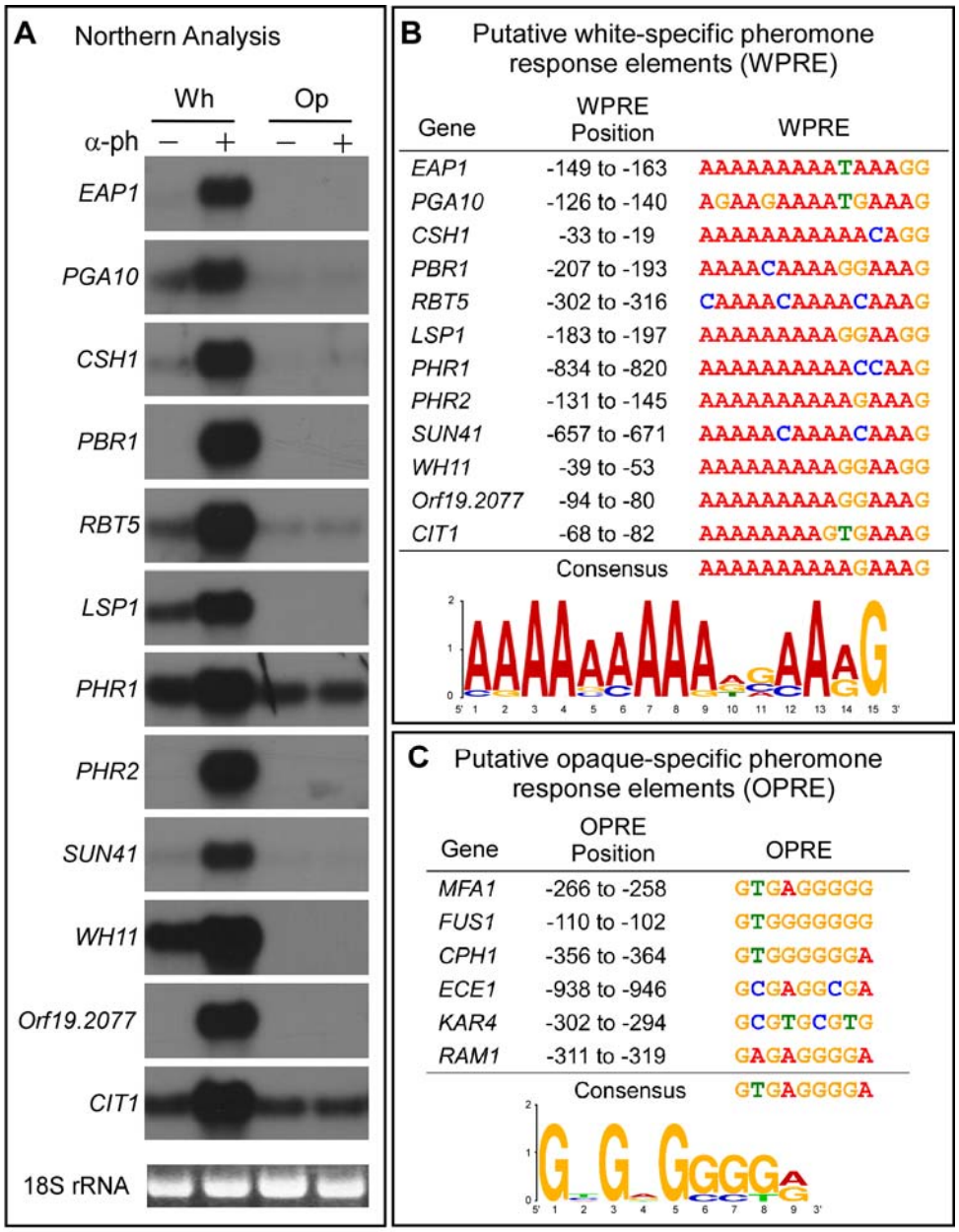

B Putative white-specific pheromone response elements (WPRE)

Gene	WPRE Position	WPRE
EAP1	-149 to -163	AAAAAAAAATAAAGG
PGA10	-126 to -140	AGAAGAAAATGAAAG
CSH1	-33 to -19	AAAAAAAAAAACAGG
PBR1	-207 to -193	AAAACAAAAGGAAAG
RBT5	-302 to -316	CAAAACAAAACAAAG
LSP1	-183 to -197	AAAAAAAAAGGAAGG
PHR1	-834 to -820	AAAAAAAAAACCAAG
PHR2	-131 to -145	AAAAAAAAAAGAAAG
SUN41	-657 to -671	AAAAACAAAACAAAG
WH11	-39 to -53	AAAAAAAAAGGAAGG
Orf19.2077	-94 to -80	AAAAAAAAAGGAAAG
CIT1	-68 to -82	AAAAAAAAAGTGAAAG
	Consensus	AAAAAAAAAAGAAAG

C Putative opaque-specific pheromone response elements (OPRE)

Gene	OPRE Position	OPRE
MFA1	-266 to -258	GTGAGGGGG
FUS1	-110 to -102	GTGGGGGGG
CPH1	-356 to -364	GTGGGGGGA
ECE1	-938 to -946	GCGAGGCGA
KAR4	-302 to -294	GCGTGCGTG
RAM1	-311 to -319	GAGAGGGGA
	Consensus	GTGAGGGGA

D Genes upregulated by α-pheromone in both opaque and white cells

Gene	OPRE Position	OPRE	WPRE Position	WPRE
STE2	-168 to -176	GGGAGGGGG	-772 to -786	AAAAAAAAAACCAAC
CEK2	-175 to -183	GGAAGGGGA	-200 to -186	AAAAAAATAAAAAAA
SST2	-238 to -246	GGGGGAGGG	-309 to -323	AAAGAAACCAAAAAA
RBT1	-910 to -918	CTGGAGGGA	-706 to -692	AGAAAAAACAGAAAG

Table 10. The white-specific pheromone response elements (WPRE) found in genes up-regulated by α-pheromone exclusively in white cells and in genes up-regulated by pheromone in both white and opaque cells.

Gene	WPRE position	WPRE	P value (threshold < e-03)	WPRE range	Orientation
EAP1	-163	AAAAAAAAATAAAGG	2.98e-05	-163 to -149	-
PGA10	-140	AGAAGAAAATGAAAG	2.84e-05	-140 to -126	-
CSH1	-33	AAAAAAAAAAACAGG	2.49e-05	-33 to -19	+
PBR1	-207	AAAACAAAAGGAAAG	4.10e-05	-207 to -193	+
RBT5	-316	CAAAACAAAACAAAG	2.29e-05	-316 to -302	-
LSP1	-197	AAAAAAAAAGGAAGG	2.02e-05	-197 to -183	-
	-491	AAAGAAAAGAAAAAG	4.79e-05	-491 to -477	-
	-444	AAGAAAGAAAGAAAG	5.25e-05	-444 to -430	-
	-174	GAAGAAGAAAGAAAG	7.59e-05	-174 to -160	-
PHR1	-834	AAAAAAAAAACCAAG	4.10e-05	-834 to -820	+
	-766	AAGAAAAAAAAAATG	7.98e-05	-766 to -742	-
PHR2	-145	AAAAAAAAAAGAAAG	2.02e-06	-145 to -131	-
	-224	AAAAAAAAAACAAAG	5.25e-06	-224 to -210	-
	-165	GAAAGATGAAGAAAG	2.85e-04	-165 to -151	-
SUN41	-671	AAAAACAAAACAAAG	4.10e-05	-671 to -657	-
WH11	-53	AAAAAAAAAGGAAGG	1.43e-04	-53 to -39	-
Orf19.2077	-94	AAAAAAAAAGGAAAG	6.99e-05	-94 to -80	+
	-432	CAAAAAAAACAGAAG	2.25e-04	-432 to -418	-
CIT1	-82	AAAAAAAAGTGAAAG	9.86e-05	-82 to -68	-
	-420	GGAGAAAAAAAAAAG	1.92e-04	-420 to -406	-
	-61	AGGAAAAGAAGAAAT	3.82e-05	-61 to -47	-
STE2	-786	AAAAAAAAAACCAAC	1.85e-04	-786 to -772	-
CEK2	-200	AAAAAAATAAAAAAA	3.43e-04	-200 to -186	+
SST2	-323	AAAGAAACCAAAAAA	4.61e-04	-323 to -309	-
RBT1	-706	AGAAAAAACAGAAAG	2.66e-05	-706 to -692	+
	Consensus	AAAAAAAAAAGAAAG			

Table 10 --- continued

Gene	WPRE position	WPRE	P value (e-03 < threshold < e-02)	WPRE range	Orientation
EAP1	-500	AAAAAAAACATAAAC	4.03e-03	-500 to -486	+
PGA10	-432	GGAAACAAGACCAAG	6.17e-03	-432 to -418	-
CSH1	-408	GAAACAGACGGAAGG	3.32e-03	-408 to -394	+
PBR1	-262	CTAAAAAAAAAAAAG	1.35e-03	-262 to -248	-
	Consensus	AAAAAAAAAAGAAAG			

the promoters of the six genes selectively up-regulated by pheromone in opaque but not white cells. The consensus sequence had no homology to the consensus sequences for the pheromone response elements (PRE) of *S. cerevisiae* (Dolan *et al*., 1989, Errede and Ammerer, 1989; Hagen *et al*., 1991) or *Ustilago maydis* (Urban *et al*., 1996). The white-specific gene promoters also contained WPRE-like sequences with lower homology to the consensus sequence (Table 10). Only the WPRE sequence with the highest homology to the consensus sequence was included for initial analyses.

Again using the MEME program at an E value of ≤0.001 as a threshold and with an upper length limit of 15 bp (28-30), the promoters of all six opaque-specific genes were found to contain at least one copy of a putative opaque pheromone-regulated element (OPRE) with the unique consensus sequence GTGAGGGGA (Figure 39C; Table 11). At this E value, this element was absent in the promoters of the 12 genes selectively up-regulated by pheromone in white cells. It exhibited no significant homology with the PREs of mating genes in *S. cerevisiae* (Dolan *et al*., 1989; Errede and Ammerer, 1989; Hagen *et al*., 1991) or *U. maydis* (Urban *et al*., 1996). Bennett and Johnson (2006) had reported the presence of a putative PRE element similar to that in *S. cerevisiae* in some, but not all, pheromone up-regulated genes in opaque cells. In an expanded list of ten pheromone-regulated opaque genes (*MFA1, FUS1, STE2, SST2, CPH1, KAR4, ECE1, RAM1, CEK2, RBT1*), we found sequences weakly homologous to the *S. cerevisiae* PRE-like element with an average E value of 10^{+2}, which indicates that the homology is probably spurious (Bailey and Elkan, 1994; Grundy *et al*., 1997; Bailey *et al*., 2006). In contrast, every one of the 10 genes had an OPRE sequence with an average E value of 10^{-5} (Table 11). Decreasing the length in the MEME search to a maximum of nine base pairs identified the same consensus sequences (Table 11) These results strongly suggested that the OPREs were better candidates for a *cis*-acting sequence regulating pheromone-induced expression of opaque genes than sequences weakly homologous to the *S. cerevisiae*

Table 11. The opaque-specific response elements (OPRE) found in genes up-regulated by α-pheromone exclusively in opaque cells and in genes up-regulated by pheromone both in white and opaque cells.

Gene	OPRE Position	OPRE	P value (threshold< e-03)	OPRE range	Orientation
MFA1	-266	GTGAGGGGG	1.23e-06	-266 to -258	+
FUS1	-110	GTGGGGGGG	1.59e-04	-110 to -102	+
CPH1	-364	GTGGGGGGA	8.69e-06	-364 to -356	-
ECE1	-946	GCGAGGCGA	5.70e-04	-946 to -938	-
KAR4	-302	GCGTGCGTG	1.70e-04	-302 to -294	+
RAM1	-319	GAGAGGGGA	1.32e-06	-319 to -311	-
STE2	-176	GGGAGGGGG	4.87e-05	-176 to -168	-
CEK2	-183	GGAAGGGGA	2.63e-06	-183 to -175	-
SST2	-246	GGGGGAGGG	1.44e-05	-246 to -238	-
RBT1	-918	CTGGAGGGA	3.91e-06	-918 to -910	-
Consensus		GTGAGGGGA			

Gene	OPRE Position	OPRE	P value (e-03< threshold< e-02)	OPRE range	Orientation
CPH1	-54	ACGAGGGGG	5.37e-03	-54 to -46	-
MFA1	-392	GTGAGCGTA	1.24e-03	-392 to -384	+
SST2	-267	GGGGGAGGG	3.78e-03	-267 to -259	-
Consensus		GTGAGGGGA			

Gene	OPRE Position	OPRE	P value (threshold= 4e-02)	OPRE range	Orientation
MFA1	-963	GAAAGAAAAAACAAA	6.54e+02	-963 to -949	+
FUS1	-267	GCAACCAAAAAAAAA	1.96e+01	-267 to -253	+
CPH1	-806	GAAACAAAAACAAAA	5.83e+02	-806 to -792	-
ECE1	-449	GACGCCAAGAAAAAA	3.66e+03	-449 to -435	+
KAR4	-95	AAAACCAAAAAAGAG	2.41e+02	-95 to -81	-

Table 11 --- continued

RAM1	-566	GAAACCAAAATACAA	1.33e+01	-566 to -552	-
STE2	-787	GAAAAAAAAAAAAAA	4.76e+02	-787 to -773	+
CEK2	-47	GAAAATAAAAAAAAA	2.09e+02	-47 to -33	-
SST2	-329	GAAACCAAAAAAAAA	1.02e+01	-329 to -315	+
RBT1	-896	GCAGGCAAAAAAAAA	1.45e+03	-896 to -882	-
Consensus		GAAACCAAAAAAAAA			

PRE-like sequences, which were weakly to negligibly homologous to each other and not present in all opaque genes regulated by pheromone (Table 11).

If pheromone up-regulated opaque-specific genes through OPRE and white-specific genes through WPRE, then genes up-regulated by pheromone in both opaque and white cells should have both elements with the same high E values of white- and opaque-specific genes. Four such genes, *STE2*, *CEK2*, *SST2* and *RBT1* (Daniels *et al*., 2006; Bennett and Johnson, 2006), were analyzed by MEME software using the same high stringency E value of ≤ 0.001 as a threshold. The promoters of all four genes had at least one WPRE and at least one OPRE at this stringent threshold (Figure 39D; Table 10 and 11).

WPRE Regulates Pheromone-induced White-specific Gene Expression

Although sequence analyses revealed potential *cis*-acting elements, only functional analyses can establish their roles as such. To test whether the putative WPRE functioned as a pheromone-responsive *cis*-acting sequence for white-specific genes, one allele of each of the four white-specific genes *EAP1*, *PGA10*, *CSH1* and *PBR1* selected from the group of 12 genes, was deleted in the natural **a**/**a** strain P37005 to generate the heterozygous deletion mutants *EAP1*/*eap1*, *PGA10*/*pga10*, *CSH1*/*csh1* and *PBR1*/*pbr1*. The WPRE in the promoter of the retained allele in each heterozygote with the highest homology to the WPRE consensus sequence was then selectively deleted, resulting in the WPRE deletion mutants $EAP1_{WPRE\Delta}$/*eap1*, $PGA10_{WPRE\Delta}$/*pga10*, $CSH1_{WPRE\Delta}$/*csh1* and $PBR1_{WPRE\Delta}$/*pbr1*. The WPRE deletion derivative of each of these mutants was then replaced with the native gene and promoter to generate the complemented controls $EAP1_{WPRE\Delta}$-*EAP1*/*eap1*, $PGA10_{WPRE\Delta}$-*PGA10*/*pga10*, $CSH1_{WPRE\Delta}$-*CSH1*/*csh1* and $PBR1_{WPRE\Delta}$-*PBR1*/*pbr1*. All complemented strains contained a GFP tag at the 3' end of the open reading frame for protein localization studies and western analysis. The homozygous deletion mutants

eap1/eap1, *pga10/pga10*, *csh1/csh1* and *pbr1/pbr1*, were also created by deleting the remaining alleles in the original heterozygous mutant.

EAP1 encodes a glycosylphosphatidylinositol-anchored cell wall protein that functions as an adhesin in biofilm development in *S. cerevisiae* as well as in an **a**/α strain of *C. albicans* (Li *et al*., 2007; Li and Palecek, 2008; Reynolds and Fink, 2001). *PGA10*, also known as *RBT51*, encodes a putative hydrophobic extracellular membrane protein that plays a role in adhesion and biofilm development in an **a**/α strain of *C. albicans* (Perez *et al*., 2006). In the complemented strains $EAP1_{WPRE\Delta}$-*EAP1*/*eap1* and $PGA10_{WPRE\Delta}$-*PGA10*/*pga10*, GFP-tagged Eap1 and GFP-tagged Pga10, respectively, localized at the surface of α-pheromone-induced white cells (Figure 40A). *CSH1* encodes a protein involved in cell surface hydrophobicity in **a**/α cells (Singleton *et al*., 2001; Singleton and Hazen, 2004) and *PBR1* will be shown here to play a role in biofilm development in *MTL*-homozygous cells. In the complemented controls $CSH1_{WPRE\Delta}$-*CSH1*/*csh1* and $PBR1_{WPRE\Delta}$-*PBR1*/*pbr1*, GFP-tagged Csh1 and GFP-tagged Pbr1, respectively, localized primarily in the cytoplasm of α-pheromone-induced white cells (Figure 40A).

To test whether α-pheromone activated the four white-specific genes through the putative pheromone response element *WPRE*, expression of each gene was compared by northern analysis to the parental strain P37005, the homozygous deletion mutant, the *WPRE* deletion mutant and the complemented control, in the absence and presence of α-pheromone.

EAP1

In the absence of α-pheromone, *EAP1* was expressed at a basal level in white cells of the parental (P37005) strain, the WPRE deletion mutant and the complemented control strain (Figure 40B). α-pheromone up-regulated expression in both the parental and

Figure 40. Localization of Eap1, Pga10, Csh1 and Pbr1 and the role of WPRE in the induction of transcription. A. GFP visualization reveals that Eap1 and Pga10 localize primarily to the cell surface, and Csh1 and Pbr1 localize primarily in the cytosol upon induction by α-pheromone. The complemented strains *EAP1*$_{\text{WPRE}\Delta}$-*EAP1/eap1*, *PGA10*$_{\text{WPRE}\Delta}$-*PGA10/pga10*, *CSH1*$_{\text{WPRE}\Delta}$-*CSH1/csh1* and *PBR1*$_{\text{WPRE}\Delta}$-*PBR1/pbr1*, which were tagged at the carboxy terminus with GFP, were examined. B. Northern analysis of mRNA levels of the parental control, deletion mutants and complemented strains of the four genes in the absence (-) and presence (+) of α-pheromone. C. Northern analysis of pheromone-induced expression of *CSH1* and *PBR1* in deletion mutants missing both the high consensus (strong) WPRE and the low consensus (lc) (weak) WPRE, lcWPRE, in the absence (-) and presence (+) of α-pheromone (α-ph). D. Western analysis of pheromone-induced expression of *CSH1* and *PBR1* in deletion mutants, as in panel C, using anti-GFP antibody.

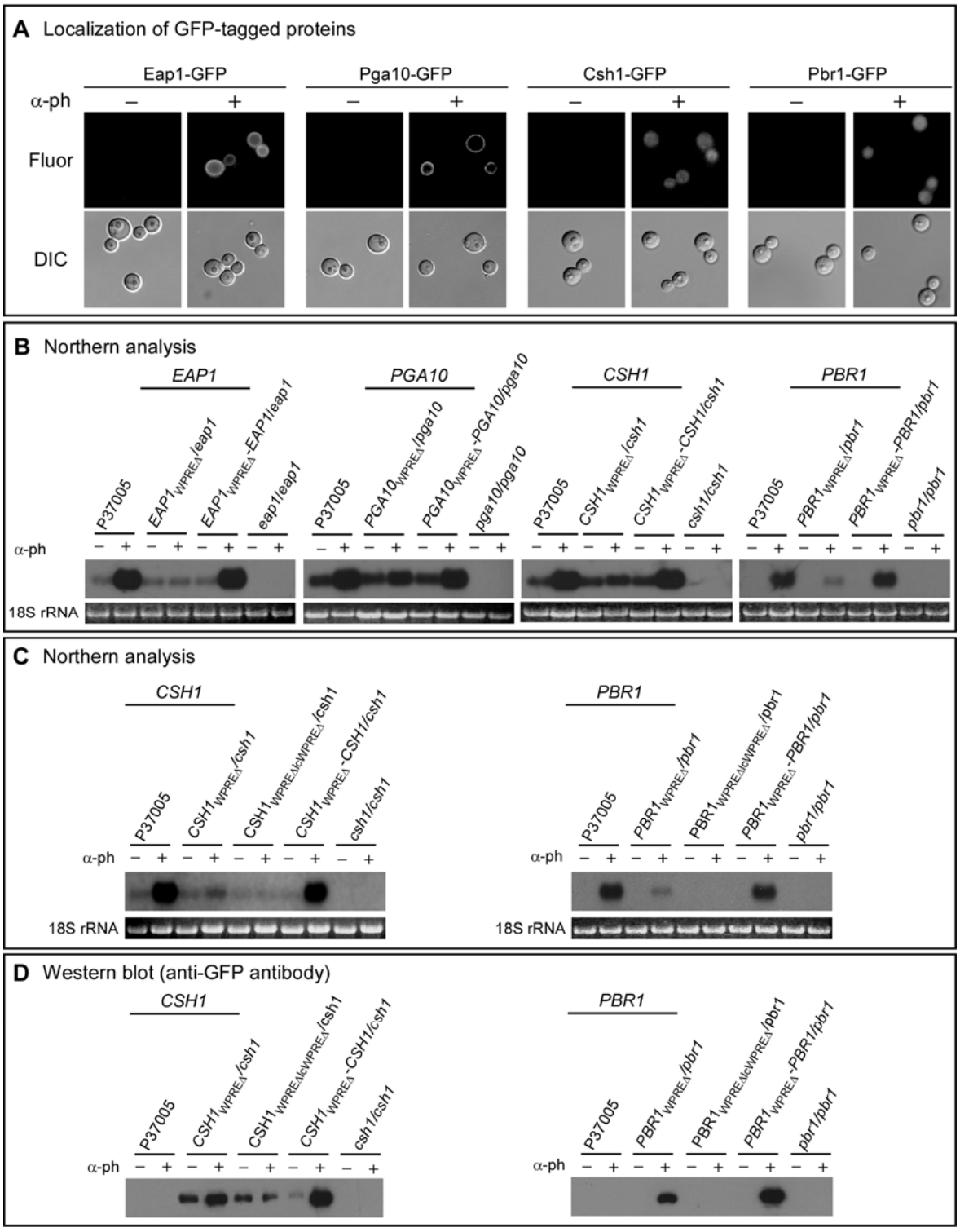
A Localization of GFP-tagged proteins
Eap1-GFP
Pga10-GFP
Csh1-GFP
Pbr1-GFP
α-ph
Fluor
DIC
B Northern analysis
EAP1
PGA10
CSH1
PBR1
P37005
EAP1WPREΔ/eap1
EAP1WPREΔ-EAP1/eap1
eap1/eap1
PGA10WPREΔ/pga10
PGA10WPREΔ-PGA10/pga10
pga10/pga10
CSH1WPREΔ/csh1
CSH1WPREΔ-CSH1/csh1
csh1/csh1
PBR1WPREΔ/pbr1
PBR1WPREΔ-PBR1/pbr1
pbr1/pbr1
18S rRNA
C Northern analysis
CSH1WPREΔΔcWPREΔ/csh1
D Western blot (anti-GFP antibody)

complemented control strains (Figure 40B). Expression in strain *EAP1*$_{WPRE\Delta}$/*eap1* remained at the basal level in the absence or presence of α-pheromone (Figure 40B).

PGA10 and *CSH1*

In the absence of α-pheromone, *PGA10* and *CSH1* were expressed at basal levels in white cells of the parental strain, the complemented control strains and the WPRE deletion mutants (Figure 40B). α-pheromone up-regulated expression of *PGA10* and *CSH1* in both the parental and complemented control strains by more than five- and six-fold, respectively (Figure 40B). α-pheromone also up-regulated expression of *PGA10* and *CSH1* in the WPRE deletion mutants, but to less than a third of the stimulated level in the parental or complemented control strains (Figure 40B).

PBR1

In the absence of α-pheromone, *PBR1* expression was undetectable in the white cells of the parental strain, complemented control and the WPRE deletion mutant (Figure 40B). There appeared, therefore, to be no basal expression, as there was for the other three genes tested. α-pheromone up-regulated PBR1 expression in the parental and complemented control strain (Figure 40B). It also up-regulated *PBR1* expression in the WPRE deletion mutant, but to a level only one tenth that of stimulated parental and complemented control cells (Figure 40B).

The low but reproducible levels of expression of *PGA10*, *CSH1* and *PBR1* induced by α-pheromone in the respective WPRE deletion mutants could have been mediated by a second, weaker pheromone-response element in the promoters of each of the three genes. We identified a lower consensus WPRE (lcWPRE) in the promoter of each of the three genes *PGA10*, *CSH1* and *PBR1*, located between -432 and -418, -408 and -394, and -262 and - 248 bp, respectively. Low consensus WPRE sequences in all 12 white-specific pheromone-induced genes are described in Table 10. To test whether these sites could be responsible for low level pheromone induction, we deleted them from strains

CSH1$_{WPRE\Delta}$/*csh1* and *PBR1*$_{WPRE\Delta}$/*pbr1*, generating strains *CSH1*$_{WPRE\Delta lcWPRE\Delta}$/*csh1* and *PBR1*$_{WPRE\Delta lcWPRE\Delta}$/*pbr1*. Deletion of the lcWPRE in the promoters of both of the WPRE mutants completely eliminated low level induction by pheromone in white cells (Figure 40C). These results indicate that the lcWPREs in the promoters of *CSH1* and *PBR1* were responsible for the low level of residual induction by pheromone observed in the WPRE deletion mutants (Figure 40B). We also compared, by western analysis using antibody against the GFP tags, the levels of the proteins Csh1 and Pbr1 in the WPRE deletion mutants *CSH1*$_{WPRE\Delta}$/*csh1* and *CSH1*$_{WPRE\Delta lcWPRE\Delta}$/*csh1*, and *PBR1*$_{WPRE\Delta}$/*pbr1* and *PBR1*$_{WPRE\Delta lcWPRE\Delta}$/*pbr1*, respectively, with the complemented controls. The levels of proteins were remarkably consistent with the transcription levels (Figure 40D).

Finally, we found that as is the case for other white-specific genes (Yi *et al*., 2008, 2009), up-regulation of the four selected genes *EAP1*, *PGA10*, *CSH1* and *PBR1* by pheromone was blocked in the mutants *ste4/ste4* and the double mutant *cek1/cek1 cek2/cek2*, but not in the mutant *cph1/cph1* (data not shown). These results demonstrate that as is the case for white-specific genes in general, up-regulation of these genes by pheromone depends upon the MAP kinase pathway, but not the target transcription factor Cph1.

OPRE Regulates Pheromone-induced Opaque-specific Gene Expression.

To assess whether the putative opaque pheromone response element OPRE mediated pheromone induction of opaque-specific genes, heterozygous deletion mutants were generated for *CPH1* and *MFA1*, genes selectively up-regulated by α-pheromone in opaque but not white cells (Yi *et al*., 2008). *CPH1* encodes the gene for the downstream transcription factor that activates opaque-specific genes and *MFA1* encodes the gene for the **a**-pheromone. The OPRE in the promoter of the retained *CPH1* and *MFA1* copy of the heterozygote *CPH1/cph1* and *MFA1/mfa1*, respectively, were then selectively deleted,

resulting in the OPRE deletion mutants *CPH1*$_{\text{OPREΔ}}$/*cph1* and *MFA1*$_{\text{OPREΔ}}$/*mfa1*. The *CPH1*$_{\text{OPREΔ}}$ and the *MFA1*$_{\text{OPREΔ}}$ copy in the respective mutants were then replaced with the wild type ORF and promoter to generate the complemented control *CPH1*$_{\text{OPREΔ}}$-*CPH1*/*cph1* and *MFA1*$_{\text{OPREΔ}}$-*MFA1*/*mfa1*. The GFP genes were fused in-frame for the localization and western studies. The wild type gene copy in both *CPH1/cph1* and *MFA1/mfa1* were also deleted to generate the homozygous deletion mutants *cph1/cph1* and *mfa1/mfa1*. The GFP-tagged Cph1 protein in strain *CPH1*$_{\text{OPREΔ}}$-*CPH1/cph1* localized in the nucleus of α-pheromone-treated opaque cells of the complemented strain, as would be expected for an opaque-specific *trans*-acting factor (Figure 41A).

Expression of *CPH1* and *MFA1* was then assessed by northern analysis in the parental strain P37005, the homozygous deletion mutants, the OPREΔ mutants and the complemented controls, in the absence or presence of α-pheromone. In the absence of α-pheromone, *CPH1* and *MFA1* expression was undetectable in opaque cells of the parental strain, complemented control and the OPRE deletion mutants (Figure 41B, C). α-pheromone up-regulated expression of *CPH1* and *MFA1* in both the parental and complemented control strains (Figure 41B, C). It also up-regulated *CPH1* and *MFA1* in the OPRE deletion mutants, but to only approximately one tenth the level of parental or complemented control cells (Figure 41B, C). These low levels of activation could have been mediated by weaker OPREs, as was the case for WPRE mutants. A site with lower OPRE homology to the consensus sequence was identified in both the *CPH1* and *MFA1* promoters (Table 11). These results indicate that the OPRE, not the *S. cerevisiae* PRE-like sequences identified by Bennett and Johnson (2006), function as the major response elements in the promoters of genes up-regulated by α-pheromone in opaque cells.

To provide further support to the suggestion that Cph1 up-regulates opaque-specific genes through the OPRE, we analyzed the expression of the genes *MFA1* and *KAR4*, which both contain an OPRE (Table 11), in the mutant *cph1/cph1*. Neither of

Figure 41. Up-regulation of the genes *CPH1* and *MFA1* by α-pheromone requires the opaque-specific pheromone response element OPRE. A. GFP visualization reveals that Cph1 localizes to the putative nucleus. The strain *CPH1*$_{\text{OPRE}\Delta}$-*CPH1/cph1*, which possesses a C-terminal GFP tag, was used for analysis. B. Northern analysis of the RNA levels of the parental control, deletion mutants and complemented strains for *CPH1* in the absence (-) and presence (+) of α-pheromone (α-ph). C. Northern analysis of the RNA levels of the parental control, deletion mutants and complemented strains for *MFA1* in the absence (-) and presence (+) of α-pheromone (α-ph).

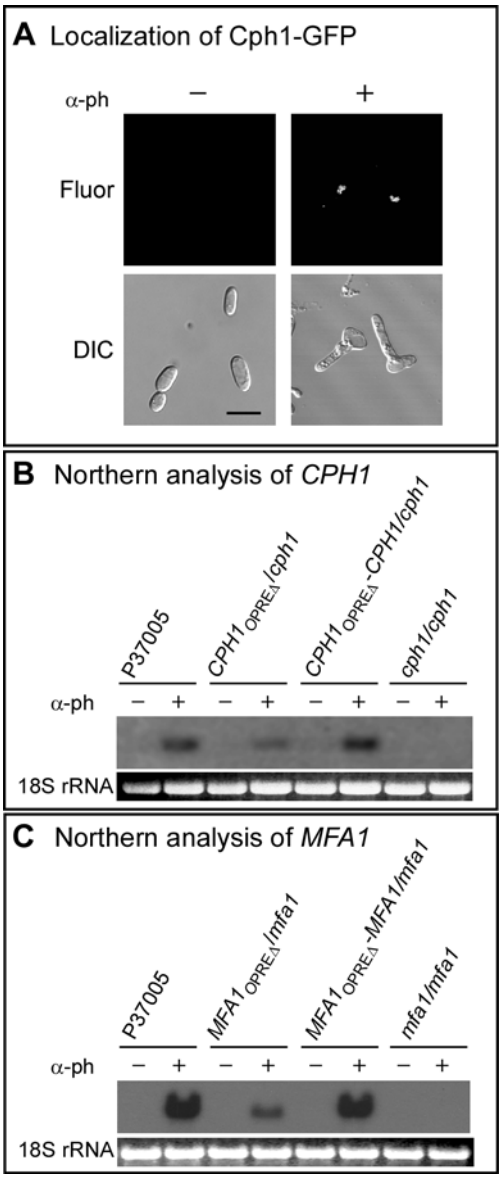
A Localization of Cph1-GFP
α-ph
–
+
Fluor
DIC
B Northern analysis of CPH1
P37005
CPH1oPREΔ/cph1
CPH1oPREΔ-CPH1/cph1
cph1/cph1
α-ph
– + – + – + – +
18S rRNA
C Northern analysis of MFA1
P37005
MFA1oPREΔ/mfa1
MFA1oPREΔ-MFA1/mfa1
mfa1/mfa1
α-ph
– + – + – + – +
18S rRNA

these genes were up-regulated by α-pheromone in this mutant (Yi *et al*., 2009; N.Sahni, S. Yi and D. R. Soll, unpublished observations). The results demonstrate that a cell must contain a functional Cph1 for α-pheromone-induced expression of genes regulated through OPRE.

The Four Pheromone-induced White-specific Genes Play No Role in the Opaque Pheromone Response

Northern analysis revealed that nine of the twelve α-pheromone-induced, white-specific genes had no detectable signal in opaque cells in the absence or presence of α-pheromone, and three (*PHR1, CIT1, RBT5*) were expressed at the same basal levels in the absence and presence of α-pheromone (Figure 39A). One would assume, therefore, that none of these white-specific genes played a role in the opaque-cell response to pheromone. To directly test this assumption, we examined whether opaque cells of the homozygous and WPRE deletion mutants of the four genes *EAP1*, *PGA10*, *CSH1* and *PBR1*, formed shmoos in response to α-pheromone or mated with opaque cells of the natural α/α strain WO-1. Both the frequency of pheromone-induced shmoo formations (Figure 42A) and that of fusion in mating mixtures (Figure 42B) were indistinguishable among opaque cells of the parental strain P37005, the homozygous deletion mutants, the WPRE deletion mutants and the complemented control strains. The shmoos (Figure 42C) formed by opaque cells of the mutants in response to α-pheromone, and the mating fusions formed between opaque **a**/**a** mutant cells and opaque α/α WO-1 cells (Figure 42D), were indistinguishable from those of the parental strain P37005. These results indicate that pheromone-induced, white-specific genes do not play a role in the mating process of opaque cells.

Figure 42. The genes *EAP1*, *PGA10*, *CSH1* and *PBR1* are not necessary for α-pheromone-induced shmoo formation or mating. A. Quantitation of shmoo formation of control and mutant strains in response to 4 hr treatment with $3x10^{-6}$ M α-pheromone (chemically synthesized 13-mer). At least 1,000 cells, the sum of four independent experiments, were analyzed and the mean ± standard deviation of the percent shmoo formation presented. N.S., not significant. B. Quantitation of fusion between control and mutant opaque cells, with opaque α/α cells of the mating partner WO-1. At least 2,000 cells of each strain, the sum of four independent experiments, were analyzed and the mean ± standard deviation of the percent presented. C. Examples of shmoo formation. D. Examples of mating fusants with α/α strain WO-1. -, absence of α-pheromone; +, presence of α-pheromone. Scale bars in C and D represent 4 μm.

A Pheromone-induced shmoo formation

Strain	Percent shmoo formation (%) -pheromone	+pheromone
P37005	0	79 ± 7
eap1/eap1	0	81 ± 8
$EAP1_{WPRE\Delta}$*/eap1*	0	82 ± 7
$EAP1_{WPRE\Delta}$*-EAP1/eap1*	0	77 ± 6
pga10/pga10	0	75 ± 7
$PGA10_{WPRE\Delta}$*/pga10*	0	78 ± 8
$PGA10_{WPRE\Delta}$*-PGA10 /pga10*	0	76 ± 5
csh1/csh1	0	83 ± 7
$CSH1_{WPRE\Delta}$*/csh1*	0	77 ± 6
$CSH1_{WPRE\Delta}$*-CSH1/csh1*	0	80 ± 6
pbr1/pbr1	0	78 ± 8
$PBR1_{WPRE\Delta}$*/pbr1*	0	79 ± 7
$PBR1_{WPRE\Delta}$*-PBR1/pbr1*	0	82 ± 7

B Mating with WO-1 (α/α)

Strain	Percent mating (%)
P37005	28 ± 2
eap1/eap1	27 ± 3
$EAP1_{WPRE\Delta}$*/eap1*	29 ± 2
$EAP1_{WPRE\Delta}$*-EAP1/eap1*	27 ± 1
pga10/pga10	26 ± 2
$PGA10_{WPRE\Delta}$*/pga10*	26 ± 1
$PGA10_{WPRE\Delta}$*-PGA10 /pga10*	25 ± 2
csh1/csh1	27 ± 2
$CSH1_{WPRE\Delta}$*/csh1*	25 ± 2
$CSH1_{WPRE\Delta}$*-CSH1/csh1*	28 ± 2
pbr1/pbr1	25 ± 2
$PBR1_{WPRE\Delta}$*/pbr1*	26 ± 2
$PBR1_{WPRE\Delta}$*-PBR1/pbr1*	25 ± 3

C Examples of shmoo formation

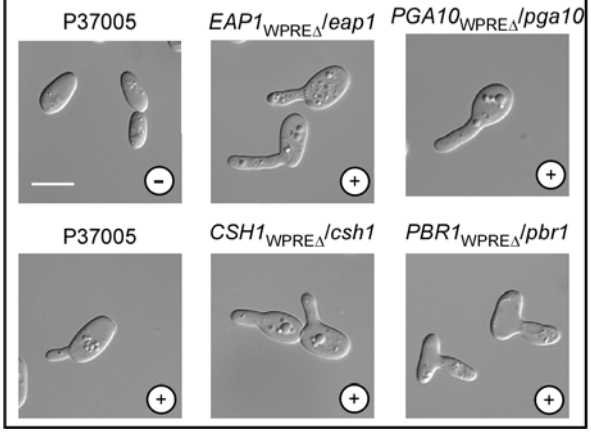

D Examples of mating fusants

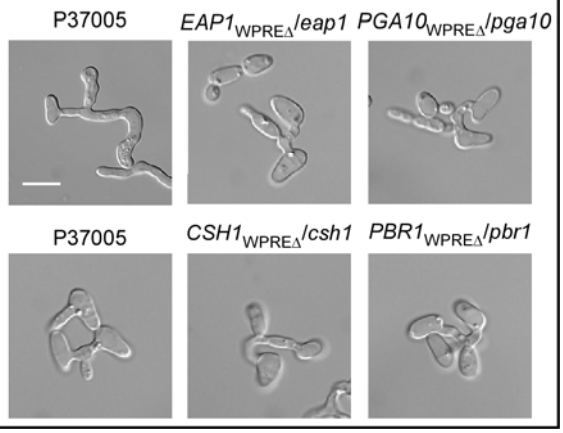

All Four Test Genes Play a Role in the White Cell Adhesion Response

In response to pheromone, white cells undergo dramatic increases in cohesion, as well as adhesion to a substratum (Daniels *et al*., 2006; Yi *et al*., 2008, 2009). To test whether the four selected white-specific genes up-regulated by α-pheromone played a role in adhesion, we compared this pheromone response between parent and mutant strains. α-pheromone induced more than 90% of the white cell populations of parental strain P37005 to adhere to the bottom of a plastic dish (Figure 43A). This represented more than a 100 fold increase over untreated cells. Although α-pheromone also induced increases in adhesion in the four homozygous deletion mutants *eap1*/*eap1*, *pga10*/*pga10*, *csh1*/*csh1* and *pbr1*/*pbr1*, the induced levels were 24%, 43%, 38% and 14%, respectively, that of the parental strain (Figure 43A). Deletion of just the WPRE region with the highest consensus in the promoter of each of the four genes resulted in approximately the same reductions in pheromone-induced adhesion as the homozygous deletion mutants (Figure 43A). Examples of the densities of cells adhering to the dish bottoms in the parent and WPRE deletion mutants are presented in Figure 43B. These results demonstrate that all four genes played a role in pheromone-induced adhesion, but no single gene was sufficient for the full pheromone-induced response. It should be noted that the lowest level of α-pheromone-induced adhesion was obtained in the homozygous and WPRE deletion mutants of *PBR1* (Figure 43A). It should also be noted that complementation of each WPRE deletion mutant with the native gene resulted in the reestablishment of wild type-level adhesion (Figure 43A).

Since the low level induction by α-pheromone of *CSH1* and *PBR1* in the WPRE deletion mutants was eliminated by deletion of a second, lower consensus WPRE (Figure 40C), lcWPRE, we tested whether there was a further reduction in pheromone-induced adhesion in the deletion mutants $CSH1_{\text{WPRE}\Delta\text{lcWPRE}\Delta}$/*csh1* and $PBR1_{\text{WPRE}\Delta\text{lcWPRE}\Delta}$/*pbr1*.

Figure 43. The genes *EAP1*, *PGA10*, *CSH1* and *PBR1* all play a role in α-pheromone-induced white cell adhesion. A. Quantitation of cells adhering to the well bottom in the absence (-) and presence (+) of α-pheromone (α-ph). The mean ± standard deviation (error bars) of three dishes is presented. B. Examples of the bottom of wells after washing of control and mutant strains.

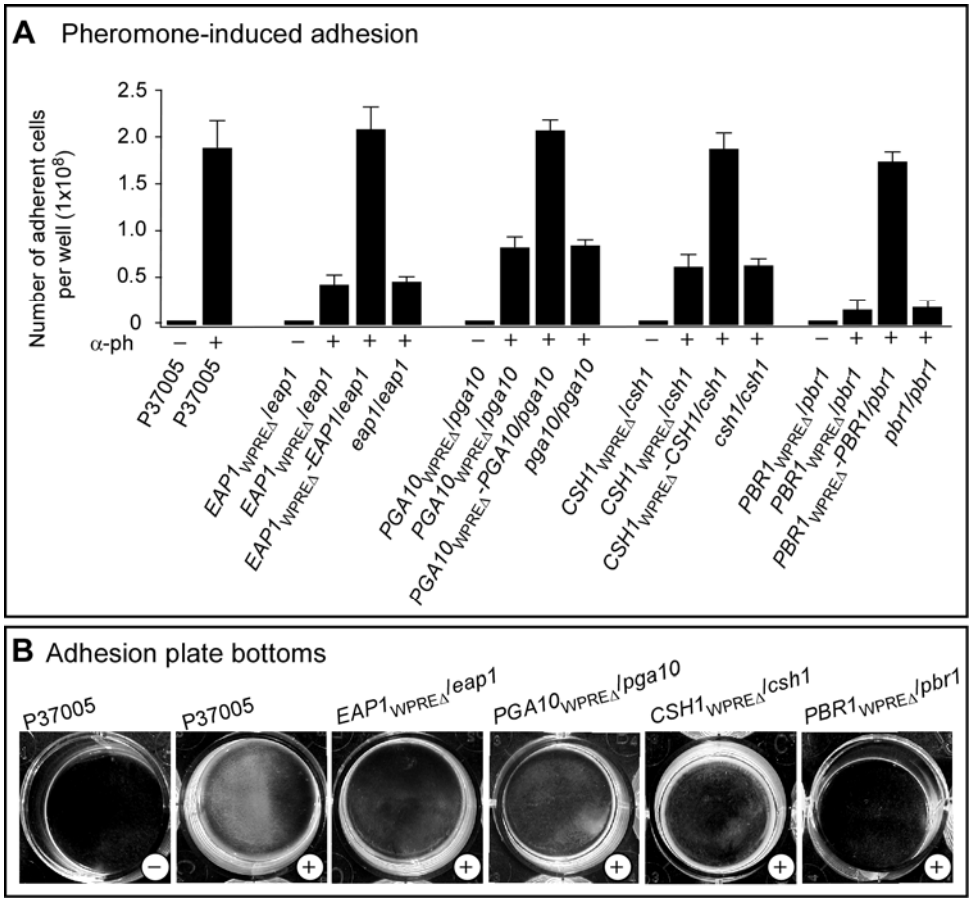
A Pheromone-induced adhesion
Number of adherent cells per well (1x10^8)
2.5
2.0
1.5
1.0
0.5
0
α-ph
– + – + + + – + + + – + + + – + + +
P37005
P37005
EAP1WPREΔ/eap1
EAP1WPREΔ/eap1
EAP1WPREΔ-EAP1/eap1
eap1/eap1
PGA10WPREΔ/pga10
PGA10WPREΔ/pga10
PGA10WPREΔ-PGA10/pga10
pga10/pga10
CSH1WPREΔ/csh1
CSH1WPREΔ/csh1
CSH1WPREΔ-CSH1/csh1
csh1/csh1
PBR1WPREΔ/pbr1
PBR1WPREΔ/pbr1
PBR1WPREΔ-PBR1/pbr1
pbr1/pbr1
B Adhesion plate bottoms
P37005
P37005
EAP1WPREΔ/eap1
PGA10WPREΔ/pga10
CSH1WPREΔ/csh1
PBR1WPREΔ/pbr1
–
+
+
+
+
+

The levels of adhesion were the same as in the mutants *CSH1*$_{WPRE\Delta}$/*csh1* and *PBR1*$_{WPRE\Delta}$/*pbr1* (Figure 44), indicating that the induced residual levels of adhesion in these mutants were due to the action of other gene products.

All Four Genes Play a Role in the White Cell Biofilm Response

In the absence of opaque cells, biofilm formation by white cells is dependent upon a functional white cell pheromone response pathway (Yi *et al*., 2009). Such white cell biofilms are enhanced by adding as little as 1% opaque cells (Daniels *et al*., 2006; Yi *et al*., 2008). We analyzed the role of the four pheromone-induced white-specific genes on white cell biofilm formation in the absence of opaque cells and in the presence of 10% opaque cells, the latter containing a 1:1 ratio of opaque **a**/**a** and opaque α/α cells. Presumably the opaque **a**/**a** cells, through the release of **a**-pheromone, up-regulate α-pheromone synthesis in the opaque α/α cells, providing a continuous source of α-pheromone for majority white **a**/**a** cell stimulation (Daniels *et al*., 2006). Biofilms were cast on a silicone elastomer surface, incubated for 48 hour, fixed and analyzed for the formation of a basal layer of white cells, hyphae formation in the upper region of the biofilm, hypha orientation, matrix formation and biofilm thickness, using laser scanning confocal microscopy.

The mean thickness of biofilms formed by majority white cells in the absence of minority opaque cells of the parent strain was 73±5 μm; that of the four complemented control strains averaged 69±1 μm (Figure 45). The differences were not significantly different (the p values were greater than 0.05). In the presence of minority opaque cells, the mean thickness of the biofilms formed by the parent strain P37005 was 106±5 μm and the average of the four complemented strains 98±4 μm, which represented increases in thickness of 45% and 43%, respectively, over that in the absence of opaque cells (Figure 45A). The differences in the absence and presence of minority opaque cells were

Figure 44. Deletion of the lcWPRE from the promoter of the strains *CSH1*$_{\text{WPRE}\Delta}$*/csh1* and *PBR1*$_{\text{WPRE}\Delta}$ */pbr1* does not remove the low level of adhesion induced by α-pheromone.

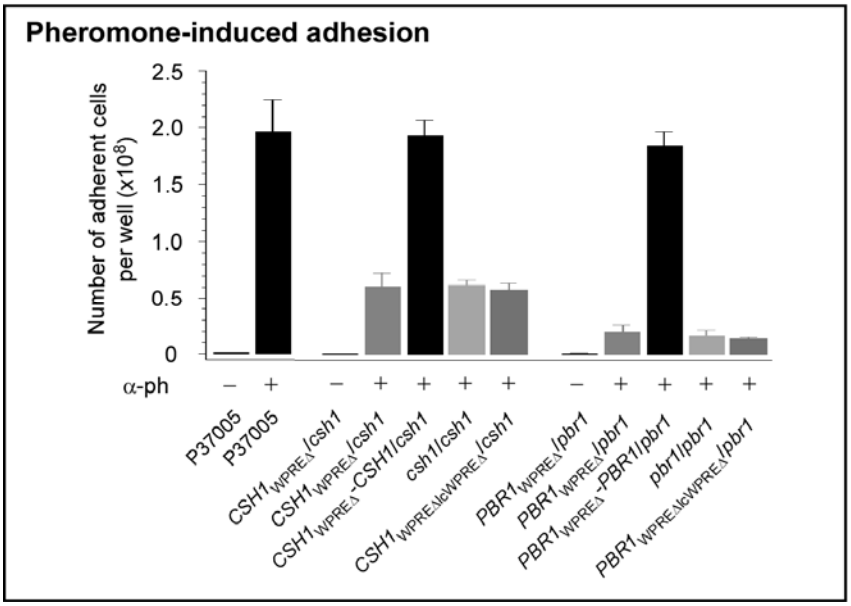
Pheromone-induced adhesion
Number of adherent cells per well (x10^6)
2.5
2.0
1.5
1.0
0.5
0
α-ph
– + – + + + + – + + + +
P37005
P37005
CSH1WPREΔ/csh1
CSH1WPREΔ/csh1
CSH1WPREΔ-CSH1/csh1
csh1/csh1
CSH1WPREΔdWPREΔ/csh1
PBR1WPREΔ/pbr1
PBR1WPREΔ/pbr1
PBR1WPREΔ-PBR1/pbr1
pbr1/pbr1
PBR1WPREΔdWPREΔ/pbr1

Figure 45. The genes *EAP1*, *PGA10*, *CSH1* and *PBR1* all are necessary for white **a**/**a** cell biofilm development in the absence or presence of minority opaque cells. A. Biofilm thickness measured in μm in the absence (-Op) and presence (+Op) of 10% opaque cells, for the complemented control strains, homozygous deletion strains and WPRE deletion strains of the four test genes. The opaque cells were half **a**/**a** and α/α. For each strain and condition, three individual biofilms were analyzed through three random regions, providing nine measurements. P values are provided for the measurements in the absence (-) and presence (+) of 0% opaque cells (Op). In Table 12, the p values are presented for comparisons of the complemented control and the two deletion mutants. B. Comparisons of biofilm compositions of the parent strain P37005, the complemented control strains, the homozygous mutants and the WPRE deletion mutants of the four test genes, in the absence (-) or presence (+) of opaque (Op) cells. Maximum matrix staining is representative as ++++ and minimum as +. The presence or absence of a white cell basal layer is denoted as + or -, respectively. Maximum and minimum hyphal density is represented as ++++ and +, respectively. Hyphal orientation (Hyph. orient.) was either vertical (vert.) and intertwined (int.), or horizontal (hor.). C, D. Scanning confocal microscopic images of the basal layer and hyphal region of biofilms of the *EAP1* complemented control and WPRE deletion mutant of *EAP1*. E. β-glucan measurements of biofilm supernatants F. Examples of the pixel intensity scans used to measure thickness, for the complemented control and WPRE deletion mutant of *EAP1*, respectively.

A Biofilm thickness (μm)

Parent strain	-Op	+Op	% increase	p value
	73±5	106±5	45%	2×10^{-10}

	Complemented control				Homozygous deletion				WPRE deletion			
Gene	-Op	+Op	% increase	p value	-Op	+Op	% increase	p value	-Op	+Op	% increase	p value
EAP1	69±5	93±3	35%	2×10^{-09}	56±3	61±5	9%	2×10^{-2}	54±3	59±5	9%	N.S.
PGA10	70±3	103±7	47%	2×10^{-07}	53±2	60±5	13%	1×10^{-4}	58±4	58±5	0%	N.S.
CSH1	68±3	98±6	44%	1×10^{-08}	54±9	58±5	7%	N.S.	52±3	55±4	6%	N.S.
PBR1	67±4	97±4	45%	4×10^{-11}	58±8	61±7	5%	N.S.	61±3	63±3	3%	N.S.
$\bar{X}$± s.d.	69±1	98±4	43.5%		56±6	60±5	8±3%		56±4	59±3	5±4%	

B Biofilm composition

Gene	Strain	Op	Matrix	Wh cell bas. layer	Hyph. dens.	Hyph. orient.
	P37005, complemented controls	–	++++	+	++++	vert., int.
		+	++++	+	++++	vert., int.
EAP1, PGA10 CSH1, PBR1	Homozygous deletion mutants	–	+	–	+	hor.
		+	+	–	+	hor.
EAP1, PGA10 CSH1, PBR1	*WPRE* deletion mutants	–	+	–	+	hor.
		+	+	–	+	hor.

C Complemented control (*EAP1*$_{WPRE\Delta}$–*EAP1*/*eap1*) + Op

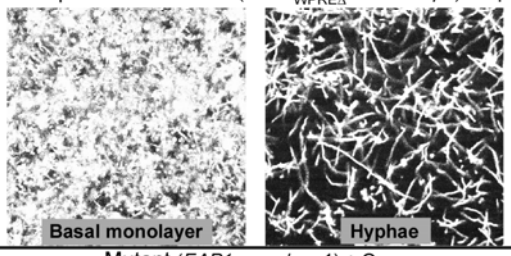

D Mutant (*EAP1*$_{WPRE\Delta}$/*eap1*) + Op

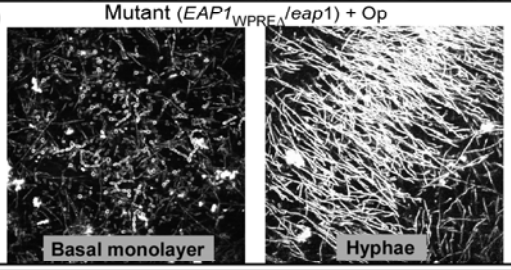

E β-glucan measurements of biofilm supernatants

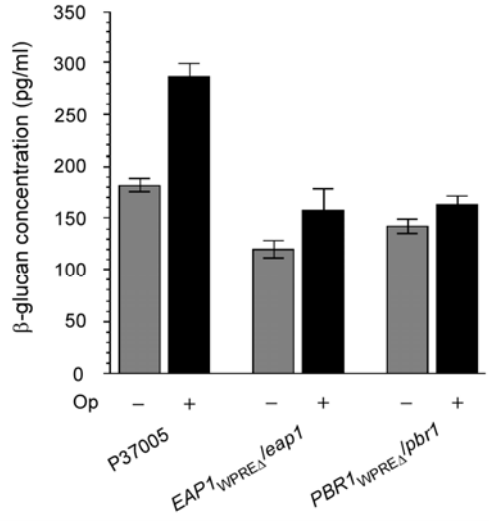

F Complemented control (*EAP1*$_{WPRE\Delta}$–*EAP1*/*eap1*) + Op

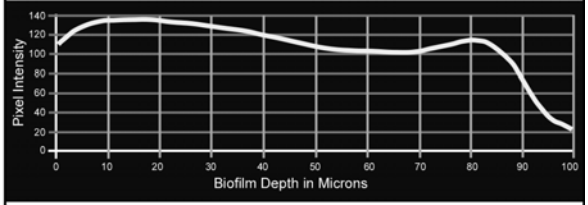

Mutant (*EAP1*$_{WPRE\Delta}$/*eap1*) + Op

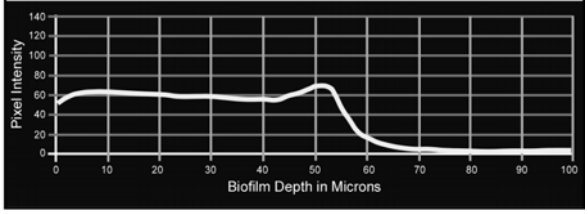

significant (Figure 45A). In both the absence and presence of minority opaque cells, the biofilms formed by white cells of the parent and complemented control strains possessed a basal layer of white cells, and above this layer a region of intertwined hyphae oriented vertically (Figure 45B, C). These biofilms contained an extracellular matrix that stained with calcofluor (Figure 46A). Measurements were also made of the concentration of β-glucan in the supernatant of biofilm cultures of the parental strain P37005 in the absence and presence of minority opaque cells (Nobile *et al*., 2009). The concentration was 58% higher in the presence of opaque cells than it was in the absence (Figure 45E). The difference was significant.

In the absence of opaque cells, the thickness of the biofilms of the four homozygous deletion mutants averaged 55±2 μm and that of the four WPRE deletion mutants 56±4 μm (Figure 45A). These biofilms were, therefore, on average 20% thinner than those of parental and complemented control cells (Figure 45A). These differences were significant (Table 12). The presence of opaque cells had only a marginal effect on the thickness of the biofilm formed by the deletion mutants (Figure 45A). Examples of the pixel intensity scans used to measure thickness for control and mutant cell biofilms are presented in Figure 45F.

In both the absence and presence of opaque cells, the biofilms formed by the deletion mutants had no consistent white cell basal layer; the cells at the substratum were sparse or patchy (Figure 45B, D). The matrix also strained far less intensely than that of control strains (Figure 45B and Figure 46B). In addition, the hyphae formed as patches and were orientated horizontally (*i.e.*, in parallel with the substratum) (Figure 45B, D), rather than vertically, in contrast to the vertical orientation in control cell biofilms (Figure 45B, C). This aberrant orientation may have been due to the dramatic decrease in matrix suggested by the staining results (Figure 46). Measurements of β-glucan in the supernatant of biofilms revealed significant differences between mutants and the parental stain both in the absence and presence of minority opaque cells. For the WPRE deletion

Figure 46. The matrix of control cell biofilms was far more pronounced than that of the four mutants. For pseudocolor, red represents cells, yellow-green represents matrix and blue represents open space.

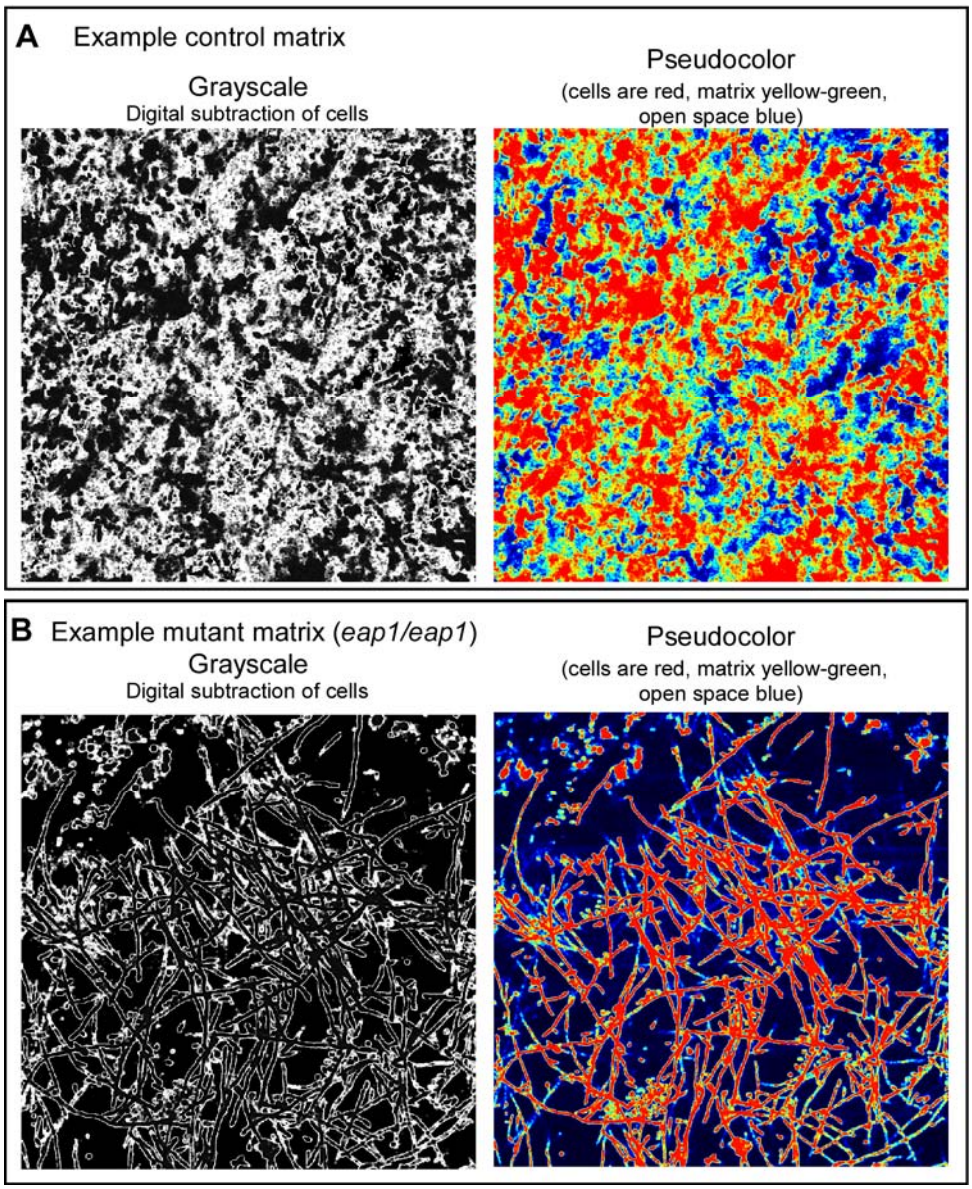
A Example control matrix
Grayscale
Digital subtraction of cells
Pseudocolor
(cells are red, matrix yellow-green, open space blue)
B Example mutant matrix (eap1/eap1)
Grayscale
Digital subtraction of cells
Pseudocolor
(cells are red, matrix yellow-green, open space blue)

Table 12. The significance of the difference in biofilm thickness between complemented controls and the deletion mutants of four white-specific pheromone-induced genes

	Versus complemented control, p value	
Mutant	-Op	+Op
eap1/eap1	$4x10^{-6}$	$2x10^{-10}$
$EAP1_{WPRE\Delta}$*/eap1*	$1x10^{-6}$	$2x10^{-10}$
pga10/ pga10	$4x10^{-10}$	$5x10^{-9}$
$PGA10_{WPRE\Delta}$*/pga10*	$2x10^{-5}$	$4x10^{-10}$
csh1/csh1	$1x10^{-2}$	$6x10^{-11}$
$CSH1_{WPRE\Delta}$*/csh1*	$8x10^{-9}$	$5x10^{-11}$
pbr1/pbr1	$2x10^{-2}$	$6x10^{-8}$
$PBR1_{WPRE\Delta}$*/pbr1*	$7x10^{-3}$	$9x10^{-13}$

mutants *EAP1*$_{WPREA}$/*eap1* and *PBR1*$_{WPREA}$/*pbr1*, the levels of β-glucan were on average 33% and 19% lower, respectively, in the absence of opaque cells, and 44% and 42% lower, respectively, in the presence of opaque cells (Figure 45E). These differences proved significant. Together these results demonstrate that each of the four α-pheromone-induced, white-specific genes analyzed was essential for normal biofilm formation and architecture in the absence as well as in the presence of opaque cells.

Expression Patterns in Deletion Mutants of Components of the Pheromone Response Pathway

Although the four WPRE-regulated white-specific genes are activated by a downstream transcription factor that is induced by the pheromone-activated MAP kinase pathway (Nett and Andes, 2006; Lynch and Robertson, 2008), this does not exclude them from playing a role in regulating upstream genes in the pheromone response pathway by a loop-back control mechanism. We, therefore, tested whether pheromone up-regulated the α-pheromone receptor gene, *STE2* and the mating factor **a** gene, *MFA1*, in the homozygous and WPRE deletion mutants of *EAP1* and *PBR1*. We also tested whether *CSH1* and *PBR1* were up-regulated by α-pheromone in the *EAP1* deletion mutants, and whether *CSH1* and *EAP1* were up-regulated in the *PBR1* deletion mutants. No effects were observed on expression (Figure 47A, B). Similar results were obtained for the homozygous and WPRE deletion mutants of *CSH1* (data not shown). These results indicate that pheromone-induced, white specific genes involved in adhesion and biofilm development do not play a role in the transduction of the pheromone signal or in up-regulation of other pheromone induced genes.

Overexpressing *PBR1* in the Other Deletion Mutants

Homozygous and WPRE deletion mutants of the four white-specific genes exhibited large but incomplete reductions in adhesion (Figure 43A). The largest effect was by the homozygous and WPRE deletion mutants of *PBR1* (Figure 43A, B). These

Figure 47. Deletion of *EAP1* or *PBR1* has no effect on pheromone regulation of *STE2*, *MFA1*, *CSH1*, and *EAP1* or *PBR1* expression, as demonstrated by northern blot hybridization. A. Expression of the four genes in *EAP1* mutants in the absence (-) or presence (+) of α-pheromone. B. Expression of the four genes in *PBR1* mutants in the absence (-) or presence (+) of α-pheromone. To demonstrate levels of loading, 18S rRNA levels are shown for opaque and white.

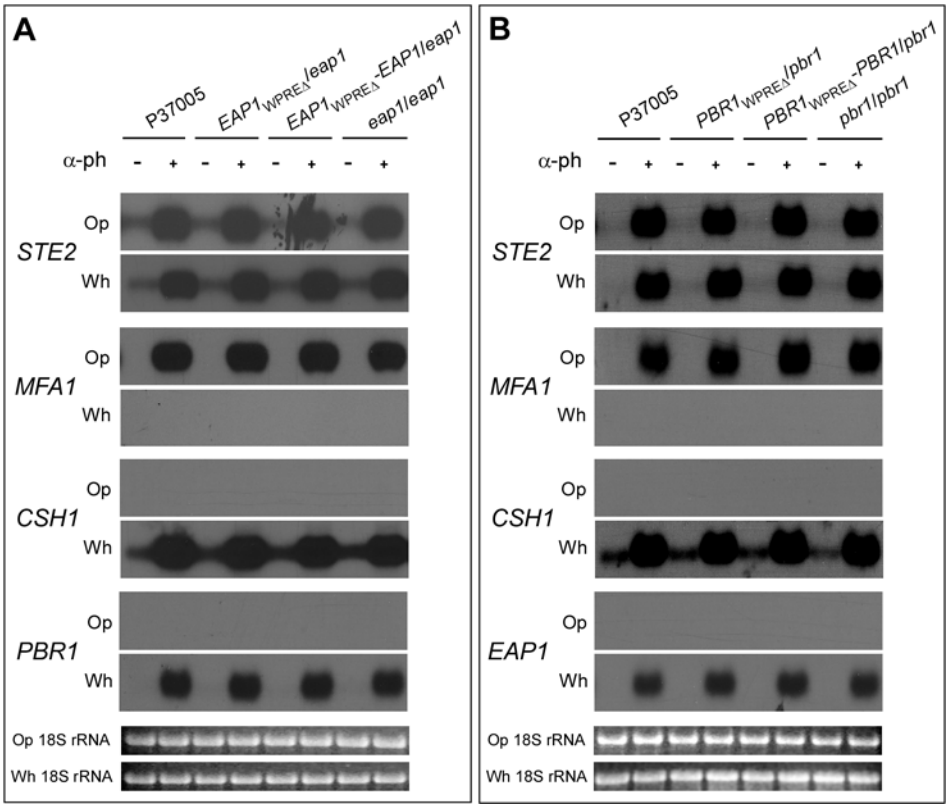
A
P37005
EAP1WPREΔ/eap1
EAP1WPREΔ-EAP1/eap1
eap1/eap1
α-ph
- + - + - + - +
Op
STE2
Wh
Op
MFA1
Wh
Op
CSH1
Wh
Op
PBR1
Wh
Op 18S rRNA
Wh 18S rRNA
B
P37005
PBR1WPREΔ/pbr1
PBR1WPREΔ-PBR1/pbr1
pbr1/pbr1
α-ph
- + - + - + - +
Op
STE2
Wh
Op
MFA1
Wh
Op
CSH1
Wh
Op
EAP1
Wh
Op 18S rRNA
Wh 18S rRNA

results suggested that the contributions of the four tested genes to the adhesion response may be both independent and additive. To explore this hypothesis, we transformed the parent strain P37005, and the WPRE deletion mutants *EAP1*$_{WPRE\Delta}$*/eap1*, *PGA10*$_{WPRE\Delta}$*/pga10*, *CSH1*$_{WPRE\Delta}$*/csh1* and *PBR1*$_{WPRE\Delta}$*/pbr1* with a construct in which *PBR1* was under the control of the inducible *tetracycline* promoter (Park and Morschhauser, 2005). The construct was targeted to one of the two alleles of the *ADH1* gene (Park and Morschhauser, 2005). The resulting strains were P37005-tet*PBR1* (the control), *EAP1*$_{WPRE\Delta}$*/eap1-tetPBR1*, *PGA10*$_{WPRE\Delta}$*/pga10-tetPBR1*, *CSH1*$_{WPRE\Delta}$*/csh1-tetPBR1* and *PBR1*$_{WPRE\Delta}$*/pbr1-tetPBR1*. Up-regulation of the tetracycline regulated gene by the tetracycline analog doxycycline was demonstrated to be dose-dependent and independent of pheromone, as demonstrated in *PBR1*$_{WPRE\Delta}$*/pbr1-tetPBR1* (Figure 48A).

Misexpression of *PBR1* in the absence of pheromone caused an increase in adhesion in the transformed parental strain P37005 that was approximately one third of the increase induced by α-pheromone (Figure 48B, C). Misexpression in the four transformed WPRE deletion mutants in the absence of α-pheromone resulted in similar levels of induction (Figure 48B, C). In the presence of α-pheromone, *PBR1* misexpression in both the transformed parental strain and the four WPRE deletion mutants resulted in a level of adhesion greater than when *PBR1* was misexpressed in the absence of α-pheromone or when cells were only treated with α-pheromone (*i.e.*, in the absence of doxycycline) (Figure 48B, C). These results indicated that the expression of *PBR1* in the absence of pheromone-induced expression of the other three test genes resulted in increased adhesion, and that simultaneous *PBR1* misexpression and α-pheromone induced native gene expression had an additive effect on adhesion. To explore this point further, we transformed the double mutant *cek1/cek1 cek2/cek2* (Yi *et al*., 2008) with the misexpression module at the *ADH1* locus. This mutant did not undergo α-pheromone induction of *EAP1*, *PGA10*, *CSH1* or native *PBR1* (Figure 48D). Misexpression of

Figure 48. Overexpression of *PBR1* at the ectopic locus *ADH1* in the parental strain and in WPRE deletion mutants of *EAP1*, *PGA10*, *CSH1* and *PBR1*, induces partial adhesion or enhances adhesion in the absence of α-pheromone and in the absence of *EAP10*, *PGA10* and *CSH1* expression. A. Northern analysis demonstrating that 100 μg/ml of doxycycline (Dox) induces *PBR1* transcription similarly in the absence (-) and presence (+) of α-pheromone (α-ph). B. Examples of white cells adhering to the bottom of wells for the control strain P37005-tet*PBR1* and *CSH1* WPRE deletion mutant $CSH1_{WPRE\Delta}$/*csh1*-tet*PBR1* in the absence (-) or presence (+) of doxycycline. C. Quantitation of adherence to well bottoms. D. Northern analysis demonstrating treatment with pheromone of the mutant *cek1/cek1 cek2/cek2* does not cause an increase in expression of the four test genes necessary for a full adhesion response to α-pheromone. E. Demonstration that misexpression of *PBR1* in the mutant *cek1/cek1 cek2/cek2*, in which the three genes, *EAP1*, *PGA10*, *CSH1* and the native *PBR1* gene are not up-regulated, results in an increase in adhesion that is 33% that of control cells. This increase is therefore independent of α-pheromone treatment in the *cek1/cek1 cek2/cek2* mutant.

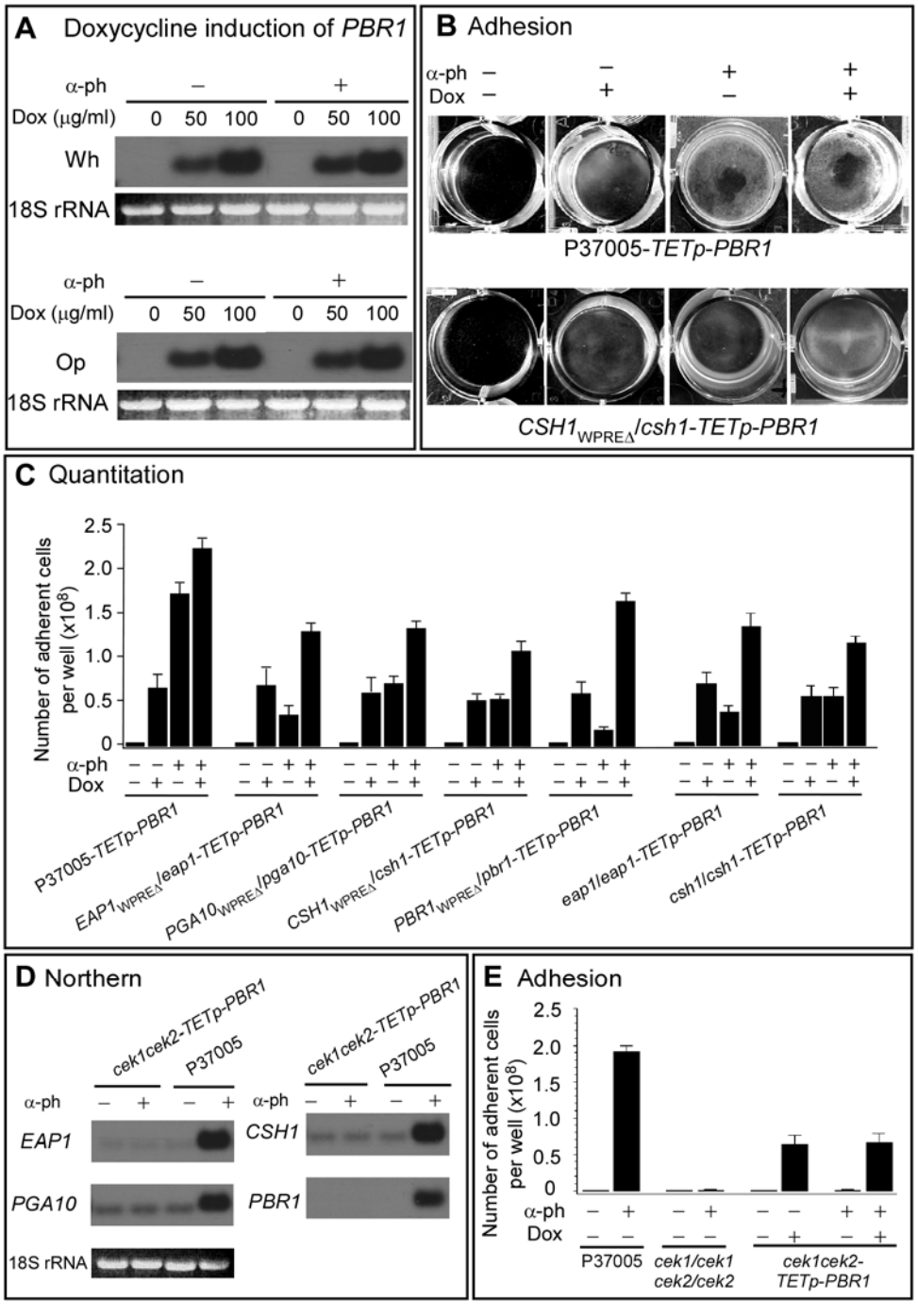
A Doxycycline induction of PBR1
α-ph
Dox (μg/ml)
0 50 100 0 50 100
Wh
18S rRNA
Op
B Adhesion
P37005-TETp-PBR1
CSH1WPREΔ/csh1-TETp-PBR1
C Quantitation
Number of adherent cells per well (x10^8)
P37005-TETp-PBR1
EAP1WPREΔ/eap1-TETp-PBR1
PGA10WPREΔ/pga10-TETp-PBR1
CSH1WPREΔ/csh1-TETp-PBR1
PBR1WPREΔ/pbr1-TETp-PBR1
eap1/eap1-TETp-PBR1
csh1/csh1-TETp-PBR1
D Northern
cek1cek2-TETp-PBR1
P37005
EAP1
PGA10
CSH1
PBR1
18S rRNA
E Adhesion
P37005
cek1/cek1 cek2/cek2
cek1cek2-TETp-PBR1

PBR1 in the double mutant in the absence or presence of α-pheromone resulted in an increase in adhesion to a level again one third of the α-pheromone-induced level in the parental control (Figure 48E). This result supports the suggestion that expression of *PBR1* alone results in increased adhesion, but not to control levels.

Since the WPRE deletion mutants of *EAP1*, *PGA10* and *CSH1* express these genes at basal or slightly induced levels (Figure 40B), misexpression of *PBR1* in these WPRE deletion mutants might still result in interactions between Pbr1 and the gene products Eap1, Pga10 or Csh1, respectively. To test further for independence, the deletion mutants *eap1/eap1* and *csh1/csh1* were transformed with the vector containing tet*PBR1* to generate *eap1/eap1*-tet*PBR1* and *csh1/csh1*-tet*PBR1*, and adhesion assessed in the absence or presence of α-pheromone and/or doxycycline. The results were highly similar to those obtained with the WPRE mutants transformed with tet*PBR1* (Figure 48C). These results support the suggestion that the white-specific α-pheromone-induced genes may confer adhesion independently and additively.

Discussion

Differences in the Opaque and White Response Pathways

The α-pheromone response pathway of white cells, from receptor through the MAP kinase cascade, includes the same gene products as the pheromone response pathway of opaque cells (Figure 49) (Yi *et al*., 2008, 2009). However, the downstream targets of the pathways differ. The target of the opaque pathway is the transcription factor Cph1, a homolog of the *S. cerevisiae* transcription factor Ste12 (Liu *et al*., 1994; Magee *et al*., 2002; Chen *et al*., 2002). The target of the white pathway, however, is a transcription factor that is distinct from Cph1 and remains unidentified (Yi *et al*., 2008). In *S. cerevisiae*, pheromone up-regulates genes involved in the mating response through the transcription factor Ste12, which binds to a common pheromone response element, PRE (Dolan *et al*., 1989; Errede and Ammerer, 1989; Hagen *et al*., 1991). Here we have

Figure 49. An updated model of the pathways regulating the pheromone-induced opaque and white responses that includes the downstream genes that are up-regulated through the opaque- and white-specific pheromone-response elements OPRE and WPRE. This model also includes genes that are up-regulated in both the opaque and white responses, and therefore contain both an OPRE and a WPRE in their promoters. The two pathways share the same components from receptor through the MAP kinase cascade (Yi *et al*., 2008). However, there are two differences, circled in red. First, an extra region of the first intracellular loop (ICI) is essential for the white, but not the opaque response (Yi *et al*., 2009). Second, the transcription factor targeted by the pathway is *CPH1* in the opaque response and a still unidentified factor in the white response (Yi *et al*., 2008).

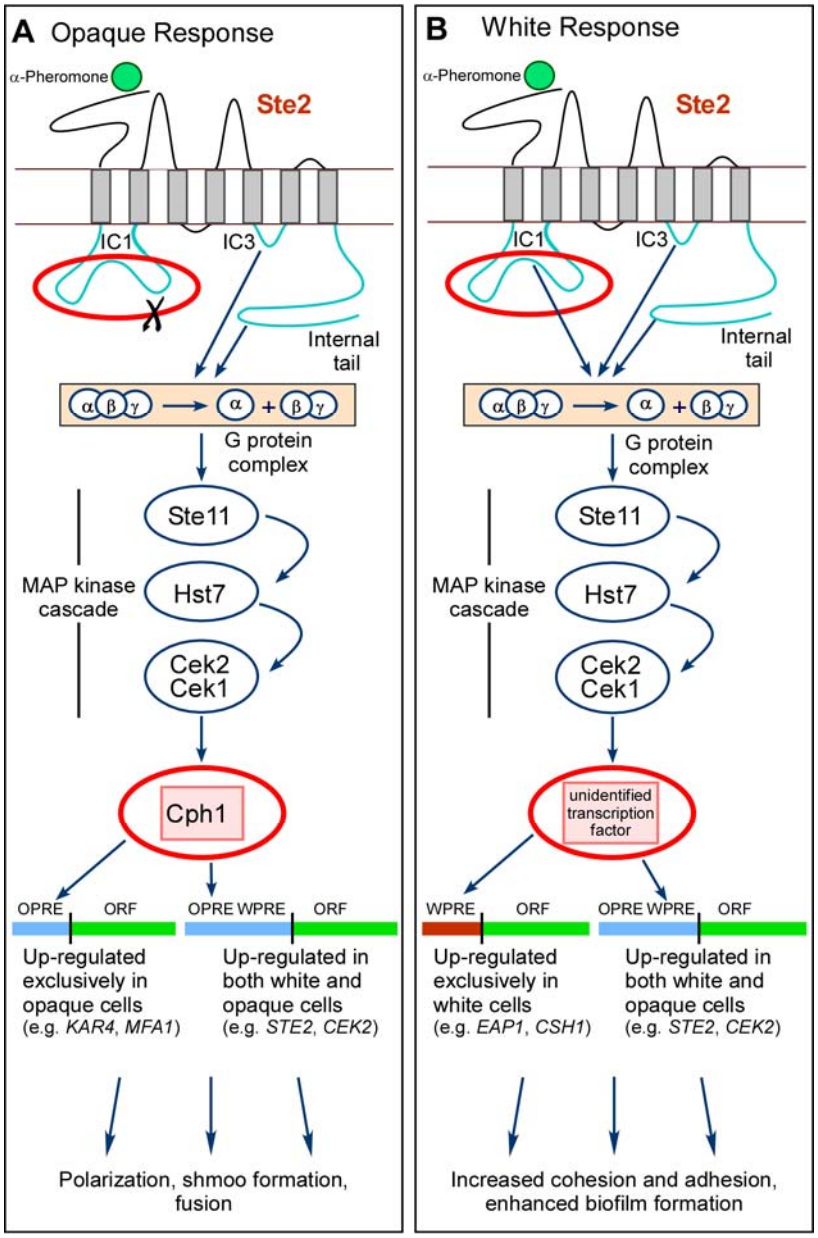
A Opaque Response
α-Pheromone
Ste2
IC1
IC3
Internal tail
G protein complex
Ste11
Hst7
Cek2 Cek1
MAP kinase cascade
Cph1
OPRE
ORF
OPRE WPRE
ORF
Up-regulated exclusively in opaque cells (e.g. KAR4, MFA1)
Up-regulated in both white and opaque cells (e.g. STE2, CEK2)
Polarization, shmoo formation, fusion
B White Response
α-Pheromone
Ste2
IC1
IC3
Internal tail
G protein complex
Ste11
Hst7
Cek2 Cek1
MAP kinase cascade
unidentified transcription factor
WPRE
ORF
OPRE WPRE
ORF
Up-regulated exclusively in white cells (e.g. EAP1, CSH1)
Up-regulated in both white and opaque cells (e.g. STE2, CEK2)
Increased cohesion and adhesion, enhanced biofilm formation

presented evidence that in opaque cells, Cph1 activates opaque-specific genes by binding to a GC-rich, opaque-specific pheromone response element, OPRE, not a *S. cerevisiae* PRE-like sequence, as has been suggested (Bennett and Johnson, 2006). We have also presented evidence that in white cells, the white-specific transcription factor activates white-specific genes by binding to a AT-rich, white-specific pheromone response element, WPRE (Figure 49). The promoter of each opaque-specific gene contains at least one OPRE and no WPRE, and the promoter of each white-specific gene contains at least one WPRE and no OPRE. Genes up-regulated by pheromone in both white and opaque cells have both a WPRE and an OPRE (Figure 49). The strategy for gene regulation in the white pheromone response therefore appears to involve a single white-specific transcription factor and a single white-specific *cis*-acting promoter element, and the strategy for gene regulation in the opaque pheromone response appears to involve a single opaque-specific transcription factor and a single opaque-specific *cis*-acting promoter element (Figure 49). These strategies are highly similar to that of the homologous mating pathway in *S. cerevisiae*, which also activates genes through one primary transcription factor and a single, dominant *cis*-acting regulatory element (Dolan *et al*., 1989; Errede and Ammerer, 1989, Hagen *et al*., 1991; Liu *et al.*, 1994; Magee *et al*., 2002).

White-specific Genes and the Adhesion Response

Each of the twelve genes that we found were strongly up-regulated by pheromone in white but not opaque cells, contained a WPRE. Deletion of four of these genes or deletion of the WPRE from their promoters resulted in a marked reduction in the white cell adhesion response to pheromone. But in no case did the full deletion of the gene, the WPRE of the representative gene, or the WPRE and lcWPRE of the representative gene in combination, lead to the complete loss of the adhesion response, suggesting that the protein product of each gene may make an independent but additive contribution to the pheromone adhesion response. Hence, none of the four gene products appeared to be essential for the

entirety of the adhesion response to pheromone. The experiments performed in which *PBR1* was misexpressed revealed that increased expression of *PBR1* alone, in the complete absence of expression of either *EAP1* or *CSH1* (*i.e.*, in the null mutants), resulted in a further, but incomplete, increase in adhesion. This was true for the WPRE and full homozygous deletion mutants as well. Moreover, misexpression of *PBR1* in the mutant *cek1/cek1 cek2/cek2*, in which *EAP1*, *PGA10*, *CSH1* and native *PBR1* cannot be induced, results in an increase in adhesion to 34% that of the induced control strain. These results indicate that the adhesion response contributed by *PBR1* in white cells may be independent of the adhesion response contributed by the other three genes. Hence, α-pheromone induced adhesion in white cells may represent the sum of multiple adhesion systems.

White-specific Genes and the Biofilm Response

Deletion of each one of the four randomly selected white-specific genes resulted in a reproducible loss in the adhesion response to α-pheromone, ranging between 57% and 86%. In contrast, deleting any one of the four genes or their WPREs resulted in relatively uniform defects in biofilm formation. Since biofilm formation is a complex process involving multiple cell phenotypes, matrix formation and a temporal sequence of steps during maturation (Hawser and Douglas, 1994; Hawser *et al*., 1998; Baillie and Douglas, 1999, 2000; Chandra *et al*., 2001; Ramage *et al.*, 2001; Kumamoto, 2002; Blankenship and Mitchell, 2006), one might have expected that deletion of each of the four genes would cause a different and partial defect. If, however, all four genes played roles in an early step in biofilm development, such as the formation of the initial basal layer of cells on the substratum (Chandra *et al*., 2001; Douglas L.J., 2003; Soll D.R., 2008), then all subsequent steps might be similarly defective in the four deletion mutants, thus accounting for the uniformity of the biofilm defects.

Induction of White Cell Biofilm Formation in the Absence of Minority Opaque Cells

Perhaps our most surprising observation was that the major defects in biofilm development by white **a**/**a** cells were exhibited by the homozygous and WPRE deletion mutants of the four white-specific genes in the absence as well as in the presence of minority opaque cells. The defects included the absence of a continuous, dense basal layer on a silicone elastomer substratum, horizontally oriented patches of hyphae rather than uniformly dense, vertically intertwined hyphae in the domains above the basal layer, and a dramatic reduction of the extracellular matrix. These defects occurred in the absence as well as the presence of minority opaque cells, indicating that white cells possess the ability to autoactivate. Given that the white response, which includes increased adhesion and up-regulation of white specific genes, depends upon an exogenous source of pheromone, these results suggest one of two mechanisms. First, there may exist an autocrine system in which *MTL*-homozygous white cells, when placed on a surface under conditions conducive to biofilm formation, are able to self-stimulate by releasing pheromone of opposite mating type. This pheromone then binds to receptors on the same cells, activating the white cell response pathway. Such a scenario is plausible since white **a**/**a** cells possess the gene for α-pheromone and α/α cells possess the gene for the **a** pheromone. We had previously suggested that an autocrine system might regulate white cell biofilm formation based on the defective phenotype of the α-receptor deletion mutant, *ste2/ste2* (Yi *et al*., 2008). The mutant formed a patchy biofilm with diminished thickness in the absence of minority opaque cells, similar to that observed for the mutants *eap1/eap1*, *pga10/pga10*, *csh1/csh1* and *pbr1/pbr1*. In a mechanism alternative to an autocrine system, white cells may depend upon the basal activity of the pheromone response pathway in the absence of pheromone, for normal biofilm formation. In *S. cerevisiae*, such basal activity has not only been observed in the pheromone response pathway (Hagen *et al*., 1991; Roberts *et al*., 2000; Dohlman and Thorner, 2001; Dohlman and Fields, 1990),

but the **α** subunit of the trimeric G protein complex, Gpa1, when overexpressed, can also activate changes in the mating response in the absence of pheromone (Dohlman and Thorner, 2001). Experiments are now in progress to distinguish between these alternatives.

MTL-homozygous and *MTL*-heterozygous Biofilms

Here, we have focused entirely on *MTL*-homozygous biofilm formation. *MTL*-heterozygous (**a**/α) strains, however, represent approximately 90% of natural strains (Lockhart *et al*., 2002; Legrand *et al*., 2004; Tavanti *et al*., 2005, Odds and Jacobsen 2008) and hence must account for the majority of biofilms formed in nature. Interestingly, the majority of the twelve genes that were identified as strongly up-regulated by α-pheromone in white, but not opaque, **a**/**a** cells have been implicated directly or indirectly in the formation of **a**/α biofilms. In **a**/α cells, it has been demonstrated that 1) deletion of *EAP1* results in a decrease in binding to epithelial cells (Li and Palecek, 2003), and defective biofilm formation both in an *in vitro* parallel plate flow chamber model and in catheters (Li *et al*., 2007); 2) deletion of *PGA10* (*RBT5*) results in fragile biofilms (Perez *et al*., 2006); 3) deletion of *CSH1* causes a reduction in hydrophilicity (Singleton *et al*., 2001), a characteristic that enhances biofilm formation (Li et al., 2003); 4) *PHR1* is down-regulated in *sun41/sun41* mutants (Norice *et al.*, 2007); 5) and *LSP1* and *CIT1* are up-regulated during biofilm formation (Seneviratne *et al*., 2008). It is therefore imperative that biofilm formation by white *MTL*-homozygous cells and *MTL*-heterozygous cells be compared both at the morphological and molecular levels, that the regulation of the genes involved in **a**/α biofilm formation be elucidated and that the roles of the two different biofilms in pathogenesis be assessed.

Evolution of the White Cell Pheromone Response

It seems reasonable to hypothesize that the white cell biofilm response to pheromone evolved from the opaque cell mating response in *C. albicans*. The opaque

response pathway is highly similar to that of *S. cerevisiae*, which branched from the *Candida* group early in the phylogenetic tree of the hemiascomycetes (Souciet *et al*., 2000; Wong *et al*., 2002). Remarkably, neither *S. cerevisiae* nor members of the *Candida* group, other than *C. albicans* and the highly related species *Candida dubliniensis* (Pujol *et al.*, 2004; Sullivan *et al.*, 1995), undergo the white-opaque transition. The white response to pheromone appears to function solely to facilitate opaque cell mating through the genesis of a protective biofilm (Daniels *et al.*, 2006), suggesting that it arose from the opaque response in order to facilitate it (Daniels *et al.*, 2006). Because the white cell pheromone response appears to be present only in *C. albicans*, it represents a pathway that has only recently evolved, and that appears to have borrowed the entire upper portion of the pheromone response pathway that functions in the mating process. The observations that the genes selectively up-regulated by α-pheromone in white, but not opaque, cells appear to play roles or to be regulated in the formation of **a**/α biofilms, also suggests that the target genes regulated by the white cell pheromone response pathway that are involved in white cell biofilm formation may have been derived from an ancestral program for **a**/α biofilm formation. Because it represents a recent event, the borrowed portions of the pathway appear to have had insufficient time to undergo refinement through gene replacement or alteration.

CHAPTER 7

TEC1 MEDIATES THE WHITE CELL PHEROMONE RESPONSE IN *C. ALBICANS*: INSIGHTS INTO THE EVOLUTION OF A NEW SIGNAL TRANSDUCTION PATHWAY

Introduction

In Chapter 6, we have demonstrated that the opaque transcription factor Cph1 up-regulated genes through the common GC-rich *cis*-acting sequence OPRE, while the unidentified white-specific transcription factor up-regulated genes through the common AT-rich *cis*-acting sequence WPRE (Sahni *et al.*, 2009b). Many of the genes that were found to be up-regulated by the white-specific transcription factor had already been implicated directly or indirectly in biofilm formation in **a**/α cells, and through mutational analyses, were shown to be involved in pheromone-induced white cell biofilm formation (Sahni *et al.*, 2009b). These observations have led to a unique glimpse into the evolution of a relatively new signal transduction pathway, the white cell pheromone response pathway (Sahni *et al.*, 2009b), which can be no older than the *C. albicans* species, given that white-opaque switching is unique to *C. albicans*. It appears that in the evolution of the white pheromone response pathway, the upper portion was borrowed intact from the mating pathway conserved in the hemiascomycetes (Butler *et al.*, 2009; Soll *et al.*, 2009), and the target genes appeared to have been borrowed from the presumably conserved biofilm process of **a**/α cells. Only one piece of this puzzle was missing, namely the identity and origin of the transcription factor connecting the upstream signal transduction pathway and the downstream genes involved in the white cell pheromone response.

To identify the transcription factor, we generated an overexpression library of 106 individual **a**/**a** strains each transformed with one of 106 constructs in which a specific transcription factor was placed under the control of the inducible tetracycline promoter. A screen for the unidentified white-specific transcription factor was then employed based on

the assumption that overexpression of the correct transcription factor in the absence of pheromone would induce the pheromone response specifically in white cells. Using the dramatic increase in adhesion associated with the white cell response as an assay, we found that only one of the 106 transcription factors, when overexpressed in the absence of pheromone, induced adhesion. The factor was Tec1, which had previously been shown to play a role in filamentation in both *S. cerevisiae* (Madhani and Fink, 1997; Lo and Dranginis, 1998) and *C. albicans* (Schweiger *et al.*, 2000). Characterization of the *TEC1* deletion mutant *tec1/tec1* confirmed that it encoded the target transcription factor in the white pheromone response pathway. With this last piece of the puzzle in hand, the evolution of the white-specific pheromone response pathway revealed a scenario in which all components of the pathway, including target genes, appear to have been borrowed from three conserved developmental programs, providing us with a possible paradigm for how new signal transduction pathways may evolve in general.

Materials and Methods

Yeast Strains and Growth Conditions

The yeast strains used in this study and their genotypes are listed in Table 13. Cells of all natural strains and the derived mutants were maintained at 25° C on agar plates containing modified Lee's medium (Lee *et al.*, 1975; Bedell and Soll, 1979) supplemented with 5 μg/ml phloxine B, which differentially stained opaque colonies and sectors red (Anderson and Soll, 1987). Cells in the white or opaque phase were also verified microscopically prior to use.

Construction of a transcription factor overexpression library

106 genes encoding putative transcription factors in *C. albicans* were selected based on their function in cell wall/membrane biogenesis, basic metabolism, adhesion, filamentation, or biofilm formation. The functions were derived by GO term searches in

Table 13. *C. albicans* strains used in the identification of the key transcription factor in the white response pathway

Strain	Parent	*MTL*	Relevant Genotype	Reference or source
P37005	–	**a**/**a**	Wild type	Lockhart *et al.* (2002)
WO-1	–	α/α	Wild type	Slutsky *et al.* (1987)
ste2/ste2	P37005	**a**/**a**	*ste2*Δ::FRT/*ste2*Δ::FRT	Yi *et al.* (2008)
ste4/ste4	P37005	**a**/**a**	*ste4*Δ::FRT/*ste4*Δ::FRT	Yi *et al.* (2008)
cek1/cek1 cek2/cek2	P37005	**a**/**a**	*cek1*Δ::FRT/*cek1*Δ::FRT *cek2*Δ::FRT/*cek2*Δ::FRT	Yi *et al.* (2008)
P37005-*TETp-STE11*	P37005	**a**/**a**	*ADH1*/*adh1*Δ::ptet-*STE11-GFP*::*SAT*^{R}	This study
P37005-*TETp-CSH1*	P37005	**a**/**a**	*ADH1*/*adh1*Δ::ptet-*CSH1-GFP*::*SAT*^{R}	This study
P37005-*TETp-PBR1*	P37005	**a**/**a**	*ADH1*/*adh1*Δ::ptet-*PBR1-GFP*::*SAT*^{R}	Sahni *et al.* (2009b)
P37005-*TETp-WH11*	P37005	**a**/**a**	*ADH1*/*adh1*Δ::ptet-*WH11-GFP*::*SAT*^{R}	This study
csh1/csh1	P37005	**a**/**a**	*csh1*Δ::FRT/*csh1*Δ::FRT	Sahni *et al.* (2009b)
pbr1/pbr1	P37005	**a**/**a**	*pbr1*Δ::FRT/*pbr1*Δ::FRT	Sahni *et al.* (2009b)
wh11/wh11	P37005	**a**/**a**	*wh11*Δ::FRT/*wh11*Δ::FRT	This study
tec1/TEC1-myc	P37005	**a**/**a**	*TEC1-myc*::*SAT*^{R} /*tec1*Δ::FRT	This study
tec1/tec1	P37005	**a**/**a**	*tec1*Δ::FRT/*tec1*Δ::FRT	This study
tec1/tec1-TEC1	*tec1/tec1*	**a**/**a**	*tec1*Δ::FRT/*tec1*Δ::FRT-*TEC1-GFP*::*SAT*^{R}	This study
L26-*TETp-TEC1*	L26	**a**/**a**	*ADH1*/*adh1*Δ::ptet-*TEC1-GFP*::*SAT*^{R}	This study
P60002-*TETp-TEC1*	P60002	**a**/**a**	*ADH1*/*adh1*Δ::ptet-*TEC1-GFP*::*SAT*^{R}	This study
WO-1-*TETp-TEC1*	WO-1	α/α	*ADH1*/*adh1*Δ::ptet-*TEC1-GFP*::*SAT*^{R}	This study
19F-*TETp-TEC1*	19F	α/α	*ADH1*/*adh1*Δ::ptet-*TEC1-GFP*::*SAT*^{R}	This study
P57072-*TETp-TEC1*	P57072	α/α	*ADH1*/*adh1*Δ::ptet-*TEC1-GFP*::*SAT*^{R}	This study
ste2/ste2-TETp-TEC1	*ste2/ste2*	**a**/**a**	*ste2*Δ::FRT/*ste2*Δ::FRT *ADH1*/*adh1*Δ::ptet-*TEC1-GFP*::*SAT*^{R}	This study

Table 13 --- continued

ste4/ste4-TETp-TEC1	*ste4/ste4*	**a**/**a**	*ste4*Δ::FRT/*ste4*Δ::FRT *ADH1*/*adh1*Δ::ptet-*TEC1-GFP*::*SAT*^{R}	This study
cek1cek2-TETp-TEC1	*cek1/cek1* *cek2/cek2*	**a**/**a**	*cek1*Δ::FRT/*cek1*Δ::FRT *cek2*Δ::FRT/*cek2*Δ::FRT *ADH1*/*adh1*Δ::ptet-*TEC1-GFP*::*SAT*^{R}	This study
tec1/tec1-TETp-TEC1	*tec1/tec1*	**a**/**a**	*tec1*Δ::FRT/*tec1*Δ::FRT *ADH1*/*adh1*Δ::ptet-*TEC1-GFP*::*SAT*^{R}	This study
P37005-*TETp-ACE2*	P37005	**a**/**a**	*ADH1*/*adh1*Δ::ptet-*ACE2-GFP*::*SAT*^{R}	This study
P37005-*TETp-ADA2*	P37005	**a**/**a**	*ADH1*/*adh1*Δ::ptet-*ADA2-GFP*::*SAT*^{R}	This study
P37005-*TETp-ASH1*	P37005	**a**/**a**	*ADH1*/*adh1*Δ::ptet-*ASH1-GFP*::*SAT*^{R}	This study
P37005-*TETp-BCR1*	P37005	**a**/**a**	*ADH1*/*adh1*Δ::ptet-*BCR1-GFP*::*SAT*^{R}	This study
P37005-*TETp-BDF1*	P37005	**a**/**a**	*ADH1*/*adh1*Δ::ptet-*BDF1-GFP*::*SAT*^{R}	This study
P37005-*TETp-BRE1*	P37005	**a**/**a**	*ADH1*/*adh1*Δ::ptet-*BRE1-GFP*::*SAT*^{R}	This study
P37005-*TETp-CAP1*	P37005	**a**/**a**	*ADH1*/*adh1*Δ::ptet-*CAP1-GFP*::*SAT*^{R}	This study
P37005-*TETp-CAS5*	P37005	**a**/**a**	*ADH1*/*adh1*Δ::ptet-*CAS5-GFP*::*SAT*^{R}	This study
P37005-*TETp-CRZ1*	P37005	**a**/**a**	*ADH1*/*adh1*Δ::ptet-*CRZ1-GFP*::*SAT*^{R}	This study
P37005-*TETp-CRZ2*	P37005	**a**/**a**	*ADH1*/*adh1*Δ::ptet-*CRZ2-GFP*::*SAT*^{R}	This study
P37005-*TETp-CSR1*	P37005	**a**/**a**	*ADH1*/*adh1*Δ::ptet-*CSR1-GFP*::*SAT*^{R}	This study
P37005-*TETp-CTA4*	P37005	**a**/**a**	*ADH1*/*adh1*Δ::ptet-*CTA4-GFP*::*SAT*^{R}	This study
P37005-*TETp-CWT1*	P37005	**a**/**a**	*ADH1*/*adh1*Δ::ptet-*CWT1-GFP*::*SAT*^{R}	This study
P37005-*TETp-EFG1*	P37005	**a**/**a**	*ADH1*/*adh1*Δ::ptet-*EFG1-GFP*::*SAT*^{R}	This study
P37005-*TETp-EFH1*	P37005	**a**/**a**	*ADH1*/*adh1*Δ::ptet-*EFH1-GFP*::*SAT*^{R}	This study
P37005-*TETp-FCR1*	P37005	**a**/**a**	*ADH1*/*adh1*Δ::ptet-*FCR1-GFP*::*SAT*^{R}	This study
P37005-*TETp-FCR3*	P37005	**a**/**a**	*ADH1*/*adh1*Δ::ptet-*FCR3-GFP*::*SAT*^{R}	This study
P37005-*TETp-FGR15*	P37005	**a**/**a**	*ADH1*/*adh1*Δ::ptet-*FGR15-GFP*::*SAT*^{R}	This study
P37005-*TETp-FGR17*	P37005	**a**/**a**	*ADH1*/*adh1*Δ::ptet-*FGR17-GFP*::*SAT*^{R}	This study
P37005-*TETp-FKH2*	P37005	**a**/**a**	*ADH1*/*adh1*Δ::ptet-*FKH2-GFP*::*SAT*^{R}	This study
P37005-*TETp-FLO8*	P37005	**a**/**a**	*ADH1*/*adh1*Δ::ptet-*FLO8-GFP*::*SAT*^{R}	This study
P37005-*TETp-GAL4*	P37005	**a**/**a**	*ADH1*/*adh1*Δ::ptet-*GAL4-GFP*::*SAT*^{R}	This study
P37005-*TETp-GAT2*	P37005	**a**/**a**	*ADH1*/*adh1*Δ::ptet-*GAT2-GFP*::*SAT*^{R}	This study

Table 13 --- continued

P37005-*TETp-GCF1*	P37005	**a**/**a**	*ADH1*/*adh1*Δ::ptet-*GCF1-GFP*::*SAT*^{R}	This study
P37005-*TETp-GCN4*	P37005	**a**/**a**	*ADH1*/*adh1*Δ::ptet-*GCN4-GFP*::*SAT*^{R}	This study
P37005-*TETp-GLN3*	P37005	**a**/**a**	*ADH1*/*adh1*Δ::ptet-*GLN3-GFP*::*SAT*^{R}	This study
P37005-*TETp-HAC1*	P37005	**a**/**a**	*ADH1*/*adh1*Δ::ptet-*HAC1-GFP*::*SAT*^{R}	This study
P37005-*TETp-HAL9*	P37005	**a**/**a**	*ADH1*/*adh1*Δ::ptet-*HAL9-GFP*::*SAT*^{R}	This study
P37005-*TETp-HAP31*	P37005	**a**/**a**	*ADH1*/*adh1*Δ::ptet-*HAP31-GFP*::*SAT*^{R}	This study
P37005-*TETp-HAP43*	P37005	**a**/**a**	*ADH1*/*adh1*Δ::ptet-*HAP43-GFP*::*SAT*^{R}	This study
P37005-*TETp-HAP5*	P37005	**a**/**a**	*ADH1*/*adh1*Δ::ptet-*HAP5-GFP*::*SAT*^{R}	This study
P37005-*TETp-IRO1*	P37005	**a**/**a**	*ADH1*/*adh1*Δ::ptet-*IRO1-GFP*::*SAT*^{R}	This study
P37005-*TETp-LYS14*	P37005	**a**/**a**	*ADH1*/*adh1*Δ::ptet-*LYS14-GFP*::*SAT*^{R}	This study
P37005-*TETp-MAC1*	P37005	**a**/**a**	*ADH1*/*adh1*Δ::ptet-*MAC1-GFP*::*SAT*^{R}	This study
P37005-*TETp-MCM1*	P37005	**a**/**a**	*ADH1*/*adh1*Δ::ptet-*MCM1-GFP*::*SAT*^{R}	This study
P37005-*TETp-MDM34*	P37005	**a**/**a**	*ADH1*/*adh1*Δ::ptet-*MDM34-GFP*::*SAT*^{R}	This study
P37005-*TETp-MIG1*	P37005	**a**/**a**	*ADH1*/*adh1*Δ::ptet-*MIG1-GFP*::*SAT*^{R}	This study
P37005-*TETp-MNL1*	P37005	**a**/**a**	*ADH1*/*adh1*Δ::ptet-*MNL1-GFP*::*SAT*^{R}	This study
P37005-*TETp-MSN4*	P37005	**a**/**a**	*ADH1*/*adh1*Δ::ptet-*MSN4-GFP*::*SAT*^{R}	This study
P37005-*TETp-NDT80*	P37005	**a**/**a**	*ADH1*/*adh1*Δ::ptet-*NDT80-GFP*::*SAT*^{R}	This study
P37005-*TETp-NHP6A*	P37005	**a**/**a**	*ADH1*/*adh1*Δ::ptet-*NHP6A-GFP*::*SAT*^{R}	This study
P37005-*TETp-NOT3*	P37005	**a**/**a**	*ADH1*/*adh1*Δ::ptet-*NOT3-GFP*::*SAT*^{R}	This study
P37005-*TETp-NOT5*	P37005	**a**/**a**	*ADH1*/*adh1*Δ::ptet-*NOT5-GFP*::*SAT*^{R}	This study
P37005-*TETp-NRG1*	P37005	**a**/**a**	*ADH1*/*adh1*Δ::ptet-*NRG1-GFP*::*SAT*^{R}	This study
P37005-*TETp-RBF1*	P37005	**a**/**a**	*ADH1*/*adh1*Δ::ptet-*RBF1-GFP*::*SAT*^{R}	This study
P37005-*TETp-RIM101*	P37005	**a**/**a**	*ADH1*/*adh1*Δ::ptet-*RIM101-GFP*::*SAT*^{R}	This study
P37005-*TETp-RIM13*	P37005	**a**/**a**	*ADH1*/*adh1*Δ::ptet-*RIM13-GFP*::*SAT*^{R}	This study
P37005-*TETp-RIM8*	P37005	**a**/**a**	*ADH1*/*adh1*Δ::ptet-*RIM8-GFP*::*SAT*^{R}	This study
P37005-*TETp-RLM1*	P37005	**a**/**a**	*ADH1*/*adh1*Δ::ptet-*RLM1-GFP*::*SAT*^{R}	This study
P37005-*TETp-SPT14*	P37005	**a**/**a**	*ADH1*/*adh1*Δ::ptet-*SPT14-GFP*::*SAT*^{R}	This study
P37005-*TETp-SPT20*	P37005	**a**/**a**	*ADH1*/*adh1*Δ::ptet-*SPT20-GFP*::*SAT*^{R}	This study
P37005-*TETp-STB5*	P37005	**a**/**a**	*ADH1*/*adh1*Δ::ptet-*STB5-GFP*::*SAT*^{R}	This study

Table 13 --- continued

P37005-*TETp-STP3*	P37005	**a**/**a**	*ADH1*/*adh1*Δ::ptet-*STP3-GFP*::*SAT*^{R}	This study
P37005-*TETp-STP4*	P37005	**a**/**a**	*ADH1*/*adh1*Δ::ptet-*STP4-GFP*::*SAT*^{R}	This study
P37005-*TETp-TAF14*	P37005	**a**/**a**	*ADH1*/*adh1*Δ::ptet-*TAF14-GFP*::*SAT*^{R}	This study
P37005-*TETp-TEA1*	P37005	**a**/**a**	*ADH1*/*adh1*Δ::ptet-*TEA1-GFP*::*SAT*^{R}	This study
P37005-*TETp-TEC1*	P37005	**a**/**a**	*ADH1*/*adh1*Δ::ptet-*TEC1-GFP*::*SAT*^{R}	This study
P37005-*TETp-TFG1*	P37005	**a**/**a**	*ADH1*/*adh1*Δ::ptet-*TFG1-GFP*::*SAT*^{R}	This study
P37005-*TETp-THI20*	P37005	**a**/**a**	*ADH1*/*adh1*Δ::ptet-*THI20-GFP*::*SAT*^{R}	This study
P37005-*TETp-TYE7*	P37005	**a**/**a**	*ADH1*/*adh1*Δ::ptet-*TYE7-GFP*::*SAT*^{R}	This study
P37005-*TETp-UGA3*	P37005	**a**/**a**	*ADH1*/*adh1*Δ::ptet-*UGA3-GFP*::*SAT*^{R}	This study
P37005-*TETp-UGA32*	P37005	**a**/**a**	*ADH1*/*adh1*Δ::ptet-*UGA32-GFP*::*SAT*^{R}	This study
P37005-*TETp-UGA33*	P37005	**a**/**a**	*ADH1*/*adh1*Δ::ptet-*UGA33-GFP*::*SAT*^{R}	This study
P37005-*TETp-UPC2*	P37005	**a**/**a**	*ADH1*/*adh1*Δ::ptet-*UPC2-GFP*::*SAT*^{R}	This study
P37005-*TETp-ZCF5*	P37005	**a**/**a**	*ADH1*/*adh1*Δ::ptet-*ZCF5-GFP*::*SAT*^{R}	This study
P37005-*TETp-ZCF6*	P37005	**a**/**a**	*ADH1*/*adh1*Δ::ptet-*ZCF6-GFP*::*SAT*^{R}	This study
P37005-*TETp-ZCF9*	P37005	**a**/**a**	*ADH1*/*adh1*Δ::ptet-*ZCF9-GFP*::*SAT*^{R}	This study
P37005-*TETp-ZCF11*	P37005	**a**/**a**	*ADH1*/*adh1*Δ::ptet-*ZCF11-GFP*::*SAT*^{R}	This study
P37005-*TETp-ZCF12*	P37005	**a**/**a**	*ADH1*/*adh1*Δ::ptet-*ZCF12-GFP*::*SAT*^{R}	This study
P37005-*TETp-ZCF14*	P37005	**a**/**a**	*ADH1*/*adh1*Δ::ptet-*ZCF14-GFP*::*SAT*^{R}	This study
P37005-*TETp-ZCF16*	P37005	**a**/**a**	*ADH1*/*adh1*Δ::ptet-*ZCF16-GFP*::*SAT*^{R}	This study
P37005-*TETp-ZCF17*	P37005	**a**/**a**	*ADH1*/*adh1*Δ::ptet-*ZCF17-GFP*::*SAT*^{R}	This study
P37005-*TETp -ZCF21*	P37005	**a**/**a**	*ADH1*/*adh1*Δ::ptet-*ZCF21-GFP*::*SAT*^{R}	This study
P37005-*TETp-ZCF22*	P37005	**a**/**a**	*ADH1*/*adh1*Δ::ptet-*ZCF22-GFP*::*SAT*^{R}	This study
P37005-*TETp-ZCF23*	P37005	**a**/**a**	*ADH1*/*adh1*Δ::ptet-*ZCF23-GFP*::*SAT*^{R}	This study
P37005-*TETp-ZCF24*	P37005	**a**/**a**	*ADH1*/*adh1*Δ::ptet-*ZCF24-GFP*::*SAT*^{R}	This study
P37005-*TETp-ZCF28*	P37005	**a**/**a**	*ADH1*/*adh1*Δ::ptet-*ZCF28-GFP*::*SAT*^{R}	This study
P37005-*TETp-ZCF32*	P37005	**a**/**a**	*ADH1*/*adh1*Δ::ptet-*ZCF32-GFP*::*SAT*^{R}	This study
P37005-*TETp-ZCF38*	P37005	**a**/**a**	*ADH1*/*adh1*Δ::ptet-*ZCF38-GFP*::*SAT*^{R}	This study
P37005-*TETp-ZCF39*	P37005	**a**/**a**	*ADH1*/*adh1*Δ::ptet-*ZCF39- GFP*::*SAT*^{R}	This study
P37005-*TETp-ZPR1*	P37005	**a**/**a**	*ADH1*/*adh1*Δ::ptet-*ZPR1- GFP*::*SAT*^{R}	This study

Table 13 --- continued

P37005-*TETp-1007*	P37005	**a**/**a**	*ADH1*/*adh1*Δ::ptet-*1007- GFP*::*SAT*^{R}	This study
P37005-*TETp-1178*	P37005	**a**/**a**	*ADH1*/*adh1*Δ::ptet-*1178- GFP*::*SAT*^{R}	This study
P37005-*TETp-1757*	P37005	**a**/**a**	*ADH1*/*adh1*Δ::ptet-*1757- GFP*::*SAT*^{R}	This study
P37005-*TETp-2260*	P37005	**a**/**a**	*ADH1*/*adh1*Δ::ptet-*2260- GFP*::*SAT*^{R}	This study
P37005-*TETp-2315*	P37005	**a**/**a**	*ADH1*/*adh1*Δ::ptet-*2315- GFP*::*SAT*^{R}	This study
P37005-*TETp-2393*	P37005	**a**/**a**	*ADH1*/*adh1*Δ::ptet-*2393- GFP*::*SAT*^{R}	This study
P37005-*TETp-2399*	P37005	**a**/**a**	*ADH1*/*adh1*Δ::ptet-*2399- GFP*::*SAT*^{R}	This study
P37005-*TETp-2458*	P37005	**a**/**a**	*ADH1*/*adh1*Δ::ptet-*2458- GFP*::*SAT*^{R}	This study
P37005-*TETp-2612*	P37005	**a**/**a**	*ADH1*/*adh1*Δ::ptet-*2612- GFP*::*SAT*^{R}	This study
P37005-*TETp-2961*	P37005	**a**/**a**	*ADH1*/*adh1*Δ::ptet-*2961- GFP*::*SAT*^{R}	This study
P37005-*TETp-3088*	P37005	**a**/**a**	*ADH1*/*adh1*Δ::ptet-*3088- GFP*::*SAT*^{R}	This study
P37005-*TETp-3407*	P37005	**a**/**a**	*ADH1*/*adh1*Δ::ptet-*3407- GFP*::*SAT*^{R}	This study
P37005-*TETp-3683*	P37005	**a**/**a**	*ADH1*/*adh1*Δ::ptet-*3683- GFP*::*SAT*^{R}	This study
P37005-*TETp-3928*	P37005	**a**/**a**	*ADH1*/*adh1*Δ::ptet-*3928- GFP*::*SAT*^{R}	This study
P37005-*TETp-4125*	P37005	**a**/**a**	*ADH1*/*adh1*Δ::ptet-*4125- GFP*::*SAT*^{R}	This study
P37005-*TETp-4778*	P37005	**a**/**a**	*ADH1*/*adh1*Δ::ptet-*4778- GFP*::*SAT*^{R}	This study
P37005-*TETp-4972*	P37005	**a**/**a**	*ADH1*/*adh1*Δ::ptet-*4972- GFP*::*SAT*^{R}	This study
P37005-*TETp-4998*	P37005	**a**/**a**	*ADH1*/*adh1*Δ::ptet-*4998- GFP*::*SAT*^{R}	This study
P37005-*TETp-5326*	P37005	**a**/**a**	*ADH1*/*adh1*Δ::ptet-*5326- GFP*::*SAT*^{R}	This study
P37005-*TETp-5953*	P37005	**a**/**a**	*ADH1*/*adh1*Δ::ptet-*5953- GFP*::*SAT*^{R}	This study
P37005-*TETp-5975*	P37005	**a**/**a**	*ADH1*/*adh1*Δ::ptet-*5975- GFP*::*SAT*^{R}	This study
P37005-*TETp-6781*	P37005	**a**/**a**	*ADH1*/*adh1*Δ::ptet-*6781- GFP*::*SAT*^{R}	This study
P37005-*TETp-684*	P37005	**a**/**a**	*ADH1*/*adh1*Δ::ptet-*684- GFP*::*SAT*^{R}	This study
P37005-*TETp-6845*	P37005	**a**/**a**	*ADH1*/*adh1*Δ::ptet-*6845- GFP*::*SAT*^{R}	This study
P37005-*TETp-6888*	P37005	**a**/**a**	*ADH1*/*adh1*Δ::ptet-*6888- GFP*::*SAT*^{R}	This study

the *Candida* genome database (http://www.candidagenome.org/). The annotations of these transcription factors are listed in Table 14.

The plasmid pNIM1 harboring a *GFP* gene and a tetracycline-inducible promoter (Park and Morschhäuser, 2005), was used to generate the overexpression module for each transcription factor gene. This plasmid was a generous gift from Joachim Morschhäuser from the University of Würzburg, Germany. The ORFs of the 106 genes encoding transcription factors were amplified by PCR using the primer sets listed in Table 15. Each of the PCR products was digested with SalI or XhoI, and cloned into the SalI-cut, dephosphorylated plasmid pNIM1. The derived plasmids were verified by sequencing for fusion of the *GFP* ORF in-frame to the 3' of each gene. The plasmids were then linearized by ApaI or SacII enzyme digestion, and transformed into the **a**/**a** natural *C. albicans* strain P37005 to generate an overexpression strain library (Table 13). The library strains were confirmed by PCR. Activation of gene expression in these strains by doxycycline, an analog of tetracycline, was also verified by northern blots and fluorescence microscopy.

Adhesion Assay

α-pheromone-induced adhesion was assessed following incubation of white cells of **a**/**a** strains at 25^{o}C for 16 hours in the wells of a Costar 12-well cluster plate (Corning Life Sciences, Corning, NY) in the presence or absence of 3×10^{-6} M synthetic 13-mer α-pheromone (Open Biosystems, Huntsville, AL) according to methods previously discussed (Daniels *et al.*, 2006; Yi *et al.*, 2009). The synthetic α-pheromone was dissolved in dimethyl sulfoxide (DMSO). For controls in the absence of pheromone, an equivalent amount of DMSO was added. Adhesion was quantitated by releasing cells from the dish bottoms using 0.05% trypsin-EDTA solution (Invitrogen, Carlsbad, CA), and counting them in a hemocytometer.

Table 14. Construction of an overexpression library for *C. albicans* transcription factors

No.	Gene/ ORF	Sc. homolog	DNA-binding motif	Function (*Candida* genome database)
1	*ACE2*	*ACE2*	Zinc finger	morphogenesis, adherence, biofilm formation and virulence
2	*ADA2*	*ADA2*	Zinc finger	cell wall integrity and resistance to caspofungin
3	*ASH1*	*ASH1*	Zinc finger	filamentous growth and virulence
4	*BCR1*	*USV1*	Zinc finger	biofilm formation and regulation of cell-surface genes
5	*BDF1*	*BDF1*	TATA binding	adherence to polystyrene
6	*BRE1*	*BRE1*	Zinc finger	filamentous growth
7	*CAP1*	*YAP1*	bZIP	multidrug resistance and oxidative stress response
8	*CAS5*	*YGL035C*	Zinc finger	cell wall integrity and resistance to caspofungin
9	*CRZ1*	*CRZ1*	Zinc finger	multidrug resistance and oxidative stress response
10	*CRZ2*	*CRZ1*	Zinc finger	multidrug resistance and oxidative stress response
11	*CSR1*	*ZAP1*	Zinc finger	biofilm matrix formation and filamentous growth
12	*CTA4*	*OAF1*	Zinc cluster	adherence to polystyrene
13	*CWT1*	*RDS2*	Zinc finger	cell wall biogenesis
14	*EFG1*	*SOK2*	bHLH	filamentous growth, adherence and virulence
15	*EFH1*	*SOK2*	APSES domain	filamentous growth, adherence and virulence
16	*FCR1*	*CAT8*	Zinc cluster	filamentous growth and fluconazole resistance
17	*FCR3*	*YAP3*	bZIP	fluconazole resistance
18	*FGR15*	*RPN4*	Zinc finger	filamentous growth
19	*FGR17*	*CHA4*	Zinc cluster	filamentous growth
20	*FKH2*	*FKH2*	Forkhead-like	filamentous growth and virulence
21	*FLO8*	*FLO8*	LUFS domain	filamentous growth and virulence
22	*GAL4*	*GAL4*	Zinc cluster	carbohydrate metabolic process
23	*GAT2*	*GAT2*	Zinc finger	filamentous growth
24	*GCF1*	N/A	HMG-like	binding to the promoter of *HWP1*

Table 14 --- continued

25	*GCN4*	*GCN4*	bZIP	filamentous growth induced upon amino acid starvation
26	*GLN3*	*GLN3*	Zinc finger	filamentous growth
27	*HAC1*	*HAC1*	bZIP	filamentous growth
28	*HAL9*	*HAL9*	Zinc cluster	stress response and salt stress tolerance
29	*HAP31*	*HAP3*	Histone-like	carbohydrate metabolic process and iron-regulated
30	*HAP43*	*YAP3*	bZIP	stress response and iron limitation regulation
31	*HAP5*	*HAP5*	Histone-like	filamentous growth
32	*IRO1*	*YJL225C*	Unknown	filamentous growth and pathogenesis
33	*LYS14*	*LYS14*	Zinc cluster	amino acid metabolic process
34	*MAC1*	*MAC1*	Copper-first domain	filamentous growth
35	*MCM1*	*MCM1*	MADS domain	filamentous growth
36	*MDM34*	*MDM34*	Zinc finger	a putative virulence gene, macrophage-downregulated
37	*MIG1*	*MIG1*	Zinc finger	hyphal growth and upregulated during biofilm formation
38	*MNL1*	*MSN2*	Zinc finger	stress response
39	*MSN4*	*MSN4*	Zinc finger	stress response
40	*NDT80*	*NDT80*	PhoG-like	drug resistance
41	*NHP6A*	*NHP6A*	Unknown	anti-fungal drug regulated
42	*NOT3*	*NOT3*	Unknown	filamentous growth
43	*NOT5*	*NOT5*	Unknown	filamentous growth, adhesion and pathogenesis
44	*NRG1*	*YPR015C*	Zinc finger	filamentous growth and virulence
45	*RBF1*	*DEF1*	Unknown	filamentous growth
46	*RIM101*	*RIM101*	Zinc finger	filamentous growth
47	*RIM13*	*RIM13*	Unknown	filamentous growth
48	*RIM8*	*RIM8*	Unknown	filamentous growth
49	*RLM1*	*RLM1*	MEF2_like	resistance to cell wall stress
50	*SPT14*	*SPT14*	Unknown	cell wall biogenesis and upregulated in biofilm
51	*SPT20*	*SPT20*	Unknown	adherence to polystyrene
52	*STB5*	*STB5*	Zinc cluster	stress response
53	*STP3*	*STP2*	Zinc finger	RNA metabolic process

Table 14 --- continued

54	*STP4*	*STP4*	Zinc finger	RNA metabolic process
55	*TAF14*	*TAF14*	TATA binding	a putative virulence gene, macrophage induced
56	*TEA1*	*TEA1*	Zinc cluster	drug resistance
57	*TEC1*	*TEC1*	TEA domain	biofilm formation and filamentous growth
58	*TFG1*	*TFG1*	TFIIFa	filamentous growth
59	*THI20*	*THI20*	TENA	thiamine biosynthesis
60	*TYE7*	*TYE7*	bHLH	filamentous growth and drug resistance
61	*UGA3*	*UGA3*	Zinc cluster	gamma-aminobutyrate metabolism
62	*UGA32*	*UGA3*	Zinc finger	gamma-aminobutyrate metabolism
63	*UGA33*	*UGA3*	Zinc finger	gamma-aminobutyrate metabolism
64	*UPC2*	*UPC2*	Zinc cluster	cell wall biosynthesis
65	*ZCF5*	*HAP1*	Zinc cluster	carbohydrate metabolic process
66	*ZCF6*	*ASG1*	Zinc cluster	inferred function in stress response and drug resistance
67	*ZCF9*	*LYS14*	Zinc cluster	response to drug and up-regulated by pheromone
68	*ZCF11*	*YBR239C*	Zinc cluster	filamentous growth
69	*ZCF12*	*ECM22*	Zinc cluster	cell wall biosynthesis
70	*ZCF14*	*HAP1*	Zinc cluster	caspofungin induced
71	*ZCF16*	*CAT8*	Zinc finger	multidrug resistance and aerobic growth
72	*ZCF17*	*UPC2*	Zinc cluster	cell wall biosynthesis
73	*ZCF21*	*MUC1*	Zinc finger	invasive growth, flocculation and biofilms
74	*ZCF22*	*UPC2*	Zinc finger	cell wall biosynthesis
75	*ZCF23*	*GSM1*	Zinc finger	inferred function in energy metabolism
76	*ZCF24*	*ASG1*	Zinc finger	stress response
77	*ZCF28*	*ECM22*	Zinc cluster	cell wall biosynthesis
78	*ZCF32*	*LYS14*	Zinc finger	amino acid metabolic process
79	*ZCF38*	*TEA1*	Zinc cluster	stress response
80	*ZCF39*	*STB5*	Zinc cluster	induced during filamentation
81	*ZPR1*	*ZPR1*	Zinc finger	drug resistance
82	*19.1007*	*YDR017C*	bZIP	stress response and telomere maintenance
83	*19.1178*	Unknown	bZIP	unknown function
84	*19.1757*	*MET32*	Zinc finger	amino acid metabolic process

Table 14 --- continued

85	*19.226*	*BCD1*	Zinc finger	filamentous growth
86	*19.2315*	*RTG3*	bZIP	RNA metabolic process
87	*19.2393*	*YTH1*	Zinc finger	RNA metabolic process
88	*19.2399*	*YNL227C*	Zinc finger	ribosome biogenesis
89	*19.2458*	*SIP5*	Zinc finger	stress response
90	*19.2612*	*SWI5*	Zinc finger	RNA metabolic process
91	*19.2961*	*MIG2*	Zinc finger	inferred function in resistance to chemicals
92	*19.3088*	Unknown	bZIP	biofilm formation and hyphal formation
93	*19.3407*	*RAD18*	Zinc finger	stress response
94	*19.3683*	*GCS1*	Zinc finger	stress response
95	*19.3928*	*AZF1*	Zinc finger	response to chemical stimulus
96	*19.4125*	*PZF1*	Zinc finger	RNA metabolic process
97	*19.4778*	*LYS14*	Zinc cluster	lysine biosynthesis
98	*19.4972*	*CRZ1*	Zinc finger	response to chemical stimulus
99	*19.4998*	*TEA1*	Zinc cluster	amino acid metabolic process
100	*19.5326*	*MIG1*	Zinc finger	carbohydrate metabolic process
101	*19.5953*	*SFP1*	Zinc finger	RNA metabolic process
102	*19.5975*	*ADR1*	Zinc finger	fluconazole-downregulated
103	*19.6781*	*LYS14*	Zinc finger	amino acid metabolic process
104	*19.684*	*PCF11*	Zinc finger	response to drug
105	*19.6845*	Unknown	bZIP	unknown function
106	*19.6888*	*YLLO54C*	Gal4p-like	drug resistance

Table 15. Oligonucleotides used for the library construction in the identification of the key transcription factor in the white response pathway

Gene/ORF	Primer	Sequence
ACE2	ACE2f	5'-TCCGTCGACAAAGATGCATTGGAAATTTCTG-3'
	ACE2r	5'-TCCGTCGACAATTGCAACATTAAAAACTC-3'
ADA2	ADA2f	5'-TCCGTCGACAAAGATGGATTCAAGAACAAAA-3'
	ADA2r	5'-TCCGTCGACAACCCCTGAGAACACCATCCCA-3'
ASH1	ASH1f	5'-TCCGTCGACAAAGATGAGTTTAGTCCAGTCA-3'
	ASH1r	5'-TCCGTCGACAAAGATTTAGGAAGTACTTC-3'
BCR1	BCR1f	5'-TCCGTCGACAAAGATGTCAGGGACATCACAA-3'
	BCR1r	5'-TCCGTCGACAATTGTGATATTAAATTATT-3'
BDF1	BDF1f	5'-TCCGTCGACAAAGATGAATGCTGGCGACAAA-3'
	BDF1r	5'-TCCGTCGACAACTCTTCTTCTGAACTTTC-3'
BRE1	BRE1f	5'-TCCGTCGACAAAGATGGCTGTTGATAACGAA-3'
	BRE1r	5'-TCCGTCGACAACAAGTGAATTGATAACAA-3'
CAP1	CAP1f	5'-TCCGTCGACAAAGATGACAGATATTAAAAGA-3'
	CAP1r	5'-TCCGTCGACAAATGTTTTATACTTCGCTC-3'
CAS5	CAS5f	5'-TCCGTCGACAAAGATGGAGAATTATTTATTA-3'
	CAS5r	5'-TCCGTCGACAAGGAAACTTCTTTGTTTTC-3'
CRZ1	CRZ1f	5'-TCCGTCGACAAAGATGTCTAACAATCCTCAT-3'
	CRZ1r	5'-TCCGTCGACAAAGTAATTTCAACACCACT-3'
CRZ2	CRZ2f	5'-TCCCTCGAGAAAGATGTTATCAACCATGTCT-3'
	CRZ2r	5'-TCCCTCGAGAATTTATTAGATTGTAATAA-3'
CSR1	CSR1f	5'-TCCGTCGACAAAGATGGAACCTATTTCTAAAT-3'
	CSR1r	5'-TCCGTCGACAATTTCTCAACTGAATGTTC-3'
CTA4	CTA4f	5'-TCCGTCGACAAAGATGACATCTGAACATAAA-3'
	CTA4r	5'-TCCGTCGACAATCCATAAAAATATCCATC-3'
CWT1	CWT1f	5'-TCCGTCGACAAAGATGTCTACCATGAGTACT-3'
	CWT1r	5'-TCCGTCGACAAAGGATCAATGGGGATAAA-3'
EFG1	EFG1f	5'-TCCGTCGACAAAGATGTCAACGTATTCTATA-3'
	EFG1r	5'-TCCGTCGACAAATGACTGAACTTGGGGTG-3'
EFH1	EFH1f	5'-TCCGTCGACAAAGATGAATGGTATTATGACG-3'

Table 15 --- continued

	EFH1r	5'-TCCGTCGACAATAATGTTTTGTGAACAGT-3'
FCR1	FCR1f	5'-TCCGTCGACAAAGATGTCTGACGATCATTCA-3'
	FCR1r	5'-TCCGTCGACAAAATATTGAAGAAAGGATC-3'
FCR3	FCR3f	5'-TCCGTCGACAAAGATGAATTTTAAGACAGAAAATTC-3'
	FCR3r	5'-TCCGTCGACAAATTCAAACTACTTTCAATTGCCT-3'
FGR15	FGR15f	5'-TCCGTCGACAAAGATGGAATCCACATTAAGT-3'
	FGR15r	5'-TCCGTCGACAACTTATTGAAAGTTACTTC-3'
FGR17	FGR17f	5'-TCCGTCGACAAAGATGCTGTCAAAATCTAGA-3'
	FGR17r	5'-TCCGTCGACAATAACATATCAAGTATGCC-3'
FKH2	FKH2f	5'-TCCGTCGACAAAGATGTCAGCACAATTTATC-3'
	FKH2r	5'-TCCGTCGACAACAGATCAATCATTTCAGT-3'
FLO8	FLO8f	5'-TCCGTCGACAAAGATGGTTCCCAACACAACT-3'
	FLO8r	5'-TCCGTCGACAAATCGCCATTTTCAATTGG-3'
GAL4	GAL4f	5'-TCCGTCGACAAAGATGTCTGAAACTAATGAA-3'
	GAL4r	5'-TCCGTCGACAAAACGTTAACAGTTTCATC-3'
GAT2	GAT2f	5'-TCCGTCGACAAAGATGTCCAGTTCATCATCT-3'
	GAT2r	5'-TCCGTCGACAAACATATGGTTGTTTGTTG-3'
GCF1	GCF1f	5'-TCCGTCGACAAAGATGTTGAGATCATTTGTA-3'
	GCF1r	5'-TCCGTCGACAAAAAGTCATCCTCCACTTT-3'
GCN4	GCN4f	5'-TCCGTCGACAAAGATGCCTGCTACTACTCCT-3'
	GCN4r	5'-TCCGTCGACAAAAATTGAATACCATTAACTCTTA-3'
GLN3	GLN3f	5'-TCCCTCGAGAAAGATGACTACATCGAATAGT-3'
	GLN3r	5'-TCCCTCGAGAAAATGTCAAACTTCAACCA-3'
HAC1	HAC1f	5'-TCCGTCGACAAAGATGGAGTTAACTGTTGAT-3'
	HAC1r	5'-TCCGTCGACAAGACTTTATGAACTTCAAC-3'
HAL9	HAL9f	5'-TCCGTCGACAAAGATGGATCCTGCTTATGAT-3'
	HAL9r	5'-TCCGTCGACAAGTTATAAAATATATCAGG-3'
HAP31	HAP31f	5'-TCCGTCGACAAAGATGAATCAACAAAACGCA-3'
	HAP31r	5'-TCCGTCGACAACTTCCTGGCTTCTCGGTA-3'
HAP43	HAP43f	5'-TCCGTCGACAAAGATGCCCGCAAAAGGTCCT-3'
	HAP43r	5'-TCCGTCGACAAATTATATGCTCTTCTATC-3'
HAP5	HAP5f	5'-TCCGTCGACAAAGATGAACGAAGATCCACAG-3'
	HAP5r	5'-TCCGTCGACAAATAATTGTTTTGGTAACC-3'

Table 15 --- continued

IRO1	IRO1f	5'-TCCGTCGACAAAGATGTTGGATAGATTAAAT-3'
	IRO1r	5'-TCCGTCGACAAGTTCAAACTGTTTAAATA-3'
LYS14	LYS14f	5'-TCCGTCGACAAAGATGTCACAATCACCATCT-3'
	LYS14r	5'-TCCGTCGACAAGTATATCAATGTATCATC-3'
MAC1	MAC1f	5'-TCCGTCGACAAAGATGATACTAATAGATGAT-3'
	MAC1r	5'-TCCGTCGACAATTTGGTCTTTTTTGAGCAA-3'
MCM1	MCM1f	5'-TCCGTCGACAAAGATGGCTATTAAGAAGAA-3'
	MCM1r	5'-TCCGTCGACAATTGATATTGCTGTTGATT-3'
MDM34	MDM34f	5'-TCCCTCGAGAAAGATGTCGTTCAAAGTAAAT-3'
	MDM34r	5'-TCCCTCGAGAAACAATATGGTGGTGGTGG-3'
MIG1	MIG1f	5'-TCCGTCGACAAAGATGTCCATGTCCACACCT-3'
	MIG1r	5'-TCCGTCGACAAACTTAATAAATTGGTTAA-3'
MNL1	MNL1f	5'-TCCGTCGACAAAGATGGATTCACATAATAAC-3'
	MNL1r	5'-TCCGTCGACAATCCTGAAGCATCATCCAT-3'
MSN4	MSN4f	5'-TCCGTCGACAAAGATGTCTCAAGAATTCCAA-3'
	MSN4r	5'-TCCGTCGACAATACCGATTTTTTCTTTTC-3'
NDT80	NDT80f	5'-TCCCTCGAGAAAGATGCATCCATCAGCTGGT-3'
	NDT80r	5'-TCCCTCGAGAACTGTGGAGGAGTAGGGGT-3'
NHP6A	NHP6Af	5'-TCCGTCGACAACACTTTGCATTTTCTGAT-3'
	NHP6Ar	5'-TCCGTCGACAAGGCGGAATTCTTTTTAGC-3'
NOT3	NOT3f	5'-TCCGTCGACAAAGATGTCAAATCGAAAACTA-3'
	NOT3r	5'-TCCGTCGACAAAAATAATGTTTTTGATGG-3'
NOT5	NOT5f	5'-TCCGTCGACAAAGATGAGTGCAAGAAAACTA-3'
	NOT5r	5'-TCCGTCGACAATTGGAAAATCTGTCTGTT-3'
NRG1	NRG1f	5'-TCCGTCGACAAAGATGCTTTATCAACAATCA-3'
	NRG1r	5'-TCCGTCGACAATACTAGGCTCTTGGTGTTG-3'
RBF1	RBF1f	5'-TCCGTCGACAAAGATGTCATCTAATAAGAAC-3'
	RBF1r	5'-TCCGTCGACAACAAAAACCCACTTCTTTT-3'
RIM101	RIM101f	5'-TCCGTCGACAAAGATGAATTACAACATTCAT-3'
	RIM101r	5'-TCCGTCGACAAGAAAGCAGTTATAGTTGG-3'
RIM13	RIM13f	5'-TCCGTCGACAAAGATGCCCACACCATGTCTA-3'
	RIM13r	5'-TCCGTCGACAATTTTAATATCACTTTATTATTGCAGC-3'
RIM8	RIM8f	5'-TCCGTCGACAAAGATGAGACGAGCAGTATCAA-3'

Table 15 --- continued

	RIM8r	5’-TCCGTCGACAACGTTCTCTGAATTCGAGTTATT-3’
RLM1	RLM1f	5'-TCCCTCGAGAAAGATGGGTAGAAGAAAGATT-3'
	RLM1r	5'-TCCCTCGAGAATGTATTTTTATTAGGTCC-3'
SPT14	SPT14f	5'-TCCGTCGACAAAGATGGGATACAATATAGCA-3'
	SPT14r	5'-TCCGTCGACAAATTTACTTTGTTCGGAAA-3'
SPT20	SPT20f	5'-TCCGTCGACAAAGATGATAAAATCTGAAGTT-3'
	SPT20r	5'-TCCGTCGACAAATTAGCAGGCGCATTTTT-3'
STB5	STB5f	5'-TCCGTCGACAAAGATGAGACCAATAGACTCC-3'
	STB5r	5'-TCCGTCGACAAAAAATTGTACATGAAATC-3'
STP3	STP3f	5'-TCCGTCGACAAAGATGTTGATACTTTCCATA-3'
	STP3r	5'-TCCGTCGACAAATCTAGTAATAGATTGCT-3'
STP4	STP4f	5'-TCCGTCGACAAAGATGTTATCAATGGCCGTA-3'
	STP4r	5'-TCCGTCGACAAATGTTCTTTTTTGATCAA-3'
TAF14	TAF14f	5'-TCCGTCGACAAAGATGTCAGAAGTAAAAAGG-3'
	TAF14r	5'-TCCGTCGACAAAGCTTCACCAGTGTGTTT-3'
TEA1	TEA1f	5’-TCCGTCGACAAAGATGTCAATCAATTCATCA-3’
	TEA1r	5’-TCCGTCGACAAATTTTTCGAATTAAATAT-3’
TEC1	TEC1f	5'-TCCGTCGACAAAGATGATGTCGCAAGCTACT-3'
	TEC1r	5'-TCCGTCGACAAAAACTCACTAGTAAATCC-3'
TFG1	TFG1f	5'-TCCGTCGACAAAGATGAGTCAATCAGATGTT-3'
	TFG1r	5'-TCCGTCGACAAGTCTTTAAGAACTAGCTT-3'
THI20	THI20f	5'-TCCCTCGAGAAAGATGACAATTGCTGGTAGC-3'
	THI20r	5'-TCCCTCGAGAATATGTTCAACACTTCATC-3'
TYE7	TYE7f	5'-TCCGTCGACAAAGATGAGTTCATTCCAGCAA-3'
	TYE7r	5'-TCCGTCGACAATATTTCACCACCCAATTT-3'
UGA3	UGA3f	5'-TCCGTCGACAAAGATGATAGTAACATTTAAT-3'
	UGA3r	5'-TCCGTCGACAATGCAAAATTTATATCCCA-3'
UGA32	UGA32f	5'-TCCGTCGACAAAGATGTTCTACGTATTCGAT-3'
	UGA32r	5'-TCCGTCGACAAGCAAAATGAGATGTTCC-3'
UGA33	UGA33f	5'-TCCGTCGACAAAGATGTCCTCACAATCCCCA-3'
	UGA33r	5'-TCCGTCGACAAAATCATGGATATTTTCCA-3'
UPC2	UPC2f	5'-TCCCTCGAGAAAGATGATGATGACAGTGAAA-3'
	UPC2r	5'-TCCCTCGAGAATTTCATATTCATAAACCC-3'

Table 15 --- continued

ZCF5	ZCF5f	5'-TCCGTCGACAAAGATGGAACTTGAAGCTAGT-3'
	ZCF5r	5'-TCCGTCGACAATTTACTCTCTCTATATATTT-3'
ZCF6	ZCF6f	5'-TCCGTCGACAAAGATGAGTCAAGATCAAACCCCA-3'
	ZCF6r	5'-TCCGTCGACAATACACATAATTGTTTTGAATTGGCAA-3'
ZCF9	ZCF9f	5'-TCCGTCGACAAAGATGCCTCTCGATAATACT-3'
	ZCF9r	5'-TCCGTCGACAACCCGAGTAGCACCTCCCA-3'
ZCF11	ZCF11f	5'-TCCGTCGACAAAGATGAAGATTAAACAGGAA-3'
	ZCF11r	5'-TCCGTCGACAATAGTATTGGTAAAAAGTT-3'
ZCF12	ZCF12f	5'-TCCCTCGAGAAAGATGGGAGACTCGCCTCCA-3'
	ZCF12r	5'-TCCCTCGAGAATTGCCTGGGATCAAAATC-3'
ZCF14	ZCF14f	5'-TCCGTCGACAAAGATGCCAATAACAAAAAAC-3'
	ZCF14r	5'-TCCGTCGACAATTTTTTCAATTGTGCCAA-3'
ZCF16	ZCF16f	5'-TCCGTCGACAAAGATGTCAAAGAAAAATAAAAAATCT-3'
	ZCF16r	5'-TCCGTCGACAAATATTGGGGACTTTGAGA-3'
ZCF17	ZCF17f	5'-TCCGTCGACAAAGATGACGAAAACTACAGTC-3'
	ZCF17r	5'-TCCGTCGACAATCTATTCAGCGAAAACAA-3'
ZCF21	ZCF21f	5'-TCCGTCGACAAAGATGATGGATATTTATCAG-3'
	ZCF21r	5'-TCCGTCGACAAAGTGATCAATTTGGAAAT-3'
ZCF22	ZCF22f	5'-TCCGTCGACAAAGATGTATTGTGGATACTAT-3'
	ZCF22r	5'-TCCGTCGACAAAAAGGCGACACTTTCGA-3'
ZCF23	ZCF23f	5'-TCCGTCGACAAAGATGACTAAAAAGTTAACT-3'
	ZCF23r	5'-TCCGTCGACAATACAATTGGCAAGAATTG-3'
ZCF24	ZCF24f	5'-TCCCTCGAGAAAGATGCCAATGAGAAATAGA-3'
	ZCF24r	5'-TCCCTCGAGAATATATCCAGCCATTTCTG-3'
ZCF28	ZCF28f	5'-TCCGTCGACAAAGATGAATCAAGATTCAACG-3'
	ZCF28r	5'-TCCGTCGACAAATTTATTCCTTCACGACC-3'
ZCF32	ZCF32f	5'-TCCGTCGACAAAGATGGAGGAAAAGAAGAAA-3'
	ZCF32r	5'-TCCGTCGACAACAACAATGTTAGATCAAC-3'
ZCF38	ZCF38f	5'-TCCCTCGAGAAAGATGTCAAATTCAACAACT-3'
	ZCF38r	5'-TCCCTCGAGTATGTTCATAGCATCATT-3'
ZCF39	ZCF39f	5'-TCCGTCGACAAAGATGTCTACCGATACAACT-3'
	ZCF39r	5'-TCCGTCGACAATGAAAATCTATTAAAATC-3'
ZPR1	ZPR1f	5'-TCCGTCGACAAAGATGTCTGAAGAAGGAGCTCATA-3'

Table 15 --- continued

	ZPR1r	5’-TCCGTCGACAAATCAGTTTTAATATCATTTAAACCTA-3’
19.1007	19.1007f	5’-TCCGTCGACAAAGATGGTGTTAATTGTAGTTGATGTA-3’
	19.1007r	5’-TCCGTCGACAACTCTGAAAGTCCTTCGTCTTCT-3’
19.1178	19.1178f	5’-TCCGTCGACAAAGATGAACGAATTGTTTGATGCTA-3’
	19.1178r	5’-TCCGTCGACAAACGACATAGATCAATCTCGA-3’
19.1757	19.1757f	5'-TCCGTCGACAAAGATGCAAAATACTAACCGT-3'
	19.1757r	5'-TCCGTCGACAAATTCTGTTGATATCCATA-3'
19.2260	19.2260f	5’-TCCGTCGACAAAGATGGATTTTGAAGAAGAGACTA-3’
	19.2260r	5’-TCCGTCGACAATGGTTCTTCTACAGTCTTGTTA-3’
19.2315	19.2315f	5’-TCCGTCGACAAAGATGGGAGATTACTTAAAC-3’
	19.2315r	5’-TCCGTCGACAAGATATTCTCAGTACTAGTACCT-3’
19.2393	19.2393f	5’-TCCCTCGAGAAAGATGTCTTCACAAGTTCCA-3’
	19.2393r	5’-TCCCTCGAGTAGAACTACATAATCTTC-3’
19.2399	19.2399f	5’-TCCGTCGACAAAGATGAAAACATGTTACTAT-3’
	19.2399r	5’-TCCGTCGACAATTTGCGTTTATTTTTCTT-3’
19.2458	19.2458f	5’-TCCGTCGACAAAGATGGGTAATGTACCAGCT-3’
	19.2458r	5’-TCCGTCGACAATTTTTTATTCTCTTTAT-3’
19.2612	19.2612f	5'-TCCGTCGACAAAGATGGTTAAACAGAAACAA-3'
	19.2612r	5'-TCCGTCGACAATGTATTTTCAGTGTTGTT-3'
19.2961	19.2961f	5'-TCCGTCGACAAAGATGAGCAATCCAAACGAA-3'
	19.2961r	5'-TCCGTCGACAAACCACGTAACAACTCTTC-3'
19.3088	19.3088f	5'-TCCCTCGAGAAAGATGGTATGTGCACATACT-3'
	19.3088r	5'-TCCCTCGAGAAAGCCAATGCTTTTCTTGA-3'
19.3407	19.3407f	5’-TCCGTCGACAAAGATGAACCTCAAAGATATTACC-3’
	19.3407r	5’-TCCGTCGACAAGTTACTCCGTGCTCTTGC-3’
19.3683	19.3683f	5’-TCCGTCGACAAAGATGTCCATTGATCCAGAAACT-3’
	19.3683r	5’-TCCGTCGACAAAAAGTCATCCCATTTATCATCA-3’
19.3928	19.3928f	5’-TCCGTCGACAAAGATGACCTTATCATCAAGA-3’
	19.3928r	5’-TCCGTCGACAAGAATGCCTCTCCTTTGGCTC-3’
19.4125	19.4125f	5'-TCCCTCGAGAAAGATGAGTGAAAGTGACGAA-3'
	19.4125r	5'-TCCCTCGAGAATCGAGAAATCACTGATGT-3'
19.4778	19.4778f	5’-TCCGTCGACAAAGATGTCTACTTCCAAGAGA-3’
	19.4778r	5’-TCCGTCGACAAGTAGGCAACATTATCGAT-3’

Table 15 --- continued

19.4972	19.4972f	5'-TCCGTCGACAAAGATGAATCTGAATTCTAAT-3'
	19.4972r	5'-TCCGTCGACAACAATGGTTTTTCATCACT-3'
19.4998	19.4998f	5’-TCCGTCGACAAAGATGACACCAAGTTCAACT-3’
	19.4998r	5’-TCCGTCGACAATAAACGAAATCCTTCTG-3’
19.5326	19.5326f	5'-TCCCTCGAGAAAGATGAGCATAGTAGACCAA-3'
	19.5326r	5'-TCCCTCGAGAATTTATTAAATTCAGGTAA-3'
19.5953	19.5953f	5’-TCCCTCGAGATGTTTAATACCAAGATA-3’
	19.5953r	5’-TCCCTCGAGATGAGTGGTATGCCCACG-3’
19.5975	19.5975f	5'-TCCCTCGAGAAAGATGTCTTTACCAATGTCA-3'
	19.5975r	5'-TCCCTCGAGAAACTGACCAACATATTA-3'
19.6781	19.6781f	5’-TCCGTCGACAAAGATGTCTAAAAGAAGAACG-3’
	19.6781r	5’-TCCGTCGACAAATTAACATCTAGTTCAGG-3’
19.684	19.684f	5’-TCCGTCGACAAAGATGACAGACATTTTGGAAGCAT-3’
	19.684r	5’-TCCGTCGACAAATCATCATTGTCCGCTGGTCTCT-3’
19.6845	19.6845f	5’-TCCGTCGACAAAGATGGGATTTATTAATCCAGGAA-3’
	19.6845r	5’-TCCGTCGACAAACCAAATCTATGTAGTATATCGT-3’
19.6888	19.6888f	5’-TCCCTCGAGATGGCAGCCAAGAAGGGA-3’
	19.6888r	5’-TCCCTCGAGTATGCATTGTAGTAAAGT-3’

Motif Elicitation by MEME Analysis

To identify common *cis*-acting DNA motifs, genes co-regulated in *C. albicans* by Cph1 or Tec1 and genes co-regulated in *S. cerevisiae* by Ste12 or Tec1, were analyzed (see Table 16). 1000 base pairs upstream of the translation start codon of the open reading frames of set of genes were subjected to MEME analysis to identify a putative consensus sequence (http://meme.sdsc.edu/meme/cgi-bin/meme.cgi). A stringency threshold E value less than 10^{-3} was used as previous described (Sahni *et al.*, 2009; Bailey *et al.*, 2006; Grundy *et al.*, 1997). Logos were prepared using Weblogo (http://weblogo.berkeley.edu/logo.cgi).

Northern Blot Hybridization

Northern blot hybridization was performed as described previously (Srikantha *et al*., 2006; Yi *et al*., 2008). The primers for synthesizing the probes are described in Table 17.

Hyperactivation of the MAP Kinase Pathway

Hyperactivation of the MAP kinase pathway was achieved by overexpression of the MAPKKK gene *STE11* in the **a**/**a** strain P37005 (Table 13), using the same strategy as that for construction of the overexpression library. Gene induction by doxycycline was confirmed by northern blot hybridization and fluorescence microscopy. The primer pairs used for generating the *STE11* ORF are described in Table 17.

Western Blot

The method for western blot analysis was previously described in detail (Yi *et al.*, 2009). In brief, *C. albicans* cells were harvested following 4 hours of α-pheromone treatment. Total protein was extracted and subjected to 8% SDS-polyacrylamide gel electrophoresis. The protein samples were then transferred to a PVDF membrane (Immobilon-P, Millipore Corporation, Bedford, MA). After blocking, the membrane was

Table 16. List of genes used for MEME analysis in the identification of the key transcription factor in the white response pathway

C. albicans WPRE	*S. cerevisiae* TCS	*C. albicans* OPRE	*S. cerevisiae* PRE
CSH1	*GSC2*	*MFA1*	*PRM1*
PBR1	*TIP1*	*FUS1*	*PRM3*
RBT5	*FLO11*	*CPH1*	*PRM6*
WH11	*CLN1*	*ECE1*	*FUS2*
TEC1	*TEC1*	*KAR4*	*CIK1*
EAP1	*PGU1*	*RAM1*	*PRM4*
PGA10	*SRL1*	*FGR23*	*AFR1*
LSP1	*CHS7*	*CAG1*	*AGA1*
PHR1	*PHD1*	*CEK1*	*SCW10*
PHR2	*CWP1*	*FIG1*	*ASG7*
SUN41	*FUS1*	*RBT4*	*FUS1*
Orf19.2077	*FUS3*	*HWP1*	*FUS3*
CIT1	*PRM2*	*ECE1*	*PRM2*
STE2	*PCL2*	*STE2*	*PCL2*
CEK2	*GIC2*	*CEK2*	*GIC2*
SST2	*SVS1*	*SST2*	*SVS1*
RBT1	*GFA1*	*RBT1*	*GFA1*

Table 17. Oligonucleotides used for mutant construction, northern and ChIP-PCR in the identification of the key transcription factor in the white response pathway

Primer	Gene/Purpose	Sequence
TEC1f1	*TEC1* heterozygote	5'-TGTGTCTTGTGGTTAAGT-3'
TEC1r1	*TEC1* heterozygote	5'-TCCCCCGGGACAAATGTGAGATTGCAA-3'
TEC1f2	*TEC1* heterozygote	5'-TCCCCCGGGACTTACTCACTGTTGGAT-3'
TEC1r2	*TEC1* heterozygote	5'-TGATGCATTGAACAAGCT -3'
TEC1f3	*TEC1* homozygote	5'-ATGATGTCGCAAGCTACT -3'
TEC1r3	*TEC1* homozygote	5'-TCCCCCGGGTTCTGAATTTCCCGGTTT-3'
TEC1f4	*TEC1* homozygote	5'-TCCCCCGGGGAAAGTGAAGGTGGTCTTA-3'
TEC1r4	*TEC1* homozygote	5'-AAACTCACTAGTAAATCCT -3'
TEC1Q1f	*TEC1* complementation	5'-TCCCCCGGGGAAAGTGAAGGTGGTCTTA-3'
TEC1Q1r	*TEC1* complementation	5'-TCCGGATCCAAACTCACTAGTAAATCCT-3'
TEC1Q2f	*TEC1* complementation	5'-TCCGGATCCACTTACTCACTGTTGGAT-3'
TEC1Q2r	*TEC1* complementation	5'- TGATGCATTGAACAAGCT-3'
SATBgF1	*GFP-SAT1* PCR	5'-TCAAGATCTTCCATCATAAAATGTCGA-3'
GFBhF1	*GFP-SAT1* PCR	5'-TCAGGATCCATGTCTAAAGGTGAAGAA-3'
TEC1nf	Northern probe	5'-ATGATGTCGCAAGCTACT-3'
TEC1nr	Northern probe	5'-AAAACTCACTAGTAAATCC-3'
CEK1nf	Northern probe	5'-CGTAGCTACAAGATGGTATAG-3'
CEK1nr	Northern probe	5'-TCGTACCGCCAGTATTACTAG-3'
CEK2nf	Northern probe	5'-GGGCTGTATATTGGCTGAACT-3'
CEK2nr	Northern probe	5'-TCTAATGCGTCTTGAACGGTG-3'
CSH1nf	Northern probe	5'-TCGACTCTGAAAAAACTA-3'
CSH1nr	Northern probe	5'-CATGCCAATGAAACTTGC-3'
PBR1nf	Northern probe	5'-AATGTGACTTTATACATT-3'
PBR1nr	Northern probe	5'-CAGCATATAAGTAATCAT-3'
RBT5nf	Northern probe	5'-TGATGCCGCTGCTGAAAC-3'
RBT5nr	Northern probe	5'-ACAGCGGCAATGACACCA-3'
WH11nf	Northern probe	5'-ATGTCCGACTTAGGTAGA-3'
WH11nr	Northern probe	5'-TTATTTGGAGTCACCAAA-3'
KAR4nf	Northern probe	5'-ATGTATACTTACAATAAGTTTGGG-3'

Table 17 --- continued

KAR4nr	Northern probe	5'-TACCTCTGTAGCACCAGA-3'
MFA1nf	Northern probe	5'-ATGGCTGCTCAACAACAA-3'
MFA1nr	Northern probe	5'-TTACATAACAGAACAAGT-3'
STE2nf	Northern probe	5'-GTGTTCAACATAAGAAGA-3'
STE2nr	Northern probe	5'-ATTATTAGCAGTTTGAGC-3'
RBT1nf	Northern probe	5'-AGCCACTGAATCAGTTCC-3'
RBT1nr	Northern probe	5'-ATCAAGAATGCAGCAATACC-3'
ACT1nf	Northern probe	5'-TTGGTGTTTGACGAGTTT-3'
ACT1nr	Northern probe	5'-TACCGTGTTCAATTGGGTAT-3'
STE11f	MAPK hyperactivation	5'-TCCGTCGACAAAGATGACAGAGATTAATGATT-3'
STE11r	MAPK hyperactivation	5'-TCCGTCGACAATTGTTTCGACATAATTAATG-3'
TEC1mycf1	TEC1-myc	5’- TCCCCCGGGGAAAGTGAAGGTGGTCTTA-3'
TEC1mycr1	TEC1-myc	5’-TCCTCTAGAAAAGTGAAGGTGGTCTTA-3’
TEC1mycf2	TEC1-myc	5’-TCCTCTAGAACTTACTCACTGTTGGAT-3’
TEC1mycr2	TEC1-myc	5’- TGATGCATTGAACAAGCT-3’
PBR1chpf	ChIP-PCR	5’-TATCGCTCATACAATGATT-3’
PBR1chpr	ChIP-PCR	5’-TTTCAAGGAAGGAATGGA-3’
CSH1chpf	ChIP-PCR	5’-AGAGAACATTCAAGCTTG-3’
CSH1chpr	ChIP-PCR	5’-AGCAAAAACAGGCAGTAT-3’
RBT5chpf	ChIP-PCR	5’-AAGCCAAGCTGCATAAGTAT-3’
RBT5chpr	ChIP-PCR	5’-TGCCTATGTATTTATACCCT-3’
WH11chpf	ChIP-PCR	5’-TGTGGCACTTGATTTCTAGT-3’
WH11chpr	ChIP-PCR	5’-TTTAATTGTTCTGTTTGTTGTT-3’
STE2chpf	ChIP-PCR	5’-TACCCGTTTGATATTCAATT-3’
STE2chpr	ChIP-PCR	5’-AGTAAATCGTTTGGTGACGA-3’
RBT1chpf	ChIP-PCR	5’-TTGGGACCACGGTCATTCAA-3’
RBT1chpr	ChIP-PCR	5’-AACACGCCTTATAATGACAA-3’
ACT1chpf	ChIP-PCR	5’-TATTAAGTAGTGTGTGCACT-3’
ACT1chpr	ChIP-PCR	5’-TTGGCAATAAATCTTGGTGA-3’
TEC1chpf	ChIP-PCR	5’-TTCTCATTGCCTTAGTCA-3’
TEC1chpf	ChIP-PCR	5’-AATTAAGGGAAGTCAAGGT-3’
KAR4chpf	ChIP-PCR	5’-TTAGGGCGTTTCAGTGTTGT-3’
KAR4chpr	ChIP-PCR	5’-TGTTTCAAATATTTGGTGTTC-3’

Table 17 --- continued

MFA1chpf	ChIP-PCR	5’-TGTAGAGAACGTAAAGAGCT-3’
MFA1chpr	ChIP-PCR	5’-TATGCTCTATTTTTCGCAATT-3’

incubated first with rabbit anti-GFP antibody (SC-8334, Santa Cruz Technology, Santa Cruz, CA), and then incubated with horseradish peroxidase-labelled goat anti-rabbit IgG (Promega, Madison, WI). Finally, the protein signal on the membrane was detected with SuperSignal West Pico Chemiluminescent Substrate (Pierce, Rockford, IL) and exposed to autoradiographic film (Eastman Kodak, Rochester, NY).

Generation of Homozygous Deletion Mutants and Complemented Strains

The recyclable cassette SAT1-2A harboring the marker SAT^r was used for generating the mutant strains. The plasmid pSFS2A was also a generous gift from Joachim Morschhäuser. To generate the homozygous deletion mutant of *TEC1*, a two step PCR disruption strategy was used. For the first deletion cassette, the 5' and 3' flanking regions of *TEC1* were amplified by PCR using the primer pairs listed in Table 17. The 5' and 3' regions were then digested with SmaI and ligated using T4 ligase. The 5'-3' ligation product was then amplified by PCR and cloned into the pGEM-T Easy vector (Promega, Madison, WI), yielding the plasmid pTEC1-T1. SAT1-2A was then ligated into the SmaI digested, dephosphorylated plasmid pTEC1-T1, yielding pTEC1-T1-2A. This plasmid was digested with SacI plus SacII, and transformed into the wild type strain P37005 by electroporation (De Backer *et al.*, 1999). The transformants were confirmed as heterozygous by both PCR and southern analysis. The heterozygotes were then to grown in YPM medium (Yi *et al.*, 2008, 2009) to excise the SAT^r marker. The second deletion cassette was generated similarly with primer pairs listed in Table 17, and was used to transform the heterozygous mutants, deriving homozygotes. The homozygous deletion mutants were verified by both PCR and southern analysis.

For generating a *TEC1*-complemented strain, the 5' and 3' regions flanking the stop codon were amplified by PCR using the primers listed in Table 17. The 5'-3' fusion product was then amplified by PCR and subcloned into pGEM-T Easy (Promega). The DNA

fragment *GFP-CaSAT1* was amplified by PCR from the plasmid pK91.6 (Yi *et al.*, 2008), digested with BamHI plus BglII, and ligated into the BamHI-cut, dephosphorylated plasmid containing the 5'-3' ligation product, yielding the plasmid pTEC1-comp. The *TEC1-GFP* in-frame fusion was verified by sequencing. Finally, the plasmid pTEC1-comp was digested with SacI plus SacII, and transformed into *tec1/tec1* to generate *tec1/tec1-TEC1*, which was verified by both PCR and Southern analysis.

Generation of *MYC*-tagged Strains and ChIP-PCR Analysis

To generate a *MYC*-tagged *TEC1* strain, the 5' and 3' regions flanking the stop codon of the *TEC1* gene were amplified by PCR, using the primers listed in Table 17. The 5' and 3' regions were then digested with XbaI and ligated using T4 ligase. The ligation product was cloned into the pGEM-T Easy vector (Promega, Madison, WI), yielding pTEC1-T. A DNA fragment harboring a 13 × Myc epitope tag and a dominant nourseothricin marker SAT^r, was amplified by PCR using primers listed in Table 17 and the plasmid p13myc-natMX as the template (Borneman *et al.*, 2007). This fragment was cloned into the XbaI-cut, dephosphorylated plasmid pTEC1-T, yielding pTEC1-myc. This plasmid was verified by sequencing for correct in-frame fusion and the number of Myc units, and by western blot analysis for expected molecular weight and protein expression levels. The plasmid pTEC1-myc was then linearized, digested with SacI and SacII, and transformed into the heterozygous deletion mutant of *TEC1*, generating the *MYC*-tagged *TEC1* strain. This *MYC*-tagged strain behaved similarly to its parental wild-type strain under all experimental conditions.

To test whether the Myc-tagged Tec1 protein complex bound to a specific DNA target, a chromatin immunoprecipitation (ChIP)-PCR analysis was performed. The myc-tagged Tec1 strain and control strains were grown to saturation phase. Cells were resuspended in fresh liquid Lee's medium at a concentration of 5×10^7/ml, and incubated in the presence or absence of α-pheromone at 25°C for 4 hr, with a final OD_{600} of 0.6-1.0. The

cultures were then fixed to crosslink the protein-DNA complexes in cells by adding formaldehyde at a final concentration of 1%, and incubated in a slow shaker for 15 minutes. Glycine was then added to quench crosslinks at a concentration of 125 mM followed by incubating for five minutes. The cells were harvested by centrifugation at 4°C for 10 minutes at 4000 rpm. The pellets were then washed twice in ice cold 1X TBS (20 mM Tris-HCl, 150 mM NaCl, pH 7.6) prior to lysis. Cell lysis was done by resuspending the pellet in ice-cold lysis buffer (0.1% deoxycholic acid, 1 mM EDTA, 50 mM HEPES/KOH, pH 7.5, 140 mM NaCl, 1% Triton X-100) with protease inhibitors cocktail (Sigma-Aldrich, St. Louis, MO) and 1 mM phenylmethylsulphonyl fluoride (PMSF). Zirconium beads were added to the cell pellets and the cells were lysed by bead beating 7-8 times using Mini Beadbeater-8 (BioSpec Products Inc., Bartlesville, OK), 2 minutes each. Between the bead beatings, the cells were incubated on ice for one minute. The lysate was collected by centrifugation at 4°C for 10 minutes at 4000 rpm.

In the lysate, the chromatin was sheared by sonication in Vibra Cell sonicator (Sonics & Materials Inc., Newtown, CT) (amplitude 20%) 9 times, 10 seconds each. In between sonication pulses, the cells were incubated on ice for one minute. The sheared chromatin averaged 500 to 800 bp in length. 50 µl of extract was stored at -20°C as the ChIP "Input" material. For chromatin IPs, the rest of the cell extract was pre-cleared by incubation with protein G sepharose beads (Active Motif, Carlsbad, CA) for 2 hr at 4°C, and then mixed with anti-c-myc antibody coupled EZview red beads (E6654**,** Sigma-Aldrich, St. Louis, MO) and incubated on a rotating platform overnight at 4°C. The following day, the beads were washed at room temperature first in lysis buffer, next in high salt lysis buffer (0.1% deoxycholic acid, 1 mM EDTA, 50 mM HEPES/KOH, pH 7.5, 500 mM NaCl, 1% Triton X-100) , then in wash buffer (0.5% deoxycholic acid, 1 mM EDTA, 10 mM Tris-HCl, pH 8.0, 250 mM LiCl, 0.5% NP-40, 0.5% sodium deoxycholate) and last in 1X TBS. Finally the immunoprecipitates were eluted by adding 25µl of elution buffer (50 mM Tris/HCl, pH 8.0, 10 mM EDTA, 1% SDS) and incubating at 65°C for 10

min. The beads were spun for 1 minute at 10,000*g* at room temperature. A second elution was done by adding 25µl of elution buffer 2 (50 mM Tris/HCl, pH 8.0, 10 mM EDTA, 0.67% SDS). Both the ChIP and the input samples were incubated overnight at 65°C to reverse the crosslinks. To further remove the proteins, the samples were treated with proteinase K at 37°C for 2h. The DNA was finally purified using the PCR purification kit (QIAGEN, Valencia, CA) and used as PCR template. Primers were designed for the promoter region of each tested gene (Table 17). The immunoprecipitated DNA was amplified by PCR under the following thermalcycling conditions: 95°C for 5 min, 30 cycles of 25 sec at 94°C, 30 sec at 50°C, 25 sec at 72°C, followed by a 7-min extension time at 72°C. Input DNA from sonicated lysate was amplified in parallel. The PCR products were subjected to a 0.8% agarose gel electrophoresis and visualized by ethidium bromide staining. The Tec1-binding sites in different species are summarized in Table 18.

Visualization of *GFP*-tagged Proteins

For *GFP* visualization, white and opaque cells of the *TEC1* complemented strain, which harbored a *GFP*-tagged Tec1, were grown for 48 hours in modified Lee's medium (Bedell and Soll, 1979). The cells were pelleted and resuspended in fresh medium, treated with 3×10^{-6} M synthetic α-pheromone for 4 hours, and then fixed in 1% formaldehyde in Dulbecco's phosphate buffered saline (Gibco, Grand Island, WY). Nuclei were counter-stained for DNA with DAPI. The untagged strain P37005 was included in this analysis as a negative control. Fluorescence was visualized through a Nikon TE2000 microscope attached to a Bio-Rad MP2100 laser scanning confocal microscope equipped with a Mai-Tai infrared laser (Spectra Physics, Mountain View, CA). Sequential images of *GFP*, DAPI and transmitted light were acquired.

Table 18. *cis*-acting DNA motifs bound by Tec1 homologs in different species

Tec1 homologs	Organism	Target gene	Motif sequence	References
Tec1	*Candida albicans*	*PHR2*	AAAAAAAAAAGAAAG	Sahni *et al.* (2009b)
		RBT1	AGAAAAAACAGAAAG	Sahni *et al.* (2009b)
		Consensus:	AAAAAAAAAAGAAAG	Sahni *et al.* (2009b)
Tec1	*Saccharomyces cerevisiae*	*SRL3*	AGAATG	Chou *et al.* (2006)
		SVS1	AGAATG	Chou *et al.* (2006)
		Consensus:	AGAATG	Baur *et al.* (1997) Madhani and Fink (1997)
AbaA	*Aspergillus nidulans*	*rodA* variant 1	GGTATG	Andrianopoulos and Timberlake (1994)
		rodA variant 2	AGAATT	Andrianopoulos and Timberlake (1994)
		Consensus:	$A_{/G}$GAATG	Andrianopoulos and Timberlake (1994)
TEF-1	*Homo sapiens*	GT-IIC	GGAATG	Davidson *et al.* (1988)
		Polyomavirus wild type	AGAATG	Davidson *et al.* (1988)
		Consensus:	$A_{/G}$GAATG	Davidson *et al.* (1988); Hwang *et al.* (1993)

Shmoo and Mating Analyses

The methods for assaying shmoo formation in response to 3×10^{-6} M synthetic α-pheromone, and mating with opaque cells of the α/α strain WO-1 have been described previously in detail (Daniels *et al.*, 2006; Yi *et al*., 2008).

Quantitation of Biofilm Formation

White cell biofilm formation was assessed after 48 hours of incubation on silicone elastomer squares in RPMI medium, according to the methods of Daniels *et al.* (2006). Biofilm enhancement by minority opaque cells was assessed by adding 5% opaque **a**/**a** P37005 cells and 5% opaque α/α WO-1 cells. Biofilm matrix formation was quantitated by measuring the concentration of (1,3)-β-glucan in the biofilm supernatant, according to the methods previously described in detail (Nobile *et al*., 2009; Sahni *et al*., 2009b).

The biofilm was fixed by addition of 10% formaldehyde to the culture, rinsed with PBS and stained with calcofluor (Fluorescent Brightener 28, Sigma, St. Louis) in 0.1 M Tris pH 9.0 and imaged as above. Calcofluor was excited at 818 nm. Using BioRad LaserSharp™ software, an initial x-y optical section was gathered at the biofilm-substrate interface. Thickness of the biofilm in the same field was determined by a 125 μm Z-series 2.0 μm steps. The characteristics of the biofilm (matrix, hyphae, etc.) were determined by scrolling through the Z-series. A singe Z-X slice through the Z-series was then digitally acquired.

Results

Generating an Overexpression Library for Transcription Factors

Our strategy to identify the transcription factor targeted by the MAP kinase pathway involved a screen, in which overexpression strains were tested for the white cell response in the absence of pheromone. To accomplish this, we first identified 106 putative

transcription factor genes involved in biofilm formation, adhesion, filamentation, cell wall integrity, membrane biogenesis, drug resistance, stress responses, metabolism and some which had no known function (Table 14). Each gene was synthesized by the polymerase chain reaction using the primers listed in Table 15, verified by sequencing and inserted into the expression site of the plasmid pNIM1 under control of the tetracycline (doxycycline)-inducible promoter of the gene *N1M1* (Park and Morschhauser, 2005), which we will refer to as *TETp*. Each transcription factor gene was fused in frame at the 3' end with the GFP ORF. Each of the 106 plasmids were then used to transform the natural **a**/**a** strain P37005 by integration at the *ADH1* locus, generating an overexpression library for the 106 transcription factors (Table 15).

Screen for the White-specific Pheromone-induced Transcription Factor

The 106 overexpression strains were each tested for increased adhesion to a plastic surface in the absence of α-pheromone after treatment with 100 μg per ml of doxycycline. To obtain a measure of maximal induction, white cells of the parental control strain P37005 were analyzed in the absence and presence of α-pheromone. Adhesion was negligible ($<10^6$ cells per well bottom) in the absence and maximal ($>10^8$ cells per well bottom) in the presence of α-pheromone. In the absence of α-pheromone, doxycycline induced adhesion in only one of the 106 overexpression strains, and did so to the same extent as α-pheromone did in control cells (Figure 50A). That single strain overexpressed the gene *TEC1*. Adhesion to the well bottom of doxycycline-induced cells in that strain is compared to that of α-pheromone-induced P37005 cells in Figure 50B. *TEC1* has been shown to be involved in filamentation in *S. cerevisiae* (Oehlen and Cross, 1998; Chou *et al.*, 2006) and *C. albicans* (Schweizer *et al.*, 2000), and in hypha formation in *C. albicans* **a**/α biofilms (Nobile and Mitchell, 2005).

Figure 50. Screen of a transcription factor overexpression library for white response regulators in *C. albicans*. A screen of an overexpression library of 106 putative transcription factor genes of *Candida albicans* revealed that overexpression of only one gene, *TEC1*, in the absence of α-pheromone, induced a higher than 100 fold increase in adhesion similar to that induced by α-pheromone. The overexpression strains each contained a different transcription factor gene under the regulation of the tetracycline promoter, which is induced by adding 100 μg per ml of doxycycline (Park and Morschhauser, 2005; Yi *et al*., 2009; Sahni *et al*., 2009b). Adhesion was measured as the number of cells adhering to the plastic well bottom. The strains are named only by the gene overexpressed, but the full strain names and genotypes can be found in supplemental table S2. A. Number of adherent cells per well bottom for the 106 strains in the presence of doxycycline and absence of α-pheromone. The levels in the untransformed control strain P37005 are presented both in the absence and presence of α-pheromone. B. Examples of adhesion of P37005 and the overexpression P37005-TET*p-TEC1*. C. A comparison of the sequences believed to be the *cis*-acting sequences interacting with Tec1 in *C. albicans* and *S. cerevisiae*, WPRE and TCS, respectively, and Cph1 and the homolog Ste12 in *C. albicans* and *S. cerevisiae*, OPRE and PRE, respectively. D. Homology of the Tec1 DNA-binding domains for *C. albicans* and *S. cerevisiae*.

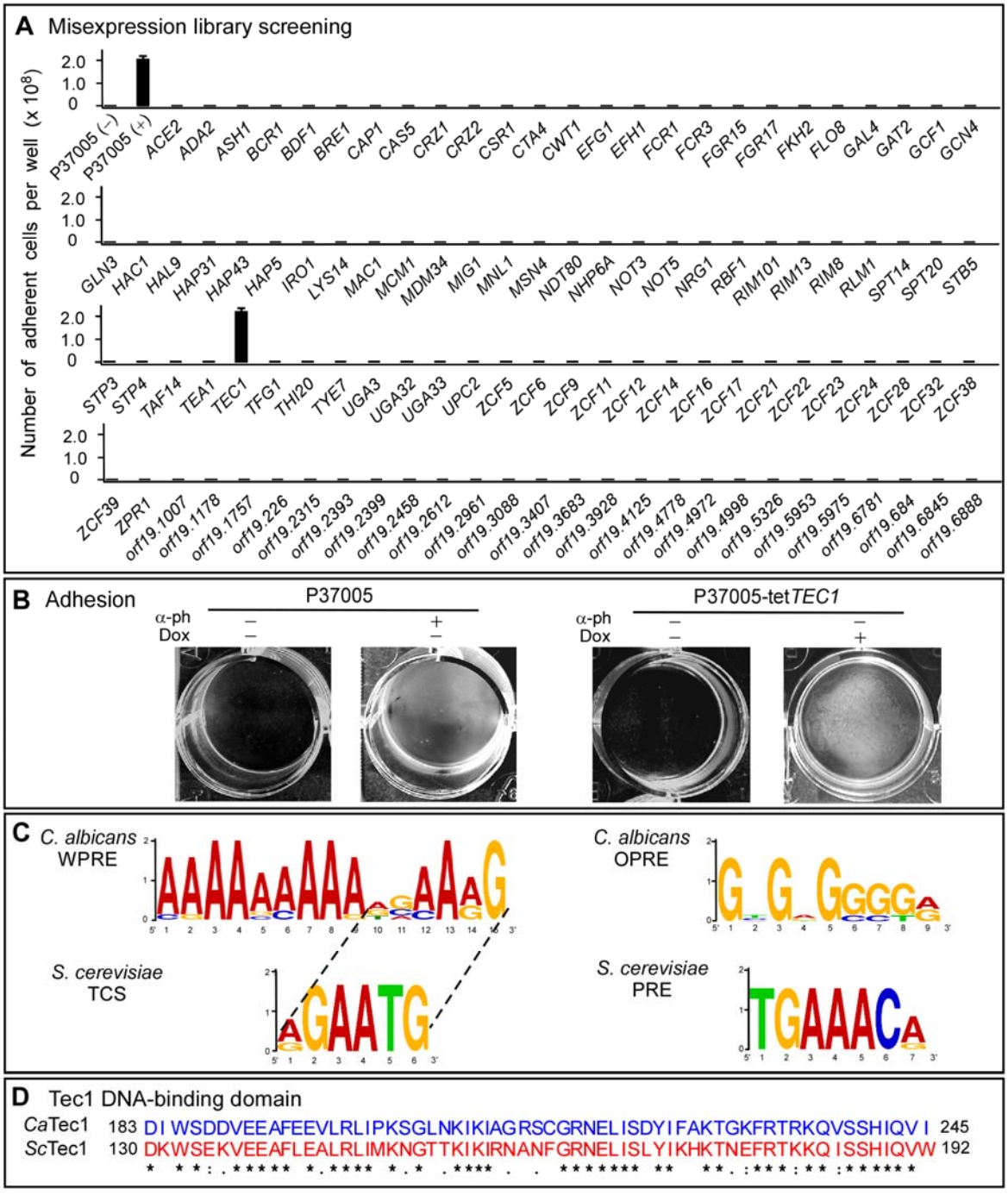
A Misexpression library screening
Number of adherent cells per well (x 10^8)
2.0
1.0
0
P37005 (–)
P37005 (+)
ACE2 ADA2 ASH1 BCR1 BDF1 BRE1 CAP1 CAS5 CRZ1 CRZ2 CSR1 CTA4 CWT1 EFG1 EFH1 FCR1 FCR3 FGR15 FGR17 FKH2 FLO8 GAL4 GAT2 GCF1 GCN4
GLN3 HAC1 HAL9 HAP31 HAP43 HAP5 IRO1 LYS14 MAC1 MCM1 MDM34 MIG1 MNL1 MSN4 NDT80 NHP6A NOT3 NOT5 NRG1 RBF1 RIM101 RIM13 RIM8 RLM1 SPT14 SPT20 STB5
STP3 STP4 TAF14 TEA1 TEC1 TFG1 THI20 TYE7 UGA3 UGA32 UGA33 UPC2 ZCF5 ZCF6 ZCF9 ZCF11 ZCF12 ZCF14 ZCF16 ZCF17 ZCF21 ZCF22 ZCF23 ZCF24 ZCF28 ZCF32 ZCF38
ZCF39 ZPR1 orf19.1007 orf19.1178 orf19.1757 orf19.226 orf19.2315 orf19.2393 orf19.2399 orf19.2458 orf19.2612 orf19.2961 orf19.3088 orf19.3407 orf19.3683 orf19.3928 orf19.4125 orf19.4778 orf19.4972 orf19.4998 orf19.5326 orf19.5953 orf19.5975 orf19.6781 orf19.684 orf19.6845 orf19.6888
B Adhesion
P37005
P37005-tetTEC1
α-ph
Dox
C C. albicans WPRE
C. albicans OPRE
S. cerevisiae TCS
S. cerevisiae PRE
D Tec1 DNA-binding domain
CaTec1 183 DIWSDDVEEAFEEVLRLIPKSGLNKIKIAGRSCGRNELISDYIFAKTGKFRTRKQVSSHIQVI 245
ScTec1 130 DKWSEKVEEAFLEALRLIMKNGTTKIKIRNANFGRNELISLYIKHKTNEFRTKKQISSHIQVW 192

In *S. cerevisiae*, Tec1 binds to an AT-rich element, TCS, in the promoters of Tec1-regulated genes (Figure 50C) (Madhani and Fink, 1997; Baur *et al*., 1997). In *C. albicans*, WPRE, the presumed Tec1 binding site, is also AT-rich, in contrast to the presumed Cph1 binding site, which is GC-rich (Figure 50C) (Sahni *et al.*, 2009b). The WPRE consensus sequence contains a six base region that is homologous to the six bases that make up TCS (Figure 50C). The DNA binding domain of Tec1 in *S. cerevisiae* is 413 amino acids in length (aa 74 to 486), whereas the DNA binding domain of Tec1 in *C. albicans* is 63 amino acids in length (aa 183 to 245). The *C. albicans* binding domain, however, shows strong homology (60% identity, 84% similarity) to a subdomain of the *S. cerevisiae* binding domain between amino acids 130 and 192 (Figure 50D).

Regulation of *TEC1*

To test whether *TEC1* expression was regulated by α-pheromone and the MAP kinase pathway, a northern analysis was performed to assess its expression in deletion mutants of key elements in the signal transduction pathway in the absence and presence of α-pheromone. In white cells of the control strain P37005, *TEC1* was expressed at a basal level in the absence of α-pheromone, and at an elevated level in the presence of α-pheromone (Figure 51A). In opaque cells of P37005, *TEC1* was expressed at the basal level in the absence and presence of α-pheromone, demonstrating that unlike white cells, α-pheromone did not up-regulate *TEC1* transcription in opaque cells (Figure 51A). In white cells of the deletion mutants of *STE2*, which encodes the α-pheromone receptor, *STE4*, which encodes the beta subunit of the trimeric G protein complex, and the double mutant for *CEK1* and *CEK2*, α-pheromone did not up-regulate *TEC1* (Figure 51A). In addition, when Ste11, a component of the MAP kinase pathway was overexpressed in white cells of strain P37005-TET*p*-*STE11* in the absence of α-pheromone, adhesion increased by over 100 fold (Figure 51B) and *TEC1* transcription was up-regulated (Figure 51C). Overexpression of *STE11* in the absence of α-pheromone also resulted in the

Figure 51. Up-regulation of *TEC1* by α-pheromone requires, the α-pheromone receptor, trimeric G protein complex and MAP kinase cascade. A. Northern analysis of pheromone (α-ph) induction of *TEC1* in P37005 white (Wh) and opaque (Op) cells, and in white cells of the mutants *ste2/ste2*, *ste4/ste4* and *cek1/cek1 cek2/cek2*. B. Overexpression of *STE11* induces adhesion in the absence of α-pheromone. Overexpression was induced in white cells by 100 μg per ml of doxycycline (Dox) in the overexpression strain P37005-TET*p-STE11*. C. Overexpression of *STE11* in the absence of α-pheromone activates genes in the white response pathway in strain P37005-TET*p-STE11* with 100 μg per ml doxycycline. D. Western blot analysis of Tec1-GFP using anti-GFP antibody in strain *tec1/tec1-TEC1* in which *TEC1* is tagged with GFP.

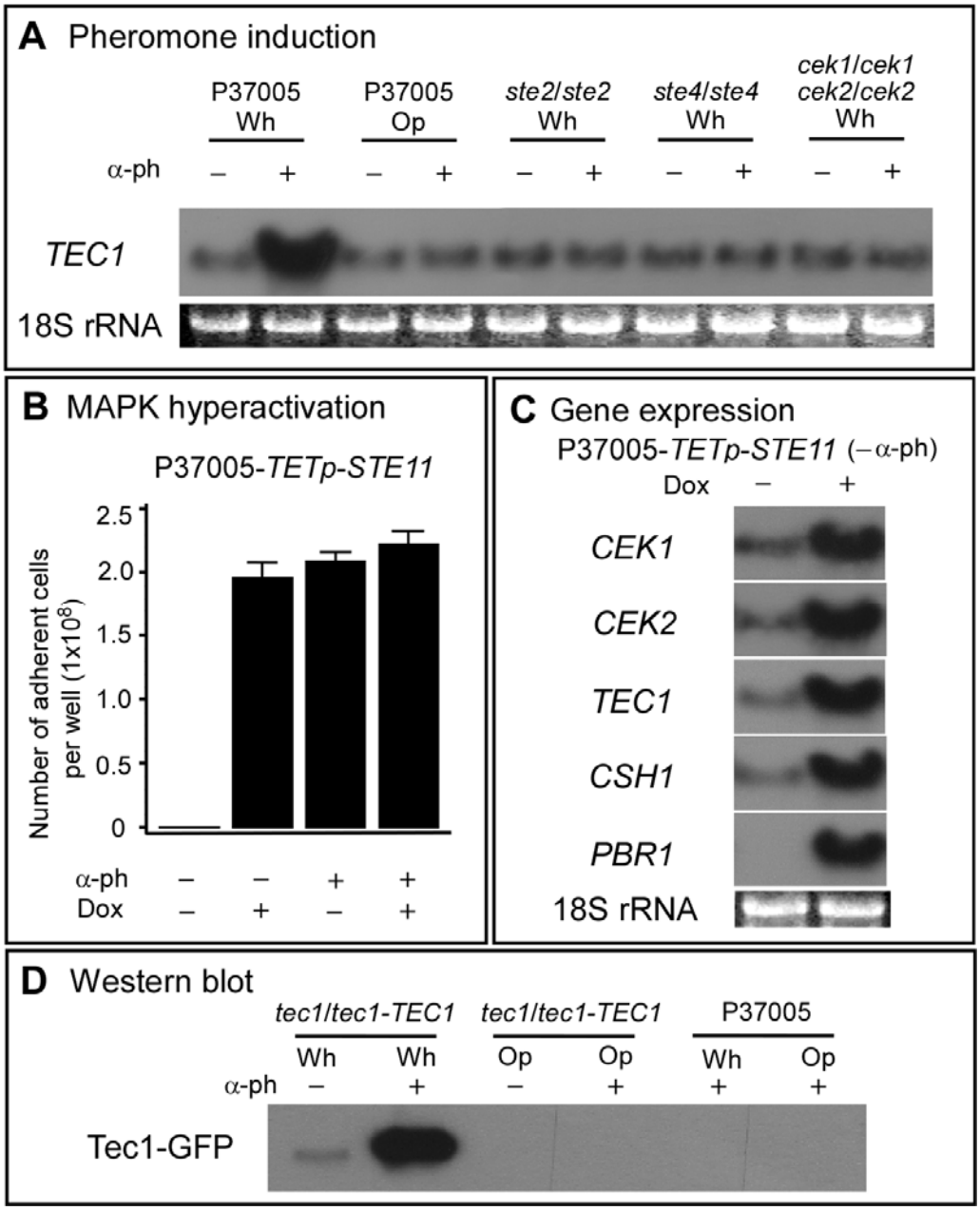
A Pheromone induction
P37005 Wh
P37005 Op
ste2/ste2 Wh
ste4/ste4 Wh
cek1/cek1 cek2/cek2 Wh
α-ph – + – + – + – + – +
TEC1
18S rRNA
B MAPK hyperactivation
P37005-TETp-STE11
Number of adherent cells per well (1x10^8)
2.5
2.0
1.5
1.0
0.5
0
α-ph – – + +
Dox – + – +
C Gene expression
P37005-TETp-STE11 (–α-ph)
Dox – +
CEK1
CEK2
TEC1
CSH1
PBR1
18S rRNA
D Western blot
tec1/tec1-TEC1
tec1/tec1-TEC1
P37005
Wh Wh Op Op Wh Op
α-ph – + – + + +
Tec1-GFP

up-regulation of *CEK1*, *CEK2*, *CSH1* and *PBR1* (Figure 51C), genes previously shown to be up-regulated by α-pheromone through the MAP kinase pathway (Yi *et al.*, 2008; Sahni *et al.*, 2009b).

To demonstrate that the protein product of *TEC1*, in addition to the transcript, was selectively up-regulated by α-pheromone in white but not opaque cells, we analyzed the level of Tec1-GFP in the strain *tec1/tec1-TEC1* in which *TEC1*-GFP had been inserted at its native site under the control of its own promoter (Table 17). The level of Tec1 was assessed by western blot analysis, using anti-GFP antibody. In the absence of α-pheromone, the basal level of Tec1 in white cells of strain *tec1/tec1-TEC1* was extremely low, it was more than 100 fold higher in the presence of α-pheromone (Figure 51D). In the absence and presence of α-pheromone in opaque cells, the level of Tec1-GFP was negligible (Figure 51D). Together, these results demonstrate that *TEC1* is selectively up-regulated by α-pheromone at the RNA and protein levels through the MAP kinase pathway in white cells, but not in opaque cells.

Tec1 Regulation of Downstream Genes

To demonstrate that Tec1 regulated the expression of genes that had previously been shown to be up-regulated by α-pheromone in white cells. We tested the effects of *TEC1* overexpression in the absence of α-pheromone in strain P37005-TETp-*TEC1* (Table 15). When *TEC1* was overexpressed in white cells of P37005-TET*p-TEC1* in the absence of α-pheromone, there was an increase in adhesion equivalent to that induced by α-pheromone (Figure 52A). Overexpression of *TEC1* in white cells of strain P37005-TET*p-TEC1* in the absence of α-pheromone also up-regulated the white-specific genes *CSH1*, *PBR1*, *RBT5* and *WH11* (Yi *et al*., 2008; Sahni *et al*., 2009b) but not the opaque-specific genes *KAR4* and *MFA1* (Bennett and Johnson, 2006; Yi *et al*., 2008; Sahni *et al*., 2009b) (Figure 52B). The genes *STE2* and *RBT1*, which are up-regulated by α-pheromone in both white and opaque cells (Daniels *et al*., 2006; Sahni *et al*., 2009b),

Figure 52. Overexpression of *TEC1* in the absence of α-pheromone results in an increase in adhesion and in up-regulation of genes that had been shown to be pheromone-induced. A. Adhesion in white cells of *TEC1* overexpressors generated in P37005, *ste2/ste2*, *ste4/ste4*, *cek1/cek1 cek2/cek2* and *tec1/tec1-TEC1* in different combinations of α-pheromone (α-ph) and doxycycline (Dox). B. Northern analysis of gene expression upon overexpression of *TEC1* in strain P37005-TET*p-TEC1*. C. Northern analysis of *TEC1* expression when the target genes *CSH1*, *PBR1*, or *WH11* are overexpressed in strains P37005-*TETp-CSH1*, P37005-*TETp-PBR1* and P37005-*TETp-WH11*. D. Northern analysis of *TEC1* expression in the target gene deletion mutants *csh1/csh1*, *pbr1/pbr1* and *wh11/wh11* and the receptor deletion mutant *ste2/ste2*.

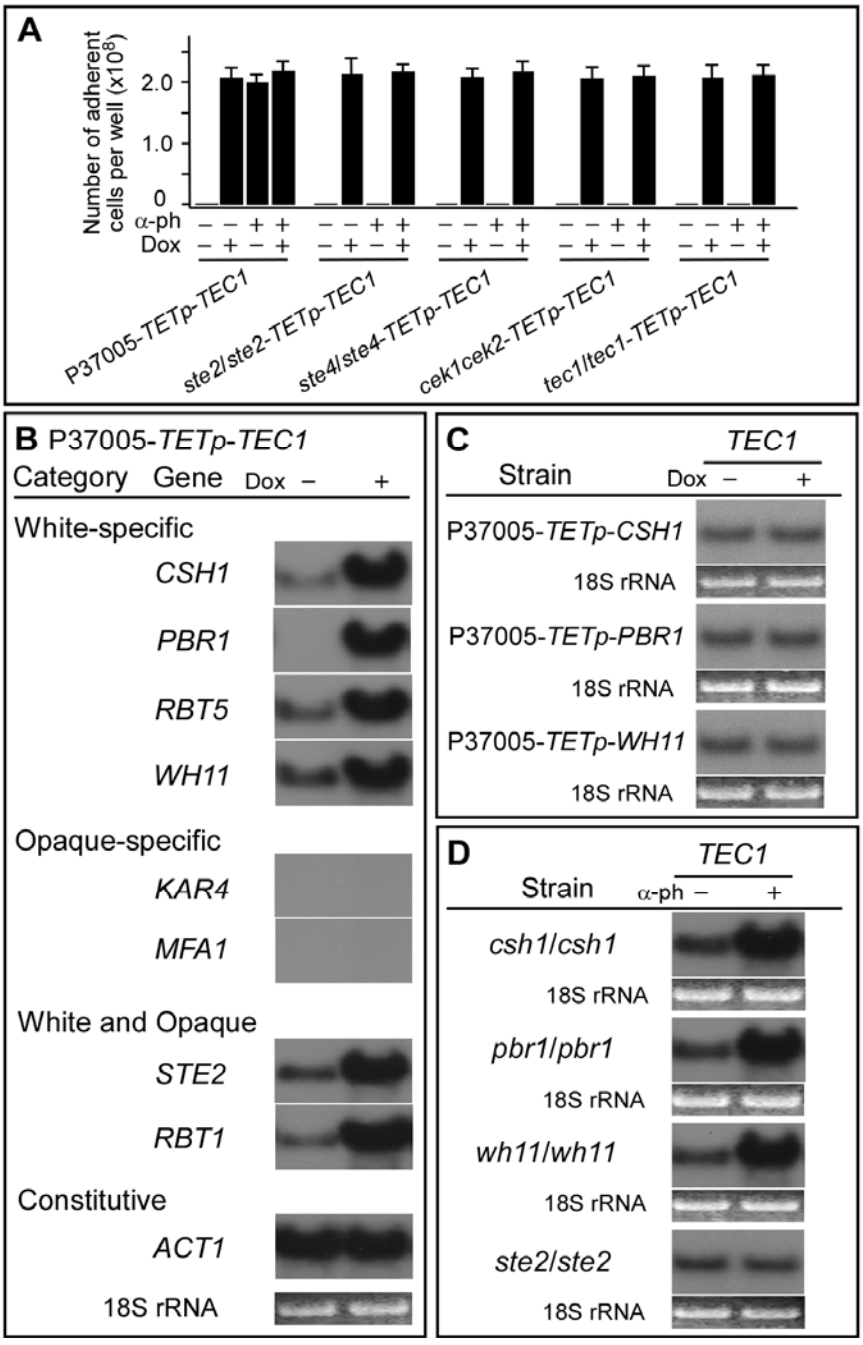
A
Number of adherent cells per well (x10^8)
2.0
1.0
0
α-ph
Dox
P37005-TETp-TEC1
ste2/ste2-TETp-TEC1
ste4/ste4-TETp-TEC1
cek1cek2-TETp-TEC1
tec1/tec1-TETp-TEC1
B P37005-TETp-TEC1
Category Gene Dox – +
White-specific
CSH1
PBR1
RBT5
WH11
Opaque-specific
KAR4
MFA1
White and Opaque
STE2
RBT1
Constitutive
ACT1
18S rRNA
C
TEC1
Strain Dox – +
P37005-TETp-CSH1
18S rRNA
P37005-TETp-PBR1
18S rRNA
P37005-TETp-WH11
18S rRNA
D
TEC1
Strain α-ph – +
csh1/csh1
18S rRNA
pbr1/pbr1
18S rRNA
wh11/wh11
18S rRNA
ste2/ste2
18S rRNA

were also up-regulated when *TEC1* was overexpressed in the absence of α-pheromone (Figure 52B). When *TEC1* was overexpressed in the mutants *ste2/ste2*-TET*p-TEC1*, *ste4/ste4*-TET*p-TEC1*, *cek1/cek1cek2/cek2*-TET*p-TEC1*, in the absence of α-pheromone, adhesion increased as it did in control cells in response to α-pheromone (Figure 52A). These results demonstrated that Tec1 mediates the induction of downstream white-specific gene expression by α-pheromone, and does so downstream of the trimeric G protein complex and MAP kinase pathway.

To test whether the downstream genes that were regulated by Tec1 in turn were involved in up-regulating *TEC1*, we analyzed *TEC1* expression in the strains P37005-TET*p-CSH1*, P37005-TET*p-PBR1* and P37005-TET*p-WH11*. When these downstream genes were overexpressed in the absence of α-pheromone, the *TEC1* transcript remained at basal level (Figure 52C). In addition, when *CSH1*, *PBR1* and *WH11* were deleted, *TEC1* expression was still up-regulated by α-pheromone (Figure 52D). Together these results demonstrated that Tec1 functions downstream of the MAP kinase pathway, but up-stream of the target genes regulated by α-pheromone, and that the target genes play no role in α-pheromone-induced regulation of *TEC1* expression.

Tec1 Binds Target Gene Promoters

Since the transcription factor Tec1 mediates α-pheromone-induced expression of genes in white cells, and WPRE represents the *cis*-acting regulatory sequence in promoters of white-specific genes that mediates up-regulation, we tested whether there was a direct interaction between Tec1 and the promoters of these select genes using a chromatin immunoprecipitation PCR (ChIP-PCR) assay (Solomon and Varshavsky, 1985; Srikantha *et al*., 2006; Zordan *et al*., 2006). To accomplish this, one copy of *TEC1* was tagged with myc at the 3' end in the heterozygous deletion mutant of *TEC1* to generate *tec1/TEC1*-myc. White cells of this strain were treated with α-pheromone to induce the putative interaction between Tec1-myc and the promoters of regulated genes. An antibody against myc was

then used to immunoprecipitate chromatin fragments bound to Tec1-myc. Immunoprecipitated DNA was then amplified by the polymerase chain reaction with primers (Table 17) designed to span approximately 400 base pairs of the promoter harboring the WPRE in the case of white-specific genes and the OPRE in the case of opaque-specific genes. The white-specific genes analyzed were *CSH1*, *PBR1*, *RBT5* and *WH11*, and the opaque-specific genes tested were *KAR4* and *MFA1* (Bennett and Johnson, 2006; Daniels *et al*., 2006; Yi *et al*., 2008; Sahni *et al*., 2009b). We also tested for the promoters of *STE2* and *RBT1*, which contain both a WPRE and OPRE (Sahni *et al.*, 2009b). Finally, we tested for the promoter of *ACT1*, which contains neither a WPRE nor OPRE (Sahni *et al*., 2009b). The only genes coimmunoprecipitated by the anti-myc antibody were those selectively up-regulated by α-pheromone in white but not opaque cells (*CSH1*, *PBR1*, *RBT5* and *WH11*), and the genes up-regulated by α-pheromone in both white and opaque cells (*STE2*, *RBT1*) (Figure 53A). The promoters of genes up-regulated through Cph1 in opaque cells only (*KAR4*, *MFA1*) and the promoter of the gene *ACT1* were not coimmunoprecipated by the anti-myc antibody (Figure 53A). These results demonstrate that Tec1 binds selectively to the promoters of the genes up-regulated by the α-pheromone in white cells, but not to the promoters of genes up-regulated by α-pheromone only in opaque cells.

Tec1 Localizes to White Cell Nuclei

Since Tec1 functions as a white-specific transcription factor, is expressed selectively in white cells, and binds to the promoters of genes up-regulated by α-pheromone in white cells, it was expected to localize to the nuclei of white cells. To test this, we compared DAPI staining, which is specific to DNA, and GFP fluorescence of the complemented strain *tec1/tec1-TEC1* that expressed a GFP-tagged Tec1 (Table 13). Opaque cells of this strain in the absence of α-pheromone or undergoing shmoo formation in the presence of α-pheromone did exhibit fluorescence either in the cytoplasm or nucleus

Figure 53. Tec1 interacts with the WPRE-containing promoter regions of genes up-regulated by α-pheromone in white cells, and localizes to the nucleus. A. ChIP PCR analysis of gene promoters that bind to Tec1. The gene categories for the promoters screened for are presented. The primers used for the promoter regions are listed in Table 17. An anti-myc antibody was used to immunoprecipitate chromatin. "Input" represents chromatin preparation before immunoprecipitation, "- and + Ab" represents immunoprecipitation procedure in the absence and presence of antibody. B. Opaque and white cells of strain *tec1/tec1-TEC1* in which *TEC1* is tagged with GFP, stained for DNA using DAPI, and imaged for DAPI staining and GFP fluorescence.

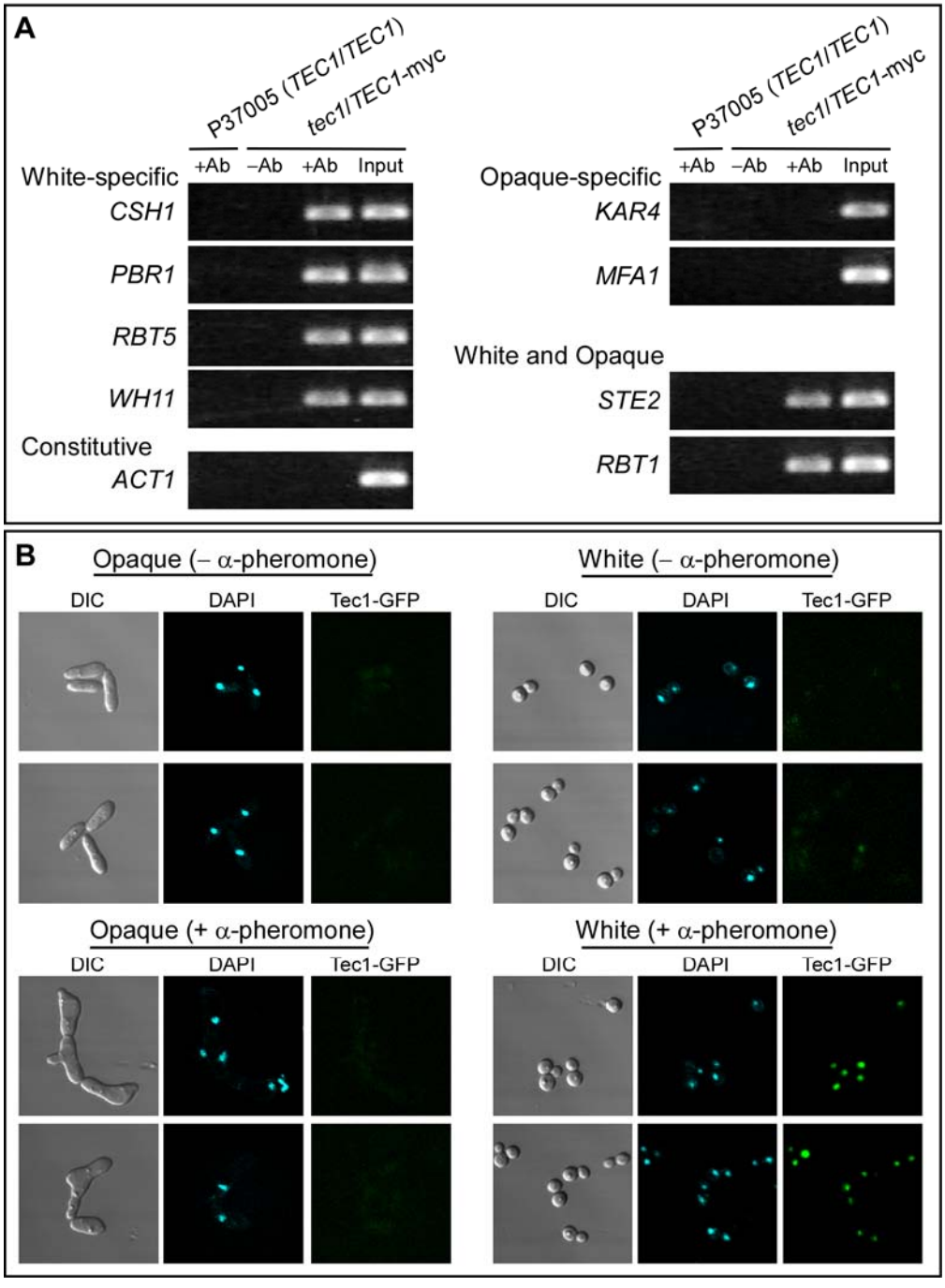
A
P37005 (TEC1/TEC1)
tec1/TEC1-myc
+Ab
–Ab
+Ab
Input
White-specific
CSH1
PBR1
RBT5
WH11
Constitutive
ACT1
Opaque-specific
KAR4
MFA1
White and Opaque
STE2
RBT1
B
Opaque (– α-pheromone)
White (– α-pheromone)
Opaque (+ α-pheromone)
White (+ α-pheromone)
DIC
DAPI
Tec1-GFP

(Figure 53B). In the absence of α-pheromone, white cells of this strain exhibited very weak fluorescence in the nuclei and in the presence of α-pheromone intense nuclear fluorescence (Figure 53B). The relative fluorescence intensities in the absence and presence of α-pheromone (Figure 53B) reflected the basal and induced levels of protein assessed in western blots (Figure 51D). These results demonstrate that Tec1 localizes to the nuclei.

Deletion of *TEC1* abolishes the white cell but not opaque cell response

Deletion of the two copies of *TEC1*, generating the mutant *tec1/tec1* (Table 17), abolished α-pheromone-induced increases in the transcription of *STE2*, *CEK2*, *CSH1* and *PBR1* (Figure 54A). If *TEC1* solely mediated the white, but not the opaque, pheromone response, then deletion of *TEC1* should selectively abolish the former, but not the latter. Both the level of shmoo formation in opaque cell populations treated with α-pheromone and the level of mating of opaque cells of *tec1/tec1*, which is **a**/**a**, mixed with minority α/α opaque cells, were indistinguishable between the parent control strain P37005 and *tec1/tec1* (Figure 54B and C, respectively). In marked contrast, α-pheromone-induced adhesion in white cells was abolished in *tec1/tec1* mutant (Figure 54D), and biofilm formation was defective (Figure 54E through G). The release of β-glucan into the supernatant, a measure of biofilm matrix formation (Nobile *et al.*, 2009), was diminished in *tec1/tec1* cells four fold in the absence α-pheromone and eight fold in the presence of α-pheromone, when compared to P37005 cells (Figure 54E). Moreover, the thickness of the biofilm, as well as the presence of matrix, formation of a basal layer of cells and orientation of hyphae were diminished or defective in *tec1/tec1* cells (Figure 54F, G). Together, these results confirmed that *TEC1* was essential for both the formation of a white cell biofilm in the absence of minority opaque cells and for the enhancement of white cell biofilm formation in the presence of minority opaque cells.

Figure 54. Deletion of *TEC1* results in the loss of the white cell response, but not the opaque cell response, to pheromone. A. Northern analysis of pheromone-induced gene expression in P37005, *tec1/tec1* and the complemented strain *tec1/tec1-TEC1*. B. Shmoo formation in opaque cells. C. Mating between opaque cells of P37005 and *tec1/tec1*, which are **a**/**a**, and opaque cells of strain WO-1, which is α/α. D. Adhesion of white cells on a plastic well bottom. E. β-glucan concentration of the supernatant of biofilms in the absence and presence of 10% **a**/**a** and α/α opaque cell mixture (50:50). F. Characterization of *tec1/tec1* biofilms. G. Side and substrate view of white cell biofilms formed by complemented control cells *tec1/tec1-TEC1* or deletion mutant cells (*tec1/tec1*).

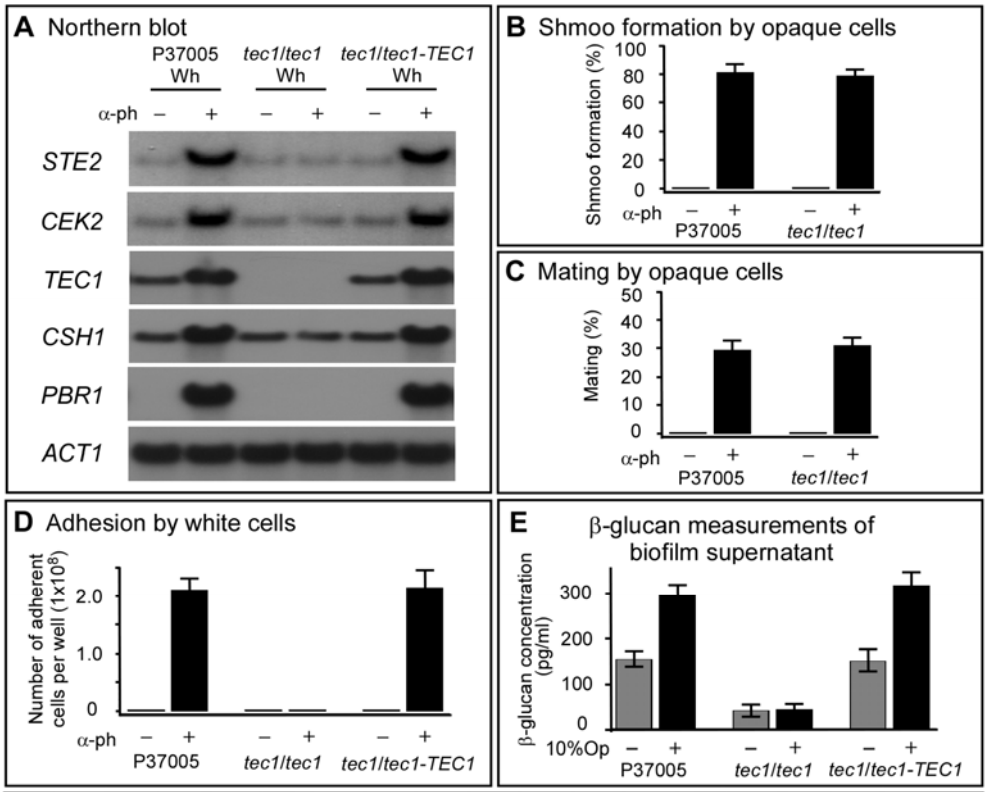

F Biofilm characteristics

Strain	Op	Thickness (μm)	% increase	p value	Matrix	Wh cell basal layer	Hypha density	Hypha orientation
P37005	–	74±4	–		+++	++++	++++	vertical
	+	100±6	35%	$2x10^{-8}$	++++	++++	++++	vertical
tec1/tec1	–	45±3	–		+	++	++	horizontal
	+	50±4	11%	$4x10^{-3}$	+	+	++	horizontal
tec1/tec1-TEC1	–	68±2	–		++++	++++	++++	vertical
	+	92±0	35%	$2x10^{-7}$	++++	++++	++++	vertical

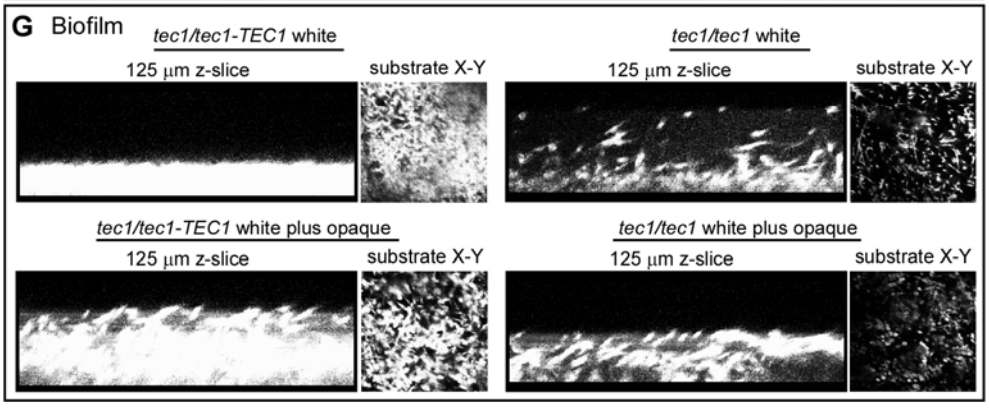

Generality of Tec1 Function

Because **a**-pheromone cannot be chemically synthesized due to complex post-translational modifications (Dignard *et al*., 2007), studies of the role of **a**-pheromone in both *S. cerevisiae* and *C. albicans* have been performed primarily with **a**/**a** strains treated with α-pheromone, which is readily synthesized chemically (Bennett *et al*., 2003; Lockhart *et al*., 2003b; Panwar *et al*., 2003). To test whether Tec1 played the same role in white α/α cells as it did in white **a**/**a** cells, we generated Tec1 overexpression strains in three natural α/α strains, WO-1 (Slutsky *et al.*, 1987), 19F (Lockhart *et al*., 1996) and P57072 (Pujol *et al*., 2002). The generated strains were WO1-*TETp-TEC1*, 19F-*TETp-TEC1* and P57072-*TETp-TEC1* (Table 13). Adherence was then compared between cells in the absence and presence of doxycycline. To assess the **a**-pheromone response, we also tested adherence in the presence of a 1% mixture of opaque **a**/**a** cells and opaque α/α (50:50), which has been shown to be a source of natural **a**-pheromone (Daniels *et al.*, 2006). For each strain, there was over a 100 fold increase in adhesion in doxycycline treated white cells, approximately the same increase observed for white cells treated with minority opaque cells (Figure 55A). These results indicate that Tec1 mediates the white cell **a**-pheromone response in α/α cells, as it does in the white cell α-pheromone response in **a**/**a** cells.

To demonstrate that Tec1 mediated the white cell pheromone response in **a**/**a** strains other than P37005 (*i.e.*, was a general phenomenon), we tested overexpression of *TEC1* in the absence of α-pheromone in two **a**/**a** strains in addition to P37005, L26 (Lockhart *et al*., 2002) and P60002 (Wu *et al*., 2007), generating strains L26-*TETp-TEC1* and P60002-*TETp-TEC1*. As it did in white cells of the **a**/**a** strain P37005, overexpression of *TEC1* in the absence of α-pheromone resulted in an increase in adhesion similar to that induced by α-pheromone (Figure 55B), demonstrating the generality of the role of Tec1 in mediating the α-pheromone response among **a/a** strains.

Figure 55. The role of Tec1 is similar in **a**/**a** and α/α white cell responses to pheromone and general among natural strains. A. The effects of α-pheromone and the overexpression of *TEC1* on adhesion in three natural α/α strains. In this case, pheromone induction was accomplished by adding a minority (1%) mixture of opaque **a**/**a** and opaque α/α cells (50:50). B. The effects of α-pheromone and the overexpression of *TEC1* on adhesion in three natural **a**/**a** strains.

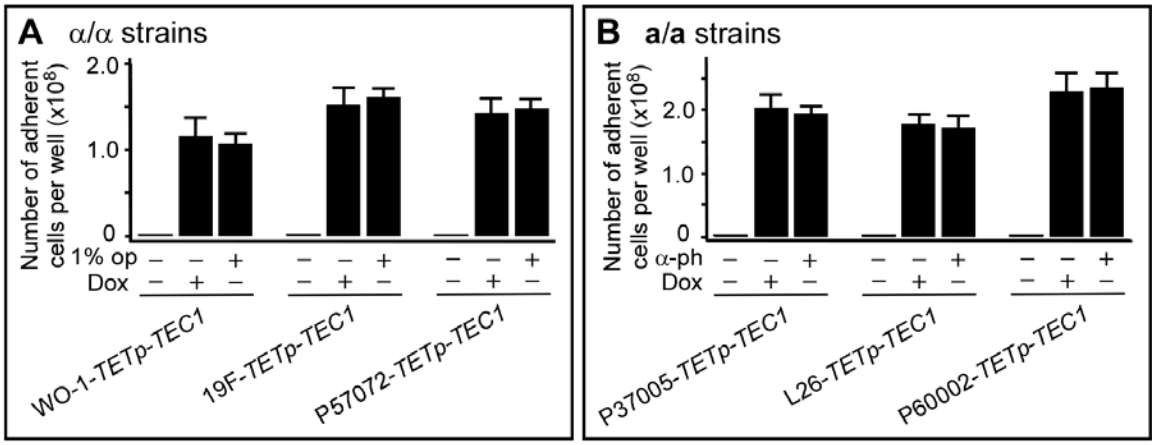
A α/α strains
Number of adherent cells per well (x10^8)
2.0
1.0
0
1% op – – + – – + – – +
Dox – + – – + – – + –
WO-1-TETp-TEC1
19F-TETp-TEC1
P57072-TETp-TEC1
B a/a strains
Number of adherent cells per well (x10^8)
2.0
1.0
0
α-ph – – + – – + – – +
Dox – + – – + – – + –
P37005-TETp-TEC1
L26-TETp-TEC1
P60002-TETp-TEC1

Discussion

In *S. cerevisiae*, Tec1, a member of the ATTS/TEA family of transcription factors, plays a role in the formation of pseudohyphae (Madhani and Fink, 1997; Lo and Dranginis, 1998). Tec1 regulates filamentation by binding in a complex, which includes Ste12 and the two Ste12 inhibitors Dig1 and Dig2, to the TCS binding motif in the promoters of filamentation genes (Chou *et al.*, 2006). In *C. albicans*, Tec1 has also been implicated in the enhancement of filamentation, but Tec1 is not essential either *in vitro* or *in vivo* (Schweizer *et al.*, 2000). Here, we have found that Tec1 is the sole downstream target of the MAP kinase pathway that mediates the white cell pheromone response in *C. albicans*.

Regulation of Tec1

TEC1 is expressed at a basal level in the absence of pheromone in both white and opaque cells, but is up-regulated by pheromone only in white cells. Western analysis revealed that Tec1 was expressed at a basal level in the absence of pheromone and up-regulated over 20 fold in the presence of pheromone. There was no Tec1 signal in western blots of opaque cells in the absence or presence of α-pheromone. Deletion of the genes up-stream of *TEC1* in the MAP kinase pathway, including *STE2*, *STE4* and *CEK1* plus *CEK2*, abolished pheromone induction of *TEC1* expression and overexpression of *STE11* in the absence of pheromone up-regulated *TEC1* expression. These results suggest that as is the case for Cph1 in the opaque cell mating response to pheromone (Chen *et al*., 2002; Magee *et al*., 2002), Tec1 appears to be the only transcription factor targeted by the pheromone-regulated MAP kinase pathway in the white response.

Tec1 Functions Through WPRE

We recently demonstrated that genes up-regulated by pheromone in white cells are regulated through the *cis*-acting motif WPRE, which includes the AT-rich consensus sequence AAAAAAAAAAGAAAG (Sahni *et al.*, 2009b). This sequence differs markedly

from the *cis*-acting sequence OPRE, which appears to regulate pheromone-inducible genes in the opaque cell response. OPRE includes the GC-rich consensus sequence GTGAGGGA (Sahni *et al.*, 2009b). WPRE contains the six base subsequence AGAAAG, which is remarkably similar to the *cis*-acting sequence that mediates Tec1 binding in *S. cerevisiae*, TCS, which includes the consensus sequence AGAATG (Baur *et al.*, 1997; Madhani and Fink, 1997). To demonstrate that Tec1 interacts directly with WPRE-containing promoters of genes up-regulated by pheromone in white cells, we performed chromatin immunoprecipitation experiments (ChIP) followed by PCR, amplifying a region in white or opaque-specific gene promoters spanning either the WPRE or OPRE, respectively, and demonstrated this to be the case. Whereas Tec1 bound to the promoter regions of *CSH1*, *PBR1*, *RBT5*, *WH11*, *STE2* and *RBT1*, which all contained a WPRE and were up-regulated by pheromone in white cells, Tec1 did not bind to the promoter regions of *KAR4* or *MFA1*, which contained an OPRE and lacked a WPRE, and the promoter of *ACT1*, which lacked both an OPRE and a WPRE (Sahni *et al.*, 2009b).

In *S. cerevisiae*, Tec1 combines with Ste12 in a regulatory complex that binds to the TCS consensus sequence of the promoters of Tec1-regulated genes (Chou *et al.*, 2006), but a similar complex containing the *C. albicans* homolog to Ste12, Cph1, is unlikely in *C. albicans* since *CPH1* is not transcribed in white cells (Yi *et al*., 2008). The apparent homology between WPRE and TCS is noteworthy given the speed at which transcription factor binding sites have been found to diverge in the evolution of the yeast (Borneman *et al.*, 2007). We have also found that the DNA binding domain of *C. albicans* Tec1, which is 63 amino acids in length, is highly similar (84%) to a subdomain of similar length in the very long complete DNA binding domain of *S. cerevisiae*, which is in 413 amino acids long.

Tec1 Regulates Biofilm Genes in White Cells

Tec1 activates both genes that are involved in the signal transduction pathway shared with the opaque cell pheromone response, and genes that were involved in adhesion and biofilm formation (Sahni *et al.*, 2009b). In a northern analysis of 103 genes implicated in adhesion, cell wall biogenesis, biofilm formation, filamentation and switching, nine genes were found to be strongly up-regulated by pheromone in white but not opaque cells (Sahni *et al.*, 2009b). All of the promoters of these genes as well as those of three additional genes that had been shown to be similarly up-regulated in white cells by pheromone (Yi *et al.*, 2008; Sahni *et al.*, 2009b) contained a WPRE and lacked an OPRE. Four of these genes randomly selected and deleted were found to play fundamental roles in white cell biofilm formation, suggesting that all or a great majority of genes containing a WPRE but not an OPRE, play a role in α-pheromone-induced white cell biofilm formation.

The Evolution of the White Phase Pheromone Response Pathway

The identification of the transcription factor, Tec1, represents the last piece of the puzzle in identifying the components in the white cell pheromone response pathway. This pathway provides the first complete picture of how mating pheromone regulates a response in mating-incompetent cells, the formation of a biofilm that facilitates rather than plays a direct role in the actual mating process. It also provides unique insights into how signal transduction pathways may evolve in general (Figure 56). The white response pathway must be new since white-opaque switching is unique to *C. albicans* and the closely related species *Candida dubliniensis* (Pujol *et al.*, 2004). It has not been observed in any of the other members of the hemiascomycetes, indicating that the white response pathway emerged with the species *C. albicans*. We propose that in the evolution of the white pheromone response pathway, all of the components were derived from components in ancestral pathways involved in other developmental programs. First, we propose that the

Figure 56. A hypothesis for the evolution of the entire white cell pheromone response pathway in *C. albicans*. Note that each major component of the pathway, from receptor to activated genes, was borrowed from an ancestral process still active in *C. albicans*. Hence, all of the components were borrowed and are shared.

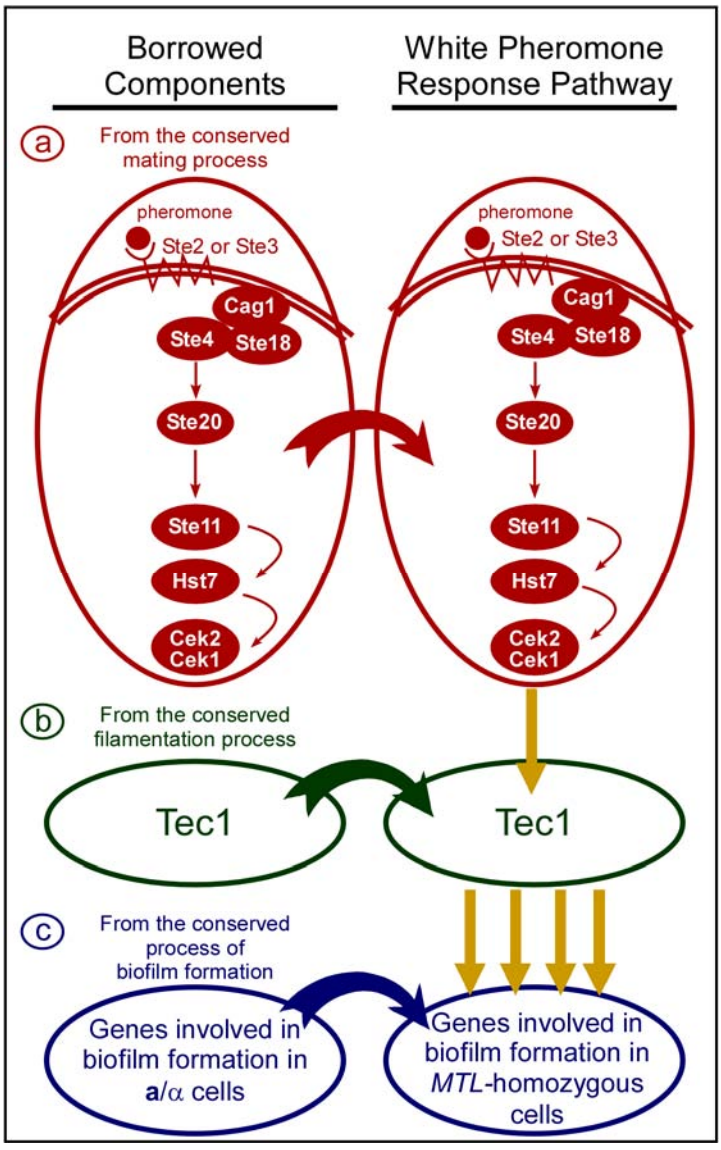
Borrowed Components
White Pheromone Response Pathway
a
From the conserved mating process
pheromone
Ste2 or Ste3
Cag1
Ste4
Ste18
Ste20
Ste11
Hst7
Cek2
Cek1
pheromone
Ste2 or Ste3
Cag1
Ste4
Ste18
Ste20
Ste11
Hst7
Cek2
Cek1
b
From the conserved filamentation process
Tec1
Tec1
c
From the conserved process of biofilm formation
Genes involved in biofilm formation in a/α cells
Genes involved in biofilm formation in MTL-homozygous cells

components of upper portion of the white pathway, including receptors, the trimeric G protein complex and MAP kinase cascade, were borrowed intact from the ancestral mating pathway (step a in Figure 56), as evidenced by the strict homology between components of that portion of the white cell pathway with the opaque cell pathway, and the pheromone response pathway of haploid *S. cerevisiae* cells (Yi *et al.*, 2008, 2009). Second (step b in Figure 56), we propose that the transcription factor regulated by the MAP kinase cascade in the white cell pheromone response pathway, Tec1, was borrowed from an ancestral filamentation pathway, as is suggested by its conserved role in *S. cerevisiae* filamentation (Oehlen and Cross, 1998; Chou *et al*., 2006) and *C. albicans* filamentation (Schweizer *et al*., 2000). And finally (step c in Figure 56), we propose that the genes directly regulated by Tec1 involved in the formation of a white cell biofilm to facilitate opaque cell mating were borrowed from an ancestral system for biofilm formation, which is conserved in **a**/α cells of *C. albicans* .

The signal transduction pathway of the white cell pheromone response evolved to facilitate the outcome of the pathway from which it was derived, namely the mating process. Hence, upper portions of the original (opaque) and derived (white) pathways can share the same signal and receptor. However, since the specific outcomes of the original and derived pathways differ (*i.e.*, mating versus biofilm development), the derived pathway borrowed target genes from another pathway with the necessary phenotypic outcome, namely the ancestral biofilm program, still functioning in **a**/α strains (Hawser and Douglas, 1994; Kumamoto, 2002; Nobile and Mitchell, 2006). To glue the upstream and downstream components together, the transcription factor, Tec1, was borrowed from a third developmental program, namely filamentation, and the *cis*-acting sequence, WPRE, which binds to Tec1 in the regulation of pheromone-induced white cell genes, appears to have evolved from the ancestral *cis*-acting sequence that bound to Tec1. All of the components, therefore, appear to have been borrowed from ancestral programs and appear intact. All of the components of the white pheromone response pathway are therefore, still

shared with other developmental programs in *C. albicans*, supporting our hypothesis that the white pathway is young and has had insufficient time to duplicate, replace or modify components in response to new selective pressures or changing roles. We suggest that the evolution of the white cell pheromone response pathway affords a unique glimpse into the evolution of a signal transduction pathway, and may provide at least one paradigm for how such pathways evolve in general.

CHAPTER 8

DISCUSSION AND FUTURE DIRECTIONS

Regulatory Network for White-Opaque Switching: an Era Post Discovery of Master Switch Locus

Why Do We Care about White-Opaque Switching in *C. albicans*?

In *S. cerevisiae*, haploid cells are immediately mating competent after meiosis (Sprague, 1991; Elion, 2000). In *C. albicans*, *MTL*-homozygosis from **a**/α to **a**/**a** or α/α is not sufficient to confer mating competency. The switch from white to opaque is a prerequisite for *MTL*-homozygotes to mate (Miller and Johnson, 2002; Lockhart *et al.*, 2003a). The white-opaque transition and the incorporation of switching into the mating process are both unique to *C. albicans* (Soll, 1992, 2002; Miller and Johnson, 2002) and its close relative, *C. dubliniensis* (Pujol *et al.*, 2004). It was initially perplexing that *C. albicans* should employ this extra step to regulate mating. The reason seems to lie in the pathogenic nature of *C. albicans*. Unlike *S. cerevisiae*, *C. albicans* is an opportunistic pathogen that resides in a variety of anatomical niches, and survives under ever-changing host physiological conditions (Odds, 1988; Soll, 1992, 2002) that *S. cerevisiae* cells seldom encounter (Schuit, 1979; Maejima *et al.*, 1980). Although mating-competent opaque cells are unstable at the host physiological temperature, 37°C (Slutsky *et al.*, 1987; Rikkerink *et al.,* 1988), evidence has been presented supporting the possibility that opaque cells can be stable in appropriate niches within the animal host (Dumitru *et al.*, 2007; Ramírez-Zavala *et al.*, 2008; Huang *et al.*, 2009). In the host, the physiological CO_2 content ranges between 4.5% and 30% (Levitt and Bond, 1970; Stenni *et al.*, 2001). These levels induce switching from white to opaque and stabilize the opaque phenotype at physiological temperature, thus facilitating mating (Huang *et al.*, 2009). Indeed, *C. albicans* mating has been demonstrated *in vivo* in the mouse kidney (Hull *et al.*, 2000) and

in the gastrointestinal tract (Dumitru *et al.*, 2007). The white-opaque transition, therefore, may have evolved in *C. albicans* to adapt to specific environmental niches found in the host.

Although white-opaque switching is required for mating, it appears that switching may play roles beyond that of mating. Microarray expression profiling has revealed that over 6% of the genes in the *C. albicans* genome are differentially regulated during the white-opaque transition (Lan *et al.*, 2002), which includes a number of putative virulence genes (Morrow *et al.*, 1992, 1993; White *et al.*, 1993; Hube *et al.*, 1994; Kvaal *et al.*, 1997, 1999; Soll, 2002). A unique opaque-white pheromone signaling system has been discovered that plays an important role in the process of *in vitro* biofilm formation (Daniels *et al.*, 2006), a key virulence trait (Hawser *et al.*, 1998; Douglas, 2003). It has been hypothesized that in this system, opaque cells could arise from rare switching of white cells in overlapping populations of *MTL*-homozygous **a**/**a** and α/α cells (Daniels *et al.*, 2006; Soll and Daniels, 2007; Soll, 2009). These opaque cells would then secrete pheromones to signal majority white cells of the opposite mating type to form a more robust biofilm. The resulting white cell biofilm, in turn, would facilitate opaque cell chemotropism in the mating process (Daniels *et al.*, 2006). This opaque-white communication system with its influence on biofilm formation, and the differential expression of many putative virulence genes in the white and opaque phenotypes, would provide a possible explanation for the establishment of the white-opaque transition in the evolution of *C. albicans* and its role in nature.

The Regulation of White-Opaque Switching Is Highly Complex

Given the intimate relationship between white-opaque switching and pathogenesis in *C. albicans*, it is imperative to study the molecular mechanisms regulating the white-opaque switching. Since the discovery of the master switch locus, *WOR1* (*TOS9*),

in *C. albicans* (Zordan *et al.*, 2006; Huang *et al.*, 2006; Srikantha *et al.*, 2006), additional transcription factors and signaling pathways have been identified that play a role in the white-opaque transition. In 2007, three additional regulators, Wor2, Czf1 and Efg1, were demonstrated to be involved in white-opaque switching by genetically interacting with Wor1, forming interlocking feedback loops (Zordan *et al.*, 2007). The pathways through which the three regulators function, however, are still not known, and whether these regulators physically interact with Wor1 in a complex has not been demonstrated. Recently, we discovered that physiological levels (4.5%-20%) of CO_2 promote, even at 37^{o}C, the white-to-opaque switch and stabilize the opaque phenotype, in a Wor1-dependent manner (Huang *et al.*, 2009). This work is significant, since it provides a possible answer to the previous paradox that the opaque phenotype is unstable at physiological temperatures (Rikkerink *et al.,* 1988; Bergen *et al.,* 1990; Soll, 2002). In this study (Huang *et al.*, 2009), it was noted that low levels (< 5%) of CO_2 regulate switching through the cAMP-PKA pathway, while high levels (~ 20%) of CO_2 function through a cAMP-PKA-independent pathway that remains unidentified. The receptor(s) of the CO_2 signal also remains unknown. Recently, we also found that N-acetyl-glucosamine (GlcNAc), another molecule present in the host gastrointestinal tract, promotes the white-to-opaque transition (Huang *et al.*, submitted). The regulation of switching by GlcNAc is mediated primarily by the cAMP-PKA pathway, but it is also regulated by a minor, unidentified cAMP-PKA-independent pathway. It is still unknown, however, how GlcNAc mediates switching *in vivo*. GlcNAc is a major component of the cell wall of intestinal bacteria (Ghuysen and Hakenbeck, 1994; Finne *et al.*, 1989), and hence, the possibility exists that GlcNAc produced by bacteria plays a role in regulating white-opaque switching. It will be revealing to test whether switching occurs in a mouse model with GlcNAc negative bacteria. However, given the high levels of CO_2 in the human host, there is the possibility of multiple signals. Hence, this experiment may not be straight-forward to interpret *in vivo*. In addition, other components such as

gastrointestinal glucose, released by bacteria or the host, may also contribute to the regulation of switching *in vivo* (Huang *et al.*, submitted), making it even more difficult to interpret the real signals for switching in the host. As an alternative approach, the interaction between bacteria and *C. albicans* in the regulation of switching can be studied *in vitro*. Either bacterial cell wall extracts or live bacterial cells can be applied to the agar media on which *C. albicans* switching is assessed. Different types of bacteria with variable levels of GlcNAc and glucose could be included in this analysis. Results from this experiment would provide a clue to the effect of bacteria-yeast interaction on switching frequencies of *C. albicans in vivo*.

Finally, it is now known that the regulation of switching by the master switch regulator Wor1 is dependent on the phosphorylation by the PKA kinases in the cAMP pathway, Tpk1 and Tpk2 (Huang *et al.*, submitted). However, it remains unknown whether other key regulators, including Efg1, Czf1 and Wor2, are regulated in a similar manner. Preliminary data in the Soll lab have demonstrated that Efg1, but not Czf1 or Wor2, has a putative PKA phosphorylation site. It will, therefore, be necessary to mutate that site in Efg1 and assess the effect on white-opaque switching (Huang and Soll, unpublished observations). This experiment is now being performed in the Soll lab.

Understanding Switching and Mating in *C. albicans* from a Unique Angle

Integration of Switching and Mating into Biofilm Development

Mating appears to be a rare event in *C. albicans* (Pujol *et al.*, 2005). Studies of population structure have also revealed low rates of recombination between strains from different clades (Pujol *et al.*, 2005) and even within the same clade (Bougnoux *et al.*, 2008). Because mating and recombination are rare, one must ask how *C. albicans* maintains the integrity of the mating machinery. In the pheromone-mediated opaque-white signaling

system, the mating process is intimately linked to biofilm formation, which represents a pathogenic trait under continuous selective pressure (Hawser and Douglas, 1994; Costerton *et al.*, 1999; Chandra *et al.*, 2001). By incorporating the mating system into biofilm formation, the mating system may come under the selective pressure of colonization and virulence, rather than that of recombination (Soll, 2009).

The correlation between mating and biofilm formation does not seem to be limited to the white cell pheromone response. Nobile *et al.* (2008) provided another link between mating and biofilm development in *C. albicans*. They found that biofilm development of *C. albicans* **a**/α cells requires two types of adhesin molecules, Als proteins and Hwp1, which function in a complementary fashion (Nobile *et al.*, 2008). The Als proteins share structural features with the *S. cerevisiae* α mating agglutinin, an adhesin required for mating in that species (Sheppard *et al.*, 2004; Dranginis *et al.*, 2007), whereas Hwp1 is expressed on the conjugation tubes of cells in the process of mating, and may represent a mating adhesin (Daniels *et al.*, 2003). These observations suggest that the cell-cell adhesion system involving Als proteins and Hwp1, which plays a critical role in biofilm development *in vitro* in **a**/α cells, may have evolved from ancestral mating agglutinins. Subsequently, we found a third link between biofilm formation and mating (Yi *et al.*, 2008). We showed that in *MTL*-homozygous white cells, deletion of the α-pheromone receptor results not only in the loss of the white cell biofilm response to pheromone, but also in a strong defect in biofilm formation in the absence of exogenously added pheromone. In other words, the mating pheromone appears to be necessary for *MTL*-homozygous white cell basal biofilm formation. Taken together, it appears that the mating system of *C. albicans* has become intimately intertwined with biofilm formation, and hence pathogenesis, in a variety of ways.

The link between mating and biofilm formation is not unique to *C. albicans*. In bacteria, a link has also been well established (Soll, 2008). Mating of the bacterium *Escherichia coli* is 1000 times more frequent in a biofilm than it is under classical plating

conditions (Hausner and Wuertz, 1999), indicating that biofilms facilitate mating in bacteria, as they do in *C. albicans* (Daniels *et al.*, 2006). In addition, mating conjugation between donor and recipient cells of *E. coli* induces the formation of bacterial biofilms (Ghigo, 2001), and the addition of mating pheromone stimulates biofilm development in the bacterium *E. faecalis* (Tendolkar *et al.*, 2006). Gene transfer not only occurs more efficiently in bacterial biofilms, but also enhances the stability of these biofilms (Molin and Tolker-Nielsen, 2003). Finally, pili adhesins, analogous to the mating adhesins in *S. cerevisiae*, are essential for biofilm development in *E. coli* (Reisner *et al.*, 2003).

Mating and Virulence in *C. albicans*

In *S. cerevisiae*, haploid **a** and α cells retain the genetic information of the opposite mating-type in one of the silent loci, *HML* (α information) or *HMR* (**a** information) (Nasmyth, 1982; Hicks *et al.*, 1977; Haber, 1998). The mating type can be switched from **a** to α or α to **a** through a cassette system, in which gene conversion at the mating type locus occurs with a gene copy of the opposite mating type at one of the silent loci (Hicks *et al.*, 1977; Haber, 1998). Hence, in both diploid (**a**/α) and haploid (**a** or α) *S. cerevisiae* cells, the entire mating type information remains conserved at the cellular level (Hicks *et al.*, 1977; Strathern *et al.*, 1982). In contrast, *C. albicans* does not possess such a cassette system for mating-type switching (Hull and Johnson, 1999; Soll, 2002; Bennett and Johnson, 2005). When *C. albicans MTL*-heterozygous **a**/α cells undergo homozygosis to **a**/**a** or α/α, they lose the genes for the opposite mating-type (Lockhart *et al.*, 2002; Legrand *et al.*, 2004; Tavanti *et al.*, 2005). A number of natural **a**/α strains (approximately 4%) can generate *MTL*-homozygous offspring at relatively high frequency (Lockhart *et al.*, 2002; Wu *et al.*, 2005). In contrast, mating in nature between *MTL*-homozygous strains seems to be rare (Blignaut *et al.*, 2008). Based on these observations, however, one should expect an accumulation of *MTL*-homozygous strains. This is obviously not the case, since the large majority of *C. albicans* strains are *MTL*-heterozygotes in nature.

Lockhart *et al.* (2005) hypothesized that the predominance of *MTL*-heterozygous **a**/α strains might lie in their competitive advantage over their **a**/**a** and α/α offspring. They isolated spontaneous **a**/**a** and α/α offspring from several natural **a**/α parental strains that exhibit frequent *MTL*-homozygosis *in vitro* and discovered that the *MTL*-heterozygous parental strains were indeed more virulent than their *MTL*-homozygous offspring in a mouse model for systemic infection (Lockhart *et al.*, 2005). These strains were shown to have lost heterozygosity at the *MTL* locus through loss of one Chromosome 5 homolog and duplication of the retained homolog (Wu *et al.*, 2005). They not only lost heterozygosity at the *MTL* locus, but also at other loci along Chromosome 5 (Wu *et al.*, 2005). Hence, there are two possible explanations for the difference in virulence: i) heterozygosity of the *MTL* genes themselves provides a competitive edge, and ii) heterozygosity of genes other than the *MTL* genes on Chromosome 5 provides a competitive edge. Wu *et al.* (2007) demonstrated that although both explanations were correct, the competitive advantage of **a**/α strains over their spontaneous **a**/**a** and α/α offspring is mainly due to the heterozygosity of genes other than the *MTL* genes on Chromosome 5.

Switching, Mating and Biofilm Development: Three Passengers Board the Same Train

A Unique "Loop": Selective Regulation of White Cell Biofilm Response by a Region in the α Mating Receptor

The integration of switching and mating into pathogenesis and biofilm formation (Wu *et al.*, 2007; Daniels *et al.*, 2006) provides a competitive edge for *C. albicans* as an opportunistic pathogen. The focus of this thesis is on the mating pheromone-mediated white cell biofilm response in *C. albicans*. We have shown that the IC1 loop of the α-pheromone receptor, Ste2, plays a selective role in the white cell pheromone response, but not the opaque response (Yi *et al.*, 2009). The IC1 loop mediates pheromone signaling through the classic MAP kinase cascade in white cells, but there appears to be a

minor pathway(s) activated by IC1 that is independent of the MAP cascade and remains unidentified (Yi *et al.*, 2009). The unique IC1 loop contains glutamine- and asparagine-rich regions that have been shown to play a role as "polar zippers" in protein-protein interactions (Perutz *et al.*, 1994; Michelitsch and Weissman, 2000). The IC1 loop also contains five mini-repeats of lysine (K)-leucine (L), a highly charged region, that could bind phosphoserine-containing proteins (Dalton *et al.*, 2007; Yeung and Grinstein, 2007; Wakelam *et al.*, 2007). Therefore, finding the IC1 loop protein interaction partners is necessary to better characterize signal transduction differences between white and opaque pheromone responses. To address this question, mutants can be generated, in which a wild-type Ste2 and an IC1Δ derivative of Ste2, respectively, can be tagged with c-myc, at its carboxy terminus and used in co-immunoprecipitation experiments to isolate potential protein partners. The putative partners interacting with IC1 loop should be present in pull-down complexes of wild-type Ste2, but not the IC1Δ derivative of Ste2.

In the search for Ste2 IC1 loop-mediated signaling circuits other than the MAP kinase pathway, one may consider the cAMP-PKA pathway. It was recently shown that the cAMP-PKA pathway mediates white to opaque switching in *MTL*-homozygous strains when N-Acetyl-glucosamine (Huang *et al.*, submitted) or low levels (~1%) of CO_2 (Huang *et al.*, 2009) are used as inducers. In addition, this pathway regulates filamentation in *C. albicans* in a number of liquid and solid hypha-inducing media (Leberer *et al.*, 2001; Rocha *et al.*, 2001). It is, therefore, necessary to test whether this pathway also plays a role in pheromone signal transduction through activation by the Ste2 IC1 loop in the white response. To study this, the *RAS1-V13* construct (Chen *et al.*, 2000), which constitutively activates the cAMP-PKA pathway, will be used to transform into the IC1 loop full deletion mutant. If the IC1 loop defect in the white cell response can be rescued, then the IC1 loop region transduces the signal, at least in part, through the cAMP-PKA pathway. If this is true, it will then be necessary to analyze the null mutants of gene components of this

pathway for the white biofilm response. However, it should be noted that genes in this pathway are not induced in white cells in response to pheromone. Hence, if this pathway plays a role in the white response, the regulation should be either at the translational or post-translational level.

Hyperactivation of the MAP Kinase Cascade: A Model Strategy for Studies of Pheromone Responses

Hyperactivation of the MAP kinase cascade has been demonstrated to be a useful tool in studying pheromone responses in *S. cerevisiae* (Gustin *et al.*, 1998; Schwartz and Madhani, 2004). In *S. cerevisiae*, overexpression of *STE4*, encoding the β subunit of the heterotrimeric G protein complex, leads to a mating response in haploid cells in the absence of exogenous pheromone (Whiteway *et al.*, 1990). In addition, overexpression of *STE12*, encoding the essential transcription factor involved in mating, also leads to constitutive transcription activation of mating-associated genes and generates a mating response in the absence of pheromone (Dolan and Fields, 1990). In *C. albicans*, on the other hand, overexpression of *STE4* alone does not hyperactivate the MAP kinase pathway, or induce the pheromone responses in opaque or white cells (Yi *et al.*, 2009). Indeed, hyperactivation of the MAP kinase pathway by *STE4* overexpression depends on the presence of pheromone (Yi *et al.*, 2009). Overexpression of *CPH1*, the homolog of *S. cerevisiae STE12*, does trigger shmoo formation in *C. albicans* opaque cells in the absence of pheromone (Yi S, Sahni N and Soll DR, unpublished observations). It does not, however, activate the pheromone response in white cells (Yi S, Sahni N and Soll DR, unpublished observations), since *CPH1* is not involved in the regulation of the white cell biofilm response (Yi *et al.*, 2008). In the search for a MAP kinase cascade hyperactivation model for the white response, we constructed a number of overexpression mutants for genes in the MAP kinase pathway, and each of the genes was placed under the control of an inducible tetracycline promoter. We found that overexpression of one gene,

STE11, encoding the MAP kinase kinase kinase (MAPKKK) results in hyperactivation of the MAP cascade in the absence of pheromone. *STE11* overexpression in opaque cells causes shmoo formation, cell cycle arrest and upregulation of mating-associated genes, while *STE11* overexpression in white cells leads to adhesion on a plastic substratum in the absence of pheromone, and upregulation of white-specific biofilm-associated genes (Yi S, Sahni N and Soll DR, unpublished observations). Therefore, overexpression of *STE11* itself in the absence of pheromone is sufficient for the activation of the MAP kinase pathway in the signal transduction of alternative pheromone responses in *C. albicans*.

Regulation of Biofilm-associated Genes by the Key Player Tec1 in the White Cell Response

We have identified Tec1 as the central transcription factor regulating pheromone-induced biofilm formation in white cells. This transcription factor is activated by the MAP kinase pathway in response to pheromone, and plays a role in the white cell biofilm response, comparable to that of Cph1 in the opaque cell mating response. In order to better understand the regulation of the white cell biofilm response, a study of target genes of the white-specific transcription factor Tec1 is very important. Several feasible strategies can be employed. First, to identify the DNA-binding targets of Tec1 on a genome-wide scale, a ChIP-chip analysis can be performed. All protein-DNA complexes in cells of a myc-tagged Tec1 strain will be cross-linked, then extracted from the cells, and anti-c-myc antibody used to pull down Tec1 protein-DNA complexes from the total cell extracts. The DNAs released from the complexes will be subjected to microarray hybridization. Results from this experiment will provide the genome-wide DNA targets bound by Tec1. The DNA binding sites will then be scrutinized for the putative *cis*-acting element, WPRE, presumably present in all the white-specific pheromone-inducible genes (Sahni *et al.*, 2009b). Second, a transcriptional profiling method, such as expression microarrays, can be employed. In this case, white cells from a

tec1 null mutant and the parental wild type strain will be included for comparison both in the absence and presence of pheromone. Genes that are upregulated or downregulated in the *tec1* mutant background will be identified. These Tec1-regulated genes, however, may or may not bind directly to Tec1. Third, a large scale proteomic approach can be applied. Comparisons of a 2-D gel electrophoresis-based proteomic profile can be done between pheromone-treated and non-treated white cells of both the *tec1* mutant and the wild type control. Differentially expressed proteins can be identified by MS-MS sequencing and a blast search in the *Candida* genome database (http://candidagenome.org/). Again, the genes encoding the identified proteins will not necessarily represent Tec1-binding sites. Taken together, the results from these experiments should identify new target genes involved in the white cell biofilm formation, and undoubtedly provide a more global view of the regulation of the white cell response to pheromone.

Positive Feedback: The White Biofilm Response Is an Autocrine System

In an **a**/**a** strain, deletion of each of the genes, *EAP1*, *PGA10*, *CSH1* and *PBR1*, which are induced by pheromone specifically in white cells, results in a defective biofilm with reduced thickness, decreased β-glucan secretion in the biofilm supernatants, diminished hypha formation and defective horizontal hypha orientation, in the presence of minority opaque cells, a source of mating pheromones (Sahni *et al.*, 2009b). Interestingly, similar defects were also observed in the absence of minority opaque cells (Sahni *et al.*, 2009b). This means that each of these genes play a role in the formation of a basal biofilm by *MTL*-homozygous white cells. The same biofilm defect exhibited by each of these mutants in the absence of minority opaque cells, suggests an autocrine system in which white cells continuously release a basal level of pheromone of the opposite mating type, that in turn binds to the pheromone receptors on the same cells, resulting in baseline

activation of the white cell pheromone response pathway and a basal biofilm response (Sahni *et al.*, 2009b). The autocrine system in the white cell biofilm response can be verified by deleting of the α-pheromone gene *MFα* in **a**/**a** cells. If **a**/**a** white cells secrete α-pheromone in an autocrine system, deletion of the α-pheromone gene *MFα* should abolish this autocrine signaling, resulting in defective biofilm formation in the absence of minority opaque cells, a phenotype similar to that of the mutant for the α-pheromone receptor gene, *STE2*.

The White Cell Biofilm Response *In Vivo*: An Essential Step toward Understanding Switching and Mating in the Host

The discovery of the white cell biofilm response *in vitro* (Daniels *et al.*, 2006) has established a unique relationship between white-opaque switching, mating and biofilm formation in *C. albicans*. Since biofilm formation is a pathogenic trait (Hawser *et al.*, 1998; Douglas, 2003), the white cell biofilm response suggests a link between switching, mating and pathogenesis in *C. albicans*. The steps involved in the white cell pheromone response have been initially formulated and verified *in vitro* (Daniels *et al.*, 2006), but they still need to be assessed *in vivo*. In the hypothesis described by Daniels *et al.* (2006), **a**/α cells would first undergo *MTL*-homozygosis to **a**/**a** or α/α. Second, *MTL*-homozygous cells would undergo white-opaque switching, generating opaque cells at a frequency of one in 1000 cell divisions. Third, rare opaque cells would signal majority white cells of the opposite mating type to form enhanced biofilms. To test this hypothesis *in vivo*, we can take advantage of specific molecular marker genes, such as *FAR1*, a gene specifically expressed in *MTL*-homozygous cells (Tsong *et al.*, 2003; Lockhart *et al.*, 2003b), *WOR1*, a gene specifically expressed in opaque cells (Huang *et al.*, 2006; Zordan *et al.*, 2006; Srikantha *et al.*, 2006), and *PBR1*, a gene specifically induced by pheromone in white cells (Sahni *et al.*, 2009b). In order to monitor the expression levels of these genes during the course of biofilm development, three different tags would be used: *RFP*, *GFP* and *CFP*,

which encode red, green and cyan fluorescent proteins, respectively. *RFP*, *GFP* and *CFP* can be placed under the control of the promoters of the three genes, *FAR1*, *WOR1* and *PBR1*, respectively, in the same cell. These engineered DNA constructs can be transformed into an **a**/α strain, which can then be in a murine model of *in vivo* biofilm formation in a catheter (Nobile *et al.*, 2006, 2009). Laser scanning confocal microscopy (Daniels *et al.*, 2006; Nobile and Mitchell, 2005) can then be used to observe the expression of each gene in biofilm samples isolated at different timepoints over time. If red fluorescence (p*FAR1-RFP* expression) is observed, it will indicate that spontaneous **a**/**a** or α/α strains arise by *MTL*-homozygosis. If green fluorescence (p*WOR1-GFP* expression) is observed, it will indicate that opaque cells are generated from rare switching in the **a**/**a** or α/α strains. If cyan fluorescence (p*PBR1-CFP* expression) is observed, it will indicate that opaque cells signal white cells to form enhanced biofilms. Hence, this system can be readily used to test the biofilm hypothesis and monitor different steps in biofilm formation *in vivo*. After *in vivo* inoculation, one can dissect the animal host, obtain the biofilm samples and perform direct observation with confocal microscopy or use fluorescence activated cell sorting (FACS) techniques. In a FACS analysis, cells with different fluorescence expression patterns can be sorted, and the intensity of each fluorescence marker quantitated and compared. As a result, one should be able to assess key steps regarding the hypothesis on biofilm development *in vivo*.

Evolutionary Significance of the White Response Pathway

The white cell pheromone response evolved specifically in *C. albicans* (Daniels *et al.*, 2006; Yi *et al.*, 2008, 2009; Sahni *et al.*, 2009a, b; Soll, 2009), and probably in the closely related species *C. dubliniensis*, to facilitate mating between opaque cells (Miller and Johnson, 2002; Lockhart *et al.*, 2003a; Pujol *et al.*, 2004; Daniels *et al.*, 2006). In contrast to *C. albicans*, the white-opaque transition is not a step in the mating process of *S. cerevisiae* (Fields, 1990; Sprague, 1994) or *C. lusitaniae* (Reedy *et al.*, 2009), which all

evolved from a common hemiascomycete ancestor (Souciet *et al.*, 2000; Wong *et al.*, 2002). The white cell pheromone response in *C. albicans* is, therefore, a relatively recent developmental program. This white response pathway evolved from three ancestral pathways (Yi *et al.*, 2008; Sahni *et al.*, 2009b; Sahni *et al.*, in preparation). First, the white pathway borrowed the upper portion of the opaque pheromone response pathway for mating, from the pheromone signal and receptor through the MAP kinase cascade (Yi *et al.*, 2008). Because the pheromone response pathway of opaque cells of *C. albicans* (Chen *et al.*, 2002; Magee *et al.*, 2002; Yi *et al.*, 2008) includes the same conserved components as the pheromone response pathway of haploid cells of *S. cerevisiae* (Fields, 1990; Elion, 2000), it seems reasonable to conclude that the mating pathway in opaque cells, rather than the biofilm response pathway in white cells, was conserved in evolution, and that the mating response pathway was reutilized in the subsequent evolution of the white cell response. Second, the white response pathway borrowed the transcription factor Tec1 from the ancestral filamentation process (Schweizer *et al.*, 2000; Sahni *et al.*, in preparation). Third, the white pathway borrowed the downstream target genes from the transduction circuits regulating biofilm formation in *C. albicans* **a**/α cells (Sahni *et al.*, 2009b; Nobile *et al.*, 2006).

The evolution of the white cell pheromone response involves a scenario in which the three major components of the pathway regulating the response were derived from three independent ancestral processes. This white response pathway serves as an elegant model to provide insights into the evolution of a new transduction pathway. In this model, the upper portion of a new signal transduction pathway can evolve from a pre-existing pathway to facilitate the outcome of the latter, and hence can share the same signal and receptor. The outcomes of the two pathways are then coordinated. Since the outcomes of the two pathways are related, but phenotypically distinct, the new pathway borrows the target genes from another pathway with the necessary phenotypic outcome. To connect the upstream and downstream components together, a transcription factor is derived from a

third developmental process. Taken together, the pheromone response pathway of white cells has therefore provided us with a unique perspective on the evolution of a novel signal transduction pathway.

Insights into the Regulation of Biofilm Formation by the Mating Type Locus

The white cell pheromone biofilm response occurs in *MTL*-homozygous strains, while biofilm formation also occurs in *MTL*-heterozygous **a**/α strains, the predominant in nature. It is, therefore, important to study the mechanisms underlying **a**/α biofilm formation and compare with *MTL*-homozygous biofilm formation. It has been demonstrated by Wu *et al.* (2007) that the mating type locus (*MTL*) in *C. albicans* plays a role in virulence assessed in a mouse model for systemic candidiasis. Since biofilm formation is an important virulence trait, the possibility that the *MTL* locus may also contribute to the regulation of biofilm development in *C. albicans* was considered. It was first observed that cells of *MTL*-hemizygous strains, derived from deleting either the *MTL* **a** or α locus from a *MTL* **a**/α parental strain P76067 (Wu *et al.*, 2007), form a thinner and more fragile biofilm than that formed by their *MTL*-heterozygous parents (Daniels and Soll, unpublished observations). This biofilm defect suggests that genes at the *MTL* locus may regulate biofilm formation. The *MTL* locus possesses sex genes (**a**1 and **a**2, or α1 and α2) as well as non-sex genes (*OBP**a***, *OBPα*, *PIK**a***, *PIKα*, *PAP**a*** and *PAPα*). In order to distinguish the roles of these genes, individual deletion derivatives will be generated and their phenotypes in biofilm formation and virulence assessed. Preliminary data obtained in the Soll lab indicate that deletion of the gene **a**1 or α2 from the natural **a**/α strains P76067 and P37039, causes a defect in biofilm formation (Soll and colleagues, unpublished observations). On the other hand, simultaneous deletion of one copy of all three non-sex genes, *OBP*, *PIK* and *PAP*, at the *MTL***a** or *MTL*α locus of the **a**/α strain P37037, results in dramatic defects in adhesion, biofilm thickness and architecture (Soll

and colleagues, unpublished observations). Deletion of these three genes also affects biofilm matrix formation (Soll and colleagues, unpublished observations), as assessed by measurements of the β-glucan concentration in biofilm supernatants (Nobile *et al.*, 2009). The defects observed in the heterozygous deletion mutant for the three genes, suggest that these gene products may have a dosage effect on biofilm formation (Soll and colleagues, unpublished observations). Unfortunately, the homologs of at least the PIK and PAP genes have been found to be essential in *S. cerevisiae* (Garcia-Bustos *et al.*, 1994; Giaever *et al.*, 2002), and the homozygous deletion mutants of these genes in *C. albicans* have not been obtained. To assess their function, therefore, an inducible tetracycline promoter can be used to regulate the expression of each of the genes in heterozygous deletion mutants. Together, results from these experiments will provide clues to the molecular mechanisms underlying the role of genes of the *MTL* locus in biofilm formation.

Regulation of the Mating Response by Far1: Another Piece of Distinction between White and Opaque Pheromone Responses

Although this thesis work has focused primarily on the white cell pheromone response, we recently revisited the role of *FAR1* in the opaque cell pheromone response, because of a report by Cote and Whiteway (2008). Far1 is a cyclin-dependent kinase inhibitor necessary for cell polarization (Butty *et al*., 1998), block in G1 (Chang and Herskowitz, 1990, 1992) and efficient mating (Peter *et al*., 1993; Valtz *et al*., 1995). In that report, they concluded that the *far1* null mutant in *C. albicans* abolishes pheromone induction of all mating-associated genes, and Far1 plays a different role from that in *S. cerevisiae*, in which Far1 is involved in up-regulating some but not all mating-associated genes (Peter *et al.*, 1993; Roberts *et al.*, 2000). In *S. cerevisiae*, deletion of *FAR1* does not affect the upregulation of most of the genes involved in mating, including *STE2*, *MFA1*, and *KAR4* (Roberts *et al.*, 2000). In contrast, Cote and Whiteway (2008) found that in *C.*

albicans, pheromone induction of almost all of the mating genes, including *STE2*, *MFA1*, and *KAR4*, was blocked in opaque cells of the *far1* null mutant. Their results were, however, not consistent with the unpublished northern blot analysis we had performed, which demonstrated that as in *S. cerevisiae*, Far1 regulates only a subset of mating-associated genes in the opaque cell pheromone response. We found that, pheromone induction of some of the genes in the MAP kinase pathway, including *STE4* and *CPH1*, was blocked in the *far1* null mutant, whereas pheromone induction of other genes in this pathway, including *STE2* and *CEK2*, was not blocked in the *far1* mutant. Pheromone induction of other genes that were not part of the MAPK pathway, but were upregulated by pheromone, including *MFA1*, *KAR4* and *SST2*, was also not affected in the *far1* mutant of *C. albicans*. The distinction made by Whiteway and colleagues regarding Far1 function in *S. cerevisiae* and *C. albicans*, was therefore not valid.

What may have caused the discrepancy between these two studies? It seems that the different results Cote and Whiteway (2008) obtained could be due to the genetic background they used. They generated the *far1* mutant in a null mutant of *SST2* (Cote and Whiteway, 2008), which plays a role in desensitization to pheromone signaling (Dignard and Whiteway, 2006). This could have two important consequences that affect pheromone signaling in a *far1* null background. First, it has been shown in *S. cerevisiae* that genes that are upregulated in the *far1* mutant in response to pheromone are also upregulated in the *sst2* mutant without pheromone (Roberts *et al.*, 2000). Second, both in *S. cerevisiae* and in *C. albicans*, deletion of *SST2* leads to a strong induction of the protease gene *BAR1*, which is involved in the degradation of α-pheromone (Roberts *et al.*, 2000; Dignard and Whiteway, 2006). This suggests that the lack of *SST2* can have opposite effects on the pheromone response. Deletion of *SST2* not only hypersensitizes pheromone signaling by stimulating the MAPK pathway, but it also induces a faster degradation of α-pheromone and hence affects pheromone- receptor complexes. As a consequence, the

deletion of *SST2* may mask the regulation of gene expression in response to pheromone in a *far1* mutant (Cote and Whiteway, 2008).

Thesis Conclusion

This thesis has focused on the molecular mechanisms regulating white-opaque switching, mating and biofilm formation, their interdependencies and their significance in the pathogenesis of *C. albicans*. Daniels *et al*. (2006) demonstrated a unique form of communication between the two switch phenotypes, white and opaque, in *C. albicans*, in which minority opaque cells through the release of pheromone signal majority white cells to form an enhanced biofilm. The white cell biofilms in turn facilitate opaque cell chemotropism, an important step in mating. Since we believe that the white cell response to pheromone may provide a key to understanding the essential role white-opaque switching plays in *C. albicans* mating (Daniels *et al*., 2006; Soll, 2008), we found it imperative to test the generality of the white cell response in a wide variety of strains representing all of the major clades of *C. albicans* (Soll and Pujol, 2003), and in a variety of common media. The result is remarkable, because it demonstrates that the white cell response is a general characteristic of all *MTL*-homozygous strains of *C. albicans* and the response occurs in all tested media (Sahni *et al*., 2009a). This thesis work also includes the identification of the signaling pathway regulating this unique white cell pheromone response in *C. albicans* (Yi *et al*., 2008). The results of this study reveal that the pathway regulating the white cell pheromone response shares all of the upstream components, from the receptor through the MAP kinase cascade, with the opaque cell mating pathway. The two pathways bifurcate later at the downstream transcription factor (Yi *et al*., 2008). This discovery is significant, because it represents for the first time in fungi, a configuration in which two distinct cell types utilize the same signal, receptor and signaling pathway to elicit two distinct responses. This configuration is found in a variety of multicellular systems (Rincón and Pedraza-Alva, 2003) and may therefore represent an antecedent to

multicellularity in higher eukaryotes. My thesis work also dissects the role of a unique region (the first intracellular loop IC1) in the *C. albicans* α-pheromone receptor Ste2. Our results demonstrate that this *C. albicans*-specific 55-amino-acid region of the first intracellular loop, IC1, of the α-pheromone receptor Ste2 plays a selective role in the white cell pheromone response. Our work also identified and characterized the *cis*-acting elements in the promoters of genes induced by pheromone in white and opaque cells. Our results demonstrated for the first time a unique *cis*-acting element WPRE in the promoters of white-specific genes distinct from the OPRE, the *cis*-acting element in the promoters of genes induced in opaque cells in response to pheromone (Sahni *et al*., 2009b). Perhaps the biggest breakthrough in this thesis is the identification of the key transcription factor in the white pheromone response pathway, Tec1. A misexpression library screen involving ~103 transcription factors previously implicated in adhesion, filamentation or biofilm formation led to the discovery of Tec1 (Sahni *et al*., in preparation). Tec1 is induced only in white cells in response to pheromone and functions through the MAP kinase pathway. Moreover, Tec1 also binds to the WPRE in the promoters of genes induced in white cells in response to pheromone. This discovery has several ramifications in terms of the evolution of the white cell pheromone response. It seems striking that the white cell response is a relatively recent developmental program that has borrowed all of the components from several ancestral pathways. The white response pathway has borrowed the upstream components from the receptor through the MAP kinases from the opaque mating pathway, the transcription factor Tec1 from the filamentation pathway and the downstream target genes from the biofilm pathway of **a**/α cells. This pathway therefore offers a unique insight into the evolution of a new signal transduction pathway.

APPENDIX A

CO_2 REGULATES WHITE-TO-OPAQUE SWITCHING IN *CANDIDA ALBICANS*

Guanghua Huang, Thyagarajan Srikantha, Nidhi Sahni, Song Yi and David R. Soll

Introduction

A majority of natural strains of *Candida albicans* are heterozygous (***a***/α) at the mating type (*MTL*) locus (Lockhart *et al*., 2002; Legrand *et al*., 2004; Tavanti *et al*., 2005). To mate, ***a***/α cells must undergo homozygosis to ***a***/***a*** or α/α (Hull and Johnson, 1999; Hull *et al*., 2000; Magee and Magee, 2000), and switch from white to opaque (Miller and Johnson, 2002).

However, the mating-competent opaque cells are unstable at physiological temperature (37 °C) (Slutsky *et al*., 1987; Soll, 2004; Rikkerink *et al*., 1988; Srikantha and Soll, 1993). This leads to the paradox that if white-opaque switching and mating are important for commensalism and pathogenesis, then opaque cells should not be unstable *in vivo*. Some characteristic of the host environment should stabilize the opaque phenotype at physiological temperature and block opaque cell switching to white.

Two observations led us to test the hypothesis that it was the high CO_2 level in the host that served this role. First, we had observed that when a petri dish containing a low density agar culture of *C. albicans* was wrapped with parafilm, and then incubated for extended periods of time, opaque sectors formed around the rim of each colony (Soll, 1991), suggesting that the accumulation of a gas, most likely CO_2, stimulated switching. Second, the level of CO_2, which is relatively low in air (~0.03%) (Stenni *et al*., 2001), accumulates in the gut of a host to levels of 4.5 to 30% (Levitt and Bond, 1970; Avunduk, 2002), and in the tissue to approximately 5% (Guyton and Hall, 2000). We hypothesized that high levels of CO_2 in the host might stabilize the opaque phenotype at physiological temperature. Here, we demonstrate that CO_2 at physiological levels not only stabilizes the

opaque phenotype at 37 °C, but also induces switching from white to opaque, inhibits switching from opaque to white, and facilitates mating.

Deletion of carbonic anhydrase, the enzyme that catalyzes the interconversion of CO_2 and HCO_3^- results in a decrease in the CO_2 effect at low, but not high, CO_2 concentrations. Finally, deletion of the master switch locus for the white-opaque transition, *WOR1* (Huang *et al*., 2006; Zordan *et al*., 2006) or *TOS9* (Srikantha et al., 2006), results in the loss of CO_2-induced switching, indicating that CO_2 may function through the master switch locus.

I along with the senior author Guanghua Huang played an important role in this study. I participated in majority of the switching and mating experiments. I was also involved in northern blot analysis of phase-specific gene expression. This work is discussed as one section of the appendix in my thesis (Appendix A).

Materials and Methods

Strain Maintainence

The strains used in this study are described in Table A1. The mutant *nce103*/*nce103* was grown in 99% air, 1% CO_2 in a CO_2 incubator. Strain WO-1 (FC4) was used in all experiments.

Mutant Construction

The genes *NCE103* and *CDC35* were independently deleted in *C. albicans* by a PCR product-directed disruption strategy (Wilson *et al*., 1999). The host strain BWP17, auxotrophic for *ura3, his1* and *arg4*, and the plasmids pRS-ARG4ΔSpeI, pGEM-HIS1 and pDDB57 required for creating the disruption cassettes, were generously provided by Aaron P. Mitchell of Carnegie Mellon University, Pittsburgh, PA (Wilson *et al*., 1999). Prior to the construction of *NCE103* and *CDC35* homozygous deletion mutants, the parental strains BWP17, which was heterozygous (***a***/*α*) at the *MTL* locus, was converted to ***a***/***a*** by sorbose

Table A1**.** Strains used in the study of CO_2 effect on switching

Strain	Parent strain	Genotype	Reference
WO-1 (FC4)		*MTLα/α WOR1/WOR1*	Slutsky *et al.* (1987)
WO-1 (Soll 1)		*MTLα/α WOR1/WOR1/WOR1*	Ramirez-Zavala *et al.* (2008)
P37005		*MTL**a**/**a***	Lockhart *et al.* (2002)
P97099		*MTLα/α*	Pujol *et al.* (2002)
P78048		*MTLα/α*	Lockhart *et al.* (2002)
GH1012	CAI4	*MTL**a**/**a** ura3::1 imm434/ ura3::1 imm434*	This study
3UM5A	P37005	*MTL**a**/**a** ura3-1Δ::FRT/ura3-2 Δ::FRT*	This study
WUM5A	WO-1	*MTLα/α ura3-1 Δ::FRT/ura3-2 Δ::FRT*	Strauss *et al.* (2001)
TOHO3	WUM5A	*MTLα/α ura3-1 Δ::FRT/ura3-2 Δ::FRT wor1Δ::FRT/wor1Δ::FRT*	Srikantha *et al.* (2006)
CAI4	SC5314	*MTL**a**/α ura3::1 imm434/ ura3::1 imm434*	Fonzi and Irwin (1993)
GH1060	CAI4	*mtl**a**:: dpl200 ura3::1 imm434/ ura3::1 imm434*	This study
BWP17	CAI4	*MTL**a**/α ura3::1 imm434/ura3::1 imm434 his1::hisG/his1::hisG arg4::hisG/arg4::hisG*	Wilson *et al.* (1999)
GH1013	BWP17	*MTL**a**/**a** ura3::1 imm434/ura3::1 imm434 his1::hisG/his1::hisG arg4::hisG/arg4::hisG*	This study
CHY477	CAI4	*MTLα/mtl**a**1::hisG ura3::1 imm434/ ura3::1 imm434 ade2::hisG-URA3-hisG/ade2::hisG*	Miller and Johnson (2002)
MMY278	CAI4	*MTL**a**/mtlα1::hisG mtlα2::hisG ura3::1 imm434/ ura3::1 imm434 ade2::hisGURA3hisG/ade2::hisG*	Miller and Johnson (2002)
CAN52	CAI4	*MTL**a**/α ras1* : : *hisG*/*ras1* : : *hph ura3* : : *imm434*/*ura3* : : *imm434*	Feng *et al.* (1999)
GH1120	CAN52	*MTLα/mtl**a**:: dpl200 ras1* : : *hisG*/*ras1* : : *hph ura3* : : *imm434*/*ura3* : : *imm434*	This study
GH1109	GH1013	*MTL**a**/**a** ura3::1 imm434/ura3::1 imm434 his1::hisG/his1::hisG arg4::hisG/arg4::hisG cdc35:: ARG4/ cdc35:: HIS1*	This study

Table A1 --- continued

GH1102	GH1013	*MTL**a**/**a** ura3::1 imm434/ura3::1 imm434 his1::hisG/his1::hisG arg4::hisG/arg4::hisG nce103:: ARG4/ nce103:: HIS1*	This study
GH1102V	GH1102	*MTL**a**/**a** ura3::1 imm434/ura3::1 imm434 his1::hisG/his1::hisG arg4::hisG/arg4::hisG nce103:: ARG4/ nce103:: HIS1 ADE/ade2::URA3-pACT*	This study
GH1102N	GH1102	*MTL**a**/**a** ura3::1 imm434/ura3::1 imm434 his1::hisG/his1::hisG arg4::hisG/arg4::hisG nce103:: ARG4/ nce103:: HIS1 ADE/ade2::URA3-pACT-NCE103*	This study
WCZF1M4B	WO-1 (Soll 1)	*MTLα/α czf1::FRT/czf1::FRT*	Ramirez-Zaval a *et al.* (2008)
SC5314		*MTL**a**/α*	Strauss *et al.* (2001)
5314a	SC5314	*MTL**a**/**a***	This study
5314α	SC5314	*MTLα/α*	This study

(Sou+) selection on YEPS medium (yeast extract – peptone + 2% sorbose) (Magee and Magee, 2000; Janbon *et al*., 1998). The heterozygous *nce103/NCE103* mutant was constructed by transforming GH1013, the ***a/a*** derivative of BWP17, with the *NCE103* disruption cassette containing selectable *ARG4* marker. The cassette was amplified by PCR with pRS-ARG4ΔSpeI as template and the primers NCE103-5DR and NCE103-3DR (Table A2). The disruption primers contained a 60 nucleotide sequence homologous to a sequence in *NCE103*, and a 20 nucleotide sequence homologous to the selectable gene in the marker plasmid. The homozygous mutant *nce103/nce103,* referred to as *nce103/nce103,* was constructed by transforming the heterozygous derivative with a PCR-derived disruption cassette containing the *HIS1* marker using pGEM-HIS1 as template and the primers NCE103-5DR and NCE103-3DR (Table A2). To select the homozygous mutant, transformed cells were cultured in 1% CO_2, because the *NCE103* null derivative had been shown to be inviable in air (Klengel *et al*., 2005). Mutant strains were verified by PCR.

To complement the *nce103/nce103* mutant, the *NCE103* ORF was cloned under the control of *C. albicans ACT1* promoter. The plasmid, pACT1, was constructed as described previously (Huang *et al*., 2006). In brief, pACT1 was first constructed by cloning the PCR amplified promoter of *C. albicans ACT1*, using CAI4 genomic DNA as template and the primers ACT1pF and ACT1pR (Table A2) for the polymerase chain reaction. PCR products were digested and subcloned into the PstI-EcoRV site of the vector BES116 (Feng *et al*., 1999), yielding pACT1. p*ACT1-NCE103* was constructed by PCR amplification of the *NCE103* coding region with primers NCE103F and NCE103R (Table A2), and subcloning the PCR fragment into the EcoRV-HindIII site of pACT1. The plasmid p*ACT1-NCE103* was digested with AscI and used for targeted transformation into the null mutant *nce103*/ *nce103* at the *ADE2* locus.

To generate a *CDC35* null mutant, the primers CDC35-5DR and CDC35-3DR (Table A2) were used to amplify the *HIS1* and *ARG4* selectable markers from the

Table A2. Primers used in the study of CO_2 effect on switching

Name	Sequence	Purpose and features
NCE103F	5′-tcatccGATATCATGGGTAGAGAAAATATTTTGAAATA-3′	pACT-*NCE103*
NCE103R	5′-tcattgAAGCTTTCAATGAGGGTTATATTCTTCTTC-3′	
NCE103-5DR	5′-ATGGGTAGAGAAAATATTTTGAAATATCAATTGGAACATGATCATGAATCTGATCTTGTTGTTTTCCCAGTCACGACGTT-3′	*NCE103* knockout
NCE103-3DR	5′-TCAATGAGGGTTATATTCTTCTTCATCATGTTCATCATGAACATGGAATAAATCCTCAAATGTGGAATTGTGAGCGGATA-3′	
CDC35-5DR	5′-AGTTTTTTAAGGAGAGATAAATCTAAAGCCAACTTTAGAGATGGTTCAGCTACTGGATTAGTTTTCCCAGTCACGACGTT-3′	*CDC35* knockout
CDC35-3DR	5′-CAAAAACAATGTTGTGGTACAACTTTCAATTCTAGTTGTAACGTGATTGAGCAATGAGATGTGGAATTGTGAGCGGATA-3′	
ACT1pF	5′ -AACTGCAGCCTCGTTTATAATAAACTTAGTC-3′	pACT1
ACT1pR	5′ -CCGATATCCATTTTGAATGATTATATTTTTTTAA-3′	
WOR1pF	5′ -CAAGTTCAATAGTGAAGTTTC-3′	*WOR1* probe
WOR1pR	5′-CACTGGTATTAGAACTAGTAAC-3′	
WH11pF	5′- ATGTCCGACTTAGGTAGAAAAG-3′	*WH11* probe
WH11pR	5′-TTATTTGGAGTCACCAAAAATAGC-3′	
OP4pF	5′- ATGAAGTTTTCACAAGCCACC-3′	*OP4* probe
OP4pR	5′- CAGAGTTCCAGACAGCTTGG-3′	
EFG1pF	5′- ATGTCAACGTATTCTATACCC-3′	*EFG1* probe

Table A2 --- continued

EFG1pR	5′-CAACGTATCCTGAACAGGAG-3′	
MTL**a**F	5′-TTGAAGCGTGAGAGGCTAGGAG -3′	*MTL**a***
MTL**a**R	5′-ATCAATTCCCTTTCTCTTCGATTAGG-3′	
MTL*α*F	5′-TTCGAGTACATTCTGGTCGCG -3′	*MTLα*
MTL*α*R	5′-TGTAAACATCCTCAATTGTACCCGA-3′	
MTL**a**-5DR	5′-TTTATAGTTAGAGTTTGCTATTTAATATCAAATTA TAAATACGAGAAAGCACATGCAAAAGTTTTCCCAGTCACGACG TT-3′	*MTLa1a2* knockout
MTL**a**-3DR	5′-TTAGTTAGCAATATTCTGTTTGATAATACATACCCAAACTCT TAT TTGGGAAAGGCTAACTGTGGAATTGTGAGCGGATA-3′	

plasmids pGEM-HIS1 and pRS-ARG4ΔSpeI, respectively. Unlike the strategy used to create *NCE103* deletion, *HIS1* selection was used first to derive the *cdc35*/*CDC35* heterozygous mutant, ARG4 selection to generate the homozygous null mutant *cdc35*/*cdc35*. Mutants were verified by PCR.

To generate a *RAS1* null mutant in an *MTL*α strain, the entire *MTL***a** locus was deleted by a PCR product-directed disruption strategy in strain CAN52, a *ras1*/*ras1* mutant (Feng *et al*., 1999). The primers *MTL***a**-5DR and *MTL***a**-3DR (Table A2) were used to generate the disruption cassette containing the *URA3* marker from the plasmid pDDB57.

White-opaque Switching Assays

White-opaque switching on agar was analyzed as described previously, with a slight modification (Anderson and Soll, 1987). For white-to-opaque switching, the strains were streaked on supplemental Lee's medium (Bedell and Soll, 1979) containing phloxine B (Anderson and Soll, 1987) and cultured in air for 5 days. Cells of homogenous white colonies were resuspended, plated onto Lee's medium plates, and incubated at 25 °C for six days. For opaque to white switching, the strains were streaked on supplemental Lee's medium containing phloxine B and cultured in air for six days. Cells of homogeneous opaque colonies cultured in 20% CO_2 were resuspended, plated and incubated at 25 °C for six days. For mass conversion experiment, opaque cells were plated and cultured at 37 °C for six days.

White and opaque switching in suspension was analyzed by resuspending cells in Lee's medium and diluting the cultures to 2 x 10^5 cells/ml 10 ml of diluted cells were incubated in an 80 ml beaker with constant stirring at 37 °C. Aliquots were removed, diluted and replated onto Lee's medium plates at varying time points. Plates were cultured at 25 °C for six days and the proportion of white, opaque and sectored colonies counted.

Mating Assays

Mating assays were performed according to Miller *et al.* (2002), as previously described (Srikantha *et al*., 2006). Mating assays between *C. albicans MTL***a** and *MTLα* strains were performed on supplemented in Lee's medium. Mixtures were incubated at 25 °C for six days. Cells were then suspended and replated onto selection media lacking either adenine or uridine, or both. The former media finished counts of parent colonies, and the last media selected for conjugants.

Northern Analysis

Northern blot analysis was performed as previously described (Srikantha *et al*., 2006). Total RNA from *C. albicans* cells was used. PCR products were used to probe the Northern blots. Primers used for generating the PCR products are listed in Table A2.

Results

CO_2 Stimulates White to Opaque Switching

Because wrapping a plate inhibits gas exchange and would lead to an increase in CO_2 in the space above the agar if metabolism of the cultures were aerobic, we first tested the possibility that an increase in CO_2 tension in the air surrounding an agar culture at 25 °C would stimulate white to opaque switching. Five homozygous strains of *C. albicans* were incubated in 5% CO_2 at 25 °C. The switching frequency measured as the proportion of white colonies with opaque regions or opaque colonies, was 4-16 fold higher than in air (Figure A1A, B). When plated and incubated in 20% CO_2 , the frequency was 10 to 105 fold higher than in air. CO_2 also induced switching at 37°C (Figure A2). Variability existed between strains, but switching was induced in all five test strains (Figure A1B).

CO_2 Blocks Opaque to White Switching

To test whether increased levels of CO_2 inhibited spontaneous switching from opaque to white, opaque cells of the same of five natural *MTL*-homozygous strains were

Figure A1. High Concentrations of CO_2 Induce Switching from the White, Wh, to Opaque, Op, phenotype in *C. albicans*. White cells of either *α/α* or ***a/a*** strains were plated on agar and then incubated in air, which contained 0.03% CO_2, air (95%) containing 5% CO_2, or air (80%) containing 20% CO_2. The agar contained phloxine B, which stained opaque colonies or opaque regions of white colonies red. (A) Representative fields of colonies for one *α/α* (WO-1, FC4) and one ***a/a*** strain (GH1012). (B) Quantitation of the frequency of switching measured as the proportion (%) of total colonies that were white with opaque regions or predominately opaque. The total number of colonies is the sum of three experiments. The "% Op colonies or Wh colonies with Op regions" represents the mean for the three experiments ± standard deviation. The fold difference with air is presented for the means at 5% and 20% CO_2. The p values calculated by the Student's two-tailed t test for switching frequencies in 5% and 20% CO_2 compared with those in air were all less than 0.05.

A

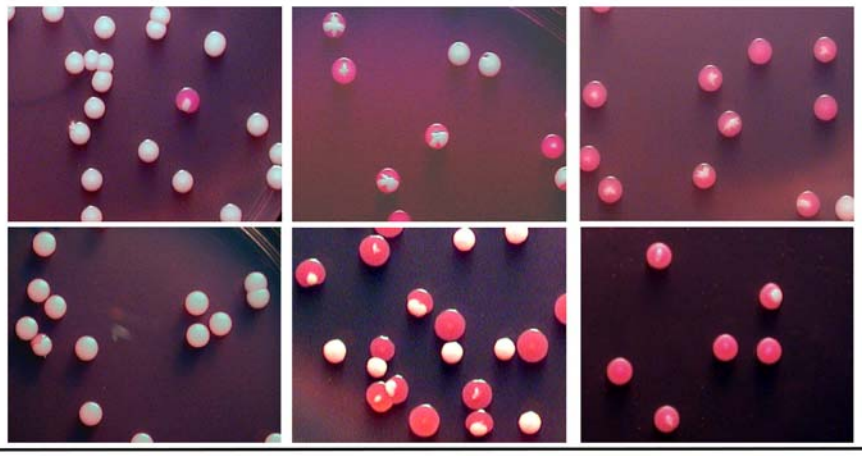

B Quantitation

Strain	*MTL* genotype	Air (0.03% CO_2) Total colonies	Air (0.03% CO_2) %Op colonies or wh colonies with op regions	5% CO_2 Total colonies	5% CO_2 %Op colonies or wh colonies with op regions	20% CO_2 Total colonies	20% CO_2 %Op colonies or wh colonies with op regions
WO-1	α/α	1379	5.4 ± 1.6	1101	88.8 ± 1.9 (16 x)	957	93.5 ± 3.0 (17 x)
GH1012	**a/a**	1300	9.1 ± 1.6	989	84.9 ± 2.2 (9 x)	720	90.6 ± 2.7 (10 x)
P37005	**a/a**	2677	0.9 ± 0.4	1811	6.6 ± 1.2 (7 x)	772	53.4 ± 3.0 (59 x)
P97099	α/α	1340	0.9 ± 0.5	1286	6.1 ± 0.7 (7 x)	690	94.5 ± 3.5 (105 x)
P78048	α/α	1170	0.6 ± 0.2	950	2.3 ± 0.3 (4 x)	690	20.3 ± 2.5 (34 x)

Figure A2. CO_2 stimulates switching from white to opaque at 37°C. White cells of strain WO-1 were plated on agar containing supplemented Lee's medium and cultured at 25°C in air (A), and 37°C in air (B), and 37°C air containing 5% CO_2 (C). After 48 hrs, the microcolonies were washed from the plates and replated at 25°C in air for five days. Percentages of opaque colonies are indicated on the bottom of the figure.

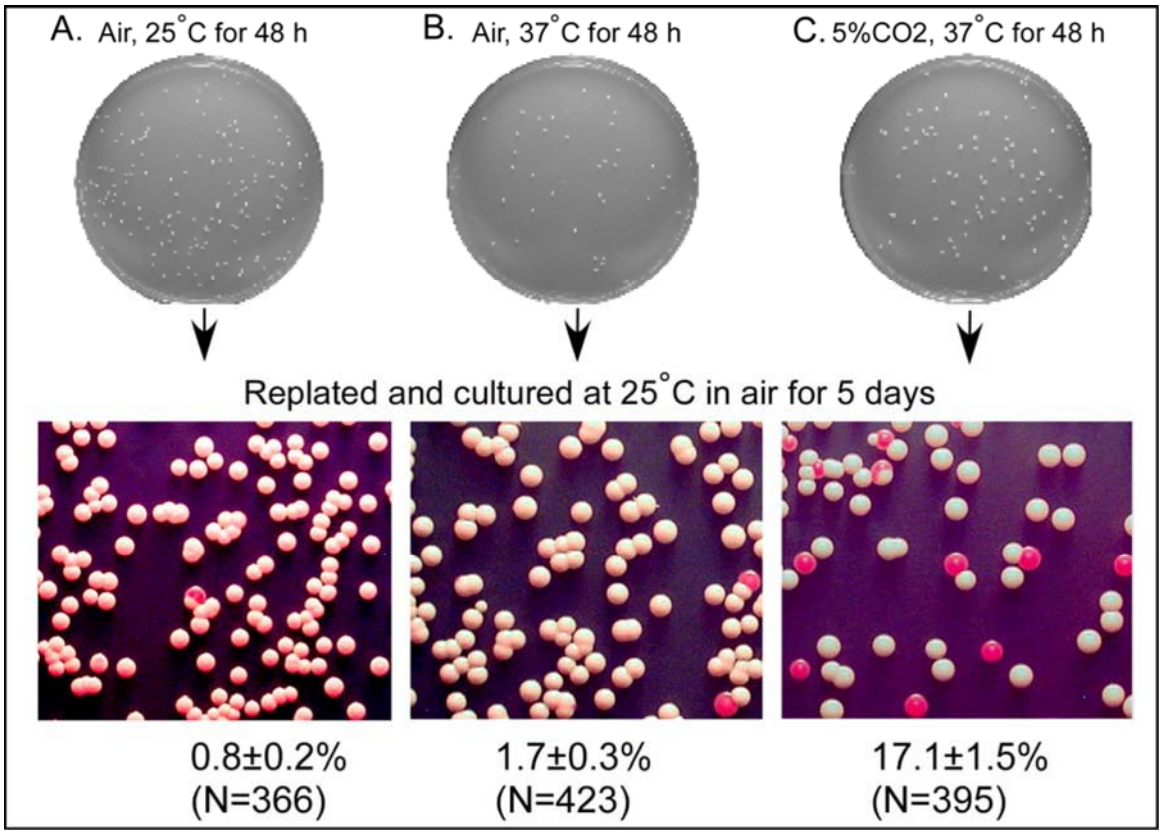
A. Air, 25°C for 48 h
B. Air, 37°C for 48 h
C. 5%CO2, 37°C for 48 h
Replated and cultured at 25°C in air for 5 days
0.8±0.2%
(N=366)
1.7±0.3%
(N=423)
17.1±1.5%
(N=395)

plated on nutrient agar and incubated, in air or 5% CO_2. Two of these strains (WO-1, GH1012) exhibited moderate rates of switching after 6 days in air (0.8 and 2.0% sectored colonies, respectively) (Figure A3A), whereas three (P37005, P97099, P78048) exhibited high rates (40 to 96%) (Figure A3A). In 5% CO_2, the rates were below 0.5% for all five strains (Figure A3A). These results demonstrate that 5% CO_2 blocks spontaneous switching from opaque to white at 25 °C.

When the temperature of opaque cultures is raised from 25 °C to 37 °C, mass conversion occurs to the white phenotype (Figure A3B) (Slutsky *et al*., 1987; Soll, 2004; Rikkerink *et al*., 1988; Srikantha and Soll,1993). For strains WO-1 and GH1012, 100 and 98% of plated opaque cells formed white colonies or opaque colonies with white sectors after 6 days (Figure A3B). Increasing the temperature to 37 °C in the presence of 5% CO_2, however, reduced the frequency of colony sectoring in strain WO-1 and GH1012 to 2 and 6%, respectively, reduction of 53 and 18 fold, respectively. In 5% CO_2, however, both white and opaque cells multiplied, and maintained their respective phenotypes (Figure A3C).

Phase-specific Gene Expression

Switching is also accompanied by the expression of phase-specific gene (Lan *et al*., 2002; , Srikantha and Soll, 1993; Morrow *et al*., 1992, Morrow et al., 1993). To verify that the induction of white to opaque switching by CO_2 included the transition from white to opaque gene expression, we analyzed the expression patterns of two white-specific genes, *WH11* (Srikantha and Soll, 1993) and *EFG1* (Sonneborn *et al*., 1999; Srikantha *et al*., 2000), and two opaque-specific genes, *OP4* (Morrow *et al*., 1993) and *TOS9 (WOR1)* (Huang *et al*., 2006; Zordan *et al*., 2006; Srikantha *et al*., 2006) in agar cultures of strain WO-1 incubated at 25 °C in air, 5% CO_2 and 20% CO_2. After 72 hours of incubation in air, the transcript levels of both white-specific genes *WH11* and *EFG1* remained high, and the transcript levels of both opaque-specific genes *OP4* and *TOS9* remained negligible

Figure A3. CO_2 Stabilizes the Opaque Phenotype at 25° and 37°C and Does Not Interfere with Cell Multiplication. (A) Opaque cells of ***a/a*** and *α/α* cells were plated on agar and monitored for switching The p values calculated by the Student's two-tailed t test of the switching frequencies of P37005, P97099, and P78048 in 5% CO_2 compared with those in air were less than 0.05. The data are the mean and standard deviation of three independent experiments. (B) Opaque cells were plated at 37°C and analyzed for switching to white. The p values calculated by the Student's two-tailed t test of WO-1 and GH1012 in 5% CO_2 compared with those in air were less than 0.05. The data are the mean and standard deviation of three independent experiments. (C) White or opaque cells were grown in liquid cultures at 37°C in air or air containing 5% CO_2, and monitored for cell number and cell phenotype. Cell phenotype was monitored by plating aliquots at time intervals and counting the proportion of colonies with regions of alternative phenotype. The data points and error bars represent the mean and standard deviation of three experiments.

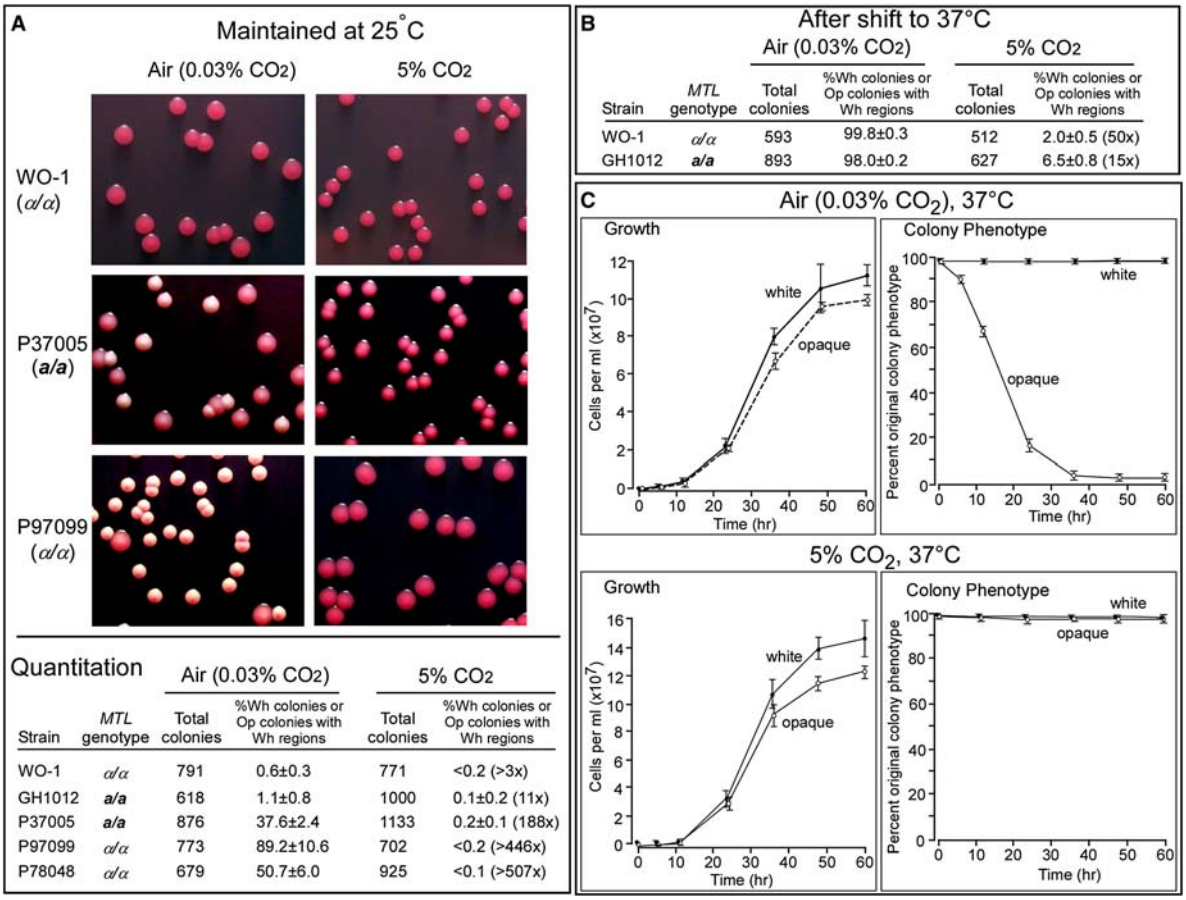

Quantitation

Strain	*MTL* genotype	Air (0.03% CO_2) Total colonies	Air (0.03% CO_2) %Wh colonies or Op colonies with Wh regions	5% CO_2 Total colonies	5% CO_2 %Wh colonies or Op colonies with Wh regions
WO-1	α/α	791	0.6±0.3	771	<0.2 (>3x)
GH1012	**a/a**	618	1.1±0.8	1000	0.1±0.2 (11x)
P37005	**a/a**	876	37.6±2.4	1133	0.2±0.1 (188x)
P97099	α/α	773	89.2±10.6	702	<0.2 (>446x)
P78048	α/α	679	50.7±6.0	925	<0.1 (>507x)

B

Strain	*MTL* genotype	Air (0.03% CO_2) Total colonies	Air (0.03% CO_2) %Wh colonies or Op colonies with Wh regions	5% CO_2 Total colonies	5% CO_2 %Wh colonies or Op colonies with Wh regions
WO-1	α/α	593	99.8±0.3	512	2.0±0.5 (50x)
GH1012	**a/a**	893	98.0±0.2	627	6.5±0.8 (15x)

(Figure A4). However, after 72 hours of incubation in 5 or 20% CO_2, the transcript levels of both white-specific genes had decreased to negligible levels, and the transcript levels of both opaque-specific genes increased to high levels (Figure A4). These results demonstrate that CO_2 stimulation of white to opaque switching is accompanied by down-regulation of white-specific genes and up-regulation of opaque-specific genes.

CO_2 Facilitates Mating

Since CO_2 both induces switching from white to opaque and stabilizes the opaque phenotype, we predicted that mating would be enhanced in mixtures of white ***a/a*** (or ***a/-***) and white α/α ($-/\alpha$) cells incubated in 5% CO_2. To measure the frequency of mating, crosses were performed between ***a/a*** (or ***a/-***) and α/α ($-/\alpha$) auxotrophs, and the frequency of complementation measured. Two sets of strains were tested for mating, WUM5A (α/α, *ura3*$^-$) X MMY278 (***a/-***, *ade2*$^-$), and CHY477 ($-/\alpha$, *ade2*$^-$) X 3UM5A (***a/a***, *ura3*$^-$) (Table A1). All variations of white and opaque phenotypes of both strains were tested in crosses. For white WUM5A X white MMY278 cross, the efficiency of mating was 9.6×10^{-9} in air and 5.6×10^{-6} in 5% CO_2, and for the white CHY477 X white 3UM5A cross, 3.8×10^{-9} and 1.5×10^{-6}, respectively (Table A3). This represented increases of 583 and 395 fold (Table A3). Small or negligible increases were observed when opaque cells were used in one or both crosses (Table A3). These results demonstrate that 5% CO_2 increases the efficiency of mating between populations of white ***a/a*** and white α/α cells by over three orders of magnitude.

Carbonic anhydrase, Adenylate cyclase and Ras1 in Switching

Carbonic anhydrase (CA) catalyzes the interconversion of CO_2 to carbonic acid (HCO_3^-). Deletion of the gene for carbonic anhydrase, *NCE103*, in *C. albicans* has been shown to block growth in air, but not in air supplemented with 5% CO_2 (Klengel *et al*., 2005). These previous observations suggested that CA might play a role in the induction

Figure A4. CO_2-Induced Switching from White to Opaque Is Accompanied by Downregulation of White-Specific and Upregulation of Opaque-Specific Genes. Northern blot hybridization was performed for white- and opaque-specific genes in white cell cultures of strain WO-1 for 0.5, 1, 2, and 3 days on agar in air, air containing 5% CO_2, or air containing 20% CO_2. The ethidium-bromide-stained 18S ribosomal RNA bands are shown to demonstrate equal loading of lanes.

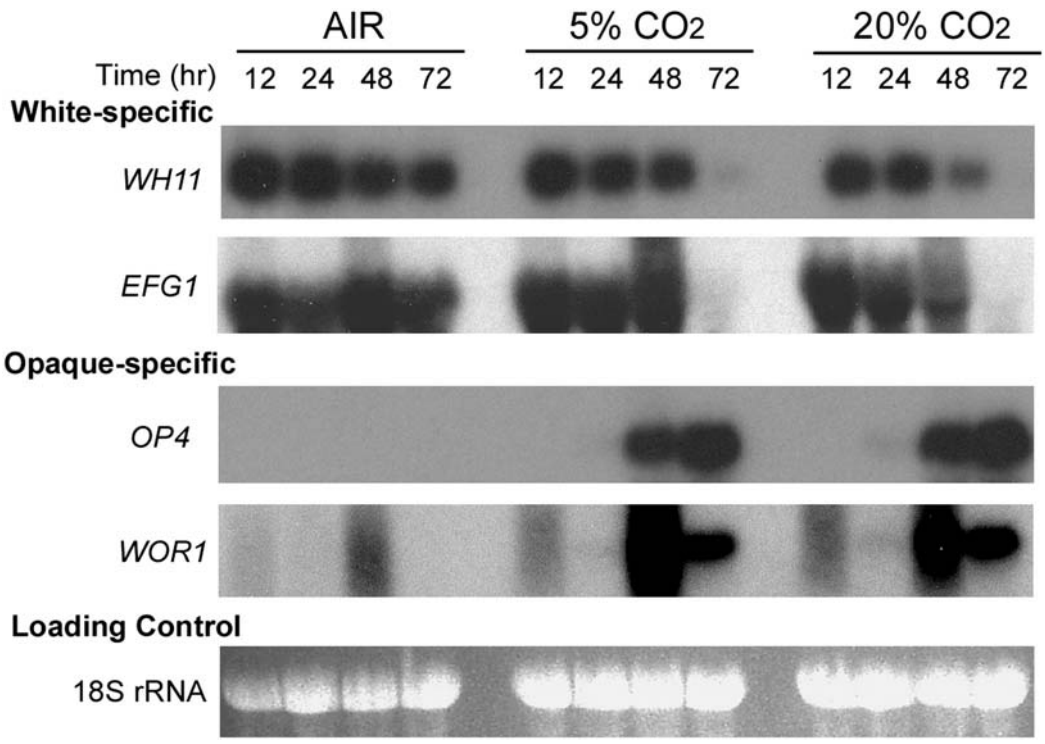
AIR
5% CO2
20% CO2
Time (hr)
12 24 48 72
12 24 48 72
12 24 48 72
White-specific
WH11
EFG1
Opaque-specific
OP4
WOR1
Loading Control
18S rRNA

Table A3. CO_2 increases the efficiency of mating between initially white populations of opposite mating type

Strains and genotypes	Cross phenotypes[a] WUM5AxMMY278		Mating efficiency in air (0.03% CO_2)	Mating efficiency in 5% CO2	Fold increase in 5% CO_2
WUM5A	Wh	Wh	9.6×10^{-9}	5.6×10^{-6}	583
(*α/α ura3-*)	Op	Wh	3.1×10^{-4}	1.2×10^{-3}	4
X	Wh	Op	3.5×10^{-5}	4.5×10^{-5}	1
MMY278 (***a****/αΔ ade2-*)	Op	Op	1.6×10^{-1}	1.7×10^{-1}	1
	CHY477 x 3UM5A				
CHY477	Wh	Wh	3.8×10^{-9}	1.5×10^{-6}	395
(***a****Δ/α ade2-*)	Op	Wh	1.2×10^{-5}	3.4×10^{-5}	3
X	Wh	Op	1.1×10^{-5}	9.6×10^{-4}	87
3UM5A (***a****/**a** ura3-*)	Op	Op	4.5×10^{-2}	5.6×10^{-1}	12

Note: Mating was quantitated according to the methods of Miller and Johnson (2002). Strains were mixed and incubated at 25 °C for six days on modified Lee's medium (Bedell and Soll, 1979).

of switching by CO_2 at low CO_2 concentrations (e.g., 0.03 or 1% CO_2), but not at high CO_2 concentrations (e.g., ≥ 5% CO_2). To test this prediction, we generated the deletion mutant *nce103Δ* in the *ura3⁻his1⁻arg4⁻* strain GH1013, a derivative of BWP17 (Wilson *et al*., 1999), the complemented strain *nce103*/*ACTp-NCE103*, in which *NCE103*, under the regulation of the actin promoter, was targeted to one of the two *ADE2* alleles, and *nce103*/*nce103*+vector, a control for the complemented strain, in which the mutant *nce103/nce103* was transformed with the vector lacking *NCE103*. As previously demonstrated (Klengel *et al*., 2005), we found that cells of the mutant *nce103/nce103* could not grow in air, but could grow in wrapped cultures or in cultures incubated in 5% CO_2 (Figure A5A). To test if CO_2 induced white to opaque switching in this mutant, white cells were first grown on agar in 1% CO_2, then cells from white colonies were plated at 1 or 5% CO_2. In 1 and 5% CO_2, 96 and 99% of wild type, and 93 and 98% of the complemented strain *nce103/ACTp-NCE103* formed opaque colonies or white colonies with outer opaque region (Figure A5B). In marked contrast, at 1% CO_2, only 21% of colonies formed by the mutant *nce103*/*nce103* and only 16% of those formed by the mutant transformed only with vector, were opaque or possessed an outer opaque region (Figure A-5B). At 5% CO_2, however, 97 and 99%, respectively, of the colonies of these mutant strains were opaque or possessed an outer opaque region (Figure A5B). These results indicate that carbonic anhydrase facilitates switching, at low (1%) but not high (≥ 5%) CO_2 levels. In 2005, Klengel *et al*. demonstrated that CO_2 induced the bud-hypha transition by stimulating adenylyl cyclase. This cAMP-dependent pathway in turn required Ras1. We therefore tested the CO_2 effect on switching in null mutants of the adenylyl cyclase gene (*CDC35*) and *RAS1*. In both the mutants, the switching frequency was lower than that of the control strain in air (Figure A5C). At 20% CO_2, however, switching was maximal, as in control cells (Figure A5C). Therefore, both adenylyl cyclase and Ras1, like carbonic anhydrase, enhanced switching in air and enhanced induction by low but not high concentrations of CO_2.

Figure A5. CO_2 Induction of Switching from White to Opaque in Null Mutants of Carbonic Anhydrase, Adenylate Cyclase, *RAS1*, the Master Switch Locus *WOR1*, and the Transcription Regulator *CZF1*. The representative mutants were *nce103/ nce103*, *cdc35/ cdc35*, *ras1/ ras1*, *wor1/ wor1*, and *czf1/ czf1*. (A) Agar cultures demonstrating that the *nce103/ nce103* mutant does not grow in air, but does grow in 5% CO_2.(B) Representative fields of colonies formed by white cells of parent strain GH1013 and *nce103/ nce103* in air containing 1% or 5% CO_2. Fields of control strains *nce103/ nce103*+*pACT-NCE103* (the complemented *nce103/ nce103* mutant) and *nce103/ nce103*+vector (*nce103/ nce103* transformed only with the vector) are also presented. (C) The switching frequencies of the tested mutants, wild-type controls, and an ***a****/α* control, monitored. The data are the mean and standard deviation of three independent experiments.

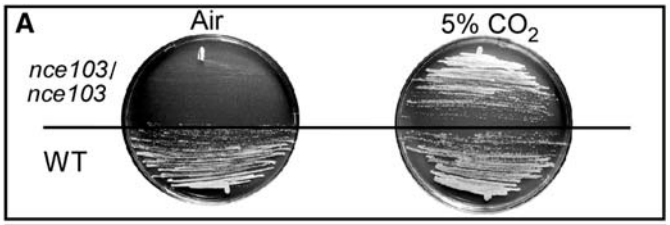

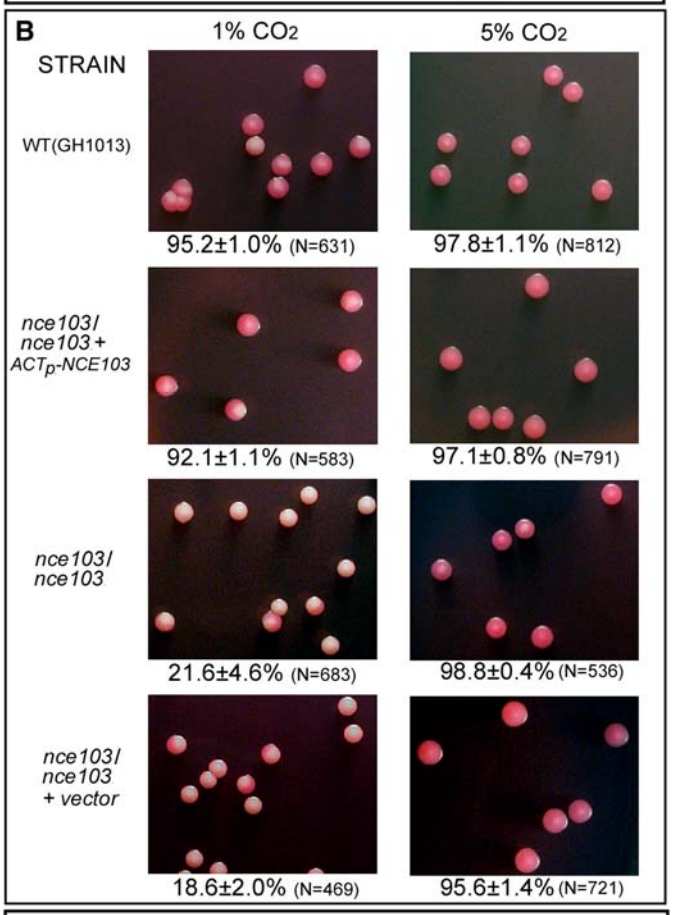

C

Strain	% op colonies or colonies with op regions		
	Air (0.03% CO_2)	1% CO_2	20% CO_2
WT(GH1013)	1.7 ± 0.7	21.9 ± 4.6	97.2 ± 1.0
ras1/ras1	0.8 ± 0.7	3.4 ± 0.5	90.4 ± 3.4
cdc35/cdc35	0.03 ± 0.05	0.3 ± 0.3	97.6 ± 0.8
WO-1(Soll1)	4.4 ± 1.1	19.5 ± 5.3	97.2 ± 1.3
czf1/czf1	0.1 ± 0.1	3.3 ± 0.8	34.0 ± 3.0
wor1/wor1	0.0 ± 0.0	0.0 ± 0.0	0.0 ± 0.0
SC5314(***a/α***)	0.0 ± 0.0	0.0 ± 0.0	0.0 ± 0.0
5314**a** (***a/a***)	0.4 ± 0.6	16.3 ± 3.4	98.2 ± 1.7
5314α(*α/α*)	0.6 ± 0.5	9.8 ± 2.9	99.4 ± 1.1

TOS9 (*WOR1*) and *CZF1*

TOS9 (WOR1) has been demonstrated to be the master switch locus for white-opaque switching (Huang *et al*., 2006; Zordan *et al*., 2006; Srikantha *et al*., 2006). Cells of *TOS9 (WOR1)* deletion mutants are blocked in the white phase and cells of a *TOS9* overexpression mutant accumulate in the opaque phase. If CO_2 stimulation of the white to opaque switch requires *TOS9 (WOR1)*, then switching from white to opaque in the deletion mutant *tos9*/*tos9*, which was generated in strain WUM5A (Srikantha *et al*., 2006), should not be stimulated by 5% CO_2. In 5% CO_2, over 80% of colonies formed from white cells of the control strain WUM5A were opaque or contained an opaque region after six days (Figure A5C), but zero percent of colonies formed from white cells of the mutant *tos9*/*tos9* were opaque or contained an opaque region (Figure A5C). Therefore, CO_2 induction of white to opaque switching requires *TOS9*. CO_2, did however, induce switching in white cells of *czf1*/*czf1* deletion mutant, but the induced frequencies in 1% and 20% CO_2 were lower than that of control cells, as was the basal frequency in air (Figure A5C). As expected, CO_2 did not induce switching in **a**/α cells (Figure A5C).

CO_2 and O_2

To address whether hypoxia alone can stimulate switching, white cells were plated and incubated in either N_2 (99.97%) containing no O_2 and 0.03% CO_2, or N_2 (99.47%) containing 0.5% O_2 (a 40-fold reduction from that in air). Rather than stimulating switching, the frequency was reduced 8 and 12 fold respectively, from that in air (Table A4). When white cells were plated and incubated in either N_2 (90%) containing no O_2 and 10% CO_2, or N_2 (89.75%) containing 0.5% O_2 and 9.75% CO_2, the frequencies of switching were 98.9% and 97.9%, respectively (Table A4). These results demonstrate that hypoxia does not induce white-to-opaque switching and that CO_2 induces switching equally in the absence and presence of O_2.

Table A4. CO_2 induces white-to-opaque switching equally in absence or presence of O_2. In addition, hypoxia does not induce white-to-opaque switching

Condition	Total colonies (N)	Frequency of opaque colonies with white regions or opaque colonies (%)	Fold increased (+) or decreased (-) compared to Air
Air (78% N_2, 20.8% O_2, 0.03% CO_2)	395	5.8±1.4	--
99.97% N_2, 0% O_2, 0.03% CO_2*	379	0.7±0.6	-8 x
90% N_2, 0% O_2, 10% CO_2	436	98.9±0.3	+17 x
99.5% N_2, 0.5% O_2, 0.03% CO_2*	405	0.5±0.5	-12 x
89.75% N_2, 0.5% O_2, 9.75% CO_2	461	97.9±0.4	+17 x
Air + 10%CO_2	370	97.2±1.8	+17 x

Note: WO-1 white cells were used for this experiment. To test the effect of depletion of O_2 and increasing CO_2 on white to opaque switching, white cells were plated onto agar containing Lee's medium. The plates were incubated in air-tight chambers, which were flushed with mixture of gases as indicated. The plates incubated in air at 25 °C were served as control. After 48 hours, all the plates were transferred to regular air incubators at 25 °C, and continued to culture for 3-4 days. Colonies were counted.

Discussion

Two factors had previously been considered possible mechanisms for preserving the opaque phenotype in a host. The first factor was the response of an opaque cell to pheromone produced by another opaque cell of opposite mating type. If opaque cells of opposite mating type appeared spontaneously through switching in the same vicinity, the pheromone each produced would block the opaque cell of opposite mating type in G1 (Zhao *et al*., 2005b; Daniels *et al*., 2006), thus facilitating mating. The second factor was anaerobiosis. Dumitru *et al.* demonstrated that opaque cells cultured under anaerobic conditions at 37 °C switched to white far slower than opaque cells cultured under aerobic conditions, resulting in elevated frequencies of mating (Anderson *et al*., 1989). Anaerobiosis, however, caused a severe reduction in the rate of growth of opaque cells at 37 °C, and retarded, but did not block, the temperature-induced transition to white (C. Pujol, K.J. Daniels and D.R. Soll, in preparation). Recently Ramirez-Zavala *et al.* demonstrated that anaerobic conditions induced white cells to switch to opaque under anaerobic conditions (Ramirez *et al*., 2008).

Here we have tested whether the high levels of CO_2 in host tissues and the gut (Levitt and Bond, 1970; Avunduk, 2002; Guyton and Hall, 2000), might be responsible for maintaining cells in the opaque phenotype *in vivo*. We have found that increasing CO_2 tension to physiological levels not only blocks cells in the opaque phenotype, but also induces switching from white to opaque and blocks switching from opaque to white at 37 °C. Moreover, cells blocked in the opaque phase by CO_2 at 37 °C continue to divide at near maximum rates. Our results, therefore, provide a plausible resolution to the paradox that physiological temperature causes opaque cells to switch to white.

APPENDIX B

N-ACETYLGLUCOSAMINE INDUCES WHITE TO OPAQUE SWITCHING THROUGH THE CAMP PATHWAY IN *C. ALBICANS*

Guanghua Huang, Song Yi, Nidhi Sahni, Karla Daniels, Thyagarajan Srikantha and David R. Soll

Introduction

As mentioned in Appendix A1, *in vitro*, the white-opaque transition is sensitive to physiological temperature (Slutsky *et al*., 1987; Rikkerink *et al*., 1988). When the temperature of opaque cells is raised to 37 °C, cells switched *en masse* to white (Srikantha and Soll, 1993), suggesting that the opaque phenotype is unstable at physiological temperatures, and hence mating would be compromised in a host. In Appendix A1, we have presented evidence that high levels of CO_2 similar to those found in some host tissues, induce switching from white to opaque, maintain cells in the opaque phenotype and block switching from opaque to white (Huang *et al*., 2009). CO_2 has been demonstrated to be an inducer of filamentation as well (Mock *et al*., 1990; Klengel *et al*., 2005). GlcNAc, which is found in the human gut (Ghuysen and Hakenbeck, 1994; Finne *et al*., 1989) and plasma (Liu *et al*., 2008), is also an inducer of filamentation (Simonetti *et al*., 1974). We therefore considered that GlcNAc, may function as an inducer of white-opaque switching in the human host.

The filamentation response by GlcNAc is mediated by the Ras1/cAMP pathway, which includes Ras1, a GTP binding protein (Cho *et al*., 1992; Feng *et al*., 1999), Cdc35, adenylate cyclase (Rocha *et al*., 2001), cAMP, Pde2, the phosphodiesterase that degrades cAMP (Bahn et al., 2003; Jung and Stateva, 2003), and protein kinase A, which includes two isoforms Tpk1 and Tpk2 (Bockmuhl *et al*., 2001).

We demonstrate that the response to GlcNAc is transduced by the same Ras1/cAMP pathway that is involved in the induction of filamentation. Finally, we

demonstrate that the target of the GlcNAc response pathway is Wor1, and that Wor1 must be phosphorylated to induce switching. We suggest that GlcNAc represents an inducer of the white to opaque transition that functions through the activation of Wor1 by phosphorylation.

I played a major role in this study along with the senior author Guanghua Huang. I participated in the generation of deletion and overexpression mutant strains, the white-opaque switching experiments, northern and western blot analysis to measure the levels of Wor1 in the wild type strain and the mutant with a point mutation in the PKA phosphorylation site of Wor1.

Materials and Methods

Strain Maintenance and Growth

The strains of *C. albicans* used in this study are listed in supplemental Table B1. For routine growth, modified Lee's medium without methionine was used (Bedell and Soll, 1979), unless stated otherwise. For repressing of *MET3* promoter-controlled gene expression, 2.5 mM methionine and 2.5 mM cysteine was added to the medium. For GlcNAc induction, the carbon source glucose was replaced with GlcNAc (1.25% w/v) in nutrient medium. Here, solid Lee's glucose medium was referred to as glucose agar or GlcNAc agar. Agar cultures were grown at a density of 80~120 colonies per 85 mm-plate. Phloxine B was added to nutrient agar for opaque colony staining (Anderson and Soll, 1987).

Mutant Construction

The *PDE2* gene was disrupted using a modified Ura-blaster method (Wilson *et al*., 2000). Two long primers (PDE2-5DR, PDE2-3DR), containing a 60 nucleotide sequence homologous to the gene *PDE2*, were used for PCR amplification (Table B2) pDDB57,

Table B1. Strains used in the study of GlcNAc effect on switching

Strain	Parent strain	Genotype	Reference
5314**a**	SC5314	*MTL***a/a**	Huang *et al.* (2009)
5314α	SC5314	*MTL*α/α	Huang *et al.* (2009)
WO-1		*MTL*α/α	Slutsky *et al.* (1987)
WUM5A	WO-1	*MTL*α/α *ura3-1::FRT/ura3-2::FRT*	Wilson *et al.* (1999)
TOHO3	WUM5A	*MTL*α/α *ura3-1::FRT/ura3-2::FRT wor1::FRT/wor1::FRT*	Srikantha *et al.* (2006)
GH1079	WUM5A	*MTL*α/α *ura3-1::FRT/ura3-2::FRT pde2::dpl200/pde2::URA3-dpl200*	This study
GH1060	CAI4	*MTL*α*/mtl***a***:: dpl200 ura3:imm434/ura3::imm434*	Huang *et al.* (2009)
GH1120	CAN52	*MTL*α*/mtl***a***::dpl200 ras1::hisG/ras1::hph ura3::imm434/ura3::imm434*	Huang *et al.* (2009)
GH1013	BWP17	*MTL***a/a** *ura3::imm434/ura3::imm434 his1::hisG/his1::hisG arg4::hisG/arg4::hisG*	Huang *et al.* (2009)
GH1109	GH1013	*MTL***a**/**a** *ura3::imm434/ura3::imm434 his1::hisG/his1::hisG arg4::hisG/arg4::hisG cdc35::ARG4/cdc35::HIS1*	Huang *et al.* (2009)
GH1126	GH1013	*MTL***a**/**a** *ura3::imm434/ura3::imm434 his1::hisG/his1::hisG arg4::hisG/arg4::hisG tpk1::ARG4/tpk1::HIS1*	This study
GH1148	GH1013	*MTL***a**/**a** *ura3::imm434/ura3::imm434 his1::hisG/his1::hisG arg4::hisG/arg4::hisG tpk2::ARG4/tpk2::HIS1*	This study

Table B2. Primers used in the study of GlcNAc effect on switching

Name	Sequence	Purpose and features
WOR1F	ttaccaagatctATGTCTAATTCAAGTATAGTCCCTAC	pMET3-WOR1
WOR1R	attacccccgggCTAAGTACCGGTGTAATACGACCC	
PDE2F	acagattGGATCCATGGCAGAAGTATTATCATTGGTTG	pMET3-PDE2
PDE2R	acagattGCATGCATTGTTATTTCTTTGCTCTTTCCAACC	
RAS1V13F	acgaatactgcagatgttgagagaatataaattag	pMET3-RAS1 V13
RAS1V13R	acgaatagcatgctcaaacaataacacaacatcc	
TPK1F	tcatcaaGATATCATGACATCCATGGAACCAGCAGAC	pACT1-TPK1
TPK1R	tcattagaagcttAAAAGTCCTGGAATTGATCACGATA	
TPK2F	ATGGTGAATCTTTTAAAGAAACTTC	pACT1-TPK2
TPK2R	tcattagaagcttCAAAAGTCAAGGAAATACAGAGC	
PDE2-5DR	GCAGAAGTATTATCATTGGTTGACCTCGAGATTCCTCAAGTCACTGATAAGTATTATAAAGTTTTCCCAGTCACGACGTT	PDE2 KO
PDE2-3DR	CTTTGCTCTTTCCAACCAAAATAGTTTGTTTTCCATAATAATATCACAAGTATACTGCAATGTGGAATTGTGAGCGGATA	
TPK1-5DR	CAATTAATATTATCATTGAATAATAGATACTTATAGCAGTTATAGTAGAATTTAATTTCTGTTTTCCCAGTCACGACGTT	TPK1 KO
TPK1-3DR	CTATAAAACTAGTTATCATAATTAACATTGTTGTGCCAATAAATACAATTTTATTTTTACTGTGGAATTGTGAGCGGATA	
TPK2-5DR	ACAAAGAAGATTAGACAAACAATCACCCACTCACACCTACTACTCACCCAATTTCCATTCGTTTTCCCAGTCACGACGTT	TPK2 KO
TPK2-3DR	TCTTACAGTTACTATCGTTATTATTTAGTCATTTATTCATTTATGAAAGTTCATCTCCTCTGTGGAATTGTGAGCGGATA	
WOR1-SalF	aatcttgtcgacATGTCTAATTCAAGTATAGTCCC	pNIM1-WOR1
WOR1-SalR	aatcttgtcgacaaAGTACCGGTGTAATACGACCC	
WOR1TAF	GAATCAAAAGATGGGCAGATGGTATTTCATGG	WOR1 TA mutation
WOR1TAR	CCATGAAATACCATCTGCCCATCTTTTGATTC	

which contains the recyclable URA3-dpl200 marker, was used as template. The PCR product was transformed into WUM5A, a WO-1 derivative (Strauss *et al*., 2001).

Transformants were grown on selective synthetic defined (SD) medium SD-Ura agar plates. To delete the second allele of *PDE2*, the PCR product was transformed into a spontaneous Ura- derivative of *PDE2/pde2* obtained from SD agar containing 5-fluoro-orotic acid. The *pde2/pde2* null mutants were selected from SD-Ura agar plates and confirmed by PCR.

TPK1 and *TPK2* were deleted by a PCR product-directed disruption protocol, as described in (Huang *et al*., 2009). Briefly, the *HIS1* and *ARG4* markers were amplified by PCR from pGEM-HIS1 and pRS-ARG4-SpeI, respectively. The oligonucleotide pairs TPK1-5DR, TPK1-3DR; TPK2-5DR, TPK2-3DR (Table B2) were used for PCR amplification. The *HIS1* and *ARG4* markers were sequentially transformed into the host strains GH1013 (Wilson *et al*., 1999), and heterozygous mutants. The null mutants were selected on SD-His-Arg plates and confirmed by PCR.

Construction of Plasmids

The primers used for plasmid constructions are listed in Table B2. To generate pMET3-RAS1V13, the *RAS1* ORF containing a mutant at the thirteenth amino acid (glycine to valine mutation) was amplified from pQF145.2 by using primers including *Pst*I and *Sph*I sites, and then cloned into pCaEXP. To generate pMET3-PDE2, the *PDE2* ORF was amplified from CAI4 genomic DNA by using the primers PDE2F and PDE2R that contained *Bam*HI and *Sph*I sites (Table B2) and the *PDE2* ORF cloned into pCaEXP. To generate pACT1-TPK1, the *TPK1* ORF was amplified from CAI4 genomic DNA by using the primers TPK2F and TPK2R that included EcoRV and HindIII sites (Table B2), and the *TPK1* ORF cloned into pACT1 (Huang *et al*., 2009). The *TPK2* ORF was amplified from CAI4 genomic DNA by using primers TPK2F and TPK2R (Table B6). To generate pACT1-TPK2, the PCR product was digested by HindIII and cloned into

EcoRV/HindIII-digested pACT1. The pNIM1-WOR1 was constructed by inserting a SalI digested PCR fragment of *WOR1* into the SalI site of pNIM1. The *WOR1* ORF was amplified from CAI4 genomic DNA. The primers WOR1salF and WOR1salR were used for PCR amplification (Table B2). To generate a site mutation in *WOR1* gene, a two-step PCR method (Ke and Madison, 1997) was used with slight modification. The primers WOR1TAF and WOR1TAR (Table B2) were used to generate site-directed mutation. The second-round PCR product was digested with SalI and subcloned into the SalI site of pNIM1. The resulting plasmid was referred to as pNIM1-WOR1TA. The correct direction of *WOR1* ORF and WOR1TA fragment in pNIM1 was confirmed by sequencing.

White/Opaque Switching Assay

White-opaque switching on agar was analyzed as described previously (Slutsky *et al*., 1987). Briefly, strains were first grown on agar containing supplemented Lee's medium for 6 days at 25 °C. Colonies were then replated onto plates containing supplemented Lee's medium (Bedell and Soll, 1979). These plates were then incubated at 25 °C for five days, and the proportion of colonies exhibiting different phenotypes counted.

White-Opaque Switching in Different Growth Phases

White colonies were inoculated into a test tube containing 1 ml of supplemented Lee's medium with glucose as carbon source and again at 25 °C. The overnight culture was diluted (to 2 x 10^5 cells/ml) in 20 ml of fresh medium with glucose as the carbon source and incubated at 22 °C in a shaker. Aliquots were taken out at different time points, diluted and plated onto both glucose agar and GlcNAc agar plates (Figure B1A). The plates were then incubated at 25 °C for five days, and the colonies exhibiting different colony phenotypes counted.

Figure B1. GlcNAc induces switching from white to opaque in **a** and α cells of *Candida albicans*. A. The experimental protocol for assessing GlcNAC induction. B. Growth kinetics of **a** and α cells in liquid glucose medium. C. Switching frequencies (Switch. Freq.) on glucose or GlcNAc agar of cells grown in liquid glucose medium for 1, 2, 5 and 10 days. D. A graph of switching frequencies from panel C. E. Examples of 3 day cultures on glucose or GlcNAc agar. All experiments in liquid were performed at approximately at 22 °C. Agar plates were cultured at 25 °C. Switching frequencies were measured after 5 days on agar. No. Cols., number of colonies.

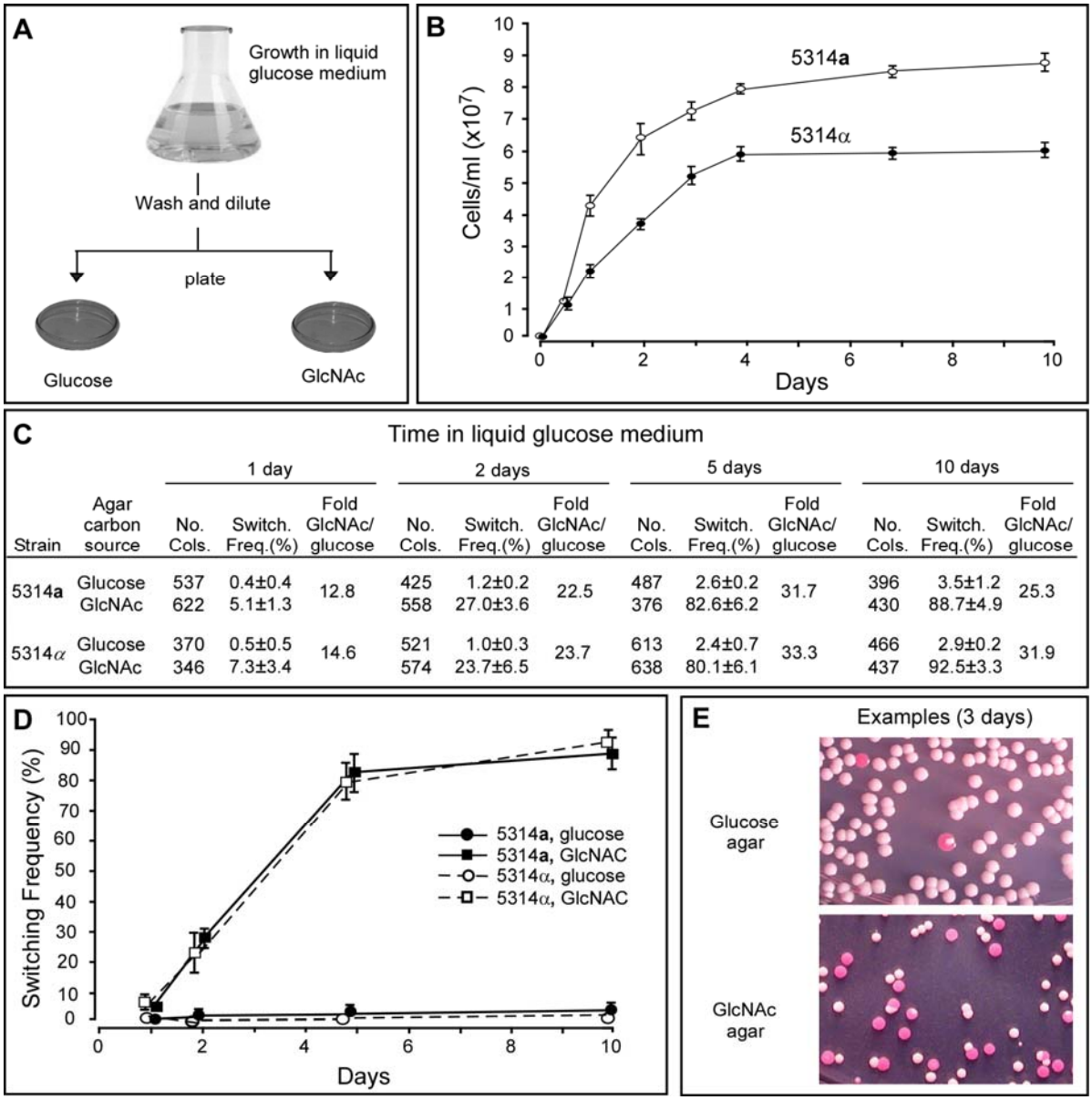

Strain	Agar carbon source	1 day No. Cols.	1 day Switch. Freq.(%)	1 day Fold GlcNAc/ glucose	2 days No. Cols.	2 days Switch. Freq.(%)	2 days Fold GlcNAc/ glucose	5 days No. Cols.	5 days Switch. Freq.(%)	5 days Fold GlcNAc/ glucose	10 days No. Cols.	10 days Switch. Freq.(%)	10 days Fold GlcNAc/ glucose
5314**a**	Glucose	537	0.4±0.4	12.8	425	1.2±0.2	22.5	487	2.6±0.2	31.7	396	3.5±1.2	25.3
	GlcNAc	622	5.1±1.3		558	27.0±3.6		376	82.6±6.2		430	88.7±4.9	
5314α	Glucose	370	0.5±0.5	14.6	521	1.0±0.3	23.7	613	2.4±0.7	33.3	466	2.9±0.2	31.9
	GlcNAc	346	7.3±3.4		574	23.7±6.5		638	80.1±6.1		437	92.5±3.3	

Northern Blot Analysis

Northern blot analyses were performed as previously described (Huang *et al*., 2009). Total RNA from *C. albicans* cells was used. PCR products were used to probe the northern blots. Primers used for generating the PCR products are listed in Table B2.

Western Blot Analysis

Cells from liquid cultures were spun down following doxycycline treatment for 12 hours. Total protein extract was obtained using a bead beater in lysis buffer that contained 50 mM Tris-HCl, 100 mM NaCl, 5mM $MgCl_2$, 1mM DTT, 1 mM EDTA, 1 mM EGTA, 0.1% Tween-20, and 5% glycerol, supplemented with a protease inhibitor cocktail (Sigma-Aldrich, St Louis, MO) and 1 mM phenyl-methylsulphonyl fluoride. An equal amount of total protein from each sample was then subjected to protein G beads (Active Motif, Carlsbad, California) for pre-clearing, followed by immuno-precipitation (IP) using goat GFP antibody-conjugated agarose beads (Santa Cruz Biotechnology, Santa Cruz, California). IP protein samples were subjected to SDS-PAGE (8% polyacrylamide) electrophoresis. After electrophoresis, the SDS-PAGE protein gel was transferred to a PVDF membrane (Immobilon-P, Millipore Corporation, Bedford, MA), blocked for 1 h in 3% non-fat dry milk in TBS-T (20 mM Tris-HCl, pH 7.5, 150 mM NaCl, 0.05% Tween-20), and then incubated with goat polyclonal GFP antibody (Santa Cruz Biotechnology, Santa Cruz, CA) overnight at 4°C (Yi *et al.*, 2009). After washing six times in TBS-T, the proteins on the membrane were detected with horseradish peroxidase-labelled goat IgG (Promega, Madison, WI) and SuperSignal West Pico Chemiluminescent Substrate (Pierce, Rockford, IL).

Colocalization of GFP-Wor1p and nuclei

Cells expressing tetracycline (doxycycline)-inducible GFP-labeled Wor1p were grown to midlog phase in the presence of 50 µg/ml doxycycline (Sigma-Aldrich, St Louis,

MO, USA), harvested and simultaneously permeabilized and the nuclei labeled with 4',6'-Diamidino-2-phenylindole (DAPI, Invitrogen, Inc.) by incubating them for 10 min at room temperature in the dark in a solution containing 5 µg/ml DAPI in 1M Sorbitol, 0.1% Saponin, 150 mM NaCl and 20 mM Tris buffer, pH 7.4, followed by a 15-20 min incubation period on ice. Without washing, the cells were imaged using a Bio-Rad Radiance 2100MP multi-photon microscope (Bio-Rad, Hermel, Hamstead, UK). Cells were excited at 780 nm by a Mai-Tai laser (Spectra- Physics, Newport Corp., Mountain View, CA) and three channel emission images (GFP, DAPI and transmitted) were gathered using a sequential 2.0 µm Z-series, gathered at 0.2 µm intervals to include the entire cell nucleus. GFP and DAPI images were visualized as Z-series projections. Transmitted images were a single scan at the focal plane selected from the Z-series.

Results

GlcNAc Induction of Switching

To test whether GlcNAc induces the white to opaque transition and does so as a function of culture age, as is the case for the induction of filamentation by GlcNAc (Simonetti *et al*., 1974; Cassone *et al*., 1985), white cells of **a**/**a** and an α/α derivative strains of SC5314, 5314**a** and 5314α, respectively, were first grown in suspension in liquid modified Lee's medium in which glucose was the sole carbon source (liquid glucose medium) (Bedell and Soll, 1979) (Figure B1A). To assess GlcNAc induction as a function of the growth phase, cells were removed at time intervals from the liquid culture through exponential growth and saturation phase, and plated on nutrient agar containing either glucose (glucose agar) or GlcNAc (GlcNAc agar) as the sole carbon source (Figure B1A). After five days on agar, the proportion of opaque colonies plus white colonies with opaque sectors was measured. This proportion will be referred to as the "switching frequency" for convenience, but should not be confused with the rate of switching (Rikkerink *et al.*, 1988; Bergen *et al.*, 1990; Soll *et al.*, 1991). Although they reached

different final cell densities, both **a**/**a** and α/α cell cultures reached saturation phase in liquid glucose medium at approximately the same time (Figure B1B).

For **a**/**a** cells plated on glucose agar, the frequency of switching increased from 0.4±0.4% for cells taken from exponential phase cultures after one day, to 3.5±1.2% for cells taken from late saturation phase cultures after 10 days (Figure B1C, D). For α/α cells, the proportion increased similarly from 0.5±0.5% to 2.9±0.2% (Figure B1C, D). Hence, the frequency in liquid glucose medium increased 9.5 and 6.0 fold, respectively, over the course of exponential growth and entrance into saturation phase of the a/a and α/α cultures. For **a**/**a** cells plated on GlcNAc agar, the frequency of switching increased from 5.1±1.3% after one day to 88.7±4.9% after 10 days, and for α/α cells, the frequency increased from 7.3±3.4% to 92.5±3.3% (Figure B1C, D). Plating on GlcNAc agar, therefore, caused an increase in the frequency of switching of the **a**/**a** and α/α cells after one day that was, respectively, approximately 13 and 16 fold, higher than the frequencies on glucose agar after one day, and after 10 days that was 25 and 32 fold, the frequency on glucose agar (Figure B1C, D). In Figure A-6E, examples are presented of cells from three day liquid glucose cultures of **a**/**a** cells plated on glucose agar or GlcNAc agar. Note that on GlcNAc agar, the majority of colonies were completely opaque rather than sectored, indicating that in these cases GlcNAc induction occurred very early in the life history of the colonies. Similar results were obtained for cells grown in liquid glucose medium for five days and plated on agar containing either glucose or GlcNAc ranging in concentration from 0.2% to 5%.

The Role of Ras1

The cAMP pathway that plays a role in filamentation includes an unidentified receptor, Ras1, Cdc35, Pde2, cAMP and the protein kinases Tpk1 and Tpk2 (Feng *et al*.,1999; Rocha *et al*., 2001; Bockmuhl *et al*., 2001; Castilla *et al*., 1998; Bahn *et al*., 2007; Wilson *et al*., 2007). To test whether GlcNAc induction of white-opaque switching

was mediated by the cAMP pathway, we first analyzed the *RAS1* deletion mutant, *ras1/ras1*. White cells of *ras1/ras1* and the **a**/**a** reference strain GH1060 (WT) were grown in liquid glucose medium to saturation phase (seven days), plated on either glucose or GlcNAc agar, and analyzed for switching frequency after five days (Figure B2A). The switching frequency on GlcNAc agar was 90.5±3.8% for WT cells, and 11.2±1.5% for *ras1/ras1* cells (Figure B2A), indicating that Ras1 played a major but not exclusive role in GlcNAc induction. Although the frequency of switching of *ras1/ras1* cells on GlcNAc agar was 9 fold lower than that of WT cells, it was also 16 fold higher than that on glucose agar (Figure B2A), indicating that although Ras1 is necessary for the major response to GlcNAc, a *RAS1*-independent response pathway is responsible for a minor response. It should also be noted that on glucose agar the frequency of switching of switching of WT cells was two fold higher than that of *ras1/ras1* cells (Figure B2A), indicating that the *RAS1*-independent pathway also played a role in spontaneous switching on glucose agar.

To explore further the role of *RAS1*, we transformed the wild type stain WUM5A, a derivative of strain WO-1, with *RAS1V13*, which encodes a constitutively activated form of Ras1, Ras1v13, (Feng *et al*., 1999) under the control of the *MET3* promoter (Care *et al*., 1999), to generate strain WT+*MET3p-RAS1V13*. The WT strain was transformed with the vector lacking the *RAS1V13* to generate the control strain WT-vector. The addition of methionine plus cysteine (+Met, +Cys) represses the *MET3* promoter and the absence (-Met, -Cys) activates it (Care *et al*., 1999). White cells of WT+*MET3p-RAS1V13* and WT-vector were first plated directly onto glucose agar in the presence or absence of methionine plus cysteine. In the repressed state (+Met, +Cys), the majority of colonies were white, with few sectors, but in the activated state (-Met, -Cys), nearly every colony was highly sectored (Figure B2B), demonstrating that misexpression of *RAS1* in the absence of GlcNAc induced switching. Next, white cells of strains WT+vector and WT+*MET3p-RAS1V13* were grown in liquid glucose medium in the repressed state for one day to mid-exponential phase, then plated on either glucose or GlcNAc agar in the induced

Figure B2. Ras1 plays a major role in GlcNAc induction. A. Switching frequencies (Switch. Freq.) of wild type (WT) and *ras1/ras1* cells grown in a glucose liquid medium for 7 days and then plated on glucose agar and GlcNAc agar. B. Cultures of the inducible strain WT+*MET3p-RAS1V13* grown on glucose agar in the presence (repressing condition) or absence (activating condition) of methionine and cysteine. C. Switching frequencies of cells of the control strain WT+vector and the *RAS1V13* overexpression strain WT+*MET3p-RAS1V13* grown in glucose liquid medium for one day and then plated on glucose or GlcNAc agar. D. Examples of colonies on glucose and GlcNAc agar under activating conditions. E. Examples of cells from colonies on glucose and GlcNAc agar under activating conditions. The even bars represent 10 μm. Switching frequencies were measured after 5 days on agar. No. Cols., number of colonies.

A

Strain	Glucose Agar No. Cols.	Glucose Agar Switch. Freq.(%)	GlcNAc Agar No. Cols.	GlcNAc Agar Switch. Freq.(%)	Fold GlcNAc/ Glucose
WT(*RAS1/RAS1*)	647	1.4 ± 0.4	751	90.5 ± 3.8	65 x
ras1/ras1	843	0.7 ± 0.3	952	11.2 ± 1.5	16 x

B

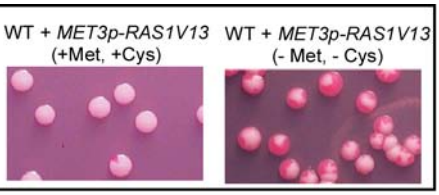

C

Strain	Glucose Agar (-Met, -Cys) No. Cols.	Glucose Agar (-Met, -Cys) Switch Freq.(%)	GlcNAc Agar (- Met, - Cys) No. Cols.	GlcNAc Agar (- Met, - Cys) Switch Freq.(%)
WT + vector	320	2.1 ± 1.0	337	3.2 ± 0.2
WT + *MET3p-RAS1V13*	294	100.0 ± 0.0	351	100.0 ± 0.0
Ratio: overexpressor / control	47.6 x		31.3 x	

D

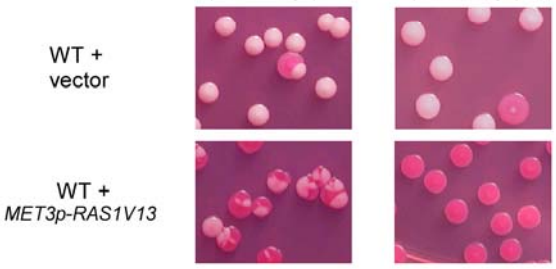

E

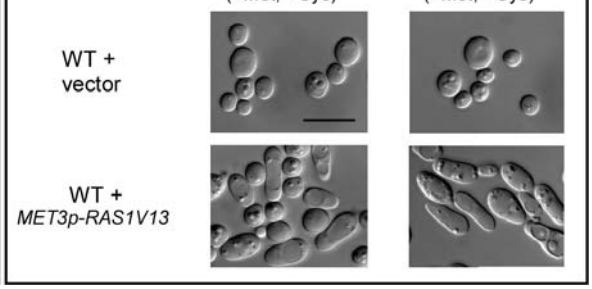

state. On glucose agar, the switching frequency of control WT-vector cells was 2.1±1.0%, and for the overexpression mutant, 100% (Figure B2C). The majority of colonies of the overexpression mutant on glucose agar were highly sectored white colonies (Figure B2D). Only 2.3±1.2% were homogeneous opaque colonies (Figure B2C, D). On GlcNAc agar, the switching frequency of control cells was 3.2±0.2%, while that of the misexpression mutant was 100% (Figure B2C). All of the latter colonies were homogeneously opaque (Figure B2C, D). The uniformity of the opaque phenotype in the latter colonies was evident at the cellular level (Figure B2E). These results reinforce the conclusion that induction of white to opaque switching by GlcNAc is mediated by Ras1.

The Role of cAMP

In the cAMP pathway that is involved in filamentation, Ras1 activates adenylate cyclase, which is encoded by a single gene, *CDC35* (Rocha *et al*., 2001). The resulting increase in cAMP is kept in check by a cAMP-phosphodiesterase, which is encoded by *PDE2* (Bahn et al., 2003; Jung and Stateva, 2003). If GlcNAc induction of white-opaque switching is mediated by the same cAMP pathway, then deletion of *CDC35* should reduce the effect and deletion of *PDE2* should enhance it. When white *cdc35/cdc35* cells were grown to saturation phase in liquid glucose medium (seven days) and then plated on GlcNAc agar, the frequency of switching was 8.0±3.5%, whereas that of the WT parental control was 86.9±4.3% (Figure B3A). These results indicate that, *CDC35* is necessary for the major response to GlcNAc, as was the case for *RAS1*. GlcNAc did, however, induce low level switching in white *cdc35/cdc35* cells, indicating that although *CDC35* is necessary for the major response to GlcNAc, there is a minor response that is *CDC35* –independent, as was observed in the *ras1/ras1* mutant (Figure B2).

When white *pde2/pde2* cells were grown to saturation phase in liquid glucose medium (five days) and then plated on GlcNAc agar, the switching frequency was 100% (Figure B3A). Moreover, when white *pde2/pde2* cells were grown to saturation phase in

Figure B3. The genes *CDC35*, *PDE2*, *TPK1* and *TPK2* play roles in GlcNAc induction of switching. A. Switching frequencies (Switch. Freq.) of cells of the mutants *cdc35/cdc35* and *pde2/pde2* grown in glucose liquid medium for 7 days (*cdc35/cdc35*) or 5 days (*pde2/pde2*) and then plated on glucose on GlcNAc agar. B. Streaks of cells grown for 5 days of the parental control strain (WT), the mutant control strain *pde2/pde2*+vector and the inducible strain *pde2/pde2*+*MET3p-PDE2* under inducing conditions. C. Switching frequencies of cells of the mutant control *pde2/pde2*+vector and the rescued strain *pde2/pde2*+*MET3p-PDE2* grown in liquid glucose medium for 2 days and then plated on glucose and GlcNAc agar under activating conditions. D. Examples of colonies of *pde2/pde2*+vector and *pde2/pde2*+*MET3p-PDE2* from panel C under activating conditions. E. Examples of cells from colonies in Figure D. F. Switching frequencies of parental control strains, the mutants *tpk1/tpk1* and *tpk2/tpk2* and the overexpression strains WT+*ACTp-TPK1* and WT+*ACTp-TPK2* grown in glucose medium for 5 days and then plated on glucose or GlcNAc agar.

A

Strain	Glucose agar No. Cols.	Glucose agar Switch. Freq.(%)	GlcNAc agar No. Cols.	GlcNAc agar Switch. Freq.(%)
WT(GH1013)	330	0.6±0.5	403	86.9±4.3
cdc35/cdc35	352	<0.3	290	8.0±3.5
Ratio: mutant / control	<0.5 x		0.09 x	
WT(WUM5A)	341	0.6±0.6	264	78.3±6.5
pde2/pde2	271	96.0±1.5	229	100.0±0.0
Ratio: mutant / control	160 x		1.3 x	

B

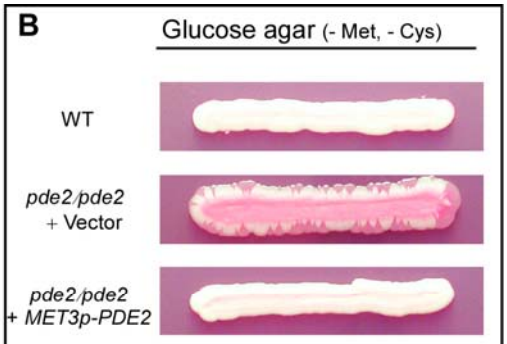

C

Strain	Glucose Agar (-Met, -Cys) No. Cols.	Glucose Agar (-Met, -Cys) Switch. Freq.(%)	GlcNAc Agar (- Met, - Cys) No. Cols.	GlcNAc Agar (- Met, - Cys) Switch. Freq.(%)
pde2/pde2 + Vector	436	98.9 ± 1.9	380	100.0 ± 0.0
pde2/pde2 + MET3p-PDE2	425	2.8 ± 1.2	390	26.8 ± 5.8
Ratio: mutant / rescued strain	34.2 x		3.7 x	

D

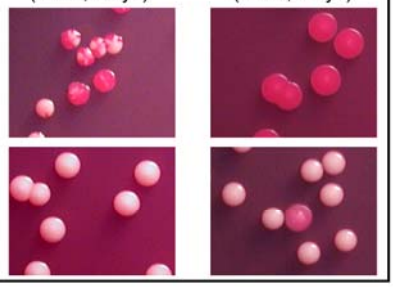

E

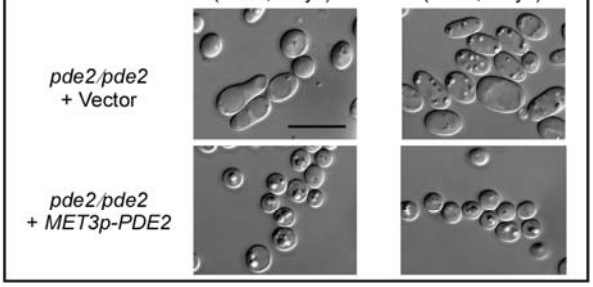

F

Strain	Glucose No. Cols.	Glucose Switch. Freq.(%)	GlcNAc No. Cols.	GlcNAc Switch. Freq.(%)
WT(GH1013)	330	0.6 ± 0.5	751	86.9 ± 4.3
tpk1/tpk1	406	0.4 ± 0.4	337	80.1 ± 5.2*
tpk2/tpk2	332	0.9 ± 0.1	368	94.1 ± 2.8

Strain	Glucose No. Cols.	Glucose Switch. Freq.(%)	GlcNAc No. Cols.	GlcNAc Switch. Freq.(%)
WT(WUM5A)	341	0.6 ± 0.6	264	78.3 ± 6.5
WT +*ACTp-TPK1*	345	0.8 ± 0.8	320	0.8 ± 0.7
WT +*ACTp-TPK2*	298	62.4 ± 4.9	407	97.5 ± 2.0

liquid glucose medium (five days), and then plated on glucose agar, the frequency of switching was 96.0±1.5%, compared to 0.6±0.6 for WT cells (Figure B3A). These results demonstrate that *PDE2* plays a major role in repressing spontaneous switching in glucose medium, and in modulating induction in GlcNAc medium.

To explore further the role of pde2 in switching, the deletion mutant *pde2/pde2* was transformed with a vector containing *PDE2* under the control of the *MET3* promoter to generate the strain *pde2/pde2*+*MET3p-PDE2*. The deletion mutant *pde2/pde2* was transformed with the vector lacking *PDE2* to generate the control strain *pde2/pde2*+vector. When white cells of the parental wild type control (WT) were grown as a streak on glucose agar lacking methionine and cysteine (activating conditions), only rare opaque sectors formed at the periphery (Figure B3B). When the mutant *pde2/pde2*+vector was streaked, opaque sectors lined the entire periphery (Figure B3B). In contrast, opaque sectors were absent at the periphery of the streak of the overexpression mutant *pde2/pde2*+*MET3p-PDE2*, under activating conditions (Figure B3B). When the misexpression mutant *pde2/pde2*+*MET3p-PDE2* was grown in liquid glucose medium under activating conditions to early exponential phase (one day), then plated on glucose agar under activating conditions, the frequency of sectoring was 2.8±1.2%, compared to 98.9±1.9% for the deletion mutant (Figure B3C). When plated on GlcNAc agar under activating conditions, the frequency of switching the overexpression strain was 26.8±5.8% compared to 100% for the control strain (Figure B3D). Examples of colonies of strain *pde1/pde2*+vector *pde2/pde2*- *MET3p-PDE2* on glucose or GlcNAc agar under activating conditions, are presented in Figure B3D, and examples of cells are presented in Figure B3E. Note that on GlcNAc agar, 100% of the colonies formed by cells of the mutant control *pde2/pde2*+vector were opaque and phenotypically homogeneous, whereas on glucose agar, the majority of colonies were sectored, again suggesting that an alternate cAMP-independent GlcNAc induction pathway exists.

The Role of the Protein Kinase As

In the *RAS1*-cAMP pathway, cAMP activates a protein kinase A (PKA) (Bockmuhl *et al*., 2001; Pan *et al*., 2000). In *S. cerevisiae* there are three PKA catalytic subunits, Tpk1, Tpk2 and Tpk3 that play roles in the cAMP pathway regulating pseudohypha formation (Pan *et al*., 2000; Nikawa *et al*., 1987). *C. albicans* possesses two isoforms, Tpk1 and Tpk2, which have been demonstrated to play functionally different roles in filamentation, depending upon environmental conditions (Bockmuhl *et al*., 2001; Cloutier *et al*., 2003). To test whether the two PKAs played a role in the induction of switching by GlcNAc, we analyzed the individual deletion mutants *tpk1/tpk1* and *tpk2/tpk2*. Consistent with previous reports (Bockmuhl *et al*., 2001), our lack of success generating a double mutant of *TPK1* and *TPK2* suggested this mutant was not viable. White cells of the two individual deletion mutants were grown in liquid glucose medium to saturation phase (seven days), then plated on glucose or GlcNAc agar and examined for switching after five days (Figure B1A). Deletion of either *TPK1* or *TPK2* had no detectable effect on the frequency of switching on glucose or on GlcNAc agar (Figure B3F). There was, however, one noticeable difference in the GlcNAc-induced opaque colonies of *tpk1/tpk1*. They possessed a mixture of opaque cells and hyphae (data not shown). Given that the alternative PKA isoform may assume the role of the other in a redundant fashion in the two mutants *tpk1/tpk1* or *tpk2/tpk2*, we generated misexpression mutants in the wild type background WUM5A (WT) in which *TPK1* or *TPK2* was placed under the regulation of the strong constitutive *ACT1* promoter. White cells of the overexpression strains WT+*ACTp-TPK1* and WT+*ACTp-TPK2*, as well as white cells of the parental wild type control strain, were grown to saturation phase in liquid glucose medium (seven days), then plated on glucose or GlcNAc agar and examined after five days for switching (Figure B1A). Overexpression of *TPK1* had no effect on switching on glucose agar, and actually suppressed switching on GlcNAc agar (Figure B3F). Overexpression of *TPK2*, however, caused a tenfold increase in the switching frequency on glucose agar over that of wild type

cells, and enhanced the frequency of switching by approximately 20% on GlcNAc agar (Figure B3F). These results suggest that Tpk2 may function as the downstream kinase in the GlcNAc induction pathway, that Tpk1 can substitute for Tpk2 in the deletion mutant *tpk2/tpk2* and that overexpression of *TPK1* suppresses switching.

The Role of *WOR1*

The *WOR1* (*TOS9*) locus has been demonstrated to regulate spontaneous white-opaque switching (Huang *et al*., 2006; Zordan *et al*., 2006; Srikantha *et al*., 2006). In the basic model for spontaneous switching, it has been proposed that a stochastic increase in *WOR1* expression above a threshold causes a switch from white to opaque, and that continued expression above that threshold maintains the opaque phenotype. Wor1 has been shown to autoinduce at the level of transcription (Huang *et al*., 2006; Zordan *et al*., 2006; Srikantha *et al*., 2006). The cAMP pathway, which traditionally functions by cAMP-activation of a protein kinase A, presumably would increase the frequency of switching by phosphorylating either Wor1 or one of the several proteins that modulate *WOR1* function through the transcriptional regulating loops (Zordan *et al*., 2007; Vinces and Kumamoto, 2007) or chromatin modification genes (Klar *et al*., 2001; Srikantha *et al*., 2001; Hnisz *et al*., 2009). Interestingly, Wor1 possesses a potential consensus PKA phosphorylation motif between amino acids 64 and 69 with a phosphorylatable threonine at amino acid 67 (Huang *et al*., 2006).

To pursue this hypothesis, we first had to demonstrate that Wor1 was essential for GlcNAc-activated switching. White cells of the parental strain (WT) and the *WOR1* deletion mutant *wor1/wor1* were, therefore, grown to saturation phase (seven days) in liquid glucose medium, then plated on nutrient agar containing glucose or GlcNAc. The *wor1/wor1* mutant did not switch on either glucose or GlcNAc agar (Figure B4A, B). Not a single opaque colony or opaque sector was observed among more than 1,000 colonies. We then tested whether overexpression of *WOR1* drove the phenotype to opaque in the

Figure B4. *WOR1*, the master switch locus, is essential for GlcNAc induction and involves phosphorylation. A. Switching frequency of the parental control and mutant *wor1/wor1*. B. Examples of cultures of the control and deletion mutant *wor1/wor1* plated on GlcNAc agar. C. Switching frequencies of cells of the overexpression derivatives *ras1/ras1+MET3p-WOR1*, *cdc35/cdc35+MET3p-WOR1*, *pde2/pde2+MET3p-WOR1*, *tpk1/tpk1+MET3p-WOR1* and *tpk2/tpk2+MET3p-WOR1* grown in glucose medium for 1 day and plated on either glucose or GlcNAc agar under activating conditions. D. Switching frequencies of cells of the mutant control *wor1/wor1+TETp-WOR1* and *wor1/wor1+TETp-WOR1TA* grown in glucose liquid medium and plated on glucose or GlcNAC agar containing 50 or 200 μg per ml of doxycycline, the *TET* inducer. E. Examples of cells from colonies of cells of *wor1/wor1+TETp-WOR1* and *wor1/wor1+TETp-WOR1TA* grown in glucose liquid medium and plated on GlcNAc agar containing 200 μg of doxycycline. F. GFP fluorescence of Wor1 and Wor1TA, in parallel with DAPI staining of nuclei, of strains *wor1/wor1+TETp-WOR1* and *wor1/wor1+TETp-WOR1TA*, respectively. Cells were grown in glucose liquid medium containing 200μg per ml of doxycycline. G. Western blot analysis of Wor1 and Wor1TA using anti-GFP antibody in strains *wor1/wor1+TETp-WOR1* and *wor1/wor1+TETp-WOR1TA*. Protein extracts were derived from cells grown in glucose liquid medium containing 200 μg per ml of doxycycline.

A

Strain	Glucose No. Cols.	Glucose Switch. Freq. (%)	GlcNAc No. Cols.	GlcNAc Switch. Freq. (%)
WOR1/WOR1 (WT)	283	5.0±2.2	330	87.8±8.9
wor1/wor1	375	0.0±0.0	321	0.0±0.0

B

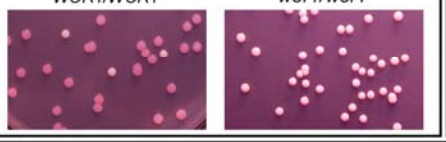

C

Strain	Glucose No. Cols.	Glucose Switch. Freq. (%)	GlcNAc No. Cols.	GlcNAc Switch. Freq. (%)
WOR1/WOR1 + vector	248	2.4 ± 1.1	353	4.7 ± 0.9
ras1/ras1 + *MET3p-WOR1*	130	100.0 ± 0.0	141	100.0 ± 0.0
cdc35/cdc35 + *MET3p-WOR1*	167	100.0 ± 0.0	144	100.0 ± 0.0
pde2/pde2 + *MET3p-WOR1*	146	100.0 ± 0.0	192	100.0 ± 0.0
tpk1/tpk1 + *MET3p-WOR1*	122	100.0 ± 0.0	137	100.0 ± 0.0
tpk2/tpk2 + *MET3p-WOR1*	129	100.0 ± 0.0	159	100.0 ± 0.0

D

Strain	Doxycyline (ug/ml) Liquid medium	Doxycyline (ug/ml) Agar medium	Glucose No. Cols.	Glucose Switch. Freq.(%)	GlcNAc No. Cols.	GlcNAc Switch. Freq. (%)
wor1/wor1 + vector	50	50	193	0.0 ± 0.0	250	0.0 ± 0.0
	200	200	232	0.0 ± 0.0	218	0.0 ± 0.0
wor1/wor1 + *TETp-WOR1*	50	50	188	100.0 ± 0.0	296	100.0 ± 0.0
	200	200	160	100.0 ± 0.0	176	100.0 ± 0.0
wor1/wor1 + *TETp-WOR1TA*	50	50	198	0.0 ± 0.0	139	0.0 ± 0.0
	200	200	243	0.0 ± 0.0	220	(100.0 ± 0.0 pink)

E

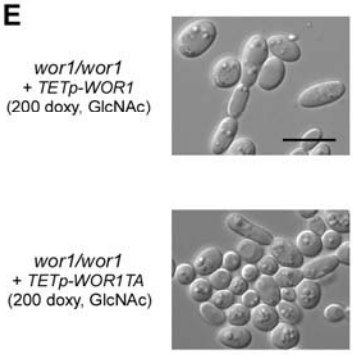

F

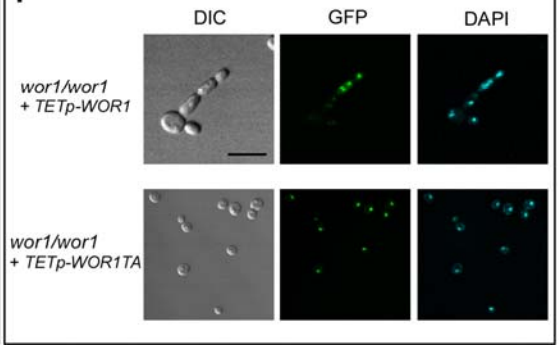

G

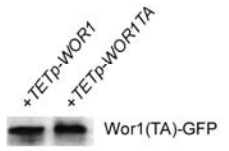

Western blot with GFP antibody

ras1/ras1, *pde2/pde2*, *cdc35/cdc35*, *tpk1/tpk1* and *tpk2/tpk2* mutants by transforming these mutants with a construct in which *WOR1* was under the regulation of the inducible *MET3* promoter (Care *et al*., 1999). In the activated state, 100% of white cells of all five overexpression mutants plated on either glucose or GlcNAc agar switched to opaque (Figure B4C). These results demonstrated that *WOR1* is essential for the induction of switching by GlcNAc, and is downstream of the Ras1/cAMP pathway.

To test if threonine phosphorylation is necessary for Wor1 activation, the homozygous deletion mutant *wor1/wor1* was transformed with a construct in which *WOR1*TA, in which the phosphorylatable threonine 67 residue was replaced with the nonphosphorylatable amino acid alanine, was placed under the control of the inducible tetracycline promoter, to generate strain *wor1/wor1+TETp*-W*OR1*TA. A control strain *wor1/wor1+TETp-WOR1*, was generated in which the native *wor1/wor1* was transformed with a construct containing the *WOR1* ORF under the regulation of the tetracycline promoter, and a second control strain, *wor1/wor1*+vector, was generated, in which *wor1/wor1* was transformed with the vector lacking a *WOR1* derivative. White cells of the three test strains were grown in liquid glucose medium to saturation phase (seven days), then plated on glucose or GlcNAc agar. Both the liquid and agar media contained either 50 or 200 μg per ml of the tetracycline derivative doxycycline, which had previously been shown to induce submaximal and maximal levels of expression, respective (Sahni *et al*., 2009b). When native *WOR1* was misexpressed both in glucose liquid medium and on glucose agar, 100% of colonies underwent switching at both 50 and 200 μg per ml of doxycycline (Figure B4D). When *WOR1TA* was misexpressed in both liquid glucose medium and on glucose agar at either 50 or 200 μg per ml of doxycycline, the frequency of switching was zero percent (Figure B4D). When native *WOR1* was misexpressed in both GlcNAc liquid medium and on GlcNAc agar at 50 and 200 μg per ml of doxycycline, 100% of the colonies underwent switching (Figure B4D). At 200 μg per ml of doxycycline, over 70% of the cells in the opaque colonies exhibited the elongate opaque

phenotype (Figure B4E). When *WOR1TA* was misexpressed in both GlcNAc liquid medium and on GlcNAc agar at 50 μg per ml of doxycycline, 0% of the colonies exhibited switching (Figure B4D). However, when misexpressed in both GlcNAc media at 200 μg per ml of doxycycline, 100% of the colonies were light pink (Figure B4D). Microscopic analysis revealed that 10% of the cells in these pink colonies were opaque (Figure B4E). These results suggest that misexpression of Wor1TA at 50 μg per ml of doxycycline did not stimulate switching, in contrast to 100% induction upon misexpression of native Wor1 at this doxycycline concentration. At 200 μg per ml of doxycycline, however, 10% of white cells switched to opaque, indicating that expression of Wor1TA was capable of inducing switching, but at far lower efficiency. Northern analysis revealed that the level of mRNA was dependent upon the dose of doxycycline for both *WOR1* and *WOR1TA* (data not shown), but that the level of *WOR1TA* transcript was between 5 and 10 times higher than that of *WOR1* at both doxycycline concentrations.

Since *WOR1* and *WOR1*TA were fused in frame with GFP in the overexpression mutants, we used confocal microscopy to test whether Wor1TA, when misexpressed, localized normally to the nucleus. Both Wor1 and Wor1TA localized to the nucleus of misexpression mutants treated with doxycycline, as demonstrated by simultaneous staining with DAPI, a DNA stain (Figure B4F). These results demonstrated that although the replacement of threonine with alanine caused a dramatic decrease in its capacity to induce switching, it did not lower the transcription level or affect nuclear localization. Western blot analysis, using anti-GFP antibody, further demonstrated that the level of Wor1 and Wor1TA protein in white cells treated with 200 μg per ml of doxycycline, were similar in strains *wor1/wor1+TETp-WOR1* and *wor1/wor1+TETp -WOR1TA*, respectively (Figure B4G). These results demonstrate that the decrease in Wor1 function by replacing threonine with adenine in the PKA consensus motif of Wor1 was due to an actual decrease in the efficiency of the transcription factor Wor1, and not increased in instability or a decrease in the level of the Wor1 protein.

GlcNAc induction is enhanced at 37 °C

All of the preceding experiments were performed at 22 °C or 25 °C. To test whether GlcNAc also induced white to opaque switching at physiological temperature (37 °C), white cells of **a**/**a** and α/α derivative of strain SC5314**a** were grown to mid-log phase on liquid glucose medium for either 24 or 48 hr at 25 °C, then plated on glucose or GlcNAc agar at either 25 °C or 37 °C. Increasing the temperature from 25 °C in liquid glucose media to 37 °C on glucose agar resulted in a reduction in the frequency of switching for white cells of both the **a**/**a** and α/α strain (Table B3). In direct contrast, when the temperature was increased from 25 °C in liquid glucose media to 37 °C on GlcNAc agar, there was a dramatic increase in switching to opaque in white cells of both **a**/**a** and α/α strains (Table B3). These data indicates that physiological temperature enhance GlcNAc induction of switching to opaque.

Low CO_2 enhances GlcNAc induction

We previously demonstrated that 1% CO_2 induced switching submaximally, and that at this concentration induction was dependent upon the Ras1/cAMP signal transduction pathway (Huang *et al*., 2009). We have shown here that GlcNAc induction is also submaximal when cells are grown for only one or two days in glucose liquid medium to mid-log phase before plating on GlcNAc agar (Figure B1C, D). We therefore tested whether growing cells in a suboptimal level (1%) CO_2 and for a suboptimal period of time in glucose liquid medium, followed by growth on GlcNAc agar in 1% CO_2, would result in enhancement of GlcNAc induction. White cells of an **a**/**a** and an α/α strain were first grown in glucose liquid medium at 25 °C in air for two days, then were plated on either glucose or GlcNAc agar in either air or 1% CO_2. On glucose agar in 1% CO_2 in air, the two strains exhibited switching frequencies of 17.8±5.2% and 16.7±22%, respectively, and on GlcNAc agar just in air, the respective frequencies were 27.0±3.6% and 23.7±6.5%, respectively (Table B4). However, when plated on GlcNAc agar in 1% CO_2 in air, the

Table B3. GlcNAc induction of white-to-opaque switching is enhanced at 37 °C

			1 day		2 days	
Strain	Agar medium	Temp	Total colonies	Switching frequency (%)	Total colonies	Switching frequency
5314**a**	Glucose	25 °C	283	0.4	187	1.1
		37°C	266	0.0	253	0.4
	GlcNAc	25 °C	291	6.2	258	29.8
		37°C	250	98.0	206	99.0
5314α	Glucose	25 °C	245	0.0	295	0.3
		37°C	190	0.0	287	0.0
	GlcNAc	25 °C	274	8.4	240	99.2
		37°C	223	98.7	231	100.0

Note: white cells were cultured for 1 or 2 days in glucose liquid medium at 22 °C, then plated onto glucose or GlcNAc agar, and incubated at 25 °C or 37 °C in air.

Table B4. Synergistic effect of GlcNAc and CO_2 on induction of white-to-opaque switching

Strain	Glucose		GlcNAc	
	Switching frequency (%)		Switching frequency	
	Air	Air+1%CO_2	Air	Air+1%CO_2
5314**a**	1.2±0.2	17.8±5.2	27.0±3.6	100.0±0.0
5314α	1.0±0.3	16.7±2.2	23.7±6.5	100.0±0.0

Note: white cells were cultured for 2 days in glucose liquid medium at 22 °C, plated onto glucose agar or GlcNAc agar, and then incubated in air or air+1%CO_2 at 25 °C.

switching frequency was 100% in both strains (Table B4), demonstrating a high degree of synergy or enhancement.

Discussion

The frequency of switching by *MTL*-homozygous cells of *C. albicans* is, therefore, influenced by at least two conditions found in the host, CO_2 levels higher than that in air (Huang *et al*., 2009), and GlcNAc. Both CO_2 and GlcNAc induction function through a Ras1/cAMP-dependent and independent pathway (Figure B5). The Ras1/cAMP-dependent pathway is the major one for GlcNAc induction and the Ras1/cAMP-independent pathway the minor one. The reverse is true for CO_2 induction. The Ras1/cAMP-dependent pathway is the minor one, functioning at submaximum levels of CO_2, and the Ras1/cAMP-independent one the major one, functioning at maximum levels of CO_2 (Huang *et al*., 2009) (Figure B5). Furthermore, our data suggest that glucose represents a weak inducer of switching that also functions through the Ras1/cAMP pathway (Figure B5). The major unidentifiable CO_2 induction pathway, and the minor GlcNAc induction pathway, therefore, may not function through Wor1 phosphorylation, although both require *WOR1* for induction, suggesting different mechanisms for Wor1 regulation. Finally, suboptimum CO_2 induction and submaximal GlcNAc induction during early exponential growth, which are both transduced by the Ras1/GlcNAc pathway, together are synergistic, suggesting that in both cases, signal activation of the receptor is limiting, but the shared transduction pathway is not.

Filamentation and the evolution of switching

The induction of switching by environmental cues share several characteristics with that of filamentation. First, both CO_2 and GlcNAc also induce filamentation (Mock *et al*., 1990; Klengel *et al*., 2005; Simonetti *et al*., 1974). Second, the Ras1/cAMP pathway has been demonstrated to play a role in the induction of filamentation by CO_2

Figure B5. A model of the regulatory circuitry involved in the induction of the white to opaque switch. The number of plus signs and the thickness of initial pathway arrows reflect the degree of induction. Note that we have all pathways converging on the master switch gene *WOR1* because of their dependency on that gene. Note that only the Ras1/cAMP pathway affects Wor1 through phosphorylation, but that point is restricted to the discussion in the text and not noted in the model.

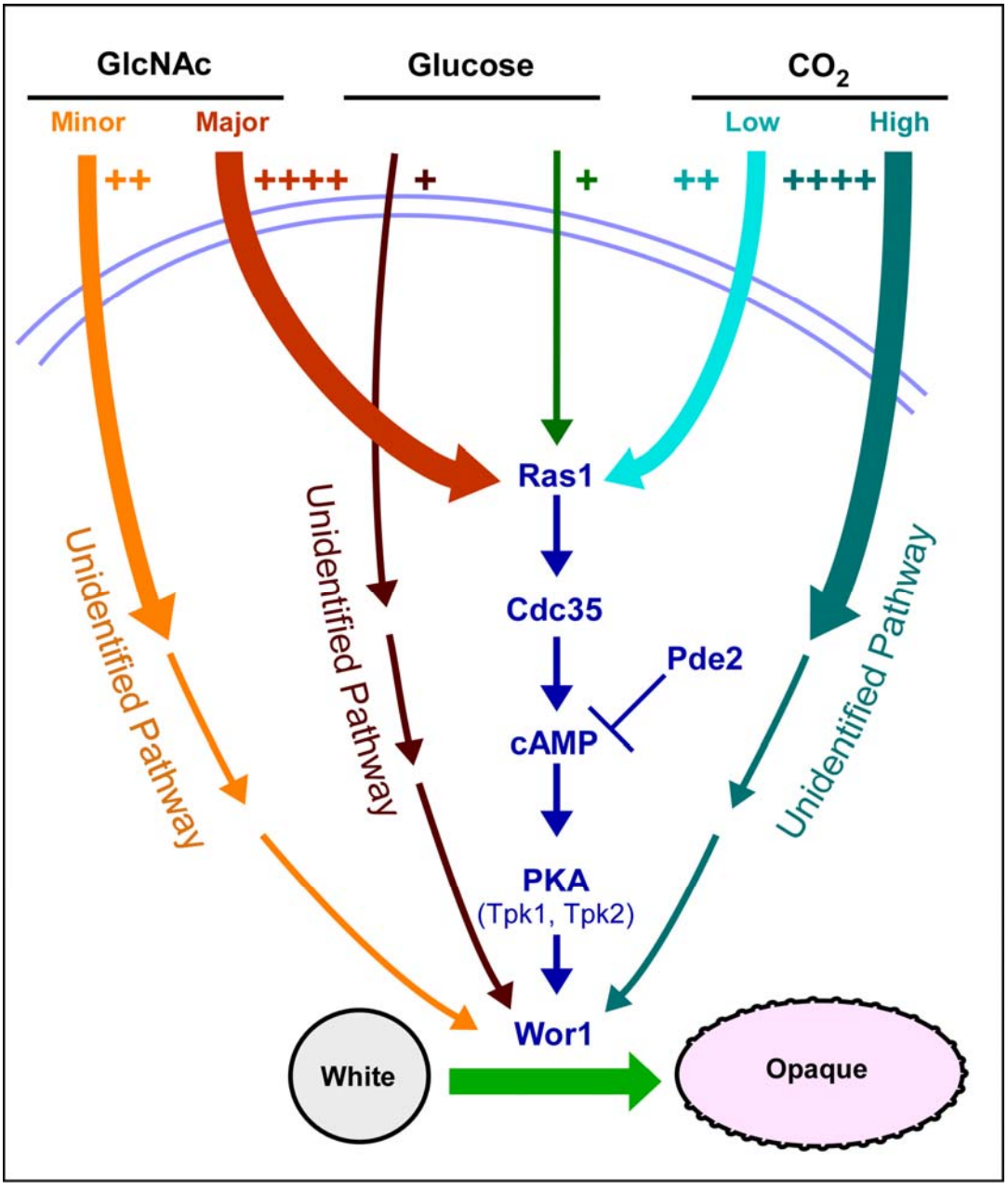
GlcNAc
Glucose
CO_2
Minor
Major
Low
High
++
++++
+
+
++
++++
Ras1
Cdc35
Pde2
cAMP
PKA
(Tpk1, Tpk2)
Wor1
Unidentified Pathway
Unidentified Pathway
Unidentified Pathway
White
Opaque

(Klengel *et al*., 2005), as is the case for switching. The Ras1/cAMP pathway has also been demonstrated to play a role in the induction of filamentation in *S. cerevisiae* (Pan *et al*., 2003; Madhani and Fink, 1998b), suggesting that the regulation of filamentation may have been an ancestral characteristic conserved in *C. albicans* and *S. cerevisiae*. And finally, many of the characteristics of the opaque phenotype are shared with hyphae, including an elongate shape, a prominent vacuole and cell surface antigens (Anderson and Soll, 1987; Anderson *et al*., 1990). Since white-opaque switching is a specific and unique characteristic of *C. albicans* and the closely related species *C. dubliniensis* (Pujol *et al*., 2004), it represents a newly evolved developmental process, whereas filamentation represents an ancestral characteristic. The similarities noted between white-opaque switching and filamentation support a scenario in which the former may have evolved from the latter.

REFERENCES

Aebersold,R. and Mann,M. (2003). Mass spectrometry-based proteomics. Nature *422*, 198-207.

Akins,R.A. (2005). An update on antifungal targets and mechanisms of resistance in *Candida albicans*. Med. Mycol. *43*, 285-318.

Al-Fattani,M.A. and Douglas,L.J. (2004). Penetration of *Candida* biofilms by antifungal agents. Antimicrob. Agents Chemother. *48*, 3291-3297.

Alonso-Monge,R., Navarro-Garcia,F., Molero,G., Diez-Orejas,R., Gustin,M., Pla,J., Sanchez,M., and Nombela,C. (1999). Role of the mitogen-activated protein kinase Hog1p in morphogenesis and virulence of *Candida albicans*. J. Bacteriol. *181*, 3058-3068.

Alonso-Monge,R., Navarro-Garcia,F., Roman,E., Negredo,A.I., Eisman,B., Nombela,C., and Pla,J. (2003). The Hog1 mitogen-activated protein kinase is essential in the oxidative stress response and chlamydospore formation in *Candida albicans*. Eukaryot. Cell *2*, 351-361.

Ammerer,G. (1990). Identification, purification, and cloning of a polypeptide (PRTF/GRM) that binds to mating-specific promoter elements in yeast. Genes Dev. *4*, 299-312.

Andaluz,E., Ciudad,T., Gomez-Raja,J., Calderone,R., and Larriba,G. (2006). Rad52 depletion in *Candida albicans* triggers both the DNA-damage checkpoint and filamentation accompanied by but independent of expression of hypha-specific genes. Mol. Microbiol. *59*, 1452-1472.

Anderegg,R.J., Betz,R., Carr,S.A., Crabb,J.W., and Duntze,W. (1988). Structure of *Saccharomyces cerevisiae* mating hormone a-factor. Identification of S-farnesyl cysteine as a structural component. J. Biol. Chem. *263*, 18236-18240.

Anderson,J., Cundiff,L., Schnars,B., Gao,M.X., Mackenzie,I., and Soll,D.R. (1989). Hypha formation in the white-opaque transition of *Candida albicans*. Infect. Immun. *57*, 458-467.

Anderson,J., Mihalik,R., and Soll,D.R. (1990). Ultrastructure and antigenicity of the unique cell wall pimple of the *Candida* opaque phenotype. J. Bacteriol. *172*, 224-235.

Anderson,J.M. and Soll,D.R. (1986). Differences in actin localization during bud and hypha formation in the yeast *Candida albicans*. J. Gen. Microbiol. *132*, 2035-2047.

Anderson,J.M. and Soll,D.R. (1987). Unique phenotype of opaque cells in the white-opaque transition of *Candida albicans*. J. Bacteriol. *169*, 5579-5588.

Andrianopoulos,A. and Timberlake,W.E. (1994). The *Aspergillus nidulans* abaA gene encodes a transcriptional activator that acts as a genetic switch to control development. Mol. Cell Biol. *14*, 2503-2515.

Antony,G., Saralaya,V., Bhat,G.K., and Shivananda,P.G. (2007). Phenotypic switching and its influence on expression of virulence factors by Candida albicans causing candidiasis in human immunodeficiency virus-infected patients. Indian J. Med. Microbiol. *25*, 241-244.

Arkowitz,R.A. (1999). Responding to attraction: chemotaxis and chemotropism in *Dictyostelium* and yeast. Trends Cell Biol. *9*, 20-27.

Avunduk C. (2002). Manual of Gastroenterology: Diagnosis and Therapy. Philadelphia: Lippincott Williams & Wilkins. 544 p.

Bacci,A., Huguenard,J.R., and Prince,D.A. (2005). Modulation of neocortical interneurons: extrinsic influences and exercises in self-control. Trends Neurosci. *28*, 602-610.

Bader,T., Schroppel,K., Bentink,S., Agabian,N., Kohler,G., and Morschhauser,J. (2006). Role of calcineurin in stress resistance, morphogenesis, and virulence of a *Candida albicans* wild-type strain. Infect. Immun. *74*, 4366-4369.

Bahler,J., Schuchert,P., Grimm,C., and Kohli,J. (1991). Synchronized meiosis and recombination in fission yeast: observations with pat1-114 diploid cells. Curr. Genet. *19*, 445-451.

Bahn,Y.S., Staab,J., and Sundstrom,P. (2003). Increased high-affinity phosphodiesterase *PDE2* gene expression in germ tubes counteracts *CAP1*-dependent synthesis of cyclic AMP, limits hypha production and promotes virulence of *Candida albicans*. Mol. Microbiol. *50*, 391-409.

Bahn,Y.S., Kojima,K., Cox,G.M., and Heitman,J. (2005). Specialization of the HOG pathway and its impact on differentiation and virulence of *Cryptococcus neoformans*. Mol. Biol. Cell *16*, 2285-2300.

Bahn,Y.S. and Muhlschlegel,F.A. (2006). CO2 sensing in fungi and beyond. Curr. Opin. Microbiol. *9*, 572-578.

Bahn,Y.S., Molenda,M., Staab,J.F., Lyman,C.A., Gordon,L.J., and Sundstrom,P. (2007). Genome-wide transcriptional profiling of the cyclic AMP-dependent signaling pathway during morphogenic transitions of *Candida albicans*. Eukaryot. Cell *6*, 2376-2390.

Bailey,T.L. and Elkan,C. (1994). Fitting a mixture model by expectation maximization to discover motifs in biopolymers. Proc. Int. Conf. Intell. Syst. Mol. Biol. *2*, 28-36.

Bailey,T.L., Williams,N., Misleh,C., and Li,W.W. (2006). MEME: discovering and analyzing DNA and protein sequence motifs. Nucleic Acids Res. *34*, W369-W373.

Baillie,G.S. and Douglas,L.J. (1999). Role of dimorphism in the development of *Candida albicans* biofilms. J. Med. Microbiol. *48*, 671-679.

Baillie,G.S. and Douglas,L.J. (2000). Matrix polymers of *Candida* biofilms and their possible role in biofilm resistance to antifungal agents. J. Antimicrob. Chemother. *46*, 397-403.

Balan,I., Alarco,A.M., and Raymond,M. (1997). The *Candida albicans CDR3* gene codes for an opaque-phase ABC transporter. J. Bacteriol. *179*, 7210-7218.

Balazsi,G. and Oltvai,Z.N. (2005). Sensing your surroundings: how transcription-regulatory networks of the cell discern environmental signals. Sci. STKE. *2005*, e20.

Banerjee,M., Thompson,D.S., Lazzell,A., Carlisle,P.L., Pierce,C., Monteagudo,C., Lopez-Ribot,J.L., and Kadosh,D. (2008). UME6, a novel filament-specific regulator of *Candida albicans* hyphal extension and virulence. Mol. Biol. Cell *19*, 1354-1365.

Banuett,F. (1998). Signalling in the yeasts: an informational cascade with links to the filamentous fungi. Microbiol. Mol. Biol. Rev. *62*, 249-274.

Bao,M.Z., Schwartz,M.A., Cantin,G.T., Yates,J.R., III, and Madhani,H.D. (2004). Pheromone-dependent destruction of the Tec1 transcription factor is required for MAP kinase signaling specificity in yeast. Cell *119*, 991-1000.

Bardwell,L., Cook,J.G., Inouye,C.J., and Thorner,J. (1994). Signal propagation and regulation in the mating pheromone response pathway of the yeast *Saccharomyces cerevisiae*. Dev. Biol. *166*, 363-379.

Barlow,A.J. and Chattaway,F.W. (1969). Observations on the carriage of *Candida albicans* in man. Br. J. Dermatol. *81*, 103-106.

Bastidas,R.J. and Heitman,J. (2009). Trimorphic stepping stones pave the way to fungal virulence. Proc. Natl. Acad. Sci. U. S. A *106*, 351-352.

Bauer,J. and Wendland,J. (2007). *Candida albicans* Sfl1 suppresses flocculation and filamentation. Eukaryot. Cell *6*, 1736-1744.

Baur,M., Esch,R.K., and Errede,B. (1997). Cooperative binding interactions required for function of the Ty1 sterile responsive element. Mol. Cell Biol. *17*, 4330-4337.

Beck-Sague,C. and Jarvis,W.R. (1993). Secular trends in the epidemiology of nosocomial fungal infections in the United States, 1980-1990. National Nosocomial Infections Surveillance System. J. Infect. Dis. *167*, 1247-1251.

Becker,W. and Joost,H.G. (1999). Structural and functional characteristics of Dyrk, a novel subfamily of protein kinases with dual specificity. Prog. Nucleic Acid Res. Mol. Biol. *62*, 1-17.

Bedell,G.W. and Soll,D.R. (1979). Effects of low concentrations of zinc on the growth and dimorphism of *Candida albicans*: evidence for zinc-resistant and -sensitive pathways for mycelium formation. Infect. Immun. *26*, 348-354.

Bender,A. and Sprague,G.F., Jr. (1986). Yeast peptide pheromones, a-factor and alpha-factor, activate a common response mechanism in their target cells. Cell *47*, 929-937.

Bender,A. and Sprague,G.F., Jr. (1987). *MAT alpha* 1 protein, a yeast transcription activator, binds synergistically with a second protein to a set of cell-type-specific genes. Cell *50*, 681-691.

Bennett,R.J. and Johnson,A.D. (2003). Completion of a parasexual cycle in *Candida albicans* by induced chromosome loss in tetraploid strains. EMBO J. *22*, 2505-2515.

Bennett,R.J. and Johnson,A.D. (2005). Mating in *Candida albicans* and the search for a sexual cycle. Annu. Rev. Microbiol. *59* , 233-255.

Bennett,R.J., Miller,M.G., Chua,P.R., Maxon,M.E., and Johnson,A.D. (2005). Nuclear fusion occurs during mating in *Candida albicans* and is dependent on the *KAR3* gene. Mol. Microbiol. *55*, 1046-1059.

Bennett,R.J. and Johnson,A.D. (2006). The role of nutrient regulation and the Gpa2 protein in the mating pheromone response of *C. albicans*. Mol. Microbiol. *62*, 100-119.

Bensen,E.S., Filler,S.G., and Berman,J. (2002). A forkhead transcription factor is important for true hyphal as well as yeast morphogenesis in *Candida albicans*. Eukaryot. Cell *1*, 787-798.

Bergen,M.S., Voss,E., and Soll,D.R. (1990). Switching at the cellular level in the white-opaque transition of *Candida albicans*. J. Gen. Microbiol. *136*, 1925-1936.

Birse,C.E., Irwin,M.Y., Fonzi,W.A., and Sypherd,P.S. (1993). Cloning and characterization of *ECE1*, a gene expressed in association with cell elongation of the dimorphic pathogen *Candida albicans*. Infect. Immun. *61*, 3648-3655.

Biswas,S., Van,D.P., and Datta,A. (2007). Environmental sensing and signal transduction pathways regulating morphopathogenic determinants of *Candida albicans*. Microbiol. Mol. Biol. Rev. *71*, 348-376.

Blankenship,J.R. and Mitchell,A.P. (2006). How to build a biofilm: a fungal perspective. Curr. Opin. Microbiol. *9*, 588-594.

Blignaut,E., Pujol,C., Lockhart,S., Joly,S., and Soll,D.R. (2002). Ca3 fingerprinting of *Candida albicans* isolates from human immunodeficiency virus-positive and healthy individuals reveals a new clade in South Africa. J. Clin. Microbiol. *40*, 826-836.

Bockmuhl,D.P., Krishnamurthy,S., Gerads,M., Sonneborn,A., and Ernst,J.F. (2001). Distinct and redundant roles of the two protein kinase A isoforms Tpk1p and Tpk2p in morphogenesis and growth of *Candida albicans*. Mol. Microbiol. *42*, 1243-1257.

Bockmuhl,D.P. and Ernst,J.F. (2001). A potential phosphorylation site for an A-type kinase in the Efg1 regulator protein contributes to hyphal morphogenesis of *Candida albicans*. Genetics *157*, 1523-1530.

Boone,C., Davis,N.G., and Sprague,G.F., Jr. (1993). Mutations that alter the third cytoplasmic loop of the a-factor receptor lead to a constitutive and hypersensitive phenotype. Proc. Natl. Acad. Sci. U. S. A *90*, 9921-9925.

Borneman,A.R., Gianoulis,T.A., Zhang,Z.D., Yu,H., Rozowsky,J., Seringhaus,M.R., Wang,L.Y., Gerstein,M., and Snyder,M. (2007). Divergence of transcription factor binding sites across related yeast species. Science *317*, 815-819.

Bougnoux,M.E., Pujol,C., Diogo,D., Bouchier,C., Soll,D.R., and d'Enfert,C. (2008). Mating is rare within as well as between clades of the human pathogen *Candida albicans*. Fungal. Genet. Biol. *45*, 221-231.

Bramley,T.A., Menzies,G.S., Williams,R.J., Kinsman,O.S., and Adams,D.J. (1991). Characterization of a factor(s) from partially purified human gonadotrophin preparations which inhibit(s) the binding of radiolabelled human LH and human chorionic gonadotrophin to *Candida albicans*. J. Endocrinol. *128*, 139-151.

Brand,A., Lee,K., Veses,V., and Gow,N.A. (2009). Calcium homeostasis is required for contact-dependent helical and sinusoidal tip growth in *Candida albicans* hyphae. Mol. Microbiol. *71*, 1155-1164.

Braun,B.R. and Johnson,A.D. (1997). Control of filament formation in *Candida albicans* by the transcriptional repressor *TUP1*. Science *277*, 105-109.

Braun,B.R. and Johnson,A.D. (2000). *TUP1*, *CPH1* and *EFG1* make independent contributions to filamentation in candida albicans. Genetics *155*, 57-67.

Braun,B.R., Kadosh,D., and Johnson,A.D. (2001). *NRG1*, a repressor of filamentous growth in *C.albicans*, is down-regulated during filament induction. EMBO J. *20*, 4753-4761.

Braun,B.R. *et al.* (2005). A human-curated annotation of the *Candida albicans* genome. PLoS. Genet. *1*, 36-57.

Brown,A.J. and Gow,N.A. (1999). Regulatory networks controlling *Candida albicans* morphogenesis. Trends Microbiol. *7*, 333-338.

Brown,D.H., Jr., Giusani,A.D., Chen,X., and Kumamoto,C.A. (1999). Filamentous growth of *Candida albicans* in response to physical environmental cues and its regulation by the unique *CZF1* gene. Mol. Microbiol. *34*, 651-662.

Brummel,M. and Soll,D.R. (1982). The temporal regulation of protein synthesis during synchronous bud or mycelium formation in the dimorphic yeast *Candida albicans*. Dev. Biol. *89*, 211-224.

Buffo,J., Herman,M.A., and Soll,D.R. (1984). A characterization of pH-regulated dimorphism in *Candida albicans*. Mycopathologia *85*, 21-30.

Bukusoglu,G. and Jenness,D.D. (1996). Agonist-specific conformational changes in the yeast alpha-factor pheromone receptor. Mol. Cell Biol. *16*, 4818-4823.

Burglin,T.R. (1991). The TEA domain: a novel, highly conserved DNA-binding motif. Cell *66*, 11-12.

Burkholder,A.C. and Hartwell,L.H. (1985). The yeast alpha-factor receptor: structural properties deduced from the sequence of the *STE2* gene. Nucleic Acids Res. *13*, 8463-8475.

Butler,G., Kenny,C., Fagan,A., Kurischko,C., Gaillardin,C., and Wolfe,K.H. (2004). Evolution of the *MAT* locus and its Ho endonuclease in yeast species. Proc. Natl. Acad. Sci. U. S. A *101*, 1632-1637.

Butler,G. Rasmussen, M.D., Lin, M.F., Santos, M.A., Sakthikumar, S, Munro, C.A., Rheinbay, E, Grabherr, M, Forche, A, Reedy, J.L., Agrafioti,I, Arnaud, M.B., Bates, S, Brown, A.J., Brunke, S, Costanzo, M.C., Fitzpatrick, D.A., de Groot, P.W., Harris, D, Hoyer, L.L, Hube B, Klis FM, Kodira C, Lennard N, Logue ME, Martin R, Neiman AM, Nikolaou E, Quail MA, Quinn J, Santos MC, Schmitzberger FF, Sherlock G, Shah P, Silverstein KA, Skrzypek MS, Soll D, Staggs R, Stansfield I, Stumpf MP, Sudbery PE, Srikantha T, Zeng Q, Berman J, Berriman M, Heitman J, Gow NA, Lorenz MC, Birren BW, Kellis M, Cuomo CA. (2009). Evolution of pathogenicity and sexual reproduction in eight *Candida* genomes. Nature *459*, 657-662.

Butty,A.C., Pryciak,P.M., Huang,L.S., Herskowitz,I., and Peter,M. (1998). The role of Far1p in linking the heterotrimeric G protein to polarity establishment proteins during yeast mating. Science *282*, 1511-1516.

Calderone,R.A. and Fonzi,W.A. (2001). Virulence factors of *Candida albicans*. Trends Microbiol. *9*, 327-335.

Calderone,R.A. 2002. *Candida* and candidiasis. R.A.Calderone (ed.), ASM Press, Washington, DC.

Cannon,R.D. *et al.* (1994). Molecular biological and biochemical aspects of fungal dimorphism. J. Med. Vet. Mycol. *32 Suppl 1*, 53-64.

Cao,F., Lane,S., Raniga,P.P., Lu,Y., Zhou,Z., Ramon,K., Chen,J., and Liu,H. (2006). The Flo8 transcription factor is essential for hyphal development and virulence in Candida albicans. Mol. Biol. Cell *17*, 295-307.

Cappellaro,C., Hauser,K., Mrsa,V., Watzele,M., Watzele,G., Gruber,C., and Tanner,W. (1991). Saccharomyces cerevisiae **a**- and alpha-agglutinin: characterization of their molecular interaction. EMBO J. *10*, 4081-4088.

Cappellaro,C., Baldermann,C., Rachel,R., and Tanner,W. (1994). Mating type-specific cell-cell recognition of *Saccharomyces cerevisiae*: cell wall attachment and active sites of a- and alpha-agglutinin. EMBO J. *13*, 4737-4744.

Carlisle,P.L., Banerjee,M., Lazzell,A., Monteagudo,C., Lopez-Ribot,J.L., and Kadosh,D. (2009). Expression levels of a filament-specific transcriptional regulator are sufficient to determine Candida albicans morphology and virulence. Proc. Natl. Acad. Sci. U. S. A *106*, 599-604.

Carmen,A.A., Rundlett,S.E., and Grunstein,M. (1996). *HDA1* and *HDA3* are components of a yeast histone deacetylase (HDA) complex. J. Biol. Chem. *271*, 15837-15844.

Care,R.S., Trevethick,J., Binley,K.M., and Sudbery,P.E. (1999). The *MET3* promoter: a new tool for *Candida albicans* molecular genetics. Mol. Microbiol. *34*, 792-798.

Cassone,A., Sullivan,P.A., and Shepherd,M.G. (1985). N-acetyl-D-glucosamine-induced morphogenesis in *Candida albicans*. Microbiologica *8*, 85-99.

Casaz,P., Sundseth,R., and Hansen,U. (1991). trans activation of the simian virus 40 late promoter by large T antigen requires binding sites for the cellular transcription factor *TEF-1*. J. Virol. *65*, 6535-6543.

Castilla,R., Passeron,S., and Cantore,M.L. (1998). N-acetyl-D-glucosamine induces germination in *Candida albicans* through a mechanism sensitive to inhibitors of cAMP-dependent protein kinase. Cell Signal. *10*, 713-719.

Celic,A., Martin,N.P., Son,C.D., Becker,J.M., Naider,F., and Dumont,M.E. (2003). Sequences in the intracellular loops of the yeast pheromone receptor Ste2p required for G protein activation. Biochemistry *42*, 3004-3017.

Chaffin,W.L. (1984). The relationship between yeast cell size and cell division in *Candida albicans*. Can. J. Microbiol. *30*, 192-203.

Chaffin,W.L. (2008). *Candida albicans* cell wall proteins. Microbiol. Mol. Biol. Rev. *72*, 495-544.

Chaleff,D.T. and Tatchell,K. (1985). Molecular cloning and characterization of the *STE7* and *STE11* genes of *Saccharomyces cerevisiae*. Mol. Cell Biol. *5*, 1878-1886.

Chandra,J., Kuhn,D.M., Mukherjee,P.K., Hoyer,L.L., McCormick,T., and Ghannoum,M.A. (2001). Biofilm formation by the fungal pathogen *Candida albicans*: development, architecture, and drug resistance. J. Bacteriol. *183*, 5385-5394.

Chang,F. and Herskowitz,I. (1990). Identification of a gene necessary for cell cycle arrest by a negative growth factor of yeast: *FAR1* is an inhibitor of a G1 cyclin, *CLN2*. Cell *63*, 999-1011.

Chang,F. and Herskowitz,I. (1992). Phosphorylation of *FAR1* in response to alpha-factor: a possible requirement for cell-cycle arrest. Mol. Biol. Cell *3*, 445-450.

Chen,J., Zhou,S., Wang,Q., Chen,X., Pan,T., and Liu,H. (2000). Crk1, a novel Cdc2-related protein kinase, is required for hyphal development and virulence in *Candida albicans*. Mol. Cell Biol. *20*, 8696-8708.

Chen,J., Chen,J., Lane,S., and Liu,H. (2002). A conserved mitogen-activated protein kinase pathway is required for mating in *Candida albicans*. Mol. Microbiol. *46*, 1335-1344.

Chen,P., Choi,J.D., Wang,R., Cotter,R.J., and Michaelis,S. (1997). A novel **a**-factor-related peptide of *Saccharomyces cerevisiae* that exits the cell by a Ste6p-independent mechanism. Mol. Biol. Cell *8*, 1273-1291.

Chen,P., Sapperstein,S.K., Choi,J.D., and Michaelis,S. (1997). Biogenesis of the *Saccharomyces cerevisiae* mating pheromone a-factor. J. Cell Biol. *136*, 251-269.

Chen,Q. and Konopka,J.B. (1996). Regulation of the G-protein-coupled alpha-factor pheromone receptor by phosphorylation. Mol. Cell Biol. *16*, 247-257.

Chen,R.E. and Thorner,J. (2007). Function and regulation in MAPK signaling pathways: lessons learned from the yeast *Saccharomyces cerevisiae*. Biochim. Biophys. Acta *1773*, 1311-1340.

Chen,X., Magee,B.B., Dawson,D., Magee,P.T., and Kumamoto,C.A. (2004). Chromosome 1 trisomy compromises the virulence of *Candida albicans*. Mol. Microbiol. *51*, 551-565.

Chenevert,J., Valtz,N., and Herskowitz,I. (1994). Identification of genes required for normal pheromone-induced cell polarization in *Saccharomyces cerevisiae*. Genetics *136*, 1287-1296.

Chibana,H., Beckerman,J.L., and Magee,P.T. (2000). Fine-resolution physical mapping of genomic diversity in *Candida albicans*. Genome Res. *10*, 1865-1877.

Chinault,S.L., Overton,M.C., and Blumer,K.J. (2004). Subunits of a yeast oligomeric G protein-coupled receptor are activated independently by agonist but function in concert to activate G protein heterotrimers. J. Biol. Chem. *279*, 16091-16100.

Cho,T., Hamatake,H., Kaminishi,H., Hagihara,Y., and Watanabe,K. (1992). The relationship between cyclic adenosine 3',5'-monophosphate and morphology in exponential phase *Candida albicans*. J. Med. Vet. Mycol. *30*, 35-42.

Choi,K.Y., Satterberg,B., Lyons,D.M., and Elion,E.A. (1994). Ste5 tethers multiple protein kinases in the MAP kinase cascade required for mating in *S. cerevisiae*. Cell *78*, 499-512.

Chou,S., Huang,L., and Liu,H. (2004). Fus3-regulated Tec1 degradation through SCFCdc4 determines MAPK signaling specificity during mating in yeast. Cell *119*, 981-990.

Chou,S., Lane,S., and Liu,H. (2006). Regulation of mating and filamentation genes by two distinct Ste12 complexes in Saccharomyces cerevisiae. Mol. Cell Biol. *26*, 4794-4805.

Chou,S., Zhao,S., Song,Y., Liu,H., and Nie,Q. (2008). Fus3-triggered Tec1 degradation modulates mating transcriptional output during the pheromone response. Mol. Syst. Biol. *4*, 212.

Ciudad,T., Andaluz,E., Steinberg-Neifach,O., Lue,N.F., Gow,N.A., Calderone,R.A., and Larriba,G. (2004). Homologous recombination in *Candida albicans*: role of CaRad52p in DNA repair, integration of linear DNA fragments and telomere length. Mol. Microbiol. *53*, 1177-1194.

Clark,C.D., Palzkill,T., and Botstein,D. (1994). Systematic mutagenesis of the yeast mating pheromone receptor third intracellular loop. J. Biol. Chem. *269*, 8831-8841.

Cloutier,M., Castilla,R., Bolduc,N., Zelada,A., Martineau,P., Bouillon,M., Magee,B.B., Passeron,S., Giasson,L., and Cantore,M.L. (2003). The two isoforms of the cAMP-dependent protein kinase catalytic subunit are involved in the control of dimorphism in the human fungal pathogen *Candida albicans*. Fungal. Genet. Biol. *38*, 133-141.

Cohen,R., Roth,F.J., Delgado,E., Ahearn,D.G., and Kalser,M.H. (1969). Fungal flora of the normal human small and large intestine. N. Engl. J. Med. *280*, 638-641.

Coleman,D.A., Oh,S.H., Zhao,X., Zhao,H., Hutchins,J.T., Vernachio,J.H., Patti,J.M., and Hoyer,L.L. (2009). Monoclonal antibodies specific for *Candida albicans* Als3 that immunolabel fungal cells in vitro and in vivo and block adhesion to host surfaces. J. Microbiol. Methods *78*, 71-78.

Cook,J.G., Bardwell,L., Kron,S.J., and Thorner,J. (1996). Two novel targets of the MAP kinase Kss1 are negative regulators of invasive growth in the yeast *Saccharomyces cerevisiae*. Genes Dev. *10*, 2831-2848.

Cormack,B.P., Bertram,G., Egerton,M., Gow,N.A., Falkow,S., and Brown,A.J. (1997). Yeast-enhanced green fluorescent protein (yEGFP)a reporter of gene expression in *Candida albicans*. Microbiology *143 (Pt 2)*, 303-311.

Corner,B.E. and Magee,P.T. (1997). *Candida* pathogenesis: unravelling the threads of infection. Curr. Biol. *7*, R691-R694.

Coste,A., Turner,V., Ischer,F., Morschhauser,J., Forche,A., Selmecki,A., Berman,J., Bille,J., and Sanglard,D. (2006). A mutation in Tac1p, a transcription factor regulating *CDR1* and *CDR2*, is coupled with loss of heterozygosity at chromosome 5 to mediate antifungal resistance in *Candida albicans*. Genetics *172*, 2139-2156.

Costerton,J.W., Stewart,P.S., and Greenberg,E.P. (1999). Bacterial biofilms: a common cause of persistent infections. Science *284*, 1318-1322.

Cote,P. and Whiteway,M. (2008). The role of *Candida albicans FAR1* in regulation of pheromone-mediated mating, gene expression and cell cycle arrest. Mol. Microbiol. *68*, 392-404.

Cowen,L.E., Nantel,A., Whiteway,M.S., Thomas,D.Y., Tessier,D.C., Kohn,L.M., and Anderson,J.B. (2002). Population genomics of drug resistance in *Candida albicans*. Proc. Natl. Acad. Sci. U. S. A *99*, 9284-9289.

Crosby,J.A., Konopka,J.B., and Fields,S. (2000). Constitutive activation of the *Saccharomyces cerevisiae* transcriptional regulator Ste12p by mutations at the amino-terminus. Yeast *16*, 1365-1375.

Crowe,M.L., Perry,B.N., and Connerton,I.F. (2000). Golf complements a *GPA1* null mutation in *Saccharomyces cerevisiae* and functionally couples to the *STE2* pheromone receptor. J. Recept. Signal. Transduct. Res. *20*, 61-73.

Cruz,M.C., Goldstein,A.L., Blankenship,J.R., Del,P.M., Davis,D., Cardenas,M.E., Perfect,J.R., McCusker,J.H., and Heitman,J. (2002). Calcineurin is essential for survival during membrane stress in *Candida albicans*. EMBO J. *21*, 546-559.

Csank,C., Schroppel,K., Leberer,E., Harcus,D., Mohamed,O., Meloche,S., Thomas,D.Y., and Whiteway,M. (1998). Roles of the *Candida albicans* mitogen-activated protein kinase homolog, Cek1p, in hyphal development and systemic candidiasis. Infect. Immun. *66*, 2713-2721.

Cutler,J.E. (1991). Putative virulence factors of *Candida albicans*. Annu. Rev. Microbiol. *45*, 187-218.

Dailey,L., Ambrosetti,D., Mansukhani,A., and Basilico,C. (2005). Mechanisms underlying differential responses to FGF signaling. Cytokine Growth Factor Rev. *16*, 233-247.

Dalton,A.K., Ako-Adjei,D., Murray,P.S., Murray,D., and Vogt,V.M. (2007). Electrostatic interactions drive membrane association of the human immunodeficiency virus type 1 Gag MA domain. J. Virol. *81*, 6434-6445.

Daniels,K.J., Lockhart,S.R., Staab,J.F., Sundstrom,P., and Soll,D.R. (2003). The adhesin Hwp1 and the first daughter cell localize to the a/a portion of the conjugation bridge during *Candida albicans* mating. Mol. Biol. Cell *14*, 4920-4930.

Daniels,K.J., Srikantha,T., Lockhart,S.R., Pujol,C., and Soll,D.R. (2006). Opaque cells signal white cells to form biofilms in *Candida albicans*. EMBO J. *25*, 2240-2252.

Davidson,I., Xiao,J.H., Rosales,R., Staub,A., and Chambon,P. (1988). The HeLa cell protein TEF-1 binds specifically and cooperatively to two SV40 enhancer motifs of unrelated sequence. Cell *54*, 931-942.

Davidson,R.C., Nichols,C.B., Cox,G.M., Perfect,J.R., and Heitman,J. (2003). A MAP kinase cascade composed of cell type specific and non-specific elements controls mating and differentiation of the fungal pathogen *Cryptococcus neoformans*. Mol. Microbiol. *49*, 469-485.

Davis,D., Wilson,R.B., and Mitchell,A.P. (2000). RIM101-dependent and-independent pathways govern pH responses in *Candida albicans*. Mol. Cell Biol. *20*, 971-978.

Davis,D.A., Bruno,V.M., Loza,L., Filler,S.G., and Mitchell,A.P. (2002). *Candida albicans* Mds3p, a conserved regulator of pH responses and virulence identified through insertional mutagenesis. Genetics *162* , 1573-1581.

De Backer,M.D., Maes,D., Vandoninck,S., Logghe,M., Contreras,R., and Luyten,W.H. (1999). Transformation of *Candida albicans* by electroporation. Yeast *15*, 1609-1618.

De Backer,M.D., Ilyina,T., Ma,X.J., Vandoninck,S., Luyten,W.H., and Vanden Bossche,H. (2001). Genomic profiling of the response of *Candida albicans* to itraconazole treatment using a DNA microarray. Antimicrob. Agents Chemother. *45*, 1660-1670.

Dignard,D. and Whiteway,M. (2006). *SST2*, a regulator of G-protein signaling for the *Candida albicans* mating response pathway. Eukaryot. Cell *5*, 192-202.

Dignard,D., El-Naggar,A.L., Logue,M.E., Butler,G., and Whiteway,M. (2007). Identification and characterization of *MFA1*, the gene encoding *Candida albicans* **a**-factor pheromone. Eukaryot. Cell *6*, 487-494.

Dignard,D., Andre,D., and Whiteway,M. (2008). Heterotrimeric G-protein subunit function in *Candida albicans*: both the alpha and beta subunits of the pheromone response G protein are required for mating. Eukaryot. Cell *7*, 1591-1599.

Dixon,K.P., Xu,J.R., Smirnoff,N., and Talbot,N.J. (1999). Independent signaling pathways regulate cellular turgor during hyperosmotic stress and appressorium-mediated plant infection by *Magnaporthe grisea*. Plant Cell *11*, 2045-2058.

Doedt,T., Krishnamurthy,S., Bockmuhl,D.P., Tebarth,B., Stempel,C., Russell,C.L., Brown,A.J., and Ernst,J.F. (2004). APSES proteins regulate morphogenesis and metabolism in *Candida albicans*. Mol. Biol. Cell *15*, 3167-3180.

Dohlman,H.G. and Thorner,J.W. (2001). Regulation of G protein-initiated signal transduction in yeast: paradigms and principles. Annu. Rev. Biochem. *70*, 703-754.

Dohlman,H.G. and Slessareva,J.E. (2006). Pheromone signaling pathways in yeast. Sci. STKE. *2006*, cm6.

Dolan,J.W., Kirkman,C., and Fields,S. (1989). The yeast STE12 protein binds to the DNA sequence mediating pheromone induction. Proc. Natl. Acad. Sci. U. S. A *86*, 5703-5707.

Dolan,J.W. and Fields,S. (1990). Overproduction of the yeast STE12 protein leads to constitutive transcriptional induction. Genes Dev. *4*, 492-502.

Dorer,R., Pryciak,P.M., and Hartwell,L.H. (1995). *Saccharomyces cerevisiae* cells execute a default pathway to select a mate in the absence of pheromone gradients. J. Cell Biol. *131*, 845-861.

Dorsky,R.I., Moon,R.T., and Raible,D.W. (2000). Environmental signals and cell fate specification in premigratory neural crest. Bioessays *22*, 708-716.

Dosil,M., Schandel,K.A., Gupta,E., Jenness,D.D., and Konopka,J.B. (2000). The C terminus of the *Saccharomyces cerevisiae* alpha-factor receptor contributes to the formation of preactivation complexes with its cognate G protein. Mol. Cell Biol. *20*, 5321-5329.

Douglas,L.J. (2003). *Candida* biofilms and their role in infection. Trends Microbiol. *11*, 30-36.

Dranginis,A.M., Rauceo,J.M., Coronado,J.E., and Lipke,P.N. (2007). A biochemical guide to yeast adhesins: glycoproteins for social and antisocial occasions. Microbiol. Mol. Biol. Rev. *71*, 282-294.

Du,W., Coaker,M., Sobel,J.D., and Akins,R.A. (2004). Shuttle vectors for *Candida albicans*: control of plasmid copy number and elevated expression of cloned genes. Curr. Genet. *45*, 390-398.

Dumitru,R., Navarathna,D.H., Semighini,C.P., Elowsky,C.G., Dumitru,R.V., Dignard,D., Whiteway,M., Atkin,A.L., and Nickerson,K.W. (2007). In vivo and in vitro anaerobic mating in *Candida albicans*. Eukaryot. Cell *6*, 465-472.

Duntze,W., MacKay,V., and Manney,T.R. (1970). *Saccharomyces cerevisiae*: a diffusible sex factor. Science *168*, 1472-1473.

Eck,R., Bruckmann,A., Wetzker,R., and Kunkel,W. (2000). A phosphatidylinositol 3-kinase of *Candida albicans*: molecular cloning and characterization. Yeast *16*, 933-944.

Edmond,M.B., Wallace,S.E., McClish,D.K., Pfaller,M.A., Jones,R.N., and Wenzel,R.P. (1999). Nosocomial bloodstream infections in United States hospitals: a three-year analysis. Clin. Infect. Dis. *29*, 239-244.

Edwards,C.R. and Besser,G.M. (1974). Diseases of the hypothalamus and pituitary gland. Clin. Endocrinol. Metab *3*, 475-505.

Eisman,B., Alonso-Monge,R., Roman,E., Arana,D., Nombela,C., and Pla,J. (2006). The Cek1 and Hog1 mitogen-activated protein kinases play complementary roles in cell wall biogenesis and chlamydospore formation in the fungal pathogen *Candida albicans*. Eukaryot. Cell *5*, 347-358.

Elion,E.A., Brill,J.A., and Fink,G.R. (1991). FUS3 represses CLN1 and CLN2 and in concert with KSS1 promotes signal transduction. Proc. Natl. Acad. Sci. U. S. A *88*, 9392-9396.

Elion,E.A., Satterberg,B., and Kranz,J.E. (1993). FUS3 phosphorylates multiple components of the mating signal transduction cascade: evidence for STE12 and FAR1. Mol. Biol. Cell *4*, 495-510.

Elion,E.A. (1995). Ste5: a meeting place for MAP kinases and their associates. Trends Cell Biol. *5*, 322-327.

Elion,E.A. (2000). Pheromone response, mating and cell biology. Curr. Opin. Microbiol. *3*, 573-581.

Enjalbert,B., Nantel,A., and Whiteway,M. (2003). Stress-induced gene expression in *Candida albicans*: absence of a general stress response. Mol. Biol. Cell *14*, 1460-1467.

Enloe,B., Diamond,A., and Mitchell,A.P. (2000). A single-transformation gene function test in diploid *Candida albicans*. J. Bacteriol. *182*, 5730-5736.

Eras,P., Goldstein,M.J., and Sherlock,P. (1972). *Candida* infection of the gastrointestinal tract. Medicine (Baltimore) *51*, 367-379.

Errede,B. and Ammerer,G. (1989). STE12, a protein involved in cell-type-specific transcription and signal transduction in yeast, is part of protein-DNA complexes. Genes Dev. *3*, 1349-1361.

Errede,B., Cade,R.M., Yashar,B.M., Kamada,Y., Levin,D.E., Irie,K., and Matsumoto,K. (1995). Dynamics and organization of MAP kinase signal pathways. Mol. Reprod. Dev. *42*, 477-485.

Esch,R.K., Wang,Y., and Errede,B. (2006). Pheromone-induced degradation of Ste12 contributes to signal attenuation and the specificity of developmental fate. Eukaryot. Cell *5*, 2147-2160.

Feng,Q., Summers,E., Guo,B., and Fink,G. (1999). Ras signaling is required for serum-induced hyphal differentiation in *Candida albicans*. J. Bacteriol. *181*, 6339-6346.

Fey,S.J., Nawrocki,A., Larsen,M.R., Gorg,A., Roepstorff,P., Skews,G.N., Williams,R., and Larsen,P.M. (1997). Proteome analysis of *Saccharomyces cerevisiae*: a methodological outline. Electrophoresis *18*, 1361-1372.

Fields,S., Chaleff,D.T., and Sprague,G.F., Jr. (1988). Yeast *STE7*, *STE11*, and *STE12* genes are required for expression of cell-type-specific genes. Mol. Cell Biol. *8*, 551-556.

Fields,S. (1990). Pheromone response in yeast. Trends Biochem. Sci. *15*, 270-273.

Finney,R., Langtimm,C.J., and Soll,D.R. (1985). The programs of protein synthesis accompanying the establishment of alternative phenotypes in *Candida albicans*. Mycopathologia *91*, 3-15.

Finne,J., Breimer,M.E., Hansson,G.C., Karlsson,K.A., Leffler,H., Vliegenthart,J.F., and van,H.H. (1989). Novel polyfucosylated N-linked glycopeptides with blood group A, H, X, and Y determinants from human small intestinal epithelial cells. J. Biol. Chem. *264*, 5720-5735.

Flatauer,L.J., Zadeh,S.F., and Bardwell,L. (2005). Mitogen-activated protein kinases with distinct requirements for Ste5 scaffolding influence signaling specificity in *Saccharomyces cerevisiae*. Mol. Cell Biol. *25*, 1793-1803.

Fonzi,W.A. and Irwin,M.Y. (1993). Isogenic strain construction and gene mapping in *Candida albicans*. Genetics *134*, 717-728.

Forche,A., Alby,K., Schaefer,D., Johnson,A.D., Berman,J., and Bennett,R.J. (2008). The parasexual cycle in *Candida albicans* provides an alternative pathway to meiosis for the formation of recombinant strains. PLoS. Biol. *6*, e110.

Fu,Y., Ibrahim,A.S., Sheppard,D.C., Chen,Y.C., French,S.W., Cutler,J.E., Filler,S.G., and Edwards,J.E., Jr. (2002). *Candida albicans* Als1p: an adhesin that is a downstream effector of the EFG1 filamentation pathway. Mol. Microbiol. *44*, 61-72.

Fujimura,H. (1990). Molecular cloning of the DAC2/FUS3 gene essential for pheromone-induced G1-arrest of the cell cycle in *Saccharomyces cerevisiae*. Curr. Genet. *18*, 395-400.

Gale,C., Finkel,D., Tao,N., Meinke,M., McClellan,M., Olson,J., Kendrick,K., and Hostetter,M. (1996). Cloning and expression of a gene encoding an integrin-like protein in *Candida albicans*. Proc. Natl. Acad. Sci. U. S. A *93*, 357-361.

Gale,C.A., Bendel,C.M., McClellan,M., Hauser,M., Becker,J.M., Berman,J., and Hostetter,M.K. (1998). Linkage of adhesion, filamentous growth, and virulence in *Candida albicans* to a single gene, *INT1*. Science *279*, 1355-1358.

Garcia-Bustos,J.F., Marini,F., Stevenson,I., Frei,C., and Hall,M.N. (1994). PIK1, an essential phosphatidylinositol 4-kinase associated with the yeast nucleus. EMBO J. *13*, 2352-2361.

Garcia-Sanchez,S., Aubert,S., Iraqui,I., Janbon,G., Ghigo,J.M., and d'Enfert,C. (2004). *Candida albicans* biofilms: a developmental state associated with specific and stable gene expression patterns. Eukaryot. Cell *3*, 536-545.

Gari,E., Volpe,T., Wang,H., Gallego,C., Futcher,B., and Aldea,M. (2001). Whi3 binds the mRNA of the G1 cyclin CLN3 to modulate cell fate in budding yeast. Genes Dev. *15*, 2803-2808.

Gavrias,V., Andrianopoulos,A., Gimeno,C.J., and Timberlake,W.E. (1996). *Saccharomyces cerevisiae* TEC1 is required for pseudohyphal growth. Mol. Microbiol. *19*, 1255-1263.

Ghigo,J.M. (2001). Natural conjugative plasmids induce bacterial biofilm development. Nature *412*, 442-445.

Ghuysen J.-M and Hakenbeck R (1994) Bacterial cell wall. Amsterdam: Elsevier. 581 p.

Giaever,G., Chu AM, Ni L, Connelly C, Riles L, Véronneau S, Dow S, Lucau-Danila A, Anderson K, André B, Arkin AP, Astromoff A, El-Bakkoury M, Bangham R, Benito R, Brachat S, Campanaro S, Curtiss M, Davis K, Deutschbauer A, Entian KD, Flaherty P, Foury F, Garfinkel DJ, Gerstein M, Gotte D, Güldener U, Hegemann JH, Hempel S, Herman Z, Jaramillo DF, Kelly DE, Kelly SL, Kötter P, LaBonte D, Lamb DC, Lan N, Liang H, Liao H, Liu L, Luo C, Lussier M, Mao R, Menard P, Ooi SL, Revuelta JL, Roberts CJ, Rose M, Ross-Macdonald P, Scherens B, Schimmack G, Shafer B, Shoemaker DD, Sookhai-Mahadeo S, Storms RK, Strathern JN, Valle G, Voet M, Volckaert G, Wang CY, Ward TR, Wilhelmy J, Winzeler EA, Yang Y, Yen G, Youngman E, Yu K, Bussey H, Boeke JD, Snyder M, Philippsen P, Davis RW, Johnston M. (2002). Functional profiling of the *Saccharomyces cerevisiae* genome. Nature *418*, 387-391.

Gilchrist,R.B., Ritter,L.J., and Armstrong,D.T. (2004). Oocyte-somatic cell interactions during follicle development in mammals. Anim Reprod. Sci. *82-83*, 431-446.

Giusani,A.D., Vinces,M., and Kumamoto,C.A. (2002). Invasive filamentous growth of *Candida albicans* is promoted by Czf1p-dependent relief of Efg1p-mediated repression. Genetics *160*, 1749-1753.

Gorbach,S.L., Spanknebel,G., Weinstein,L., Plaut,A.G., Nahas,L., and Levitan,R. (1969). Studies of intestinal microflora. 8. Effect of lincomycin on the microbial population of the human intestine. J. Infect. Dis. *120*, 298-304.

Gorner,W., Durchschlag,E., Martinez-Pastor,M.T., Estruch,F., Ammerer,G., Hamilton,B., Ruis,H., and Schuller,C. (1998). Nuclear localization of the C2H2 zinc finger protein Msn2p is regulated by stress and protein kinase A activity. Genes Dev. *12*, 586-597.

Gortz,H.D. and Fujishima,M. (1983). Conjugation and meiosis of Paramecium caudatum infected with the micronucleus-specific bacterium *Holospora elegans*. Eur. J. Cell Biol. *32*, 86-91.

Gow,N.A. and Gooday,G.W. (1982). Vacuolation, branch production and linear growth of germ tubes in *Candida albicans*. J. Gen. Microbiol. *128*, 2195-2198.

Gow,N.A, Perera,T.H., Sherwood-Higham,J., Gooday,G.W., Gregory,D.W., Marshall,D. (1994a). Investigation of touch-sensitive responses by hyphae of the human pathogenic fungus *Candida albicans*. Scanning Microsc. *8*, 705-710.

Gow,N.A., Robbins,P.W., Lester,J.W., Brown,A.J., Fonzi,W.A., Chapman,T., and Kinsman,O.S. (1994b). A hyphal-specific chitin synthase gene (*CHS2*) is not essential for growth, dimorphism, or virulence of *Candida albicans*. Proc. Natl. Acad. Sci. U. S. A *91*, 6216-6220.

Gow,N.A. (1997). Germ tube growth of *Candida albicans*. Curr. Top. Med. Mycol. *8*, 43-55.

Gow,N.A., Bates,S., Brown,A.J., Buurman,E.T., Thomson,L.M., and Westwater,C. (1999). *Candida* cell wall mannosylation: importance in host-fungus interaction and potential as a target for the development of antifungal drugs. Biochem. Soc. Trans. *27*, 512-516.

Goyard,S. *et al.* (2008). The Yak1 kinase is involved in the initiation and maintenance of hyphal growth in *Candida albicans*. Mol. Biol. Cell *19*, 2251-2266.

Granger,B.L., Flenniken,M.L., Davis,D.A., Mitchell,A.P., and Cutler,J.E. (2005). Yeast wall protein 1 of *Candida albicans*. Microbiology *151*, 1631-1644.

Green,C.B., Cheng,G., Chandra,J., Mukherjee,P., Ghannoum,M.A., and Hoyer,L.L. (2004). RT-PCR detection of *Candida albicans ALS* gene expression in the reconstituted human epithelium (RHE) model of oral candidiasis and in model biofilms. Microbiology *150*, 267-275.

Groes,M., Teilum,K., Olesen,K., Poulsen,F.M., and Henriksen,A. (2002). Purification, crystallization and preliminary X-ray diffraction analysis of the carbohydrate-binding domain of flocculin, a cell-adhesion molecule from *Saccharomyces carlsbergensis*. Acta Crystallogr. D. Biol. Crystallogr. *58*, 2135-2137.

Grozinger,C.M., Hassig,C.A., and Schreiber,S.L. (1999). Three proteins define a class of human histone deacetylases related to yeast Hda1p. Proc. Natl. Acad. Sci. U. S. A *96*, 4868-4873.

Grundy,W.N., Bailey,T.L., Elkan,C.P., and Baker,M.E. (1997). Meta-MEME: motif-based hidden Markov models of protein families. Comput. Appl. Biosci. *13*, 397-406.

Gunther,J., Nguyen,M., Hartl,A., Kunkel,W., Zipfel,P.F., and Eck,R. (2005). Generation and functional in vivo characterization of a lipid kinase defective phosphatidylinositol 3-kinase Vps34p of *Candida albicans*. Microbiology *151*, 81-89.

Gustin,M.C., Albertyn,J., Alexander,M., and Davenport,K. (1998). MAP kinase pathways in the yeast *Saccharomyces cerevisiae*. Microbiol. Mol. Biol. Rev. *62*, 1264-1300.

Guyton, A.C., and Hall, J.E. (2000). Textbook of Medical Physiology (Philadelphia, PA: W.B. Saunders).

Haber,J.E. (1992). Mating-type gene switching in *Saccharomyces cerevisiae*. Trends Genet. *8*, 446-452.

Haber,J.E. (1998). Mating-type gene switching in *Saccharomyces cerevisiae*. Annu. Rev. Genet. *32*, 561-599.

Hagen,D.C., McCaffrey,G., and Sprague,G.F., Jr. (1986). Evidence the yeast *STE3* gene encodes a receptor for the peptide pheromone a factor: gene sequence and implications for the structure of the presumed receptor. Proc. Natl. Acad. Sci. U. S. A *83*, 1418-1422.

Hagen,D.C., McCaffrey,G., and Sprague,G.F., Jr. (1991). Pheromone response elements are necessary and sufficient for basal and pheromone-induced transcription of the *FUS1* gene of *Saccharomyces cerevisiae*. Mol. Cell Biol. *11*, 2952-2961.

Hall-Stoodley,L. and Stoodley,P. (2005). Biofilm formation and dispersal and the transmission of human pathogens. Trends Microbiol. *13*, 7-10.

Hartwell,L.H. (1980). Mutants of *Saccharomyces cerevisiae* unresponsive to cell division control by polypeptide mating hormone. J. Cell Biol. *85*, 811-822.

Hassig,C.A., Tong,J.K., Fleischer,T.C., Owa,T., Grable,P.G., Ayer,D.E., and Schreiber,S.L. (1998). A role for histone deacetylase activity in HDAC1-mediated transcriptional repression. Proc. Natl. Acad. Sci. U. S. A *95*, 3519-3524.

Hausner,M. and Wuertz,S. (1999). High rates of conjugation in bacterial biofilms as determined by quantitative in situ analysis. Appl. Environ. Microbiol. *65*, 3710-3713.

Hawser,S.P. and Douglas,L.J. (1994). Biofilm formation by *Candida* species on the surface of catheter materials in vitro. Infect. Immun. *62*, 915-921.

Hawser,S.P., Baillie,G.S., and Douglas,L.J. (1998). Production of extracellular matrix by *Candida albicans* biofilms. J. Med. Microbiol. *47*, 253-256.

Haynes,P.A., Gygi,S.P., Figeys,D., and Aebersold,R. (1998). Proteome analysis: biological assay or data archive? Electrophoresis *19*, 1862-1871.

Hernaez,M.L., Gil,C., Pla,J., and Nombela,C. (1998). Induced expression of the *Candida albicans* multidrug resistance gene *CDR1* in response to fluconazole and other antifungals. Yeast *14*, 517-526.

Hicke,L. and Riezman,H. (1996). Ubiquitination of a yeast plasma membrane receptor signals its ligand-stimulated endocytosis. Cell *84*, 277-287.

Hicke,L. (1999). Gettin' down with ubiquitin: turning off cell-surface receptors, transporters and channels. Trends Cell Biol. *9*, 107-112.

Hicks,J.B., Strathern,J.N., and Herskowitz,I. (1977). Interconversion of Yeast Mating Types III. Action of the Homothallism (HO) Gene in Cells Homozygous for the Mating Type Locus. Genetics *85*, 395-405.

Hill,D.R., Brunner,M.E., Schmitz,D.C., Davis,C.C., Flood,J.A., Schlievert,P.M., Wang-Weigand,S.Z., and Osborn,T.W. (2005). In vivo assessment of human vaginal oxygen and carbon dioxide levels during and post menses. J. Appl. Physiol *99*, 1582-1591.

Hill,R.B., Jr., Rowlands,D.T., Jr., and Rifkind,D. (1999). Infectious pulmonary disease in patients receiving immunosuppressive therapy for organ transplantation. 1964. Rev. Med. Virol. *9*, 5-10.

Hiller,E., Heine,S., Brunner,H., and Rupp,S. (2007). *Candida albicans* Sun41p, a putative glycosidase, is involved in morphogenesis, cell wall biogenesis, and biofilm formation. Eukaryot. Cell *6*, 2056-2065.

Hnisz,D., Schwarzmuller,T., and Kuchler,K. (2009). Transcriptional loops meet chromatin: a dual-layer network controls white-opaque switching in *Candida albicans*. Mol. Microbiol. *74*, 1-15.

Ho,J. and Bretscher,A. (2001). Ras regulates the polarity of the yeast actin cytoskeleton through the stress response pathway. Mol. Biol. Cell *12*, 1541-1555.

Hogan,D.A., Vik,A., and Kolter,R. (2004). A *Pseudomonas aeruginosa* quorum-sensing molecule influences *Candida albicans* morphology. Mol. Microbiol. *54*, 1212-1223.

Honigberg,S.M., McCarroll,R.M., and Esposito,R.E. (1993). Regulatory mechanisms in meiosis. Curr. Opin. Cell Biol. *5*, 219-225.

Hoyer,L.L. (2001). The *ALS* gene family of *Candida albicans*. Trends Microbiol. *9*, 176-180.

Hoyer,L.L., Green,C.B., Oh,S.H., and Zhao,X. (2008). Discovering the secrets of the *Candida albicans* agglutinin-like sequence (*ALS*) gene family--a sticky pursuit. Med. Mycol. *46*, 1-15.

Hrmova,M. and Drobnica,L. (1982). Induction of mycelial type of development in *Candida albicans* by the antibiotic monorden and N-acetyl-D-glucosamine. Mycopathologia *79*, 55-64.

Huang,G., Wang,H., Chou,S., Nie,X., Chen,J., and Liu,H. (2006). Bistable expression of *WOR1*, a master regulator of white-opaque switching in *Candida albicans*. Proc. Natl. Acad. Sci. U. S. A *103*, 12813-12818.

Huang,G., Srikantha,T., Sahni,N., Yi,S., and Soll,D.R. (2009). CO(2) regulates white-to-opaque switching in *Candida albicans*. Curr. Biol. *19*, 330-334.

Hube,B., Monod,M., Schofield,D.A., Brown,A.J., and Gow,N.A. (1994). Expression of seven members of the gene family encoding secretory aspartyl proteinases in *Candida albicans*. Mol. Microbiol. *14*, 87-99.

Hube,B. and Naglik,J. (2001). *Candida albicans* proteinases: resolving the mystery of a gene family. Microbiology *147*, 1997-2005.

Hull,C.M. and Johnson,A.D. (1999). Identification of a mating type-like locus in the asexual pathogenic yeast *Candida albicans*. Science *285*, 1271-1275.

Hull,C.M., Raisner,R.M., and Johnson,A.D. (2000). Evidence for mating of the "asexual" yeast *Candida albicans* in a mammalian host. Science *289*, 307-310.

Huyer,G., Kistler,A., Nouvet,F.J., George,C.M., Boyle,M.L., and Michaelis,S. (2006). *Saccharomyces cerevisiae* **a**-factor mutants reveal residues critical for processing, activity, and export. Eukaryot. Cell *5*, 1560-1570.

Hwang,J.J., Chambon,P., and Davidson,I. (1993). Characterization of the transcription activation function and the DNA binding domain of transcriptional enhancer factor-1. EMBO J. *12*, 2337-2348.

Hwang-Shum,J.J., Hagen,D.C., Jarvis,E.E., Westby,C.A., and Sprague,G.F., Jr. (1991). Relative contributions of MCM1 and STE12 to transcriptional activation of **a**- and alpha-specific genes from *Saccharomyces cerevisiae*. Mol. Gen. Genet. *227*, 197-204.

Hwang,C.S., Oh,J.H., Huh,W.K., Yim,H.S., and Kang,S.O. (2003). Ssn6, an important factor of morphological conversion and virulence in *Candida albicans*. Mol. Microbiol. *47*, 1029-1043.

Irie,K., Nomoto,S., Miyajima,I., and Matsumoto,K. (1991). *SGV1* encodes a CDC28/cdc2-related kinase required for a G alpha subunit-mediated adaptive response to pheromone in *S. cerevisiae*. Cell *65*, 785-795.

Ishii,N., Yamamoto,M., Yoshihara,F., Arisawa,M., and Aoki,Y. (1997). Biochemical and genetic characterization of Rbf1p, a putative transcription factor of *Candida albicans*. Microbiology *143 (Pt 2)*, 429-435.

James,P. (1997). Of genomes and proteomes. Biochem. Biophys. Res. Commun. *231*, 1-6.

Janbon,G., Sherman,F., and Rustchenko,E. (1998). Monosomy of a specific chromosome determines L-sorbose utilization: a novel regulatory mechanism in *Candida albicans*. Proc. Natl. Acad. Sci. U. S. A *95*, 5150-5155.

Jarvis,E.E., Clark,K.L., and Sprague,G.F., Jr. (1989). The yeast transcription activator PRTF, a homolog of the mammalian serum response factor, is encoded by the *MCM1* gene. Genes Dev. *3*, 936-945.

Jones,S., White,G., and Hunter,P.R. (1994). Increased phenotypic switching in strains of *Candida albicans* associated with invasive infections. J. Clin. Microbiol. *32*, 2869-2870.

Jones,T. *et al.* (2004). The diploid genome sequence of *Candida albicans*. Proc. Natl. Acad. Sci. U. S. A *101*, 7329-7334.

Jung,W.H. and Stateva,L.I. (2003). The cAMP phosphodiesterase encoded by *CaPDE2* is required for hyphal development in *Candida albicans*. Microbiology *149*, 2961-2976.

Juretic,D., Zoranic,L., and Zucic,D. (2002). Basic charge clusters and predictions of membrane protein topology. J. Chem. Inf. Comput. Sci. *42*, 620-632.

Kadosh,D. and Struhl,K. (1998). Histone deacetylase activity of Rpd3 is important for transcriptional repression in vivo. Genes Dev. *12*, 797-805.

Kadosh,D. and Johnson,A.D. (2001). Rfg1, a protein related to the *Saccharomyces cerevisiae* hypoxic regulator Rox1, controls filamentous growth and virulence in *Candida albicans*. Mol. Cell Biol. *21*, 2496-2505.

Kaminishi,H., Iwata,A., Tamaki,T., Cho,T., and Hagihara,Y. (1994). Spiral hyphae of *Candida albicans* formed in anaerobic culture. Mycoses *37*, 349-352.

Kao,A.S. *et al.* (1999). The epidemiology of candidemia in two United States cities: results of a population-based active surveillance. Clin. Infect. Dis. *29*, 1164-1170.

Kapteyn,J.C., Van Den Ende,H., and Klis,F.M. (1999). The contribution of cell wall proteins to the organization of the yeast cell wall. Biochim. Biophys. Acta *1426*, 373-383.

Karababa,M., Valentino,E., Pardini,G., Coste,A.T., Bille,J., and Sanglard,D. (2006). CRZ1, a target of the calcineurin pathway in *Candida albicans*. Mol. Microbiol. *59*, 1429-1451.

Keleher,C.A., Passmore,S., and Johnson,A.D. (1989). Yeast repressor alpha 2 binds to its operator cooperatively with yeast protein Mcm1. Mol. Cell Biol. *9*, 5228-5230.

Kelly,M.T., MacCallum,D.M., Clancy,S.D., Odds,F.C., Brown,A.J., and Butler,G. (2004). The *Candida albicans CaACE2* gene affects morphogenesis, adherence and virulence. Mol. Microbiol. *53*, 969-983.

Kennedy,M.J., Rogers,A.L., Hanselmen,L.R., Soll,D.R., and Yancey,R.J., Jr. (1988). Variation in adhesion and cell surface hydrophobicity in *Candida albicans* white and opaque phenotypes. Mycopathologia *102* , 149-156.

Ketel,C., Wang,H.S., McClellan,M., Bouchonville,K., Selmecki,A., Lahav,T., Gerami-Nejad,M., and Berman,J. (2009). Neocentromeres form efficiently at multiple possible loci in *Candida albicans*. PLoS. Genet. *5*, e1000400.

Ke,S.H. and Madison,E.L. (1997). Rapid and efficient site-directed mutagenesis by single-tube 'megaprimer' PCR method. Nucleic Acids Res. *25*, 3371-3372.

Khalaf,R.A. and Zitomer,R.S. (2001). The DNA binding protein Rfg1 is a repressor of filamentation in *Candida albicans*. Genetics *157*, 1503-1512.

Kinsman,O.S., Pitblado,K., and Coulson,C.J. (1988). Effect of mammalian steroid hormones and luteinizing hormone on the germination of *Candida albicans* and implications for vaginal candidosis. Mycoses *31*, 617-626.

Klar,A.J., Fogel,S., and Lusnak,K. (1979). Gene conversion of the mating-type locus in *Saccharomyces cerevisiae*. Genetics *92* , 777-782.

Klar,A.J., Srikantha,T., and Soll,D.R. (2001). A histone deacetylation inhibitor and mutant promote colony-type switching of the human pathogen *Candida albicans*. Genetics *158*, 919-924.

Klengel T, Liang WJ, Chaloupka J, Ruoff C, Schroppel K, Naglik JR, Eckert SE, Mogensen EG, Haynes K, Tuite MF, Levin LR, Buck J, Muhlschlegel FA (2005). Fungal adenylyl cyclase integrates CO2 sensing with cAMP signaling and virulence. Curr. Biol. *15*, 2021-2026.

Kobayashi,H., Oyamada,H., Iwadate,N., Suzuki,H., Mitobe,H., Takahashi,K., Shibata,N., Suzuki,S., and Okawa,Y. (1998). Structural and immunochemical characterization of beta-1,2-linked mannobiosyl phosphate residue in the cell wall mannan of *Candida glabrata*. Arch. Microbiol. *169*, 188-194.

Kohler,J.R. and Fink,G.R. (1996). *Candida albicans* strains heterozygous and homozygous for mutations in mitogen-activated protein kinase signaling components have defects in hyphal development. Proc. Natl. Acad. Sci. U. S. A *93*, 13223-13228.

Kojic,E.M. and Darouiche,R.O. (2004). *Candida* infections of medical devices. Clin. Microbiol. Rev. *17*, 255-267.

Kolotila,M.P. and Diamond,R.D. (1990). Effects of neutrophils and in vitro oxidants on survival and phenotypic switching of *Candida albicans* WO-1. Infect. Immun. *58*, 1174-1179.

Konopka,J.B., Jenness,D.D., and Hartwell,L.H. (1988). The C-terminus of the *S. cerevisiae* alpha-pheromone receptor mediates an adaptive response to pheromone. Cell *54*, 609-620.

Konopka,J.B., Margarit,S.M., and Dube,P. (1996). Mutation of Pro-258 in transmembrane domain 6 constitutively activates the G protein-coupled alpha-factor receptor. Proc. Natl. Acad. Sci. U. S. A *93*, 6764-6769.

Kraus,P.R., Fox,D.S., Cox,G.M., and Heitman,J. (2003). The *Cryptococcus neoformans* MAP kinase Mpk1 regulates cell integrity in response to antifungal drugs and loss of calcineurin function. Mol. Microbiol. *48*, 1377-1387.

Kronstad,J.W., Holly,J.A., and MacKay,V.L. (1987). A yeast operator overlaps an upstream activation site. Cell *50*, 369-377.

Krueger,K.E., Ghosh,A.K., Krom,B.P., and Cihlar,R.L. (2004). Deletion of the *NOT4* gene impairs hyphal development and pathogenicity in *Candida albicans*. Microbiology *150*, 229-240.

Kruppa,M. and Calderone,R. (2006). Two-component signal transduction in human fungal pathogens. FEMS Yeast Res. *6*, 149-159.

Kuhn,D.M., George,T., Chandra,J., Mukherjee,P.K., and Ghannoum,M.A. (2002). Antifungal susceptibility of *Candida* biofilms: unique efficacy of amphotericin B lipid formulations and echinocandins. Antimicrob. Agents Chemother. *46*, 1773-1780.

Kuhn,D.M. and Ghannoum,M.A. (2004). Candida biofilms: antifungal resistance and emerging therapeutic options. Curr. Opin. Investig. Drugs *5*, 186-197.

Kullas,A.L., Martin,S.J., and Davis,D. (2007). Adaptation to environmental pH: integrating the Rim101 and calcineurin signal transduction pathways. Mol. Microbiol. *66*, 858-871.

Kumamoto,C.A. (2002). *Candida* biofilms. Curr. Opin. Microbiol. *5*, 608-611.

Kurjan,J. (1993). The pheromone response pathway in *Saccharomyces cerevisiae*. Annu. Rev. Genet. *27*, 147-179.

Kvaal,C., Lachke,S.A., Srikantha,T., Daniels,K., McCoy,J., and Soll,D.R. (1999). Misexpression of the opaque-phase-specific gene *PEP1* (*SAP1*) in the white phase of *Candida albicans* confers increased virulence in a mouse model of cutaneous infection. Infect. Immun. *67*, 6652-6662.

Kvaal,C.A., Srikantha,T., and Soll,D.R. (1997). Misexpression of the white-phase-specific gene *WH11* in the opaque phase of *Candida albicans* affects switching and virulence. Infect. Immun. *65*, 4468-4475.

Lachke,S.A., Srikantha,T., and Soll,D.R. (2003a). The regulation of *EFG1* in white-opaque switching in *Candida albicans* involves overlapping promoters. Mol. Microbiol. *48*, 523-536.

Lachke,S.A., Lockhart,S.R., Daniels,K.J., and Soll,D.R. (2003b). Skin facilitates *Candida albicans* mating. Infect. Immun. *71*, 4970-4976.

Lambert,M., Blanchin-Roland,S., Le,L.F., Lepingle,A., and Gaillardin,C. (1997). Genetic analysis of regulatory mutants affecting synthesis of extracellular proteinases in the yeast *Yarrowia lipolytica*: identification of a RIM101/pacC homolog. Mol. Cell Biol. *17*, 3966-3976.

Lan,C.Y., Newport,G., Murillo,L.A., Jones,T., Scherer,S., Davis,R.W., and Agabian,N. (2002). Metabolic specialization associated with phenotypic switching in *Candida albicans*. Proc. Natl. Acad. Sci. U. S. A *99*, 14907-14912.

Lane,S., Birse,C., Zhou,S., Matson,R., and Liu,H. (2001). DNA array studies demonstrate convergent regulation of virulence factors by Cph1, Cph2, and Efg1 in *Candida albicans*. J. Biol. Chem. *276*, 48988-48996.

Lazo,B., Bates,S., and Sudbery,P. (2005). The G1 cyclin Cln3 regulates morphogenesis in *Candida albicans*. Eukaryot. Cell *4*, 90-94.

Leberer,E., Harcus,D., Broadbent,I.D., Clark,K.L., Dignard,D., Ziegelbauer,K., Schmidt,A., Gow,N.A., Brown,A.J., and Thomas,D.Y. (1996). Signal transduction through homologs of the Ste20p and Ste7p protein kinases can trigger hyphal formation in the pathogenic fungus *Candida albicans*. Proc. Natl. Acad. Sci. U. S. A *93*, 13217-13222.

Leberer,E., Thomas,D.Y., and Whiteway,M. (1997). Pheromone signalling and polarized morphogenesis in yeast. Curr. Opin. Genet. Dev. *7*, 59-66.

Leberer,E., Harcus,D., Dignard,D., Johnson,L., Ushinsky,S., Thomas,D.Y., and Schroppel,K. (2001). Ras links cellular morphogenesis to virulence by regulation of the MAP kinase and cAMP signalling pathways in the pathogenic fungus *Candida albicans*. Mol. Microbiol. *42*, 673-687.

Lee,K.L., Buckley,H.R., and Campbell,C.C. (1975). An amino acid liquid synthetic medium for the development of mycelial and yeast forms of *Candida albicans*. Sabouraudia. *13*, 148-153.

Lee,M.J. and Dohlman,H.G. (2008). Coactivation of G protein signaling by cell-surface receptors and an intracellular exchange factor. Curr. Biol. *18*, 211-215.

Lee,T.I.., Rinaldi,N.J., Robert,F., Odom,D.T., Bar-Joseph,Z., Gerber,G.K., Hannett,N.M., Harbison,C.T., Thompson,C.M., Simon,I., Zeitlinger,J., Jennings,E.G., Murray,H.L., Gordon,D.B., Ren,B., Wyrick,J.J.,Tagne,J.B., Volkert,T.L., Fraenkel,E., Gifford,D.K., Young,R.A. (2002). Transcriptional regulatory networks in *Saccharomyces cerevisiae*. Science *298*, 799-804.

Legrand,M., Lephart,P., Forche,A., Mueller,F.M., Walsh,T., Magee,P.T., and Magee,B.B. (2004). Homozygosity at the *MTL* locus in clinical strains of *Candida albicans*: karyotypic rearrangements and tetraploid formation. Mol. Microbiol. *52*, 1451-1462.

Lengeler,K.B., Davidson,R.C., D'souza,C., Harashima,T., Shen,W.C., Wang,P., Pan,X., Waugh,M., and Heitman,J. (2000). Signal transduction cascades regulating fungal development and virulence. Microbiol. Mol. Biol. Rev. *64*, 746-785.

Levin,D.E. and Errede,B. (1995). The proliferation of MAP kinase signaling pathways in yeast. Curr. Opin. Cell Biol. *7*, 197-202.

Levitt,M.D. and Bond,J.H., Jr. (1970). Volume, composition, and source of intestinal gas. Gastroenterology *59*, 921-929.

Li,D., Bobrowicz,P., Wilkinson,H.H., and Ebbole,D.J. (2005). A mitogen-activated protein kinase pathway essential for mating and contributing to vegetative growth in *Neurospora crassa*. Genetics *170*, 1091-1104.

Li,F. and Palecek,S.P. (2003). *EAP1*, a *Candida albicans* gene involved in binding human epithelial cells. Eukaryot. Cell *2*, 1266-1273.

Li,F. and Palecek,S.P. (2005). Identification of *Candida albicans* genes that induce *Saccharomyces cerevisiae* cell adhesion and morphogenesis. Biotechnol. Prog. *21*, 1601-1609.

Li,F., Svarovsky,M.J., Karlsson,A.J., Wagner,J.P., Marchillo,K., Oshel,P., Andes,D., and Palecek,S.P. (2007). Eap1p, an adhesin that mediates *Candida albicans* biofilm formation in vitro and in vivo. Eukaryot. Cell *6*, 931-939.

Li,F. and Palecek,S.P. (2008). Distinct domains of the *Candida albicans* adhesin Eap1p mediate cell-cell and cell-substrate interactions. Microbiology *154*, 1193-1203.

Li,X., Yan,Z., and Xu,J. (2003). Quantitative variation of biofilms among strains in natural populations of *Candida albicans*. Microbiology *149*, 353-362.

Li,Y., Su,C., Mao,X., Cao,F., and Chen,J. (2007). Roles of *Candida albicans* Sfl1 in hyphal development. Eukaryot. Cell *6*, 2112-2121.

Liu,C.L., Kaplan,T., Kim,M., Buratowski,S., Schreiber,S.L., Friedman,N., and Rando,O.J. (2005). Single-nucleosome mapping of histone modifications in *S. cerevisiae*. PLoS. Biol. *3*, e328.

Liu,H., Kohler,J., and Fink,G.R. (1994). Suppression of hyphal formation in *Candida albicans* by mutation of a STE12 homolog. Science *266*, 1723-1726.

Liu,H. (2002). Co-regulation of pathogenesis with dimorphism and phenotypic switching in *Candida albicans*, a commensal and a pathogen. Int. J. Med. Microbiol. *292*, 299-311.

Liu,Y., Li,Z., Liu,G., Jia,J., Li,S., and Yu,C. (2008). Liquid chromatography-tandem mass spectrometry method for determination of N-acetylglucosamine concentration in human plasma. J. Chromatogr. B Analyt. Technol. Biomed. Life Sci. *862*, 150-154.

Lo,H.J., Kohler,J.R., DiDomenico,B., Loebenberg,D., Cacciapuoti,A., and Fink,G.R. (1997). Nonfilamentous *C. albicans* mutants are avirulent. Cell *90*, 939-949.

Lo,W.S. and Dranginis,A.M. (1998). The cell surface flocculin Flo11 is required for pseudohyphae formation and invasion by *Saccharomyces cerevisiae*. Mol. Biol. Cell *9*, 161-171.

Lockhart,S.R., Reed,B.D., Pierson,C.L., and Soll,D.R. (1996). Most frequent scenario for recurrent *Candida* vaginitis is strain maintenance with "substrain shuffling": demonstration by sequential DNA fingerprinting with probes Ca3, C1, and CARE2. J. Clin. Microbiol. *34*, 767-777.

Lockhart,S.R., Nguyen,M., Srikantha,T., and Soll,D.R. (1998). A MADS box protein consensus binding site is necessary and sufficient for activation of the opaque-phase-specific gene *OP4* of *Candida albicans*. J. Bacteriol. *180*, 6607-6616.

Lockhart,S.R., Pujol,C., Daniels,K.J., Miller,M.G., Johnson,A.D., Pfaller,M.A., and Soll,D.R. (2002). In *Candida albicans*, white-opaque switchers are homozygous for mating type. Genetics *162*, 737-745.

Lockhart,S.R., Daniels,K.J., Zhao,R., Wessels,D., and Soll,D.R. (2003a). Cell biology of mating in *Candida albicans*. Eukaryot. Cell *2*, 49-61.

Lockhart,S.R., Zhao,R., Daniels,K.J., and Soll,D.R. (2003b). Alpha-pheromone-induced "shmooing" and gene regulation require white-opaque switching during *Candida albicans* mating. Eukaryot. Cell *2*, 847-855.

Lockhart,S.R., Wu,W., Radke,J.B., Zhao,R., and Soll,D.R. (2005). Increased virulence and competitive advantage of a/alpha over a/a or alpha/alpha offspring conserves the mating system of *Candida albicans*. Genetics *169*, 1883-1890.

Loeb,J.D., Sepulveda-Becerra,M., Hazan,I., and Liu,H. (1999). A G1 cyclin is necessary for maintenance of filamentous growth in *Candida albicans*. Mol. Cell Biol. *19*, 4019-4027.

Lohse,M.B. and Johnson,A.D. (2008). Differential phagocytosis of white versus opaque *Candida albicans* by *Drosophila* and mouse phagocytes. PLoS. One. *3*, e1473.

Lorenz,M.C. and Fink,G.R. (2001). The glyoxylate cycle is required for fungal virulence. Nature *412*, 83-86.

Lorenz,M.C. and Fink,G.R. (2002). Life and death in a macrophage: role of the glyoxylate cycle in virulence. Eukaryot. Cell *1*, 657-662.

Lynch,A.S. and Robertson,G.T. (2008). Bacterial and fungal biofilm infections. Annu. Rev. Med. *59*, 415-428.

Ma,D., Cook,J.G., and Thorner,J. (1995). Phosphorylation and localization of Kss1, a MAP kinase of the *Saccharomyces cerevisiae* pheromone response pathway. Mol. Biol. Cell *6*, 889-909.

Madhani,H.D. and Fink,G.R. (1997). Combinatorial control required for the specificity of yeast MAPK signaling. Science *275*, 1314-1317.

Madhani,H.D., Styles,C.A., and Fink,G.R. (1997). MAP kinases with distinct inhibitory functions impart signaling specificity during yeast differentiation. Cell *91*, 673-684.

Madhani,H.D. and Fink,G.R. (1998a). The riddle of MAP kinase signaling specificity. Trends Genet. *14*, 151-155.

Madhani,H.D. and Fink,G.R. (1998b). The control of filamentous differentiation and virulence in fungi. Trends Cell Biol. *8*, 348-353.

Maejima,K., Shimoda,K., Morita,C., Fujiwara,T., and Kitamura,T. (1980). Colonization and pathogenicity of Saccharomyces cerevisiae, MC16, in mice and cynomolgus monkeys after oral and intravenous administration. Jpn. J. Med. Sci. Biol. *33*, 271-276.

Magee,B.B., D'Souza,T.M., and Magee,P.T. (1987). Strain and species identification by restriction fragment length polymorphisms in the ribosomal DNA repeat of *Candida* species. J. Bacteriol. *169*, 1639-1643.

Magee,B.B. and Magee,P.T. (2000). Induction of mating in *Candida albicans* by construction of MTLa and MTLalpha strains. Science *289*, 310-313.

Magee,B.B., Legrand,M., Alarco,A.M., Raymond,M., and Magee,P.T. (2002). Many of the genes required for mating in *Saccharomyces cerevisiae* are also required for mating in *Candida albicans*. Mol. Microbiol. *46*, 1345-1351.

Magee,B.B., Sanchez,M.D., Saunders,D., Harris,D., Berriman,M., and Magee,P.T. (2008). Extensive chromosome rearrangements distinguish the karyotype of the hypovirulent species *Candida dubliniensis* from the virulent *Candida albicans*. Fungal. Genet. Biol. *45*, 338-350.

Mahanty,S.K., Wang,Y., Farley,F.W., and Elion,E.A. (1999). Nuclear shuttling of yeast scaffold Ste5 is required for its recruitment to the plasma membrane and activation of the mating MAPK cascade. Cell *98*, 501-512.

Maksymiuk,A.W., Thongprasert,S., Hopfer,R., Luna,M., Fainstein,V., and Bodey,G.P. (1984). Systemic candidiasis in cancer patients. Am. J. Med. *77*, 20-27.

Malavasic,M.J., Mcelhaney-Feser,G.E., Southard,S.B., and Cihlar,R.L. (1991). Phenotypic variation of a virulent *Candida albicans* strain and two spontaneous, relatively avirulent mutant strain derivatives. J. Med. Vet. Mycol. *29*, 145-155.

Maleri,S., Ge,Q., Hackett,E.A., Wang,Y., Dohlman,H.G., and Errede,B. (2004). Persistent activation by constitutive Ste7 promotes Kss1-mediated invasive growth but fails to support Fus3-dependent mating in yeast. Mol. Cell Biol. *24*, 9221-9238.

Mao,X., Cao,F., Nie,X., Liu,H., and Chen,J. (2006). The Swi/Snf chromatin remodeling complex is essential for hyphal development in *Candida albicans*. FEBS Lett. *580*, 2615-2622.

Mao,X., Li,Y., Wang,H., Cao,F., and Chen,J. (2008). Antagonistic interplay of Swi1 and Tup1 on filamentous growth of *Candida albicans*. FEMS Microbiol. Lett. *285*, 233-241.

Marichal,P., Koymans,L., Willemsens,S., Bellens,D., Verhasselt,P., Luyten,W., Borgers,M., Ramaekers,F.C., Odds,F.C., and Bossche,H.V. (1999). Contribution of mutations in the cytochrome P450 14alpha-demethylase (Erg11p, Cyp51p) to azole resistance in *Candida albicans*. Microbiology *145 (Pt 10)*, 2701-2713.

Martin,M.V. and Wilkinson,G.R. (1983). The oral yeast flora of 10-year-old schoolchildren. Sabouraudia. *21*, 129-135.

Mateus,C., Crow,S.A., Jr., and Ahearn,D.G. (2004). Adherence of *Candida albicans* to silicone induces immediate enhanced tolerance to fluconazole. Antimicrob. Agents Chemother. *48*, 3358-3366.

McCaffrey,G., Clay,F.J., Kelsay,K., and Sprague,G.F., Jr. (1987). Identification and regulation of a gene required for cell fusion during mating of the yeast *Saccharomyces cerevisiae*. Mol. Cell Biol. *7*, 2680-2690.

Messenguy,F. and Scherens,B. (1990). Induction of "General Control" and thermotolerance in cdc mutants of *Saccharomyces cerevisiae*. Mol. Gen. Genet. *224*, 257-263.

Michaelis,S. and Herskowitz,I. (1988). The **a**-factor pheromone of *Saccharomyces cerevisiae* is essential for mating. Mol. Cell Biol. *8*, 1309-1318.

Michaelis,S., Chen,P., Berkower,C., Sapperstein,S., and Kistler,A. (1992). Biogenesis of yeast a-factor involves prenylation, methylation and a novel export mechanism. Antonie Van Leeuwenhoek *61*, 115-117.

Michelitsch,M.D. and Weissman,J.S. (2000). A census of glutamine/asparagine-rich regions: implications for their conserved function and the prediction of novel prions. Proc. Natl. Acad. Sci. U. S. A *97*, 11910-11915.

Mickle,W.A. and Jones,C.P. (1940). Dissociation of *Candida albicans* by lithium chloride and immune serum. J. Bacteriol. *39*, 633-647.

Miller,M.G. and Johnson,A.D. (2002). White-opaque switching in *Candida albicans* is controlled by mating-type locus homeodomain proteins and allows efficient mating. Cell *110*, 293-302.

Mitchell,A.P. (1998). Dimorphism and virulence in *Candida albicans*. Curr. Opin. Microbiol. *1*, 687-692.

Mitchell,L.H. and Soll,D.R. (1979). Commitment to germ tube or bud formation during release from stationary phase in *Candida albicans*. Exp. Cell Res. *120*, 167-179.

Mitrovich,Q.M. and Guthrie,C. (2007). Evolution of small nuclear RNAs in *S. cerevisiae*, *C. albicans*, and other hemiascomycetous yeasts. RNA. *13*, 2066-2080.

Miyajima,I., Nakafuku,M., Nakayama,N., Brenner,C., Miyajima,A., Kaibuchi,K., Arai,K., Kaziro,Y., and Matsumoto,K. (1987). *GPA1*, a haploid-specific essential gene, encodes a yeast homolog of mammalian G protein which may be involved in mating factor signal transduction. Cell *50*, 1011-1019.

Miyasaki,S.H., Hicks,J.B., Greenspan,D., Polacheck,I., MacPhail,L.A., White,T.C., Agabian,N., and Greenspan,J.S. (1992). The identification and tracking of *Candida albicans* isolates from oral lesions in HIV-seropositive individuals. J. Acquir. Immune. Defic. Syndr. *5*, 1039-1046.

Mock,R.C., Pollack,J.H., and Hashimoto,T. (1990). Carbon dioxide induces endotrophic germ tube formation in *Candida albicans*. Can. J. Microbiol. *36*, 249-253.

Moffat,J. and Andrews,B. (2004). Late-G1 cyclin-CDK activity is essential for control of cell morphogenesis in budding yeast. Nat. Cell Biol. *6*, 59-66.

Molin,S. and Tolker-Nielsen,T. (2003). Gene transfer occurs with enhanced efficiency in biofilms and induces enhanced stabilisation of the biofilm structure. Curr. Opin. Biotechnol. *14*, 255-261.

Moore,S.A. (1983). Comparison of dose-response curves for alpha factor-induced cell division arrest, agglutination, and projection formation of yeast cells. Implication for the mechanism of alpha factor action. J. Biol. Chem. *258*, 13849-13856.

Morrow,B., Anderson,J., Wilson,J., and Soll,D.R. (1989). Bidirectional stimulation of the white-opaque transition of *Candida albicans* by ultraviolet irradiation. J. Gen. Microbiol. *135*, 1201-1208.

Morrow,B., Srikantha,T., and Soll,D.R. (1992). Transcription of the gene for a pepsinogen, *PEP1*, is regulated by white-opaque switching in *Candida albicans*. Mol. Cell Biol. *12*, 2997-3005.

Morrow,B., Srikantha,T., Anderson,J., and Soll,D.R. (1993). Coordinate regulation of two opaque-phase-specific genes during white-opaque switching in *Candida albicans*. Infect. Immun. *61*, 1823-1828.

Mosch,H.U. and Fink,G.R. (1997). Dissection of filamentous growth by transposon mutagenesis in *Saccharomyces cerevisiae*. Genetics *145*, 671-684.

Mukherjee,P.K., Chandra,J., Kuhn,D.M., and Ghannoum,M.A. (2003). Mechanism of fluconazole resistance in *Candida albicans* biofilms: phase-specific role of efflux pumps and membrane sterols. Infect. Immun. *71*, 4333-4340.

Mulhern,S.M., Logue,M.E., and Butler,G. (2006). *Candida albicans* transcription factor Ace2 regulates metabolism and is required for filamentation in hypoxic conditions. Eukaryot. Cell *5*, 2001-2013.

Murad,A.M. *et al.* (2001). *NRG1* represses yeast-hypha morphogenesis and hypha-specific gene expression in *Candida albicans*. EMBO J. *20*, 4742-4752.

Murillo,L.A., Newport,G., Lan,C.Y., Habelitz,S., Dungan,J., and Agabian,N.M. (2005). Genome-wide transcription profiling of the early phase of biofilm formation by *Candida albicans*. Eukaryot. Cell *4*, 1562-1573.

Naglik,J.R., Challacombe,S.J., and Hube,B. (2003). *Candida albicans* secreted aspartyl proteinases in virulence and pathogenesis. Microbiol. Mol. Biol. Rev. *67*, 400-28, table.

Nakayama,N., Miyajima,A., and Arai,K. (1985). Nucleotide sequences of *STE2* and *STE3*, cell type-specific sterile genes from *Saccharomyces cerevisiae*. EMBO J. *4*, 2643-2648.

Nakayama,N., Miyajima,A., and Arai,K. (1987). Common signal transduction system shared by *STE2* and *STE3* in haploid cells of *Saccharomyces cerevisiae*: autocrine cell-cycle arrest results from forced expression of *STE2*. EMBO J. *6*, 249-254.

Nakayama,N., Kaziro,Y., Arai,K., and Matsumoto,K. (1988). Role of *STE* genes in the mating factor signaling pathway mediated by *GPA1* in *Saccharomyces cerevisiae*. Mol. Cell Biol. *8*, 3777-3783.

Nantel,A. *et al.* (2002). Transcription profiling of *Candida albicans* cells undergoing the yeast-to-hyphal transition. Mol. Biol. Cell *13*, 3452-3465.

Nasmyth,K.A. (1982). Molecular genetics of yeast mating type. Annu. Rev. Genet. *16*, 439-500.

Navarro-Garcia,F., Sanchez,M., Pla,J., and Nombela,C. (1995). Functional characterization of the *MKC1* gene of *Candida albicans*, which encodes a mitogen-activated protein kinase homolog related to cell integrity. Mol. Cell Biol. *15*, 2197-2206.

Navarro-Garcia,F., Alonso-Monge,R., Rico,H., Pla,J., Sentandreu,R., and Nombela,C. (1998). A role for the MAP kinase gene *MKC1* in cell wall construction and morphological transitions in *Candida albicans*. Microbiology *144 (Pt 2)*, 411-424.

Nett,J. and Andes,D. (2006). *Candida albicans* biofilm development, modeling a host-pathogen interaction. Curr. Opin. Microbiol. *9*, 340-345.

Nikawa,J., Cameron,S., Toda,T., Ferguson,K.M., and Wigler,M. (1987). Rigorous feedback control of cAMP levels in Saccharomyces cerevisiae. Genes Dev. *1*, 931-937.

Nobile,C.J. and Mitchell,A.P. (2005). Regulation of cell-surface genes and biofilm formation by the *C. albicans* transcription factor Bcr1p. Curr. Biol. *15*, 1150-1155.

Nobile,C.J. and Mitchell,A.P. (2006). Genetics and genomics of *Candida albicans* biofilm formation. Cell Microbiol. *8*, 1382-1391.

Nobile,C.J., Andes,D.R., Nett,J.E., Smith,F.J., Yue,F., Phan,Q.T., Edwards,J.E., Filler,S.G., and Mitchell,A.P. (2006a). Critical role of Bcr1-dependent adhesins in *C. albicans* biofilm formation in vitro and in vivo. PLoS. Pathog. *2*, e63.

Nobile,C.J., Nett,J.E., Andes,D.R., Mitchell,A.P. (2006b). Function of *Candida albicans* adhesin Hwp1 in biofilm formation. Eukaryot Cell *5*, 1604-10.

Nobile,C.J., Schneider,H.A., Nett,J.E., Sheppard,D.C., Filler,S.G., Andes,D.R., and Mitchell,A.P. (2008). Complementary adhesin function in *C. albicans* biofilm formation. Curr. Biol. *18*, 1017-1024.

Nobile,C.J., Nett,J.E., Herndday,A.D., Homann,O.R., Deneault,J.S., Nantel,A., Andes,D.R., Johnson,A.D., and Mitchell,A.P. (2009). Biofilm matrix regulation by *Candida albicans* Zap1. PLoS. Biol. *7*, e1000133.

Nolan,S., Cowan,A.E., Koppel,D.E., Jin,H., and Grote,E. (2006). *FUS1* regulates the opening and expansion of fusion pores between mating yeast. Mol. Biol. Cell *17*, 2439-2450.

Norice,C.T., Smith,F.J., Jr., Solis,N., Filler,S.G., and Mitchell,A.P. (2007). Requirement for *Candida albicans* Sun41 in biofilm formation and virulence. Eukaryot. Cell *6*, 2046-2055.

Odds,E.C. (1997). Switch of phenotype as an escape mechanism of the intruder. Mycoses *40 Suppl 2*, 9-12.

Odds,F.C., Cheesman,S.L., and Abbott,A.B. (1986). Antifungal effects of fluconazole (UK 49858), a new triazole antifungal, in vitro. J. Antimicrob. Chemother. *18*, 473-478.

Odds,F.C. 1988. *Candida* and candidosis: a review and bibliography. Bailliere Tindale,London, United Kingdom.

Odds,F.C. and Jacobsen,M.D. (2008). Multilocus sequence typing of pathogenic *Candida* species. Eukaryot. Cell *7*, 1075-1084.

Oehlen,L. and Cross,F.R. (1998). The mating factor response pathway regulates transcription of *TEC1*, a gene involved in pseudohyphal differentiation of *Saccharomyces cerevisiae*. FEBS Lett. *429*, 83-88.

Oh,K.B., Miyazawa,H., Naito,T., and Matsuoka,H. (2001). Purification and characterization of an autoregulatory substance capable of regulating the morphological transition in *Candida albicans*. Proc. Natl. Acad. Sci. U. S. A *98*, 4664-4668.

Overton,M.C., Chinault,S.L., and Blumer,K.J. (2003). Oligomerization, biogenesis, and signaling is promoted by a glycophorin A-like dimerization motif in transmembrane domain 1 of a yeast G protein-coupled receptor. J. Biol. Chem. *278*, 49369-49377.

Paliwal,S., Iglesias,P.A., Campbell,K., Hilioti,Z., Groisman,A., and Levchenko,A. (2007). MAPK-mediated bimodal gene expression and adaptive gradient sensing in yeast. Nature *446*, 46-51.

Pan,X., Harashima,T., and Heitman,J. (2000). Signal transduction cascades regulating pseudohyphal differentiation of *Saccharomyces cerevisiae*. Curr. Opin. Microbiol. *3*, 567-572.

Panwar,S.L., Legrand,M., Dignard,D., Whiteway,M., and Magee,P.T. (2003). *MFalpha1*, the gene encoding the alpha mating pheromone of *Candida albicans*. Eukaryot. Cell *2*, 1350-1360.

Park,Y.N. and Morschhauser,J. (2005). Tetracycline-inducible gene expression and gene deletion in *Candida albicans*. Eukaryot. Cell *4*, 1328-1342.

Pendrak,M.L., Yan,S.S., and Roberts,D.D. (2004). Hemoglobin regulates expression of an activator of mating-type locus alpha genes in *Candida albicans*. Eukaryot. Cell *3*, 764-775.

Perea,S., Lopez-Ribot,J.L., Kirkpatrick,W.R., McAtee,R.K., Santillan,R.A., Martinez,M., Calabrese,D., Sanglard,D., and Patterson,T.F. (2001). Prevalence of molecular mechanisms of resistance to azole antifungal agents in *Candida albicans* strains displaying high-level fluconazole resistance isolated from human immunodeficiency virus-infected patients. Antimicrob. Agents Chemother. *45*, 2676-2684.

Perepnikhatka,V., Fischer,F.J., Niimi,M., Baker,R.A., Cannon,R.D., Wang,Y.K., Sherman,F., and Rustchenko,E. (1999). Specific chromosome alterations in fluconazole-resistant mutants of *Candida albicans*. J. Bacteriol. *181*, 4041-4049.

Perez,A., Pedros,B., Murgui,A., Casanova,M., Lopez-Ribot,J.L., and Martinez,J.P. (2006). Biofilm formation by *Candida albicans* mutants for genes coding fungal proteins exhibiting the eight-cysteine-containing CFEM domain. FEMS Yeast Res. *6*, 1074-1084.

Perutz,M.F., Johnson,T., Suzuki,M., and Finch,J.T. (1994). Glutamine repeats as polar zippers: their possible role in inherited neurodegenerative diseases. Proc. Natl. Acad. Sci. U. S. A *91*, 5355-5358.

Peters,R.B., Bahn,A.N., and Barens,G. (1966). *Candida albicans* in the oral cavities of diabetics. J. Dent. Res. *45*, 771-777.

Pfaller,M.A., Diekema,D.J., Jones,R.N., Sader,H.S., Fluit,A.C., Hollis,R.J., and Messer,S.A. (2001). International surveillance of bloodstream infections due to *Candida* species: frequency of occurrence and in vitro susceptibilities to fluconazole, ravuconazole, and voriconazole of isolates collected from 1997 through 1999 in the SENTRY antimicrobial surveillance program. J. Clin. Microbiol. *39*, 3254-3259.

Phan,Q.T., Belanger,P.H., and Filler,S.G. (2000). Role of hyphal formation in interactions of *Candida albicans* with endothelial cells. Infect. Immun. *68*, 3485-3490.

Phan,Q.T., Myers,C.L., Fu,Y., Sheppard,D.C., Yeaman,M.R., Welch,W.H., Ibrahim,A.S., Edwards,J.E., Jr., and Filler,S.G. (2007). Als3 is a *Candida albicans* invasin that binds to cadherins and induces endocytosis by host cells. PLoS. Biol. *5*, e64.

Pitarch,A., Pardo,M., Jimenez,A., Pla,J., Gil,C., Sanchez,M., and Nombela,C. (1999). Two-dimensional gel electrophoresis as analytical tool for identifying *Candida albicans* immunogenic proteins. Electrophoresis *20*, 1001-1010.

Pitarch,A., Sanchez,M., Nombela,C., and Gil,C. (2003). Analysis of the *Candida albicans* proteome. I. Strategies and applications. J. Chromatogr. B Analyt. Technol. Biomed. Life Sci. *787*, 101-128.

Powderly,W.G. (1992). Mucosal candidiasis caused by non-albicans species of *Candida* in HIV-positive patients. AIDS *6*, 604-605.

Prasad,R., De,W.P., Goffeau,A., and Balzi,E. (1995). Molecular cloning and characterization of a novel gene of *Candida albicans*, *CDR1*, conferring multiple resistance to drugs and antifungals. Curr. Genet. *27*, 320-329.

Price,L.A., Kajkowski,E.M., Hadcock,J.R., Ozenberger,B.A., and Pausch,M.H. (1995). Functional coupling of a mammalian somatostatin receptor to the yeast pheromone response pathway. Mol. Cell Biol. *15*, 6188-6195.

Price,L.A., Strnad,J., Pausch,M.H., and Hadcock,J.R. (1996). Pharmacological characterization of the rat A2a adenosine receptor functionally coupled to the yeast pheromone response pathway. Mol. Pharmacol. *50*, 829-837.

Pujol,C., Joly,S., Lockhart,S.R., Noel,S., Tibayrenc,M., and Soll,D.R. (1997). Parity among the randomly amplified polymorphic DNA method, multilocus enzyme electrophoresis, and Southern blot hybridization with the moderately repetitive DNA probe Ca3 for fingerprinting *Candida albicans*. J. Clin. Microbiol. *35*, 2348-2358.

Pujol,C., Pfaller,M., and Soll,D.R. (2002). Ca3 fingerprinting of *Candida albicans* bloodstream isolates from the United States, Canada, South America, and Europe reveals a European clade. J. Clin. Microbiol. *40*, 2729-2740.

Pujol,C., Daniels,K.J., Lockhart,S.R., Srikantha,T., Radke,J.B., Geiger,J., and Soll,D.R. (2004). The closely related species *Candida albicans* and *Candida dubliniensis* can mate. Eukaryot. Cell *3*, 1015-1027.

Pujol,C., A.R.Dodgson, and D.R.Soll. 2005. Population genetics of ascomycetes pathogenic to humans and animals, p. 149-188. In: Evolutionary genetics of fungi, J. Xu (ed.), Horizonbioscience, The Cromwell Press, Norfolk, United Kingdom.

Ramage,G., Vandewalle,K., Wickes,B.L., and Lopez-Ribot,J.L. (2001). Characteristics of biofilm formation by *Candida albicans*. Rev. Iberoam. Micol. *18*, 163-170.

Ramage,G., Vandewalle,K., Lopez-Ribot,J.L., and Wickes,B.L. (2002). The filamentation pathway controlled by the Efg1 regulator protein is required for normal biofilm formation and development in *Candida albicans*. FEMS Microbiol. Lett. *214*, 95-100.

Ramage,G., Saville,S.P., Thomas,D.P., and Lopez-Ribot,J.L. (2005). *Candida* biofilms: an update. Eukaryot. Cell *4*, 633-638.

Ramer,S.W. and Davis,R.W. (1993). A dominant truncation allele identifies a gene, *STE20*, that encodes a putative protein kinase necessary for mating in *Saccharomyces cerevisiae*. Proc. Natl. Acad. Sci. U. S. A *90*, 452-456.

Ramirez-Zavala,B., Reuss,O., Park,Y.N., Ohlsen,K., and Morschhauser,J. (2008). Environmental induction of white-opaque switching in *Candida albicans*. PLoS. Pathog. *4*, e1000089.

Reedy,J.L., Floyd,A.M., and Heitman,J. (2009). Mechanistic plasticity of sexual reproduction and meiosis in the *Candida* pathogenic species complex. Curr. Biol. *19*, 891-899.

Reisner,A., Haagensen,J.A., Schembri,M.A., Zechner,E.L., and Molin,S. (2003). Development and maturation of *Escherichia coli* K-12 biofilms. Mol. Microbiol. *48*, 933-946.

Ren,B., Robert,F., Wyrick, J.J., Aparicio,O., Jennings,E.G., Simon,I., Zeitlinger,J., Schreiber,J., Hannett,N., Kanin,E., Volkert,T.L., Wilson,C.J., Bell,S.P., Young,R.A. (2000). Genome-wide location and function of DNA binding proteins. Science *290*, 2306-2309.

Reuss,O., Vik,A., Kolter,R., and Morschhauser,J. (2004). The *SAT1* flipper, an optimized tool for gene disruption in *Candida albicans*. Gene *341*, 119-127.

Reynolds,T.B. and Fink,G.R. (2001). Bakers' yeast, a model for fungal biofilm formation. Science *291*, 878-881.

Rhodes,N., Connell,L., and Errede,B. (1990). *STE11* is a protein kinase required for cell-type-specific transcription and signal transduction in yeast. Genes Dev. *4*, 1862-1874.

Richard,M.L., Nobile,C.J., Bruno,V.M., and Mitchell,A.P. (2005). *Candida albicans* biofilm-defective mutants. Eukaryot. Cell *4*, 1493-1502.

Rigden,D.J., Mello,L.V., and Galperin,M.Y. (2004). The PA14 domain, a conserved all-beta domain in bacterial toxins, enzymes, adhesins and signaling molecules. Trends Biochem. Sci. *29*, 335-339.

Riggle,P.J., Andrutis,K.A., Chen,X., Tzipori,S.R., and Kumamoto,C.A. (1999). Invasive lesions containing filamentous forms produced by a *Candida albicans* mutant that is defective in filamentous growth in culture. Infect. Immun. *67*, 3649-3652.

Riggsby,W.S., Torres-Bauza,L.J., Wills,J.W., and Townes,T.M. (1982). DNA content, kinetic complexity, and the ploidy question in *Candida albicans*. Mol. Cell Biol. *2*, 853-862.

Rikkerink,E.H., Magee,B.B., and Magee,P.T. (1988). Opaque-white phenotype transition: a programmed morphological transition in *Candida albicans*. J. Bacteriol. *170*, 895-899.

Rincon,M. and Pedraza-Alva,G. (2003). JNK and p38 MAP kinases in CD4+ and CD8+ T cells. Immunol. Rev. *192*, 131-142.

Roberts,C.J., Nelson, B., Marton, M. J., Stoughton, R., Meyer, M. R., Bennett, H. A., He, Y. D., Dai, H., Walker, W. L., Hughes, T. R., Tyers, M., Boone, C., and Friend, S. H. (2000). Signaling and circuitry of multiple MAPK pathways revealed by a matrix of global gene expression profiles. Science *287*, 873-880.

Rocha,C.R., Schroppel,K., Harcus,D., Marcil,A., Dignard,D., Taylor,B.N., Thomas,D.Y., Whiteway,M., and Leberer,E. (2001). Signaling through adenylyl cyclase is essential for hyphal growth and virulence in the pathogenic fungus *Candida albicans*. Mol. Biol. Cell *12*, 3631-3643.

Rohrer,J., Benedetti,H., Zanolari,B., and Riezman,H. (1993). Identification of a novel sequence mediating regulated endocytosis of the G protein-coupled alpha-pheromone receptor in yeast. Mol. Biol. Cell *4*, 511-521.

Roth,A.F. and Davis,N.G. (1996). Ubiquitination of the yeast **a**-factor receptor. J. Cell Biol. *134*, 661-674.

Rundlett,S.E., Carmen,A.A., Suka,N., Turner,B.M., and Grunstein,M. (1998). Transcriptional repression by *UME6* involves deacetylation of lysine 5 of histone H4 by *RPD3*. Nature *392*, 831-835.

Russell,C. and Lay,K.M. (1973). Natural history of *Candida* species and yeasts in the oral cavities of infants. Arch. Oral Biol. *18*, 957-962.

Sadhu,C., Hoekstra,D., McEachern,M.J., Reed,S.I., and Hicks,J.B. (1992). A G-protein alpha subunit from asexual *Candida albicans* functions in the mating signal transduction pathway of Saccharomyces cerevisiae and is regulated by the a1-alpha 2 repressor. Mol. Cell Biol. *12*, 1977-1985.

Sahni,N., Yi,S., Pujol,C., and Soll,D.R. (2009a). The white cell response to pheromone is a general characteristic of *Candida albicans* strains. Eukaryot. Cell *8*, 251-256.

Sahni,N., Yi,S., Daniels,K.J., Srikantha,T., Pujol,C., and Soll,D.R. (2009b). Genes selectively up-regulated by pheromone in white cells are involved in biofilm formation in *Candida albicans*. PLoS. Pathog. *5*, e1000601.

Saito,H. and Tatebayashi,K. (2004). Regulation of the osmoregulatory HOG MAPK cascade in yeast. J. Biochem. *136*, 267-272.

San-Blas,G.,Travassos,L.R., Fries,B.C., Goldman,D.L., Casadevall,A., Carmona,A.K., Barros,T.F., Puccia,R., Hostetter,M.K., Shanks,S.G., Copping,V.M., Knox,Y., Gow,N.A.. (2000). Fungal morphogenesis and virulence. Med. Mycol. *38 Suppl 1*, 79-86.

Sanglard,D., Ischer,F., Calabrese,D., Micheli,M., and Bille,J. (1998). Multiple resistance mechanisms to azole antifungals in yeast clinical isolates. Drug Resist. Updat. *1*, 255-265.

Sanglard,D., Ischer,F., Parkinson,T., Falconer,D., and Bille,J. (2003). *Candida albicans* mutations in the ergosterol biosynthetic pathway and resistance to several antifungal agents. Antimicrob. Agents Chemother. *47*, 2404-2412.

Santos,M. and de Larrinoa,I.F. (2005). Functional characterization of the *Candida albicans CRZ1* gene encoding a calcineurin-regulated transcription factor. Curr. Genet. *48*, 88-100.

Saville,S.P., Lazzell,A.L., Monteagudo,C., and Lopez-Ribot,J.L. (2003). Engineered control of cell morphology in vivo reveals distinct roles for yeast and filamentous forms of *Candida albicans* during infection. Eukaryot. Cell *2*, 1053-1060.

Schandel,K.A. and Jenness,D.D. (1994). Direct evidence for ligand-induced internalization of the yeast alpha-factor pheromone receptor. Mol. Cell Biol. *14*, 7245-7255.

Scherer,S. and Magee,P.T. (1990). Genetics of *Candida albicans*. Microbiol. Rev. *54*, 226-241.

Scherwitz,C. (1982). Ultrastructure of human cutaneous candidosis. J. Invest Dermatol. *78*, 200-205.

Schuit,K.E. (1979). Phagocytosis and intracellular killing of pathogenic yeasts by human monocytes and neutrophils. Infect. Immun. *24*, 932-938.

Schwartz,M.A. and Madhani,H.D. (2004). Principles of MAP kinase signaling specificity in *Saccharomyces cerevisiae*. Annu. Rev. Genet. *38*, 725-748.

Schweizer,A., Rupp,S., Taylor,B.N., Rollinghoff,M., and Schroppel,K. (2000). The TEA/ATTS transcription factor CaTec1p regulates hyphal development and virulence in Candida albicans. Mol. Microbiol. *38*, 435-445.

Seelig,M.S., Speth,C.P., Kozinn,P.J., Taschdjian,C.L., Toni,E.F., and Goldberg,P. (1974). Patterns of *Candida* endocarditis following cardiac surgery: Importance of early diagnosis and therapy (an analysis of 91 cases). Prog. Cardiovasc. Dis. *17*, 125-160.

Sellam,A., Al-Niemi,T., McInnerney,K., Brumfield,S., Nantel,A., and Suci,P.A. (2009). A *Candida albicans* early stage biofilm detachment event in rich medium. BMC. Microbiol. *9*, 25.

Selmecki,A., Bergmann,S., and Berman,J. (2005). Comparative genome hybridization reveals widespread aneuploidy in *Candida albicans* laboratory strains. Mol. Microbiol. *55*, 1553-1565.

Selmecki,A., Forche,A., and Berman,J. (2006). Aneuploidy and isochromosome formation in drug-resistant *Candida albicans*. Science *313*, 367-370.

Seneviratne,C.J., Wang,Y., Jin,L., Abiko,Y., and Samaranayake,L.P. (2008). *Candida albicans* biofilm formation is associated with increased anti-oxidative capacities. Proteomics. *8*, 2936-2947.

Sengupta,P. and Cochran,B.H. (1990). The PRE and PQ box are functionally distinct yeast pheromone response elements. Mol. Cell Biol. *10*, 6809-6812.

Sewall,T.C., Mims,C.W., and Timberlake,W.E. (1990). abaA controls phialide differentiation in *Aspergillus nidulans*. Plant Cell *2*, 731-739.

Shannon,J.L. and Rothman,A.H. (1971). Transverse septum formation in budding cells of the yeastlike fungus *Candida albicans*. J. Bacteriol. *106*, 1026-1028.

Sharkey,L.L., McNemar,M.D., Saporito-Irwin,S.M., Sypherd,P.S., and Fonzi,W.A. (1999). *HWP1* functions in the morphological development of *Candida albicans* downstream of *EFG1*, *TUP1*, and *RBF1*. J. Bacteriol. *181*, 5273-5279.

Sheppard,D.C., Yeaman,M.R., Welch,W.H., Phan,Q.T., Fu,Y., Ibrahim,A.S., Filler,S.G., Zhang,M., Waring,A.J., and Edwards,J.E., Jr. (2004). Functional and structural diversity in the Als protein family of *Candida albicans*. J. Biol. Chem. *279*, 30480-30489.

Sherwood-Higham,J., Zhu,W.Y., Devine,C.A., Gooday,G.W., Gow,N.A., and Gregory,D.W. (1994). Helical growth of hyphae of *Candida albicans*. J. Med. Vet. Mycol. *32*, 437-445.

Sherwood,J., Gow,N.A., Gooday,G.W., Gregory,D.W., and Marshall,D. (1992). Contact sensing in *Candida albicans*: a possible aid to epithelial penetration. J. Med. Vet. Mycol. *30*, 461-469.

Shih,S.C., Sloper-Mould,K.E., and Hicke,L. (2000). Monoubiquitin carries a novel internalization signal that is appended to activated receptors. EMBO J. *19*, 187-198.

Shimoda,C. and Yanagishima,N. (1975). Mating reaction in *Saccharomyces cerevisiae*. VIII. Mating-type-specific substances responsible for sexual cell agglutination. Antonie Van Leeuwenhoek *41*, 521-532.

Simonetti,N., Strippoli,V., and Cassone,A. (1974). Yeast-mycelial conversion induced by N-acetyl-D-glucosamine in *Candida albicans*. Nature *250*, 344-346.

Simuangco,S.A., Fernandez,M.C., Campos,P.O., Ortiz,M., and Jacaline,A. (1957). Cutaneous candidiasis; a clinical and therapeutic study. J. Philipp. Med. Assoc. *33*, 257-270.

Singh,B., Cutler,J.C., and Utidjian,H.M. (1972). Studies on development of a vaginal preparation providing both prophylaxis against venereal disease, other genital infections and contraception. 3. In vitro effect of vaginal contraceptive and selected vaginal preparations of *Candida albicans* and *Trichomonas vaginalis*. Contraception *5*, 401-411.

Singh,S.D., Robbins,N., Zaas,A.K., Schell,W.A., Perfect,J.R., and Cowen,L.E. (2009). Hsp90 governs echinocandin resistance in the pathogenic yeast *Candida albicans* via calcineurin. PLoS. Pathog. *5*, e1000532.

Singleton,D.R., Masuoka,J., and Hazen,K.C. (2001). Cloning and analysis of a *Candida albicans* gene that affects cell surface hydrophobicity. J. Bacteriol. *183*, 3582-3588.

Singleton,D.R. and Hazen,K.C. (2004). Differential surface localization and temperature-dependent expression of the *Candida albicans* CSH1 protein. Microbiology *150*, 285-292.

Singleton,D.R., Fidel,P.L., Jr., Wozniak,K.L., and Hazen,K.C. (2005). Contribution of cell surface hydrophobicity protein 1 (Csh1p) to virulence of hydrophobic *Candida albicans* serotype A cells. FEMS Microbiol. Lett. *244*, 373-377.

Skoglund,R.W. (1971). Diabetes presenting with phimosis. Lancet *2*, 1431.

Slessareva,J.E., Routt,S.M., Temple,B., Bankaitis,V.A., and Dohlman,H.G. (2006). Activation of the phosphatidylinositol 3-kinase Vps34 by a G protein alpha subunit at the endosome. Cell *126*, 191-203.

Slessareva,J.E. and Dohlman,H.G. (2006). G protein signaling in yeast: new components, new connections, new compartments. Science *314*, 1412-1413.

Slutsky,B., Buffo,J., and Soll,D.R. (1985). High-frequency switching of colony morphology in *Candida albicans*. Science *230*, 666-669.

Slutsky,B., Staebell,M., Anderson,J., Risen,L., Pfaller,M., and Soll,D.R. (1987). "White-opaque transition": a second high-frequency switching system in *Candida albicans*. J. Bacteriol. *169*, 189-197.

Smith,D.A., Nicholls,S., Morgan,B.A., Brown,A.J., and Quinn,J. (2004). A conserved stress-activated protein kinase regulates a core stress response in the human pathogen *Candida albicans*. Mol. Biol. Cell *15*, 4179-4190.

Soll,D.R. and Herman,M.A. (1983). Growth and the inducibility of mycelium formation in *Candida albicans*: a single-cell analysis using a perfusion chamber. J. Gen. Microbiol. *129*, 2809-2824.

Soll,D.R. (1986). The regulation of cellular differentiation in the dimorphic yeast *Candida albicans*. Bioessays *5*, 5-11.

Soll,D.R., Galask,R., Isley,S., Rao,T.V., Stone,D., Hicks,J., Schmid,J., Mac,K., and Hanna,C. (1989). Switching of *Candida albicans* during successive episodes of recurrent vaginitis. J. Clin. Microbiol. *27*, 681-690.

Soll,D.R., Galask,R., Schmid,J., Hanna,C., Mac,K., and Morrow,B. (1991). Genetic dissimilarity of commensal strains of *Candida* spp. carried in different anatomical locations of the same healthy women. J. Clin. Microbiol. *29*, 1702-1710.

Soll,D.R. (1992). High-frequency switching in *Candida albicans*. Clin. Microbiol. Rev. *5*, 183-203.

Soll,D.R. and Srikantha,T. (1998). Reporters for the analysis of gene regulation in fungi pathogenic to man. Curr. Opin. Microbiol. *1*, 400-405.

Soll,D.R. (2002). *Candida* commensalism and virulence: the evolution of phenotypic plasticity. Acta Trop. *81*, 101-110.

Soll,D.R. and Pujol,C. (2003). *Candida albicans* clades. FEMS Immunol. Med. Microbiol. *39*, 1-7.

Soll,D.R. 2004. Mating-type locus homozygosis, phenotypic switching and mating: a unique sequence of dependencies in *Candida albicans*. *Bioessays* **26**: 10-20.

Soll,D.R., C.Pujol, and S.R.Lockhart. 2007. Laboratory procedures for the epidemiological analysis of microorganisms, p. 129-151. *In* P. R. Murray, E. J. Baron, J. H. Jorgensen, M. L. Landry, and M. A. Pfaller (ed.), Manual of clinical microbiology, 9th ed. ASM Press, Washington, DC.

Soll,D.R., and K.J.Daniels. 2007. *MAT*, mating, switching, and pathogenesis in *Candida albicans*, *Candida dubliniensis* and *Candida glabrata*. In: Sex in Fungi, J. Heitman, J. W. Kronstad, J. W. Taylor, and L. A. Casselton, Washington, DC: ASM Press, 215–234.

Soll,D.R. (2008). *Candida* biofilms: is adhesion sexy? Curr. Biol. *18*, R717-R720.

Soll,D.R., Pujol,C., and Srikantha,T. (2009). Sex: deviant mating in yeast. Curr. Biol. *19*, R509-R511.

Soll,D.R. (2009). Why does *Candida albicans* switch? FEMS Yeast Res. *9*, 973-989.

Solomon,M.J. and Varshavsky,A. (1985). Formaldehyde-mediated DNA-protein crosslinking: a probe for in vivo chromatin structures. Proc. Natl. Acad. Sci. U. S. A *82*, 6470-6474.

Sonneborn A., Tebarth B., and Ernst J.F. (1999). Control of white-opaque phenotypic switching in *Candida albicans* by the Efg1p morphogenetic regulator**.** Infect. Immun. *67***:** 4655-4660.

Sonneborn,A., Bockmuhl,D.P., Gerads,M., Kurpanek,K., Sanglard,D., and Ernst,J.F. (2000). Protein kinase A encoded by TPK2 regulates dimorphism of Candida albicans. Mol. Microbiol. *35*, 386-396.

Souciet,J.,Aigle M, Artiguenave F, Blandin G, Bolotin-Fukuhara M, Bon E, Brottier P, Casaregola S, de Montigny J, Dujon B, Durrens P, Gaillardin C, Lépingle A, Llorente B, Malpertuy A, Neuvéglise C, Ozier-Kalogéropoulos O, Potier S, Saurin W, Tekaia F, Toffano-Nioche C, Wésolowski-Louvel M, Wincker P, Weissenbach J. (2000). Genomic exploration of the hemiascomycetous yeasts: 1. A set of yeast species for molecular evolution studies. FEBS Lett. *487*, 3-12.

Souto,G., Giacometti,R., Silberstein,S., Giasson,L., Cantore,M.L., and Passeron,S. (2006). Expression of *TPK1* and *TPK2* genes encoding PKA catalytic subunits during growth and morphogenesis in *Candida albicans*. Yeast *23*, 591-603.

Sprague,G.F., Jr., Blair,L.C., and Thorner,J. (1983). Cell interactions and regulation of cell type in the yeast Saccharomyces cerevisiae. Annu. Rev. Microbiol. *37*, 623-660.

Sprague,G.F., Jr. (1991). Assay of yeast mating reaction. Methods Enzymol. *194*, 77-93.

Srikantha,T. and Soll,D.R. (1993). A white-specific gene in the white-opaque switching system of *Candida albicans*. Gene *131*, 53-60.

Srikantha,T., Klapach,A., Lorenz,W.W., Tsai,L.K., Laughlin,L.A., Gorman,J.A., and Soll,D.R. (1996). The sea pansy Renilla reniformis luciferase serves as a sensitive bioluminescent reporter for differential gene expression in *Candida albicans*. J. Bacteriol. *178*, 121-129.

Srikantha,T., Tsai,L.K., and Soll,D.R. (1997). The *WH11* gene of *Candida albicans* is regulated in two distinct developmental programs through the same transcription activation sequences. J. Bacteriol. *179*, 3837-3844.

Srikantha,T., Tsai,L.K., Daniels,K., and Soll,D.R. (2000). EFG1 null mutants of *Candida albicans* switch but cannot express the complete phenotype of white-phase budding cells. J. Bacteriol. *182*, 1580-1591.

Srikantha,T., Tsai,L., Daniels,K., Klar,A.J., and Soll,D.R. (2001). The histone deacetylase genes *HDA1* and *RPD3* play distinct roles in regulation of high-frequency phenotypic switching in *Candida albicans*. J. Bacteriol. *183*, 4614-4625.

Srikantha,T., Borneman,A.R., Daniels,K.J., Pujol,C., Wu,W., Seringhaus,M.R., Gerstein,M., Yi,S., Snyder,M., and Soll,D.R. (2006). *TOS9* regulates white-opaque switching in *Candida albicans*. Eukaryot. Cell *5*, 1674-1687.

Staab,J.F., Ferrer,C.A., and Sundstrom,P. (1996). Developmental expression of a tandemly repeated, proline-and glutamine-rich amino acid motif on hyphal surfaces on *Candida albicans*. J. Biol. Chem. *271*, 6298-6305.

Staab,J.F. and Sundstrom,P. (1998). Genetic organization and sequence analysis of the hypha-specific cell wall protein gene *HWP1* of *Candida albicans*. Yeast *14*, 681-686.

Staab,J.F., Bradway,S.D., Fidel,P.L., and Sundstrom,P. (1999). Adhesive and mammalian transglutaminase substrate properties of *Candida albicans* Hwp1. Science *283*, 1535-1538.

Staebell,M. and Soll,D.R. (1985). Temporal and spatial differences in cell wall expansion during bud and mycelium formation in *Candida albicans*. J. Gen. Microbiol. *131*, 1467-1480.

Stefan,C.J. and Blumer,K.J. (1994). The third cytoplasmic loop of a yeast G-protein-coupled receptor controls pathway activation, ligand discrimination, and receptor internalization. Mol. Cell Biol. *14*, 3339-3349.

Stenni,B., Masson-Delmotte,V., Johnsen,S., Jouzel,J., Longinelli,A., Monnin,E., Rothlisberger,R., and Selmo,E. (2001). An oceanic cold reversal during the last deglaciation. Science *293*, 2074-2077.

Stoldt,V.R., Sonneborn,A., Leuker,C.E., and Ernst,J.F. (1997). Efg1p, an essential regulator of morphogenesis of the human pathogen *Candida albicans*, is a member of a conserved class of bHLH proteins regulating morphogenetic processes in fungi. EMBO J. *16*, 1982-1991.

Strathern,J.N., Newlon,C.S., Herskowitz,I., and Hicks,J.B. (1979). Isolation of a circular derivative of yeast chromosome III: implications for the mechanism of mating type interconversion. Cell *18*, 309-319.

Strathern,J.N., Klar,A.J., Hicks,J.B., Abraham,J.A., Ivy,J.M., Nasmyth,K.A., and McGill,C. (1982). Homothallic switching of yeast mating type cassettes is initiated by a double-stranded cut in the MAT locus. Cell *31*, 183-192.

Strauss,A., Michel,S., and Morschhauser,J. (2001). Analysis of phase-specific gene expression at the single-cell level in the white-opaque switching system of *Candida albicans*. J. Bacteriol. *183*, 3761-3769.

Su,C., Li,Y., Lu,Y., and Chen,J. (2009). Mss11, a Transcriptional Activator, is Required for Hyphal Development in *Candida albicans*. Eukaryot. Cell.

Su,S.S. and Mitchell,A.P. (1993). Molecular characterization of the yeast meiotic regulatory gene *RIM1*. Nucleic Acids Res. *21*, 3789-3797.

Sudbery,P., Gow,N., and Berman,J. (2004). The distinct morphogenic states of *Candida albicans*. Trends Microbiol. *12*, 317-324.

Sudbery,P.E. (2001). The germ tubes of *Candida albicans* hyphae and pseudohyphae show different patterns of septin ring localization. Mol. Microbiol. *41*, 19-31.

Suka,N., Carmen,A.A., Rundlett,S.E., and Grunstein,M. (1998). The regulation of gene activity by histones and the histone deacetylase *RPD3*. Cold Spring Harb. Symp. Quant. Biol. *63*, 391-399.

Sullivan,D.J., Westerneng,T.J., Haynes,K.A., Bennett,D.E., and Coleman,D.C. (1995). *Candida dubliniensis* sp. nov.: phenotypic and molecular characterization of a novel species associated with oral candidosis in HIV-infected individuals. Microbiology *141 (Pt 7)*, 1507-1521.

Sullivan,P.A. and Shepherd,M.G. (1982). Gratuitous induction by N-acetylmannosamine of germ tube formation and enzymes for N-acetylglucosamine utilization in *Candida albicans*. J. Bacteriol. *151*, 1118-1122.

Sundstrom,P., Cutler,J.E., and Staab,J.F. (2002). Reevaluation of the role of *HWP1* in systemic candidiasis by use of *Candida albicans* strains with selectable marker *URA3* targeted to the *ENO1* locus. Infect. Immun. *70*, 3281-3283.

Suzuki,T., Ueda,T., Ohama,T., Osawa,S., and Watanabe,K. (1993). The gene for serine tRNA having anticodon sequence CAG in a pathogenic yeast, *Candida albicans*. Nucleic Acids Res. *21*, 356.

Taschdjian,C.L., Burchall,J.J., and Kozinn,P.J. (1960). Rapid identification of *Candida albicans* by filamentation on serum and serum substitutes. AMA. J. Dis. Child *99*, 212-215.

Tavanti,A., Davidson,A.D., Fordyce,M.J., Gow,N.A., Maiden,M.C., and Odds,F.C. (2005). Population structure and properties of *Candida albicans*, as determined by multilocus sequence typing. J. Clin. Microbiol. *43*, 5601-5613.

Tedford,K., Kim,S., Sa,D., Stevens,K., and Tyers,M. (1997). Regulation of the mating pheromone and invasive growth responses in yeast by two MAP kinase substrates. Curr. Biol. *7*, 228-238.

Tendolkar,P.M., Baghdayan,A.S., and Shankar,N. (2006). Putative surface proteins encoded within a novel transferable locus confer a high-biofilm phenotype to *Enterococcus faecalis*. J. Bacteriol. *188*, 2063-2072.

Thompson,J.D., Higgins,D.G., and Gibson,T.J. (1994). CLUSTAL W: improving the sensitivity of progressive multiple sequence alignment through sequence weighting, position-specific gap penalties and weight matrix choice. Nucleic Acids Res. *22*, 4673-4680.

Tripathi,G., Wiltshire,C., Macaskill,S., Tournu,H., Budge,S., and Brown,A.J. (2002). Gcn4 co-ordinates morphogenetic and metabolic responses to amino acid starvation in *Candida albicans*. EMBO J. *21*, 5448-5456.

Trueheart,J., Boeke,J.D., and Fink,G.R. (1987). Two genes required for cell fusion during yeast conjugation: evidence for a pheromone-induced surface protein. Mol. Cell Biol. *7*, 2316-2328.

Tsong,A.E., Miller,M.G., Raisner,R.M., and Johnson,A.D. (2003). Evolution of a combinatorial transcriptional circuit: a case study in yeasts. Cell *115*, 389-399.

Tsong,A.E., Tuch,B.B., Li,H., and Johnson,A.D. (2006). Evolution of alternative transcriptional circuits with identical logic. Nature *443*, 415-420.

Tsuchimori,N., Sharkey,L.L., Fonzi,W.A., French,S.W., Edwards,J.E., Jr., and Filler,S.G. (2000). Reduced virulence of HWP1-deficient mutants of *Candida albicans* and their interactions with host cells. Infect. Immun. *68*, 1997-2002.

Tyers,M. and Futcher,B. (1993). Far1 and Fus3 link the mating pheromone signal transduction pathway to three G1-phase Cdc28 kinase complexes. Mol. Cell Biol. *13*, 5659-5669.

Tzung,K.W. *et al.* (2001). Genomic evidence for a complete sexual cycle in *Candida albicans*. Proc. Natl. Acad. Sci. U. S. A *98*, 3249-3253.

Uhl,M.A., Biery,M., Craig,N., and Johnson,A.D. (2003). Haploinsufficiency-based large-scale forward genetic analysis of filamentous growth in the diploid human fungal pathogen *C.albicans*. EMBO J. *22*, 2668-2678.

Umazume,M., Ueta,E., and Osaki,T. (1995). Reduced inhibition of *Candida albicans* adhesion by saliva from patients receiving oral cancer therapy. J. Clin. Microbiol. *33*, 432-439.

Umeyama,T., Kaneko,A., Watanabe,H., Hirai,A., Uehara,Y., Niimi,M., and Azuma,M. (2006). Deletion of the *CaBIG1* gene reduces beta-1,6-glucan synthesis, filamentation, adhesion, and virulence in *Candida albicans*. Infect. Immun. *74*, 2373-2381.

Urban,M., Kahmann,R., and Bolker,M. (1996). Identification of the pheromone response element in *Ustilago maydis*. Mol. Gen. Genet. *251*, 31-37.

Valtz,N., Peter,M., and Herskowitz,I. (1995). *FAR1* is required for oriented polarization of yeast cells in response to mating pheromones. J. Cell Biol. *131*, 863-873.

Van het Hoog M, Rast TJ, Martchenko M, Grindle S, Dignard D, Hogues H, Cuomo C, Berriman M, Scherer S, Magee BB, Whiteway M, Chibana H, Nantel A, Magee PT. (2007). Assembly of the *Candida albicans* genome into sixteen supercontigs aligned on the eight chromosomes. Genome Biol. *8*, R52.

Vargas,K., Wertz,P.W., Drake,D., Morrow,B., and Soll,D.R. (1994). Differences in adhesion of *Candida albicans* 3153A cells exhibiting switch phenotypes to buccal epithelium and stratum corneum. Infect. Immun. *62*, 1328-1335.

Vargas,K., Messer,S.A., Pfaller,M., Lockhart,S.R., Stapleton,J.T., Hellstein,J., and Soll,D.R. (2000). Elevated phenotypic switching and drug resistance of *Candida albicans* from human immunodeficiency virus-positive individuals prior to first thrush episode. J. Clin. Microbiol. *38*, 3595-3607.

Vinces,M.D. and Kumamoto,C.A. (2007). The morphogenetic regulator Czf1p is a DNA-binding protein that regulates white opaque switching in *Candida albicans*. Microbiology *153*, 2877-2884.

Wakelam,M.J., Pettitt,T.R., and Postle,A.D. (2007). Lipidomic analysis of signaling pathways. Methods Enzymol. *432*, 233-246.

Weiner,J.L., Guttierez-Steil,C., and Blumer,K.J. (1993). Disruption of receptor-G protein coupling in yeast promotes the function of an *SST2*-dependent adaptation pathway. J. Biol. Chem. *268*, 8070-8077.

Whelan,W.L., Partridge,R.M., and Magee,P.T. (1980). Heterozygosity and segregation in *Candida albicans*. Mol. Gen. Genet. *180* , 107-113.

Whelan,W.L. and Magee,P.T. (1981). Natural heterozygosity in *Candida albicans*. J. Bacteriol. *145*, 896-903.

Whelan,W.L. and Soll,D.R. (1982). Mitotic recombination in *Candida albicans*: recessive lethal alleles linked to a gene required for methionine biosynthesis. Mol. Gen. Genet. *187*, 477-485.

White,T.C., Miyasaki,S.H., and Agabian,N. (1993). Three distinct secreted aspartyl proteinases in *Candida albicans*. J. Bacteriol. *175*, 6126-6133.

Whiteway,M., Hougan,L., and Thomas,D.Y. (1988). Expression of *MF alpha 1* in *MAT***a** cells supersensitive to alpha-factor leads to self-arrest. Mol. Gen. Genet. *214*, 85-88.

Whiteway,M., Hougan,L., Dignard,D., Thomas,D.Y., Bell,L., Saari,G.C., Grant,F.J., O'Hara,P., and MacKay,V.L. (1989). The *STE4* and *STE18* genes of yeast encode potential beta and gamma subunits of the mating factor receptor-coupled G protein. Cell *56*, 467-477.

Whiteway,M., Hougan,L., and Thomas,D.Y. (1990). Overexpression of the *STE4* gene leads to mating response in haploid *Saccharomyces cerevisiae*. Mol. Cell Biol. *10*, 217-222.

Whiteway,M. and Oberholzer,U. (2004). *Candida* morphogenesis and host-pathogen interactions. Curr. Opin. Microbiol. *7*, 350-357.

Whiteway,M. and Bachewich,C. (2007). Morphogenesis in *Candida albicans*. Annu. Rev. Microbiol. *61*, 529-553.

Wilkieson,C., Samaranayake,L.P., MacFarlane,T.W., Lamey,P.J., and MacKenzie,D. (1991). Oral candidosis in the elderly in long term hospital care. J. Oral Pathol. Med. *20*, 13-16.

Wilkinson,L.E. and Pringle,J.R. (1974). Transient G1 arrest of S. cerevisiae cells of mating type alpha by a factor produced by cells of mating type a. Exp. Cell Res. *89*, 175-187.

Wilson R.B., Davis D., and Mitchell A.P. (1999). Rapid hypothesis testing with *Candida albicans* through gene disruption with short homology regions**.** J. Bacteriol. *181***:** 1868-1874.

Wilson,R.B., Davis,D., Enloe,B.M., and Mitchell,A.P. (2000). A recyclable *Candida albicans URA3* cassette for PCR product-directed gene disruptions. Yeast *16*, 65-70.

Wilson,D., Tutulan-Cunita,A., Jung,W., Hauser,N.C., Hernandez,R., Williamson,T., Piekarska,K., Rupp,S., Young,T., and Stateva,L. (2007). Deletion of the high-affinity cAMP phosphodiesterase encoded by *PDE2* affects stress responses and virulence in *Candida albicans*. Mol. Microbiol. *65* , 841-856.

Wirsching,S., Michel,S., and Morschhauser,J. (2000). Targeted gene disruption in *Candida albicans* wild-type strains: the role of the *MDR1* gene in fluconazole resistance of clinical *Candida albicans* isolates. Mol. Microbiol. *36*, 856-865.

Wisplinghoff,H., Bischoff,T., Tallent,S.M., Seifert,H., Wenzel,R.P., and Edmond,M.B. (2004). Nosocomial bloodstream infections in US hospitals: analysis of 24,179 cases from a prospective nationwide surveillance study. Clin. Infect. Dis. *39*, 309-317.

Wong,S., Butler,G., and Wolfe,K.H. (2002). Gene order evolution and paleopolyploidy in hemiascomycete yeasts. Proc. Natl. Acad. Sci. U. S. A *99*, 9272-9277.

Wu,W., Pujol,C., Lockhart,S.R., and Soll,D.R. (2005). Chromosome loss followed by duplication is the major mechanism of spontaneous mating-type locus homozygosis in *Candida albicans*. Genetics *169*, 1311-1327.

Wu,W., Lockhart,S.R., Pujol,C., Srikantha,T., and Soll,D.R. (2007). Heterozygosity of genes on the sex chromosome regulates *Candida albicans* virulence. Mol. Microbiol. *64*, 1587-1604.

Xiao,J.H., Davidson,I., Matthes,H., Garnier,J.M., and Chambon,P. (1991). Cloning, expression, and transcriptional properties of the human enhancer factor TEF-1. Cell *65*, 551-568.

Xu,J.R. (2000). Map kinases in fungal pathogens. Fungal. Genet. Biol. *31*, 137-152.

Xu,X.L., Lee,R.T., Fang,H.M., Wang,Y.M., Li,R., Zou,H., Zhu,Y., and Wang,Y. (2008). Bacterial peptidoglycan triggers *Candida albicans* hyphal growth by directly activating the adenylyl cyclase Cyr1p. Cell Host. Microbe *4*, 28-39.

Yeung,T. and Grinstein,S. (2007). Lipid signaling and the modulation of surface charge during phagocytosis. Immunol. Rev. *219*, 17-36.

Yi,S., Sahni,N., Daniels,K.J., Pujol,C., Srikantha,T., and Soll,D.R. (2008). The same receptor, G protein, and mitogen-activated protein kinase pathway activate different downstream regulators in the alternative white and opaque pheromone responses of *Candida albicans*. Mol. Biol. Cell *19*, 957-970.

Yi,S., Sahni,N., Pujol,C., Daniels,K.J., Srikantha,T., Ma,N., and Soll,D.R. (2009). A *Candida albicans*-specific region of the alpha-pheromone receptor plays a selective role in the white cell pheromone response. Mol. Microbiol. *71*, 925-947.

Young, G. (1958). The process of invasion and the persistence of *Candida albicans* injected intraperitoneally into mice. J. Infect.Dis *102*, 114-120.

Zeitlinger,J., Simon,I., Harbison,C.T., Hannett,N.M., Volkert,T.L., Fink,G.R., and Young,R.A. (2003). Program-specific distribution of a transcription factor dependent on partner transcription factor and MAPK signaling. Cell *113*, 395-404.

Zhao,R., Lockhart,S.R., Daniels,K., and Soll,D.R. (2002). Roles of *TUP1* in switching, phase maintenance, and phase-specific gene expression in *Candida albicans*. Eukaryot. Cell *1*, 353-365.

Zhao,X., Oh,S.H., Yeater,K.M., and Hoyer,L.L. (2005a). Analysis of the *Candida albicans* Als2p and Als4p adhesins suggests the potential for compensatory function within the Als family. Microbiology *151*, 1619-1630.

Zhao,R., Daniels,K.J., Lockhart,S.R., Yeater,K.M., Hoyer,L.L., and Soll,D.R. (2005b). Unique aspects of gene expression during Candida albicans mating and possible G(1) dependency. Eukaryot. Cell *4*, 1175-1190.

Zhao,X., Malloy,P.J., Ardies,C.M., and Feldman,D. (1995). Oestrogen-binding protein in *Candida albicans*: antibody development and cellular localization by electron immunocytochemistry. Microbiology *141 (Pt 10)*, 2685-2692.

Zhao,X., Oh,S.H., Cheng,G., Green,C.B., Nuessen,J.A., Yeater,K., Leng,R.P., Brown,A.J., and Hoyer,L.L. (2004). *ALS3* and *ALS8* represent a single locus that encodes a *Candida albicans* adhesin; functional comparisons between Als3p and Als1p. Microbiology *150*, 2415-2428.

Zhao,X., Kim,Y., Park,G., and Xu,J.R. (2005). A mitogen-activated protein kinase cascade regulating infection-related morphogenesis in *Magnaporthe grisea*. Plant Cell *17*, 1317-1329.

Zhao,X., Oh,S.H., and Hoyer,L.L. (2007). Unequal contribution of *ALS9* alleles to adhesion between *Candida albicans* and human vascular endothelial cells. Microbiology *153*, 2342-2350.

Zheng,X., Wang,Y., and Wang,Y. (2004). Hgc1, a novel hypha-specific G1 cyclin-related protein regulates *Candida albicans* hyphal morphogenesis. EMBO J. *23*, 1845-1856.

Zordan,R.E., Galgoczy,D.J., and Johnson,A.D. (2006). Epigenetic properties of white-opaque switching in *Candida albicans* are based on a self-sustaining transcriptional feedback loop. Proc. Natl. Acad. Sci. U. S. A *103*, 12807-12812.

Zordan,R.E., Miller,M.G., Galgoczy,D.J., Tuch,B.B., and Johnson,A.D. (2007). Interlocking transcriptional feedback loops control white-opaque switching in *Candida albicans*. PLoS. Biol. *5*, e256.